

Drying Technologies in Food Processing

Dedications

To my family: Lishun, Lisa, Nathan and Benjamin

XDC

To my family for all their support

ASM

Drying Technologies in Food Processing

Edited by

Xiao Dong Chen

Department of Chemical Engineering
Monash University
Melbourne, Victoria
Australia

Arun S. Mujumdar

Department of Mechanical Engineering
Faculty of Engineering
National University of Singapore
Singapore



Blackwell
Publishing

This edition first published 2008
© 2008 Blackwell Publishing Ltd

Blackwell Publishing was acquired by John Wiley & Sons in February 2007. Blackwell's publishing programme has been merged with Wiley's global Scientific, Technical, and Medical business to form Wiley-Blackwell.

Registered office

John Wiley & Sons Ltd, The Atrium, Southern Gate, Chichester, West Sussex, PO19 8SQ, United Kingdom

Editorial office

9600 Garsington Road, Oxford, OX4 2DQ, United Kingdom

For details of our global editorial offices, for customer services and for information about how to apply for permission to reuse the copyright material in this book please see our website at www.wiley.com/wiley-blackwell.

The right of the author to be identified as the author of this work has been asserted in accordance with the Copyright, Designs and Patents Act 1988.

All rights reserved. No part of this publication may be reproduced, stored in a retrieval system, or transmitted, in any form or by any means, electronic, mechanical, photocopying, recording or otherwise, except as permitted by the UK Copyright, Designs and Patents Act 1988, without the prior permission of the publisher.

Wiley also publishes its books in a variety of electronic formats. Some content that appears in print may not be available in electronic books.

Designations used by companies to distinguish their products are often claimed as trademarks. All brand names and product names used in this book are trade names, service marks, trademarks or registered trademarks of their respective owners. The publisher is not associated with any product or vendor mentioned in this book. This publication is designed to provide accurate and authoritative information in regard to the subject matter covered. It is sold on the understanding that the publisher is not engaged in rendering professional services. If professional advice or other expert assistance is required, the services of a competent professional should be sought.

Library of Congress Cataloging-in-Publication Data

Drying technologies in food processing/edited by Xiao Dong Chen, Arun S. Mujumdar
p. cm.

Includes bibliographical references and index.

ISBN-13: 978-1-4051-5763-6 (hardback : alk. paper)

ISBN-10: 1-4051-5763-1 (hardback : alk. paper) 1. Drying. 2. Food industry and trade.

I. Chen, Xiao Dong. II. Mujumdar, Arun S.

TP363.D7945 2008

664'.0284—dc22

2008006131

A catalogue record for this book is available from the British Library.

Set in 10/12 pt Times by Newgen Imaging Systems (P) Ltd, Chennai, India

Printed in Singapore by C.O.S. Printers Pte Ltd

Contents

<i>Contributors</i>	xi
<i>Preface</i>	xiii
<i>Introduction: structural images of some fresh and processed foods</i> Xiao Dong Chen	xv
1 Food drying fundamentals	1
Xiao Dong Chen	
1.1 Introduction to food materials	1
1.2 Drying of food	2
1.3 Physical properties of foods	8
1.3.1 The scales of interest	8
1.3.2 Mechanical properties	10
1.3.3 Shrinkage and densities	15
1.3.4 Thermal properties and conventional heating	20
1.3.5 Colour	26
1.3.6 Equilibrium isotherms	29
1.4 Drying rate characteristic curve approach to correlate drying rates – van Meel's method	30
1.5 Diffusion theories of drying	32
1.5.1 Effective Fickian diffusivity	32
1.5.2 Intuitive understanding of the diffusion theory	34
1.5.3 Drying of foods simulated using the effective Fickian diffusion law	36
1.5.4 Alternative effective diffusion theories	38
1.6 Driers	42
1.7 Concluding remarks	43
1.8 Notation	44
Appendix I: Typical mass transfer correlations	46
Appendix II: On the 'effectiveness' of the effective moisture diffusivity benchmarked against the Luikov theory	46
Appendix III: Drying of pulped Kiwi fruit layer for making fruit leather	52
References	52
2 Water activity in food processing and preservation	55
Bhesh R. Bhandari and Benu P. Adhikari	
2.1 Introduction	55
2.1.1 Thermodynamics of water activity	56
2.1.2 Definition and significance	57

2.1.3	Sorption isotherms	58
2.1.4	Hysteresis in sorption isotherms	58
2.2	Composition-based water activity predictive models	59
2.2.1	Raoult's Law	59
2.2.2	Norrish model	60
2.2.3	Ross model	61
2.2.4	Money–Born equation	62
2.2.5	Grover model	63
2.2.6	Salwin equation	64
2.3	Models for prediction of sorption isotherms	65
2.3.1	Two-parameter models	65
2.3.2	Three-parameter isotherms	68
2.3.3	Effect of temperature on water activity	73
2.3.4	Water activity above boiling point	75
2.4	Types of sorption isotherms and hysteresis in isotherms	75
2.5	Determination of sorption isotherms	78
2.5.1	Gravimetric method	78
2.5.2	Manometric method	83
2.5.3	Hygroscopic methods	84
2.5.4	Sample preparation and equilibrium time	84
2.6	Concluding remarks	86
	References	86
3	Biological changes during food drying processes	90
	Xiao Dong Chen and Kamlesh C. Patel	
3.1	Introduction to drying and food quality	90
3.2	Post-drying problems	91
3.3	In-drying problems	95
3.4	Food bio-deterioration by drying – a sub-cell level approach	106
3.5	Concluding remarks	108
3.6	Notation	109
	References	109
4	Spray drying of food materials – process and product characteristics	113
	Bhesh R. Bhandari, Kamlesh C. Patel and Xiao Dong Chen	
4.1	Introduction	113
4.2	Basic concepts of spray drying	114
4.3	Components of a spray drying system	117
4.3.1	Drying gas supply and heating system	117
4.3.2	Atomization system	118
4.3.3	Drying chamber	121
4.3.4	Powder separators	122
4.4	Drying of droplets	125
4.4.1	Fundamentals of droplet drying	125
4.4.2	Drying kinetics	126
4.4.3	Residence time	129

4.5	Mass and heat balances over a spray drier	130
4.5.1	Overall mass balance	130
4.5.2	Overall heat balance	133
4.6	Drier efficiency	134
4.6.1	Thermal efficiency	134
4.6.2	Evaporative efficiency	136
4.6.3	Volumetric evaporative capacity	136
4.7	Powder characterization	137
4.7.1	Particle micro-structure	137
4.7.2	Particle morphology	139
4.7.3	Physical and functional properties of powder	141
4.7.4	Drying parameters	147
4.8	Spray drying of various food products	149
4.8.1	Dairy powders	149
4.8.2	Micro-encapsulated powders	151
4.8.3	Sugar-rich products	153
4.8.4	Egg	154
4.8.5	Enzymes	154
4.9	Concluding remarks	155
4.10	Notation	155
	References	157
5	Low-pressure superheated steam drying of food products	160
	Sakamon Devahastin and Peamsuk Suvarnakuta	
5.1	Introduction	160
5.2	Basic principles of superheated steam drying	161
5.3	Low-pressure superheated steam drying of foods and biomaterials	163
5.4	Some advances in LPSSD of foods and biomaterials	177
5.5	Mathematical modeling of LPSSD of foods and biomaterials	182
5.6	Concluding remarks	186
5.7	Notation	187
	References	187
6	Heat pump-assisted drying	190
	Md Raisul Islam and Arun S. Mujumdar	
6.1	Introduction	190
6.2	Classification of heat pump driers	191
6.3	Fundamentals of heat pump driers	191
6.4	Heat and mass transfer mechanisms	197
6.5	Optimum use of heat pumps in drying systems	210
6.6	Innovative heat pump drying systems	212
6.6.1	Multi-stage compression heat pump drying	213
6.6.2	Cascade heat pump drying systems	214
6.6.3	Heat pump drying systems with multiple evaporators in series and in parallel	215
6.6.4	Vapor absorption heat pump drier	217

6.7	Closing remarks	221
6.8	Notation	222
	References	223
7	Freeze and vacuum drying of foods	225
	Cristina Ratti	
7.1	Introduction	225
7.2	States of water	225
7.3	Food and air properties in relation to vacuum and freeze-drying	227
7.4	Heat transfer mechanisms at low pressures	232
7.5	Vacuum drying: principles and dehydration models	234
7.6	Freeze drying: principles and dehydration models	236
7.7	Illustrative example	239
7.8	Advances in vacuum and freeze drying of foods	243
7.9	Closure	245
7.10	Notation	245
	References	246
8	Post-drying aspects for meat and horticultural products	252
	Mohammad Shafiqur Rahman	
8.1	Introduction	252
8.2	State diagram and stability concepts of dried products	252
8.3	Controlling quality attributes	255
	8.3.1 Microbial quality	255
	8.3.2 Chemical changes and quality	257
	8.3.3 Physical changes and quality	260
	8.3.4 Vitamins retention	265
8.4	Conclusion	265
	References	265
9	Food drier process control	270
	Brent R. Young	
9.1	Introduction – why process control?	270
	9.1.1 Disturbance variables	270
	9.1.2 Control benefits	271
	9.1.3 Examples	271
	9.1.4 Chapter organization	272
9.2	What to control (manipulated and controlled variables)	272
	9.2.1 Controlled variables	272
	9.2.2 Manipulated variables	273
9.3	Where to control (control strategy)	273
	9.3.1 Plant-wide control strategy configuration	273
	9.3.2 Common loops and examples	274
9.4	When to control (control philosophy)	276
	9.4.1 After something happens – feedback control	276
	9.4.2 As something happens – feed-forward/predictive control	278

9.5	How to control (fundamental control methods)	279
9.5.1	PID feedback control and tuning	279
9.6	How to do advanced control (advanced control methods)	292
9.6.1	Model predictive control (MPC)	293
9.6.2	Adaptive control	295
9.6.3	Artificial intelligence in control	295
	References	297
10	Fire and explosion protection in food driers	299
	Xiao Dong Chen	
10.1	Introduction – thermal hazards in driers	299
10.1.1	Conditions for an explosion to occur	299
10.1.2	How serious is the problem?	300
10.1.3	What affects the degree of violence of a dust explosion?	300
10.1.4	How to reduce the risk of dust explosion	301
10.2	A practical example: milk powder plant safety	301
10.2.1	Fires	302
10.2.2	Explosion protection	310
10.3	Testing for various explosion parameters	314
10.4	The human factors	314
10.5	Concluding remarks	316
	References	316
	<i>Index</i>	319
	<i>The colour plate section follows page 40</i>	

Contributors

Benu P. Adhikari

School of Science and Engineering
The University of Ballarat
Mount Helen, Victoria
Australia

Bhesh R. Bhandari

School of Land, Crop and Food Sciences
The University of Queensland
St Lucia, Queensland
Australia

Xiao Dong Chen

Department of Chemical Engineering
Monash University
Clayton Campus
Melbourne, Victoria
Australia

Sakamon Devahastin

Department of Food Engineering
King Mongkut's University of Technology
Thonburi
Bangkok
Thailand

Md Raisul Islam

Department of Mechanical Engineering
School of Engineering and Science
Curtin University of Technology
Sarawak Campus Malaysia
Sarawak
Malaysia

Arun S. Mujumdar

Department of Mechanical Engineering
Faculty of Engineering
National University of Singapore
Singapore

Kamlesh C. Patel

Department of Chemical
Engineering
Monash University
Clayton Campus
Melbourne, Victoria
Australia

Mohammad Shafiur Rahman

Department of Food Science and
Nutrition
College of Agricultural and Marine
Sciences
Sultan Qaboos University
Sultanate of Oman

Cristina Ratti

Food Engineering Program
Département des Sols et de Génie
Agroalimentaire
Université Laval
Québec
Canada

Peamsuk Suvarnakuta

Department of Food Science and
Technology
Thammasat University
Rangsit Campus
Pathum Thani
Thailand

Brent R. Young

Department of Chemical and Materials
Engineering
The University of Auckland
Auckland
New Zealand

Preface

Thanks to significant improvements in agricultural technologies, there are abundant food resources in many countries around the world. Global transport means that foods and ingredients can be traded over larger distances than ever before, but the need for foods to be safe and wholesome remains paramount.

Most foods are highly perishable, so awareness of storage life (shelf-life) is vital if ingredients are to be transported over large distances and stored in warehouses, or by the consumer, for substantial periods. Drying is by far the most useful large scale operation method of keeping solid foods safe for long periods of time. Drying itself may be treated as a thermal processing method as the number of live micro-organisms can be reduced during drying. Nutrient content, on the other hand, has to be maintained at the highest level possible. Drying operations therefore need to be precisely controlled and optimised in order to produce a good quality product that has the highest level of nutrient retention and flavour, whilst maintaining microbial safety.

Although drying literature (from the engineering perspective) has become very extensive in recent years, drying of foods still presents many new challenges due to ever-diversifying product ranges. In this book, our intention is to look at food drying processes in an intuitive manner, so simplicity, and how to reduce a complex model to a simple one so it can be dealt with more effectively, has been emphasised. Where possible, examples are given either in the form of calculations or diagrams to demonstrate the underlying principles. All the main industrial drying methods have been covered here. A collection of microscopic images of the foods (fresh or dried) is also presented so that readers are reminded of the nature of the food micro-structure and the possible relationship between the structure and processing properties, such as transport properties and textures.

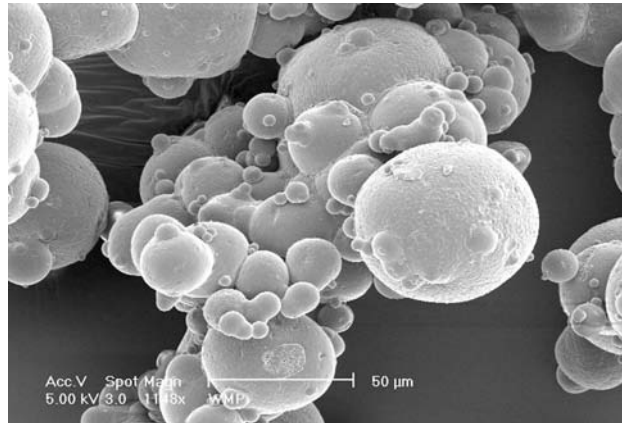
The book presents the key drying processes and their impacts on foods, and links micro-structural changes to processing parameters and product quality. It highlights many of the main issues related to food drying in what is designed to be an easily accessible manner. We hope that the book will make for enjoyable, thought-provoking reading and that it will be further improved and updated in due course.

Finally, the Editors are very grateful to the contributing authors of this book. Thanks also go to the publisher for making this book possible.

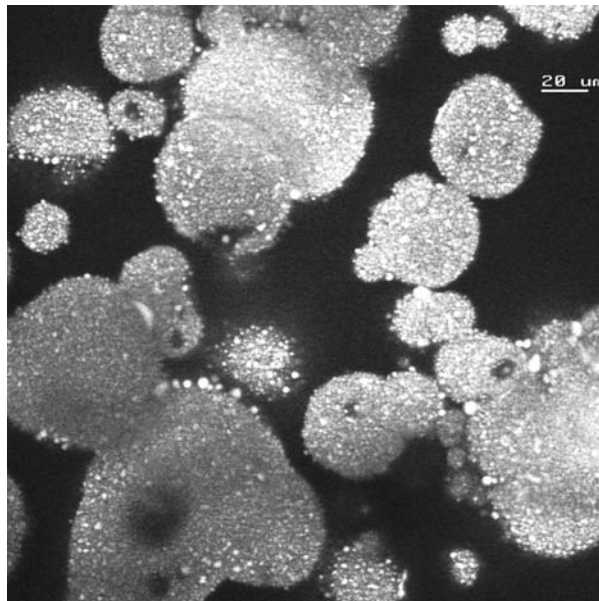
Xiao Dong Chen
Arun S. Mujumdar

Introduction: structural images of some fresh and processed foods

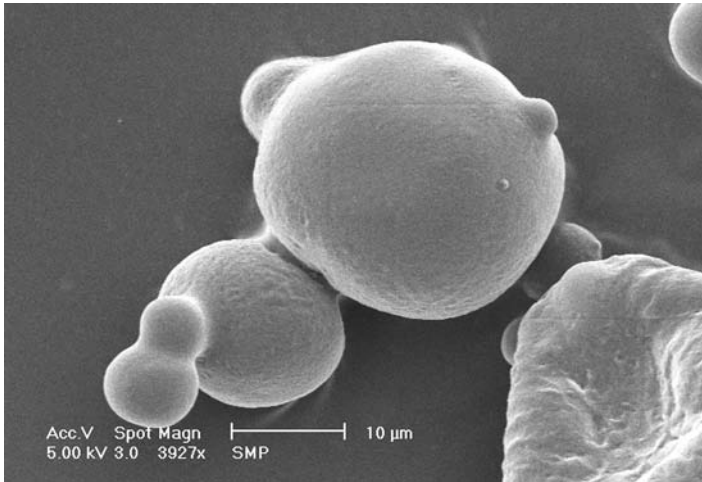
Compiled by Xiao Dong Chen



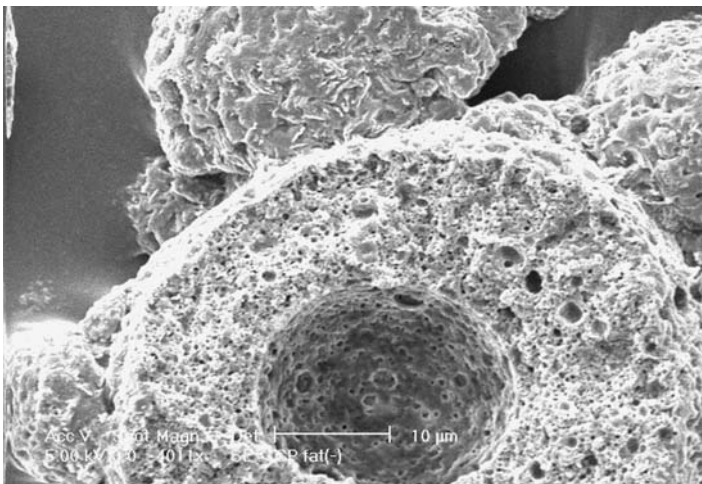
Whole milk powder particles produced in a commercial scale drier (about 6 tonnes h^{-1}). (Provided by Xiao Dong Chen, Department of Chemical Engineering, Monash University.)



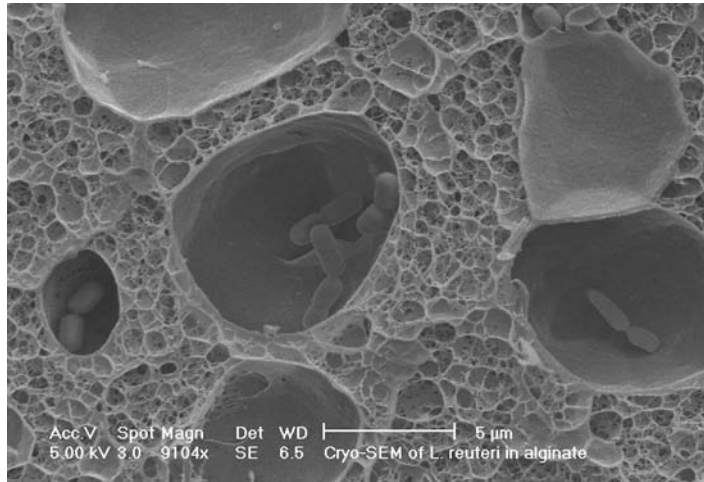
A commercial whole milk powder (confocal laser micrograph) (the bright spots are fat globules). (Provided by Dr Esther Kim, Department of Chemical and Materials Engineering, The University of Auckland, and Professor Xiao Dong Chen, Department of Chemical Engineering, Monash University.)



Skim milk powder produced in a commercial scale drier (about 6 tonnes h⁻¹). (Provided by Professor Xiao Dong Chen, Department of Chemical Engineering, Monash University.)



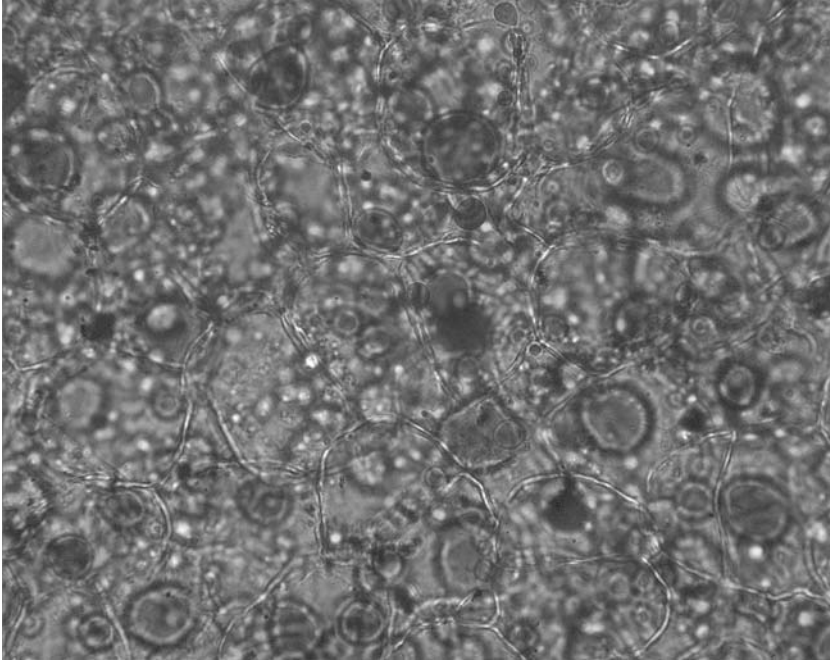
Cross-sectional view of cream powder particles (fat content is greater than 50 wt%). Commercial product from a drier of about 4 tonnes h⁻¹. (Provided by Dr Esther Kim, Department of Chemical and Materials Engineering, The University of Auckland, and Professor Xiao Dong Chen, Department of Chemical Engineering, Monash University.)



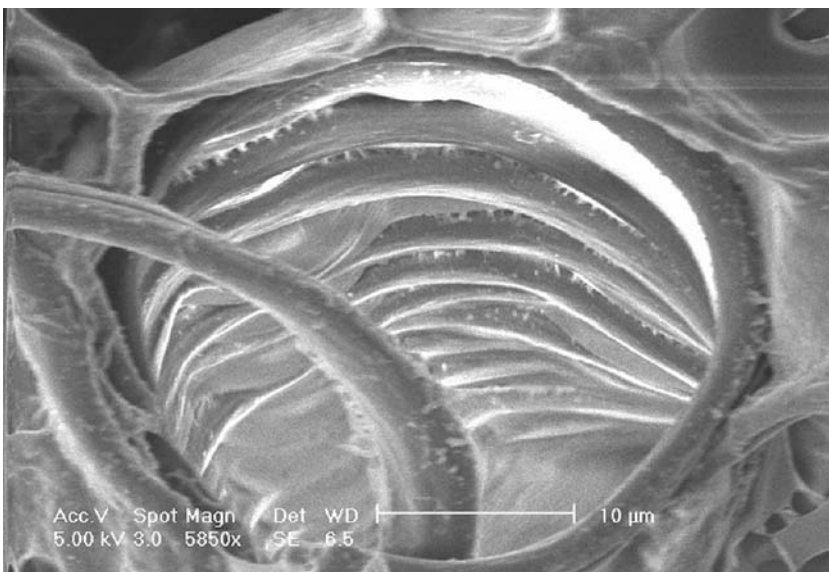
Cross-sectional view of a gel-bead particle (alginate cross-linked using CaCl and dried in vacuum) showing the probiotic bacteria encapsulated. (Provided by Professor Xiao Dong Chen, Department of Chemical Engineering, Monash University.)



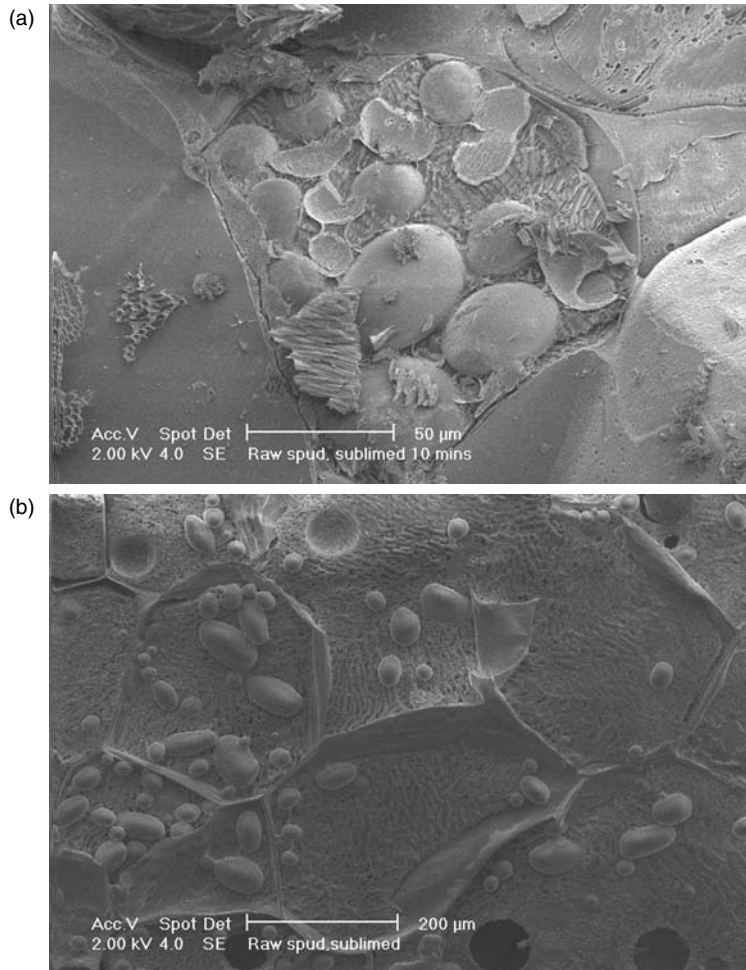
Potato crisps (2 cm in diameter) after 5 min of deep-oil frying. (Provided by Mai Tran, Department of Chemical and Materials Engineering, The University of Auckland, and Professor Xiao Dong Chen, Department of Chemical Engineering, Monash University.)



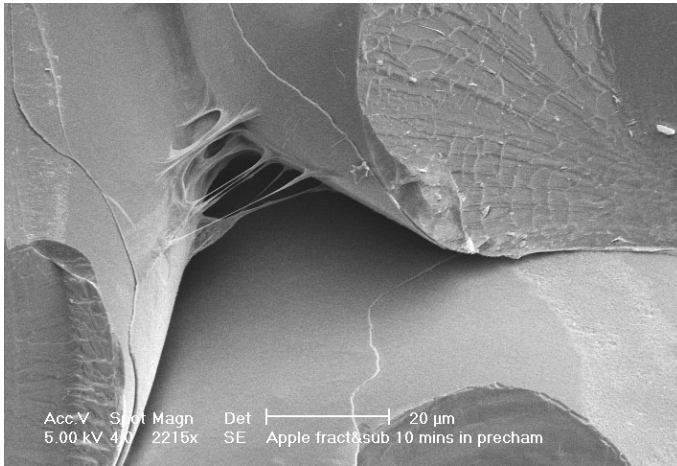
Avocado flesh stained with Sudan red 7 B (the lipid stains red). (Provided by Dr Bronwen Smith, Department of Chemistry, The University of Auckland.)



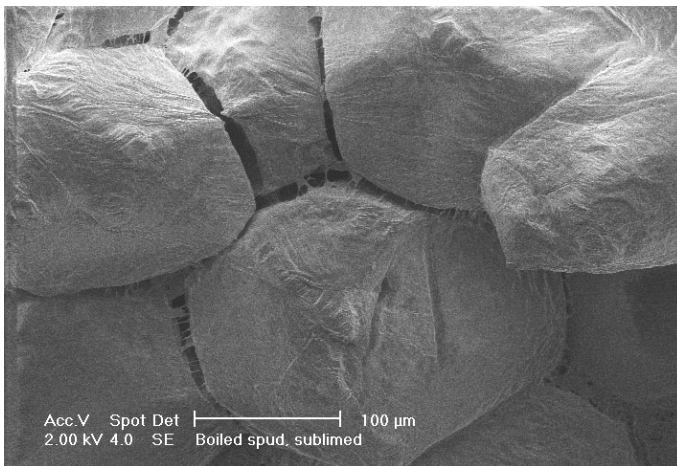
Xylem tracheary element from celery done by cryo-SEM. (Provided by Dr Bronwen Smith, Department of Chemistry, The University of Auckland.)



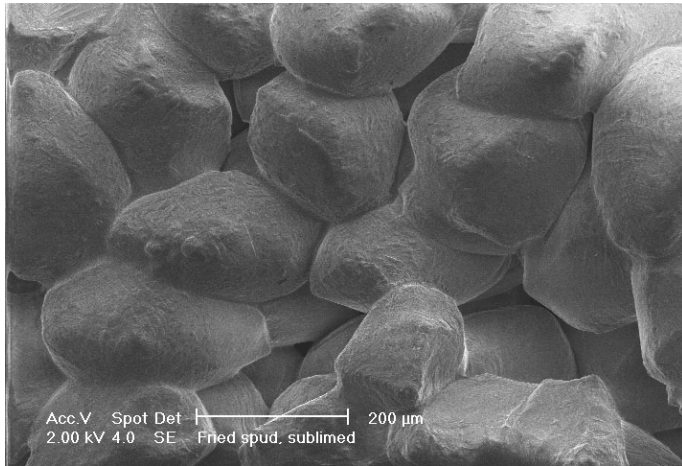
Cryogenic SEM image of the cross-sectional structure of raw potato cells: (a) one cell contains a number of starch granules; (b) a number of ripped-open cells. (Provided by Dr Bryony James, Department of Chemical and Materials Engineering, The University of Auckland.)



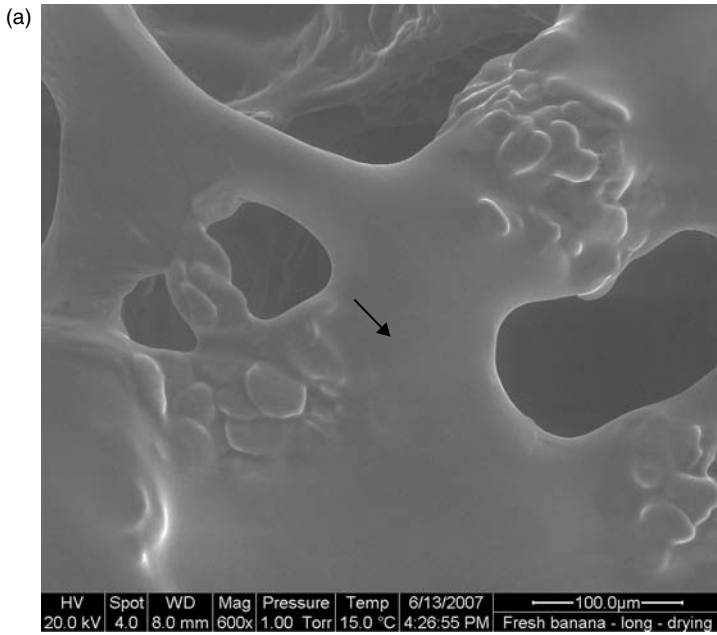
Cryogenic SEM image of the cross-sectional structure of apple cells being torn apart in the juice expression/compression process. (Provided by Dr Bryony James, Department of Chemical and Materials Engineering, The University of Auckland.)



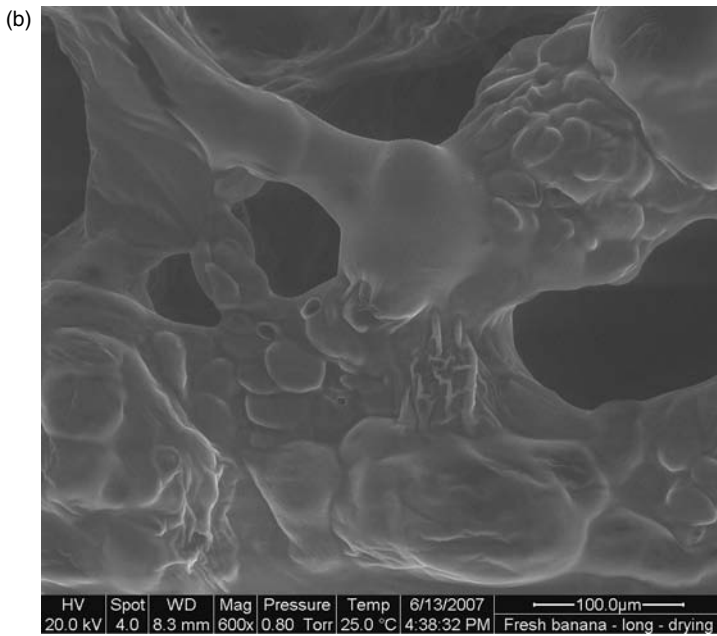
Cryogenic SEM image of close-up cross-sectional structure of cooked potato showing the breakages between cells. (Provided by Dr Bryony James, Department of Chemical and Materials Engineering, The University of Auckland.)



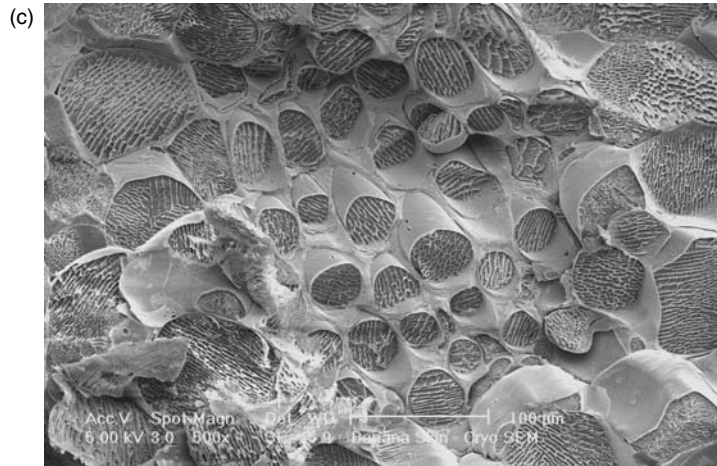
Cryogenic SEM image of cross-sectional structure of cooked potato showing the cells 'accumulated' to 'still' form the potato tissue. (Provided by Dr Bryony James, Department of Chemical and Materials Engineering, The University of Auckland.)



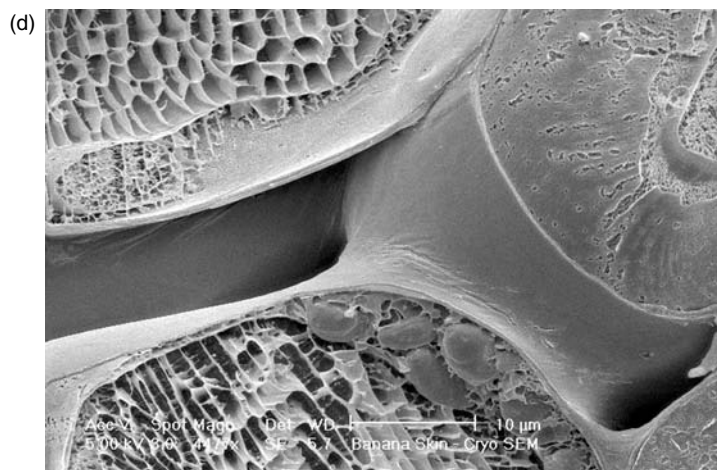
(a) Fresh banana cross-section (at the start of the vacuum drying) (ESEM).



(b) Fresh banana cross-section (at the end of the vacuum drying) (ESEM).



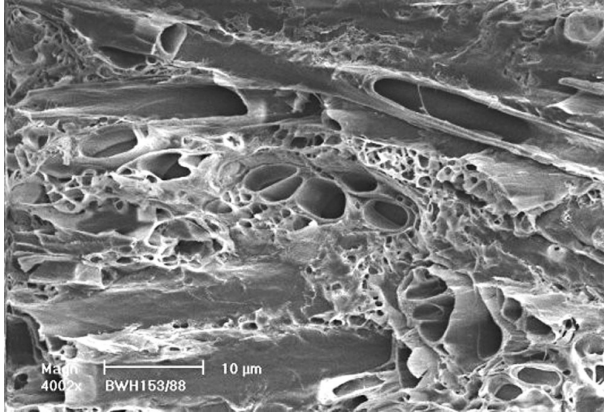
(c) Banana skin cross-section (at the end of the vacuum drying) (cryogenic SEM).



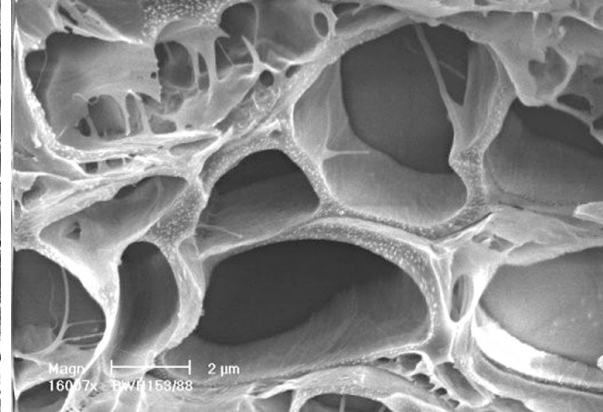
(d) Banana skin cross-section (at the end of the vacuum drying) (cryogenic SEM).

(All banana-related images were provided by Dr Bryony James, Department of Chemical and Materials Engineering, The University of Auckland.)

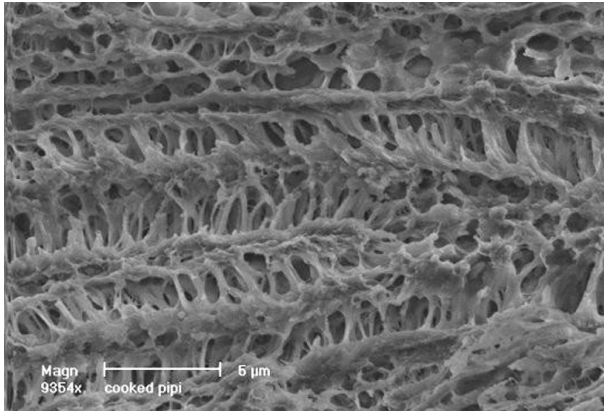
(a)



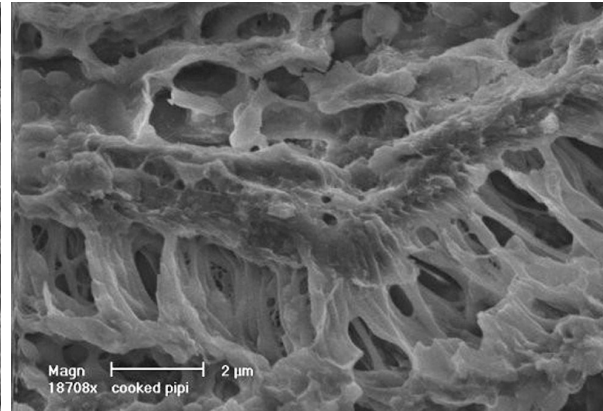
(b)



(c)



(d)



Cryo-SEM of the shellfish pipi (tissue): (a,b) uncooked; (c,d) cooked. (Provided by Dr Bronwen Smith, Department of Chemistry, The University of Auckland.)

1 Food drying fundamentals

Xiao Dong Chen

1.1 INTRODUCTION TO FOOD MATERIALS

Nutrition is essential to human survival. People consume food to gain energy and minerals so they can grow and stay healthy. These nutrients are the naturally occurring chemical substances found in foods.

Proteins, lipids, carbohydrates, vitamins, minerals and water form natural foods. The chemistry of each of these constituents plays key roles in our nutrition. The first three constituents (proteins, lipids and carbohydrates) provide the energy for our bodies to function on a daily basis. The energy levels are respectively 4 kcal per gram of protein, similar for carbohydrate and 9 kcal per gram of fat (Parker, 2003). A range of natural foods and processed foods are illustrated in Figure 1.1.

More and more manufactured foods are made available at low prices, catering to the practical needs of the market, such as those for school children. Nutritional values are a primary consideration. Food design, especially functional food design – for instance foods containing Omega-3 to help manage cholesterol – must include good nutritional value (based on medical evidence), interesting texture and attractive colour, good taste and acceptable



Fig. 1.1 My daughter's school lunch box showing the common range of foods which are either in the natural or processed forms. (Nectarine, yogurt, sticky cake made from glutinous rice flour, Sandwiches made from cheese slices, ham slices and bread slices, seed coated cake etc.) (photographed by X.D. Chen).

shelf-life. Large-scale food preparation methods, including mixing, baking, frying, roasting and air drying, are usually employed. The food ingredients, usually in the form of particles, need grinding (if they are of solid origin), concentration (if they are of dilute liquid origin), and drying (for powdered products) processes to manufacture. Many semi-ready foods are made from a combination of food ingredients. The storage of these semi-ready foods requires an understanding of the moisture–deterioration relationships that are similar to those known by drying experts.

Simple carbohydrates include monosaccharides and disaccharides and complex carbohydrates include starches and dietary fibres. The functions of carbohydrates are many, including sweetening, water binding, texture contribution, hygroscopic nature/water sorption, gelation regulation, spoilage prevention, colour, coagulation delay of protein and crystal structure creation etc. Starch is commonly found in plants and exists as granules of 2–130 μm in size. The granules of starch are in crystalline forms. Starch begins to gelatinise around 60–70°C depending on the type of starch density. Gelatinisation will bring the starch granules to their fully swollen stage. Below this range, starch can swell when absorbing water but the process is reversible. All this, in relation to water content and temperature, has a great impact on texture.

Proteins contain amino acids. They can be of plant or animal origin. Proteins are large molecules. They are polymers of amino acids. The shape and the function of a protein is determined by the sequence of its amino acids. Enzymes are kinds of proteins that catalyse certain reactions. Proteins can also be a main contributor to food texture. Proteins are heat sensitive and water sorption capacities are also high. Protein structure confirmation may be changed during the drying process, especially when the heat effect is significant at high water content, which may result in the loss of the desirable functions that are expected during the formulation stage of product development. This is the kind of product–process interaction that needs great attention paid to it.

Lipids include fats and oils from plants and animals. Lipids are soluble in organic solvents. These are triglycerides, fatty acids and phospholipids, and also some pigments, vitamins and cholesterol (Parker, 2003). The fats have different melting points (–8 to 80°C approximately) thus playing a key role in the material integrity (texture) in response to temperature changes. Some fats are encapsulated in protein membranes which behave differently from those in free flow form (such as free fat).

Minerals are present in small quantities, but they also play a key role in forming texture perception, through their interactions with proteins for example. They also, of course, play many other important nutritional roles in supporting our lives.

Water, or the removal of it from food material, makes foods more stable and means they can be kept for longer without spoilage. The prime objective of drying of foods is usually giving a long shelf-life to foods that easily deteriorate in their natural forms.

Foods or food materials come in all shapes and sizes. Size matters in the choice of engineering treatments and the engineering properties of the foods of concern. For example, food powder technology is a whole subject of interest by itself.

1.2 DRYING OF FOOD

There are numerous methods or processes to dry food materials and their merits can be judged on energy efficiency, time to dry, product quality achieved etc. depending on the market requirement. A balance among these factors is often required to achieve the economic aim

of the manufacturing procedures while ensuring safe and tasty foods are delivered to the consumer. In general, the dehydration processes may be divided into two large groups: in-air or in-vacuum. In-air processes can be further generalised to those where a gas medium other than air as the fundamental could be similar. A vacuum is useful for removing water vapour when the products are better processed without air. Also, the relatively low temperatures used can be preferential. Vacuum drying is perhaps more useful for preserving micro-organisms than destroying them. This is the case when probiotic bacteria are involved as the prime advantage of the products to be dried. Usually, freeze drying (in vacuum) is employed. The maximum level of activity of the valuable microbes is maintained. In-air process can involve elevated temperatures which are usually intended for achieving a high rate of drying.

The heat can be supplied in different ways: convection, radiation, conduction, microwave, radio-frequency, or even Joule (ohmic) heating. The implications of using different methods of heating will be illustrated in the section on Synergistic drying.

Drying of a food material occurs when water vapour is removed from its surface into the surrounding space, resulting in a relatively dried form of the material. Drying, as we describe it in this chapter and other chapters in this book, differs from the so-called 'dewatering' process. In dewatering, liquid water is 'drained' or 'squeezed' out of the material.

In general, the drying process should follow one of the trends illustrated in Figure 1.2, depending on initial and drying conditions.

The principle of this, no matter what drying mechanisms are involved, can be generally expressed by the following surface vapour flux equation:

$$N_v'' = h_m \cdot (\rho_{v,s} - \rho_{v,\infty}) \quad (1.1)$$

where N_v'' is the vapour (or drying) flux ($\text{kg m}^{-2} \text{s}^{-1}$); h_m is the mass transfer coefficient (m s^{-1}); $\rho_{v,s}$ is the interfacial vapour concentration at the moist material surface (kg m^{-3}) and $\rho_{v,\infty}$ is the vapour concentration in the surrounding space that the vapour travels into (kg m^{-3}). h_m is determined by the flow field around the material being dried (m s^{-1}), which may be viewed as a velocity of mass movement.

When this vapour concentration difference is positive, vapour leaves the material, and thus drying occurs. The reverse is the wetting/humidification process. The drying process as a

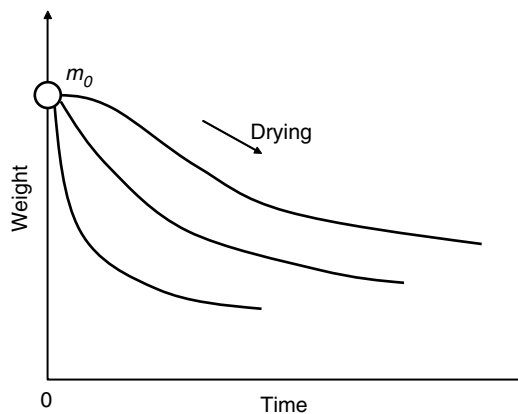


Fig. 1.2 Weight loss curves as drying proceeds (drawn by X.D. Chen).

whole has to involve the generation of vapour (transforming from the liquid phase inside the moist material to gaseous phase) on and within the moist material being dried, and the transport of the water phases outwards of the material. Some debates are around how liquid water may move within the material structure.

The generation of vapour requires heat input into the material to combat the latent heat of water vaporisation which is quite large, for example 2200 kJ kg^{-1} . Water vaporisation consumes the heat input from the drying medium so the moist material being dried could remain at relatively low temperatures thus maintaining the quality of the material to some extent. The heat supply can be provided using hot air, where the heat is conveyed to the material firstly by convection (boundary layer phenomena) and then conducted into the material. As mentioned earlier, heat can be provided using a heat radiator. Heat can also be supplied through a volumetric heating mechanism such as microwave.

It is known that the vapour generated has to travel by diffusion, convection or a combined mode through the pore channels or pore networks inside the moist material. The vapour transfer is better understood when compared with the mechanisms for liquid water transfer (such as the 'capillary effect' etc.) inside the material.

One can see also from equation (1.1) that lowering the surrounding vapour concentration $\rho_{v,\infty}$ is one way to increase the drying rate. The surface vapour concentration $\rho_{v,s}$ is highest at the saturation condition for the surface temperature T_s . If T_s is at a freezing temperature, say zero degrees Celsius, the saturated vapour concentration is about 1/6 of that at a room temperature of, say, 30°C . Vacuum is used sometimes to achieve this, such as that in vacuum freeze drying. Superheated steam can also be used, and this will be discussed further in another chapter *in this book*.

The micro-structure of the food materials is particularly relevant to drying, as both liquid water and water vapour move within the structure. The micro-structure, as far as the transport of heat and chemical species is concerned, is mainly made up of compounds such as protein, fat and carbohydrate, and minerals and air. Porosity and tortuosity are usual characteristics. The material's composition and its affinity to water (sorption characteristics) play a key role in water holding capacity and local evaporation rates which will be described later in this chapter.

When drying using hot air, the surface of the material being dried is usually denser than that of the core.

Drying also creates a new micro-structure as it progresses and the spatial distribution of the micro-structure characteristics, density included, is important in texture perception of the product and affects how it may be used as an ingredient for mixing into other foods (for instance, the reconstitution properties for food powders created by spray drying). Flavour retention of a food product after drying can also vary depending on how the drying is conducted. The pro-life bioactivity of the food materials is one highly valuable attribute of the final product, so attempts to maintain it at the highest level are currently being investigated by engineers. For instance, micro-encapsulation is employed to protect the active and beneficial ingredients, such as probiotic bacteria, during drying (Chen, 2007; Chen and Patel, 2007). Drying is also preferably done at the lowest temperature possible, for the same purpose of achieving higher retention of bioactivity.

Bacterial cells or micro-organisms are vulnerable in the drying process, especially when a high temperature environment is encountered. Drying may be viewed as a thermal processing stage. On the other hand, as mentioned above, preservation of the activities of the good beneficial bacteria – such as probiotic bacteria – becomes important when the drying process can be detrimental. A generic view of the effects of water content (or water activity or relative

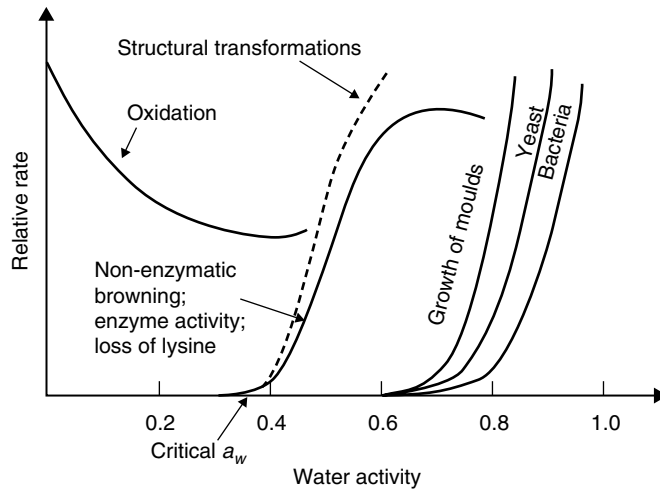


Fig. 1.3 Chemical and biochemical reaction rates as functions of water activity (modified from Roos, 2002).

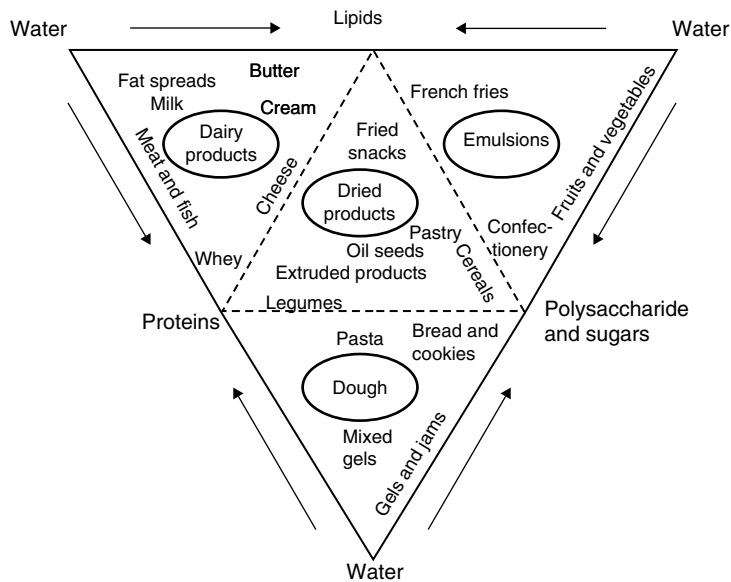


Fig. 1.4 Typical food products and their relative water contents (high or low) (modified from Aguilera and Stanley, 1999).

humidity) on the chemical and physical activities in food systems, is shown in Figure 1.3 (modified from Roos, 2002). It can be seen that if the product is held at the intermediate water content (a few per cent on wet basis) the deterioration reactions are slowest.

A diagram modified from Aguilera and Stanley (1999) is shown in Figure 1.4. It shows that different foods actually exhibit different water contents.

As mentioned earlier, the surface vapour flux for all the food drying processes (except immersion frying – if we include it as a food drying process), can be expressed at the surface

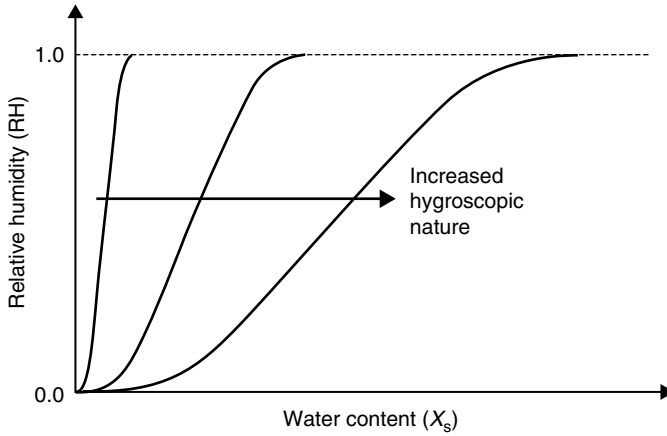


Fig. 1.5 Qualitative equilibrium isotherms for various types of food materials. (Sugar crystalline would be one of the ‘nearly non-hygroscopic’ materials, whilst its amorphous form would be one of the ‘hygroscopic porous medium’ materials.)

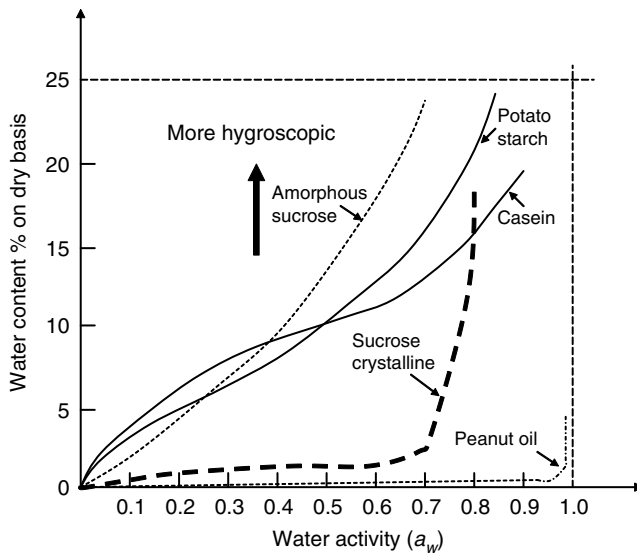


Fig. 1.6 Typical sorption isotherms for some food materials (modified from Aguilera and Stanley, 1999).

of the material being dried using equation (1.16). The interfacial vapour concentration is determined by many factors including chemical composition at the surface and the rate of water supply (more in the form of vapour perhaps) from the inside of the material to the surface, etc.

Assuming that the surface is at equilibrium condition, that is, that the vapour concentration is the one determined by the equilibrium water sorption isotherm ($\phi(X, T)$):

$$RH_s = \frac{\rho_{v,s}}{\rho_{v,sat}(T_s)} = \phi(X_s, T_s) \tag{1.2}$$

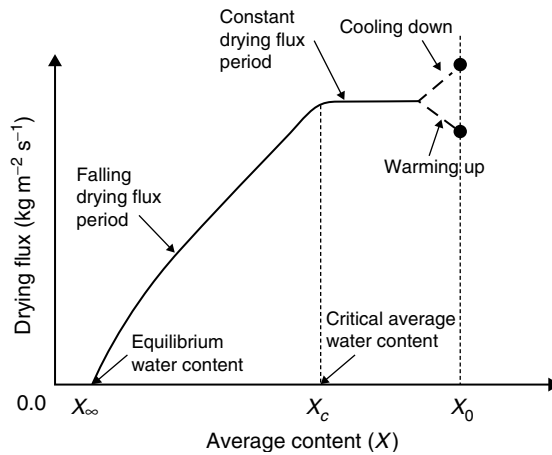


Fig. 1.7 Drying (flux) rate characteristics (drawn by X.D. Chen).

where RH is the relative humidity, ρ_v is the vapour concentration (kg m^{-3}), and the subscripts of 'v, s, sat' represent 'vapour, surface and saturated condition' respectively. One can say that this relationship is material dependent (Rahman, 1995). When the surface water content X_s is reduced to the value that corresponds to the equilibrium relationship defined in the above equation, with surrounding (drying medium) relative humidity RH_∞ and temperature T_∞ ,

$$RH_\infty = \varphi(X_s, T_\infty) \quad (1.3)$$

drying should cease. Essentially at this point of time, the surface temperature X_s approaches X_∞ , and T_s approaches T_∞ . A broad classification of the materials in relation to water sorption isotherm is shown in Figure 1.5. A selection of the materials of interest is given in Figure 1.6. This property is important as it defines when, for a given drying medium condition (temperature and humidity), the drying process would cease. It also demonstrates how hygroscopic a dried material is.

Drying under constant drying medium conditions has been traditionally described as having three typical stages: a warming up/cooling down period, a constant rate drying period and a falling rate drying period. This is depicted in Figure 1.7. Here it is noted that the flux is the rate per unit surface area of the food material (May and Perré, 2002).

This has been known for many years, and still remains the first introduction of the drying phenomena to university students. There has been much research effort spent on understanding the fundamentals of drying, and more complicated mathematical models published in the literature, but a concise introduction of drying still centres on the notion of these three drying stages. A recent study by May and Perré (2002) has emphasised that the rates in diagrams such as Figure 1.7 should represent the drying flux (vapour flux).

The maintenance of the constant drying rate period (at the end of it) may be due to two reasons: one is the increasing temperature at the air-product interface (increasing the interfacial vapour concentration even though the relative humidity might have gone below unity); the other is due to the material's surface nature, where relative humidity can be kept constant for quite a long time.

The variations in the mass transfer coefficient or the proportionality h_m in equation (1.1) can be predicted using existing theories of transport phenomena (Incropera and De Wit, 2002; Bird *et al.*, 1996). For vapour transport from the material surface to the bulk drying medium (convection), italic number correlation is needed, and the correlations for a large number of geometries have been established through previous efforts (see examples in Appendix I).

There have been a large number of studies published in the past two decades on the drying of food and biological materials. In these papers, drying rates are represented using empirical models of explicit time-dependent functions (curve fits, essentially). In particular, the *Page* model (1949) appears to be the one that is the most successful in describing the weight loss versus time data obtained in a constant environment for drying (constant temperature and humidity of the drying medium) (the general trends such as that shown in Figure 1.2):

$$\frac{M_t - M_e}{M_o - M_e} = e^{-k \cdot t^n} \quad (1.4)$$

or its modified forms such as:

$$\frac{M_t - M_e}{M_o - M_e} = e^{-(k \cdot t)^n} \quad (1.5)$$

Both the model coefficients k and n can be correlated as functions of the drying conditions such as environment temperature, drying gas velocity and the like. M is the wet basis water content. Often, the above equations can describe the trends almost exactly. It is an empirical approach, but for constant drying conditions (constant temperature and constant humidity environment) it yields rather good correlation coefficients. One could use the Page equation as a fitting equation to work out drying rates at different stages of drying for analytical purposes.

It is noted that the Page equation shows the overall weight loss, thus the rate worked out would usually be in the unit of kg s^{-1} . The constant rate period should be referred to the area based drying rate ($\text{kg m}^{-2} \text{s}^{-1}$). For example, vegetables are highly shrinkable during drying. Once the area change is accounted for, Perré and May (2002) have shown that constant rate periods do exist for several vegetables, such as the potato tissue. Constant drying flux is a better term to use.

More in-depth understanding of the drying process is shown in a later section: Diffusion theory of drying.

1.3 PHYSICAL PROPERTIES OF FOODS

In general, the physical properties of foods, which can be interactive with the drying operations, are the mechanical, thermal, electrical and optical properties. Foods are usually seen to fall into two major categories: natural foods – structure occurs naturally, such as fruit, vegetables, meat, fish etc.; structured foods – structure occurs as a result of processing, such as dairy products, bread, confectionery etc. Drying alters food structure or even creates new food structures.

1.3.1 The scales of interest

As mentioned earlier, drying also creates a new micro-structure and the spatial distribution of the micro-structure characteristics is important in texture perception of the products and

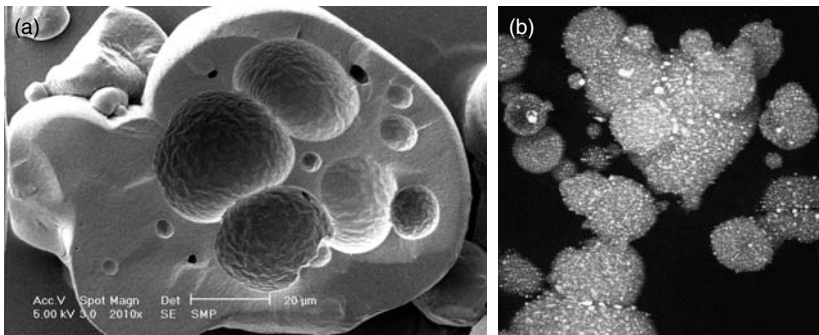


Fig. 1.8 Scanning electron microscope (SEM) image of skim milk powder and a confocal laser microscopy image of the agglomerate in the upper part full-cream milk particles (the size of the large agglomerate in the upper part is in the order of 300 μm). (a) A cross-section of an industrial skim milk powder and (b) agglomerated whole milk powder (courtesy of X.D. Chen).

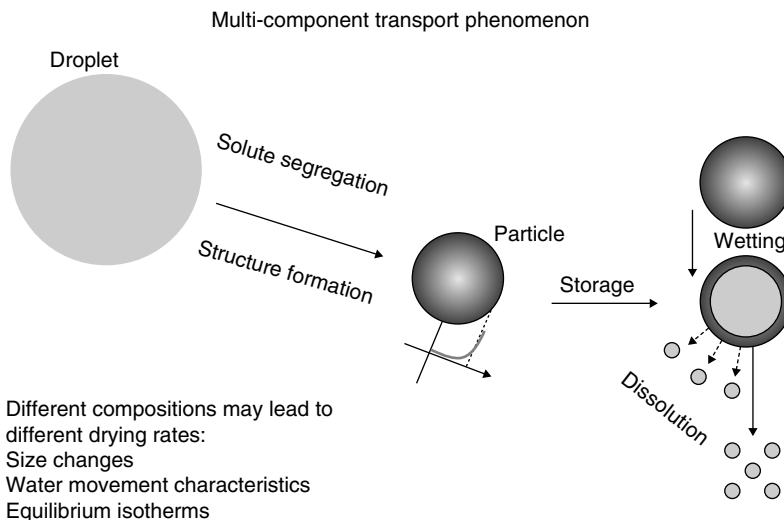


Fig. 1.9 Particle formation during droplet drying and subsequent wetting and dissolution in water (it shows that different surface composition and micro-structures can lead to different rates of wetting and disintegration in water) (drawn by X.D. Chen).

affects how it may be used as an ingredient for mixing into other foods (for instance the reconstitution properties of food powders created through spray drying). Figure 1.8 shows (a) a cross section of a skim milk powder, (b) the micro-structure of a full-cream milk powder made using spray drier obtained with a Confocal laser microscope. The lighter (actually yellow in colour) spots are the fat globules. One does not usually want these globules to stay at the outer surface as they prevent a fast wetting process, making the particle less user friendly. The reconstitution process is shown schematically in Figure 1.9, which demonstrates the distribution of the structural components that can influence dissolution.

Flavour retention of a food product after drying can also vary depending on how the drying is conducted, as it can create a porous structure that limits certain flavour compounds

from escaping out of the structure. This is sometimes referred to in the context of process engineering as the ‘selective diffusion’. Micro-encapsulation is employed to protect the active and beneficial ingredients during drying.

It is therefore important to understand the physical dimensions of the food materials in order to apply process engineering principles to food industry drying processes.

Plate 1.1 shows the typical scales of interest to food processing including drying as a food manufacture step.

1.3.2 Mechanical properties

Food usually contains solids, liquids and gases, which is a kind of dispersed system. The mechanical properties are multi-phase by nature. Foods vary from the very liquid (e.g. beer, fruit juices etc.) to the very solid (e.g. biscuits, chocolate etc.). When drying liquid to form solids, such as through spray drying (e.g. milk powder manufacture) or freeze drying (e.g. coffee extracts), as the liquid is concentrated, mechanical changes occur. When the liquid is concentrated (but not yet solid), viscosity becomes a prime issue for handling or processing purposes.

Viscosity is a reflection of the frictional effect of the interacting food constituent molecules or particles. Viscosity is thus a measure of the resistance to flow. It is dependent on internal frictional resistance to motion.

Viscosity μ (Pa s) is the coefficient relating the shear stress (shearing force over the area acted upon) to the shear rate (the velocity gradient) (refer to the one-dimensional situation shown in Figure 1.10):

$$\tau_y = \frac{F}{A} = -\mu \cdot \frac{\Delta u}{\Delta y} \quad (\text{Pa or N m}^{-2}) \quad (1.6)$$

For Newtonian fluids, the viscosity is constant against the shear rate. The fluids may be divided into two groups: solutions and suspensions. The latter contains particulate or in general undissolved materials.

The viscosity is usually temperature dependent (Holdsworth, 1971; Rao, 1977):

$$\mu \propto \exp\left(\frac{a}{T}\right) \quad (1.7)$$

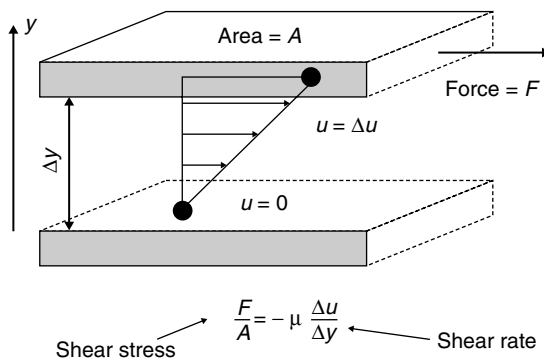


Fig. 1.10 A schematic diagram showing the one-dimensional process of shearing (drawn by X.D. Chen).

For a liquid medium the higher the temperature is, the lower the viscosity. It is also (dissolved) solute concentration dependent, for example (Rao *et al.*, 1984):

$$\mu \propto C^b \quad (1.8)$$

where a and b are model constants. C is the solute concentration (kg m^{-3}).

For dilute suspension of rigid spheres (generally less than 10% volume occupancy), the viscosity is expressed using the Einstein equation:

$$\mu = \mu_0 \cdot (1 + 2.5\phi) \quad (1.9)$$

where μ_0 is the ‘base fluid’ or the dissolved solute medium viscosity; ϕ is the volume fraction of the spherical particles.

More generally, the effect of the suspended particles is accounted for by the following empirical formula (Aguilera and Stanley, 1999):

$$\mu = \mu_0 \cdot (1 + 2.5\phi + \beta\phi^2 + \gamma\phi^3 + \dots) \quad (1.10)$$

The maximum packing of the particles (where it may be said that a solid structure is formed as the viscosity has become ‘sky high’) is considered in the Krieger–Dougherty-type relation (Aguilera and Stanley, 1999):

$$\mu = \mu_0 \cdot \left(1 - \frac{\phi}{\phi_{max}}\right)^{-\alpha \cdot \phi_{max}} \quad (1.11)$$

α is in fact the ‘intrinsic’ viscosity reflecting the ability of the material in solvent to increase viscosity of the mixture. For polymer solutions, α may be a power function of the average molecular weights (power constants of 0.5–0.8 have been found in previous studies) (Aguilera and Stanley, 1999). The maximum packing condition ϕ_{max} is in the range of 0.63–0.71 for low and high shear rates (Aguilera and Stanley, 1999). Formulae (1.23)–(1.26) may be suitable for either the undissolved particles, or the dissolved but somewhat large molecules such as protein micelles or even protein-coated fat globules.

The order of magnitudes of the viscosities of some typical materials is shown in Table 1.1.

For sugar solutions (sucrose, glucose and fructose), Telis *et al.* (2007) have recently established correlations that adequately describe the experimental data obtained using the Brookfield viscometer.

Table 1.1 Viscosity – order of magnitudes.

Air	10^{-5}	(Pa s)
Water	10^{-3}	
Olive oil	10^{-1}	
Glycerol	10^0	
Liquid honey	10^1	
Golden syrup	10^2	
Glass	10^{40}	

1 centipoise = 0.01 poise = 1×10^{-3} Pa s.

Table 1.2 The reference viscosities (mPa s) at different concentrations at 45°C.

Concentration (wt%)	10	20	30	40	50	60
Sucrose	0.74	1.06	1.51	2.84	5.04	17.20
Glucose	0.71	1.05	1.43	2.47	3.91	10.56
Fructose	0.67	0.99	1.24	2.30	3.65	9.57

Table 1.3 Van der Waals molar volumes and molecular weights.

Component	M (g mol ⁻¹)	\bar{V} (cm ³ mol ⁻¹)
Sucrose	342.30	160.35
Glucose	180.16	88.03
Fructose	180.16	88.03
Water	18.02	11.49

The viscosity was seen to be highly correlated against the Arrhenius equation in the following form:

$$\mu = \mu_{ref} \cdot \exp \left[\frac{E_a}{R} \cdot \left(\frac{1}{T} - \frac{1}{T_{ref}} \right) \right] \quad (1.12)$$

The reference temperature was taken to be 45°C (313 K). The reference viscosities for sucrose, glucose and fructose are given respectively in Table 1.2.

The activation energy E_a is expressed as a function of volume of the fraction taken up by the solute in solution ϕ :

$$E_a = E_{ao} \cdot \frac{1 + 0.5\phi}{1 - \phi} \quad (1.13)$$

A common value of E_{ao} was found to be 15080.24 ± 86.12 J mol⁻¹. The following equations are also needed for the correlation.

$$\phi = \frac{\phi_{sf}}{1 + \phi_{sf}} \quad (1.14)$$

$$\phi_{sf} = \frac{w}{1 - w} \cdot \frac{M_{H_2O}}{M_{solute}} \cdot \frac{\bar{V}_{solute}}{\bar{V}_{H_2O}} \quad (1.15)$$

w is the solute mass fraction. The molecular weights (molar masses, g mol⁻¹) and Van der Waals molar volumes (cm³ mol⁻¹) are given in Table 1.3.

For non-Newtonian fluids, the viscosity changes with shear rate.

Foods are made of large molecules and the interactions involving proteins or starches, for example, are non-Newtonian. Rheology then becomes the subject of interest. Rheology is the study of deformation and flow of matter (in general, the behaviour of the non-Newtonian materials). Materials deform when they are stirred, pumped, eaten or handled. The quality and functionality of food products is dependent on rheology.

For non-Newtonian fluid, the viscosity is called the ‘apparent viscosity’ at a single shear rate and can be calculated in this way:

$$\mu_a = \frac{\tau}{\dot{\gamma}} \quad (1.16)$$

This apparent viscosity μ_a can change with shear rate, such as that for the power-law fluid:

$$\mu_a = \frac{K\dot{\gamma}^n}{\dot{\gamma}} = K\dot{\gamma}^{n-1} \quad (1.17)$$

For the more solid foods, such as dough, a yield stress is required to trigger the material to ‘flow’. A number of rheological models are used such as the Herschel–Bulkley model (1926):

$$\tau = K \cdot \dot{\gamma}^n + \tau_0 \quad (1.18)$$

where τ_0 is the yield stress. One can see that only when the shear stress applied overcomes the yield stress, does the material becomes a power-law fluid.

The typical fluid behaviours are depicted in a standard graph (Figure 1.11), which can be found in many textbooks that introduce rheology.

For solid foods, the typical behaviours are shown in Figure 1.12 (modified from Aguilera and Stanley, 1999). Strain can be commonly expressed as the ‘engineering strain’, which is ratio of the change in length (size) made due to stress applied on the material to the original length (size). Stress (F/A) can be applied in a number of ways, such as compression, shear and tension respectively or simultaneously. Hooke’s law relates the stress F/A to strain ε via the proportionality labelling stiffness or ‘Young’s modulus E ’:

$$\text{Stress} = \frac{F}{A} = E \cdot \varepsilon = E \cdot \frac{\Delta L}{L_0} \quad (1.19)$$

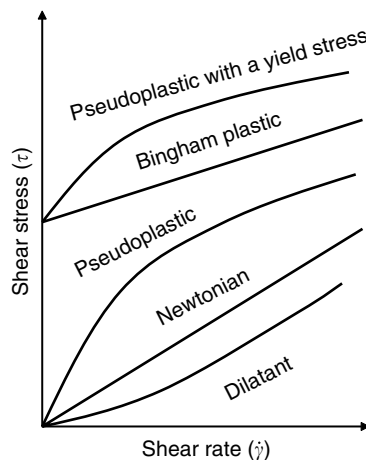


Fig. 1.11 Typical rheological properties of fluids.

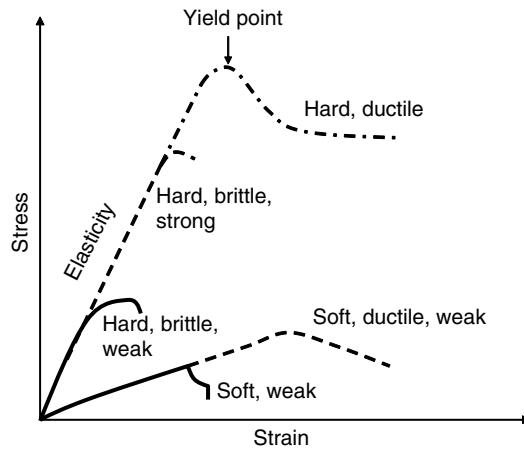


Fig. 1.12 Stress–strain curves for several types of solid materials (modified from Aguilera and Stanley, 1999).

The Young's modulus E may be taken as an effective value and correlated as a function of water content and temperature of the food materials (Ponsart *et al.*, 2003). As drying proceeds, creating spatial non-uniformity of either the water content or the temperature, E would vary locally in the material being dried, thus affecting the local stress–strain relationship causing structure non-uniformity. As drying proceeds, a wet product such as spaghetti would change from the state of being soft or weak to the state of being stiff. The effective Young's modulus would vary in this process by a factor of 2×10^4 . The spatial distribution of Young's modulus results in the distribution of the stress (compression, tension occurs at different places within the product). The overall sensory perception of a dried food product could be affected significantly by the drying process. The differences between the temperature–time, moisture–time history of the product surface and the product centre can influence the texture felt by consumers. Air drying of fruit slices or pieces usually results in a harder 'shell' formed at the surface and a somewhat softer centre. Depending on the product unit size (thick or thin for example), the feeling of a 'bite' would be different.

The images of a cross-section of apple tissue (fresh (a) and pre-boiled (b)) are shown in Figure 1.13, which were taken using an environmental scanning electron microscope (ESEM) at the University of Auckland (courtesy of X.D. Chen and Y.L. Chiu). The cells and their boundaries were all visible in both cases. However, due to the structural change after the tissue was boiled in water for some time, the drying behaviour of the pre-boiled sample was very different from that of the fresh sample. The pre-boiling is expected to have caused gelatinisation of the starch granules residing in the cells. The cell structure is also expected to be substantially softened so the shrinking behaviour would be drastically different. In the ESEM real-time observation of the drying processes for the two types of samples, for the same time frame, the pre-boiled sample showed more uniform shrinking or collapsing behaviour. The intact cells in the fresh sample made moisture removal more difficult (Figure 1.14).

The load–deformation relationships of the raw and cooked apple tissue are shown schematically in Figure 1.15 (modified from Aguilera and Stanley, 1999). The cooked sample has lost the 'crunchiness'. The boiling would have gelatinised the starch granules which resided in the cells in discrete locations, and they would have become mixed and somewhat dissolved in water (forming a 'mushy' zone) that may retard water removal. On the other hand, the

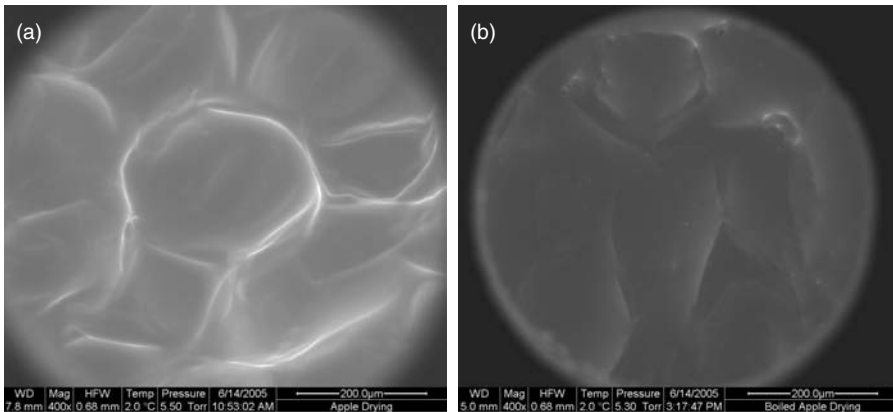


Fig. 1.13 ESEM images of (a) the fresh cut sample and (b) the pre-boiled sample of apple tissue.

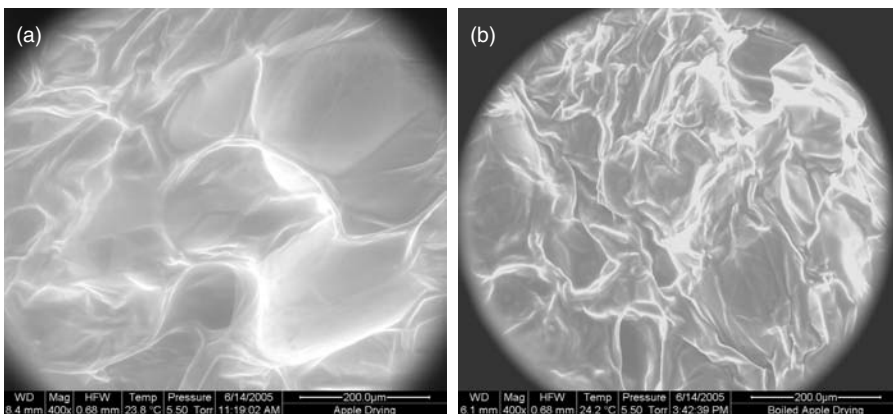


Fig. 1.14 ESEM images of (a) the fresh cut sample and (b) the pre-boiled sample of an apple tissue (dried in ESEM chamber after the same drying time (25 min) under the same drying condition: chamber pressure and temperature) (courtesy of X.D. Chen and Y.L. Chiu).

disintegration of the cell walls may be more important in helping the release of the water from within (this is reflected in the drying curves shown in Figure 1.15).

The weight loss curves of the two types of samples (in cylindrical shapes) are shown in Figure 1.16 (modified from Chen *et al.*, 2006).

1.3.3 Shrinkage and densities

Shrinkage is a phenomenon which is expected of drying of food materials such as fruits and vegetables. Hardening is associated with shrinkage, or is a result of shrinkage, and is also well known where the dried foods are generally perceived to be ‘harder to chew’ compared with their original states before drying. Sometimes, ‘case hardening’ is suggested, which is known to correspond to the lowest water contents that are achieved first at the surfaces exposed to the drying medium, such as in a normal hot air drying or solar drying scenarios. The different degrees of the case hardening processes at the initial stages of drying, due to

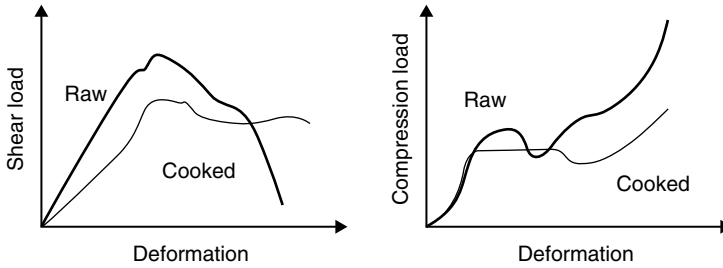


Fig. 1.15 Behaviour of raw and cooked apple (a) during shear and (b) during compression (modified from Aguilera and Stanley, 1999). (In the shear load figure (a), the peak value for the raw sample is about 6 N and occurs at about 4 mm deformation; in the compression load figure (b), the plateau value for the fresh sample is about 30 N and occurs at 3 mm deformation; The highest value of the compression load for the raw sample reached about 70 N at about 9.5 mm deformation.)

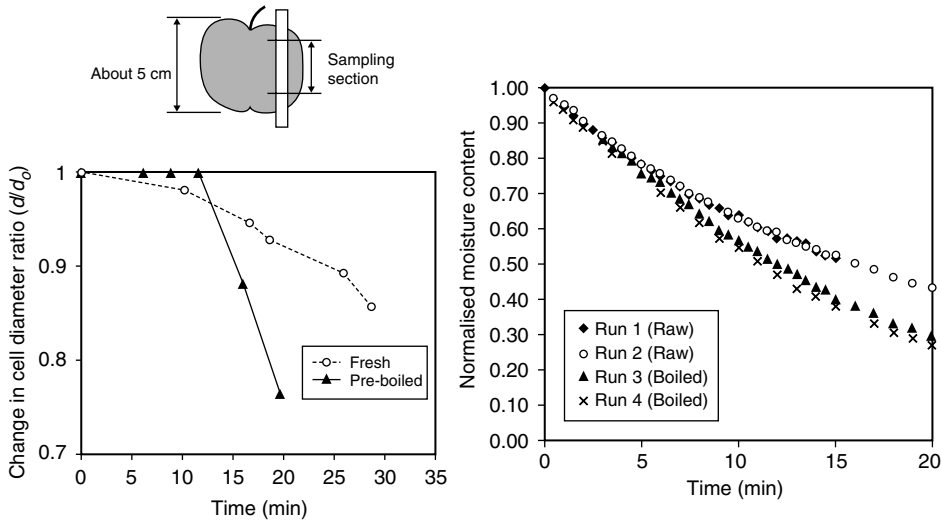


Fig. 1.16 Drying behaviour of the fresh and pre-boiled apple tissue samples. Left (top): sample cylinder was taken from the location as shown; Left (bottom): cell size change during ESEM drying; Right: air drying behaviour of the two types of samples (modified from Chen *et al.*, 2006). (The LHS upper figure shows where the sample cylinder was taken; the LHD lower figure shows the change in a cell size over time; the RHS figure shows the air-drying behaviour of the apple tissue.)

different drying conditions and the kind of compounds involved, determine the type and the extent of shrinkage.

The mobility of the solid structure/matrix is related to the shrinkage behaviour. The mobility of the solid matrix is a dynamic process with rates that depend on the temperature difference ($T - T_g$) (Aguilera and Stanley, 1999). T is the temperature of the sample (could be the local temperature within the material also when spatially distributed behaviour is of interest) undergoing drying. T_g is the material's glass-transition temperature. T_g is a function of water content (X) or a function of water activity (a_w). At high water contents, the material (carbohydrate or other polymers) is in the rubbery state, shrinkage could compensate entirely for the water loss due to drying so the volume of the material decreases.

Shrinkage is usually defined as the overall volume reduction of the whole food material subjected to drying. As a result, the concentrations of the solids in foods (inter-exchangeable with the ‘densities of solids’, kg m^{-3}), usually increase as drying proceeds. There are exceptions though when water content is reduced to the low end, and perhaps also depending on how one measures the shrinkage (*in situ*, on-line or off-line after equilibration) and beyond or below the glass-transition temperatures of the materials (which will be described more later on). The *bulk density* is defined as:

$$\rho_b = \frac{m_w + m_s}{V_s + V_w + V_{voids}} \quad (1.20)$$

and the *solids concentration* (for porous particles, this may be called the *particle density*) is expressed as:

$$\rho_{s,b} = \frac{m_s}{V_s + V_w + V_{voids}} \quad (1.21)$$

The *shrinkage (SKG)* is expressed as the relative change of volume, area or thickness (or diameter if spherical). For volume reduction, it is expressed as:

$$S_b = \frac{V}{V_o} \quad (1.22)$$

The *porosity* change is a local phenomenon which depends on the local water content and the voids created or destroyed during drying. These changes are linked to the overall process of shrinking. The average porosity over the entire sample volume is defined as:

$$\varepsilon = \frac{V_{voids}}{V_s + V_w + V_{voids}} \quad (1.23)$$

If the shrinkage simply corresponds to the volume of water removal (for carrot, squid, sweet potato, apple etc.), the following should be true (i.e. the scenario of pure water evaporation):

$$\frac{\Delta V_w}{V_o} \equiv \frac{V_o - V}{V_o} \quad (1.24)$$

where ΔV_w , V_o , and V are respectively the volume of water removed (calculated based on drying data), initial volume of the food sample (measured) and the volume of the sample at the time (measured) (m^3).

It appears that if the initial void space or porosity is very small, the above relationship works well. For apple tissue, as the initial porosity is high (much higher than that for potato tissue), the relationship between $\Delta V_w/V_o$ and $(V_o - V)/V_o$ deviates from the above equation (i.e. a correction function ξ is needed to make the equality). The deviations for food materials from this equality might not be that large as the initial water contents of the food materials are quite high – about 80 wt% usually.

$$\frac{V_o - V}{V_o} = \xi \cdot \frac{\Delta V_w}{V_o} \quad (1.25)$$

Translating this to water content on dry basis, one may have:

$$1 - S_b = \left(\frac{X_o \cdot m_s}{\rho_w \cdot V_o} \right) \cdot \left(1 - \frac{X}{X_o} \right) \cdot \xi \quad (1.26)$$

The first bracket on the RHS is in fact the water concentration at the start of the drying process divided by the pure water density (a ratio defining how ‘far away’ the wetness of the material is from that of pure water). This ratio is denoted as ϕ_s . One may expect that the correction function ξ should be a weak function of water content ratio, thus the above equation becomes:

$$S_b = 1 - \left(\frac{X_o \cdot m_s}{\rho_w \cdot V_o} \right) \cdot \left(1 - \frac{X}{X_o} \right) \cdot \xi \left(\frac{X}{X_o} \right) \quad (1.27)$$

which lends support to the empirical formulae given by Mayor and Sereno (2004); the quadratic model:

$$S_b = c_1 + c_2 \cdot \left(\frac{X}{X_o} \right) + c_3 \cdot \left(\frac{X}{X_o} \right)^2 \quad (1.28)$$

which has been shown to work quite well for carrot, potato, squid and apple. c_1 should be the final ratio (V_∞/V_o) (i.e. when $X \rightarrow 0$). They also tried an exponential function of X/X_o but the correlation results were much poorer. As mentioned earlier, for high moisture content materials such as these foods, ξ should be a weak function of water content ratio and is perhaps dependent on temperature and other drying conditions. The coefficients in the quadratic equation shown above may be made drying condition dependent, for example, temperature dependent and so on.

When water content becomes minimal, that is, when $X \rightarrow 0$, the following equation exists based on equation (1.27):

$$S_{b,\infty} = 1 - \left(\frac{X_o \cdot m_s}{\rho_w \cdot V_o} \right) \cdot \xi(0) = \frac{V_\infty}{V_o} \quad (1.29)$$

Thus, one has

$$\xi(0) = \left(1 - \frac{V_\infty}{V_o} \right) \cdot \phi_s^{-1} \quad (1.30)$$

It is conceivable that the following may be written:

$$\xi \left(\frac{X}{X_o} \right) = \left(1 - \frac{V_\infty}{V_o} \right) \cdot \phi_s^{-1} + \theta \left(\frac{X}{X_o} \right) \quad (1.31)$$

With the simplest function of $\theta(X/X_o)$ being a power function:

$$\theta \left(\frac{X}{X_o} \right) = b \cdot \left(\frac{X}{X_o} \right)^n \quad (1.32)$$

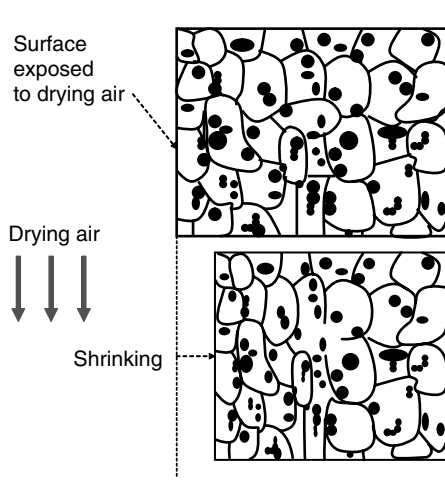


Fig. 1.17 Line drawing of the cross-sectional micro-structure distribution as drying occurs on the left-hand side of the potato tissue same (drawn by X.D. Chen based on the microscope images taken by Wang and Brennan, 1995).

where n may be 1 or varying around 1. When $n = 1$, the shrinkage model would become the same as the quadratic one. Shrinkage may also be expressed in terms of thickness, diameter, area etc. depending on how one intends to use the data.

Due to the effect of ‘case hardening’ or ‘shell formation’ at the early stage of drying, which is affected by drying conditions such as temperature and drying medium velocity, the solids concentration changes with a spatially non-uniform distribution. For instance, for drying of potato tissue, the light microscope images taken of cross-sections of the samples being dried, at different times of the drying processes, show that the denser cell packing is formed near the air–sample interface (illustrated qualitatively in Figure 1.17) (Wang and Brennan, 1995). After some time drying, the surface (LHS) exposed to the drying air (thus lower water content) had greater shrinkage than the bottom of the sample which is ‘water tight’ (RHS). When the temperature was higher, the drying occurred more quickly in these experiments and the structures were ‘fixed’ while the water was still being continuously extracted, resulting in lower sample density. The density of the sample increased first until the water content was reduced to about 0.5 kg per kg dry mass, and then actually decreased ending at around to $1.23 \times 10^3 \text{ kg m}^{-3}$ (corresponding to the volume shrinkage value S_b of about 0.2; or in other words, V_∞ is about $0.2V_0$ or 80% reduction in volume since the beginning of the drying process). The initial density was about $1.1 \times 10^3 \text{ kg m}^{-3}$, corresponding to the initial water content of about 4.2 kg per kg dry mass. The maximum density was achieved at the lowest temperature tested (40°C) and was about $1.38 \times 10^3 \text{ kg m}^{-3}$.

Therefore, it is important to realise that the shrinkage of food materials subjected to drying is not uniform within the material dimension (i.e. the concept of local shrinkage) depending on how uniformly the water removal occurs within it. The shrinkage at the boundary region, where the water is extracted most quickly in the case of hot air drying, plays a key role in restricting moisture transfer as well as giving the perception of the sensory texture when testing or tasting. In freeze drying, as it pre-fixes the structure of the material at the freezing stage and indeed the freezing condition is maintained throughout the drying process, the sublimation-drying occurs through the pores or pore networks, which does not seem to shrink

much of the material. Microwave drying is more aggressive but, when used well, can also maintain a larger portion of the volume compared with the normal hot air drying processes.

In summary, the shrinkage behaviour is due to the physical–chemical nature of the solids matrices in food materials and is affected by the processing conditions (temperature, drying rate etc.). So far, the majority of published works describe empirical correlations and the overall volume change (rather than local solids concentration change). There is a need to investigate the spatial distribution, that is, the local shrinkage, in greater depth.

For further reading, the reader may be referred to the work of Rahman *et al.* (1996).

The apparent densities (mass over volume) of the foods are more difficult to estimate. They are usually functions of water content. Rahman *et al.* (1996) have given some other example correlations.

The pure densities (kg m^{-3}) of the food constituents may be estimated using the formulas provided by Choi and Okos (1986). The individual densities are calculated as follows:

$$\rho_{\text{water}} = 997.18 + 0.0031439 \cdot T - 0.0037574 \cdot T^2 \quad (1.33)$$

$$\rho_{\text{protein}} = 1329.9 - 0.5185 \cdot T \quad (1.34)$$

$$\rho_{\text{fat}} = 925.59 - 0.41757 \cdot T \quad (1.35)$$

$$\rho_{\text{carbohydrate}} = 1599.1 - 0.31046 \cdot T \quad (1.36)$$

$$\rho_{\text{fibre}} = 1311.5 - 0.36589 \cdot T \quad (1.37)$$

$$\rho_{\text{ash}} = 2423.8 - 0.28063 \cdot T \quad (1.38)$$

where the temperature T is in degree Celsius.

1.3.4 Thermal properties and conventional heating

For food materials, two thermal properties are of particular interest: heat conductivity and specific heat capacity, as they are directly replaced in cooking. Heat conduction is the most important mechanism of heat transfer within the food materials during drying. It occurs wherever there is a ‘material’ medium and there is a temperature gradient within it. On an infinitely long slab or tube, being subjected to two constant temperatures at both sides (one high and one low), the isotherms (constant temperature lines or surface whereby on these lines or surfaces, the temperature is all the same) are shown in Figure 1.18(a) and (b). If the tube were not cylindrical, as shown in Figure 1.18(c), the isotherms would be different. Along the direction perpendicular to these isotherms, temperature changes and heat flows from the higher to the lower temperature region.

It is common sense that heat is conducted from high to low temperatures unless there is another mechanism to ‘pump’ heat from a low temperature region to high temperature region (this happens in refrigeration).

It is intuitive for one to think that the larger the temperature difference across the infinite slab the greater the heat flux (heat transfer rate per unit heat transfer area). On the other hand, the thicker the slab, the more difficult it is to transfer heat across. All these intuitions are reflected in the following equation:

$$q \propto \frac{T_h - T_l}{\delta} \quad (1.39)$$

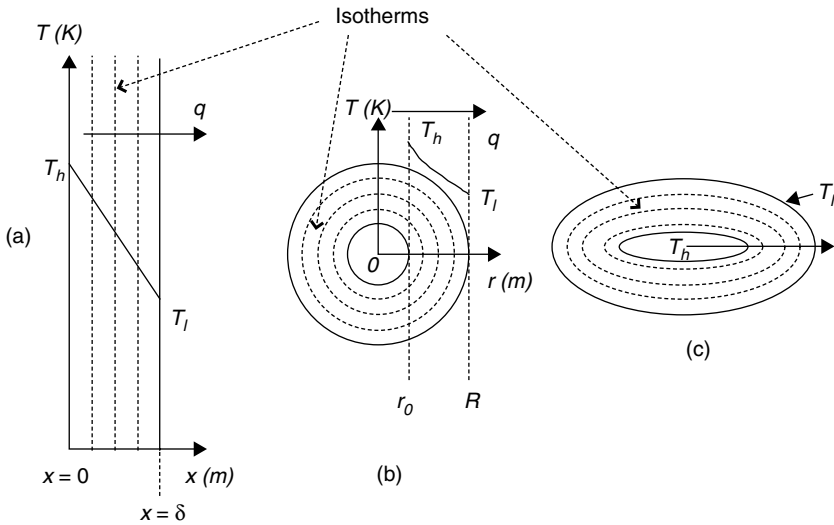


Fig. 1.18 Schematic diagrams of heat conduction through infinitely long objects. (a) Slab, (b) cylinder and (c) ellipsoid (drawn by X.D. Chen).

If the slab is a piece of wood as opposed to a piece of stainless steel, the heat flux is expected to be lower. The conducting ‘power’ of the wood is lower than that of the steel, as such:

$$q \propto k \cdot \frac{T_h - T_l}{\delta} \quad (1.40)$$

where k is the proportionality reflecting the nature of the slab. In fact, equation (1.40) is exact at steady state when we say that k is the heat conductivity of the slab material.

$$q = k \cdot \frac{T_h - T_l}{\delta} \quad (\text{W m}^{-2}) \quad (1.41)$$

To generalise the above to anywhere that is perpendicular to the isotherm (at unit vector \vec{n} direction), and at any time instance, Fourier’s law defines:

$$\vec{q}_n = -k \frac{\partial T}{\partial l} \vec{n} \quad (\text{W m}^{-2}) \quad (1.42)$$

\vec{q}_n is the heat flux vector at \vec{n} direction and $\partial T / \partial l$ is the temperature gradient at \vec{n} direction (see Figure 1.19). l is the length along \vec{n} direction (m). k has the unit of $\text{W m}^{-1} \text{K}^{-1}$. k is obviously composition dependent and is also dependent on temperature. In general it increases as temperature increases. Marked differences can be found between different materials, for example, pure copper has a k value of $399 \text{ W m}^{-1} \text{K}^{-1}$, carbon containing steel (1.5% carbon content) $36.7 \text{ W m}^{-1} \text{K}^{-1}$, water at 20°C $0.599 \text{ W m}^{-1} \text{K}^{-1}$, and finally dry air at 20°C $0.0259 \text{ W m}^{-1} \text{K}^{-1}$.

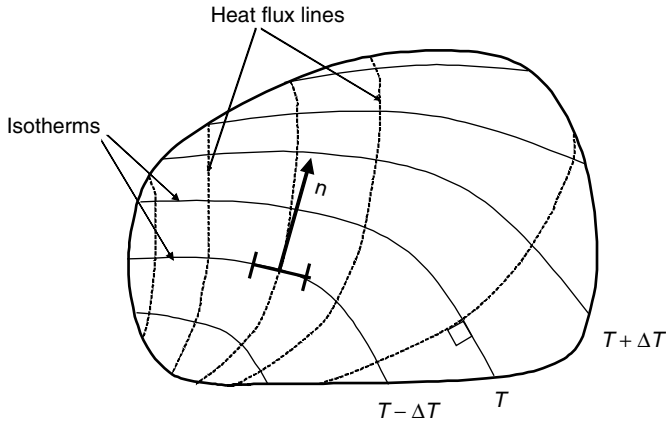


Fig. 1.19 Isotherms (solid lines) and heat flux lines (dashed lines) (drawn by X.D. Chen).

Recalling equation (1.41), Fourier's law can be written at one dimension (Figure 1.18(a)) as:

$$q = -k \frac{\partial T}{\partial x} \quad (\text{W m}^{-2}) \quad (1.43)$$

The heat flux along r -direction in Figure 1.18(b) is:

$$q = -k \frac{\partial T}{\partial r} \quad (\text{W m}^{-2}) \quad (1.44)$$

The conductivity of food materials is a unique topic to food engineering. The food usually consists of fat, protein, mineral, moisture and air components, and other minor components like volatiles. To generically describe this property of food, accurately, may be viewed as an impossible task. Choi and Okos (1986) took on this 'impossible' challenge and have provided a series of 'universal' correlations for the gross components.

Formulas of k for pure materials

Often, the sum of all the fractional contributions made by the components may be appropriate for engineering calculations. Uniform foods (down to the pore level) may not be possible. Therefore, these calculations can be viewed only as being approximate. It may be done as the following:

$$k_{water} = 0.57109 + 0.0017625 \cdot T - 6.7036 \times 10^{-6} \cdot T^2 \quad (1.45)$$

$$k_{protein} = 0.17881 + 0.0011958 \cdot T - 2.7178 \times 10^{-6} \cdot T^2 \quad (1.46)$$

$$k_{fat} = 0.18071 + 0.0027604 \cdot T - 1.7749 \times 10^{-7} \cdot T^2 \quad (1.47)$$

$$k_{carbohydrate} = 0.20141 + 0.0013874 \cdot T - 4.3312 \times 10^{-6} \cdot T^2 \quad (1.48)$$

$$k_{fibre} = 0.18331 + 0.0012497 \cdot T - 3.1683 \times 10^{-6} \cdot T^2 \quad (1.49)$$

$$k_{ash} = 0.32962 + 0.0014011 \cdot T - 2.9069 \times 10^{-6} \cdot T^2 \quad (1.50)$$

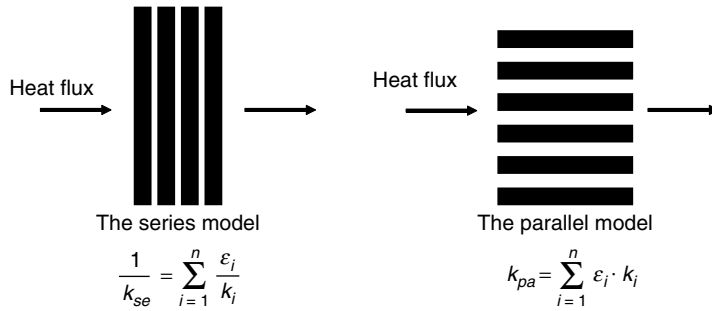


Fig. 1.20 Schematics of the two simplest structures for evaluating thermal conductivity (drawn by X.D. Chen).

The above thermal conductivities have the unit of $\text{W m}^{-1} \text{K}^{-1}$. The temperature range may be considered to be appropriate up to 50°C .

Two simplistic structures

For the two simple structures (see Figure 1.20), one can write the following:

For the *parallel* structure,

$$k_{mixture} = \varepsilon_{water} \cdot k_{water} + \varepsilon_{protein} \cdot k_{protein} + \varepsilon_{fat} \cdot k_{fat} + \varepsilon_{carbohydrate} \cdot k_{carbohydrate} + \varepsilon_{fibre} \cdot k_{fibre} + \varepsilon_{ash} \cdot k_{ash} \quad (1.51)$$

This model predicts the lowest estimate of the mixture thermal conductivity.

For the *series* structure,

$$\frac{1}{k_{mixture}} = \frac{\varepsilon_{water}}{k_{water}} + \frac{\varepsilon_{protein}}{k_{protein}} + \frac{\varepsilon_{fat}}{k_{fat}} + \frac{\varepsilon_{carbohydrate}}{k_{carbohydrate}} + \frac{\varepsilon_{fibre}}{k_{fibre}} + \frac{\varepsilon_{ash}}{k_{ash}} \quad (1.52)$$

This model predicts the highest estimate of the mixture thermal conductivity.

The sensible value is expected to occur in between the above two extremes, which sometimes suggests how many parallel structures and how many series structures are ‘mixed’ together. The fractions in between are often implied (Kee, 1992) (see Figure 1.21).

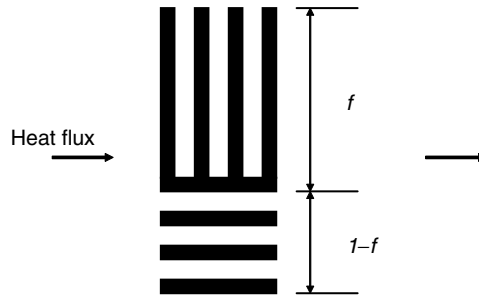
ε_i is the volume fraction of each component (i) which can be determined from mass fraction:

$$\varepsilon_i = \frac{\omega_i \cdot \rho}{\rho_i} \quad (1.53)$$

and ρ is the composite or mixture density (kg m^{-3}) and ρ_i is the individual density (kg m^{-3}). The composite density is estimated using the following formula:

$$\rho = \frac{1}{\sum X_i / \rho_i} \quad (1.54)$$

Table 1.4 provides some typical values of practical interest (Singh and Heldman, 1993).



The combined model

$$\frac{1}{k_{com}} = \frac{1-f}{k_{pa}} + \frac{f}{k_{se}}$$

Fig. 1.21 Combination of the two simplest structures to form a more realistic structure (modified from Keey (1992) by X.D. Chen).

Table 1.4 Typical thermal conductivities of food materials.

Material	Temperature (°C)	Water content (wt%)	Thermal conductivity (W m ⁻¹ K ⁻¹)
Apple	2–36	85.6	0.39
Butter	46	15	0.20
Beef (lean)	7–62	~79	0.43–0.49
Cod	2.8	83	0.54
Egg (white)	36	—	0.54
Egg (yolk)	33	—	0.34
Lamb	5, 61	72	0.42–0.45, 0.42–0.48
Milk (skim)	1.5, 80	—	0.54–0.63
Olive oil	15	—	0.19
Raw potato	1–32	81.5	0.55

In food processing, it is often of interest to calculate how quickly a food product is heated up or cooled down under a convection situation. For a food object (a pea or a peach for example), the characteristics size L may be determined by the following:

$$L = \frac{V}{A} \tag{1.55}$$

where V is the volume of the object (m³) and A is the surface area of the same object (m²). For an infinite slab with thickness of 2δ , $L = \delta$; for an infinitely long cylinder of radius of R , $L = 0.5R$; for a sphere of radius of R , $L = R/3$. The corresponding *Biot* number is thus defined as the following:

$$Bi = \frac{hL}{k} = \frac{h(V/A)}{k} \tag{1.56}$$

where h is the convection heat transfer coefficient (m s^{-1}) which is determined either experimentally for the material and geometry, flow condition are concerned, or using the established relationships for the *Nusselt* number (hL/k) in relation to flow conditions (often a function of the *Reynolds* ($\rho uL/\mu$) number and the *Prandtl* number (ν/α) (see Appendix I). u is the fluid velocity (m s^{-1}). Here the fluid properties are used; k , ρ , μ , ν and α are heat or thermal conductivity ($\text{W m}^{-1} \text{K}^{-1}$), density (kg m^{-3}), viscosity (Pa s), kinematic viscosity (μ/ρ) (m s^{-1}) and thermal diffusivity ($k/\rho C_p$) (m s^{-1}) respectively.

Conventionally, when Bi is smaller than 0.1, meaning the internal thermal resistance (due to conduction) is less than approximately 10% of that of the external thermal resistance, so the temperature within the object may be considered to be uniform. This can simplify many of the calculations of the heating or cooling time. More strictly, for 5% as limit, this criterion may be generalised to be:

$$Bi < 0.1M \quad (1.57)$$

where $M = 1$ for infinite slab and $M = 1/2$ for infinite cylinder and $M = 1/3$ for sphere. Under the condition of uniform internal temperature, for a food object being treated in a convective environment (say cooling of peach with cold water), the following equation can be written:

$$mc_p \frac{dT}{dt} = -hA(T - T_\infty) \quad (1.58)$$

m is mass (kg), c_p is the specific heat capacity ($\text{J kg}^{-1} \text{K}^{-1}$), T is the temperature of the object (K) and T_∞ is the bulk fluid temperature (K). c_p values can be estimated using the formula provided in Appendix 3. Some typical product values are given in Table 1.5. This has a simple solution:

$$\frac{T - T_\infty}{T_i - T_\infty} = \exp\left(-\frac{hA}{mc_p}t\right) \quad (1.59)$$

When the internal thermal resistance cannot be ignored, that is, when Bi is not that small, equation (A2.28) cannot be used directly. Usually, the *Heisler* charts of standard object geometries (infinite slab, infinite cylinder and sphere) can be used, in which the dimensionless

Table 1.5 Typical values of specific heat capacities of various food materials (composition in wt%) (summarised from Singh and Heldman, 1993).

Material	Water	Protein	Carbohydrate	Fat	Ash	Experimental C_p ($\text{kJ kg}^{-1} \text{K}^{-1}$)
Beef patty	68.3	20.7	0.0	10.0	1.0	3.52
Butter	15.5	0.6	0.4	81.0	2.5	2.05–2.14
Whole milk	87.0	3.5	4.9	3.9	0.7	3.85
Potato	79.8	2.1	17.1	0.1	0.9	3.52
Apple	84.4	0.2	14.5	0.6	0.3	3.73–4.02
Fish	80.0	15.0	4.0	0.3	0.7	3.6
Carrot	88.2	1.2	9.3	0.3	1.1	3.81–3.94

temperatures (average, centre, surface temperatures) versus dimensionless time (the Fourier number) are graphically expressed at different values of Bi^{-1} .

On the other hand, as an approximate approach, using the characteristic resistance dimension model (van der Sman, 2003), that is, the existence of a characteristic length into the food object (δ_c), one may choose to use equation (A2.28) even for large Biot numbers for convenience. Here the heat transfer coefficient h is replaced by an *overall* heat transfer coefficient (U), which is determined by the following:

$$\frac{1}{U} \approx \frac{1}{h} + \frac{\delta_c}{k} \quad (1.60)$$

The temperature in equation (A2.28) is now the *average* temperature within the food object. The typical values of δ_c are: $\delta_c = 0.25 \times \text{Slab Thickness}$ for infinite slab; $1/3 \times \text{radius}$ for infinite cylinder; $1/4 \times \text{radius}$ for sphere.

Formulas for calculating specific heat capacities ($J kg^{-1} K^{-1}$)

Specific heat capacity is important in the calculations of the temperature rise or drop (see equation (1.59)). The individual specific heat capacities of the food constituents are estimated using the following equations:

$$Cp_{water} = 4176.2 - 0.090864 \cdot T + 0.0054731 \cdot T^2 \quad (1.61)$$

$$Cp_{protein} = 2008.2 + 1.2089 \cdot T - 0.0013129 \cdot T^2 \quad (1.62)$$

$$Cp_{fat} = 1984.2 + 1.4733 \cdot T - 0.0048008 \cdot T^2 \quad (1.63)$$

$$Cp_{carbohydrate} = 1548.8 + 1.9625 \cdot T - 0.0059399 \cdot T^2 \quad (1.64)$$

$$Cp_{fibre} = 1845.9 + 1.8306 \cdot T - 0.0046509 \cdot T^2 \quad (1.65)$$

$$Cp_{ash} = 1092.6 + 1.8896 \cdot T - 0.0036817 \cdot T^2 \quad (1.66)$$

The composite, mixture or a native food's specific heat capacity may be estimated using the following equation based on weight fractions ($W = 0 - 1$):

$$Cp_{mixture} = W_{water} \cdot Cp_{water} + W_{protein} \cdot Cp_{protein} + W_{fat} \cdot Cp_{fat} \\ + W_{carbohydrate} \cdot Cp_{carbohydrate} + W_{fibre} \cdot Cp_{fibre} + W_{ash} \cdot Cp_{ash} \quad (1.67)$$

1.3.5 Colour

Colour, flavour, taste and shape (appearance) are the four important factors affecting people's choice of foods in the first instance. Texture plays a subsequent, but also important role, once the foods are consumed. Colour perhaps forms the first impression of a cooked dish or food product for consumers. Vision psychology, science of colour, colour psychology, the technologies that measure colour and computer imaging, have all been developed in order to design foods, quantify colour and improve the quality of the foods.

The colour of the product affects the perception of the goodness or badness of the product. Birren's statistical analysis (Li, 1998) is shown qualitatively in Figure 1.22.

The measurement of colour is these days conducted with the CIELAB system, or the $L^* - a^* - b^*$ system established in 1976. The parameters L^* , a^* and b^* are measured through

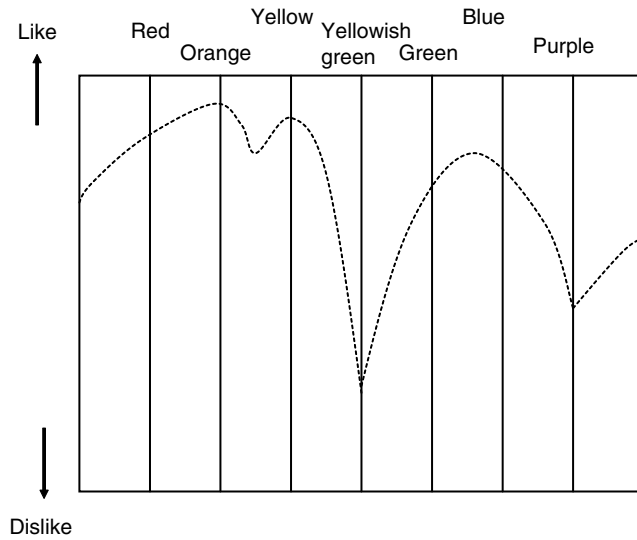


Fig. 1.22 Qualitative illustration of the impact of the colour of a natural food product upon 'Like or Dislike' (after Li, 1998). (The qualitative Birren diagram modified from that summarised by Li, 1998.)

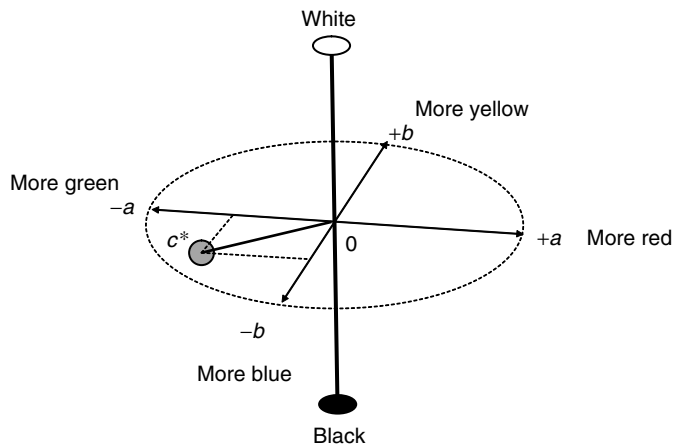


Fig. 1.23 An illustration of the CIELAB colour expression system (drawn by X.D. Chen).

a colorimeter such as the Hunter Lab instrument. A schematic diagram showing the L^* , a^* and b^* coordinate system is shown in Figure 1.23.

$L^* = 0$ corresponds to Black; $L^* = 100$ denotes White. L^* represents the brightness. There are thus 100 graduations between White and Black, in other words, the grey scales. As $a^* \rightarrow +a$, the colour approaches pure RED; and as $a^* \rightarrow -a$, the colour approaches pure Green. $-b$ towards pure Blue and $+b$ towards pure Yellow. The product colour would be a combination of a^* and b^* at the same level of brightness L^* , based on the basic idea that Red, Blue and Yellow can make up other colours by combination. Blue and Yellow mix together to form some kind of Green depending on proportions of the mixture (most painters would

use this principle). The combination value of colour evaluated using the following formula:

$$c^* = \sqrt{(a^*)^2 + (b^*)^2} \quad (1.68)$$

is useful and is called 'metric chroma'. The greater the c^* the purer the colour appears to be. The 'metric Hue-angle' is defined as:

$$hue = \arctan\left(\frac{b^*}{a^*}\right) \quad (1.69)$$

a^* and b^* may also be called the 'colour indices'. These parameters may be understood (based on Figure 1.23) based on our knowledge of two-dimensional geometry. A three-dimensional parameter is then the following:

$$\Delta E^* = \sqrt{(\Delta L^*)^2 + (\Delta a^*)^2 + (\Delta b^*)^2} \quad (1.70)$$

ΔL^* , Δa^* and Δb^* are respectively the differences between two points in the coordinate system given in Figure 1.23.

The above equation may be written as follows to be more practical, that is, by choosing a reference point to benchmark the significance of change:

$$\Delta E^* = \sqrt{(L^* - L_{ref}^*)^2 + (a^* - a_{ref}^*)^2 + (b^* - b_{ref}^*)^2} \quad (1.71)$$

For colour 'sensory' evaluation, ΔE^* is very important quantity determining (Li, 1998):

Trace level difference	$\Delta E^* = 0-0.5$
Slight difference	$\Delta E^* = 0.5-1.5$
Noticeable difference	$\Delta E^* = 1.5-3.0$
Appreciable difference	$\Delta E^* = 3.0-6.0$
Large difference	$\Delta E^* = 6.0-12.0$
Very obvious difference	$\Delta E^* > 12.0$

It is not clear what the relationship is between colour perception and water content. Colour may be intensified (colourings concentrated) as water is removed. On the other hand, as in hot air drying, the surface temperature of the product can get very high, which promotes heat-sensitive chemical reactions such as Millard reactions, so the product exhibits a 'cooked' colour. It is important to emphasise that colour as a quality of the manufactured food is a 'surface phenomena' so the surface temperature and surface water content control should be the most important parameters to control.

Based on a study of bread browning kinetics during baking (Purlis and Salvadori (2007)), colour development ΔE^* of the bread crust during baking could be expressed as a 'rule of thumb' approach or an empirical approach as:

$$\Delta E^* = k \cdot \frac{\Delta m}{m_o} \quad (1.72)$$

that is the total colour change is proportional to the weight loss $\Delta m/m_o$ (the ratio of the weight loss (kg) from the start to the initial weight (kg); thus it is a percentage) with the coefficient k being a simple function of oven temperature T_{oven} :

$$k = k_o \cdot T_{oven} + k_1 \quad (1.73)$$

where k_0 and k_1 are model constants. This model was found to be very accurate (below 10% error) for large weight loss percentages of greater than approximately 13%. This indicates the importance of the high temperature influence as baking (and water loss) proceeds. As water content at the surface of the bread gets lower, the surface temperature increases, increasing the Millard reaction rates.

A more fundamental approach may be demonstrated in a study on lycopene degradation (red colour change) in the drying process (Goula *et al.*, 2006). Here, experimentally, the temperatures and water contents of the tomato pulp samples were fixed so the degradation kinetics could be worked out as functions of temperature and water content:

$$\frac{dC}{dt} = -k \cdot C \quad (1.74)$$

Here the nutrient (lycopene) is considered to degrade following a first-order reaction mechanism. C is the concentration of lycopene (kg m^{-3}). The rate constant k is expressed as:

$$k = 0.121238 \cdot e^{0.0188 \cdot W} \cdot e^{-(2317/T)} \text{ (min}^{-1}\text{)} \quad \text{for } W \geq 55 \text{ (wt\%)} \quad (1.75)$$

and

$$k = 0.275271 \cdot e^{0.00241 \cdot W} \cdot e^{-(2207/T)} \text{ (min}^{-1}\text{)} \quad \text{for } W \leq 55 \text{ (wt\%)} \quad (1.76)$$

where W is the product moisture content in % (wet basis); T is the product temperature in K.

There has been little work conducted explicitly on taking the same approach as in the lycopene degradation to model colour change. It is expected that this gap will be filled soon.

Various combinations of the three colour parameters, L^* , a^* and b^* , may make better sense when correlating the colour changes or the rates of the changes to constituent changes. One example is that:

$$a^* \times b^* = k_1 + k_2 \cdot C \quad (1.77)$$

Here k_1 , k_2 are correlation constants and C is the lycopene concentration of tomato peel (Kaur *et al.*, 2006). k_1 , k_2 are temperature dependent.

1.3.6 Equilibrium isotherms

Water sorption (desorption and absorption) isotherm is important in determining the extent of a drying or a humidifying process that can be operated under a defined set of ambient relative humidity and temperature. Relative humidity (RH) is defined as the partial pressure of water vapour in a mixture of gases divided by the partial pressure corresponding to vapour saturation in the same mixture. At constant total pressure and when ideal gas law applies, the relative humidity is also the ratio of vapour concentrations:

$$RH = \frac{\rho_v}{\rho_{v,sat}} \quad (1.78)$$

For food systems, RH is the same as the water activity in value (a_w). Figure 1.6 shows the typical equilibrium isotherms for desorption. The absorption curve for the same temperature

can be non-identical to that of desorption, and this phenomenon is called sorption hysteresis. This phenomena may have implications for the surface area of the material ($\text{m}^2 \text{g}^{-1}$) depending on whether water sorption or desorption is involved.

The two most popular models are the GAB and BET equations for n-layers of absorbed molecules (Rahman, 1995). The GAB model generally gives the best fit over the largest number of food materials measured for equilibrium isotherms. The GAB equation for curve fitting has the following form:

$$X_{eq} = \frac{Ckm_0a_w}{(1 - ka_w)(1 - ka_w + Cka_w)} \quad (1.79)$$

where X_{eq} is the equilibrium moisture content, a_w is the water activity, m_0 is the monolayer moisture content and C and k are constants related to the temperature.

$$C = C_o \exp\left(\frac{\Delta H_1}{RT}\right) \quad (1.80)$$

$$k = k_o \exp\left(\frac{\Delta H_2}{RT}\right) \quad (1.81)$$

where T is the absolute temperature, R is the universal gas constant and ΔH_1 and ΔH_2 are heats of sorption of water. The measured results are not necessarily indicating the rather neat Arrhenius relationships proposed above.

As mentioned earlier, under equilibrium conditions, defined by a combination of gas temperature and water content, RH is a function of the two, f :

$$RH_{eq} = f(X_{eq}, T) \quad (1.82)$$

According to the common assumption that the surface vapour concentration is the one that is in equilibrium with the surface liquid water content, equation (1.1) for drying flux can be re-written as:

$$\begin{aligned} N''_v &= h_m \cdot (RH_s \cdot \rho_{v,sat}(T_s) - \rho_{v,\infty}) \\ &= h_m \cdot (f(X_s, T_s) \cdot \rho_{v,sat}(T_s) - \rho_{v,s}) \end{aligned} \quad (1.83)$$

One can see that when f is smaller than 1, the drying process progresses into the so-called 'falling drying flux' period if T_s remains the same. Usually when drying in hot air, the interface temperature T_s would be somewhat higher than the core and more moist region inside the material, $\rho_{v,sat}(T_s)$ would become larger as temperature increases. The wet-bulb temperature is usually quoted as being the temperature at the constant drying flux regime, though in reality it is an approximate value. Due to the exponential increasing dependence of $\rho_{v,sat}(T_s)$ on surface temperature, the reduction in RH_s may be compensated, exceeding the constant drying flux period.

1.4 DRYING RATE CHARACTERISTIC CURVE APPROACH TO CORRELATE DRYING RATES – VAN MEEL'S METHOD

Van Meel (1958) postulated that when working with convective batch driers, a single characteristic drying curve could be deduced for a material being dried. This model reflects the

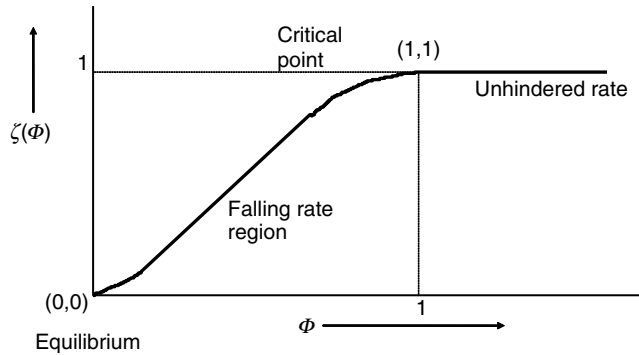


Fig. 1.24 Characteristic drying curve (adapted from Van Meel, 1958).

nature of the drying rate curves shown in Figure 1.24. It is empirical but has been successful in correlating drying kinetics of small particles (Keey, 1992). The model assumes that for any given sample water content, a corresponding specific drying rate exists. This rate is relative to the initial unhindered drying rate, and is independent of the external drying conditions. These conditions include the temperature, humidity and pressure of the drying gas. The model also implies that a region exists, where for a period of time the rate remains unhindered. The relative drying rate is defined as:

$$\zeta = \frac{N}{N_c} \quad (1.84)$$

where ξ is the relative drying rate, N is the instantaneous drying rate, and N_c is the drying rate at the critical condition (i.e. when the drying regime is in transition between the unhindered rate and falling rate periods).

The characteristic moisture content is defined by the following equation:

$$\Phi = \frac{X - X_\infty}{X_c - X_\infty} \quad (1.85)$$

where X is the liquid water content (on dry basis), X_∞ is the equilibrium water content, and X_c is the critical water content. Hence the drying is normalised to pass through the critical point and the equilibrium point, denoted by points (1,1) and (0,0) respectively in:

According to Keey (1992), the characteristic curve method is attractive since it leads to a simple lumped-parameter expression for the drying rate, in the following form:

$$N = \zeta(N_c) = \zeta[\beta\Phi(YW - YG)] \quad (1.86)$$

This expression has been used extensively as the basis for understanding the behaviour of industrial drying plants, because of the simplicity of the parameters that are used: ζ is a function of the material itself, β is dependent on the drier design, and the process conditions are accounted for by the term $\Phi(YW - YG)$. Y_W is the saturated absolute humidity at wet-bulb temperature, and Y_G is the absolute humidity of the drying gas.

However, in reality, for many drying systems, the characteristic drying curve is a gross approximation. A common drying curve will only be found if the volume-averaged water

content reflects the moistness of the drying surface in some way. A characteristic drying curve must be obtained from laboratory experiments under constant external conditions, with material of exactly the same form and size as that of interest in the real industrial drier situation.

Keey (1992) further specifies that a unique characteristic curve can be established at Kirpichev numbers of less than 2, or in effect, when the material is thinly spread and the permeability to moisture is high (i.e. the material has a large moisture diffusivity). The Kirpichev number is given by:

$$Ki = \frac{N_c L}{\rho_S X_o D_{eff}} \quad (1.87)$$

where L is the thickness of the sample, ρ_S is density of the dry solid, X_o is the initial water content, and D_{eff} is the effective diffusion coefficient.

The Kuts and Pikus model (Kuts and Pikus, 1980) describes the drying of a number of hygroscopic materials using an empirical expression as follows:

$$\zeta = \frac{N}{N_c} = \frac{(X - X_\infty)^u}{B + F(X - X_\infty)^u} \quad (1.88)$$

in which B , F , and u are the correlation coefficients. However, according to Keey (1992) in many cases the drying curve can be fitted by a simple algebraic equation over a limited moisture-content range of interest by:

$$\zeta = \frac{N}{N_c} = \left(\frac{X - X_\infty}{X_c - X_\infty} \right)^j = \Phi^j \quad (1.89)$$

where j is a parameter which is dependent on the relative difficulty of removing moisture from a material.

1.5 DIFFUSION THEORIES OF DRYING

1.5.1 Effective Fickian diffusivity

As soon as the pure water evaporation-like behaviour is finished (i.e. the so-called constant drying flux period), the falling rate period starts and the internal moisture transfer or the internal resistance to moisture transfer becomes important. Fick's diffusion law has been suggested to apply. This theory is popular as its complexity is in between that of comprehensive theories, such as the Luikov theory, and the totally empirical model, such as the Page model. It also possesses fundamental information – an effective Fickian-type diffusivity. Furthermore, the related partial differential equation, governing mass transfer process, is the simplest mathematical model of drying which could predict the transient water content distribution realistically across the material being dried.

The Fickian diffusional flux can be expressed as:

$$\vec{m}_n = -D \cdot \frac{\partial C}{\partial l} \vec{n} \quad (\text{kg m}^{-3} \text{ m}^{-2} \text{ s}^{-1}) \quad (1.90)$$

\vec{m}_n is the diffusive mass flux vector at \vec{n} direction and $\partial C / \partial l$ is the temperature gradient at \vec{n} direction within the material. l is the length along \vec{n} direction (m). D has the unit of $\text{m}^2 \text{ s}^{-1}$,

Table 1.6 Some typical values for effective liquid water diffusivities. Reproduced from Sablani *et al.* (2000) with permission from Science Publishers.

Products	Temperature (°C)	Water content on dry basis (kg kg ⁻¹)	Diffusivity (m ² s ⁻¹)
Apple	30–70	0.1–1.5	1×10^{-11} to 3.3×10^{-9}
Banana	20–40	0.01–3.5	3×10^{-13} to 2.1×10^{-10}
Beef (raw, freeze dried)	25	0.1268	3.07×10^{-11}
Biscuit	20–100	0.1–0.6	8.6×10^{-10} to 9.4×10^{-8}
Bread	20–100	0.1–0.75	2.8×10^{-9} to 9.6×10^{-7}
Fish	30	0.05–0.3	1.3×10^{-11} to 3.1×10^{-10}
Milk (dry, non-fat)	25	0.13	2.1×10^{-11}
Milk (skim)	50–90	0.25–0.8	2.8×10^{-11} to 3.1×10^{-10}
Pasta	40	0.27	2.5×10^{-11}
Potato	30–90	0.05–1.5	1.1×10^{-10} to 4.5×10^{-10}
Rice	30–50	0.1–0.25	3.8×10^{-8} to 2.5×10^{-7}
Starch gel	60–100	0.1–1	1.4×10^{-11} to 3.2×10^{-10}
Wheat flour	25	0.06–0.17	3.9×10^{-12} to 3.2×10^{-11}

which is expected to be a function of concentration and temperature. The concentration may also be expressed in molar concentration. The mass diffusivities in food processes are sometimes difficult to determine and the variability is large. Examples of the water diffusivities in foods during dehydration processes are given in Table 1.6.

The moisture diffusivity is dependent on temperature, water content and porosity, a number of models exist for describing the moisture diffusivities. The water content dependency is sometimes expressed as the following:

$$D \propto \exp(\omega) \quad (1.91)$$

where ω is the liquid water content on wet-basis (wt%). This usually reflects the apparently high mobility of water molecules when water content is high. The temperature dependency is often expressed in the chemical reaction rate type or the Arrhenius form:

$$D \propto \exp\left(-\frac{E}{RT}\right) \quad (1.92)$$

that is, the higher the temperature the greater the diffusivity.

Sometimes, the formula can get more complicated. It is important to note the compositional influence and also micro-structural influence on diffusivities of the extraction (liquid–liquid, liquid–solid and evaporation) processes (Aguilera and Stanley, 1999).

For a skim milk droplet exposed to hot drying air, for instance, the liquid water diffusivity equation has been expressed as:

$$D_{l,eff}^{f\&m\&w} = \exp\left[-\frac{82.50 + 1700 \cdot \omega_l}{1 + 79.61 \cdot \omega_l} - \frac{1.39 \times 10^5 \cdot \exp(-3.32 \cdot \omega_l)}{8.314} \cdot \left(\frac{1}{T} - \frac{1}{323}\right)\right] \quad (1.93)$$

By Ferrari *et al.* (1989).

1.5.2 Intuitive understanding of the diffusion theory

Evaporating aroma liquid in a wicking system (see Figure 1.25) is a good example for intuitive understanding of drying theory. It is often understood or taught that the capillary action created by the semi-empty capillaries at the upper section of the wick, which is exposed to the air (natural convection at the top), brings up the liquid. As time goes by, the liquid level in the bottle reduces and becomes eventually dry.

The effective liquid diffusivity may be related to ‘capillary’ diffusivity as one sometimes visualises drying as liquid water ‘supplied’ by the ‘capillary action’. Based on the observation given in Figure 1.26, it is unlikely that the capillary flow can somehow be maintained. It is clear that the liquid is depleted by the gaseous phase, rather than being supplied to the air–material interface. The effective diffusion process would have more to do with gaseous phase transport (vapour and air).

For transport in porous media, there is also the idea of surface diffusion as molecules can move from site to site (Rigby, 2005). Since the food material surfaces are in general

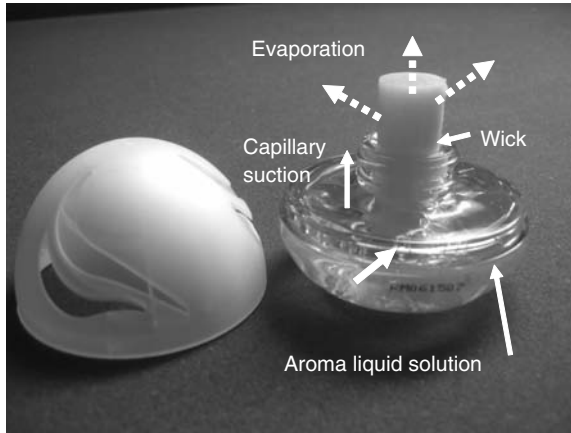


Fig. 1.25 A commercial wicking system which ‘sucks’ liquid into the wick and then evaporates into the room atmosphere for pleasure (photographed and illustrated by X.D. Chen).

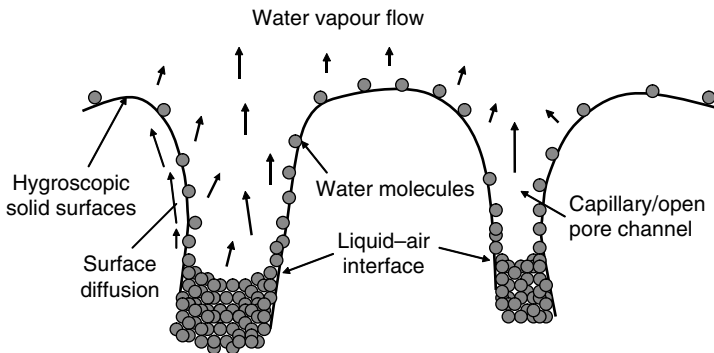


Fig. 1.26 An illustration of the kind of surface diffusion along the pore channel walls or capillary walls – the molecules moving from the more crowded areas to the less crowded (drawn by X.D. Chen).

hygroscopic (interactive with the water molecules), surface diffusion is possible. This has not been discussed much in food related literature, it is, however, a possible diffusion mechanism for water transport from the liquid level to the surface of the material being dried (as depicted in Figure 1.25).

One cannot rule out that, for highly shrinkable materials such as vegetables, due to the compression of the porous structure the capillaries may become smaller, which would ‘raise’ the liquid ‘column’ heights. This may seem like the capillaries are ‘supplying’ liquid towards the air–material interface during the drying process (see Figure 1.27), that is, $H_{r,1} > H_{r,2}$. Once the capillaries are fixed in size once drying has occurred to a large extent (i.e. when the material has shrunk to a somewhat constant size), the liquid inside the capillaries will be depleted as suggested earlier. No matter whether it is forced by pressure as temperature rises (for instance when the internal region of the material has higher temperature such as in microwave drying process and vapour bubble or air bubble expands) or it is just a simple liquid depletion process as suggested above, moisture is always ‘seen’ to move from the high liquid water content region towards the low liquid water content region. Thus an effective or equivalent diffusion process is a reasonable approach from a practical point of view.

Shrinking might have another impact as it reduces the path length (ΔH) between the material surface and the liquid surface, thus increasing the mass transfer flux, according to the following:

$$\text{Massflux} = D_{v,air} \cdot \frac{\rho_{v,sat} - \rho_{v,s}}{\Delta H} \quad (\text{kg m}^{-3} \text{ m}^{-2} \text{ s}^{-1}) \quad (1.94)$$

The vapour concentration at the liquid surface is that of the saturated one $\rho_{v,sat}$ and at the surface of the material (the outlet of the capillary) the vapour concentration is $\rho_{v,s}$ (kg m^{-3}). If the pore/capillary narrowing shown in Figure 1.27 and the shrinking effect shown in Figure 1.28 is approximately balanced, it is possible that the existence of the constant drying flux period is extended while the material shrinks.

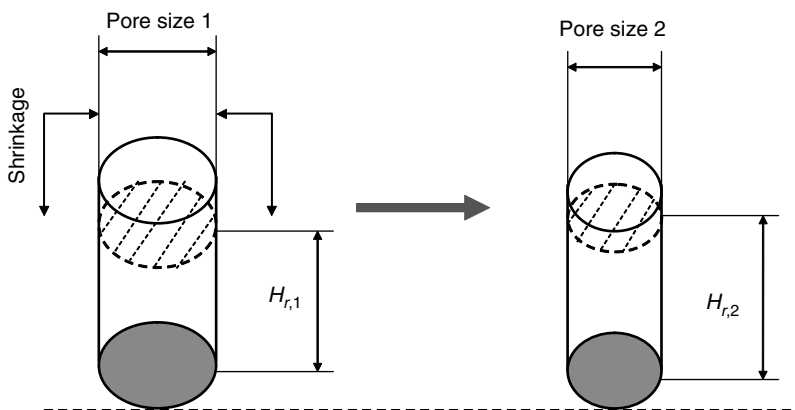


Fig. 1.27 A simplistic illustration of the effect of shrinkage on drying rate (pore/capillary narrowing) (drawn by X.D. Chen).

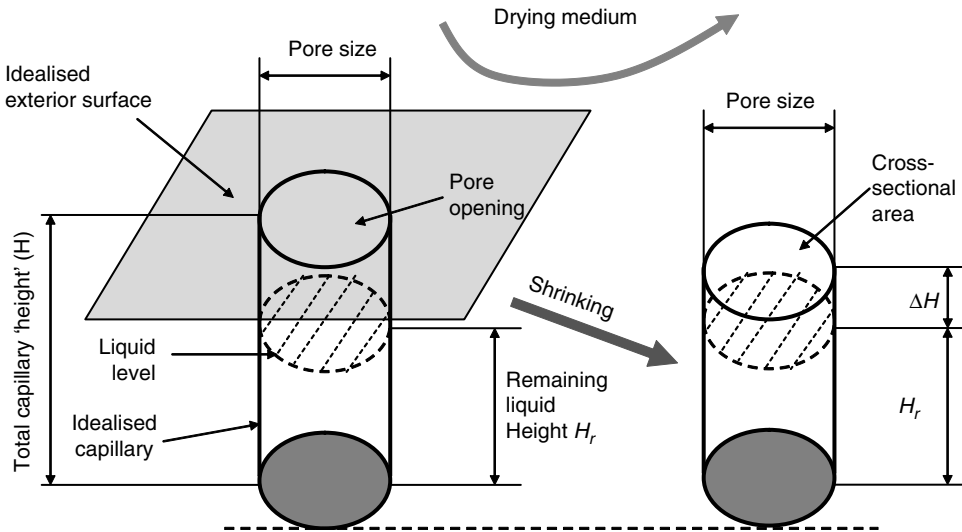


Fig. 1.28 A simplistic illustration of the effect of shrinkage on drying rate (pore channel length reducing) (drawn by X.D. Chen).

1.5.3 Drying of foods simulated using the effective Fickian diffusion law

To explore the rate of drying and the spatial distribution of water content within the material being dried, the following Fickian law is expressed based on mass conservation without the source term (e.g., the local evaporation rate/wetting rate – to be discussed later on):

$$\frac{\partial C}{\partial t} = \frac{\partial}{\partial x} \left(D \frac{\partial C}{\partial x} \right) \quad (1.95)$$

Here only a one-dimensional expression (i.e. the slab geometry) is given for simplicity. C can be considered the concentration of liquid water in the material being dried ($C = C_l$) (kg m^{-3}) and D is the effective (liquid) moisture diffusivity ($D = D_{eff,l}$) ($\text{m}^2 \text{s}^{-1}$). t and x are time (s) and distance (m) respectively. The most important parameter or physical property is the effective diffusivity D . A general system of air drying is shown in Figure 1.29.

1.5.3.1 Crank's solutions of the effective liquid diffusion equations

The following partial difference equation (for the slab geometry as an example; see Figure 1.29) governing the mass transfer process and the long time-scale solution of this PDE, which are most frequently used in the literature, are given below respectively (Crank, 1975; Karim and Hawlader, 2005).

$$\frac{\partial C}{\partial t} = D_{eff,l} \frac{\partial}{\partial x} \left(\frac{\partial C}{\partial x} \right) \quad (1.96)$$

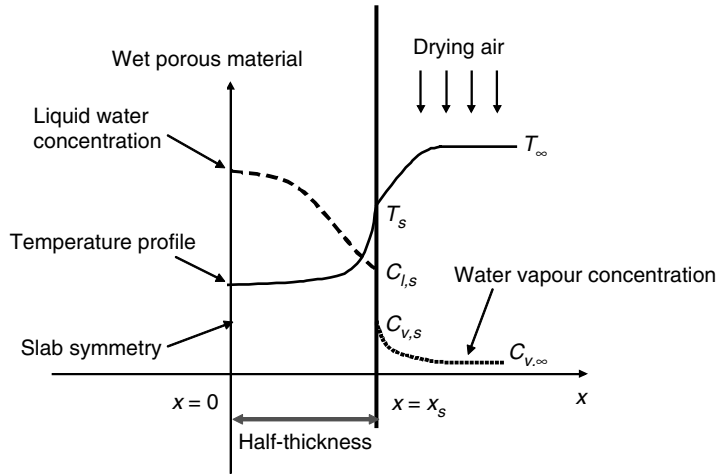


Fig. 1.29 Schematic diagram of drying of a slab symmetrically.

And its solution for negligible external mass transfer resistance:

$$\frac{\bar{X} - X_e}{X_o - X_e} = \frac{8}{\pi^2} \sum_{n=0}^{\infty} \frac{1}{(2n+1)^2} \cdot \exp\left(- (2n+1)^2 \frac{\pi^2}{4L^2} D_{eff,l} \cdot t\right) \quad (1.97)$$

where X_o is the initial water content (kg kg^{-1}), The liquid concentration (C_l) is related to the dry basis water content (X) by $C = X \cdot \rho_s$. Note here, a constant (effective diffusivity) is assumed. L is the total thickness of the material being dried ($= 2b$) (m). b ($x = x_s$) is the half-thickness (m) and the material is dried symmetrically. This model assumes zero volume change, negligible external mass transfer resistance (*Biot* number for mass transfer is infinite) and an isothermal process.

For a 'long time' after drying starts, only the first term of equation (1.97) is sufficient for a good approximation to the full solution, that is:

$$\ln\left(\frac{X - X_e}{X_o - X_e}\right) \approx \ln\left(\frac{8}{\pi^2}\right) - \left(\frac{\pi^2}{L^2} D_{eff,l}\right) t \quad (1.98)$$

This approach correlates very well to the weight loss data only towards the end of the drying period (Sikiatden and Roberts, 2006) if the process is not an isothermal one. In fact, if the above equation was applied to the entire drying process, equation (1.98) would lead to a simple exponential time function that describes the general trend of dryin. This has been proposed as a general model previously, but may yield large errors, however, (Chen, 2005a) if the samples are large and the initial warming up or cooling down periods play important part in drying. The effective diffusivity is always correlated against the drying medium temperature, which is fundamentally incorrect.

In applying the above, one needs to notice that Crank's model and its solutions are based on the following convection boundary condition:

$$-D_{eff,l} \cdot \frac{\partial C_l}{\partial x} \Big|_s = \beta \cdot (C_{l,s} - C_{l,e}) \quad (1.99)$$

or

$$-D_{eff,l} \cdot \frac{\partial X}{\partial x} \Big|_s = \beta \cdot (X_s - X_e) \quad (1.100)$$

This boundary condition is in contrast to what one would write for the vapour transfer:

$$-D_v \cdot \frac{\partial C_v}{\partial x} \Big|_s = h_m \cdot (\rho_{v,s} - \rho_{v,e}) \quad (1.101)$$

The two approaches only become equivalent when the mass transfer coefficients are very large such that the water content at the interface is instantly in equilibrium with the drying medium. Therefore, the lab, the drying condition needs to be a well-mixed one. When the effective diffusivity turns out to be a function of velocity of the drying gas, the assumption of the infinite *Biot* number for mass transfer would be incorrect. One needs to be cautious about how to apply the diffusivity derived this way (at the infinite *Biot* for mass transfer) to the cases where the *Biot* number is finite.

An isothermal drying method has been discussed by Sikiatden and Roberts (2006), which combines microwave energy internal heating and convective hot air to establish the ‘isothermal condition’, a constant D_{eff} for each air temperature has been assumed and a large number of terms taken in Crank’s solution for the cylindrical sample shape. They have shown that the effective diffusion model (Fickian diffusion) for a cylinder represents the drying trends of potato and carrot core samples reasonably accurately. The isothermal condition is promoted with the internal heating due to microwave penetration, which may offset the gradient of temperature caused by convection heat transfer, which in turn may be reasoned by the *Biot* number analysis (Chen, 2005b).

1.5.4 Alternative effective diffusion theories

It is interesting to note that the effective liquid moisture diffusivity $D_{eff,l}$ has not been expressed in the following form:

$$D_{eff,A} = D_{o,A} \cdot \frac{\varepsilon}{\tau} \quad (1.102)$$

which is the common porous media transport approach, as there no ‘reference’ liquid water diffusivity $D_{o,A} = D_{o,l}$ can be found. The porosity ε and tortuosity τ both influence moisture transfer. Sometimes, a ‘constrictivity’ factor may be multiplied to the RHS of equation (1.102) to account for the narrow pores which restrict the diffusion of the chemical species (which is thus dependent on the molecular size to pore channel diameter ratio). It is noted that for food and biological materials there is a general lack of data on pore diameters and this could become a beneficial area for future research.

τ is sometimes treated as a function of porosity, a power function for instance, and it is expected to be greater than unity. The above is a common expression for diffusion of a species *A* in a porous material immersed (or saturated) in species *B*. The reference $D_{o,A}$ should be the free diffusion coefficient of species *A* in species *B* in the absence of the porous material. It is the effective vapour diffusivity $D_{eff,v}$ that can be expressed this way, that is:

$$D_{eff,v} = D_{o,v} \cdot \frac{\varepsilon}{\tau} \quad (1.103)$$

where $D_{o,v}$ is the vapour diffusivity in air for air-drying or in another gaseous drying medium. One step further from the sole liquid diffusion model, and most likely an improvement, is a model that considers vapour as the second phase transported. It is interesting to note that although there has been much hype about the effect of micro-structure on transport properties, there has been little progress on linking micro-structure to properties such as diffusivity.

Using liquid diffusion alone may not be sufficient to explain the process of air drying. Sooner or later during drying, a vapour concentration profile has to be established within the porous material being dried and its movement may also be quite restricted. The vapour flow could have a great impact on volatile compounds. One would consider that an improvement from the 'pure' liquid diffusion model with an effective diffusivity, should consider the mechanisms of both liquid water diffusion and water vapour diffusion. The models that take into account the spatial distributions of temperature and water content (liquid water and water vapour) are generally of two types (one with the source term and one without) The following is one that does not consider the source term again for the slab geometry:

$$\frac{\partial C_l}{\partial t} = \frac{\partial}{\partial x} \left(D_{eff,l} \cdot \frac{\partial C_l}{\partial x} \right) \quad (1.104)$$

$$\frac{\partial C_v}{\partial t} = \frac{\partial}{\partial x} \left(D_{eff,v} \cdot \frac{\partial C_v}{\partial x} \right) \quad (1.105)$$

$$\frac{\partial T}{\partial t} = \frac{1}{\rho C_p} \cdot \frac{\partial}{\partial x} \left(k \cdot \frac{\partial T}{\partial x} \right) \quad (1.106)$$

A close look at the equations (1.104)–(1.106) would reveal that there is no obvious interaction between the mechanisms described in equations (1.104) and (1.105) except at least the vapour diffusivity should be treated as a function of porosity, which is a function of liquid (water) content of the porous material. The thermal conductivity k should also be a function of water content, which changes locally as drying proceeds. At the boundary of a porous structure and air flow, that is, the convective boundary condition at $x = x_s$ (see Figure 1.29) for vapour transfer, diffusive transport of vapour is balanced by the convective transport of vapour into the air stream at the boundary.

If the drying is symmetrical, $x = 0$ is chosen as the symmetry and $x = x_s$ is the convection boundary. At $x = 0$, the boundary condition is the 'impermeable and adiabatic' one:

$$\left. \frac{\partial C_l}{\partial x} \right|_s = 0 \quad (1.107)$$

$$\left. \frac{\partial C_v}{\partial x} \right|_s = 0 \quad (1.108)$$

$$\left. \frac{\partial T}{\partial x} \right|_s = 0 \quad (1.109)$$

The vapour concentration at the boundary can be determined by balancing the diffusive water vapour transfer (in the porous structure side at the boundary) with the convective vapour transfer. It is, therefore, not necessary to assume the equilibrium relationship between the water vapour at the boundary and the liquid water content at the boundary. In summary, the

boundary conditions at $x = x_s$ may be written as follows:

$$-D_l \cdot \left. \frac{\partial C_l}{\partial x} \right|_s = 0 \quad (1.110)$$

$$-D_v \cdot \left. \frac{\partial C_v}{\partial x} \right|_s = h_m \cdot (\rho_{v,s} - \rho_{v,\infty}) \quad (1.111)$$

$$k \cdot \left. \frac{\partial T}{\partial x} \right|_s = h \cdot (T_\infty - T_s) - (\Delta H_L + C_{pv} \cdot (T_\infty - T_s)) \cdot h_m \cdot (\rho_{v,s} - \rho_{v,\infty}) \quad (1.112)$$

or

$$k \cdot \left. \frac{\partial T}{\partial x} \right|_s \approx h \cdot (T_\infty - T_s) - \Delta H_L \cdot h_m \cdot (\rho_{v,s} - \rho_{v,\infty}) \quad (1.113)$$

Equation (1.113) is different from equation (1.112) as the enthalpy term $C_{pv} \cdot (T_\infty - T_s)$ is usually significantly smaller than the latent heat of evaporation, especially when the temperature difference is not large. The relationship between the vapour concentration at the interface but on the side of the solid (i.e. $C_{v,s}$) and the vapour concentration at the interface but in the gas (i.e. $\rho_{v,s}$) may be expressed as $C_{v,s} \approx \varepsilon_s \cdot \rho_{v,s}$. ε_s is the porosity at the surface of the porous material, which may be approximated to be the same as that of the bulk material). In this model, $D_{eff,v}$ may well be explained using equation (1.23), where the porosity depends on water content.

This set of model equations have turned out to be unreasonable as if one integrates equation (1.104) from the centre (symmetry) to the boundary (which should satisfy equation (1.110)), the rate of change of the mean liquid water concentration would be zero, thus no drying apparently occurs. This means that the physics based model of drying with diffusion as the fundamental mechanism should really have a source term, as pointed out by Zhang and Datta (2004), and indeed shown to be useful by Chong and Chen (1999).

On the other hand, in order to make the liquid diffusion (only) model work, one can see that the boundary condition (1.110) needs to be ‘balanced’ by the boundary condition (1.111).

$$-D_{eff,l} \cdot \left. \frac{\partial C_l}{\partial x} \right|_s = h_m \cdot (\rho_{v,s} - \rho_{v,\infty}) \quad (1.114)$$

With this, equation (1.105) is no longer used.

There needs to be an established relationship between the surface water concentration and the surface vapour concentration. This is often assumed to take the equilibrium (isotherm) relationship, that is, fundamentally $\rho_{v,s}$ is equal to the surface relative humidity RH_s multiplied by the saturated surface vapour concentration $\rho_{v,sat}$ at the surface temperature T_s . The equilibrium isotherm for RH_s is a function of equilibrium water content and temperature, which can most often be correlated nicely using the GAB model.

To this end, equation (1.114) implies that the water evaporates ‘only’ at the surface. The thermal impact of evaporation is also the largest at the boundary according to equation ((1.112) or (1.113)). This may not predict precisely the liquid distribution within the material.

As the pore spaces are freed up within the materials as drying proceeds, the evaporation would be occurring locally more and more. Assuming the local rate of evaporation \dot{E}_v is

positive when liquid is converted into vapour, the set of governing equations should be modified to become:

$$\frac{\partial C_l}{\partial t} = \frac{\partial}{\partial x} \left(D_{eff,l} \cdot \frac{\partial C_l}{\partial x} \right) - \dot{E}_v \int_0^{x_s} \frac{\partial C_l}{\partial t} \cdot dx \quad (1.115)$$

$$\frac{\partial C_v}{\partial t} = \frac{\partial}{\partial x} \left(D_{eff,v} \cdot \frac{\partial C_v}{\partial x} \right) + \dot{E}_v \quad (1.116)$$

$$\frac{\partial T}{\partial t} = \frac{1}{\rho C_p} \cdot \frac{\partial}{\partial x} \left(k \cdot \frac{\partial T}{\partial x} \right) - \frac{\Delta H_L}{\rho C_p} \cdot \dot{E}_v \quad (1.117)$$

Integration of equation (1.115) from $x = 0$ to $x = x_s$ (half thickness of a symmetrically dried slab) gives:

$$\frac{d\bar{C}_l}{dt} = - \frac{\int_0^{x_s} \dot{E}_v \cdot dx}{x_s} \quad (1.118)$$

This is the rate of average change in water content during drying, which would be conventionally measured through recording the weight loss over time (i.e. $V \cdot d\bar{C}_l/dt$ where V is the volume of the material). Integration of equation (1.116) along the thickness also, gives:

$$\frac{d\bar{C}_v}{dt} = \frac{D_{eff,v}}{x_s} \cdot \frac{\partial C_v}{\partial x} \Big|_{x_s} + \frac{\int_0^{x_s} \dot{E}_v \cdot dx}{x_s} \quad (1.119)$$

It is known that the vapour diffusion at the boundary should be balanced by the convective vapour transfer:

$$-D_{eff,v} \cdot \frac{\partial C_v}{\partial x} \Big|_{x_s} = h_m \cdot (\rho_{v,s} - \rho_{v,\infty}) \quad (1.120)$$

Equation (1.119) can then be re-written as:

$$\frac{d\bar{C}_v}{dt} = - \frac{h_m}{x_s} \cdot (\rho_{v,s} - \rho_{v,\infty}) + \frac{\int_0^{x_s} \dot{E}_v \cdot dx}{x_s} \quad (1.121)$$

For simplicity, one may assume zero rate of accumulation of water vapour inside the porous structure so one can arrive at a familiar outcome:

$$\frac{m_s}{2 \cdot A} \cdot \frac{d\bar{X}}{dt} = - \int_0^{x_s} \dot{E}_v \cdot dx \approx -h_m \cdot (\rho_{v,s} - \rho_{v,\infty}) \quad (1.122)$$

where m_s is the dry mass of the slab and A is the surface area on one side of the slab (in this case, it may be taken as a unit area 1 m^2).

Based on equation (1.122), the record of weight loss during drying, with the known h_m (which may be obtained using the established mass transfer correlation involving the *Reynolds* number (Re) and *Schmidt* number (Sc), that is, a *Sherwood* number (Sh) correlation), one can work out the surface vapour concentration as a function of time.

One may also be able to work out the average local rate of drying from the weight loss curve, as illustrated in equation (1.122). It is not yet fully understood how one may establish the local rate of evaporation (i.e. the source term) precisely. Modern instruments including MRI can only show the residual water content level (profile) without showing the direction of the liquid flow. As such, they cannot help us to establish whether local evaporation is one of the most important phenomena and whether liquid water is just depleted from the porous material.

It is better to view the effective liquid diffusivity purely as a fitting parameter, called a ‘liquid depletion coefficient’ so to remove the physical meaning relating to Fickian diffusion. This may help avoid certain confusions.

If the porous system is the packed moist porous solid particles, a local evaporation (and condensation) term can be approximated around each particle (for similar pressure and uniform particle size) (Chong and Chen, 1999):

$$-\rho_{sp} \cdot \frac{dX}{dt} = h_{eff,m} \cdot n_p \cdot \frac{A_p}{V_p} \cdot (\rho_{v,s} - \rho_{v,voids}) \quad (1.123)$$

ρ_{sp} is the concentration of the solid mass of the particle (kg m^{-3}) and X is the water content of the particle phase on dry basis (kg kg^{-1}), n_p is the number concentration of the particles (1 m^{-3}), A_p is the surface area of each particle (m^2) and V_p is the particle volume (m^3). $h_{eff,m}$ is an effective mass transfer coefficient (m s^{-1}). The surface vapour concentration can be expressed as a function of the mean temperature and mean water contents of the small packed particles, which can be established experimentally.

1.6 DRIERS

There are numerous methods or processes to dry food materials and their merits can be judged by energy efficiency, time to dry, product quality achieved etc. depending on the market requirement. A balance among these factors is often required to achieve the economic aim of the manufacturing procedures while ensuring safe and tasty foods are delivered to the consumers. Drying is achieved by supplying heat to the material and extracting water vapour out of the material. The technologies of drying may be classified based on either the mechanisms of heating or the mechanism of vapour transport.

In general, the processes may be divided in two large groups: *in-gas* (air, nitrogen etc.) or *in-vacuum*. Drying-in-air processes can also be generalised to those where a gas medium other than air as the fundamental theory would be similar. Air drying usually requires high temperature air, which not only supplies heat to the material but also carries the vapour away from the material. Vacuum is useful in removing the water vapour when the products would be better off processed without the air and also when relatively low temperatures are preferred. Vacuum drying is perhaps more useful for preserving micro-organisms than destroying them. Microwave heating is used to ensure the heat is absorbed within the material (primarily by water) so the drying can be done more efficiently.

When the temperature gradient is in the same direction of the moisture concentration gradient, heat and moisture transfer go along the same direction (see Figure 1.30). This process may be called a ‘Synergistic Drying Process’ (discussed in 2004 at Partsee-4 Conference; X.D. Chen; unpublished power-point presentation). This may be beneficial from an energy transfer viewpoint as for food materials the higher the water content, the higher the thermal conductivity. The interface temperature (at the material–air interface for example)

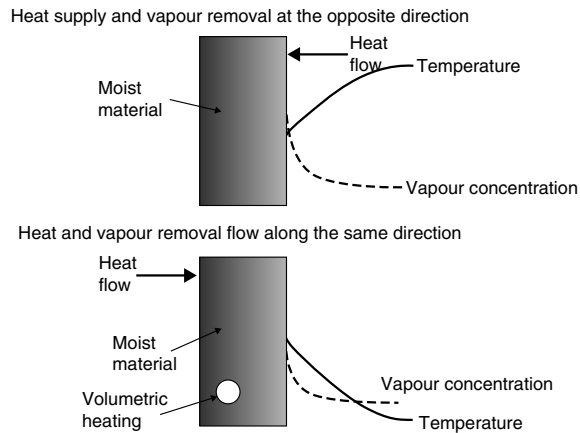


Fig. 1.30 An illustration of the concept of synergistic drying.

would not be too high, so the interfacial properties may be quite different from when the two transfer processes are going opposite ways. Microwave heating-drying may be viewed as a synergistic drying operation. A spouted-bed operation may also be viewed as a synergistic drying operation, as the spouts would be heated up and, when the material dried peels off from the hot solid spheres, new material will be dried in a synergistic way.

This idea may provide a *rule of thumb* for designing more efficient drying and, at the same time, understanding the implication of the drying setup on product property.

Any equipment that can provide a drying medium (usually hot gas) with temperature and humidity combinations that possess drying power (i.e. the vapour pressure at the product surface has to be higher than that of the drying medium), can be called driers. A large number of devices are manufactured today to achieve the basic water removal requirement. All typical driers can be found in Mujumdar's industrial drying handbook (2005) or Kudra and Strumillo (1998). In this book, the detailed geometries of these driers are not described as can be found in so many books.

Some driers consume large quantities of energy, and usually the energy required by a drying system for every kilogram of water removed is the practical criteria, benchmarked against the latent heat required for water evaporation. The heat pump principle is employed for the processes of moderate drying rates to recover the heat and for dehumidification. For large capacity operations, tonnes of liquid water removed from liquid concentrates, spray drying devices are required. Single stage spray drying is very energy hungry as it is not at all easy to recover the lower temperature energy in the warm air coming out of the spray drier. Incorporation of internal and external fluidised beds into a spray drying technology is now common as it improves the overall energy consumption.

In the pressure driven devices, on the other hand, such as the vacuum drier and vacuum freeze drier, there is higher initial capital investment, while the energy required for running the devices can be much lower than that of a straight evaporative process. Here, the pressure of vapour surrounding the material being dried is lowered by the vacuum and lower temperatures.

1.7 CONCLUDING REMARKS

In this chapter, some key elements of the drying of foods have been discussed in an intuitive manner. The rigorous treatment, usually mathematical by nature, can be found elsewhere in

the literature and has not been described in detail. There are numerous models of drying, and mechanisms proposed for water transport vary from study to study. The diffusion based transport, as described in this chapter, is a typical model and is perhaps the most common. The arguments provided here do not rule out other realistic mechanisms and the general trends proposed based on the diffusion mechanisms are expected to be reasonable.

What needs be further highlighted, and hopefully illustrated somewhat in this study, is that the drying of foods cannot be considered as a single, isolated unit operation by the practitioners in the food industry and food engineering researchers/technologists due to its inter-connectivity with what happened before drying (pre-drying operations) and after drying (post-drying operations). What has happened during drying in terms of the micro-structure of the food material being dried, bioactivity and appearance, is intimately related to the water removal. The spatial distribution of the water content and temperature distribution within the product being dried play key roles in determining the product quality. The analyses given in this chapter may help to understand the qualitative trends in these distributions and their likely influences on quality (surface quality and bulk quality). Though many who are working in the food industry do not have the necessary mathematical/engineering backgrounds to deal with the differential equations that govern drying, the basic concepts discussed in this chapter may not be too difficult to handle for practical purposes.

1.8 NOTATION

X	water content on dry basis, kg kg^{-1}
\bar{X}	average or mean water content on dry basis, kg kg^{-1}
N_v''	drying rate for constant drying-rate period, $\text{kg m}^{-2} \text{s}^{-1}$
\dot{m}_v	mass flow of water vapour, kg s^{-1}
\dot{E}_v	internal local evaporation rate, $\text{kg m}^{-3} \text{s}^{-1}$
\dot{S}_v	rate of surface evaporation, $\text{kg m}^{-2} \text{s}^{-1}$
ΔH_L	latent heat of water vaporisation, J kg^{-1}
A_p	surface area of single droplet or particle, m^2
b or x_s	half-thickness of the slab, m
B	Spalding number, Antoine equation coefficient
Bi	<i>Biot</i> number (for heat transfer $Bi = hL/k$ or for mass transfer $Bi_m = h_m L/D$)
Bi^*	modified <i>Biot</i> number
C	GAB equation parameter, Antoine equation coefficient or concentration, kg m^{-3}
C_0	GAB equation coefficient
C_p or c_p	specific heat capacity, $\text{J kg}^{-1} \text{K}^{-1}$
D	diffusivity, $\text{m}^2 \text{s}^{-1}$
d_p	diameter of droplet or particle, m
D_v	vapour-in-air diffusivity, $\text{m}^2 \text{s}^{-1}$
E	activation energy, J mol^{-1}
f	relative drying rate
g	gravitational acceleration, m s^{-2}
h	heat transfer coefficient, $\text{W m}^{-2} \text{K}^{-1}$, or distance from the tip of the atomiser (drier height), m

h_m	mass transfer coefficient, m s^{-1}
k	thermal conductivity, $\text{W m}^{-1} \text{K}^{-1}$
L	thickness of the material, m
M	molecular weight, g mol^{-1}
m_s	mass of solids, kg
n	number concentration of the particles, l m^{-3}
Nu	<i>Nusselt</i> number ($Nu = hL/k$) (k here is that of the fluid, thus differing from that for <i>Biot</i> number calculation)
N_v	drying rate, $\text{kg m}^{-2} \text{s}^{-1}$
Pr	<i>Prandtl</i> number ($Pr = \nu/\alpha$, where ν is the kinematic viscosity, $\text{m}^2 \text{s}^{-1}$)
Q	convective heat flow, J
q	heat flux, W m^{-2}
R	ideal gas law constant
Re	<i>Reynolds</i> number ($Re = \rho uL/\mu$)
RH	relative humidity
Sc	<i>Schmidt</i> number ($Sc = \nu/D$)
Sh	<i>Sherwood</i> number ($Sh = h_mL/D$) (D here is that in the fluid, thus differing from that for <i>Biot</i> number for mass transfer calculation)
T	temperature, K
t	time, s
T_{sat}	adiabatic saturation temperature of drying air, K
T_{wb}	wet-bulb temperature of drying air, K
u	velocity, m s^{-1}
V	volume, m^3
x	distance or x -coordinate, m
X_{cr}	critical moisture content on dry basis, kg kg^{-1}
X_e	equilibrium moisture content on dry basis, kg kg^{-1}
Y	air humidity, kg kg^{-1}

Symbols

ρ	density, kg m^{-3}
ϕ	volume fraction
μ	dynamic viscosity, Pa s
ϵ	porosity, or
φ	relative humidity ($=RH$)
δ	thickness, m
τ	tortuosity
μ	viscosity, Pa s
ρ_v	vapour concentration, kg m^{-3}

Subscripts

∞	bulk, surrounding or equilibrium
1,2	surface 1 and surface 2
a	ambient condition
<i>air</i>	air properties
<i>av</i>	average

<i>b</i>	bulk
<i>c</i>	characteristic parameters
<i>cond</i>	conduction
<i>conv</i>	convection
<i>cr</i>	critical conditions
<i>D</i>	drier
<i>e</i>	equilibrium or ambient conditions
<i>E</i>	exit condition
<i>eff</i>	effective
<i>l</i>	liquid
<i>L</i>	thickness
<i>m</i>	mass transfer
<i>o</i>	centre temperature or initial
<i>s</i>	solid, surface
<i>sat</i>	saturated
<i>p</i>	particle
<i>T</i>	thermal
<i>v</i>	water vapour
<i>w</i>	liquid water
<i>x</i>	space coordinate

APPENDIX I: TYPICAL MASS TRANSFER CORRELATIONS

Heat convection is a well-studied subject and is well documented in many texts. The mass transfer calculations can be done, as the first approximation, based on the heat transfer correlations. The mass transfer coefficient (h_m) is obtained from established correlations for the *Sherwood* number ($h_m \cdot L/D$) originally for the *Nusselt* number ($h \cdot L/k$). L is the characteristic length of the object (m) and k is the thermal conductivity of the bulk fluid ($\text{W m}^{-1} \text{K}^{-1}$). The two principal numbers are correlated to the *Reynolds* number ($\rho \cdot u \cdot L/\mu$), the *Prandtl* number (ν/α) or *Schmidt* number (ν/D), respectively. u is the bulk fluid velocity (m s^{-1}). ρ is the fluid density (kg m^{-3}), μ is the viscosity (Pa s) and α is the thermal diffusivity ($\text{m}^2 \text{s}^{-1}$), and D is the mass diffusivity ($\text{m}^2 \text{s}^{-1}$).

All the physical properties used in the calculations are usually determined at the film temperature ($T_f = ((T_s + T_\infty)/2)$) and film concentration ($C_f = ((C_s + C_\infty)/2)$). Table A1.1 shows the typical correlations, which may be used as the first approximation for evaluating mass transfer coefficients.

APPENDIX II: ON THE 'EFFECTIVENESS' OF THE EFFECTIVE MOISTURE DIFFUSIVITY BENCHMARKED AGAINST THE LUIKOV THEORY

Drying is a complex subject to model mathematically, there have been a number of continuum-type mechanisms proposed and the associated mathematical models established. These include liquid diffusion – as mentioned earlier in this chapter (Lewis, 1921) (thus equation (1.95) is used), – capillary flow (Buckingham, 1907), evaporation–condensation

Table A1.1 Commonly used mass transfer correlations for average Sherwood number calculations (modified from Incropera and De Witt, 2002).

Configuration	Geometry	Conditions	Correlation
External flow (<i>forced convection</i>)	Flat plate	Laminar, $0.6 \leq Pr \leq 50$, L – length of the plate (m)	$\overline{Sh}_L = 0.664 Re_L^{1/2} Sc^{1/3}$
		Mixed, $Re_{L,c} = 5 \times 10^5$, $Re_L \leq 10^8$, $0.6 \leq Pr \leq 50$, L – length of the plate (m)	$\overline{Sh}_L = (0.037 Re_L^{4/5} - 871) Sc^{1/3}$
	Cylinder (pipe or tube)	$Re_L Pr > 0.2$, L – diameter ($L = d$)	$\overline{Sh}_L = 0.3 +$ $\left[0.62 Re_L^{1/2} Sc^{1/3} \times \left[1 + \left(\frac{0.4}{Sc} \right)^{2/3} \right]^{-1/4} \right]$ $\times \left[1 + \left(\frac{Re_L}{282,000} \right)^{5/8} \right]^{4/5}$
		Sphere	L – diameter ($L = d$)
External flow (<i>natural convection</i>)	Vertical plate	L – length of the plate	$\overline{Sh}_L = \left\{ 0.825 + \frac{0.387 Ra_L^{1/6}}{[1 + (0.492/Sc)^{9/16}]^{8/27}} \right\}^2$
	Cylinder (pipe or tube)	$L = d$ (diameter), $Ra_L \leq 10^{12}$	$\overline{Sh}_L = \left\{ 0.60 + \frac{0.387 Ra_L^{1/6}}{[1 + (0.559/Sc)^{9/16}]^{8/27}} \right\}^2$
	Sphere	$L = d$ (diameter), $Pr \geq 0.7$, $Ra_L \leq 10^{11}$	$\overline{Sh}_L = 2 + \frac{0.589 Ra_L^{1/6}}{[1 + (0.469/Sc)^{9/16}]^{4/9}}$

Continued

Table A1.1 Continued.

Configuration	Geometry	Conditions	Correlation
Internal flow (<i>forced convection</i>)	Laminar	Fully developed, uniform wall heat flux, $Pr \geq 0.6$, $L = 4A_c/P$ (hydraulic diameter), A_c – flow cross-sectional area, P – wetted perimeter	$\overline{Sh}_L = 4.36$
		Fully developed, uniform wall temperature, $Pr \geq 0.6$	$\overline{Sh}_L = 3.66$
Internal flow (<i>natural convection</i>)	Horizontal cavity heated from below	Turbulent, fully developed, $0.6 \leq Pr \leq 16\,700$, Length/diameter ≥ 10 , $Re_L \geq 10\,000$, μ_s – viscosity at wall	$\overline{Sh}_L = 0.027 Re_L^{4/5} Sc^{1/3} \left(\frac{\mu}{\mu_s}\right)^{0.14}$
		$Ra_L = \frac{g\beta(T_1 - T_2)L^3}{\alpha\nu} > 1708$	$\overline{Sh}_L = 0.069 Re_L^{1/3} Sc^{0.074}$
Combined natural and forced convection	Vertical cavity heated from one side and cooled at the other	T_1 – the bottom surface temperature, T_2 – the upper surface temperature, β – thermal expansion coefficient ($\approx 1/T_f$), L – distance between two horizontal walls, $3 \times 10^5 Ra_L \geq 7 \times 10^9$	$\overline{Sh}_L = 0.22 \left(\frac{Sc}{0.2 + Sc} Ra_L\right)^{0.28} \left(\frac{H}{L}\right)^{-0.25}$
		$2 < H/L < 10$, $Pr < 10^5$, $10^3 \leq Ra_L \leq 10^{10}$, H – height of the cavity, L – distance between two vertical walls	$\overline{Sh}_L^n = \overline{Sh}_{forced}^n \pm \overline{Sh}_{natural}^n$
		n is often quoted to be 3, though 7/2 and 4 are better for transverse flows (i.e. two effects are 'opposite to each other' and the sign in the correction is '-')	

(Henry, 1939), dual (temperature, water content gradient) and triple (temperature, water content and pressure gradient) driving force mechanisms by Luikov (1986), another dual driving force mechanism by Philip and De Vries (1957) and De Vries (1958), dual phase (liquid and vapour) transfer mechanism of Krischer as summarised by Fortes and Okos (1980). Whitaker (1977, 1999) has proposed detailed transport equations to account for the macro- and micro-scale structures in biological materials. Three phase (solid, vapour and liquid) conservations and their local volume-averaged behaviours are considered. The mechanisms for moisture transfer are largely the same as that proposed by Luikov (1975), Philip and De Vries (1957), except that the small-scale phenomena (local pores, pore channels, shells, voids etc.) have been taken into account. This theory is based on a known distribution of the macro-scale and micro-scale unit structures which allow local volume-averaging to be carried out (Liu and Yang, 2005).

The more modern approach is that of the pore-network model (which can include a number of scale levels), which is, however, still in the development phase and has not been rigorously and experimentally validated (Nowicki, 1992; Prat, 1993). In addition, the detailed pore structure and network (geometries and distribution) is actually very difficult to establish quantitatively for a real material, which may hinder the applicability of the model approach to food or bio-product drying. Besides the liquid diffusion mechanism considered as the single driving force for drying, the above approaches all involve complicated mathematics (partial differential equation sets and numerical schemes for gaining a stable solution) and some model coefficients which cannot be individually determined. Because the numerous coefficients need to be considered, accurately modelling the single trend of the overall water loss during drying is generally possible with these models. However, the practical significance of the detailed physics associated with these models becomes minimal if only such simple trends are of the practical interest.

The above-mentioned models might all be helpful when spatial distributions of both the water content and temperature are required. As more information is required about the product surface and core during drying, so the differential changes of colour, bio-activity and stress etc. between the surface and the core can be determined. These models might eventually become popular, especially if commercial software was developed for researchers to more easily manipulate and run. On the other hand, as a compromise, liquid water diffusion is the model that has been used most extensively and which has had a mixture of success in both the overall trend modelling and local profile predictions. It is the simplest approach among the models mentioned earlier.

Taking Luikov's theory as an example (1975), which is based on the 'irreversible thermodynamics' principles, it considers that the temperature and pressure gradient within the porous material being dried also impact on the moisture (liquid) transfer. This is to show how an effective diffusivity might have to be formulated when the drying mechanisms are complex. In mathematical terms, the following are the set of PDEs that govern the moisture transport process (Irudayaraj *et al.*, 1990, 1992, 1999):

$$\frac{\partial T}{\partial t} = K_{11} \nabla^2 T + K_{12} \nabla^2 X + K_{13} \nabla^2 P \quad (\text{A1})$$

$$\frac{\partial X}{\partial t} = K_{21} \nabla^2 T + K_{22} \nabla^2 X + K_{23} \nabla^2 P \quad (\text{A2})$$

$$\frac{\partial P}{\partial t} = K_{31} \nabla^2 T + K_{32} \nabla^2 X + K_{33} \nabla^2 P \quad (\text{A3})$$

For one dimensional situation, that is, along the x -coordinate in the *Cartesian* coordinate system, equation (1.5) can be rewritten as:

$$\frac{\partial X}{\partial t} = K_{21} \frac{\partial^2 T}{\partial x^2} + K_{22} \frac{\partial^2 X}{\partial x^2} + K_{23} \frac{\partial^2 P}{\partial x^2} \quad (\text{A4})$$

One may further rewrite equation (A4) to the following to elucidate the complexity of the effective liquid water diffusivity (the one defined in equation (1.3)) if such mechanisms are followed:

$$\begin{aligned} \frac{\partial X}{\partial t} &= \frac{\partial}{\partial x} \left(K_{21} \frac{\partial T}{\partial x} + K_{22} \frac{\partial X}{\partial x} + K_{23} \frac{\partial P}{\partial x} \right) \\ &= \frac{\partial}{\partial x} \left(K_{21} \frac{\partial T}{\partial X} \cdot \frac{\partial X}{\partial x} + K_{22} \frac{\partial X}{\partial x} + K_{23} \frac{\partial P}{\partial X} \cdot \frac{\partial X}{\partial x} \right) \\ &= \frac{\partial}{\partial x} \left[\left(K_{21} \frac{\partial T}{\partial X} + K_{22} + K_{23} \frac{\partial P}{\partial X} \right) \cdot \frac{\partial X}{\partial x} \right] \end{aligned} \quad (\text{A5})$$

Here, these coupling coefficients (positive in general) may be taken as constants for the system of concern. One can see that the effective diffusivity $D_{eff,l}$ (in equation (1.95)) if it was used to laterally replace equation (A5), would be at least a function that represents the interactions between water content and temperature and pressure. It has been found experimentally that the coupling coefficients are temperature and water content dependent.

$$D_{eff,l} = K_{21} \frac{\partial T}{\partial X} + K_{22} + K_{23} \frac{\partial P}{\partial X} \quad (\text{A6})$$

For simplicity, assuming the effect of pressure and the effect of temperature can both be neglected, equation (A5) reduces to:

$$D_{eff,l} \approx K_{22} \quad (\text{A7})$$

Since it is a common sense that X should be reduced if T is elevated, this general trend may be qualitatively described with an exponential function or an inverse power function:

$$X \propto \exp\left(-\frac{E}{RT}\right) \quad \text{or} \quad \frac{1}{T^n} \quad (\text{A8})$$

n is the power constant, which may be a function of water content. In the first approximation, E may also be a function of water content:

$$E = E(X) \quad (\text{A9})$$

Here, it is expected that as X increases, the difficulty in removing water becomes smaller thus the activation energy would be lower.

Taking the exponential function as an example, the first derivative of temperature against water content in equation (A8) would be as follows:

$$\frac{\partial T}{\partial X} \propto -\frac{RT^2}{E} \exp\left(-\frac{E}{RT}\right) + \frac{T}{E} \frac{dE}{dX} \quad (\text{A10})$$

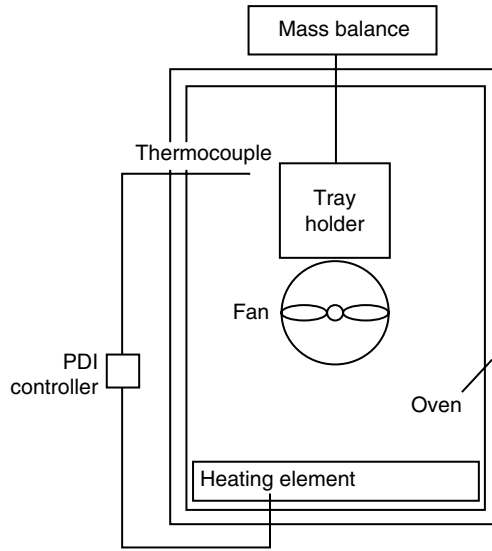


Fig. A1.1 Schematic diagram of the oven drying set up (Chen and Pirini 2004).

Based on the above expectation, dE/dX is negative. Without the influence of pressure, the effective diffusivity may then be expressed in the following form:

$$D_{eff,l} \approx K_{22} - K_{21} \cdot b \cdot \frac{RT^2}{E} \exp\left(-\frac{E}{RT}\right) + K_{21}b \cdot \frac{T}{E} \frac{dE}{dX} \quad (\text{A11})$$

b is a positive proportionality for equation (A10). When the temperature range is small, the above equation (A11) is expected to reduce to a simple Arrhenius form with single activation energy value (as reported in the literature many times, D is proportional to $\exp(-E/RT)$). K_{22} has to over-shadow the effects of the two other terms on the RHS of equation (A11) in any temperature range, so it has to be a more highly temperature sensitive term. The above analysis is not a ‘water-tight’ derivation procedure by any means. It has been done to show how effective a single diffusivity function has to be. The higher the liquid water content locally, the larger the effective water diffusivity, as one would normally expect. Equation (A11) is indicative of how complex this effective diffusivity is: it has to be a function of water content, which may account for the effect of pore network changes as water content changes; it has to be temperature dependent, and this temperature dependence may vary in strength at different liquid moisture content levels. It is further noted that the shrinkage effect is sometimes ‘lumped’ into this diffusivity as well. Besides water content and temperature (and pressure), pH, initial water content, velocity, shrinkage and shape have all been shown to have influences on the values of effective diffusivity determined. These may be linked to a multi-component diffusion system, how the material shrinks and the kind of mass transfer boundary defined, and the three-dimensional effect that may not be accounted for adequately in the experiments. Therefore, effective diffusivity is a ‘lumped’ parameter and its variability can be largely dependent on the drying condition and compositional variations. It may be noted that though Luikov’s model seems more fundamental, the complexity of correlating the coupling coefficients actually reduces its usefulness practically.

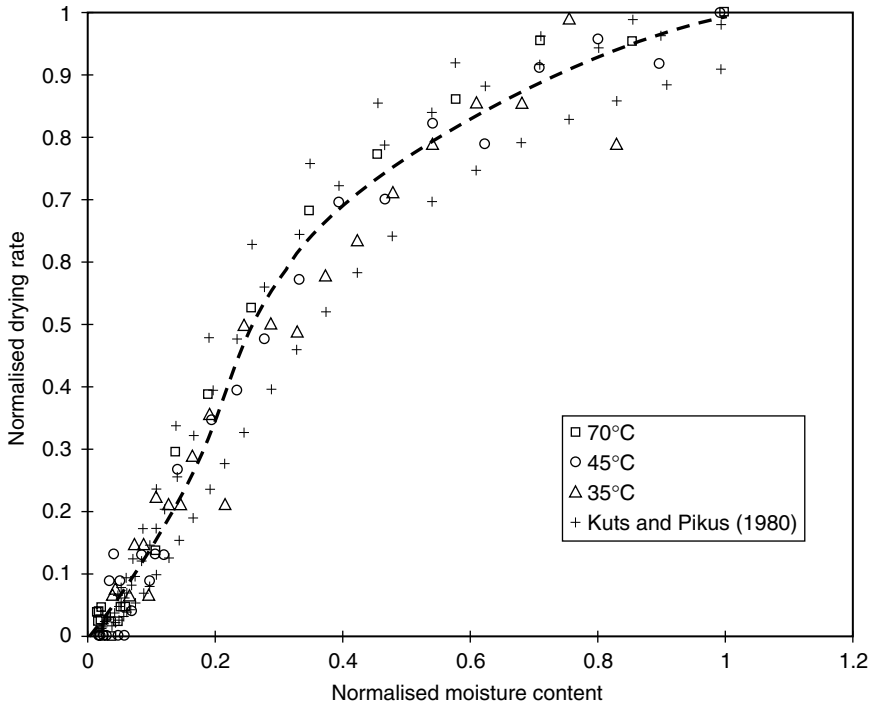


Fig. A1.2 Van Meel's method is used to normalise the drying rates according to Kuts and Pikus (1980) and the model is fitted to the data (equation (1.88)).

APPENDIX III: DRYING OF PULPED KIWI FRUIT LAYER FOR MAKING FRUIT LEATHER

In order to obtain drying kinetics, such as the van Meel model fits for the specific material of concern, an oven test or tray drying test may be conducted (a typical set up is shown in Figure A1.1). Here, the weight loss of the layer of pulped Kiwi fruit in an aluminium container specially made for these experiments is calculated (Chen *et al.*, 2001). The van Meel model has been applied through the model's of Kuts and Pikus (1980) (Figure A1.2).

REFERENCES

- Aguilera, J.M. and Stanley, D.W. (1999) *Microstructural Principles of Food Processing and Engineering*, 2nd edn. Aspen Publications, Gaithersburg, Maryland, pp. 186–250.
- Bird, R.B., Stewart, W.E. and Lightfoot, E.N. (1960 and 2002) *Transport Phenomena*, 1st and 2nd edn. John Wiley, New York.
- Buckingham, E.A. (1907) *Studies on the Movement of Soil Moisture*. US Department of Agriculture Bulletin, No. 38.
- Chen, X.D. (2005a) A discussion on a generalised correlation for drying rate modelling. *Drying Technology*, **23**, 415–426.
- Chen, X.D. (2005b) Critical *Biot* number for uniform temperature assumption in transient heat and mass transfer calculations. *International Journal of Food Engineering*, **1**(3), Article 6, 1–8.

- Chen, X.D. (2007) Drying as a means of controlling food bio-deterioration. In: *Food Bio-Deterioration* (ed. Gary Tucker). Blackwell, Oxford.
- Chen, X.D. and Patel, K.C. (2007) Micro-organism inactivation during drying of small droplets or thin-layer slabs – a critical review of existing kinetics models and an appraisal of the drying rate dependent model. *Journal of Food Engineering*, **82**, 1–10.
- Chen, X.D. and Pirini, W. (2004) The reaction engineering modelling approach to drying of thin layer of silica gel particles. In: *Topics in Heat and Mass Transfer* (eds G. Chen, S. Devahastin and B.N. Thorat). Vindhya Press, IWSID-2004, Mumbai, India, pp. 131–140.
- Chen, X.D., Chiu, Y.L., Lin, S.X.Q. and James, B.J. (2006) *In situ* ESEM examination of microstructural changes of an apple tissue sample undergoing low-pressure air-drying followed by wetting. *Drying Technology*, **24**, 965–972.
- Chen, X.D., Pirini, W. and Ozilgen, M. (2001) The reaction engineering approach to modelling drying of thin layer of pulped Kiwifruit flesh under conditions of small *Biot* numbers. *Chemical Engineering and Processing*, **40**, 311–320.
- Choi, Y. and Okos, M.R. (1986) Effects of temperature and composition on the thermal properties of foods. In: *Food Engineering and Process Applications, Vol. 1, Transport Phenomena* (eds M. Le Maguer and P. Jelen). Applied Science Publishers, Elsevier, London, pp. 93–101.
- Chong, L.V. and Chen, X.D. (1999) A mathematical model of self-heating of spray dried food powders containing fat, protein, sugar and moisture. *Chemical Engineering Science*, **54**, 4165–4178.
- Crank, J. (1975) *The Mathematics of Diffusion*, 2nd edn. Clarendon Press, Oxford.
- De Vries, D.A. (1958) Simultaneous transfer of heat and moisture transfer in porous media. *Transactions of the American Geophysics Union*, **39**(5), 909–916.
- Ferrari, G., Meerdink, G. and Walstra, P. (1989) Drying kinetics for a single droplet of skim milk. *Journal of Food Engineering*, **10**, 215–230.
- Fortes, M. and Okos, R. (1980) Drying theories: Their bases and limitations applied to food and grain. *Advances in Drying*, **1**, 119–154.
- Goula, A.M., Adamopoulos, K.G., Chatzidakis, P.C. and Nikas, V.A. (2006) Prediction of lycopene degradation during a drying process of tomato pulp. *Journal of Food Engineering*, **74**, 37–46.
- Henry, P.S.H. (1939) Diffusion in absorbing media. *Proceedings of Royal Society London*, **171A**, 215–241.
- Holdsworth, S.D. (1971) Applicability of rheological models to the interpretation of flow and processing behaviour of fluid food products. *Journal of Texture Studies*, **2**, 393–418.
- Incropera, F.P. and DeWitt, D.P. (2002) *Fundamentals of Heat and Mass Transfer*, 4th and 5th edn. John Wiley & Sons, New York.
- Irudayaraj, J., Haghighi, K. and Stroshine, R.L. (1992) Finite element analysis of drying with application to cereal grains. *Journal of Agricultural Engineering Research*, **53**(4), 209–229.
- Irudayaraj, J., Haghighi, K. and Stroshine, R.L. (1990) Nonlinear finite element analysis of coupled heat and mass transfer problems with an application to timber drying. *Drying Technology*, **8**(4), 731–749.
- Irudayaraj, J. and Wu, Y. (1999) Heat and mass transfer coefficients in drying of starch based systems. *Journal of Food Science*, **64**(2), 323–327.
- Karim, Md. A. and Hawlader, M.N.A. (2005) Drying characteristics of banana: Theoretical modelling and experimental validation. *Journal of Food Engineering*, **70**, 35–45.
- Kaur, D., Sogi, D.S. and Wani, A.A. (2006) Degradation kinetics of lycopene and visual color in tomato peel isolated from pomace. *International Journal of Food Properties*, **9**, 781–789.
- Keey, R.B. (1992) *Drying of Loose and Particulate Materials*. Hemisphere Publishing Corporation, New York.
- Kudra, T. and Mujumdar, A.S. (2002) *Advanced Drying Technologies*. Marcel Dekker Inc., New York.
- Kudra, T. and Strumillo, C. (eds) (1998) *Thermal Processing of Bio-Materials*. Gordon and Breach Science Publishers, Amsterdam.
- Kuts, P.S. and Pikus, I.F. (1980) Independence between heat and mass transfer in drying. In: *Drying'80, Vol. 1*, (ed. A.S. Mujumdar). Hemisphere, Washington, D.C., pp. 65–79.
- Lewis, W.K. (1921) The rate of drying of solid materials. *Industrial and Engineering Chemistry*, **13**, 427–432.
- Li, L.T. (1998) *Food Properties*. China Agriculture Publisher, Beijing (in Chinese).
- Liu, X.D. and Yang, B. (2005) Review and vista on drying theories of porous medium. *Journal of China Agricultural University* **10**(4), 81–92 (in Chinese).

- Luikov, A.V. (1986) *Drying Theory*. Energia, Moscow.
- Luikov, A.V. (1975) *Heat and Mass Transfer in Capillary-Porous Bodies*. Pergamon Press, Oxford.
- May, B.K. and Perré, P. (2002) The importance of considering exchange surface area reduction to exhibit a constant drying flux period in foodstuffs. *Journal of Food Engineering*, **54**(4), 271–282.
- Mayor, L. and Sereno, A.M. (2004) Modelling shrinkage during convective drying of food materials: A review. *Journal of Food Engineering*, **61**, 373–386.
- Mujumdar, A.S. (2005) *Handbook of Industrial Drying*. CRC Press, Taylor and Francis, New York.
- Nowicki, S.C., Davis, H.T. and Scriven, L.E. (1992) Microscopic determination of transport parameters in drying porous media. *Drying Technology*, **10**(4), 925–946.
- Page, G.E. (1949) Factors influencing the maximum rates of air drying shelled corn in thin layers. *MS Thesis*, Department of Mechanical Engineering, Purdue University.
- Parker, R. (2003) *Introduction to Food Science*. Delmer, New York.
- Philip, J.R. and De Vries, D.A. (1957) Moisture movement in porous materials under temperature gradients. *Trans A Geophys Union*, **38**(5), 222–232, 594.
- Ponsart, G., Vasseur, J., Frias, J.M., Duquenoy, A. and Meot, J.M. (2003) Modelling of stress due to shrinkage during drying of spaghetti. *Journal of Food Engineering*, **57**, 277–285.
- Prat, M. (1993) Percolation model of drying under isothermal conditions in porous media. *International Journal of Multi-Phase Flow*, **19**, 691–704.
- Purlis, E. and Salvadori, V. O. (2007) Bread browning kinetics during baking. *Journal of Food Engineering*, **80**, 1107–1115.
- Rahman, M.S. (1995) *Food Properties Handbook*. CRC Press, New York.
- Rahman, M.S., Perera, C.O., Chen, X.D., Driscoll, R.H. and Potluri, P.L. (1996) Density, shrinkage and porosity of Calamari Mantle meat during air drying in a cabinet dryer as a function of water content. *Journal of Food Engineering*, **30**, 135–145.
- Rao, M.A. (1977) Rheology of liquid foods. *Journal of Texture Studies*, **8**, 135–168.
- Rao, M.A., Cooley, H.J. and Vitali, A.A. (1984) Flow properties of concentrated juices at low temperatures. *Food Technology*, **38**(3), 113–119.
- Roos, Y.H. (2002) Importance of glass-transition and water activity to spray drying and stability of dairy powders. *Lait*, **82**, 475–484.
- Rigby, S.P. (2005) Predicting surface diffusivities of molecules from equilibrium adsorption isotherms. *Colloids and Surfaces A: Physicochemical and Engineering Aspects*, **262**, 139–149.
- Sablani S., Rahman, S. and Al-Habsi, N. (2000) Moisture diffusivity in foods an overview. Chapter 2. In: *Drying Technology in Agriculture and Food Sciences* (ed. A.S. Mujumdar). Science Publishers, Enfield, NH, USA, pp. 35–59.
- Sikiatden, J. and Roberts, J.S. (2006) Measuring moisture diffusivity of potato and carrot (cor and cortex) during convective hot air and isothermal drying. *Journal of Food Engineering*, **74**, 143–152.
- Singh, R.P. and Heldman, D.R. (1993) *Introduction to Food Engineering*, 2nd edn. Academic Press, Amsterdam.
- Telis, V.R.N., Telis-Romero, J., Mazzotti, H.B. and Gabas, A.L. (2007) Viscosity of aqueous carbohydrate solutions at different temperatures and concentrations. *International Journal of Food Properties*, **10**, 185–195.
- van der Sman, R.G.M. (2003) Simple model for estimating heat and mass transfer in regular-shaped foods. *Journal of Food Engineering*, **60**, 383–390.
- van Meel, D.A. (1958) Adiabatic convection batch drying with recirculation of air. *Chemical Engineering Science*, **9**, 36–44.
- Wang, N. and Brennan, J.G. (1995) Changes in structure, density and porosity of potato during dehydration. *Journal of Food Engineering*, **24**, 61–76.
- Whitaker, S. (1977) Simultaneous heat, mass and momentum transfer in porous media. A theory of drying. *Advances in Heat Transfer*, **13**, 119–203. Academic Press, New York.
- Whitaker, S. (1999) *The Method of Volume Averaging*. Kluwer, Academic Publishers, Dordrecht, Boston, London.
- Zhang, J. and Datta, A.K. (2004) Some considerations in modelling of moisture transport in heating of hygroscopic materials. *Drying Technology*, **22**(8), 1983–2008.

2 Water activity in food processing and preservation

Bhesh R. Bhandari and Benu P. Adhikari

2.1 INTRODUCTION

Water activity (a_w) is the quantification of the extent of water that is either available or unavailable for hydration interactions, microbial growth and chemical and enzymatic reactions. When water interacts with solutes it is not wholly available for these interactions. Water activity is an equilibrium property of a system in any phase that contains water, and is defined as a ratio of vapour pressure of that system over the vapour pressure of pure water at the same temperature. This means that a_w is equal to the equilibrium relative humidity (ERH) when expressed as a fraction of 100. Hence, an a_w value of 'unity' indicates that 100% of the water is available where as a 'zero' value indicates none of it is available for microbial growth, chemical or enzymatic reactions. Therefore, water activity is a major quality parameter in the assessment of stability of foods. It is an important parameter to assess the shelf-life of packaged foods.

Although water activity is equilibrium rather than a kinetic property of a system, it nevertheless is ubiquitously used to assess the extent and potential of moisture diffusion and drying. This is one of the key boundary parameters in mathematical models representing drying behaviour.

Many desired and undesired physical changes in amorphous food and pharmaceutical powders, such as stickiness, caking, agglomeration and crystallization can be correlated to the water activity of the system through the glass-transition temperature. Since the glass-transition temperature can also be expressed as a function of a_w , all of these phenomena can be better explained through the use of a_w rather than the moisture content.

Because of the above reasons, a thorough understanding of the theory, correlating and predicting models and measurement methods and protocols is essential for researchers, technologists and practising engineers. In this chapter, Section 2.2 provides information regarding the thermodynamic, definitional aspects of water activity and hysteresis of sorption isotherms. Section 2.3 lists and describes some of the food composition-based predictive models. Worked examples are provided to illustrate their use. Section 2.4 describes the mathematical models that predict sorption isotherms of foods. Since, BET and GAB models have found wider application; various aspects of these models are dealt with in considerable detail with worked examples. Similarly, Section 2.5 discusses different types of sorption isotherms encountered in practice and their implication in storage and processing. Finally, Section 2.6 describes the methods and procedures and provides hands-on information regarding the measurement of water activity and sorption isotherms.

2.1.1 Thermodynamics of water activity

The notion of water activity or the equilibrium relative humidity is derived from the fundamental concepts of chemical potential and fugacity which are basic concepts in thermodynamics. Detailed treatment of this subject can be found in the works of Van Den Berg (1985), Ross (1975), Sahin and Sumnu (2006) and Rizvi (2005). A very brief derivation of water activity in quantitative terms is presented here. For a multi-component food system comprised of n moles, Gibbs free energy (G) defined by equation (2.1) is a function of temperature (T), pressure (P) and total number of moles (n) in the system.

$$G = f(P, T, n) \quad (2.1)$$

The chemical potential (μ_i) for a component (i), which is known as partial molar Gibbs free energy, is defined as the change in the total free energy per mole of the component (i) when the temperature, pressure and the number of moles of all the components other than (i) are kept constant. For water vapour in gaseous mixture, its chemical potential (μ_w) is given by equation (2.2).

$$\mu_w = \left(\frac{\partial G}{\partial n_w} \right) \Big|_{T, P, n'} \quad (2.2)$$

where n_w is the number of moles of water vapour and n' is the number of moles of all the components (in the gas mixture) other than that of water vapour.

Following Gibbs for a food system comprised of a solid, liquid and gaseous phase the necessary condition for equilibrium of water vapour can be given equation (2.3) or (2.4).

$$\mu_w^{Vapour} = \mu_w^{Liquid} = \mu_w^{Gas} \quad (2.3)$$

or

$$d\mu_w^{Vapour} = d\mu_w^{Liquid} = d\mu_w^{Gas} \quad (2.4)$$

the superscripts indicate the available phases in the system. If the water vapour is assumed to be an ideal gas, chemical potential can be expressed in terms of easily measurable parameters as shown in equation (2.5).

$$d\mu_w = RT \frac{dP_w}{P} \quad (2.5)$$

where P_w and P are the partial pressure of water vapour in the gas mixture and the total pressure of the system, respectively. R is the universal gas constant. However, the absolute value of chemical potential is not known and hence it has to be expressed in terms of the chemical potential of a reference state. This reference state is taken at a reference pressure which is usually 1 atmospheric pressure. Integration of equation (2.5) then yields:

$$\mu_w = \mu_w^0 + RT \ln P_w \quad (2.6)$$

where μ_w^0 is the chemical potential of water vapour at a reference pressure.

Equation (2.6) is not obeyed by water vapour if it is not considered to be ideal gas. Hence, the concept of fugacity was introduced to make this equation applicable to all pressures. In terms of fugacity, this equation is written as:

$$\mu_w = \mu_w^0 + RT \ln f_w \quad (2.7)$$

where f_w is the fugacity of water vapour in gaseous mixture. Since $f_w = \gamma_{f,w} P_w$, it can be seen from this equation that the fugacity is a correction in pressure such that the correct chemical potential can be calculated. If ($f_w^\bullet = 1 \times P_{w,sat}$) and (μ_w^\bullet) are the fugacity of pure water vapour and standard state chemical potential when the gaseous phase is completely covered by pure vapour and that it is in equilibrium with pure liquid water then, equation (2.7) becomes:

$$\mu_w^\bullet = \mu_w^0 + RT \ln f_w^\bullet \quad (2.8)$$

Equation (2.8) has to be modified to determine the chemical potential in liquid. The modification is based on equation (2.3) and Raoult's law, ($P_w = P_{w,sat} \times X_w$), $P_{w,sat}$ and X_w being saturated vapour pressure and mole fraction of water, respectively. The fugacity in equation (2.7) is replaced with 'water activity' and the reference state chemical potential is replaced with the standard state chemical potential of solution as shown in equation (2.9), below.

$$\mu_w(\text{solution}) = \mu_w^\bullet + RT \ln a_w \quad (2.9)$$

When a solid or liquid food is equilibrated to the headspace, at equilibrium, the condition set forth in equation (2.3) is obeyed. Hence, from equations (2.7) and (2.9):

$$\mu_w^0 + RT \ln f_w = \mu_w^\bullet + RT \ln a_w \quad (2.10)$$

By replacing μ_w^\bullet from equation (2.8) and simplification, the final expression of water activity is obtained.

$$a_w = \left(\frac{f_w}{f_w^\bullet} \right) \Big|_T = \left(\frac{\gamma_{f,w} \times P_w}{\gamma_{f,w} \times P_{w,sat}} \right) \Big|_T = \left(\frac{P_w}{P_{w,sat}} \right) \Big|_T \quad (2.11)$$

2.1.2 Definition and significance

Water activity (a_w) and sorption behaviour are the two most powerful concepts available for understanding and controlling the shelf-life of foods (Labuza, 1968). From equation (2.11) water activity is defined as the ratio of the vapour pressure exerted by a food sample to the vapour pressure exerted by pure water at the same temperature. a_w is the physical measure of 'active' water available in foods. This active water is responsible for the growth of spoilage bacteria, chemical reactions and enzymatic activities. Although factors such as temperature, pH and osmotic pressure and several others can influence how long the foods can be preserved, a_w is the one which influences the shelf-life the most. For example, spoilage bacteria are inhibited below a_w of 0.91 and most moulds are inhibited at a_w below 0.80. Furthermore, water activity can have a major impact on the colour, taste and aroma of foods. On the processing side, it determines the extent of moisture transfer out from the food and the amount of residual moisture of the dried food. This is an equilibrium parameter and hence has to be determined

when the food and its surroundings are completely in equilibrium. Water activity is also known as equilibrium relative humidity (ERH) (%). The relationship between ERH and a_w is given by equation (2.12).

$$a_w = \frac{\text{ERH}}{100} \Big|_T \quad (2.12)$$

2.1.3 Sorption isotherms

The sorption isotherm of a food is a plot at which the absolute water content (kg water per kg dry solid) of a food material is plotted as a function of water activity or ERH at a given temperature. Both the a_w (or ERH) and water content are to be determined when the system has reached equilibrium. The isotherm curve can be sub-divided into adsorption and desorption isotherms. The adsorption isotherm follows the wetting route. In this case, a completely dry sample is subjected to the head-spaces of progressively higher relative humidities and is allowed to gain moisture. When it attains equilibrium to the given set of relative humidities, the corresponding moisture contents are determined. The desorption isotherm is obtained by following the drying route. In this case, a wet sample is subjected to the head-spaces of progressively lower relative humidities and allowed to lose its moisture. When it attains equilibrium to the set head-spaces, the corresponding moisture contents are measured.

2.1.4 Hysteresis in sorption isotherms

As stated previously, moisture sorption isotherms can be constructed either by the adsorption process (starting from dry state, $a_w \approx 0.0$) or by the desorption process (starting from wet state, $a_w \approx 1.0$). When these two curves are plotted together, the curves fail to superimpose. A typical plot for maltodextrin of DE 11-12, determined in our laboratory, is presented in Figure 2.1. As shown in this figure, at a given a_w a food sample equilibrates at a higher moisture content when the desorption route is followed. The same food sample equilibrates

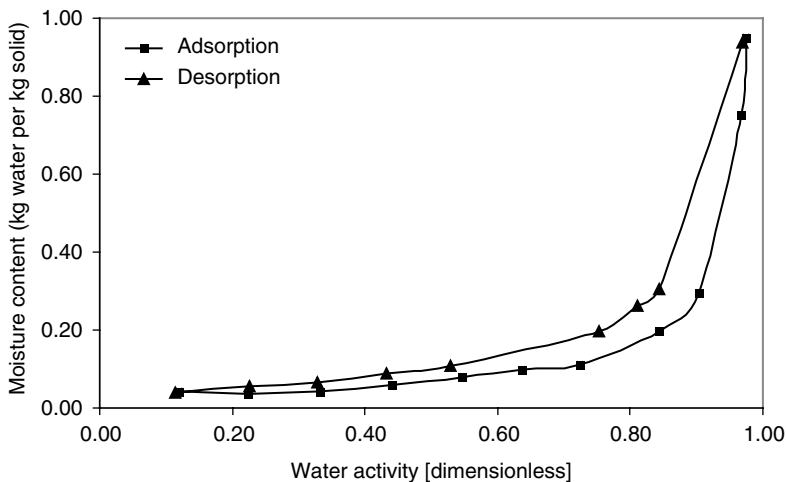


Fig. 2.1 A typical example of hysteresis in sorption isotherms (Maltodextrin, DE 11-12).

at a lower moisture content when the adsorption route is followed. As shown in Figure 2.1, the gap between the adsorption and desorption curves are narrowest or overlap at very high and very low a_w , and the gap is widest at the intermediate a_w values. Thermodynamically, there should be no hysteresis and both the adsorption and desorption isotherms should overlap. This is because the chemical potential of water or a_w is the state function and should be independent of the route taken. Thus, for a given composition, an a_w value at a given moisture content should be the same irrespective of the route taken.

2.2 COMPOSITION-BASED WATER ACTIVITY PREDICTIVE MODELS

There is no generally accepted model to predict the water activity in foods. The models in literature are mostly product specific in nature. Some of the most widely used equations are presented in this section with some working examples.

2.2.1 Raoult's Law

Raoult's law can be used to predict the water activity of food solutions as a function of the mole fraction of water. This equation is only applicable in dilute solutions, especially that of sugar and salts. However, this is applicable for $a_w \geq 0.95$.

$$a_w = \gamma_R \frac{\text{Moles of water}}{\text{Moles of water} + \text{Moles of solute}} = \gamma_R X_w \quad (2.13)$$

X_w , is the mole fraction of water and γ_R is the activity coefficient, $\gamma_R = 1$ for dilute and ideal solutions.

Raoult's equation is not suitable for a solution of macro-molecules of large molecular size. This is because equation (2.13) results in $a_w = 1$ for any practical solutions (moles of solute will be too large).

Example 2.1: Calculate the water activity of a 5.87 and 40.78 wt% sucrose solution and compare with literature data.

Solution: Molecular weight of water = 18; Molecular weight of sucrose = 342
From equation (2.13):

$$\begin{aligned} a_w(5.87\% \text{ sucrose}) &= \gamma_R \frac{\text{moles of water}}{\text{moles of sucrose} + \text{moles of water}} \\ &= 1 \times \frac{94.83/18}{94.83/18 + 5.87/342} = 0.997 \\ a_w(40.78\% \text{ sucrose}) &= \gamma_R \frac{\text{moles of water}}{\text{moles of sucrose} + \text{moles of water}} \\ &= 1 \times \frac{50/18}{50/18 + 50/342} = 0.965 \end{aligned}$$

The comparison in Table 2.1 shows that predictions using Raoult's law are reasonable within this concentration range.

Table 2.1 Comparison of experimental and predicated (Raoult's law) a_w values.

Sucrose (wt %)	Raoult's law	Chuang and Toledo (1976)	Robinson and Stokes (1965)
5.87	0.997	0.993	0.997
40.78	0.965	0.944	0.948

Table 2.2 Composition of a composite food and properties of its components.

Ingredients	Formulation (%w/w)	Molecular weight	k_i values
Water	30	18	—
Sucrose	45	342	2.6
Glucose	5	180	0.7
Glucose Syrup DE 64	10	353	1.96
Sorbitol	5	182	0.85
Glycerol	5	92	0.38

2.2.2 Norrish model

Norrish's model is based on the thermodynamic approach and considers water activity to be a function of the mole fraction of each soluble solute present in the system. This model considers a non-ideality of the water–solute system (Norrish, 1966; Leiras *et al.*, 1990; Lacroix and Castaigne, 1985; Bell and Labuza, 2000). Equations (2.14) and (2.15) are used for binary and multi-component solutions, respectively.

$$\log \left(\frac{a_w}{X_w} \right) = -K X_s^2 \quad (2.14)$$

$$\log \left(\frac{a_w}{X_w} \right) = -[(k_1^{0.5} X_{s1} + (k_2^{0.5}) X_{s2} + (k_3^{0.5}) X_{s3} + \dots]^2 \quad (2.15)$$

where K is the constant for binary solutions. k_i = constant for solute i , and X_{si} = mole fraction of solute i in the solution. The k values for each individual component or ingredient can be determined experimentally. The k values for lists of ingredients can be found elsewhere (Toledo, 1991; Bell and Labuza, 2000). This equation is valid for both electrolyte and non-electrolyte solutions (Leiras *et al.*, 1990).

Example 2.2: Determine the water activity of the composite food, the formulation of which is presented in Table 2.2.

Solution: Simply inserting the values from Table 2.2 in equation (2.15) gives $a_w = 0.804$. While calculating, moles of each component and its mole fraction are to be calculated as required by equation (2.15).

Example 2.3: Predict the water activity of honey whose composition is provided in Table 2.3.

Solution: $a_w = 0.594$.

Table 2.3 Composition of typical honey.

Ingredients	Formulation (% w/w)	Molecular weight	k_i values
Water	18	18	—
Sucrose	5	342	2.6
Glucose	35	180	0.7
Fructose	37	180	0.7
Maltose	5	342	2.6

Table 2.4 Formulation of a composite food sample.

Ingredients	Formulation (% w/w)	Molecular weight	k_i values
Water	13	18	
Sucrose	50	342	2.6
Glucose	7.5	180	0.7
Fructose	7.5	180	0.7
Salt	1	58.44	
Gelatin	1	30 000	
Starch	20	480 000	

Example 2.4: Determine the water activity of a composite food whose composition is provided in Table 2.4.

Equations (2.14) and (2.15) cannot be generalized to treat non-solute components (Ross, 1975). Some of the non-solute materials such as starches and proteins do not have defined molality, but they bind water and contribute to lowered water activity. In food formulations the solids can exist in soluble or non-soluble states. Therefore, the applicability of this equation can be limited for such complex food systems.

2.2.3 Ross model

This is a more empirical relationship (equation (2.16)). The water activity of a mixture involving several components can be determined from the product of the water activity of each component separately. This equation does not consider interactions among the solutes. It assumes that each solute behaves independently and dissolves in all the water in the system. This equation has a good prediction capability for electrolyte and non-electrolyte solutions in presence of non-solute components (Chirife *et al.*, 1985; Lacroix and Castaigne, 1985; Bell and Labuza, 2000).

$$a_w = a_{w1} \cdot a_{w2} \cdot a_{w3} \cdots \quad (2.16)$$

where $a_{w,i}$ is the water activity of component i at a water content of the system. For a solute in solution, the water activity can be calculated by using the Norrish equation (equations (2.14) and (2.15)). For non-solutes (solids not in solution), it can be determined using a sorption isotherm diagram. If the ratio of non-solute solids to total moisture is equal to or lower than 1, the non-solute component need not be taken into account to estimate water activity.

Table 2.5 Solution workout for example 2.5.

Ingredients	% w/w	M_w	K_i	Mole fraction*	$a_{w,i}$
Water	18	18			
Sucrose	5	342	2.6	0.014	0.984
Glucose	35	180	0.7	0.163	0.802
Maltose	5	342	2.6	0.014	0.984
Fructose	37	180	0.7	0.171	0.792

* Calculated assuming that ingredient i is the only solute present in the solution.

The water activity of many non-solutes is considered as close to 1. Chirife (1978) has listed many non-solutes solids such as gelatin, casein, potato, soybean, starch gel, beef and soy isolate to be close to 1 (0.98–0.99) when the ratio of solid to moisture was higher than 1.5. The Ross equation is a more practical approach than the Norrish model for products such as fruit bars where there is a presence of insoluble solids, which are added in dry form.

Example 2.5: Calculate the water activity of honey (Table 2.3) using the Ross equation.

Solution: The workout of the solution is given in Table 2.5. The water activity of each component has to be calculated from the Norrish equation at the given moisture content (18%, w/w). Or they have to be found out through sorption experiments. While using the Norrish equation the mole fraction of the solute i has to be calculated, assuming that this is the only one present in the water. Once the water activities of each are determined, the overall water activity is the product of water activities of all the components.

$$a_w(\text{overall}) = 0.984 \times 0.802 \times 0.984 \times 0.792 = 0.615$$

Example 2.6: Determine the water activity of composite food whose specification is presented in Table 2.4.

Solution: The solution procedure is exactly the same as in example 2.5 above. Since the K_i values to be used in the Norrish model are not available for starch and gelatin and also given that the mole fractions of these components are always close to zero (due to large molecular weight), water activities of these components will have to be assumed unity. The workout is given in Table 2.6.

$$a_w(\text{overall}) = 0.702 \times 0.941 \times 0.941 \times 0.986 \times 1.0 \times 1.0 = 0.613$$

2.2.4 Money–Born equation

This method requires the molecular weight of each solute present in the system. This is an empirical model based on Raoult's law which states that the water vapour pressure of a solution is inversely proportional to the molar concentration of solutes in a multi-component mixture. The water activity of a solution is described by the following equation (2.17) (Vega-Mercado and Barbosa-Canovas, 1994; Delmer, 1986).

$$a_w = \frac{1}{1 + 27 \sum N_{si}} \quad (2.17)$$

Table 2.6 Solution workout for example 2.6.

Ingredients	% w/w	M_w	K_i	Mole fraction*	$a_{w,i}$
Water	13	18			
Sucrose	50	342	2.600	0.168	0.702
Glucose	7.5	180	0.700	0.055	0.941
Fructose	7.5	180	0.700	0.55	0.941
NaCl	1	58.44	-7.590	0.23	0.986
Gelatin	1	30 000		0.000	1.000
Starch	20	480 000		0.000	1.000

* Calculated assuming that ingredient i is only solute present in the solution.

Table 2.7 Grover constants for various food materials.

Ingredients	Grover constant (K_i)
Sucrose	1.0
Lactose	1.0
Glucose, fructose	1.3
Maltodextrin DE 42	0.8
Protein	1.3
Starch	0.8
Gums	0.8
Acid	2.5
Glycol	4.0
Salt	9
Fat	0.0

where N_{si} = mole of solute i per gram of water present in the system. The applicability of this model has not been widely described.

2.2.5 Grover model

This is an empirical relationship (equation (2.18)) which was originally developed for confectionery products (Grover and Nicole, 1940). This method is based on a coefficient of equivalence with sucrose, considering the coefficient for sucrose to be 1. The equivalent sucrose values for other components can be found elsewhere (Bell and Labuza, 2000). This model has also been applied successfully to some complex food systems such as bread, biscuit dough and frankfurters (Delmer, 1986; Lacroix and Castaigne, 1985).

$$a_w = 1.04 - 0.1 \sum (K_i C_i) + 0.0045 \sum (K_i C_i)^2 \quad (2.18)$$

K_i = equivalent sucrose coefficient of component i , C_i = gram of component i /gram of total water. The K_i values for some food materials are presented in Table 2.7.

Example 2.7: Calculate the water activity of honey whose composition is given in Table 2.3.

Solution: The workout is shown in Table 2.8. The key step here is to compute the $\sum (K_i C_i)$ and $\sum (K_i C_i)^2$ and insert the values in equation (2.18). The a_w of this honey is 0.526 which is lower compared to the result obtained using the Norrish model (example 2.3).

Table 2.8 Solution workout for example 2.7.

Ingredients	% w/w	K_i	C_i	$K_i C_i$	$(K_i C_i)^2$	a_w
Water	18					
Sucrose	5	1	0.278	0.278	0.077	
Glucose	35	1.3	1.944	2.528	6.390	
Maltose	5	1	0.278	0.278	0.077	
Fructose	37	1.3	2.056	2.672	7.141	
Sum	100			5.756	13.685	0.526

Table 2.9 Solution workout for example 2.8.

Ingredients	% w/w	K_i	C_i	$K_i C_i$	$(K_i C_i)^2$	a_w
Water	13					
Sucrose	50	1	3.846	3.846	14.793	
Glucose	7.5	1.3	0.577	0.750	0.563	
Fructose	7.5	1.3	0.577	0.750	0.563	
Salt	1	9	0.077	0.692	0.479	
Gelatin	1	1.3	0.077	0.100	0.010	
Starch	20	0.8	1.538	1.231	1.515	
Sum	100			7.369	17.922	0.384

Example 2.8: Calculate the water activity of a composite food the composition of which is given in Table 2.4.

Solution: The workout of the solution is given in Table 2.9. This method has an advantage over the Norrish, Money–Born and Ross models because in a real food system the molecular weight of the components such as flour, protein, starches etc. is unknown. The Grover model does not require the molecular weight, though the sucrose equivalent needs to be determined experimentally. The Grover model is not applicable above 8 or 9 equivalent sucrose per unit weight of water present in the system (Delmer, 1986).

2.2.6 Salwin equation

This is valid for a dry mix system with or without any dissolution of added ingredients in the water present in the mixture. This equation (equation (2.19)) adopts an equilibrium approach to determine the water activity of the system (Bone, 1987; Bell and Labuza, 2000). It is based on the sorption isotherm of each ingredient present in the mix. This equation assumes that no significant interactions occur that alter the isotherms of the mix ingredients. The mix may contain simple solutes, starches, proteins, flours or complex foods (Bone, 1987). The equilibrium depends on the ratio of the materials and the slopes of their respective moisture sorption isotherms within the possible range of moisture exchange (considering the moisture sorption curve of this section linear). This is a simple model and possesses potential for application to complex food systems such as dried food product mixtures and intermediate food systems such as fruit leather or fruit bars.

$$a_w = \frac{\sum a_{w,i} b_i w_i}{\sum b_i w_i} \quad (2.19)$$

where $a_{w,i}$ = initial water activity of ingredient i , b_i = absolute value of slope of moisture isotherm of ingredient i , w_i = weight of dry solids of ingredient i .

2.3 MODELS FOR PREDICTION OF SORPTION ISOTHERMS

There are various models with corresponding mathematical equations for prediction or data fitting of sorption isotherms of foods. The mathematical expressions based on two- and three-parameter models are the most commonly used. Due to the complex nature of foods, no single model is general enough to represent the sorption isotherms of foods. Some of the most common are presented in this section. Since BET and GAB models are most commonly used in predictions of sorption isotherms of foods, these two are presented in greater detail.

2.3.1 Two-parameter models

2.3.1.1 Langmuir equation

Langmuir's equation (Langmuir, 1918) is one of the first equations that represents water activity with moisture content. It only represents the type I isotherms. This is given by equation (2.20):

$$\frac{m}{M_o} = \frac{Ca_w}{1 + Ca_w} \quad (2.20)$$

where C and M_o are constants and M_o represents the monolayer moisture content.

2.3.1.2 Smith equation

Smith (1947) proposed an empirical sorption equation (equation (2.21)) that can reasonably fit sorption data of various bio-polymers.

$$m = a - b \ln(1 - a_w) \quad (2.21)$$

where a and b are fitting constants. Becker and Sallans (1956) used this equation to fit the sorption data of wheat and reported that this equation followed the experimental sorption data between a_w value of 0.5–0.95 reasonably well. Young (1976) applied this equation to peanuts and found that this equation provided a best fit of their data and recommended its use for a_w values greater than 0.3. Similarly, Lang and Steinberg (1981) used this equation with some modification to predict water activity of binary and composite foods containing macro-molecules. The a_w range tested was 0.3–0.95 and they reported that its accuracy was within 1.86%. Furthermore, Rahman (1995) reported that this equation was suitable in the water activity range of 0.5–0.95 in wheat desorption.

2.3.1.3 Oswin equation

Oswin (1946) developed an equation (equation (2.22)) to represent water activity. This is a mathematical series expansion for sigmoid shaped curves.

$$m = k \left(\frac{a_w}{1 - a_w} \right)^n \quad (2.22)$$

k and n are constants to be obtained by fitting the experimental data. Labuza *et al.* (1972) used this equation to correlate equilibrium moisture content in non-fat powder milk and freeze-dried tea. It was found to follow the experimental data reasonably well within $a_w = 0.5$. Furthermore, the parameter k was found to be a linear function of temperature. Equation (2.8) can be modified to incorporate the temperature (T) as given by equation (2.23):

$$m = (a + bT) \left(\frac{a_w}{1 - a_w} \right)^n \quad (2.23)$$

where a and b are constants to be fitted assuming linear temperature dependence of k .

2.3.1.4 Henderson equation

Henderson's empirical equation (Henderson, 1952) is relatively widely used to relate water activity with moisture content. Henderson's equation is given by equations (2.24) and (2.25);

$$1 - a_w = \exp(-km^n) \quad (2.24)$$

or

$$\ln[-\ln(1 - a_w)] = \ln k + n \ln m \quad (2.25)$$

where k and n are fitting parameters. Equation (2.25) allows quantification of parameters k and n from the intercept and slope of a straight line when $[-\ln(1 - a_w)]$ versus m are fitted with experimental data.

Iglesias and Chirife (1976a) compared the fitting power of the Halsey and Henderson equations using 220 isotherms comprising 69 different food materials. They found that in 70.4% cases the isotherms were better represented by the Halsey equation while 21.9% of the isotherms were better represented by the Henderson equation. The remaining 7.7% isotherms were equally fitted by both the equations. Thomson *et al.* (1968) modified the Henderson equation to include the effect of temperature. The modified Henderson equation (equation (2.26)) is given below.

$$1 - a_w = \exp(-k(m + T)m^n) \quad (2.26)$$

Here, m is an additional constant. The Henderson or modified Henderson equation is applied to many food isotherms. However, it has been suggested that the Henderson equations' fitting power is rather limited compared to that of the Halsey or modified Halsey equation (Chirife and Iglesias, 1978).

2.3.1.5 Halsey equation

Assuming that the potential energy of a molecule varies as the inverse r th power of its distance from the surface, Halsey (1948) developed equation (2.27).

$$a_w = \exp\left(\frac{k}{RT}\theta^{-r}\right) \quad (2.27)$$

where k and r are constants. $\theta = m/M_o$, and M_o is the monolayer moisture content. He also stated that the magnitude of the parameter r characterizes the type of interaction between the vapour and the solid. If r is large, the attraction of the solid for the vapour does not extend far from the surface. When r is small the forces are more typical of van der Waals and are able to act at a greater distance. This equation was shown by Halsey to be a good representation of adsorption data that exhibit BET type I, II and III shapes. Later Iglesias and Chirife (1976b) found that the use of the term RT does not eliminate the temperature dependence of constant k and r . Consequently, they further simplified Halsey equation to the following form equation (2.28):

$$a_w = \exp(a'\theta^{-r}) \quad (2.28)$$

Here, $a' = k/RT$. This equation was further generalized to include the temperature effect as given by equation (2.29) below:

$$a_w = \exp[(a + bT)m^{-r}] \quad (2.29)$$

where a and b are constants that account for the temperature dependence.

2.3.1.6 Chung and Pfof equations

Chung and Pfof (1967a,b) developed equations assuming that the change in free energy for sorption is related to the moisture content, as given by equation (2.30) below.

$$a_w = \exp\left[-\frac{k}{RT} \exp(-nm)\right] \quad (2.30)$$

where k and n are fitting parameters. It was found that this equation cannot be used to predict the temperature dependence because the use of temperature term (T) does not eliminate the temperature dependence of parameters k and n (Chirife and Iglesias, 1978). Later, it was modified to accommodate the temperature effect through an additional term, as given by equation (2.31) (Basu *et al.*, 2006; Chirife and Iglesias, 1978):

$$a_w = \exp\left[-\frac{k}{q+T} \exp(-nm)\right] \quad (2.31)$$

where q is additional constant to account for the effect of temperature, in this way this equation has become three-parameter equation.

2.3.1.7 BET equation

The BET sorption equation, represented by equations (2.32) and (2.33) (Brunauer *et al.*, 1938) is one of the most widely used equations, which has some physical significance to the parameters used (Timmermann, 1989). It gives a good fit to data coming from various food sources within the region $0.05 < a_w < 0.45$ (Chirife *et al.*, 1978). Thus, this relationship cannot hold for the entire water activity range in foods. The most important aspect of this equation is that it permits us to calculate the monolayer moisture content of a food. It should

be noted that the shelf-life and product quality is normally optimum at monolayer moisture content.

$$\frac{m}{M_o} = \frac{Ca_w}{(1 - a_w)[1 + (C - 1)a_w]} \quad (2.32)$$

or

$$\frac{a_w}{(1 - a_w)m} = \frac{1}{M_o C} + \frac{(C - 1)a_w}{U_o C} \quad (2.33)$$

where M_o is the monolayer moisture content, C is the constant related to the net heat of sorption. Iglesias and Chirife (1976c) provided 300 monolayer values corresponding to about 100 different foods and food components.

The above equation can be re-written in linearized form as given by equation (2.34):

$$\frac{a_w}{(1 - a_w)m} = \alpha a_w + \beta \quad (2.34)$$

where $\alpha = [(C - 1)/(M_o C)]$ and $\beta = 1/(M_o C)$. α is determined from the slope and β is determined from the intercept of the straight line when $[a_w/(1 - a_w)m]$ is plotted as a function of a_w . Finally, the monolayer moisture content (M_o) and the net heat of sorption (C) parameters are determined.

The BET equation is criticized for the assumptions on which it is based (Rizvi, 2005), for example (1) the rate of condensation on the first layer is equal to the rate of evaporation from the second layer, (2) the binding energy of all the adsorbate on the first layer is the same and (3) the binding energy of the other layers is equal to those of the pure adsorbate. Further assumptions such as uniform adsorbent surface and absence of lateral interactions between adsorbed molecules are also known to be incorrect in view of heterogeneous food surface interactions (Rizvi, 2005).

2.3.2 Three-parameter isotherms

2.3.2.1 *Ferro Fontan et al.* equation

Ferro Fontan *et al.* (1982) developed an equation that is able to provide good fit to sorption isotherms of various foods in the range of a_w 0.1–0.95. This equation was developed for foods whose isosteric heat of sorption varies with the inverse r th function of moisture content. This equation was derived by the integration of the Clausius–Clayperon equation and is represented by equation (2.35).

$$\ln \left(\frac{\gamma}{a_w} \right) = \alpha m^{-r} \quad (2.35)$$

Here, γ is the parameter that accounts for the structure of the sorbed water, α is the proportionality constant, r is the power that relates the net isosteric heat with moisture content (r th power). When $\gamma = 1$, Ferro Fontan *et al.*'s equation reduces to the Halsey equation given above. It has been shown by Chirife *et al.* (1983) that equation (2.35) follows the sorption isotherms of oilseeds, starchy foods and proteins within a 2–4% average error. Iglesias and Chirife (1995) compiled 156 sorption isotherms of 92 different food products (proteins,

starchy cereals, oilseeds, meats, vegetables) and showed that equation (2.35) better represents the sorption isotherms of foods within an a_w range of 0.1–0.9 with the average error remaining within 3.3%.

2.3.2.2 Schuchmann–Ray–Peleg model

Since the majority of isotherm models do not fit the experimental data towards the higher water a_w range, Schuchmann *et al.* (1990) proposed a three-parameter empirical equation (equation (2.36)). They reported that this equation fits the sorption very well up to $a_w = 0.9 - 0.99$:

$$m = \frac{C_1 x}{(1 + C_2 x)(C_3 - x)} \quad (2.36)$$

where C_1 , C_2 and C_3 are empirical fitting constants. x is related to water activity by two relations as shown by equation (2.37). Either of these relations should be selected based on best fit.

$$x = \ln\left(\frac{1}{1 - a_w}\right) \quad \text{or} \quad x = \frac{a_w}{1 - a_w} \quad (2.37)$$

2.3.2.3 Guggenheim–Anderson–de Boer (GAB) model

The GAB equation is the best equation among three-parameter models. It provides the best fit for many food materials over a wide range of water activity. The equation was independently developed by Guggenheim (1966), Anderson (1946) and de Boer (1968) and is represented by equation (2.38) below. This equation has been adopted by European Project COST-90 (van den Berg and Bruin, 1981; Bizot, 1983). Fundamentally, it incorporates the basic tenets of Langmuir and BET theories. All of the parameters used in GAB equation have physical meaning associated with them.

$$\frac{m}{M_o} = \frac{CKa_w}{(1 - Ka_w)[1 - Ka_w + CKa_w]} \quad (2.38)$$

C and k are constants associated with the energies of interaction between the first and the distant sorbed molecules at the individual sorption sites. Theoretically they are related to the sorption enthalpies as given by equations (2.39) and (2.40). M_o is the monolayer value. Equation (2.38) reduces to the BET equation when $K = 1$. This constant K permits the model to be applicable to higher water activity (at multilayer moisture region). The constants C and K have Arrhenius type of temperature dependence as shown in the following equations (2.39) and (2.40).

$$C = C_o \exp\left(\frac{\Delta H_c}{RT}\right) \quad (2.39)$$

$$K = K_o \exp\left(\frac{\Delta H_k}{RT}\right) \quad (2.40)$$

C_o and K_o are the entropic accommodation factors. $\Delta H_c = H_o - H_n$, H_o and H_n are the molar sorption enthalpies of the monolayer and the multi-layer (kJ mol^{-1}) respectively. $\Delta H_k = H_n - H_l$, and H_l is the molar enthalpy (kJ mol^{-1}) of the bulk liquid phase.

Table 2.10 Monolayer moisture values of some food materials.

Food	M_o (g per 100 g solids)
Amorphous lactose	6.0
Beans	4.2
Beef ground	6.1
Chicken	5.2
Spray-dried cheese	2.2
Cocoa	3.9
Coffee	8.3
Crystallized sucrose	0.4
Egg	6.8
Fish	4.9
Whole milk powder	1.2–2.0
Instant milk powder	5.7
Skim milk powder	3.0
Pea	3.6
Potato	5.1–7.8
Gelatin	11.0
Potato starch	6.6
Starch	11.0
Shrimp	5.6

For values $K \neq 1$, the application of the BET and GAB equations yields different values of monolayer (M_o) and the enthalpy constant C . The monolayer moisture content obtained by the BET equation is always lower than that obtained by the GAB ($M_{o,BET} < M_{o,GAB}$). Similarly, the enthalpy constant C obtained by the BET is always larger than that obtained by the GAB ($C_{BET} > C_{GAB}$). The difference has been attributed to the mathematical nature of the equations rather than the nature of the sorption isotherms (Timmermann *et al.*, 2001; Timmermann, 2003). Table 2.10 lists the monolayer moisture contents of some food materials.

Procedure to determine GAB parameters

There are two approaches to determine the C , K and M_o values from a given sorption isotherm. The first approach [approach (a)] transforms the equation into quadratic form and determines the parameters. The second approach uses the statistical least-squares method to determine these parameters without the need of linearization.

Approach (a) Equation (2.38) can be cast in the quadratic form as given by equation (2.41) below.

$$\frac{a_w}{m} = \frac{K}{M_o} \left(\frac{1}{C} - 1 \right) a_w^2 + \frac{1}{M_o} \left(1 - \frac{2}{C} \right) a_w + \frac{1}{M_o K C} \quad (2.41)$$

$$\text{with } \alpha = \frac{K}{M_o} \left(\frac{1}{C} - 1 \right); \quad \beta = \frac{1}{M_o} \left(1 - \frac{2}{C} \right) \quad \text{and} \quad \gamma = \frac{1}{M_o K C} \quad (2.42)$$

Equation (2.41) can be further simplified as:

$$\frac{a_w}{m} = \alpha a_w^2 + \beta a_w + \gamma \quad (2.43)$$

α , β and γ are obtained through the least-squares method from the experimental data. The sum of the squared differences is minimized, as shown in equation (2.44) to obtain the best-fit values of α , β and γ . Once α , β and γ are obtained, the GAB parameters C , K and M_o are reverted back as shown by equation (2.42).

$$f_{\min} = \min \sum_{i=1}^n \left[\left(\frac{a_{w,i}}{m_i} \right) \Big|_{\text{Exp}} - \left(\frac{a_{w,i}}{m_i} \right) \Big|_{\text{Pred}} \right]^2 \quad (2.44)$$

Approach (b) In this approach, the GAB parameters are determined directly from the least-square method. As will be shown in the example, once the experimental sorption data are available, the C , K and M_o will be determined directly and there is no need to go through the painful process of linearization and transformation of parameters back and forth.

Example 2.9: The following data are obtained for a food product with a crisp-crust with soft centre filling. Determine GAB parameters for both components using both approach (a) and approach (b).

Solution: Approach (a). As per equation (2.43), the regression analysis is carried out first to determine α , β and γ . The regressed data from Table 2.11 are listed in Table 2.12. Subsequently, the C , K and M_o values are re-calculated from α , β and γ values using relationships shown in equation (2.42). The C , K and M_o values calculated in this way are also listed in

Table 2.11 Water activity versus moisture content data for products in example 2.9.

Water activity	Moisture content (kg water/kg solid)	
	Crisp cell	Centre fill
0.11	0.039	0.071
0.22	0.048	0.101
0.33	0.064	0.135
0.44	0.079	0.171
0.52	0.09	0.200
0.68	0.126	0.285
0.75	0.169	0.343
0.88	0.29	0.48

Table 2.12 Tabulation of parameters calculated from approach (a).

Parameters	Crisp cell	Centre fill
α	-18.94052788	-6.105687406
β	18.88075025	6.228087003
γ	1.081493	1.015984
M_o	0.048	0.135
C	20.188	7.161
K	0.951	0.828

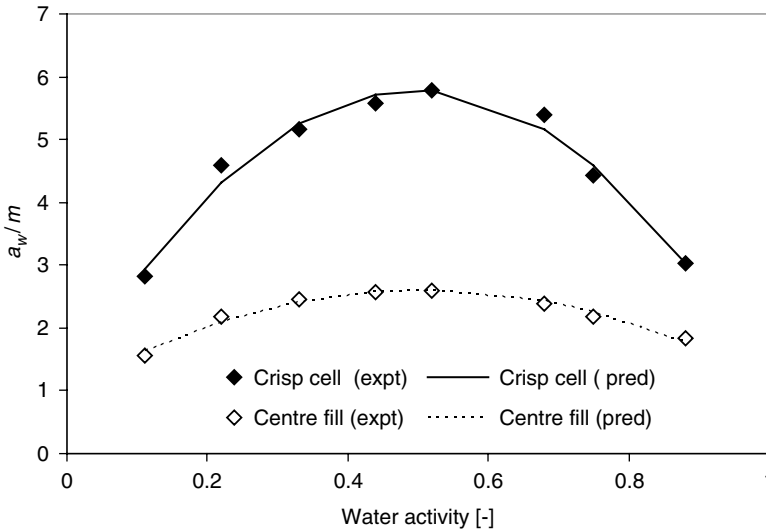


Fig. 2.2 Fitting of experimental a_w/m data from Table 2.11 with equation (2.43).

Table 2.13 Determination of C, K, M_o values for crisp cell using approach (b).

GAB parameters	M_o	K	C	
Optimized values	0.048	0.951	20.188	
a_w	Moisture expt	Moisture predicted	Diff squared	% Error (prediction)
0.11	0.039	0.038	1.97938E-06	3.61
0.22	0.048	0.051	9.33054E-06	6.36
0.33	0.064	0.063	9.51417E-07	1.52
0.44	0.079	0.077	3.61051E-06	2.41
0.52	0.090	0.090	5.45049E-08	0.26
0.68	0.126	0.132	3.61646E-05	4.77
0.75	0.169	0.164	2.74509E-05	3.10
0.88	0.290	0.291	2.59395E-07	0.18
		Σ (Diff squared)	7.980E-05	
		Average error		2.78

Table 2.12. Figure 2.2 shows the extent of the fit of experimental a_w/m with equation (2.43), which provides the parameters α, β and γ .

Solution: Approach (b). In this approach, equation (2.43) is directly fitted with experimental data with the least-square method. The parameters C, K and M_o are obtained directly. Tables 2.13 and 2.14 present the work-out of how the regression was carried out. These tables also provide the average absolute error (%) in prediction. The errors in prediction when the C, K and M_o values listed in Tables 2.13 and 2.14 are used are 2.78–2.83%, respectively. This is a reasonably good fit.

Example 2.10: The quantitative proportion of Crisp Cell and Centre Fill is 50:50. The initial water activities of the Crisp Cell and Centre Fill are 0.061 and 0.536, respectively. The Crisp

Table 2.14 Determination of C, K, M₀ values for centre fill using approach (b).

GAB parameters	M₀	K	C	
Optimized values	0.138	0.828	7.161	
a_w	Moisture expt	Moisture predicted	Diff squared	% Error (prediction)
0.11	0.071	0.063	5.97024E-05	10.88
0.22	0.101	0.103	6.00151E-06	2.43
0.33	0.135	0.138	9.66671E-06	2.30
0.44	0.171	0.174	9.80496E-06	1.83
0.52	0.200	0.204	1.66433E-05	2.04
0.68	0.285	0.284	4.33654E-07	0.23
0.75	0.343	0.335	6.59215E-05	2.37
0.88	0.480	0.483	7.64112E-06	0.58
		∑ (Diff squared)	1.758E-04	
		Average error		2.83

Cell loses its crispness at a water activity of 0.45 or above. The Centre Fill becomes too hard at a water activity of 0.39 or below. Calculate the water activity at equilibrium and comment if this value is within the specification to maintain the crispness of the crust and softness of the centre fill.

Solution: The Salwin equation (2.19) can be used to calculate the equilibrium water activity.

$$a_{weq} = \frac{\sum a_{w,i} b_i w_i}{\sum b_i w_i} = \frac{a_{w1} b_1 w_1 + a_{w2} b_2 w_2}{b_1 w_1 + b_2 w_2}$$

Substitute the values $a_{w1} = 0.061$, $a_{w2} = 0.536$, $b_1 = 0.14$, $b_2 = 0.329$, $w_1 = 50$, $w_2 = 50$ in the above equation. The b_1 and b_2 are the slopes of the sorption linear line between 0.22 and 0.52 water activity values. The equilibrium water activity (a_{weq}) is found to be 0.394. This water activity is between 0.39 and 0.45. This shows that the Crisp Cell will maintain the crispness and the centre fill will remain soft.

2.3.3 Effect of temperature on water activity

The water activity shift by temperature at constant moisture content is due to the change in water binding (increased mobility of water), dissociation of water or increase in solubility of solute in water (Labuza *et al.*, 1985). Because of the nature of water binding, at constant water activity most foods hold less water at higher temperature (in other words for the same moisture content, the water activity is higher at higher temperature). The effect of temperature follows equation (2.45).

$$\ln \frac{a_{w1}}{a_{w2}} = \frac{Q_s}{R} \left[\frac{1}{T_1} - \frac{1}{T_2} \right] \quad (2.45)$$

where Q_s (MJ mol⁻¹) is the excess binding energy for the removal of water.

In general, the effect of temperature on increasing the water activity at constant moisture content is greatest at lower to intermediate water activities (Figure 2.3). In some cases, such

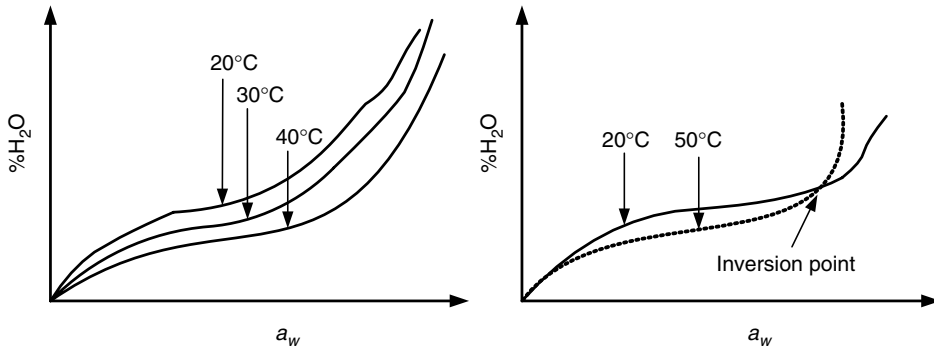


Fig. 2.3 Effect of temperature on moisture sorption isotherm of foods.

Table 2.15 Sorption isotherm data for sucrose/maltodextrin 60:40) powder at 25°C, 35°C and 45°C.

25°C		35°C		45°C	
a_w	m (kg water per kg solid)	a_w	m (kg water per kg solid)	a_w	m (kg water per kg solid)
0.113	0.026	0.113	0.025	0.112	0.024
0.225	0.045	0.214	0.041	0.204	0.038
0.311	0.059	0.321	0.058	0.328	0.055

as sugar-rich products like fruits, there is an inversion effect. This is due to the increased solubility of sugars. The solubilization reduces the mobility of water. The cross-over point (intersection) depends on the sugar content (the higher the sugar content the lower the inversion point). This point varies from a_w 0.55 (sultana raisin) to 0.75 (apricot).

Effect of pressure on water activity: The effect of pressure on the adsorption isotherm is relatively small and negligible at reasonable pressure levels.

Example 2.11: The sorption isotherm data for a sucrose/maltodextrin (60:40) powder sample is given in Table 2.15. Determine the excess binding energy (MJ mol^{-1}) for water removal of this sample. Given $R = 8314.34$ ($\text{kg m}^2 \text{s}^{-2} \text{kg mol}^{-1} \text{K}^{-1}$). Comment on the nature of the Q_s value.

Solution: To determine the Q_s value, two water activity values at two different isotherms have to be found which have the same moisture content. To determine two or more water activity values at different isotherms but at a given moisture content, isotherms have to be plotted and those values have to be found through interpolation. Suitable isotherm equations described in Sections 2.3.1 and 2.3.2 have to be utilized for this purpose. The Q_s values can then be calculated from the knowledge of two a_w values along with the corresponding temperatures as given in equation (2.46)

$$Q_s = \frac{RT_1T_2}{T_1 - T_2} \ln \left(\frac{a_{w1}}{a_{w2}} \right) \quad (2.46)$$

Table 2.16 Tabulation of the Q_s values for example 2.11.

Moisture (kg water per kg solid)	Temperature (K)	a_w	Q_s (MJ mol ⁻¹)
0.03	298	0.149	5911.006
0.03	308	0.161	5854.063
0.03	318	0.173	5883.459
0.05	298	0.254	5504.983
0.05	308	0.273	5479.041
0.05	318	0.292	5492.433

The Q_s values at two moisture content levels are given in Table 2.16. It can be seen from this table that, for this particular food product, the Q_s value is moisture dependant.

2.3.4 Water activity above boiling point

Above 100°C, water activity does not depend on the binding forces between water and solutes or solids and composition; it is only a function of temperature (Loncin, 1988). If any substance initially containing free water is heated in a closed vessel at temperature above 100°C (say 110°C) and if the pressure released in order to reach the atmospheric pressure (1.0133×10^5 Pa), then the water activity (Loncin, 1988):

$$a_w = \frac{1.0133 \times 10^5}{1.43 \times 10^5} = 0.7 \quad (2.47)$$

where 1.43×10^5 Pa is the vapour pressure of pure water at 110°C. This is important in extrusion and film/roller drying where the water activity at the outlet is a function of temperature only.

2.4 TYPES OF SORPTION ISOTHERMS AND HYSTERESIS IN ISOTHERMS

The relationship between the adsorbed amount (equivalent to moisture content) of various gases such as oxygen, nitrogen and water vapour as a function of their activity coefficient (equivalent to water activity) was first illustrated by Brunauer *et al.* (1940). Water can be adsorbed on the food surface both chemically (chemisorption) and physically (capillarity). It can be adsorbed in multi-layers. Brunauer *et al.* (1940) described five types of isotherms (Figure 2.4). Type I is well-known Langmuir isotherm, obtained by the mono-molecular adsorption of gas by porous solids within finite volume of pores. Anti-caking agents used in food powder also exhibit this type of isotherm. Type II is the sigmoid isotherm, which is obtained for soluble products and shows an asymptotic trend as water activity tends towards 1. Type III, known as the Flory–Huggins isotherm, accounts for the adsorption of a solvent or plasticizer like glycerol, for example, above the glass-transition temperature. Sugars also exhibit this type of isotherm. Type IV isotherm describes the adsorption by a swellable hydrophilic solid until a maximum of hydration sites is reached. Type V is the BET (Brunauer *et al.*, 1938) multi-layer adsorption isotherm, observed for the adsorption of water vapour on

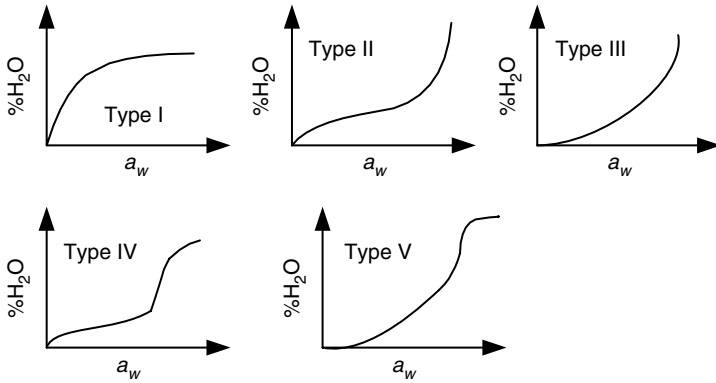


Fig. 2.4 General shapes of isotherms observed in food systems.

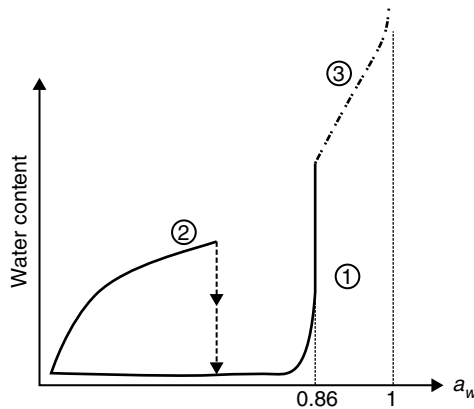


Fig. 2.5 Adsorption isotherm of (1) crystalline sucrose, (2) amorphous sucrose and (3) saturated solution. The arrow (\downarrow) shows the crystallization of the amorphous sucrose).

charcoal which is related to types II and III isotherms. Type II and Type IV isotherms are the most common isotherms found in food products (Mathlouthi and Roge, 2003). Beside the V types of BET isotherms, there are some product specific isotherms, for example that of sucrose (Figure 2.5). Anhydrous sucrose crystals only contain traces of water at low and medium values of relative humidity. The adsorption by anhydrous crystals corresponds to saturation equilibrium (a vertical line on the adsorption curve) at a characteristic ERH (86% for sucrose). The amorphous sucrose exhibits type I isotherm until it crystallizes and loses the water. Icing sucrose and sucrose with particle size $<250 \mu\text{m}$ also exhibit adsorption isotherm of amorphous sucrose (Mathlouthi and Roge, 2003).

Hysteresis in sorption isotherms

The hysteresis in the sorption isotherm results from the presence of a network of pores and voids in foods. The physical phenomena, such as glass-transition and swelling of the food matrix, also lead to sorption hysteresis. In this respect, the ink bottle theory (McBain, 1935; Cohan, 1938, 1944; Rao, 1941) and glass-transition theory (Bell and Labuza, 2000) explain that the hysteresis in sorption isotherms is inevitable. The ink bottle theory makes use of

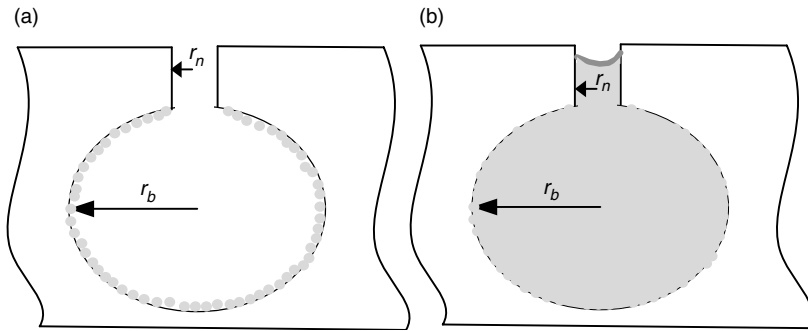


Fig. 2.6 Schematic diagram illustrating ink bottle effects that cause hysteresis in sorption isotherms. (a) adsorption route (b) desorption route.

Kelvin's equation (equation (2.48)) and explains that food materials have an extensive network of pores. This pore network likens to the ink bottle with larger (or bulk) inner pores connected to the smaller (neck) ones which are open to the adsorbate (Figure 2.6). During adsorption the condensation of the adsorbate takes place at the smaller pores and extends to the inner pores. According to equation (2.3), the pressure (P_v) at which this progresses is controlled by the radius of the larger pore ($r = r_b$). As shown in Figure 2.6, the bulk pore diameter (r_b) is an order of magnitude larger than that of the neck (r_n). During the desorption process, however, so long as the liquid column in the pore network remains intact, evaporation cannot take place until the vapour pressure (P_v in equation (2.48)) falls to the value corresponding to the $r = r_n$. Hence the amount of the moisture content that has completely filled the pore and the neck, a_w value, will be higher for adsorption isotherms than the desorption isotherms. The contact angle has also synergistic effect regarding the hysteresis. The smaller θ values give lower vapour pressures (equation (2.48)) and vice versa. Since the condensing adsorbate has to wet the solid surface the contact angle tends to be higher. During desorption, however, since the pores are completely wet, the contact angle is either very small or close to zero. The smaller r and θ values both act to lower the vapour pressure during desorption. From the same reasoning, greater r and θ values both act to raise the vapour pressure during desorption (equation (2.48)).

$$a_w = \frac{P_v}{P_v^0} = \text{Exp} \left(-\frac{2\sigma \cos \theta}{rRT} \right) \quad (2.48)$$

σ = surface tension of water (N m^{-1}), r = radius of the pore or neck (m), θ = contact angle, R = universal gas constant $8314.34 \text{ (kg m}^2 \text{ s}^{-2} \text{ kg mol}^{-1} \text{ K}^{-1})$ and T = absolute temperature (K).

The transition between a glassy and rubbery state of a material can also lead to hysteresis. Moisture adsorption into a glassy material is usually very slow due to much reduced moisture diffusivities and restricted moisture mobility. The food sample may fail to reach its equilibrium moisture within the experimental time frame. This leads to a lower moisture content for a given a_w than if equilibrium was reached. However, food samples are usually in a rubbery state during the desorption process and have an inherently higher moisture mobility due to a higher diffusion coefficient. This allows rubbery samples to reach equilibrium faster, which usually leads to higher moisture content (desorption) than for the glassy state during adsorption (Bell and Labuza, 2000). Similarly, swelling of polymeric materials, such as

proteins, during sorption can lead to hysteresis. As a polymeric material swells, polar sites, once obscured, may now be available to interact with water. The hydrated proteins, prior to desorption, contain many sites to which water can hydrogen bond. The dehydrated protein, prior to adsorption, has some polar sites hidden and unavailable to water. The structural differences, the aggregation and slow uptake of water cause hysteresis in proteins (Cerofolini and Cerofolini, 1980; Kocherbitov *et al.*, 2004).

2.5 DETERMINATION OF SORPTION ISOTHERMS

There are numerous methods to determine the sorption isotherms. These methods could be subjectively grouped into three categories: (a) gravimetric; (b) manometric; and (c) hygroscopic, and these methods are detailed in the ensuing section.

2.5.1 Gravimetric method

Gravimetric methods utilize measurement of change in mass. The gravimetric measurements can be of both discontinuous and continuous type. However, the discontinuous method is the one which is most widely used. This is probably due to the fact that the controlled humidity chamber and the need to create a vacuum impede the continuous measurements. The continuous measurement methods have advantages in that they allow measurement of sorption and desorption kinetics and the time at which the equilibrium is attained.

2.5.1.1 Controlled humidity chamber

A simple approach to establish a moisture adsorption–desorption isotherm for a food is to put it into a controlled humidity chamber at a constant temperature and measure weight gain or loss with time until equilibrium is attained. The use of a controlled humidity chamber was standardized by the COST-90 project (Wolf *et al.*, 1985; Spiess and Wolf, 1987). This project investigated the use of various salt solutions and saturated solutions of sulphuric acid to standardize the water activity measuring system. It was found that the accuracy of saturated salt solution is 0.05–2% of RH depending on the type of salt used. The accuracy of sulphuric acid solution was found to be within 0.1% of RH over the temperature range of 15–60°C.

In this method the measurement of the adsorption isotherm must commence at its lowest water activity and the desorption isotherm from the highest one. It is recommended that, if possible, the initial water activity of the sample be kept at zero through subjecting it to dryrite™ or phosphorous pentoxide. This provides one added advantage of having a sample with zero moisture content. The sample must be in solution form to start the desorption isotherm and the equilibrium moisture content should be measured at the end of the completion of the isotherm.

The COST-90 project also recommends the standardized procedure, the humidity chamber and also the standard material for calibration. It recommends that the sorption container be 1 L in volume and tightly sealed against water vapour by means of vapour seal rings and glass covers. It recommends that a total of 5 replicates be made for each water activity value. In order to make sure that the resistance to vapour movement within the enclosure is negligible compared with sample, the maximum distance between the surface of the food sample to the surface of the solution should be <10 cm. Similarly, the ratio of the area of the smallest equipment diameter to the visible salt solutions surface area should not exceed

Table 2.17 General guidelines for preparing salt solutions for sorption isotherm measurement at 25°C.

Salt	RH (%)	Salt (g)	Water (ml)
LiCl	11.15	>175	100
CH ₃ COOK	22.60	>300	100
MgCl ₂	32.73	>82	100
K ₂ CO ₃	43.80	>168	100
Mg(NO ₃) ₂	52.86	>188	100
NaBr	57.70	>110	100
SrCl ₂	70.83	>81	100
NaCl	75.32	>54	100
KCl	84.32	>53	100
BaCl ₂	90.26	>57	100

5:1. The height of the salt solution columns should not be greater than 1/4 of the height of the container. The container height and the container diameter should be equal to one another. The salt solutions must be prepared by using analytical grade salts and solutions. Since these salt solutions must have an excess of salt above their solubility, their solubility (at a given isotherm) has to be taken into account and excess salt amounting to 1.5–2 times that of their solubility should be maintained (Table 2.17). The temperature fluctuation should not exceed $\pm 0.2^\circ\text{C}$ for routine measurements and $\pm 0.02^\circ\text{C}$ for standard experimentations. The precision of the balance should be adequate to register the change in water content of $\pm 0.1\%$ absolute for routine measurements and ± 0.01 absolute for reference methods. Similarly, micro-crystalline cellulose Avicel PH 101 is recommended as a standard material for sorption isotherm construction (Spiess and Wolf, 1987).

There is already an established practice of using some specific containers to carry out the sorption isotherm. A total of 10 containers are to be used to determine 8–10 water activity values to cover the 0.0 to 1.0 a_w range. Specially designed desiccators and jars that meet the above mentioned container standards, are used for this purpose.

Desiccators. Both glass and polycarbonate desiccators (Figure 2.7) are available. Although glass containers allow the use of sulphuric acid solutions, they are expensive and fragile and not ideal to create a vacuum environment. Hence, polycarbonate desiccators are most widely used. A desiccator with a 230 mm internal diameter can accommodate 3 sample replicates held in glass Petri dishes. Plastic desiccators are cheap, easy to handle and inert to saturated salts up to 60–70°C. Plastic desiccators come with on/off valves to generate vacuum within.

Jars. Glass jars with an inert plastic support can also be used. However, make sure that the seal is good and the metal top is not rusted.

Methods of creating constant ERH/adjustment of water activity

1. Saturated salt solutions

Saturated solutions of various inorganic and organic salts produce a constant vapour pressure in the head-space at a constant temperature. This is the most common method employed to adjust the water activities of food samples. The ERH decreases as the temperature increases.

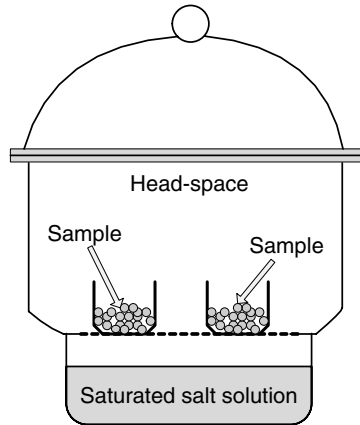


Fig. 2.7 Schematic diagram of a desiccator with saturated salt solution to create a controlled RH environment.

Table 2.18 Water activity values of saturated salt solutions as a function of temperature.

Salt	Temperatures (°C)						
	5	10	20	25	30	40	50
Lithium chloride/ $(\ln a_w = 500.95/T - 3.85)$	0.113	0.113	0.113	0.113	0.113	0.112	0.111
Potassium acetate ($\ln a_w = 861.39/T - 4.33$)	—	0.234	0.231	0.225	0.216	—	—
Magnesium chloride ($\ln a_w = 303.35/T - 2.13$)	0.336	0.335	0.331	0.328	0.324	0.316	0.305
Potassium carbonate ($\ln a_w = 145.0/T - 1.3$)	0.431	0.431	0.432	0.432	0.432	—	—
Magnesium nitrate ($\ln a_w = 356.6/T - 1.82$)	0.589	0.574	0.544	0.529	0.514	0.484	0.454
Potassium iodide	0.733	0.721	0.699	0.689	0.679	0.661	0.645
Sodium chloride ($\ln a_w = 228.92/T - 1.04$)	0.757	0.757	0.755	0.753	0.751	0.747	0.744
Ammonium sulphate	0.824	0.821	0.813	0.810	0.806	0.799	0.792
($\ln a_w = 367.58/T - 1.39$)	0.877	0.868	0.851	0.843	0.836	0.823	0.812
Potassium nitrate	0.963	0.960	0.946	0.936	0.923	0.891	0.848
Potassium sulphate	0.985	0.982	0.976	0.970	0.970	0.964	0.958

This is due to the increased solubility of salts with an increase in temperature and their negative heats of solution. The water activity values for readily available salt solutions from 5°C to 50°C are provided in Table 2.18.

Limitations. During the experiment the loss or gain of moisture may change the water activity of the top layer, so the solution should be stirred occasionally to keep it well mixed. Some salts such as potassium dichromate and potassium chloride are caustic. Lithium chloride and sodium nitrate are highly toxic. Alkaline solutions such as K_2CO_3 absorb large amounts of CO_2 with time, which decreases the water activity significantly.

Table 2.19 Water activity of sulphuric acid solutions at different concentrations and temperatures.

H ₂ SO ₄ (%)	Density at 25°C (g cm ⁻³)	Temperature (°C)						
		5	10	20	25	30	40	50
5.00	1.0300	0.9803	0.9804	0.9806	0.9807	0.9808	0.9811	0.9814
10.00	1.0640	0.9554	0.9555	0.9558	0.9560	0.9562	0.9565	0.9570
15.00	1.0994	0.9227	0.9230	0.9237	0.9241	0.9245	0.9253	0.9261
20.00	1.1365	0.8771	0.8779	0.8796	0.8805	0.8814	0.8831	0.8848
25.00	1.1750	0.8165	0.8183	0.8218	0.8235	0.8252	0.8285	0.8317
30.00	1.2150	0.7396	0.7429	0.7491	0.7521	0.7549	0.7604	0.7655
35.00	1.2563	0.6464	0.6514	0.6607	0.6651	0.6693	0.6773	0.6846
40.00	1.2991	0.5417	0.5480	0.5599	0.5656	0.5711	0.5816	0.5914
45.00	1.3437	0.4319	0.4389	0.4524	0.4589	0.4653	0.4775	0.4891
50.00	1.3911	0.3238	0.3307	0.3442	0.3509	0.3574	0.3702	0.3827
55.00	1.4412	0.2255	0.2317	0.2440	0.2502	0.2563	0.2685	0.2807
60.00	1.4940	0.1420	0.1471	0.1573	0.1625	0.1677	0.1781	0.1887
65.00	1.5490	0.0785	0.0821	0.0895	0.0933	0.0972	0.1052	0.1135
70.00	1.6059	0.0355	0.0377	0.0422	0.0445	0.0470	0.0521	0.0575
75.00	1.6644	0.0131	0.0142	0.0165	0.0177	0.0190	0.0218	0.0249
80.00	1.7221	0.0035	0.0039	0.0048	0.0053	0.0059	0.0071	0.0085

2. Sulphuric acid–water solution

Sulphuric acid–water solutions provide a very precise relative humidity environment. The vapour pressure of H₂SO₄ solutions depends on the solution concentration. The ERH in the head-space increases with an increase in temperature.

Limitations. Sulphuric acid–water solutions are hazardous to use and extremely corrosive. The solutions require titration after each run to determine the accurate a_w value. This arises due to gain and loss of water during tests. Table 2.19 provides information regarding water activity of H₂SO₄–water solutions as a function of concentration and temperature.

3. Glycerol–H₂O solutions

Glycerol solution at various solid concentrations can be used to determine water activity. These solutions are non-corrosive as well. The water activity values of glycerol solutions as a function of glycerol concentrations are given in Table 2.20.

Limitations. It can volatilize and absorb into food causing error if weight gain is used as the moisture measurement. It has to be analysed after completion of the test to ascertain the a_w . Gas–liquid chromatography is used for this purpose. This is because it gets diluted or dehydrated during use.

4. Mechanical humidifiers

A desired relative humidity can be maintained in a chamber by the use of a wet-bulb controlling mechanism. For this purpose a calculated amount of water is sprayed with a calculated amount of dry air at a certain temperature. Nozzle atomizers are used for this purpose. Alternatively, the dry air can be bubbled through a water pool maintained at a certain temperature. However, it has low precision (± 2 –5% RH), the size of the assembly is usually large and it costs more. The relative humidity of the air has to be measured by psychrometric instruments either directly (dew-point) or indirectly (wet-bulb temperature, capacitive

Table 2.20 Water activity of glycerol solutions of various concentrations.

20°C		23°C	
Glycerol (% w/w)	a_w	Glycerol (% w/w)	a_w
30.8	0.89	8.4	0.95
44.3	0.85	31.7	0.9
49.8	0.81	40.8	0.85
56.2	0.77	48.1	0.80
60.6	0.74	54.9	0.75
65.0	0.69	61.0	0.70
70.9	0.64	70.9	0.6
75.0	0.58	78.7	0.50
82.1	0.46	84.7	0.40
86.2	0.37	89.3	0.30
88.2	0.36	90.9	0.20
93.9	0.19	96.2	0.10

hygrometers). The main difficulty of the method is in keeping a constant level of moisture in the chamber and measuring it with a good level of accuracy.

Dry desiccators (for zero water activity)

Calcium sulphate (Drierite™). This comes doped with cobalt chloride and turns from blue to pink when it reaches the upper saturation limit. It can then be regenerated by drying at 150°C for 24 h. It produces water activity of 0.001.

Phosphorous pentoxide (P₂O₅). It is also used in laboratories to achieve zero relative humidity. This is a very effective desiccant. However, one should be very careful while using this chemical. It generates a large amount of heat and become explosive when it absorbs large amount of water and organic volatiles. Furthermore, it emits gas with pungent odour. It is non-regenerative.

Dynamic vapour sorption instrument (DVS)

The dynamic vapour sorption (DVS) is one of the advanced sorption measurement systems. The principle of the sorption isotherm generation, the reaching of moisture equilibrium by a sample at controlled head-space water activity, are the same as the static method (saturated salt solutions) described above.

As shown in Plate 2.1 the sample and reference compartments of the DVS contain a sample pan that hangs on a loop connected to a sensitive micro-balance. The sample size ranges from 1.5 to 10 g and the precision ranges from 0.1 to 1 µg. The desired RH is controlled via two thermal conductivity mass flow controllers. These controllers use the RH sensors based on the conductance principle to determine and control the RH of each stream. One of the controllers directs the flow of the dry carrier gas (nitrogen) while the other controls the flow of water vapour saturated carrier gas. The desired RH (0–90%) is generated by mixing appropriate amounts of dry and water vapour saturated gas streams. Nitrogen gas at desired RH flows through both the sample and reference compartments. The temperature and RH of both the sample and reference compartments are monitored by using temperature and RH probes located underneath the sample and reference cells. Since both the flow streams and temperature

and RH are precisely controlled through appropriate software, the adsorption and desorption isotherms are pre-programmed. DVS instruments usually work by pre-programmed step-wise increments of relative humidity. Usually, the step size is kept at 10% RH. Commercially available DVS instruments operate at 5–85°C range.

2.5.2 Manometric method

This is the most accurate and precise method to determine water activity (Zanoni *et al.*, 1999). This involves the measurement of vapour pressure over food using manometry. The structure and working principle of this method is described by Taylor (1961), Karel and Nikerson (1964) and Labuza (1975). The schematic diagram of the instrument is shown in Figure 2.8. It consists of a sample flask connected to a manometer. Before the run of the measurement the whole system other than the sample is thoroughly evacuated down to $<200 \mu\text{Hg}$. The vapour space around the food is subsequently evacuated for 1–2 min to remove the gases present on the sample head-space. Then the valve across the manometer is closed. The whole system is maintained at constant temperature. The food sample exerts vapour pressure to equilibrate the system which can be read directly from the differential height in the manometer column. A low density and low vapour pressure (not easy to vaporize) oil is used so that large differential heights can be obtained with small change in vapour pressure over the sample head-space. The sample size to vapour space ratio should be large enough so that the evaporation of water vapour from the sample doesn't affect its a_w or moisture content significantly. Usually, 5–10 g of sample is used and it takes about 30–40 min for this sample size to reach equilibrium. Liquid samples have to be frozen and solidified in order to measure a_w . This lengthens the

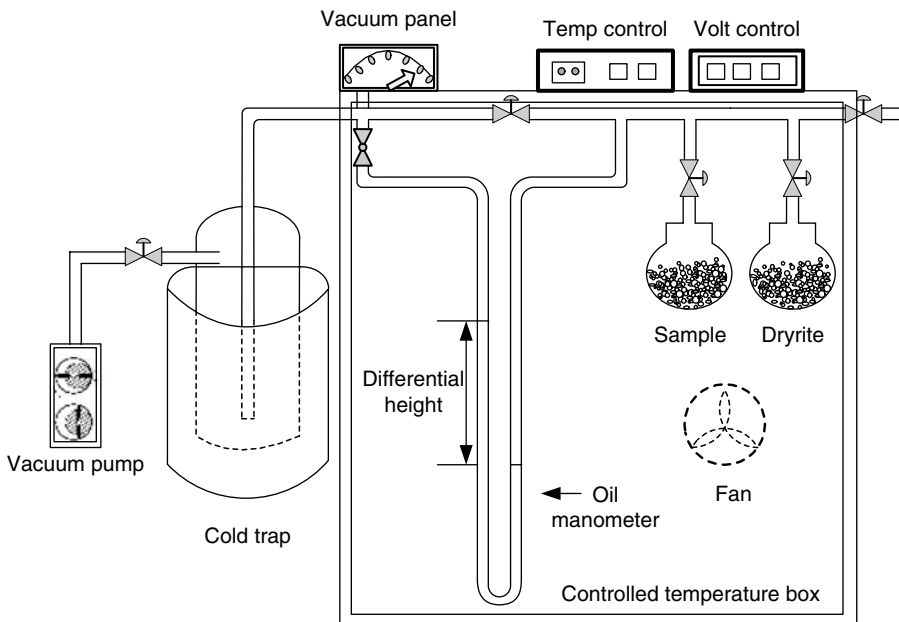


Fig. 2.8 Schematic diagram of manometric water activity measuring instrument.

equilibrium time. This system has a very high degree of accuracy ($\pm 0.002 a_w$ units), if the temperature is accurately controlled.

2.5.3 Hygroscopic methods

The most commonly used hygroscopic methods can be classified as the chilled-mirror type and capacitive sensor type, as described below.

2.5.3.1 Chilled-mirror type

The AquaLab™ series (Decagon Company, Pullman, USA) of water activity measuring instruments use chilled-mirror theory to determine a_w . Here a sample is equilibrated within the head-space of a sealed chamber that contains a mirror, an optical sensor, an internal fan and an infrared temperature sensor. At the temperature and moisture equilibrium, the RH of the head-space should be the same as that of the sample. The accuracy of this instrument lies in the accuracy of determining at which point the first condensation (dew-point) appears. Provision is made to detect, by monitoring the change in reflectance of the mirror, when the dew-point appears. Infrared beams are used for this purpose. Thermocouple sensors are used to monitor the dew-point temperature on the mirror and a thermopile sensor is used to determine the temperature of the sample surface. Both the dew-point and sample temperatures are then used to determine the water activity. Standard saturated salt solutions are used to see the accuracy of the instrument to determine water activity. The contamination of the mirror is a concern in this type of instrument for which frequent cleaning is required. The equilibrium time of these instruments is in the range of 5–10 min and the accuracy is claimed to be within $\pm 0.003 a_w$.

2.5.3.2 Capacitive sensor type

Instruments that measure a_w using capacitive humidity sensors are available commercially. These instruments use sensors made from a hygroscopic dielectric material and associated circuitry that gives a signal relative to the ERH. Most capacitive sensors use a polymer as the dielectric material whose dielectric constant ranges from 2 to 15. The water has a dielectric constant of 80 at room temperature. Hence, the adsorption or desorption of water vapour in the sensor changes its capacitance which is correlated to the equilibrium relative humidity (ERH). The typical uncertainty of capacitive sensors is $\pm 2\%$ RH from 5% to 95% RH. The ERH so measured is equal to the water activity of the sample only when the temperatures of the sample and the sensor are the same. Hence it is essential to ensure that the sensor and the sample temperature remain the same by carefully controlling the temperature of the system. The capacitive sensors require a relatively longer time than the chilled-mirror dew-point relative humidity sensors. However, they work well at elevated temperatures as high as 200°C and the drift in measurement due to temperature is relatively small. Accurate measurements with this type of system require good temperature control. ERH measuring instruments based on these sensors and marketed by Rotronic Company (USA) are widely used in the food and chemical industries.

2.5.4 Sample preparation and equilibrium time

The procedure for sample preparation depends if an adsorption or desorption isotherm is desired. For a desorption isotherm, it is essential to dry down the sample to as close to zero

moisture level as possible, or at least lower than the lowest water activity of the saturated salt solution being used. It is recommended that the sample be dried within 70–100°C at pressure of 25 mm Hg. Depending on the nature of the product it may be essential to further dry it over P₂O₅ for few days or weeks. Alternatively, freeze-drying can provide ideally low moisture content when the sample is dried at 100 μHg for 48 h (26–32°C). Further drying over P₂O₅ at least for a week may be essential. While constructing a desorption isotherm, the sample can be used as it is or equilibrating it at water activity higher than the highest a_w salt solution used. However, it is essential to measure the water content of the sample.

2.5.4.1 Equilibration time

The equilibrium time is dictated to the greatest extent by the moisture diffusivity from within the sample. It is also influenced to some extent by the external mass transfer resistance or ease at which the vapour from and to the sample diffuses through the headspace. The design of most desiccators is such that the external mass transfer resistance is insignificant. In this case the moisture diffusivity (D_{eff}) and the thickness of the sample (L) dictates the time it takes to reach equilibrium. In most cases, this varies from 1 to 4 weeks.

If external diffusion of water in the air space is not limiting, the rate of uptake or loss of moisture can be predicted from equation (2.49). This equation was derived by Crank (1956) by assuming that the effective moisture diffusivity in the sample is independent of the moisture content, and that the adsorption or desorption take a relatively long time to reach equilibrium.

$$\frac{m - m_e}{m_o - m_e} = \frac{8}{\pi^2} \exp \left[-\frac{\pi^2}{4L^2} D_{eff} t \right] \quad (2.49)$$

where D_{eff} is the effective diffusivity of water in sample. m_e is the equilibrium moisture content (kg water per kg solid). m_o is the initial moisture content (kg water per kg solid). m is the moisture content at time (t). L is the thickness of the slab where adsorption/desorption takes place from one side (m) and t is the time (s). Equation (2.49) can be solved for time as follows (equation (2.50)).

$$t = \frac{4L^2}{\pi^2 D_{eff}} \left[\ln \left(\frac{8}{\pi^2} \right) - \ln \left(\frac{m - m_e}{m_o - m_e} \right) \right] \quad (2.50)$$

Equation (2.50) states that an infinite time is needed for the sample to reach a true equilibrium, however a pseudo-equilibrium stage is considered adequate when the measurement is at $\pm 0.2\%$ or 2 mg g⁻¹. The effective diffusivity is 10⁻¹⁰ cm² s⁻¹ for most of vegetable tissues. Under vacuum, the diffusivity coefficients increase by a factor of around 10; thus a vacuum desiccator reduces the equilibrium time significantly. At higher relative humidity it takes a longer time to reach the equilibrium. The thickness of the sample significantly affects equilibrium time (square of thickness) – doubling the thickness increases the equilibrium time by a factor of 4. Although drawing vacuum reduces the equilibrium time because of increased internal diffusivity of moisture in the sample, it also inherits some disadvantages such as condensation of moisture inside the desiccator at higher equilibrium temperature due to mixing of cold air to the hot head-space, adsorption of the moisture by the sample from the ambient air while breaking vacuum, spattering of the powder sample if a strong vacuum is created too fast and spattering of the solution due to boiling after pulling the vacuum.

Example 2.12: During desorption, the isotherm is measured at 25°C. 40% (w/w) sucrose solution is subjected to a saturated salt solution. Assuming that the equilibrium moisture content of the sucrose solution at the headspace relative humidity is 10%, (w/w). The thickness of the solution column is 1 mm. Determine the equilibrium time if D_{eff} of sucrose solution at average moisture content (25%, w/w) is 4.46×10^{-11} ($m^2 s^{-1}$). Assume that the effective moisture diffusivity of sucrose is independent of moisture content. What happens if the thickness of the solution column is reduced by one half?

Solution: Here the initial moisture (m) = 1.5 kg water per kg solid; equilibrium moisture content is = 0.111 kg water per kg solid. Thickness (L) = $1 \times 10^{-3}m$. From equation (2.50), the equilibrium time is:

$$t = \frac{4(1 \times 10^{-3})^2}{\pi^2 4.46 \times 10^{-11}} \left[\ln \left(\frac{8}{\pi^2} \right) - \ln \left(\frac{0.1112 - 0.111}{1.5 - 0.111} \right) \right] = 21.8 \text{ h}$$

Note that the $m \neq m_e$. Hence, in this solution $m = 0.1112$ is used which is effectively the m_e . It can be seen that equilibrium is reached for this sample within a day.

If the thickness of the solution column is reduced by half, the time for the sample to reach equilibrium = 5.5 h.

2.6 CONCLUDING REMARKS

Water activity is a well researched theme and a widely applied and powerful tool in food processing, preservation and storage. There are numerous books, book chapters and research articles in peer reviewed journals dealing with various aspects of this theme. The availability and sheer amount of information often confuses students, technologists and application engineers and makes it harder for them to find the relevant information. We have long felt that hands-on information, such as selecting appropriate test methods and establishing optimal test protocols, determination of the parameters in predictive models and information regarding the equilibrium time, is not easily available. In this chapter, we have tried to make this information available through worked-out examples.

REFERENCES

- Anderson, R.B. (1946) Modifications of the Brunauer, Emmett and Teller equation. *Journal of the American Chemical Society*, **68**(4), 686–69.
- Basu, S., Shivhare, U.S. and Mujumdar, A.S. (2006) Models for sorption isotherms for foods: A review. *Drying Technology*, **24**(12), 1705–1705.
- Becker, H.A. and Sallans, H.R. (1956) S study of the desorption isotherms of wheat at 25°C and 50°C. *Cereal Chemistry*, **33**(2), 79–91.
- Bell, L.N. and Labuza, T.P. (2000) *Moisture Sorption: Practical Aspects of Isotherm Measurement and Use*. American Association of Cereal Chemists, Inc., 3340 Pilot Knob Road, St. Paul, MN, USA.
- Bizot, H. (1983) Using the ‘GAB’ model to construct sorption isotherms. In: *Physical Properties of Foods* (eds Jowitt *et al.*). Applied Science, New York, pp. 43–54.
- Bone, D.P. (1987) Practical applications of water activity and moisture relations in foods. Chapter 15. In: *Water Activity: Theory and Applications to Food* (eds L.B. Rockland and L.R. Beuchat). Marcel Dekker, Inc., New York and Basel, pp. 369–395.

- Brunauer, S., Deming, L.S., Deming, W.E. and Teller, E. (1940) On a theory of the van der Waals adsorption of gases. *Journal of the American Chemical Society*, **62**, 1723–1732.
- Brunauer, S., Emmett, P.H. and Teller, E. (1938) Adsorption of gases in multimolecular layers. *Journal of the American Chemical Society*, **60**, 309–319.
- Cerofolini, G.F. and Cerofolini, M. (1980) Heterogeneity, allostericity, and hysteresis in adsorption of water by proteins. *Journal of Colloid and Interface Science*, **78**(1), 65–73.
- Chirife, J. (1978) Prediction of water activity in intermediate moisture foods. *Journal of Food Technology*, **13**, 417–424.
- Chirife, J. and Iglesias, H.A. (1978) Equations for fitting water sorption isotherms of foods: Part 1 – a review. *Journal of Food Technology*, **13**, 159–174.
- Chirife, J., Boquet, R., Ferro Fontan, C. and Iglesias, H.A. (1983) A new model for describing the water sorption isotherms of foods. *Journal of Food Science*, **48**, 1382–1383.
- Chirife, J. and Resnik, S.L. (1984) Saturated solutions of sodium chloride as reference sources of water activity at various temperatures. *Journal of Food Science*, **49**, 1486–1488.
- Chirife, J., Resnik, S.L. and Ferro-Fontan, C. (1985) Application of Ross equation for prediction of water activity in intermediate moisture food systems containing a non-solute solid. *Journal of Food Technology*, **20**(6), 773–779.
- Chuang, L. and Toldeo, R.T. (1976) Predicting the water activity of multicomponent systems from water sorption isotherms of individual components. *Journal of Food Science*, **41**, 922–927.
- Chung, D.S. and Pfof, H.B. (1967a) Adsorption and desorption of water vapour by cereal grains and their products. Part I. Heat and free energy changes of adsorption and desorption. *Transactions of the ASAE*, **10**, 549–551, 555.
- Chung, D.S. and Pfof, H.B. (1967b) Adsorption and desorption of water vapour by cereal grains and their products. Part II. Hypothesis for explaining the hysteresis effect. *Transactions of ASAE*, **10**, 552–555.
- Cohan, L.H. (1938) Sorption hysteresis and the vapor pressure of concave surfaces. *Journal of the American Chemical Society*, **60**, 433–435.
- Cohan, L.H. (1944) Hysteresis and capillary theory of adsorption of vapours. *Journal of the American Chemical Society*, **66**, 98–105.
- de Boer, J.H. (1968) *The Dynamical Character of Adsorption*, 2nd edn. Clarendon Press, Oxford.
- Delmer, F. (1986) Methods of calculating water activity in food products. *Revue Generale du Froid*, **76**(2), 83–86.
- Ferro Fontan, C., Chirife, J., Sancho, E. and Iglesias, H.A. (1982) Analysis of a model for water sorption phenomena in foods. *Journal of Food Science*, **47**, 1590–1594.
- Grover, D.W. and Nicole, J.M. (1940) The vapour pressure of glycerin solutions at 20°C. *Journal of Society of Chemical Industry*, **59**, 175–177.
- Guggenheim, E.A. (1966) *Applications of Statistical Mechanics*. Clarendon Press, Oxford.
- Halsey, G. (1948) Physical adsorption on non-uniform surfaces. *Journal of Chemical Physics*, **16**(10), 931–937.
- Iglesias, H.A. and Chirife, J. (1976a) A model for describing the water sorption behaviour of foods. *Journal of Food Science*, **41**, 984–992.
- Iglesias, H.A. and Chirife, J. (1976b) Prediction of effect of temperature on water sorption of food materials. *Journal of Food Technology*, **11**, 109–116.
- Iglesias, H.A. and Chirife, J. (1976c) BET monolayer values in dehydrated foods and food components. *Lebensm.-Wiss. Technology*, **9**, 107–113.
- Iglesias, H.A. and Chirife, J. (1995) An alternative to the G.A.B. model for the mathematical description of moisture sorption isotherms of foods. *Food Research International*, **28**(3), 317–321.
- Kocherbitov, V., Arnebrant, T. and Soderman, O. (2004) Lysozyme–water interactions studied by sorption calorimetry. *Journal of Physical Chemistry B*, **108**(49), 19036–19042.
- Labuza, T.P. (1968) Sorption phenomena in foods. *Food Technology*, **22**(3), 15–24.
- Labuza, T.P. (1975) Sorption phenomena in foods: Theoretical and practical aspects. In: *Theory, Determination and Control of Physical Properties of Food Materials* (ed. C. Rha). D. Reidel Publishing Company, Dordrecht-Holland/Boston-USA, pp. 197–219.
- Labuza, T.P., Kaanane, A. and Chen, J.Y. (1985) Effect of temperature on the moisture sorption isotherms and water activity shift of two dehydrated foods. *Journal of Food Science*, **50**, 385–391.

- Labuza, T.P., Mizrahi, S. and Karel, M. (1972) Mathematical models for optimization of flexible film packaging of foods for storage. *Transactions of the ASAE*, **15**(1), 150–155.
- Lacroix, C. and Castaigne, F. (1985) Evaluation of various methods of predicting the water activity of Frankfurter type cooked meat emulsions in relation to contents of salt. *Canadian Institute of Food Science and Technology Journal*, **18**(1), 44–52.
- Lang, K.W. and Steinberg, M.P. (1981) Predicting water activity from 0.30 to 0.95 of a multi-component food formulation. *Journal of Food Science*, **46**(3), 670–672.
- Langmuir, I. (1918) The adsorption of gases on plane surfaces of glass, mica and platinum. *Journal of the American Chemical Society*, **40**, 1361–1402.
- Loncin, M. (1988) Activity of water and its importance in preconcentration and drying of foods. In: *Preconcentration and Drying of Food Materials* (ed. S. Bruin). Elsevier Science Publishers, Amsterdam.
- Leiras, M.C., Alzamora, S.M. and Chirife, J. (1990) Water activity of galactose solutions. *Journal of Food Science*, **55**(4), 1174, 1176.
- Mathlouthi, M. and Roge, B. (2003) Water vapour sorption isotherms and the caking of food powders. *Food Chemistry*, **82**, 61–71.
- McBain, J.W. (1935) An explanation of hysteresis in the hydration and dehydration of gels. *Journal of the American Chemical Society*, **57**, 699–700.
- Oswin, C.R. (1946) The kinetics of package life III. Isotherm. *Journal of Society of Chemical Industry*, **65**, 419–421.
- Rahman, S. (1995) Water activity and sorption properties of foods. In: *Food Properties Handbook*. CRC Press, Boca Raton, FL, pp. 1–83.
- Rao, K.S. (1941) Hysteresis in sorption. V Permanence, scanning, and drift of the hysteresis loop. Ferric oxide gel-carbon tetrachloride and ferric oxide gel-water systems. *Journal of Physical Chemistry*, **45**(3), 522–531.
- Rizvi, S.S.H. (2005) Thermodynamic properties of foods in dehydration. In: *Engineering Properties of Foods*, 3rd edn (eds M.A. Rao, S.S.H. Rizvi and A.K. Datta). Taylor & Francis.
- Ross, K.D. (1975) Estimation of water activity in intermediate moisture foods. *Food Technology*, **29**(3), 26–34.
- Sahin, S. and Sumnu, S.G. (2006) Water activity and sorption properties of foods. In: *Physical Properties of Foods* (eds D.R. Heldman). Heldman Associates, San Marcos, CA, pp. 193–228.
- Schuchmann, H., Roy, Y. and Peleg, M. (1990) Empirical models for moisture sorption isotherms at very high water activities. *Journal of Food Science*, **55**(3), 759–762.
- Smith, S.E. (1947) The sorption of water vapor by high polymers. *Journal of the American Chemical Society*, **69**(3), 646–651.
- Spies, W.E.L. and Wolf, W. (1987) Critical evaluation of methods to determine moisture sorption isotherms. In: *Water Activity: Theory and Applications to Food* (eds L.B. Rockland and L.R. Beuchat). Marcel Dekker, Inc., New York.
- Taylor, A.A. (1961) Determination of moisture equilibria in dehydrated foods. *Food Technology*, **15**(12), 536–540.
- Thomson, T.L., Pert, R.M. and Foster, G.H. (1968) Mathematical simulation of corn drying—a new model. *Transactions of ASAE*, **24**(3), 582–586.
- Timmermann, E.O., Chiffie, J. and Iglesias, H.A. (2001) Water sorption isotherms of foods and food stuffs: BET or GAB parameters? *Journal of Food Engineering*, **48**, 19–31.
- Timmermann, E.O. (2003) Multi-layer sorption parameters: BET or GAB values? *Colloids and Surfaces*, **A222**, 235–260. A
- Timmermann, E.O. (1989) A B.E.T.-like three sorption stage isotherm. *Journal of the Chemical Society, Faraday Transactions I*, **85**(7), 1631–1645.
- Toledo, R.T. (1991) *Fundamentals of Food Engineering*, 2nd edn. Van Nostrand Reinhold, New York.
- Van den Berg, C. and Bruin, S. (1981) Water activity and its estimation in foods systems: Theoretical aspects. In: *Water Activity: Influence on Food Quality* (eds L.R. Rockland and G.F. Stewart). Academic Press, New York.
- Van den Berg, C. (1985) Water activity. In: *Concentration and Drying of Foods* (ed. D. Mac Carthy), Elsevier Applied Science Publishers, pp. 11–36.

- Vega-Mercado, H. and Barbosa-Canovas, G.V. (1994) Prediction of water activity in food systems. A review on theoretical models. *Revista Espanola de Ciencia y Tecnologia de Alimentos*, **34**(4), 368–388.
- Wolf, W., Spiess, W.E.L. and Jung, G. (1985) Standardization of isotherm measurements (Cost-Project 90 and 90 BIS). In: *Properties of Water in Foods* (eds D. Simatos and J.L. Multon). Martinus Nijhoff Publishers. Boston.
- Young, J.H. (1976) Evaluation of models to describe adsorption and desorption equilibrium moisture contents isotherms of Virginia-type peanuts. *Transactions of ASAE*, **19**, 146.
- Zanoni, B., Peri, C., Giovanelli, G. and Pagliarini, E. (1999) Design and setting up of a water vapour pressure capacitance manometer for measurement of water activity. *Journal of Food Engineering*, **38**, 407–423.

3 Biological changes during food drying processes

Xiao Dong Chen and Kamlesh C. Patel

3.1 INTRODUCTION TO DRYING AND FOOD QUALITY

Foodstuffs are complex biological materials, which are the main sources of various nutrients, and are used for energy and health purposes. Drying, as discussed in Chapter 1, is a traditional method of food preservation against micro-biological spoilages and pathogenic bacteria. When food materials are exposed to drying conditions, the native physical state of the food material is altered, leading to changes in the quality and safety of food materials. In general, drying processes help maintain the 'acceptable-to-excellent' edible status of various foodstuffs which have useful bioactive components such as proteins, vitamins, probiotics, enzymes, etc. for benefit to humans and animals. The shelf-life of the food is extended by a drying process, which can be used to control the bioactivity of various useful and harmful biological compounds including micro-organisms. Drying involves removal of excess water from the food matrix until a 'safe' moisture level is achieved, at which minimum or no physical, chemical or micro-biological reactions occur. The required level of moisture level (water content or water activity) in dried products for preventing spoilage is different due to dissimilar responses and inactivation mechanisms exhibited by different bioactive compounds.

For thermal deactivation of micro-organisms, three stages are considered: pre-treatment, heat treatment and post-treatment. Treating the drying process as a thermal treatment process, it is appropriate to also discuss the effects of drying on micro-organisms for three stages, that is, pre-drying, in-drying and post-drying. Pre-drying operations such as osmotic dehydration, evaporation, freeze concentration, membrane separation and extraction are employed to remove the excess water from the liquid feed prior to the drying operation. The selection of the pre-drying operation depends on the extent of the water removal, the type and physical form of the material and the expected damage during processing. Fundamental principles of water removal during the pre-drying processes vary from process to process. During osmotic dehydration of food materials, for instance dipping fruits or vegetables in concentrated syrup, the mutual diffusion of both sugar and water molecules in opposite directions removes the water from the fruits or vegetables. Post-drying processes include cooling, handling (including conveying), packaging, storage, rehydration, etc., which are basically product-specific operations. There have been many studies published on understanding the stability of various food products during the pre-drying and post-drying stages. Emphasis in this chapter is given to the in-drying process, that is, the drying stage, which is a crucial step for maintaining the biological activity of the food material.

High-temperature drying processes require a strong heat supply for the removal of moisture from the food sample. The heat can be supplied in many ways, such as microwave,

radio-frequency, hot gas stream including air, superheated steam, etc. The hot gas stream is the most frequently used heat source for large-scale commercial industries due to its easier availability, easier heat recovery and cheaper costs compared to other heat sources. The driers are often named according to how heat is supplied or what the drying medium is, for instance, solar drier, superheated-steam drier, heat-pump drier and microwave drier. Heat can be supplied through direct contact conduction, for example, drum drying, spray drying and tunnel drying. Radiation is also frequently used as a way of heating for batch-scale drying operations, for example, infrared drying.

The influences of drying on the microbial activities that are of interest in practice, may be classified into two categories: *in-drying* (i.e. deactivation of bioactive compounds embedded in liquid food materials, which experience certain temperature–time and moisture content–time profiles during drying) and *post-drying* (i.e. deactivation of bioactive compounds captured in dried materials which may undergo slow and progressive deterioration depending on different water activity levels). In the following sections, some basic issues involved with post-drying inactivation processes and modelling aspects of in-drying inactivation processes are discussed with respect to changes in the quality of food materials.

3.2 POST-DRYING PROBLEMS

In food storage studies, extensive research has already been conducted by industrial microbiologists and food technologists. There is a body of common knowledge for preserving food over a longer period of time by controlling spoilage. Spoilage of food results from changes in food composition, structure, appearance and/or quality due to the growth of microorganisms or other physical transformations, or chemical reactions occurring during storage. In general, spoilage of food can be due to physical, chemical or microbial transformations. The physical, chemical and microbial transformations in various food systems are affected by product and environmental conditions. The overall spoilage rate for a specific food system can be influenced by various physico-chemical parameters. A better understanding of the effects of individual physico-chemical parameters on the spoilage rate, as well as the effects of a combination of such parameters, is crucial for maintaining food in safe conditions over a certain period. The following physico-chemical parameters are known to be very important:

- Temperature
- Water activity
- pH
- Oxygen availability
- Nutrient availability
- Micro-structure
- Chemical inhibitors

Water activity (a_w) values are used extensively to predict the stability of foodstuffs with respect to microbial growth and enzymatic, chemical and physical changes (such as glass transition) that can lead to food degradation during storage (Christian, 2000). The water activity of the food system indicates how tightly water is bound, structurally or chemically, in the food matrix (Scott, 1957; Labuza, 1975). In other words, the water activity of the food describes the energy status of water in a food system, and hence its availability to

act as a solvent and participant in chemical or biochemical reactions (Labuza, 1977). The ability of water to act as a solvent, medium or reactant decreases as water activity is reduced. Water activity is believed to be a better index to microbial growth or food quality because the microbes or other living cells respond to the availability of water, not the amount of water. Water content is product specific, while water activity is fundamentally related to the processes, which are more likely to be energy driven. For the same water activity value, different food may hold different amounts of water. For instance, the water-holding capacity of fruits is higher than the same of cellulose at equal water activity.

The water activity of the food system can be measured by estimating the relative humidity (or water vapour pressure) of air in equilibrium with a food sample stored in a sealed chamber. Raoult's law is normally used to predict the water activity, mainly for ideal solutions (Caurie, 1983). However, Raoult's law may not be adequate when strong solute-solvent interactions, or intermolecular forces such as Van der Waals forces, ions dissolution and capillary phenomena (when the solvent or solution is trapped in a porous matrix) exist (Fennema, 1996). Food samples cannot be ideal solutions due to strong interactions between local molecules in the matrix. This challenge forced researchers to develop appropriate water activity models for specific food systems. The models developed by Ross (1975), Bone (1987) and Lilley and Sutton (1991) to estimate the water activity of two- or three-component systems are well documented in the literature. Roa and Tapia (1998) developed a model, based on the mobility of each solute, for estimating water activity in multi-component systems. The recent trend is to use the sorption isotherm data (i.e. water content vs. water activity) rather than only a water activity value for optimizing dehydration processes, packaging, microbial growth conditions and the physical/chemical stability of the product (Hardy *et al.*, 2002).

The water activity value ranges from 0 (no water) to 1 (pure water). The a_w is reduced by drying, by adding solutes such as sugar and salt or by a combination of drying and adding solutes. As summarized by Hendrickx and Knorr (2001), a small reduction in water activity, for instance from 0.98 to 0.97, is already sufficient to prevent the multiplication of many important spoilage micro-organisms such as various species of *Pseudomonas*, which can rapidly spoil meat products. One of the food-poisoning bacteria, *Staphylococcus aureus*, is the most tolerant to a_w changes. The water activity must be reduced to about 0.86 to limit its growth in the presence of oxygen and 0.91 to limit its growth anaerobically. Micro-organisms that can grow at low a_w levels can divert energy to the synthesis or accumulation of intracellular solutes such as glycine, betaine, proline and polyols. These solutes may osmoregulate during their synthesis in order to avoid water loss by osmosis and to maintain their functionality in their cytoplasmic membranes (Booth, 1998).

At $a_w < 0.86$, a few groups of bacteria, none of which are of public health concern, can multiply. Food spoilage in products below the a_w of 0.86 is mainly caused by yeasts and various type of moulds. Some of these organisms can grow slowly at or above a_w of approximately 0.6. No microbial proliferation is expected below a water activity of 0.6. The optimum water activity range of different living organisms for their growth in different food systems is illustrated in Table 3.1, obtained from Beuchat (1981). This information could be useful to determine the 'safe' water level for preserving the food over a longer period of time. Table 3.2, acquired from Gibbs and Gekas (2001), presents the minimum water activity values for some known food-borne infections and food-poisoning bacteria. Food poisoning is the result of ingesting food with pre-mixed toxins, produced by food-poisoning microbes. Food-borne infections are the result of the survival and growth of microbes in the digestive tract and toxin production inside the body. The water activity has to be higher than the minimum optimum level for an individual group of micro-organisms to produce toxins in food systems.

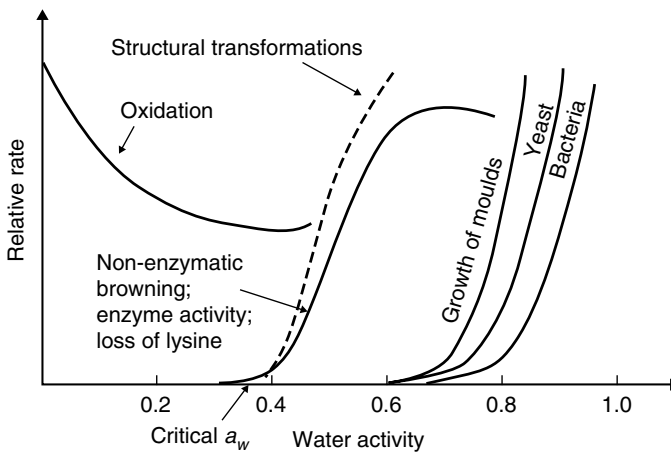
Table 3.1 Water activity range and growth of micro-organisms in different food.

Range of a_w	Micro-organisms generally inhibited by lowest a_w in this range	Foods generally within this range
1.00–0.95	<i>Pseudomonas</i> , <i>Escherichia</i> , <i>Proteus</i> , <i>Shigella</i> , <i>Klebsiella</i> , <i>Bacillus</i> , <i>Clostridium perfringens</i> , some yeasts	Highly perishable (fresh) foods and canned fruits, vegetables, meat, fish, and milk; cooked sausages and breads; foods containing up to 40% (w/w) sucrose or 7% sodium chloride
0.95–0.91	<i>Salmonella</i> , <i>Vibrio parahaemolyticus</i> , <i>C. botulinum</i> , <i>Serratia</i> , <i>Lactobacillus</i> , <i>Pediococcus</i> , some moulds, yeasts (<i>Rhodotorula</i> , <i>Pichia</i>)	Some cheeses (Cheddar, Swiss, Muenster, Provolone), cured meat (ham), some fruit juice concentrates; foods containing 55% (w/w) sucrose or 12% sodium chloride
0.91–0.87	Many yeasts (<i>Candida</i> , <i>Torulopsis</i> , <i>Hansenula</i>), <i>Micrococcus</i>	Fermented sausage (salami), sponge cakes, dry cheeses, margarine; foods containing 65% (w/w) sucrose (saturated) or 15% sodium chloride
0.87–0.80	Most moulds (mycotoxigenic penicillia), <i>Staphylococcus aureus</i> , most <i>Saccharomyces</i> (<i>bailii</i>) spp., <i>Debaryomyces</i>	Most fruit juice concentrates, sweetened condensed milk, chocolate syrup, maple and fruit syrups; flour, rice, pulses containing 15–17% moisture; fruit cake; country-style ham, fondants, high-ratio cakes
0.80–0.75	Most halophilic bacteria, mycotoxigenic aspergilli	Jam, marmalade, marzipan, glacé fruits, some marshmallows
0.75–0.65	Xerophilic moulds (<i>Aspergillus chevalieri</i> , <i>A. candidus</i> , <i>Wallemia sebi</i>), <i>Saccharomyces bisporus</i>	Rolled oats containing approximately 10% moisture, grained nougats, fudge, marshmallows, jelly, molasses, raw cane sugar, some dried fruits, nuts
0.65–0.60	Osmophilic yeasts (<i>Saccharomyces rouxii</i>), few moulds (<i>Aspergillus echinulatus</i> , <i>Monascus bisporus</i>)	Dried fruits containing 15–20% moisture; some toffees and caramels; honey
0.50	No microbial proliferation	Pasta containing approximately 12% moisture; species containing approximately 10% moisture
0.40	No microbial proliferation	Whole egg powder containing approximately 5% moisture
0.30	No microbial proliferation	Cookies, crackers, bread crusts, etc. containing 3–5% moisture
0.20	No microbial proliferation	Whole milk powder containing 2–3% moisture; dried vegetables containing approximately 5% moisture; corn flakes containing approximately 5% moisture; fruit cake; country-style cookies, crackers

Table 3.2 Minimum water activity level for growth of food-related micro-organisms (modified from Gibbs and Gekas, 2001).

Food poisoning organisms	Minimum a_w	Food-borne infectious organisms	Minimum a_w
<i>Campylobacter jejuni</i>	0.98	<i>Yersinia enterocolitica</i>	0.96
<i>Campylobacter coli</i>	0.97	<i>Clostridium perfringens</i>	0.95
<i>Bacillus cereus</i>	0.95	<i>Escherichia coli</i>	0.95
<i>Clostridium botulinum</i>			
Type A	0.95	<i>Salmonella</i> spp.	0.95
Type B	0.94	<i>Vibrio parahaemolyticus</i>	0.94
Type E	0.97	<i>Shigella</i> spp.	0.92
<i>Listeria monocytogenes</i>	0.92	<i>Eurotium amstelodami</i> (fungi)*	0.80 (15°C) 0.75 (30°C)
<i>Staphylococcus aureus</i>	0.86	<i>Eurotium chevalieri</i> (fungi)*	0.85 (15°C) 0.75 (30°C)
		<i>Eurotium herbariorum</i> (fungi)*	0.80 (15°C) 0.75 (30°C)

* Obtained from Abellana et al. (1999).

**Fig. 3.1** Stability map for food materials (modified from Roos, 2002).

Shelf-stable food products tend to be formulated at an a_w of about 0.3, where lipid oxidation, chemical changes and other enzymatic changes are minimal (Hendrickx and Knorr, 2001).

Several groups of living cells or spores, which have survived the drying process during production, may also be preserved in the dried food matrix. For instance, food-borne bacteria *Salmonellae* can survive spray drying or other high drying rate processes (Li Cari and Potter, 1970). The microbial cell is in fact not a simple osmometer that loses a functionality as soon as the water activity level is reduced (Keey, 1992).

A semi-qualitative illustration of the effect of water activity (a_w), for instance at a temperature of 25°C, on micro-organisms is shown in Figure 3.1 – modified from Roos (2002), but originally from Rockland and Beuchat (1987). In the diagram proposed by Roos (2002) for dairy products, the structural transformation was introduced in relation to the phenomenon of

glass-transition of amorphous sugars. Towards the right-hand side of the water activity line, stickiness, caking, structure collapse, crystallization of carbohydrates and browning reactions may be expected.

When the food structure disintegrates the fat, encapsulated in the matrix made up of sugar and protein, can be exposed to oxygen causing oxidative flavour and odours that may be objectionable (Sun *et al.*, 2002). The food matrix is exposed to oxygen due to more channels opening up, or cracks being formed during processing in the interior of the matrix that induce a greater extent of oxidation of lipids. The stability of proteins and enzymes is also highly affected by water activity changes due to their relatively fragile nature or easy changes in their conformation. Enzymatic reactions are significant above a_w of 0.8, however some enzymatic activities may occur at low a_w values (Monsan and Combes, 1986). Figure 3.1 also shows that the non-enzymatic browning reaches a maximum level at a_w in the range of 0.6–0.7. The degradation rate of water-soluble vitamins in food systems drastically increases with elevating a_w values (Kirk, 1981). This information could be very helpful when designing a food system with specific requirements.

The most important concept to recognize from this figure is that as the water activity (or the relative humidity of air) increases above the critical water activity for survival, micro-organism growth can cause significant problems in maintaining food quality and safety during processing and storage. This is the primary motive in employing drying operations for producing dried products, which should have the water activity lower than the threshold value. Dried food materials are then kept in controlled environmental conditions (for instance, in sealed packages) so that no water (vapour) re-adsorption can occur. The food systems are said to be safe from microbial spoilages only for a defined shelf-life, which depends on the product's properties, composition, microbial counts and handling and storage conditions.

When food is preserved at low water activities, it is not necessary that all micro-organisms are destroyed. Some bacteria may have lost microbial activity in the food matrix, however, they may gain their functionalities upon rehydration or at higher water activity conditions (Hendrickx and Knorr, 2001). Micro-organisms have different levels of resistance to the heat treatment when the water activity of the system is different. Heat tolerance is also affected by other physico-chemical parameters of the food systems. For instance, the thermal resistance of *B. stearothermophilus* spores, which is known as a highly thermal-resistant microbe, is strongly affected by the water activity (Xu and Wang, 2005). The partially dehydrated microbes or cellular components, when exposed to the hot environment, were observed to show higher resistance against heat (Corry, 1974, 1976; Murrell and Scott, 1966; Hendrickx and Knorr, 2001). As an example, when the experiments were conducted using egg albumin powder under controlled humidity and temperature conditions, it was observed that at a_w equals 0.98 (20°C), the decimal reduction (D value) was 15 min; at a_w of 0.68 (20°C), D was 51 min; at a_w of 0.33 (20°C), D was 460 min; and at a_w of 0 (20°C), D was 7 min. It may be then concluded that the initial reduction in water content increases the thermal stability of the dried product, in other words, improves storage and handling properties. When the water content is lower than the tolerance of the cells, one should expect a rapid kill of the microbes.

3.3 IN-DRYING PROBLEMS

The inactivation of biological compounds during drying is commonly termed as the *in-process* inactivation stage, where micro-organisms within the food materials are deactivated by the influence of heat and mass transfer occurring simultaneously. The in-drying or in-process

inactivation may be better for keeping high product quality and safety by deactivating harmful micro-organisms. At the same time, the inactivation process may be undesirable when useful bioactive compounds such as vitamins, proteins, enzymes, etc. have to be preserved. A fundamental understanding and keeping of a good balance between these two aspects of inactivation can certainly help improve the overall quality of dried products (Chen, 2006a,b).

Drying rate, the rate of water removal (weight of water removed per unit surface/volume of the food matrix per unit time), is an important parameter for 'in-process' inactivation of biological substances. The processing time, product quality, optimization and equipment designs are directly influenced by the rate of drying. Low drying-rate processes are usually more energy-intensive and have higher processing times, leading to a high production cost. Different drying rates may have different impacts on the cellular activities and/or other physical/biological transformations which may be responsible for overall degradation of the food quality. The first group of drying processes, which deal with high drying rates, are the high temperature processes such as spray drying, hot-air tunnel drying, drum drying, superheated-steam drying, fluidized-bed drying, spouted-bed drying and heat-pump drying. Another group of drying processes, which have low drying-rates and higher processing times, involve relatively lower temperatures compared to the first group of drying processes: freeze drying, vacuum drying, atmospheric freeze drying, solar drying and microwave drying can be placed in a group with low drying rates. In order to achieve higher efficiencies, improved product quality, lower processing times and reduce production costs, a combined drying approach is often used. Microwave–vacuum drying, microwave–convection drying and spray–freeze drying are examples of combined drying processes. Often, two or more drying techniques are operated in a series to minimize the overall drying time and degradation of useful biological substances.

Low-temperature drying processes are favourable for keeping the high bioactivity of desired bio-components in the final product. A minimal change in nutritional values is targeted during low-temperature processes. The unwanted microbial activity could also be preserved in the food material. Drying of food using hot air does not necessarily involve high temperatures due to the evaporative cooling effect during water evaporation. Evaporation of water from the food surface to the surrounding air minimizes the temperature rise of the food system. Superheated-steam drying can, however, lead to high food temperatures during processing. The severity of inactivation of micro-organisms during drying is lower than the severity during other thermal treatments where no evaporation is involved and where the temperature of the moist food sample is maintained at as high as 121°C for a certain time. High-temperature thermal treatments, although highly effective in deactivating unwanted bacterial activity, also severely degrades other essential food ingredients.

For the removal of water from the given food geometry, the moisture (liquid and vapour) contained in the solid material must migrate from the interior to the surface. The transport of moisture in the moist food materials can be considered as moisture transport in porous media, and thus the recognized principles of heat and mass transfer in a porous medium can be readily used (Welti-Chanes *et al.*, 2005; Aversa *et al.*, 2007). A common model for the migration of moisture from the internal structure to the surface is by assuming liquid water flow or water vapour diffusion. The transport of liquid water is often accounted for by using a capillary flow (Chen and Pie, 1989; Shi and Wang, 2004). Many mechanisms have been proposed for describing the internal transport of water, which is generally believed to be a major rate-limiting step, nevertheless no generalized theory exists that effectively explains the internal moisture transfer, owing to the complexity of the process and the nature of the material. Diffusion phenomena are considered to be extremely complex due to the wide

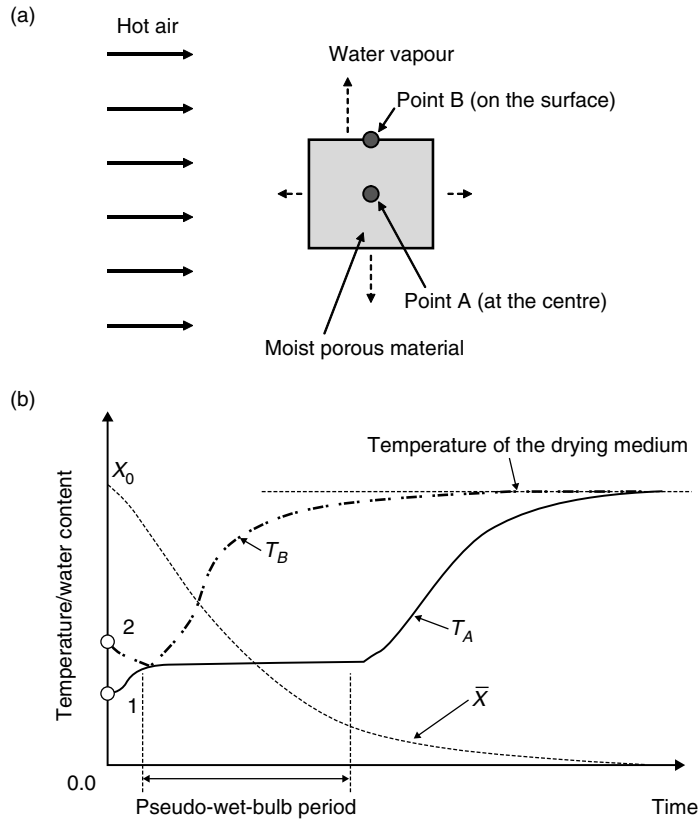


Fig. 3.2 Qualitative illustration of (a) drying of a moist food slab and (b) temperature–time and moisture content–time profiles during drying.

diversity of chemical compositions and physical structures of food systems, and hence reliable data are limited. The transport of water has been widely modelled using the effective liquid diffusion model (Yusheng and Poulsen, 1988; Chen, 2006b). Extensive studies have already been published for developing the theoretical model to estimate the effective diffusivity or diffusion coefficient for various food systems (Zogzas *et al.*, 1996; Reyes *et al.*, 2002; Simal *et al.*, 2006).

Figure 3.2a shows a typical scenario where the heat coming from the surrounding hot air is transferred to the product–air interface and subsequently to the moist food product. In order to overcome the latent heat of vaporization, heat must be supplied to the food surface and also into the porous food structure. For hot air drying, the temperature history at the surface and the centre of the moist porous material, presented by points A and B respectively, and average water loss versus time, may be depicted in Figure 3.2b. It was assumed that the initial water content was fairly high. This assumption is reasonable because the water contents of natural food materials are generally in the order of 80 wt%. For low water content food materials, such as 50 wt% (dry basis) concentrated milk, the pseudo-wet-bulb drying period is very short or does not exist. The local evaporation rate within the moist food material should be determined by the local driving force, that is the vapour pressure difference in the solid structure and the local ‘head-space’ such as pores or channel space at the same location

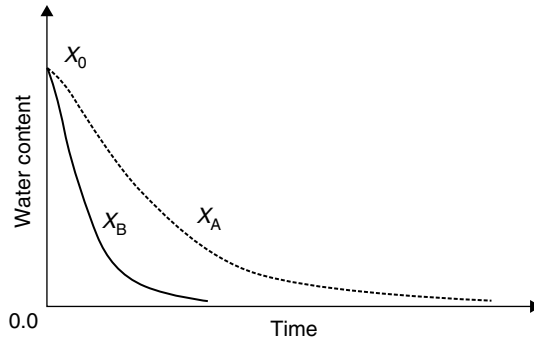


Fig. 3.3 Qualitative illustration of the surface and centre moisture content–time profiles of the same material in Figure 3.2.

(refer to Figure 3.3). It is shown in Figure 3.3 that the surface water content would drop more rapidly than the water content at the centre point. The spatial distribution of water content over the material thickness in the moist food slab would have implications for the deactivation rate of living cells or spores within the matrix.

Living cells are composed of high molecular weight polymeric compounds. These are proteins, nuclei acids, polysaccharides, lipids and other storage materials such as fat, polyhydroxybutyrate and glycogen. These are called biopolymers and are major structural elements of the living cells. A typical microbial cell wall contains polysaccharides, proteins and lipids. The cell cytoplasm contains proteins, which are mostly in the form of enzymes; whilst in eukaryotes, the cell nucleus contains nucleic acids mostly in the form of DNA. Inorganic salts are also a part of the cell content that acts in a crucial way to keep the cell functioning as usual. The macro-molecules can only be functional if they are in their proper three dimensional configurations. The interactions between these molecules are complex. It is known that a living cell may be viewed as a chemical reactor in which more than 2000 reactions take place (Shuler and Kargi, 1992). These interactions can be disturbed or influenced by environmental variations such as changes in pH, humidity and temperature, or chemical composition. For an enzyme, it is known that both pH and temperature have significant effects on their stability. There is a local optimal of the two-parameter space for their highest stability. In severe situations, where the protein molecular structures, for instance, are altered irreversibly (unfolding and aggregation), the functioning of the living cell would cease. Indeed, most of the macro-molecules would change to some extent when subjected to elevated temperatures or extreme pH conditions.

The death of a particular cell is likely to be due to the denaturation of one or more kinds of essential protein, such as enzymes (Bailey and Ollis, 1986). The kinetics for deactivation of individual macro-molecules may make different contributions to the overall ‘cell death’. The environmental parameters such as pH, temperature and water activity all have impacts on this ‘cell death’. Often, these environmental parameters are interdependent. As an example, the temperature needed for coagulation of the egg protein albumin was found to be water content dependent (Bailey and Ollis, 1986). The deactivation process is also influenced by the age distribution of the cell populations.

The thermal stability of micro-organisms is known to be affected by the pH of the food system. Heat-induced changes in protein molecules, cell surface structure and other cell functions are altered with varying pH conditions. Food pH generally ranges from 2 to 9.5.

Table 3.3 Food and its natural pH.

Food	pH
Egg whites	9.5
Shrimps	7.0
Fish	6.0–7.0
Corn	6.0–7.0
Milk	6.5
Melon fruits	6.5
Butter	6.2
Meat	5.1–6.4
Oyster	5.0–6.0
Cheese	5.9
Cabbage	5.5
Potatoes	5.3
Fermented milk	4.5
Tomatoes	4.2
Yoghurt	3.9
Apples	3.0
Lemon	2.0

Table 3.4 Optimum pH for micro-organisms.

Micro-organisms	pH
<i>S. faecalis</i>	6.8
<i>S. aureus</i>	6.5
<i>B. subtilis</i>	7.0–7.5
<i>C. sporogenes</i>	6.6–7.5
<i>C. botulinum</i>	6.7–7.0

Typical pH values for common food materials are listed in Table 3.3, obtained from Enfors (2007). Micro-organisms of different types have different optimal pH values for their highest heat stabilities. The optimal pH range for most micro-organisms tends to be around the neutral pH, but at the slightly acidic range (Xu and Wang, 2005). An optimum pH range for a few micro-organisms is given in Table 3.4. For example, cow's milk has a pH of 6.6, which is ideal for the growth of many micro-organisms. Yeasts can grow in a more acidic environment compared to microbes. Molds are able to grow over a wide range of pH, but slightly acidic conditions are preferable. Enzymes are active over only a restricted range of pH, and exhibit an optimum pH where the activity is maximal. Enzymes usually contain various amino acid residues in their active sites, which are in different states of ionization depending on the concentration of H^+ ions in the micro-environment of enzymes (Bergamasco *et al.*, 2000). The enzymatic activity is directly related to interactions of these sites with other molecules, ions or substrates. Changes in pH significantly alter these active sites and hence the bioactivity of enzymes.

Changes in pH away from the optimal value reduce the thermal stability of micro-organisms or enzymes within a food system. Thermal inactivation of bacteria has been extensively studied for the corresponding kinetics, such as the studies published by Chiruta *et al.* (1997) and Khoo *et al.* (2003). In their work on *Escherichia coli*, they have shown the following first-order

inactivation kinetics model to be useful for constant treatment conditions (temperature T and pH):

$$\ln \frac{N}{N_0} = -k_d t \quad (3.1)$$

where N is the number of the live micro-organisms in suspension (cell m^{-3}), k_d is the inactivation rate constant (s^{-1}) and N_0 is the initial cell concentration (cell m^{-3}). If it was for an enzyme inactivation, N may be replaced by the 'live' enzyme concentration (units m^{-3}). The death-rate constant k_d was expressed using the following formula:

$$\ln k = C_0 + \frac{C_1}{T} + \frac{C_2}{T^2} + C_3 pH + C_4 pH^2 \quad (3.2)$$

where T is the absolute exposure temperature in K. Equation coefficients C_0 , C_1 , C_2 , C_3 and C_4 for inactivation of *E. coli* in Carbopol liquid were reported to be -3613 , 2.44×10^6 , -4.11×10^8 , -1.523 and 0.124 respectively. Experiments on thermal treatments of micro-organisms at different relative humidity (RH) or water activity (a_w) values have revealed a general trend for micro-organisms. The thermal stability (survival of the micro-organisms in the pre-equilibrated food systems) is increased and reaches a peak as the water activity is reduced at the beginning of heat treatment, but the thermal stability is then rapidly reduced as the material is dried to very low water activity levels. This optimal water activity for highest thermal stability is between 0.2 and 0.5.

The drying stage may alter the pH of the food system and cause osmotic imbalance during processing due to water removal and the subsequent increment in the concentration of solutes. Acidic foods tend to get more acidic within the food matrix due to a higher concentration of solutes. Drying would 'fix' the structures of long chain molecules causing irreversible changes in their preferred three-dimensional positions. The effect of fixing may be viewed simply as a 'scaring of the burnt tissue' to make it more visual. When water activity is reduced, there is less available water associated with the cell constituents that are considered to be protective to cell functions, thus reducing the thermal stability of heat-sensitive components. The combination of temperature and water activity is important in determining the extent of deactivation of micro-organisms or denaturation of proteins and enzymes. This phenomenon is interactive and may act synergistically depending on the internal and external circumstances.

The rate of water removal and the temperature rise are more rapid at the surface of a moist material compared to other locations within the food material. Typical water content profiles with respect to drying time for surface and centre locations are shown qualitatively in Figure 3.3. It is expected that the water content distribution and temperature distribution inside the material being dried are both important phenomena for influencing the local rate of micro-organism deactivation. The deactivation of the micro-organisms located at the surface or near the surface would be different from the deactivation rate profiles inside the material. The status of mineral components and the possibility of generating insoluble metal compounds may also have an impact on the availability of bioactivity (Watzke, 1998).

The inactivation of the microbial population in food during drying is dependent on how micro-organisms are distributed within the food matrix. Living cells or active enzymes may be totally encapsulated and stay in the core region of a food material or stay near the boundary region of a food material. The thermal damage to the living cells or active enzymes is also influenced by the food ingredients or additives, which may have protective effects during

drying (Leslie *et al.*, 1995; Zhao and Zhang, 2005; Oldenhof *et al.*, 2005). For instance, addition of trehalose to yeast suspension significantly reduced the damage to the active yeast cells (Bayrock and Ingledew, 1997a,b; Berny and Hennebert, 1991). The protective effect of a specific food additive may vary for different micro-organisms, depending on the type and mode of drying, drying conditions, type and concentration of microbes and the type of food material itself.

It is, to date, a difficult task to correlate the cell death data before and after a drying stage. This is largely due to the complex nature of the inactivation kinetics itself when parameters such as water content and temperature, and often their distribution within the material during drying, have to be taken into account. When the material is of a particulate form, they have complicated trajectories when drying in a spray drier, a pneumatic drier or a fluidized-bed drier. The measurement of various drying and inactivation parameters for moving particles is sometimes impossible. Therefore, formulation and validation of mathematical models for inactivation of micro-organisms or enzymes are complex studies, and are not yet fully established.

Lievense *et al.* (1992) proposed an inactivation kinetics model for degradation of *Lactobacillus plantarum* during drying by considering thermal and dehydration inactivation as two separate influences, but operating simultaneously. The model had ten parameters to be obtained from the experimental work. Measurements of the drying parameters were obtained from the fluidized-bed drying with drying temperatures lower than 50°C. The effective diffusivity concept was used to take into account the spatial moisture distribution. The inactivation parameters were measured from 'non-drying', heating experiments in which an approximately 1 mm thick *L. plantarum* starch granulate was placed in a Petri dish and stored at $5.0 \pm 0.5^\circ\text{C}$ in a vacuum desiccator for 48 h. After 48 h, the glucose fermenting activity and moisture concentrations of the sample were measured. They illustrated in their work that thermal inactivation is insignificant at drying temperatures lower than 50°C. Furthermore, they stated that the dehydration inactivation depends on the reached moisture content of the material only and is independent of the drying rate. However, Lievense *et al.* (1992) did not show if this observation could be true for high-temperature drying processes such as spray drying, where drying rates are much higher.

A similar trend was followed by Yamamoto and Sano (1992), who proposed a five-parameter model for enzyme inactivation during drying using a single suspended droplet drying experiment. A sucrose solution of fixed water content containing different enzymes such as β -galactosidase, glucose oxidase and alkaline phosphatase was incubated at a constant temperature. The thickness of the material used and air temperatures were not reported in the study. The deactivation energy E_d was described as a function of average water content. Again, a binary (water and dissolved solids) diffusion coefficient was introduced to the drying analysis to take care of the water distribution inside the droplet. They concluded that air temperatures and droplet size significantly affect the inactivation rate. The effect of initial water content is shown to be insignificant. The enzyme activity was experimentally measured using constant temperature and constant moisture content heating experiments, where no evaporation was involved. Again, this work may be classified into the pre-equilibration experiments.

In general, inactivation kinetics of micro-organisms during drying has been conventionally expressed using a first-order reaction equation:

$$\frac{d(N/N_0)}{dt} = -k_d(N/N_0) \quad (3.3)$$

Equation (3.3) is sometimes argued to be not the most appropriate kinetics equation for describing the inactivation kinetics. It is believed to be the unstructured model. A structured model which can deal with the non-log-linear behaviour has been developed, especially accounting for the tail ends of the survival curves (Geeraerd *et al.*, 2000). However, the in-process behaviour during an industrial drying process may be considered as a short-time behaviour, so the tailing effect is not very significant. Furthermore, the water removal rate itself introduces the non-log-linear effect when it is incorporated with the inactivation kinetics. Therefore, it should be sufficient to consider the first-order inactivation kinetics for deactivation of bioactive constituents during drying processes.

For micro-organisms distributed in a moist material that is not yet dried (i.e. in a saturated medium), k_d is usually considered to be a function of temperature and is described using the Arrhenius equation (Wijlhuizen *et al.*, 1979; Yamamoto and Sano, 1992; Johnson and Etzel, 1993; Meerdink and Van't Riet, 1995):

$$k_d = k_0 \exp\left(-\frac{E_d}{RT}\right) \quad (3.4)$$

where R is the universal gas constant ($\approx 8.314 \text{ J mol}^{-1} \text{ K}^{-1}$). When the in-drying process is considered, the inactivation kinetics should include the material's temperature and also moisture concentration effects. The water content profile could be significantly non-uniform within the moist material being dried due to the nature of the drying process. In the literature, the temperature dependence of the inactivation rate constant k_d during drying was described using an equation (3.4). The temperature distribution may also have an impact on the local distribution of the inactivation rates. The temperature gradient can be significant if the *Biot* number is quite large ($Bi = hL/k$; h is the convective heat transfer coefficient ($\text{W m}^{-2} \text{ K}^{-1}$) which can be determined similarly to that for h_m ; k is the thermal conductivity of the moist material ($\text{W m}^{-1} \text{ K}^{-1}$)). Usually, a *Bi* of less than 0.1 is considered, beyond which temperature non-uniformity cannot be ignored (Incropera and De Wit, 2002). However, when evaporation takes place, this non-uniformity is damped and even for some large *Bi* values such as 0.5 or 1, a small evaporating water droplet can have a negligible temperature gradient (Chen and Peng, 2005; Patel *et al.*, 2005).

The traditional inactivation kinetics model, equation (3.4), contains only two parameters, k_0 (pre-exponential factor) and E_d (deactivation energy), but this model does not include the moisture content effects. Meerdink and Van't Riet (1995) studied the inactivation of the enzyme α -amylase during droplet drying, describing the deactivation energy parameter (E_d) to be water content dependent. Meerdink and Van't Riet (1995) concluded that the inactivation rate is more sensitive to changes in a material's temperature compared to the drying rate. An approach considered by Meerdink and Van't Riet (1995) is attractive, as it requires only four parameters (a , b , k_0 and E_d) to be obtained from the experimental work. The inactivation rate constant was expressed using the following formula:

$$k_d = k_0 \exp\left(aX - \frac{E_d + bX}{RT}\right) \quad (3.5)$$

where X is the water content on a dry basis. The activation energy (E_d) for inactivation represents the difficulty in deactivating living cells or denaturing proteins and enzymes. Higher activation energy indicates greater difficulty for deactivating micro-organisms or living cells. Table 3.5 shows some typical activation energy values required for deactivation of various

micro-organisms, enzymes and other bioactive substances, which are heat and/or water activity sensitive. The activation energy may change with environmental conditions around living cells such as temperature, water activity, pH and pressure. At higher temperatures, the activation energy may be lower to destroy the functionalities of living cells or enzymes. Teixeira *et al.* (1995) reported that the activation energy for inactivation of *Lactobacillus bulgaricus* at $T > 70^\circ\text{C}$ was 33.5 kJ mol^{-1} , while it was 85.8 kJ mol^{-1} for $T < 70^\circ\text{C}$. The activation energy also depends on the food micro-structure and the state of the bioactive constituent (e.g. encapsulated, immobilized, etc.). For instance, the activation energy for deactivation of peroxidase present in potato, carrot and two varieties of tomatoes were different from the activation energy for the same enzyme present in pumpkin (illustrated in Table 3.5).

In order to show the effect of local water content and temperature during drying, equation (3.5) may be used, assuming this model is valid for both enzyme and cell materials. Equation (3.5) can be further written as:

$$k_d = k_0 e^{aX} \exp\left(-\frac{E_d}{RT} - \frac{bX}{RT}\right) \quad (3.6)$$

As a reference, the parameters of equation (3.6) for inactivation of α -amylase during drying were reported as: $k_0 = 1.2426 \times 10^{32} \text{ (s}^{-1}\text{)}$, $E_d = 247.3 \times 10^3 \text{ (J mol}^{-1}\text{)}$, $a = 121.8 \text{ (J mol}^{-1}\text{)}$ and $b = 341$. The nature of equation (3.6) is such that:

If $a > 0$, $b > 0$, k_d may have a peak value in the water content range considered;

If $a > 0$, $b < 0$, k_d would just reduce as water content decreases;

If $a < 0$, $b > 0$, k_d may have a minimum in the water content range considered.

These possibilities are dependent on the value of model coefficients, which may or may not show the minimum or maximum in the water content range considered. Nevertheless, in order to show the unique effect of drying on the survival of micro-organisms, equation (3.6) should be integrated over the material domain of interest. The first-order kinetics, as in equation (3.3), where $\phi = N/N_0$ is written as below:

$$\frac{d\phi}{dt} = -k_0 e^{aX} \exp\left(-\frac{E_d}{RT} - \frac{bX}{RT}\right) \cdot \phi \quad (3.7)$$

For simplicity, the infinite slab geometry is considered. $x = 0$ is the symmetry of the slab which is symmetrically heated and dried. The derivation procedure is given below. Integrating (3.7) from $x = 0$ to $x = L$, giving the average change in average activity or average cell concentration as:

$$\begin{aligned} \frac{d\bar{\phi}}{dt} &\approx -\frac{k_0}{L} \int_0^L e^{aX} \exp\left(-\frac{E_d}{RT}\right) \exp\left(-\frac{bX}{RT}\right) \cdot \phi \cdot dx \\ &= -\frac{k_0 \bar{\phi}}{L} \int_0^L e^{a(1-(b/RT))X} \exp\left(-\frac{E_d}{RT}\right) dx \end{aligned} \quad (3.8)$$

In this step, the average temperature is chosen for the second term in the exponential function in equation (3.7), so that the effect of water content X and the temperature effect

Table 3.5 Activation energy level for deactivation of heat- and/or water activity-sensitive bio-compound.

No.	Heat- and/or water activity-sensitive component	Activation energy for deactivation (kJ mol ⁻¹)	Reference
1	Lycopene	19.3 ($X \geq 55$) 18.3 ($X \leq 55$)	Goula <i>et al.</i> (2006)
2	Ascorbic acid (Vitamin C)	53.1 (80°C, 1 atm) 68.5 (40°C, 9869 atm)	Polydera <i>et al.</i> (2005)
3	<i>Lactobacillus bulgaricus</i>	33.5 ($T > 70^\circ\text{C}$) 85.8 ($T < 70^\circ\text{C}$)	Teixeira <i>et al.</i> (1995)
4	β -Galactosidase	199.0 (35–55°C)	Zhou and Chen (2001)
5	Amilosobtilin	112.5 (70–90°C)	Sadykov <i>et al.</i> (1997)
6	α -Amylase	199.0 (60–80°C)	Sadykov <i>et al.</i> (1997)
7	Maltavamorin	144.1 (50–65°C)	Sadykov <i>et al.</i> (1997)
8	Gen Seng biomaterial	74.7 (60–95°C)	Sadykov <i>et al.</i> (1997)
9	Riboflavin	21.7 (50–120°C)	Nisha <i>et al.</i> (2005)
10	α -Amylase	247.3 (75–100°C)	Meerdink and van't Riet (1995)
11	<i>Bifidobacterium infantis</i>	38.8 (70–100°C) 26.5 27.1 67.7	Li <i>et al.</i> (2006)
12	<i>Streptococcus thermophilus</i>	39.6 (70–100°C) 34.8 37.8 75.7	Li <i>et al.</i> (2006)
13	Polyphenoloxidase	319.3 (62.5–77.5°C) 363.5	Weemaes <i>et al.</i> (1998)
14	Peroxidase (potato) Peroxidase (carrot)	478 (60–85°C) 480	Anthon and Barrett (2002)
15	Peroxidase (tomato, two varieties)	546 (66–72°C) 557	Anthon <i>et al.</i> (2002)
16	Peroxidase (pumpkin)	86.2 (75–95°C)	Gonçalves <i>et al.</i> (2007)
17	Lipoxygenase (soybean)	485 (70°C)	Liou <i>et al.</i> (1985)
18	Lipoxygenase (tomato dices) Lipoxygenase (tomato extract)	137 (98°C) 147 (90°C)	Anese and Sovrano (2006)
19	<i>Saccharomyces cerevisiae</i> (in water suspensions)	58.4	Huang (2004)
20	<i>Saccharomyces cerevisiae</i> (in skim milk suspensions)	55.3	Huang (2004)
21	<i>Candida sake</i> CPA-1 (yeast) (in skim milk suspensions)	53.88	Abadias <i>et al.</i> (2005)
22	<i>Candida sake</i> CPA-1 (yeast) (skim milk + lactose suspensions)	43.08	Abadias <i>et al.</i> (2005)

can be apparently ‘separated’ for ease of analysis. Equation (3.8) can be further simplified based on the Frank–Kamenetskii transformation (Bowes, 1984) to yield the following:

$$\frac{1}{\bar{\phi}} \frac{d\bar{\phi}}{dt} = -\frac{k_0 e^{(E_d/RT_{ref})}}{L} \int_0^L e^{(a-(b/R\bar{T}))X} e^{\theta} dx \quad (3.9)$$

where

$$\theta = -\frac{E_d}{RT_{ref}^2} (T - T_{ref}) \quad (3.10)$$

In general, industrial drying operations involve reduction in the moisture content of the material during processing, as well as an increase in the temperature of the material. It should be noted that the inactivation rate usually increases with increasing temperature and is reduced with reducing the moisture content. Hence, the overall inactivation is a ‘competitive’ process between the two different inactivation mechanisms. However, the contribution of each inactivation mechanism during processing is not very well understood, although as mentioned earlier, the lowering of the water content has less affect than that of rising temperature. It is an interesting task to discover the controlling inactivation parameter during different phases of a drying process. This information could be very helpful for process design and optimization to achieve a higher ‘kill’ of the unwanted bacteria. The above equation is further written as:

$$\frac{1}{\bar{\phi}} \frac{d\bar{\phi}}{dt} = -\frac{\bar{k}_0}{L} \int_{x=0}^{x=L} \exp(\bar{a}X + \theta) dx \quad (3.11)$$

where $\bar{k}_0 = k_0 e^{E_d/R \cdot T_{ref}}$ and $\bar{a} = (a - (b/R \cdot \bar{T}))$.

By rearranging equation (3.11), one can obtain the following:

$$\frac{1}{\bar{\phi}} \frac{d\bar{\phi}}{dt} = -\frac{\bar{k}_0}{L} \left[\int_{x=0}^{x=L} d(e^{\bar{a}X + \theta}) - \int_{x=0}^{x=L} x d(e^{\bar{a}X + \theta}) \right] = -\frac{\bar{k}_0}{L} \left[e^{\bar{a}X_s + \theta_s} L - \int_{x=0}^{x=L} x d(e^{\bar{a}X + \theta}) \right] \quad (3.12)$$

Introducing a characteristic dimension ($x_c < L$) in such a way that the second integral on the RHS of the above equation can be simplified. This expression further results in a simple formula from equation (3.12) as follows:

$$\frac{1}{\bar{\phi}} \frac{d\bar{\phi}}{dt} = -\frac{\bar{k}_0}{L} [e^{\bar{a}X_s + \theta_s} (L - x_c) + x_c e^{\bar{a}X_0 + \theta_0}] \quad (3.13)$$

The dynamics of the above equation are clearly shown to be dependent upon the surface water content and surface temperature, as well as the progression of the characteristic distance x_c into the droplet/particle or a thin-layer slab as drying proceeds. This characteristic distance may be a fraction of L that would stay relatively constant in the falling drying flux period if the mass transfer process is viewed as a similar process as in the heat conduction situation

considered by van der Sman (2003). In other words, the similarity of the moisture content profile is maintained in this period of drying.

For the case of a thin film of moist food, where the surface and the centre temperature can be considered similar (i.e. $\theta_s \approx \theta_0$), equation (3.13) can be further re-written as:

$$\frac{1}{\bar{\phi}} \frac{d\bar{\phi}}{dt} \approx -\frac{\bar{k}_0}{L} [e^{\bar{a}X_s}(L - x_c) + x_c e^{\bar{a}X_0}] \cdot e^{\theta_0} \quad (3.14)$$

This expression illustrates that the dynamics of the inactivation kinetics is determined by both the surface and the centre water content. When the drying kinetics is modelled using a common lumped-parameter model – where the rate is expressed as a function of the mean water content – the different, but perhaps significant, roles played by the surface and the centre water content cannot be addressed. This is interesting information and it is argued that the moisture distribution effect can be significant depending on how quickly the water content is distributed. The apparent ‘drying rate dependent inactivation model’ has been found to be a useful correlation if one has used the lumped-parameter model to describe the bulk behaviour of inactivation for constant drying conditions (Li *et al.*, 2006). Chen and Patel (2006) have illustrated that the drying rate dependency is a reasonable approach by deriving the rate dependency from equation (3.14).

All these studies have shown that even if the cells are uniformly distributed in the porous media to be dried, the local water content can be influential to the average inactivation rate. If the initial cell distribution in a product to be dried is not uniform, it is likely that the uneven distribution will affect the rate of average cell concentration reduction in the industries.

If the local rate of deactivation, such as that described by equation (3.5), can be found independently through constant water content and temperature experiments, the local water content distribution should be resolved for process simulation and optimization purposes for either protecting or deactivating bioactive constituents during drying. Often, the local water moisture content is predicted using a Fickian-type effective liquid diffusion model as described in Chapter 1. The spatial distribution of temperature can also be resolved using the energy equations given in Chapter 1. This approach can be found in many previous studies (Chen, 2006b). In addition, the local concentration of bacteria across the material being dried is also essential to make this approach valid.

3.4 FOOD BIO-DETERIORATION BY DRYING – A SUB-CELL LEVEL APPROACH

The living microbial cell may be considered an individual sample. The drying process around each cell boundary should be a topic of interest now, in order to understand the effects of evaporation on various cell components. The micro-structure of the microbial cell should play a role in its response to heat, pH, water removal and life threatening pressure. Living cells with different shapes, sizes and structures may respond differently to drying-induced stress. To date, the mathematical analysis for drying-induced inactivation of living cells has not been performed at the microscopic level that may consider inactivation of individual components of the living cells.

Considering extensive development of the cell level or even bio-molecular level understanding, it may be possible now to study how individual components in each micro-organism

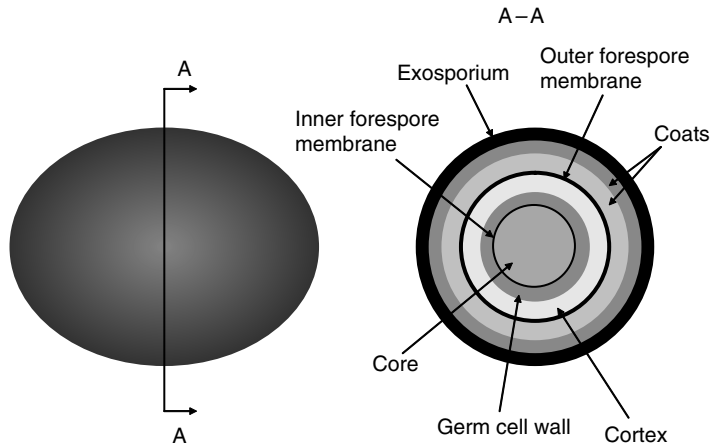


Fig. 3.4 Schematic diagrams for micro-structure of a typical spore and its cross-section (A–A).

denature or deactivate, and how their ‘weighted’ contribution to the overall inactivation kinetics may be revealed. Making an analogy to the death of an animal due to certain organ failures, the loss of the organ functions may interact to cause the ‘overall’ death. Deterioration of one organ to some extent and by itself may not be life threatening, its interactions with other neighbouring organs may trigger an overall deterioration. Cumulatively and/or interactively, the reduction in their activities may lead to the ultimate death.

For spore-forming bacteria, after sporulation, the resulting organism is extremely resistant to both physical or chemical external attacks. The resistance is due to the high degree of compartmentalization. Hendrickx and Knorr (2001) have shown simplified structures of bacterial spores, as in Figure 3.4. The small spore, for instance the one illustrated in Figure 3.4, can be considered isothermal as soon as the fluid around the spore is heated up. The heat would penetrate quickly through various layers. If a chemical invasion is the main mechanism to ‘kill’ the spore, the time for ‘failure’ of various critical bits of the structure, which are located at different radial planes, would be longer compared to thermal inactivation.

For deactivating the microbial cell, the rate expression of population change may be written as:

$$\frac{dN}{dt} = - \sum_1^I \xi_i \cdot \varepsilon_i \quad (3.15)$$

where I is the total number of components that are influential to the survival of the micro-organism of concern and ξ_i is the weighting factor for each contributing component. The parameter ε_i is the residual activity of each component such as enzymes, proteins, vitamins, etc. The residual activity of each component is determined by its own inactivation kinetics. If the inactivation kinetics models are considered as having the same format as equation (3.9):

$$\frac{d\varepsilon_i}{dt} = -k_{d,i} \cdot \varepsilon_i \quad (3.16)$$

The sum of ξ_i is unity. Equation (3.16) assumes no inactivation between the sensitive components. An interactive type of deactivation model can also be formulated where the activities

can multiply. For simplicity, where only two components in a cell are of prime interest, the inactivation model for the overall death may be expressed as:

$$\frac{dN}{dt} = -\xi_1 \cdot \varepsilon_1 \cdot \varepsilon_2 \quad (3.17)$$

Equation (3.17) shows that ε_1 and ε_2 are interactive parameters contributing to the overall cell death. Parameters ε_1 and ε_2 may be evaluated in a similar way as shown by equation (3.16). Similarly, the model for the overall cell death can be formulated for multiple bioactive components, which may undergo physical, chemical or microbial changes during processing. This kind of modelling approach may lead to a more detailed understanding for controlling food spoilage or deterioration during in-process and post-process stages.

3.5 CONCLUDING REMARKS

Drying operations would ideally be operated in such a way that useful bacteria and nutrients could be preserved during processing, yet harmful micro-organisms be deactivated. The thermal efficiency of the operation has to be higher during processing, and often this is not possible. The activity of bioactive compounds is influenced during pre-drying and post-drying processes in addition to in-drying processes. Deactivation is a complex phenomenon that requires assessment of the residual activity before and after each processing step. The pre-determined availability of nutrients or desired level of activity of harmful micro-organisms can be achieved by controlling the activity of targeted bioactive constituents during pre-drying, in-drying and post-drying processes. Drying-induced changes can cause deterioration of the food products during two main processes, which are in-drying and post-drying stages. Deterioration of foodstuffs during post-process stages is well documented and better understood compared to in-drying processes. Drying, which is the 'in-process stage', can be treated as a thermal treatment procedure, which can deactivate micro-organisms and other bioactive compounds such as proteins, enzymes, vitamins, carbohydrate and fat matrixes of different proportions, which are distributed or imbedded in the food matrix.

The process of inactivation is dependent on the cell structure, composition, interactions with water and their responses to temperature and water activity changes. The average inactivation rate of micro-organisms is dependent on the temperature and water content history of the food system during drying. The inactivation rate for various bioactive compounds is also affected by the spatial distributions of temperature and water content within the food matrix which are responsible for different heat and mass transfer properties at different regions of the food matrix. Spatial distributions of water content and temperature within a food matrix depend on the food composition, micro-structure and the physical size of the food. Distribution of micro-organisms or nutrients, which is also key to understanding detailed modelling for inactivation kinetics, is not yet fully understood. Furthermore, different components of a single cell may have different responses to heat and water changes or to drying-induced stresses. A sub-cell level understanding for the cause of overall cell death could be a useful tool for developing a micro-structure-based deactivation approach. Scope for more fundamental research in this area still exists in order to achieve better control over the inactivation rate during drying operations.

3.6 NOTATION

a	fitting parameter
\bar{a}	fitting parameter
a_w	water activity
b	fitting parameter
Bi	Biot number (heat-transfer based)
E_d	apparent activation energy, J mol^{-1}
h	heat transfer coefficient, $\text{W m}^{-2} \text{K}^{-1}$
I	total number of components
k	thermal conductivity of food material, $\text{W m}^{-1} \text{K}^{-1}$
k_0	pre-exponential factor, s^{-1}
\bar{k}_0	fitting parameter
k_d	inactivation rate constant, s^{-1}
L	thickness of the slab or film, m
N	concentration of the live micro-organism, cell m^{-3}
N_0	initial number of the live micro-organism, cell m^{-3}
R	universal gas constant, $\text{J mol}^{-1} \text{K}^{-1}$
t	time, s
T	temperature, K
x	distance within a food slab, m
x_c	characteristic radius, m
X	water content on a dry basis, kg water per kg dry solids
X_0	centre water content of the food slab, kg water per kg dry solids

Greek symbols

ε	residual activity
ξ	weighing factor
ϕ	concentration ratio ($=N/N_0$)
θ	dimensionless temperature

Subscripts

i	individual component
s	surface conditions
ref	reference conditions

REFERENCES

- Abadias, M., Teixido, N., Usall, J., Solsona, C. and Vinas, I. (2005) Survival of the postharvest biocontrol yeast *Candida sake* CPA-1 after dehydration by spray-drying. *Biocontrol Science and Technology*, **15**(8), 835–846.
- Abellana, M., Magri, X., Sanchis, V. and Ramos, A.J. (1999) Water activity and temperature effects on growth of *Eurotium amstelodami*, *E. chevalieri* and *E. herbariorum* on a sponge cake analogue. *International Journal of Food Microbiology*, **52**(1–2), 97–103.
- Anese, M. and Sovrano, S. (2006) Kinetics of thermal inactivation of tomato lipoxygenase. *Food Chemistry*, **95**(1), 131–137.

- Anthon, G.E. and Barrett, D.M. (2002) Kinetic parameters for the thermal inactivation of quality-related enzymes in carrots and potatoes. *Journal of Agricultural and Food Chemistry*, **50**(14), 4119–4125.
- Anthon, G.E., Sekine, Y., Watanabe, N. and Barrett, D.M. (2002) Thermal inactivation of pectin methyl-esterase, polygalacturonase, and peroxidase in tomato juice. *Journal of Agricultural and Food Chemistry*, **50**(21), 6153–6159.
- Aversa, M., Curcio, S., Calabrò, V. and Iorio, G. (2007) An analysis of the transport phenomena occurring during food drying process. *Journal of Food Engineering*, **78**(3), 922–932.
- Bailey, J.B. and Ollis, D.F. (1986) *Biochemical Engineering Fundamentals*. McGraw-Hill Book Company, New York.
- Bayrock, D. and Ingledew, W.M. (1997a) Fluidized bed drying of baker's yeast: Moisture levels, drying rates and viability changes during drying. *Food Research International*, **30**(6), 407–415.
- Bayrock, D. and Ingledew, W.M. (1997b) Mechanism of viability loss during fluidized bed drying of baker's yeast. *Food Research International*, **30**(6), 417–425.
- Bergamasco, R., Bassetti, F.J., de Moraes, F.F. and Zanin, G.M. (2000) Characterization of free and immobilized invertase regarding activity and energy of activation. *Brazilian Journal of Chemical Engineering*, **17**(4–7), 873–880.
- Berny, J.F. and Hennebert, G.L. (1991) Viability and stability of yeast cells and filamentous fungus spores during freeze drying: Effects of protectants and cooling rates. *Mycologia*, **83**, 805–815.
- Beuchat, L.R. (1981) Microbial stability as affected by water activity. *Cereal Foods World*, **26**(7), 345–349.
- Bone, D.P. (1987) Practical applications of water activity and moisture relations in foods. In: *Water Activity: Theory and Applications to Food* (eds L.B. Rockland and L.R. Beuchet). Marcel Dekker Inc., New York, USA, p. 369.
- Booth, I.R. (1998) Bacterial responses to osmotic stress: Diverse mechanisms to achieve a common goal. In: *The Properties of Water in Foods, ISOPOW 6* (ed. D.S. Reid), Blackie Academic & Professional, London, pp. 456–485.
- Bowes, P.C. (1984) *Self-heating Evaluating and Controlling the Hazards*. Amsterdam: Elsevier Science, pp. 26–27.
- Caurie, M. (1983) Raoult's law, water activity and moisture availability in solutions. *Journal of Food Science*, **48**, 648–649.
- Chen, P. and Pei, D.C.T. (1989) A mathematical model of drying processes. *International Journal of Heat and Mass Transfer*, **32**(2), 297–310.
- Chen, X.D. (2006a) Guest editorial on drying and microstructure. *Drying Technology*, **24**, 121–122.
- Chen, X.D. (2006b) Moisture diffusivity in food and biological materials. Plenary Keynote at *15th International Drying Symposium (IDS 2006)*, Budapest, Hungary, 20–23 August, 2006 (on CD Rom).
- Chen, X.D. and Patel, K.C. (2006) Micro-organism inactivation during drying of small droplets or thin-layer slabs – A critical review of existing kinetics models and an appraisal of the drying rate dependent model. *Journal of Food Engineering*, **82**, 1–10.
- Chen, X.D. and Peng, X. (2005) Modified *Biot* number in the context of air-drying of small moist porous objects. *Drying Technology*, **23**(1–2), 83–103.
- Chiruta, J., Davey, K.R. and Thomas, C.J. (1997) Thermal inactivation kinetics of three vegetative bacteria as influenced by combined temperature and pH in a liquid medium. *Transactions of the IChemE (Part C)*, **75**, 174–180.
- Christian, J.H.B. (2000) Drying and reduction in water activity. In: *The Microbiological Safety and Quality of Food* (eds B.M. Lund, A.C. Baird-Parker and G.W. Gauld). Aspen, Gaithersburg, MD.
- Corry, J.E.L. (1974) The effect of sugars and polyols on the heat resistance of *Salmonellae*. *Journal of Applied Bacteriology*, **37**, 31–43.
- Corry, J.E.L. (1976) The effect of sugars and polyols on heat resistance and morphology of osmophilic yeasts. *Journal of Applied Bacteriology*, **40**, 269–276.
- Enfors, S.-O. (2007) Lecture notes, Food spoilage: The ecological basis. KTH Biotechnology, Albanova University Center, Sweden, Retrieved on 10th May 2007, Retrieved from: http://www.biotech.kth.se/courses/gru/courselist/3A1315/Downloads%20copy/Livsmedelsmikro/1_EcologyBasis.pdf
- Fennema, O.R. (1996) *Food Chemistry*, 3rd edn. Marcel Dekker Inc., New York, USA.

- Geeraerd, A.H., Herremans, C.H. and Van Impe, J.F. (2000) Structural model requirements to describe microbial inactivation during a mild heat treatment. *International Journal of Food Microbiology*, **59**, 185–209.
- Gibbs, P. and Gekas, V. (2001) Nelfood library online document, water activity and microbiological aspects of foods: A knowledge base. Retrieved on 5th of May 2007, Retrieved from: <http://www.nelfood.com/help/library/nelfood-kb02.pdf>
- Gonçalves, E.M., Pinheiro, J., Abreu, M., Brandão, T.R.S. and Silva, C.L.M. (2007) Modelling the kinetics of peroxidase inactivation, colour and texture changes of pumpkin (*Cucurbita maxima* L.) during blanching. *Journal of Food Engineering*, **81**(4), 693–701.
- Goula, A.M., Adamopoulos, K.G., Chatzidakis, P.C., and Nikas, V.A. (2006) Prediction of lycopene degradation during a drying process of tomato pulp. *Journal of Food Engineering*, **74**(1), 37–46.
- Hardy, J., Scher, J. and Banon, S. (2002) Water activity and hydration of dairy powders. *Lait*, **82**, 441–452.
- Hendrickx, M.E.G. and Knorr, D. (eds) (2001) *Ultra High Pressure Treatments of Foods*. Kluwer Academic/Plenum Publishers, New York.
- Huang, H. (2004) Experimental and theoretical investigation of the inactivation of yeast drying. *Master Thesis*, University of Auckland, New Zealand.
- Incropera, F.P. and DeWitt, D.P. (2002) *Fundamentals of Heat and Mass Transfer*, 4th and 5th edn. John Wiley & Sons, New York.
- Johnson, J.A.C. and Etzel, M.R. (1993) Inactivation of lactic acid bacteria during spray drying. *AIChE Symposium Series*, **297**(89), 98–107.
- Keey, R.B. (1992) *Drying of Loose and Particulate Materials*. Hemisphere Publishing Corporation, New York.
- Khoo, K.Y., Davey, K.R. and Thomas, C.J. (2003) Assessment of four model forms for predicting thermal inactivation kinetics of *Escherichia coli* in liquid as affected by combined exposure time, liquid temperature and pH. *Transactions of the IChemE (Part C)*, **81**, 129–137.
- Kirk, J.R. (1981) Influence of water activity on stability of vitamins in dehydrated foods. In: *Water Activity: Influences on Food Quality* (eds Rockland, L.B. and Stewart, G.F.). Academic Press, New York, USA.
- Labuza, T.P. (1975) Oxidative changes in foods at low and intermediate moisture levels. In: *Water Relations of Foods* (ed. Duckworth, R.B.). Academic Press, New York, pp. 455–474.
- Labuza, T.P. (1977) The properties of water in relationship to water binding in foods: A review. *Journal of Food Processing and Preservation*, **1**, 167–190.
- Leslie, S.B., Israeli, E., Lighthart, B., Crowe, J. H. and Crowe, L.M. (1995) Trehalose and sucrose protect both membranes and proteins in intact bacteria during drying. *Applied and Environmental Microbiology*, **61**(10), 3592–3597.
- Li, X., Lin, S.X.Q., Chen, X.D., Chen, L. and Pearce, D. (2006) Inactivation kinetics of probiotic bacteria during the drying of single milk droplets. *Drying Technology*, **24**(6), 695–701.
- Li Cari, J.J. and Potter, N.N. (1970) Salmonellae survival during spray drying and subsequent handling of skim milk powder. *Journal of Dairy Science*, **53**(7), 871–876.
- Lievens, L.C., Verbeek, M.A.M., Taekema, T., Meerdink G. and Van't Riet, K. (1992) Modelling the inactivation of *Lactobacillus plantarum* during a drying process. *Chemical Engineering Science*, **47**(1), 87–97.
- Lilley, T.H. and Sutton, R.L. (1991) The prediction of water activities in multicomponent systems. In: *Water Relationships in Food*. Plenum Press, New York, pp. 291–304.
- Liou, J.K., Luyben, K.Ch.A.M. and Bruin, S. (1985) A simplified calculation method applied to enzyme inactivation during drying. *Biotechnology and Bioengineering*, **27**, 109–116.
- Meerdink, G. and Van't Riet, K. (1995) Prediction of product quality during spray drying. *Transactions of the IChemE (Part C): Food and Bioproduct Processing*, **73**, 165–170.
- Monsan, P. and Combes, D. (1986) Effect of water activity on enzyme action and stability. *Journal of Food Science*, **434**(1), 48.
- Murrell, W.G. and Scott, W.J. (1966) Heat resistance of bacterial spores at various water activities. *Journal of General Microbiology*, **43**, 411–425.
- Nisha, P., Singhal, R.S. and Pandit, A.B. (2005) A study on degradation kinetics of riboflavin in spinach (*Spinacea oleracea* L.). *Journal of Food Engineering*, **67**(4), 407–412.

- Oldenhof, H., Wolkers, W.F., Fonseca, F., Passot, S.P. and Marin, M. (2005) Effect of sucrose and maltodextrin on the physical properties and survival of air-dried *Lactobacillus bulgaricus*: An *in situ* Fourier transform infrared spectroscopy study. *Biotechnology Progress*, **21**(3), 885–892.
- Patel, K.C., Chen, X.D. and Kar, S. (2005) The temperature uniformity during air drying of a colloidal liquid droplet. *Drying Technology*, **23**(12), 2337–2367.
- Polydera, A.C., Stoforos, N.G. and Taoukis, P.S. (2005) Quality degradation kinetics of pasteurised and high pressure processed fresh Navel orange juice: Nutritional parameters and shelf life. *Innovative Food Science and Emerging Technologies*, **6**(1), 1–9.
- Reyes, A., Alvarez, P.I. and Marquardt, F.H. (2002) Drying of carrots in a fluidized bed. I. Effects of drying conditions and modeling. *Drying Technology*, **20**(7), 1463–1483.
- Roa, V. and Tapia, M.S. (1998) Estimating water activity in systems containing multiple solutes based on solute properties. *Journal of Food Science*, **63**, 559–564.
- Rockland, L.B. and Beuchat, L.R. (eds) (1987) *Water Activity – Theory and Applications to Food*. Marcel Dekker Inc., New York, USA.
- Roos, Y.H. (2002) Importance of glass transition and water activity to spray drying and stability of dairy powders. *Lait*, **82**, 475–484.
- Ross, K.D. (1975) Estimation of water activity in intermediate moisture foods. *Food Technology*, **39**, 26–34.
- Sadykov, R.A., Pobedimsky, D.G. and Bakhtiyarov, F.R. (1997) Drying of bioactive products: Inactivation kinetics. *Drying Technology*, **15**(10), 2401–2420.
- Scott, W.J. (1957) Water relations of food spoilage microorganisms. *Advances in Food Research*, **7**, 83–127.
- Shi, M. and Wang, X. (2004) Investigation on moisture transfer mechanism in porous media during rapid drying process. *Drying Technology*, **22**(1–2), 111–122.
- Shuler, M.L. and Kargi, F. (1992) *Bioprocess Engineering – Basic Concepts*. Prentice-Hall, Englewood Cliffs, NJ.
- Simal, S., Garau, M.C., Femenia, A. and Rossell, C. (2006) A diffusional model with a moisture-dependent diffusion coefficient. *Drying Technology*, **24**(11), 1365–1372.
- Sun, Q., Senecal, A., Chinachoti, P. and Faustman, C. (2002) Effect of water activity on lipid oxidation and proteins solubility in freeze-dried beef during storage. *Journal of Food Science*, **67**(7), 2512–2516.
- Teixeira, P.C., Castro, M.H. and Kirby, R.M. (1995) Death kinetics of *Lactobacillus bulgaricus* in a spray drying process. *Journal of Food Protection*, **57**(8), 934–936.
- Van der Sman, R.G.M. (2003) Simple model for estimating heat and mass transfer in regular-shaped foods. *Journal of Food Engineering*, **60**, 383–390.
- Watzke, H.J. (1998) Impact of processing on bioavailability examples of minerals in foods. *Trends in Food Science and Technology*, **9**, 320–327.
- Weemaes, C.A., Ludikhuyze, L.R., Van den Broeck, I., Hendrickx, M.E. (1998) Effect of pH on pressure and thermal inactivation of avocado polyphenoloxidase: A kinetic study. *Journal of Agricultural and Food Chemistry*, **46**(7), 2785–2792.
- Welti-Chanes, J., Vergara-Balderas, F. and Bermúdez-Aguirre, D. (2005) Transport phenomena in food engineering: Basic concepts and advances. *Journal of Food Engineering*, **67**(1–2), 113–128.
- Wijlhuizen, A.E., Kerkhof, P.J.A.M. and Bruin, S. (1979) Theoretical study of the inactivation of phosphatase during spray drying of skim milk. *Chemical Engineering Science*, **34**(5), 651–660.
- Xu, H. and Wang, Y. (2005) *New Food Sterilization Technologies*. Scientific and Technical Documents Publishing House, Beijing (ISBN 7-5023-4955-3).
- Yamamoto, S. and Sano, Y. (1982) Drying of enzymes: Enzyme retention during drying of a single droplet. *Chemical Engineering Science*, **47**(1), 177–183.
- Yusheng, Z. and Poulsen, K.P. (1988) Diffusion in potato drying. *Journal of Food Engineering*, **7**(3), 249–262.
- Zhao, G. and Zhang, G. (2005) Effect of protective agents, freezing temperature, rehydration media on viability of malolactic bacteria subjected to freeze-drying. *Journal of Applied Microbiology*, **99**(2), 333–338.
- Zhou, Q.Z.K. and Chen, X.D. (2001) Effects of temperature and pH on the catalytic activity of the immobilized β -galactosidase from *Kluyveromyces lactis*. *Biochemical Engineering Journal*, **9**(1), 33–40.
- Zogzas, N.P., Maroulis, Z.B. and Marinou-Kouris, D. (1996) Moisture diffusivity data compilation in foodstuffs. *Drying Technology*, **14**(10), 2225–2253.

4 Spray drying of food materials – process and product characteristics

Bhesh R. Bhandari, Kamlesh C. Patel and
Xiao Dong Chen

4.1 INTRODUCTION

Spray drying is a common unit operation to convert liquid materials into powders for preservation, ease of storage, transport and handling and other economic considerations. The concept of spray drying was first recorded in a patent by Samuel Perry in 1872. This process was introduced for commercial purposes in the 1920s, and spray drying was fully established on a large-scale basis in the early 1980s (Masters, 1991, 2004). Now, spray drying is a common practice in the food and dairy industries to make powders for capturing bioactive components and nutrients for a longer period of time. Besides the food and dairy industries, spray drying is used by many other industrial sectors such as the pharmaceutical, agrochemical, light and heavy chemicals, detergent, pigment, biotechnology and ceramic. Among all food industries, the dairy industry is the largest sector to use spray drying for converting liquid milk and other milk-based products into a powder form. One of the unique characteristics of this process is that the production capacity of the spray drier can be as low as a few hundred grams of powder per hour, up to several tons per hour. The final product could be free-flowing powder of individual particles, agglomerates or granules. The main advantages of spray drying processes over other drying processes are listed in Table 4.1. Since this unit operation provides a flexible and economical production approach and offers many advantages to the manufacturer, over 20 000 spray driers are employed around the world for large-scale production of various powders (Mujumdar, 2004).

In spite of huge research and development progress, the energy requirement for spray drying operations is even now relatively high compared to other dehydration processes. The high-energy requirement is due to the fact that there is no mechanical dewatering involved during spray drying, since the majority of the water is removed using thermal energy only. The energy consumption for the evaporation of water during spray drying is reported to be 1.5 to 2 times higher than the expected latent heat of water evaporation ($\approx 2250 \text{ kJ kg}^{-1}$). A comparison of energy consumption for various dehydration processes is depicted in Table 4.2. Freeze drying is a more energy-intensive operation compared to spray drying. The spray drier, being a convective drier, has a poor thermal efficiency unless very high inlet drying gas temperatures are used. The concentrated feed must be pumpable in order to dry. An exhaust gas stream from the drying chamber contains large amounts of low-grade waste heat, which is very difficult and expensive to recover at this stage due to the presence of particles in the stream. Another limitation of the spray drying operation is the high installation costs involved in setting up the plant.

Table 4.1 Key advantages of spray drying.

1. Dried products of predetermined characteristics (size, density, moisture content and nutrients content) and types (fine powders, granules and agglomerates) can be produced.
2. Powder quality remains constant throughout the entire production run when drying conditions are held constant.
3. Powders with a narrow size distribution can be achieved.
4. Dried products are ready for packaging – no additional grinding is required.
5. Both heat-sensitive and heat-resistive liquid materials can be processed without a significant damage to the product.
6. Heat-spoilage to the product is relatively small due to short exposure times in a hot environment, cooling effects in a critical drying period and also due to the solvent removal at temperatures lower than the normal boiling point.
7. Versatile process – same equipment can be used to dry a wide range of liquid materials.
8. Continuous operation – high production rates (over 25 tons powder per hour per drier) – economical process.
9. Operation and maintenance of the plant can be fully automated.
10. Vast knowledge has been established to characterize different phenomena of spray drying using various mathematical models and computational tools.

Table 4.2 Indicative energy consumption of various dehydration processes.

Processes	Energy consumption (kJ per kg water evaporation)
Membrane processes	1400
Evaporator (six effects with thermo compression)	220
Freeze drying	>>6000
Drum drying	2800–6000
Spray drying process	
Single effect	5000
Integrated with fluidized bed	3500

Source: Filkova and Mujumdar (1995) and Straatsma (1990).

4.2 BASIC CONCEPTS OF SPRAY DRYING

Spray drying involves formation of droplets from the bulk liquid followed by the removal of moisture from the liquid droplets. The material in the liquid state is sprayed in the drying chamber, where the low-humidity hot gas (drying gas/medium) is mixed with the dispersed droplets. The spray of individual droplets is produced by the rotary wheel/disc atomizers, pressure nozzle or pneumatic-type atomizers. The atomizer is generally located at the top-centre of the drying chamber for most spray drying operations. The moisture, in the form of vapor, quickly evaporates from the suspended droplets due to simultaneous and fast heat and mass transfer processes. Spray drying is thus often referred to as a suspended droplet/particle processing technique. Drying of the droplets continues inside the drying chamber until the desired particle characteristics are achieved. The final dried product is produced using a single-stage drying process, schematically shown in Figure 4.1, for small to medium-scale spray drying operations. Separation of the dried particles from the drying gas and their subsequent collection take place in external equipment such as cyclones and/or bag-filter houses.

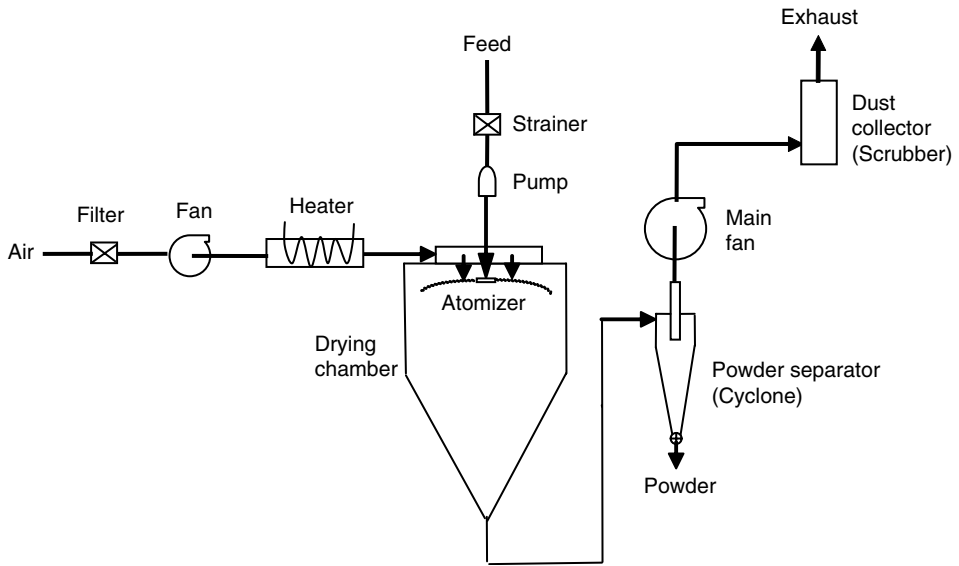


Fig. 4.1 A schematic diagram of a single-stage spray drying system.

Modern large-scale spray driers are often equipped with internal and/or external fluid-beds, which may be used for second-stage drying, cooling, agglomeration, granulation and/or coating of particulate materials. The rapid acceptance of the multi-stage drying technology has been due to the production of free-flowing and dust (very fine particles)-free powders, the contribution to economy improvement and the successful scale-up procedures. Extremely small particles (fines) are usually recovered from the cyclones, filter houses and fluidized-bed driers, and are sent to the top of the drying chamber for mixing with the freshly produced droplets. Mixing of fine particles with fresh droplets is beneficial where agglomerates are of interest. The exhaust drying gas from the cyclone or filter house is discharged to the environment. Many times, scrubbers are installed to recover fines from the exhaust drying gas in order to meet environmental laws for minimizing pollution.

Spray drying can also be considered as an air humidification process. At ideal adiabatic conditions (assuming no heat losses), the temperature of the dry air during moisture evaporation will be reduced but the heat content of the air (dry air + vapor) will remain constant. The increased water vapor present in the air carries the lost energy from the dry air. Therefore, the temperature of the air follows an isenthalpic line during the cooling down period (Figure 4.2).

To produce a hot drying medium, the ambient air (at $T_{ambient}$) is heated to the desired temperature (T_{inlet}). In modern spray driers, the hot air stream is mixed with a cooling air stream (to keep the atomizer temperature at a low value) and a recycled air stream (containing fine particles) which is relatively cold. Therefore, the temperature of the hot air stream is usually kept slightly higher than the temperature required at the atomizer zone. During this heating, the absolute humidity of the air remains constant while its vapor pressure (relative humidity) is reduced to a very low value (near zero). When the psychrometric chart is referred to (as presented in Figure 4.2), moisture can be evaporated until the air is saturated to its dew-point (following the isenthalpic line). However, the water activity of the dried product is normally reduced to less than 0.2; therefore the relative humidity of the air is maintained below 20% RH to reach the desired level of water activity. The outlet air temperature (T_{outlet}),

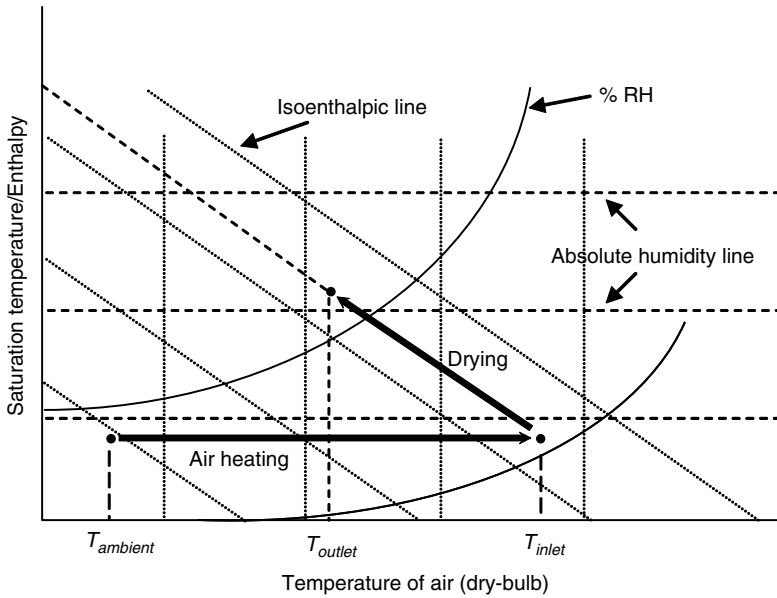


Fig. 4.2 A psychrometric illustration of drying air (ideal adiabatic condition) in a spray drying process.

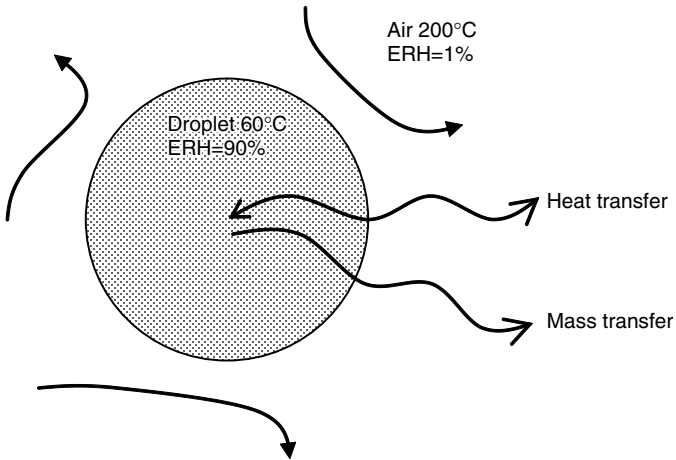


Fig. 4.3 A schematic diagram for drying of a single droplet where the drying rate decreases with reducing the temperature and vapor pressure (relative humidity) depressions.

which is controlled by the liquid flow, is regulated to keep the moisture or water activity of the product at the desired level. At the end of the drying, the drying gas and the dried product can approach an equilibrium state. Therefore, the temperature of the product can be slightly lower than the outlet air temperature, whereas the vapor pressure of the water in the product can be slightly higher than the vapor pressure of the water in the air. For example, if the outlet air humidity is 15%, the water activity of the product at the exit can be fixed at 0.2.

The rate of evaporation during spray drying is influenced by the temperature and vapor pressure differences between the surface of the droplets and the drying gas (Figure 4.3). The

other important factors influencing the heat and mass transfer rates are diffusivity of water in air, relative velocity of droplet with respect to drying gas and the kinematic viscosity, the conductivity and heat capacity of air. The water can be diffused to the surface by the bulk liquid mobility or the vapor diffusion, depending on the feed type, physical form, composition, concentration, solvent type and drying medium conditions. The diffusion of water can be accompanied by the diffusion of certain solutes towards the surface of the droplets. This means that in a complex food system, certain components can be at higher concentrations towards the surface than at the centre of the droplets. During the earlier stages of drying, when the material moisture content is high, the liquid water diffusion mechanism dominates, whereas at low moisture content there might be both liquid diffusion and vapor diffusion or only vapor diffusion, depending on the type and other physical characteristics of the material being dried (Kundu *et al.*, 2005; Zhang and Datta, 2004). The conversion of the liquid droplet to the dried particle is accompanied by an approximate weight loss of 50% (due to loss of water) and volume loss of 25% (due to shrinkage).

4.3 COMPONENTS OF A SPRAY DRYING SYSTEM

A schematic diagram of a typical single-stage spray drier is presented in Figure 4.1. A typical spray drier should consist of at least four main components, which are:

1. drying gas supply and heating system
2. atomization system
3. drying chamber
4. powder separators

Depending on the drier design, the number of stages and the drying mode, there could be additional drying components such as a fluidized-bed drier, belt drier, etc. Evaporators and fluidized-bed driers are other key equipment used before and after spray drying respectively, and are briefly discussed later in this chapter. It should be noted that the fluidized-bed drier could be internally integrated with the spray drier, and it could be quoted as a part of a two-stage spray drying system.

4.3.1 Drying gas supply and heating system

In most food-related spray drying operations, ambient air is used as a drying medium. Superheated steam may be used where oxygen could be an objectionable element, although the heat damage to the food product could be more severe when using superheated steam as a drying gas. Normally, ambient air is drawn with the help of centrifugal fan(s) through an air filter system. An air-supply fan is usually fitted prior to the air heater. The air could be heated from 150°C to 270°C for drying of various liquid-based food materials. The absolute humidity of hot air at the inlet of the drier usually varies from 4 to 8 g water per kg of dry air, depending on the weather pattern in a specific region. Hot air with higher humidity (higher than 8 g water per kg of dry air) may result in a dried product with a slightly higher moisture content. For high humidity air drying, other process parameters have to be adjusted in order to compensate for the humidity changes and achieve a final product with the desired moisture content. An air dehumidification unit could be installed prior to heating of air in order to produce a very low humidity drying gas. In fact, low humidity drying may allow use of lower

inlet air temperatures for achieving the same evaporation capacity as the drying process that involves high air temperatures and ambient humidity. The cost and product analysis have to be studied in detail before applying the concept of using low humidity air to drying of specific food systems.

The air can be heated using a direct-contact or an indirect-contact system. Electrical, steam, oil-fired or gas heaters are used for heating air, depending on the size of the drier, the product characteristics and the availability and economics of the energy source. Application of a combination of heating methods such as steam and electrical heating is also common. An exhaust fan is usually mounted after the cyclone. The exhaust fan is normally operated at a higher power than that of the air-supply fan in order to compensate for the pressure drop in the drying chamber, ducts and cyclones. The air pressure in the drying chamber is, therefore, slightly lower than the atmospheric pressure. A lower pressure helps to avoid leakage of product/air from the drier. The hot air enters the drying chamber through an air disperser to provide a homogeneous flow of air and the effective mixing of hot air with droplets inside the chamber.

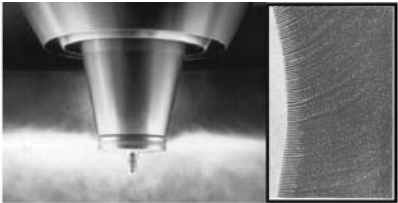

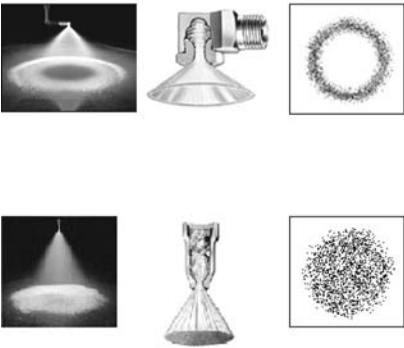

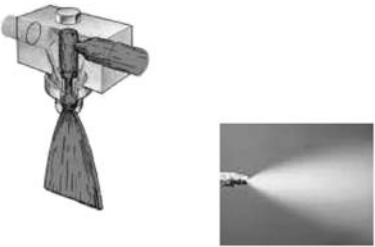

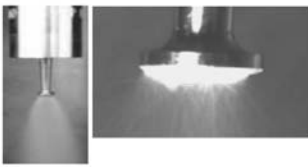

4.3.2 Atomization system

Atomization is the most important processing step during spray drying. The atomization step produces a large surface area between the moist droplets and the drying medium for heat and mass transfer processes to and from the dispersed droplets. For example, one cubic metre of liquid forms approximately 2×10^{12} uniform droplets of 100 μm diameter and a total surface area of 60 000 m^2 (Bayvel and Orzechowski, 1993). This vast interfacial area drastically reduces the water removal time (drying time) since the rate of evaporation is directly proportional to the surface area available for heat and mass transfers. Drying efficiency, powder properties and powder collection efficiency are all dependent on the performance of the atomizers. The atomization process also influences the droplet's size, size distribution, trajectory and velocity, the overall product quality, the drying chamber design as well as the energy requirement to form the spray of droplets.

The resultant spray is usually characterized by the mean droplet size and the droplet size distribution because of the random nature of the atomization. The mean droplet size and its distribution are functions of the type of atomizer used, atomization conditions and the feed characteristics (such as viscosity, density and surface tension). The feed density has the least distinct effect on spray characteristics because the atomized droplets do not show a large density difference. The liquid viscosity and surface tension have the most discrete effects on spray characteristics. The feed viscosity influences not only the mean droplet size and its size distribution but also the feed flow rate and the spray pattern. High viscosity lowers the Reynolds number and also hinders the development of any natural instability in the liquid jet or sheet. The combined effect delays disintegration of droplets leading to increased drop sizes. Similarly, feed with higher surface tension generates larger droplets.

The device used for liquid atomization is commonly known as an atomizer. Atomizers can be used either as an individual device or in groups. The selection and operation of the atomizer is of supreme importance in achieving economic production of a top quality product. The atomizer must work effectively and reliably under harsh conditions. Atomizers can be classified based on the type of the energy used for atomization, the number and shape of orifices, the mode of operation (continuous or intermittent) and the geometry of atomizers. The usual classification is based on the type of the energy utilized for disintegration of droplets from the bulk liquid. There are mainly four types of atomizers used in commercial spray drying

Table 4.3 Various types of atomizers used in spray driers.

Type	Spray pattern	Image
Rotary wheel/disc		
Pressure nozzle		
Pneumatic nozzle		
Ultrasonic horn		

Courtesy: Niro, Spraying System Co. and Sonotek.

operations: rotary wheel/disc (centrifugal energy), pressure nozzles (pressure energy), two-fluid nozzles (pressure and gas energy) and sonic nozzles (sonic energy). A few widely used atomizers and their spray patterns are presented in Table 4.3. The droplet formation mechanism of sonic atomizers is different to that of traditional atomizers. Sonic atomizers use high-frequency sound energy created by a sonic resonance cup placed in front of the nozzle

Table 4.4 Comparison of atomizers used in spray driers.

Atomizer/ Characteristics	Rotary	Pressure	Two-fluid	Sonic
Design	Disc with or without channels	0.3–0.4 mm tube with or without turbulence	Tube with double entry of air/vapor and liquid	Liquid injector and sonic emitter
Energy	Centrifugal speed: 5000–60 000 rpm	Pressure: 10–60 kPa	Air kinetic: 1–3 kPa air:liquid = 10:1	Sonic: 18–42 kHz Air: 1–5 kPa
Droplet trajectory	>120°	5–140°	20–60°	
Particle size	30–120 μm	180–250 μm	20–250 μm	20–250 μm
Advantages	Control of particle size easier, high capacity	No moving parts, simple	Handle viscous, thick or abrasive products	Economical
Limitations	Large droplet trajectory	Viscosity limits, blockage, wear and tear	Fine particles, need extra air supply	Small volume
Energy consumption	More than pressure nozzles	Most economical	Most expensive	
General application	Food	Food	Chemical, food pilot driers	In development stage, small size driers

to disintegrate droplets from the bulk liquid. Rotary atomizers and pressure nozzles are widely employed in large-scale industrial operations. Pneumatic nozzles are being used in small to medium scale spray driers. Sonic atomizers are even now at developmental stage and are being used in small-scale productions for dispersing liquids which are difficult to atomize using traditional atomizers and for manufacturing specialized products. Several characteristics, advantages and drawbacks of common atomizers are illustrated in Table 4.4.

The spray pattern is determined by the shape and the size of the spray produced by the atomizer. Spray patterns have a vital role in achieving the desired penetration of droplets in the drying chamber for effective droplets–gas mixing and evaporation. The spray pattern is also important in designing the drying chamber, controlling the wall deposition and determining the droplet characteristics such as density, velocity, trajectory and size with respect to time and space. The uniform and homogeneous spray pattern is advantageous for minimizing the droplet size distribution. A typical spray pattern is a result of hydrodynamic and aerodynamic interactions between the concentrated feed and the drying gas. Pressure-swirl, sonic and two-fluid nozzles generally produce a hollow cone-type spray pattern or a fully developed cone, depending on the feedback pressure and the gas contact mode. The hollow-cone can be transferred into a fully developed cone by adjusting the axial velocity of the feed in the nozzle. Rotary atomizers produce a wide cone, which is sometimes referred as a ‘spray cloud’. Usually, a thin sheet or large ligament comes out from the disc or vanes of the rotary atomizer, which then further disintegrates into small individual droplets. It was noticed that the droplet size distribution appeared to be somewhat narrower with rotary-type atomizers. Sonic-type atomizers can produce droplets with a very narrow size distribution.

The atomization process generally produces spherical droplets. Dried particles, however, may not have the same shape or size. The size and/or shape distribution of droplets is affected by the nature of the feed, its solids concentration, type of atomizer and the air patterns. The

Table 4.5 Correlations for predicting the mean droplet size for various atomizers.

Atomizer type	Mean droplet size prediction equation	References
Rotary	$\frac{D_{3,2}}{r} = 0.4 \left(\frac{M}{N_v b \rho N r^2} \right)^{0.6} \left(\frac{N v \mu b}{M} \right)^{0.2} \left(\frac{\sigma b^3 \rho N_v^3}{M^2} \right)^{0.1}$	Masters (1991) Perry (1984)
Pressure	$D_{3,2} = 286[(2.54 \times 10^{-2})D + 0.17] \exp \left[\frac{39}{v_{AX}} - (3.13 \times 10^{-3})v_1 \right]$ $D_{3,2} = \frac{9575}{\Delta P^{1/3}}$	Perry (1984)
Two-fluid (pneumatic)	$D_{3,2} = 585\,000 \frac{\sqrt{\sigma}}{v_{rel} \sqrt{\rho_1}} + 597 \left[\frac{\mu}{\sqrt{\sigma \rho_1}} \right]^{0.45} \left(1000 \frac{Q_F}{Q_a} \right)^{1.5}$	Perry (1984)
Sonic	$D_{3,2} = \left(\frac{\pi \sigma}{\rho f^2} \right)^{0.33} [1 + A(N_{We})^{0.22} (N_{oh})^{0.165} (N_{in})^{-0.0277}]$	Avvaru <i>et al.</i> (2006)

particle-size distribution follows a slightly different pattern depending on the type of the atomizer, the droplet mean residence time, the droplet collision history and the chamber design. There could also be a vast difference in the surface morphology of the final particles. The mean size of droplets and the resultant particles is best described by the volume–surface mean diameter (Sauter mean diameter, D_{32}). Rotary, pressure and pneumatic atomizers follow log-normal, Rosin–Rammler and Nukiyama–Tanasawa distributions, respectively (Perry, 1984; Masters, 1991). The size and the size distribution of droplets generated by four different atomizers are depicted in Table 4.5.

4.3.3 Drying chamber

In the last four decades, a significant advance in spray drying technology and drier designs has been observed in order to dry a large variety of feedstock, achieve the highest production rate, meet the prerequisite product quality, reduce energy requirements, minimize the production and equipment designing costs and reduce the difficulties involved with scale-up and optimization. The traditional and most commonly used configuration of a spray drier consists of a cylindrical drying chamber with a cone of 40°–60° at the bottom. Gravity makes the powder exit from the bottom of the drying chamber. Tall-form, short-form and flat-bottom spray driers have also been employed in designing new products in order to satisfy specific requirements. Several commonly used geometries are shown in Figure 4.4. Huang *et al.* (2003) proposed several other geometries such as simple cone, hour-glass and lantern-shaped chambers with vertical orientation that may replace the traditional configuration. Recently, some publications have reportedly sought the possibility of employing horizontal spray driers, which may be suitable for handling heat-sensitive materials and reducing the difficulties involved with scale-up (Cakaloz *et al.*, 1997; Huang and Mujumdar, 2005).

The drier chamber design primarily depends on the type of the atomizer, the trajectory of droplets, the properties (such as heat sensitivity, solids content, etc.) of the material to be dried, the capacity of the drier, single- or two-stage drying, the cost and the type of air flow (co- or counter-current) with respect to the feed. The driers equipped with pressure nozzles have a high height to width ratio, while those with rotary atomizers are generally wider and have a low height to width ratio. The tendency today is to design a drying chamber in such a

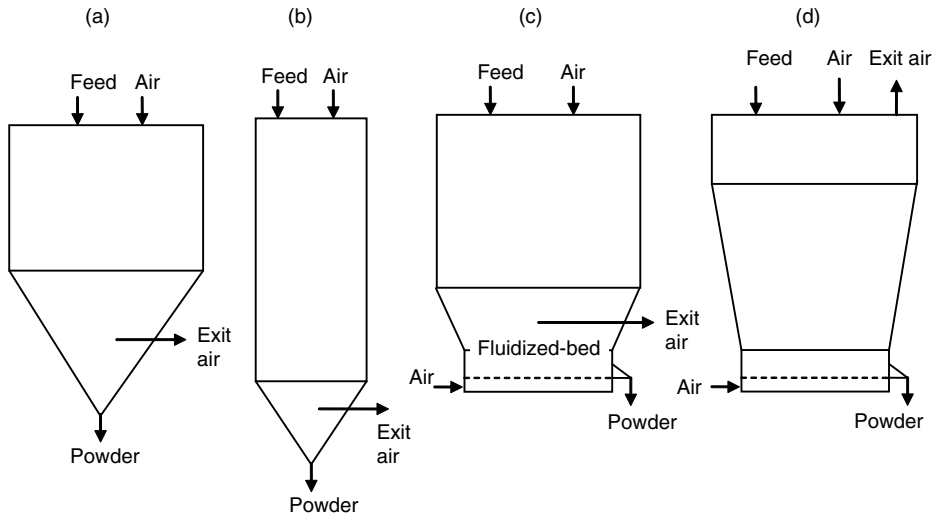


Fig. 4.4 Drying chamber layouts: (a) parallel flow drier with a rotary atomizer; (b) parallel flow tall-form drier with a pressure nozzle or a two-fluid atomizer; (c) mixed flow drier with a rotary atomizer; (d) mixed flow drier with multiple pressure nozzles.

way that the airflow is not influenced by the interior accessories of the chamber. To facilitate powder removal and minimize the wall deposition, the drier chambers are usually equipped with an air or mechanical sweeping system, a set of hammers to dislodge the particles and a cooling system to regulate the temperature of the chamber. Modern drying chambers also include light sources, inspection doors, over-pressure vents and safety doors. Two-stage driers are integrated with a fluidized-bed drying system (internally or externally mounted) in order to continue to dry the powder (Figure 4.5). The location of the exhaust air stream is one of the prime issues when designing drying chambers for two-stage spray driers.

For drying of food materials, spray driers are mostly operated with a co-current mode, that is, the drying gas and the atomized droplets move in the same direction in the drying chamber. The mean residence time of the particles is small, and the dried particles do not have to pass through the high temperature zone during a co-current drying process. This mode is highly suitable for drying heat-sensitive materials where the residual activity of bioactive components is targeted. A non-rotating airflow is generally used when the hot drying air is discharged in tall-form spray driers or when the pressure atomizers are equipped to spray the liquid feed. When rotary-type atomizers are used, a rotational airflow is commonly used that provides more uniform temperatures in the drying chamber compared to that of the non-rotational airflow.

4.3.4 Powder separators

For modern multi-stage spray driers, the air stream from the drying chamber usually contains about 10–50% of the total powder depending on the material and spray drier type and operating conditions (Pisecky, 1997). It is important to recover the powder from the exhaust stream not only for economy purposes, but also to clean the air in order to minimize the pollution problems. The powder separation from the air takes place either by the use of gravity separators (e.g. cyclones) only or by a combination of gravity and filter separators. In

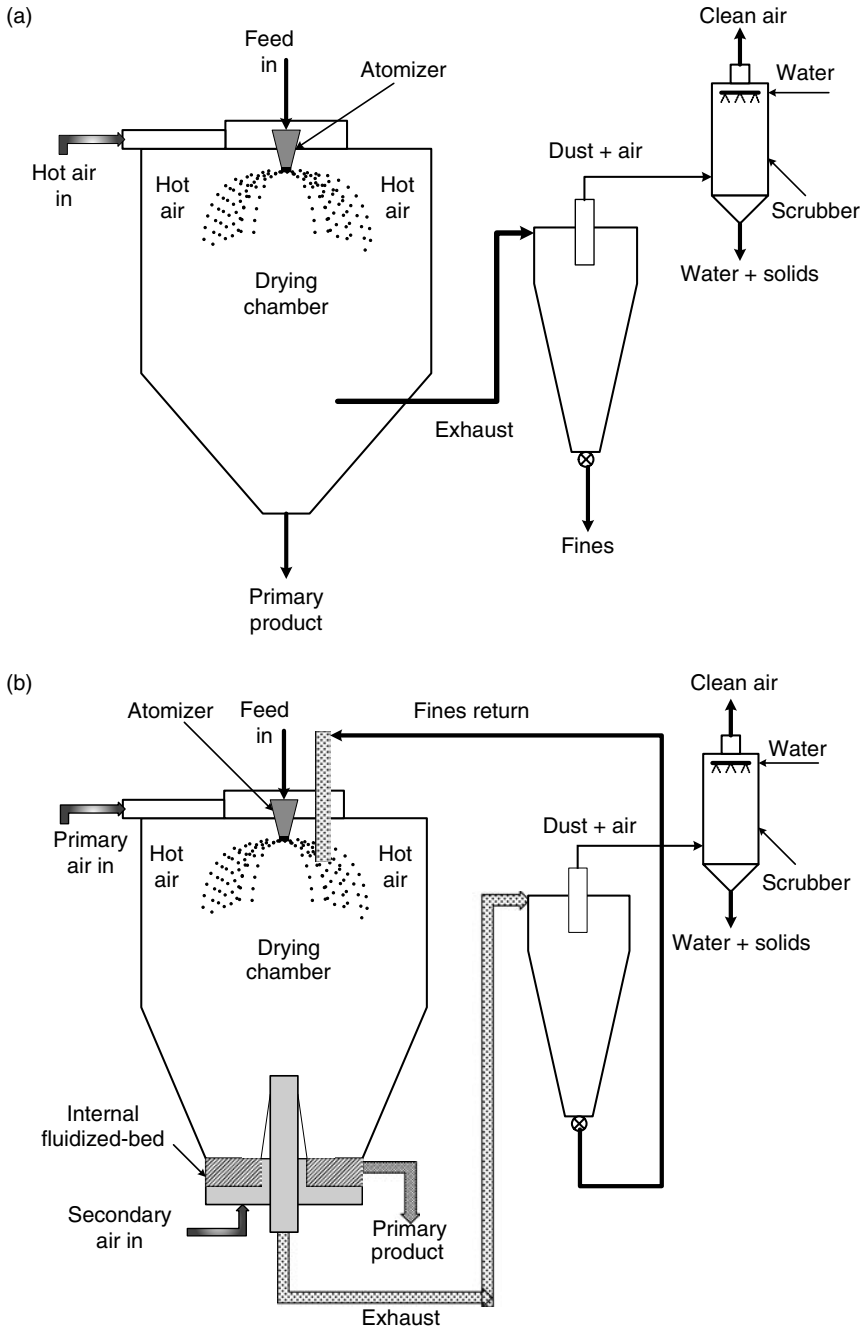


Fig. 4.5 Spray drying systems: (a) single-stage; (b) two-stage.

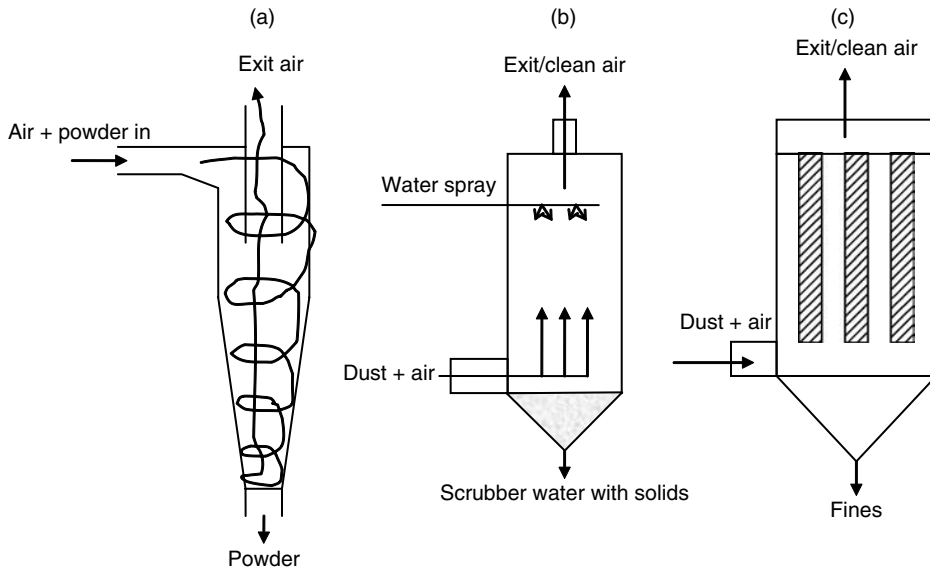


Fig. 4.6 Schematic diagrams of (a) cyclone, (b) wet scrubber and (c) bag filter.

general, particles are recovered by incorporating one or more of the following installations (Figure 4.6):

1. cyclone separators
2. bag filters
3. wet scrubbers

Cyclones, also known as dust separators, are used in many industries to recover particles from the gas stream. To guide the air and particle separation in the cyclone, the top of the cyclone is usually cylindrical while the bottom is conical. The apex angle lies from 10° – 20° . The height of the cyclone is generally 2–6 times the diameter of the cylindrical body. The air stream tangentially enters the cyclone separator and has a vortex-type spiral path down to the bottom of the cyclone. Particles hit the cyclone wall due to the centrifugal force and drop off by gravity while the clean air moves up from the bottom to the top of the cyclone due to differential pressures created between the radial and axial directions. The centrifugal force exerted to each particle is calculated by the following equation:

$$C = m_d v_t^2 / r \quad (4.1)$$

where m_d is the mass of the particle, v_t is the tangential velocity and r is the radial distance to the wall of the cyclone from any given point. The efficiency of a cyclone mainly depends on the centrifugal force exerted on the particles. Smaller particles (fines) have a higher radial velocity component and are carried away by the exhaust air. Higher efficiency can be achieved for high inlet velocity gas streams, exhaust streams with large particles and cyclones with a smaller radial dimension. Small apex angles are also known to be favourable for achieving high efficiencies. A sufficient residence time in the cyclone should be allowed to get efficient separation of particles. To handle a large volume of exhaust air, a number of cyclones in

series are often used. The efficiency of the cyclone is generally estimated by evaluating the cut-off size, the critical particle diameter and the overall cyclone efficiency. The cut-off size is defined as the size for which 50% collection is achieved. Since the efficiency of the cyclone is not 100%, very fine particles may escape with the exhaust air.

In many environmental regulations, the dust limit in the exhaust is not to be more than 10 mg powder per kg exhaust air. In order to meet the dust emission regulation and eventually to control air pollution, the outlet air stream from the cyclone requires further cleaning through a series of bag filters or wet scrubbers. Fine powders can be recovered from the bag filters when the exhaust air stream is passed through the bag-filter house. Where the wet scrubber is used, the exhaust is injected at very high velocities through a venturi inlet. A solvent fluid, normally water, is sprayed at the same time in such a way that the gas stream and water spray makes intimate contact. The fines are dissolved in the water leading to the clean air that escapes from the scrubber. Micro-biological growth is an issue when using wet scrubbers because of the warm temperature (40–45°C). Recently, Niro A/S has introduced cleaning-in-place (CIP) bag filter systems which are reported to be very efficient (99.8%) and also do not require the cyclone separator (Masters, 1998, 2004). The CIP-bag filter system can be used instead of cyclones or alongside cyclones.

4.4 DRYING OF DROPLETS

4.4.1 Fundamentals of droplet drying

Simultaneous heat and mass transfer processes are taking place during the drying of droplets (Chen, 2004). Modeling for the drying of single droplets therefore requires the solution of coupled heat and mass transfer models. Drying starts with evaporation of ‘free’ moisture on the droplet surface. When the droplet surface is fully covered with water, the drying rate would be similar to the rate for pure water evaporation. When a droplet that has dissolved or a suspended solid is being dried, the vapor pressure at the droplet surface would become smaller than that for the pure water droplet as evaporation proceeds (Shi and Wang, 2004). As a result, the mass transfer rate gradually becomes lower during drying of the droplets. The surface temperature of the droplet under evaporation conditions consequently increases to, or above, the wet-bulb temperature or the evaporation temperature of the pure water droplet. Once the surface vapor concentration falls below the saturated vapor concentration corresponding to the surface temperature, mainly after the formation of solid structures on the surface, the drying also commences within the droplets.

The moisture transfer mechanism during different periods of drying is crucial for determining the drying-rate limiting step. The removal of moisture from the droplet has been the subject of intense research over the last few years. Many theories have been proposed based on different moisture movement possibilities. During rapid drying processes, the moisture transfer is caused by gradients of temperature, concentration and pressure (Konovalov and Gatapova, 2006). During drying of the wet ‘porous’ droplets, there are generally five moisture transfer mechanisms: (1) liquid diffusion caused by the liquid density gradient; (2) vapor diffusion caused by the vapor density gradient; (3) capillary flow caused by the capillary force; (4) moisture transfer caused by the internal pressure gradient; and (5) moisture transfer caused by evaporation and condensation in pores. Different mechanisms dominate during different drying periods. In general, at the initial stage of drying when the droplet surface is fully covered with free water, the mass transfer is believed to take place mainly due to

liquid diffusion. During a later stage when the solids content within the droplet is high, the moisture transfer is said to be governed by the vapor diffusion. The rate of heat and mass transfer primarily depends on the gas-droplet temperature difference, the droplet's relative velocity (with respect to gas velocity) and the film or boundary layer conditions surrounding the droplets (such as humidity, air velocity, temperature and vapor pressure).

4.4.2 Drying kinetics

Droplet drying stages are mainly divided into three drying periods (Masters, 1991). These drying stages are schematically shown in Figure 1.7 in Chapter 1. Drying may start with warming up or cooling down stages, depending on the initial feed temperature. These initial stages are usually small and mostly ignored for calculation purposes. The first stage is called the constant drying-rate period when the rate of moisture removal is constant. In this period the surface of the droplet is saturated with free water, and the droplet temperature is believed to be maintained at the wet-bulb temperature of the hot air. The amount of heat transferred to the droplet is compensated by the latent heat of vaporization during this period. Once the droplet moisture content falls below the critical moisture content, the rate of moisture removal drops gradually with time. This is called the 'falling' drying-rate period. During this drying stage, the temperature of the droplet rises close to the outlet air temperature, since the surface of the droplet is no longer saturated to maintain the temperature at the corresponding wet-bulb temperature (diffusion-limited phenomenon).

Although there are two periods assumed during the droplet drying process, there is no significant constant drying-rate period observed during drying of small droplets which have a high amount of suspended and/or dissolved solids. There is not sufficient free water available on the droplet surface to act as a 'source' of free water for the feed with high solids concentration, and hence the vapor pressure of the surface will not be same as that for pure water (Chen and Lin, 2005). Furthermore, the majority of the free water is removed in a short period of time, leading to a very short (most times negligible) constant-rate drying period and a relatively longer falling rate period during drying of small droplets. A 'linear' falling rate period is believed to represent the drying rate curve for drying of small porous substances (Ferrari *et al.*, 1989; Langrish and Kockel, 2001). Since the temperature of the drying air is very high, there is a possibility that the droplet surface temperature exceeds the corresponding wet-bulb temperature (Figure 4.7), and hence the droplet temperature could be higher than the evaporating temperature (Chen, 2004). For this reason, relatively lower inlet air temperatures are used for drying of heat-sensitive materials.

During spray drying, the maximum water evaporation takes place in a fraction of a second and within a short distance from the atomizer. Longer residence time in the drier (around 20 s) provides longer time for evaporation during the falling drying-rate period. Determining the drying time is very complex because the dynamics of the air-droplets system change over a short period of time. To simplify the calculation, the heat transfer during the constant drying-rate period is usually considered the same as that for the pure water. The mass and heat transfer coefficients are estimated using the well-known Ranz–Marshall correlations (Masters, 1991):

$$Nu = \frac{h \cdot d_{av}}{k_d} = 2 + 0.6Re^{1/2} \cdot Pr^{1/3} \quad (4.2)$$

$$Sh = \frac{h_m \cdot d_{av}}{D_d} = 2 + 0.6Re^{1/2} \cdot Sc^{1/3} \quad (4.3)$$

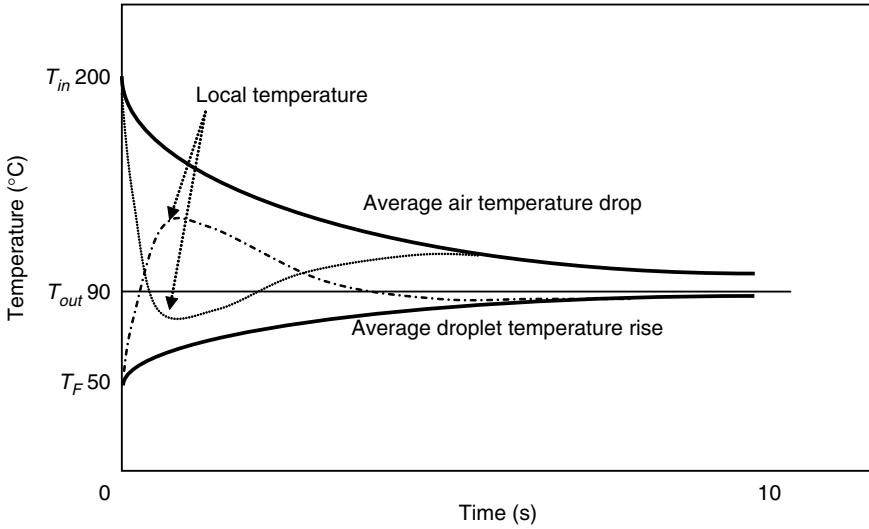


Fig. 4.7 Illustration of local temperature of droplets and drying air during the initial drying stage of droplets.

where h and h_m are convective heat and mass transfer coefficients, respectively. The parameters k_d and D_d are thermal conductivity of the droplet and diffusion coefficient respectively, which are temperature and moisture concentration dependent. The relative velocity between air and droplet is often neglected during calculation (the Reynolds number becomes zero in that case). During the constant drying-rate period, the average water removal rate and average drying time are expressed by the following equations:

$$\frac{dX}{dt} = \frac{2\pi d_{av} k_d}{\lambda} (\Delta T_{LMTD}) \quad (4.4)$$

$$t_c = \frac{\lambda}{8k_b (\Delta T_{LMTD})} [\rho_0 d_0^2 - \rho_1 d_1^2] \quad (4.5)$$

where, d_{av} is the average diameter of the droplet (average of initial d_0 and at the end of constant rate period (d_1) by considering shrinkage due to the removal of water), k_b is the thermal conductivity of the drying gas, ΔT_{LMTD} is the log mean temperature difference between air and droplet temperature and ρ_0 and ρ_1 are the densities of the droplet at the beginning and end of the constant-rate period.

In the falling drying-rate period, the average water removal rate is expressed by the following equation:

$$\frac{dX'}{dt} = \frac{-12k_d}{\lambda d_1^2 \rho_s} (\Delta T_{LMTD}) \quad (4.6)$$

The rate of change of water loss during the constant-rate period (dX/dt) will then be equal to the rate of change of water loss (dX'/dt) times the weight of dry solids at the critical moisture content. The drying time in the falling drying-rate period cannot be precisely expressed in an equation form because it depends on the nature of the solid phase. Ranz and Marshall,

however, estimated the average drying time during the falling drying-rate period incorporating the critical moisture content by the following correlation (Heldman and Singh, 1980):

$$t_f = \frac{\rho_p d_1^2 \lambda (X_1 - X_b)}{6k_d \Delta T_{AMTD}} \quad (4.7)$$

where ρ_p is the density of the particle, X_1 is the critical moisture content (that is the moisture content at the end of constant drying-rate period) (kg water per kg dry solids), X_b is the equilibrium moisture content (kg water per kg dry solids) at the end of drying and ΔT_{AMTD} is the arithmetic mean temperature difference between droplet and air (because the temperature change is low).

For drying of small droplets or thin-layer materials, Chen and Xie (1997) established correlations to calculate the rate of change in water loss based on a reaction engineering approach. Recently, Chen and Lin (2005) validated this drying kinetics approach based on experimental work for drying of single skim milk and whole milk droplets. Their drying kinetics model described the rate of change of water loss as a function of the vapor concentration difference. The fundamental correlations were:

$$-\frac{dX}{dt} = \frac{A_d \cdot h_m}{m_s} \left(\rho_{v,sat} \cdot \exp\left(-\frac{\Delta E_v}{R_g \cdot T}\right) - \rho_{v,b} \right) \quad (4.8)$$

where, T is droplet temperature (K), m_s is mass of solids in a droplet (kg), A_d is the droplet surface area (m^2), and $\rho_{v,b}$ and $\rho_{v,sat}$ represent bulk phase vapor concentration and saturated vapor concentration at the solid–gas interface, respectively. The parameter ΔE_v in equation (4.8) is an apparent activation energy factor that represents the increasing difficulty of removing moisture from the droplet under drying conditions due to lowering moisture content effects. In the work by Chen and Lin (2005), the parameter ΔE_v was found to be a function of the droplet's free moisture content ($X - X_b$). Here, the relationship between the activation energy and the free moisture content under drying conditions is viewed as a characteristic property of the individual material. This characteristic relationship of the material has to be obtained experimentally for the individual material. This relationship between the activation energy and the free water content is already established for drying of a few dairy products such as skim milk, whole milk, lactose, cream and whey proteins concentrate (Chen and Lin, 2005; Lin and Chen, 2006, 2007):

$$\text{Lactose, } \frac{\Delta E_v}{\Delta E_{v,b}} = 1.017 \exp[-1.678(X - X_b)^{1.018}] \quad (4.9a)$$

$$\text{Skim milk, } \frac{\Delta E_v}{\Delta E_{v,b}} = 0.998 \exp[-1.405(X - X_b)^{0.930}] \quad (4.9b)$$

$$\text{Whole milk, } \frac{\Delta E_v}{\Delta E_{v,b}} = 0.957 \exp[-1.291(X - X_b)^{0.934}] \quad (4.9c)$$

$$\text{WPC, } \frac{\Delta E_v}{\Delta E_{v,b}} = 1.335 - 0.3669 \exp X^{0.3011} \quad (4.9d)$$

$$\text{Cream, } \frac{\Delta E_v}{\Delta E_{v,b}} = 1 - 0.6282X^{0.5561} \quad (4.9e)$$

It can be judged from equations (4.9) that when the free moisture content ($X - X_b$) is large, that is, the free moisture fully covers up the droplet surface, the apparent activation energy ΔE_v , and hence the difficulty in removing free water, are expected to be very small. The activation energy factor gradually increases to a large value when the droplet's free moisture decreases to a small value. The parameter $\Delta E_{v,b}$ in equations (4.9) is an equilibrium activation energy, and was obtained using the gas relative humidity ($\rho_{v,b}/\rho_{v,sat}$) and gas temperature (T_b):

$$\Delta E_{v,b} = -R_g T_b \ln \left(\frac{\rho_{v,b}}{\rho_{v,sat}} \right) \quad (4.10)$$

The reaction engineering approach estimates the drying rate for the entire drying period and does not require separate equations for individual drying stages. Furthermore, it should be easy to incorporate the above equations into common process calculations tools such as computational fluid dynamics tools and Microsoft Excel Programs. This concept was found to be attractive for simulation of a drier-wide scenario using industrial drying conditions for various dairy products (Patel and Chen, 2007, 2008).

4.4.3 Residence time

Sufficient residence time is required for atomized droplets inside the drying chamber to convert them into dried particles of specified residual moisture content. When existing drier and product experience are unavailable, an importance of the role of the residence time data is vital in order to prevent under-sizing or over-sizing of the drying chamber. The residence time of the droplets in the chamber varies depending on the volume and the geometry of the drier, the droplet size distribution and the airflow rate and pattern (Zbicinski *et al.*, 2002). Droplets of different size follow different paths inside the drying chamber leading to a residence time distribution for the dried particles. The average particle residence time usually varies from 5 to 20 s for small-scale driers whilst it is in the range of 20–35 s for large-scale drying operations (Masters, 1991). The average particle residence time data do not include the processing time in the integrated fluidized-bed drier.

The average gas residence time can be calculated assuming plug-flow conditions using the following equation:

$$t = \frac{V_{ch}}{\dot{V}} \quad (4.11)$$

where \dot{V} is the volumetric air flow rate ($\text{m}^3 \text{s}^{-1}$) and V_{ch} is the volume of the drying chamber (m^3). The volume of the conical-shaped chamber can be determined by estimating the chamber diameter, cylindrical height and the cone angle. The average particle residence time data are usually judged from the average gas residence time data, and require a great deal of practical experience. Droplet velocities inside the drier are sometimes assumed to be close to 'free-fall' velocities, and the average residence time can be obtained when considering a plug-flow drier. When assuming a plug-flow drier and the same velocity for the droplets and the drying gas, the average residence time can be obtained using equation (4.11).

Actual residence time of some particles can be much larger than this average value due to the recirculation of air and droplets, the differential droplet/air velocity in some sections of the drier and the short-time deposition of particles on the chamber wall. In the drier

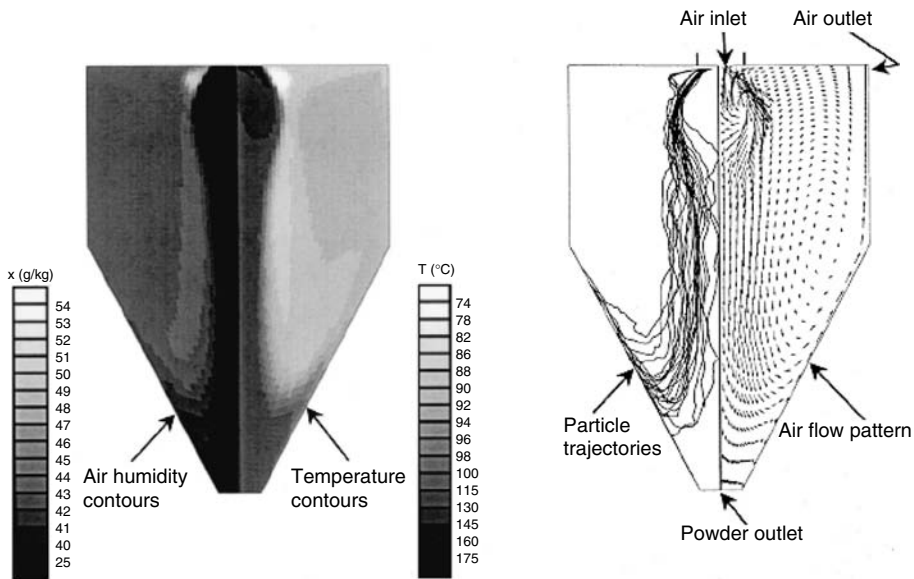


Fig. 4.8 Air humidity and temperature profiles and particle trajectory and airflow profiles in a drier (Straatsma *et al.*, 1999, with permission).

with a low height-to-width ratio, the airflow is more complex than in the tall form of driers (Langrish and Fletcher, 2001). The non-uniformity of the humidity and temperature, the droplet trajectory (rotary atomizer) and the air profile of a mixed flow drier are depicted in Figure 4.8 (Straatsma *et al.*, 1999). This was obtained using the computational fluid dynamics (CFD) model techniques. The gray color in the first drier indicates the high-humidity–low-temperature zone and the dark color indicates the high-temperature–low-humidity zone. In the right-hand side figure, a straight downward air flow and some air recirculation can be seen at the middle of the central axis and the drier wall.

4.5 MASS AND HEAT BALANCES OVER A SPRAY DRIER

The heat and mass balances over a spray drier allows estimation of the drier efficiency, forms a basis for designing a spray drier and helps in minimizing heat and product losses. Calculation of heat and mass balances over the spray drier and the integrated fluidized-bed drier are usually done separately in order to evaluate the efficiency of each process independently. The mass and heat balances could be more complex for multiple-stage drying, for instance in three-stage drying where changes in heat and mass of the particles occur in the spray drier, internal fluidized-bed drier and external fluidized-bed drier. Here, a sample calculation for determining the heat and mass balance over the two-stage drier that has an integrated fluidized-bed drier is presented. The inflow and outflow of the materials and the enthalpy are schematically represented in Figure 4.9.

4.5.1 Overall mass balance

The overall mass balance can be a ‘closed loop’ or ‘open loop’. In a closed loop balance all the variables are measured. The difference between the inlet and outlet streams estimates both

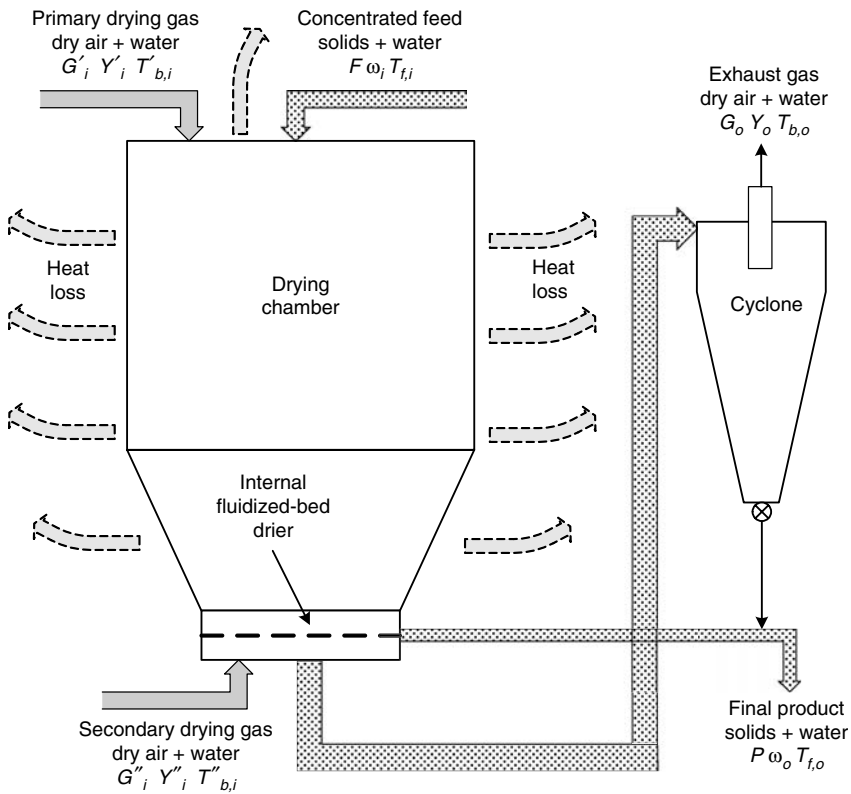


Fig. 4.9 A schematic diagram indicating materials in and out from the system.

the accuracy during measurements and the losses occurring in the process. In an open loop mass balance, the data are measured either for inlet or outlet streams and the data for another stream is calculated from the differences in the mass balance. The latter type of mass balance cannot provide the accurate information required to determine losses. The open loop mass balance is applied where it is difficult to measure the one stream, although the conclusion could be biased. A closed loop balance is more accurate since the measurements are done in both inlet and out-going streams. Depending on the ease of measurements and accessibility in the drier, either of the mass balances can be used.

There are two material streams involved in the drying operation, namely the feed to be dried and the drying gas. Spray drying is a continuous process, and therefore the information or the quantity has to be expressed per unit time. The overall mass balance can be based on the solids content or the water content of the feed. The balance of mass for the drying gas can also provide useful information about the process. The mass balance is usually performed based on the total solids content of the liquid feed because the solid component is the main interest during food drying. When specialized products with functional ingredients such as encapsulated fat, color or flavor are being dried, the mass balance can be focused mainly on the important components. In general, the overall mass balance can be expressed as:

Feed rate + Inlet air rate = Powder rate + Exit air rate

$$F + G_i = P + G_o \quad (4.12)$$

The drying gas (mixture of dry air and water vapor) flow rate can be presented as:

$$G_i = G_{dry} + W_i \quad (4.13)$$

The amount of water vapor is usually expressed using the absolute air humidity (g moisture per kg dry air), which can be determined using the relative humidity and the dry-bulb temperature of the drying air. Then the inlet air flow rate can be written as:

$$G_i = G_{dry}(1 + Y_i) \quad (4.14)$$

In a two-stage drying system (Figure 4.9), two air streams – the primary air stream for drying of the droplets in the chamber and the secondary air stream for drying of semi-dried particles in a fluidized-bed drier – are entering the drying chamber. As shown in Figure 4.5, there is only one air stream leaving the drier. For this two-stage drying system, the inlet air flow rate would be:

$$G_i = G'_{dry}(1 + Y'_i) + G''_{dry}(1 + Y''_i) \quad (4.15)$$

Similarly, the mass balance can be written for the outlet gas stream. Here, the quantity of the dry air remains constant in inlet and outlet air streams.

$$G_o = G_{dry} + W_o = G_{dry}(1 + Y_o) \quad (4.16)$$

The outlet air stream is composed of water vapor coming in through the inlet air stream and the moisture evaporated during drying. The total moisture evaporated during drying can be estimated using the difference between the feed and powder moisture concentrations ($\omega_i F - \omega_o P$). Hence, the outlet air flow rate can be written as:

$$G_o = G'_{dry}(1 + Y'_i) + G''_{dry}(1 + Y''_i) + \omega_i F - \omega_o P \quad (4.17)$$

The mass balance for the total solids can be written based on the solids fraction in the feed stream ($1 - \omega_i$) and the solids fraction in the powder stream ($1 - \omega_o$):

Feed solids in = powder solids out + losses

$$(1 - \omega_i)F = (1 - \omega_o)P + losses \quad (4.18)$$

The total loss of material accounts for the accumulation in the drying chamber, ducts and other integrated systems as well as losses of fines in the exhaust air stream. The total powder losses can be calculated only when other data are obtained for a given processing time.

The mass balance can also be written for the water phase if the amount of water in inlet feed, primary air, secondary air, final powder and outlet air streams are known. The mass balance for the water phase would be:

$$\omega_i F + G'_{dry} Y'_i + G''_{dry} Y''_i = \omega_o P + G_o Y_o \quad (4.19)$$

4.5.2 Overall heat balance

The overall heat balance over the spray drying system discussed in the above section can be presented as follows when steady-state conditions are assumed:

$$H_{feed} + H_{b,inlet} = H_{product} + H_{b,outlet} + H_{loss} \quad (4.20)$$

The enthalpy of the feed can be obtained using the following equation:

$$H_f = F \cdot C_{pf}(T_{f,i} - T_{ref}) \quad (4.21)$$

where T_{ref} is the reference temperature for which other thermo-physical properties are known. For a food system with a known fractional composition, the specific heat of the feed (C_{pf}) can be approximated by the following empirical equation:

$$C_{pf} = 1.42C + 1.549P + 1.67F + 0.837A + 4.187M \quad (4.22)$$

where C = carbohydrate, P = protein, F = fat, A = ash and M = moisture weight fractions. The enthalpy of the inlet air streams (primary and secondary) can be calculated using the following formula:

$$H_{b,i} = G'_i C_{pb}'(T'_{b,i} - T_{ref}) + G'_i Y'_i \lambda' + G''_i C_{pb}''(T''_{b,i} - T_{ref}) + G''_i Y''_i \lambda'' \quad (4.23)$$

Similarly, the enthalpy of the outlet gas stream can be presented as:

$$\begin{aligned} H_{b,o} &= G_o C_{pb}(T_{b,o} - T_{ref}) + G_o Y_o \lambda \\ &= G_o C_{pb}(T_{b,o} - T_{ref}) + (G_i Y_i + (\omega_i F - \omega_o P)) \lambda \end{aligned} \quad (4.24)$$

Here, C_{pb} is the specific heat of the bulk drying air. The bulk drying air is the mixture of vapor and dry air. The specific heat of the bulk mixture can be calculated as:

$$C_{pb} = C_{pdryair} + Y \cdot C_{pvapor} \quad (4.25)$$

Enthalpy of dry powder can be estimated by the following equation:

$$H_p = P \cdot C_{pp}(T_p - T_{ref}) \quad (4.26)$$

The overall heat balance for the two-stage spray drying system, shown in Figure 4.5, can be expressed using the above analysis:

$$\begin{aligned} &F \cdot C_{pf}(T_{f,i} - T_{ref}) + G'_i C_{pb}'(T'_{b,i} - T_{ref}) + G'_i Y'_i \lambda' + G''_i C_{pb}''(T''_{b,i} - T_{ref}) + G''_i Y''_i \lambda'' \\ &= P \cdot C_{pp}(T_{p,o} - T_{ref}) + G_o C_{pb}(T_{b,o} - T_{ref}) \\ &\quad + (G_i Y_i + (\omega_i F - \omega_o P)) \lambda + H_{losses} \end{aligned} \quad (4.27)$$

The loss of heat (H_{losses}) in the drying chamber is normally influenced by the properties of the material in the outer cladding of the chamber and the ducts. Efficient insulation can greatly minimize the heat loss through the drier walls and the ducts. The heat losses can be expressed

in the form of a heat transfer equation based on the total surface area (A) of the chamber and the ducts. The overall heat transfer coefficient (U) of the wall can be calculated from the following equation:

$$H_{loss} = UA(T_{b,o} - T_{b,a}) \quad (4.28)$$

Here, the ambient air temperature ($T_{b,a}$) is the temperature of the air around the outer wall of the chamber which will be higher than the room temperature. The outlet air temperature (T_o) is usually measured at the duct which takes the exhaust air stream to the cyclone. Small values of the heat-transfer coefficient (e.g. 4–8 kJ m⁻² s °C) indicate efficient heat insulation of the system.

Microsoft Excel spreadsheets can be used to perform calculations for the overall mass and heat balances, and to compare the energy expenditure, the drier efficiency, variations in the product characteristics and the production costs at different periods during the year. A sample Microsoft Excel spreadsheet is shown in Table 4.6. This worksheet can be easily altered for different spray drying systems knowing the inlet and outlet streams. The water content and the solids content of the material being dried at the inlet and outlet of the drier, the total energy required per kg of water removed and the average drying time are the most important parameters to be obtained from the calculation of such spreadsheets.

4.6 DRIER EFFICIENCY

The performance of spray driers is usually expressed in terms of the thermal efficiency and the evaporative efficiency. These efficiencies of spray driers are primarily affected by the drier operating conditions, mainly the inlet and outlet drying air temperatures. The efficiencies and therefore the spray drier performance can be enhanced by increasing the air inlet temperature and by operating the drier at an outlet temperature as low as the process permits. In practical terms, the drier efficiency can be described based on the heat input required for the production of a unit weight of dried product. The heat input is directly proportional to the evaporation rate. For a given evaporation rate, the heat input is greatly affected by the inlet feed concentrations. For instance, feeds with higher solid content lead to reduction in the heat input (Masters, 1991). The specific energy consumption is often used that is equal to the energy required to evaporate a unit weight of water from the feed.

4.6.1 Thermal efficiency

For an adiabatic operation (that means heat losses are negligible), the thermal efficiency ($\eta_{overall}$) or the overall efficiency is defined as the ratio of the heat utilized in evaporation to the total heat input and can be presented by the correlation (Masters, 1991; Keey, 1991):

$$\begin{aligned} \eta_{thermal} (\%) &= \frac{\text{heat used in evaporation}}{\text{heat input}} \\ &= \left(\frac{T_{b,i} - T_{b,o}}{T_{b,i} - T_{b,a}} \right) \times 100 \end{aligned} \quad (4.29)$$

where $T_{b,i}$ and $T_{b,o}$ are inlet and outlet drying gas temperatures, respectively, and $T_{b,a}$ is the ambient gas temperature (K). The thermal efficiency is directly proportional to the inlet and

Table 4.6 A Microsoft Excel spreadsheet to calculate the heat and mass balance of a drier.

MASS BALANCE				
INPUT		Units	OUTPUT	Units
1. FEED FLOW			1. POWDER FLOW	
Total solids	% w/w	55	Moisture	% w/w 5
Mass feed rate	kg h ⁻¹	100	Powder production rate	kg h ⁻¹ 50
Solids rate	kg h ⁻¹	55	Solid rate	kg h ⁻¹ 47.5
Moisture rate	kg h ⁻¹	45	Moisture rate	kg h ⁻¹ 2.5
2. INLET AIR FLOWS			2. EXIT AIR FLOW	
2.1 Primary drying air			Temperature	°C 80
Temperature	°C	200	Air flow rate	kg h ⁻¹ 744.8
Air flow rate	kg h ⁻¹	700	Absolute humidity	kg per kg dry air 0.0691
Absolute humidity	kg per kg dry air	0.008	Dry air flow rate	kg h ⁻¹ 696.68
Dry air flow rate	kg h ⁻¹	694.4	Moisture flow rate	kg h ⁻¹ 48.12
Moisture flow rate	kg h ⁻¹	5.6		
2.2 Secondary drying air				
Temperature	°C	130		
Air flow rate	kg h ⁻¹	2.3		
Absolute humidity	kg per kg dry air	0.008		
Dry air flow rate	kg h ⁻¹	2.28		
Moisture flow rate	kg h ⁻¹	0.018		
TOTAL MASS FLOW IN		802.3	TOTAL MASS FLOW OUT	794.8
			Mass difference	7.5
			% Difference	0.93
			POWDER IN EXHAUST	
			Dust/powder in the exhaust	mg per kg air 30
			Powder rate	kg h ⁻¹ 0.0223
			Moisture rate	kg h ⁻¹ 0.0011
			ACCUMULATION AND ERROR	kg h ⁻¹ 4.98
SOLIDS BALANCE				
Total dry solids in	kg h ⁻¹	55	Total dry solids out	47.5
			Solids mass difference	7.5
			% Difference	13.64
MOISTURE BALANCE				
Total moisture in	kg h ⁻¹	50.6184	Total moisture out	50.6184
			Moisture mass difference	0
			% Difference	0
HEAT BALANCE				
INPUT		Units	OUTPUT	Units
1. FEED FLOW			1. POWDER FLOW	
Feed temperature	°C	50	Powder temperature	°C 80
Feed specific heat	kJ kg ⁻¹ °C	2.856	Powder specific heat	kJ kg ⁻¹ °C 1.919
Feed enthalpy rate	kJ h ⁻¹	14280.0	Powder enthalpy rate	kJ h ⁻¹ 7675.4
2. INLET AIR FLOWS			2. EXIT AIR FLOW	
2.1 Primary drying air			Temperature	°C 85
Dry air specific heat	kJ kg ⁻¹ °C	1.032	Dry air specific heat	kJ per kg °C 1.025
Water vapor specific heat	kJ kg ⁻¹ °C	1.903	Water vapor specific heat	kJ per kg °C 1.884
Heat utilized for evaporation	kJ h ⁻¹	11994.478	Heat utilized for evaporation	kJ h ⁻¹ 109067.0
Primary air enthalpy rate	kJ h ⁻¹	157450	Exit air enthalpy rate	kJ h ⁻¹ 169512.9
2.2 Secondary drying air				
Dry air specific heat	kJ kg ⁻¹ °C	1.026		
Water vapor specific heat	kJ kg ⁻¹ °C	1.887		
Heat utilized for evaporation	kJ h ⁻¹	41.418		
Secondary air enthalpy rate	kJ h ⁻¹	350.252		
TOTAL ENTHALPY FLOW IN	kJ h ⁻¹	172080.2	TOTAL ENTHALPY FLOW OUT	kJ h ⁻¹ 177187.6
			Enthalpy difference	-5107.3
			% Difference	-2.97
			Energy per kg water removed	kJ kg ⁻¹ 4048.9

outlet gas temperature difference. By permitting the highest possible inlet gas temperature and the lowest possible outlet gas temperature, the maximum thermal efficiency can be achieved. Running the drier on extreme gas temperature ranges is not practical because the heat damage to the food product would be very high when operating the drier with very high inlet gas temperatures, whilst the very low outlet gas temperatures can lead to the product having higher residual moisture content. If the heat losses cannot be neglected during the operation, the following correlation should be used to estimate the thermal efficiency of the spray drier (Katta and Gauvin, 1976):

$$\eta_{thermal} (\%) = \left(\frac{\dot{E}_c \lambda}{G \cdot C_{pb}(T_{b,i} - T_{wb}) + F \cdot C_{pf}(T_{f,i} - T_{wb})} \right) \quad (4.30)$$

where \dot{E}_c is the evaporation capacity of the drier, $T_{f,i}$ is the inlet feed temperature and T_{wb} is wet-bulb temperature corresponding to the drying gas temperature, and C_{pb} and C_{pf} are the heat capacity of the drying gas and the liquid feed, respectively.

4.6.2 Evaporative efficiency

The spray drier performance is often expressed by evaporative efficiency. The evaporative efficiency is defined as the ratio of the actual evaporative capacity to the capacity obtained with air of saturated condition. Then, the evaporative efficiency (η_{evap}) can be determined by replacing the ambient air temperature in equation (4.29) with the adiabatic saturation temperature (T_{sat}) corresponding to the inlet air temperatures (Masters, 1991):

$$\begin{aligned} \eta_{evap} (\%) &= \frac{\text{heat used in evaporation}}{\text{heat required for maximum possible evaporation}} \\ &= \left(\frac{T_{b,i} - T_{b,o}}{T_{b,i} - T_{b,sat}} \right) \times 100 \end{aligned} \quad (4.31)$$

4.6.3 Volumetric evaporative capacity

The spray drier can also be evaluated by its specific evaporative capacity, which can be defined as the rate of water evaporation per unit volume of the drying chamber:

$$\begin{aligned} \text{Vol. evap. capacity (kg/m}^3\text{h)} &= \frac{\text{Water evaporation rate}}{\text{Chamber volume}} \\ &= \frac{dm_w/dt}{V_{ch}} \end{aligned} \quad (4.32)$$

The overall or thermal efficiency of the spray drier can be improved by considering one or more of the following steps:

1. Increase the difference between inlet and outlet air temperature to a maximum value. However, this step is limited by the possible heat damage to, or the undesirable quality of, the final product.
2. Installation of the heat recovery system at the exit of the drying gas. A special design for a heat-exchanger is required due to the presence of fine particles in the exhaust gas stream.

3. Recycle a part of the exhaust gas stream into the drying chamber. This step is limited by the increment in the absolute humidity of the inlet drying gas).
4. Draw the drying air from the top section of the drier room, which is the hottest part of the plant building.
5. Use high feed solid concentrations and temperatures. This application is limited by the atomization capacity of the atomizer and the product damage at high feed temperatures.
6. Use more effective insulation for the drying chamber and the ducts.

4.7 POWDER CHARACTERIZATION

4.7.1 Particle micro-structure

The micro-structure of the particle is the link between processing and functionality (Chen and Özkan, 2007). The droplets experience substantial changes during processing in the drying chamber. These changes produce dried particles with porous or non-porous solid structures. Several spray-dried particles of different food materials are illustrated in Figure 4.10 using scanning electron microscope (SEM) images. A typical micro-structure formed during spray drying is drying-rate dependent, and affected by drying conditions such as drying gas temperature, humidity and velocity, and feed conditions such as liquid concentration, composition and temperature. For given drying conditions, particles may distort, shrivel, fracture or inflate depending on the shrinkage behavior, the stress distribution on the surface and the type of the particle's shell or crust (impervious or permeable, porous or non-porous, etc.) formed during drying. With some materials, a smooth skin may form on the particle surface (see Figures 4.10b, 4.10c, 4.10d), whilst with some other materials particles may crack, or even fracture giving broken shell fragments (see Figure 4.10f). Certain qualitative relations were observed between the micro-structural changes in particles and the particle's moisture content and air temperature profiles in the drying chamber (Alamilla-Beltrán *et al.*, 2005). Shriveled particles (see Figure 4.10f), in general, were more likely to occur at low drying temperatures because water diffusion is slower, allowing more time for structures to deform, shrink and even collapse (Walton, 2000). Particles tend to inflate, crack or break when dried at high drying temperatures. When drying rates are fast, particles experience a smaller shrinkage and smooth and regular surfaces are usually observed for complete or broken particles. On the other hand, particles with a thick, compact and irregular crust are observed for slow drying processes (Oakley, 1997).

Particles may have indentations or pores on the outer surface (see Figure 4.10a) which may or may not be connected with inner pores or a centre vacuole, as shown schematically in Figure 4.11. The high inlet and outlet air temperatures may cause expansion of particles due to flash boiling of water and expansion of occluded air/vapor mixture inside the particle. Hollow particles may be formed when drying rates are very fast, air is trapped in the liquid feed and the shell formed on the surface is partially impervious to the vapor (Kentish *et al.*, 2005). Air can be trapped in the liquid feed during pumping to the atomizer and also during atomizing the liquid feed in the drying chamber, especially for pneumatic kind of atomizers. The bulk density of the powder could be small where the powder is comprised of mainly hollow particles.

An accurate interpretation of the transport of key constituents in the droplet/particle may be helpful in understanding the micro-structure formation during drying. A great deal of research work has been done in this area, however this multi-component transport phenomenon is still

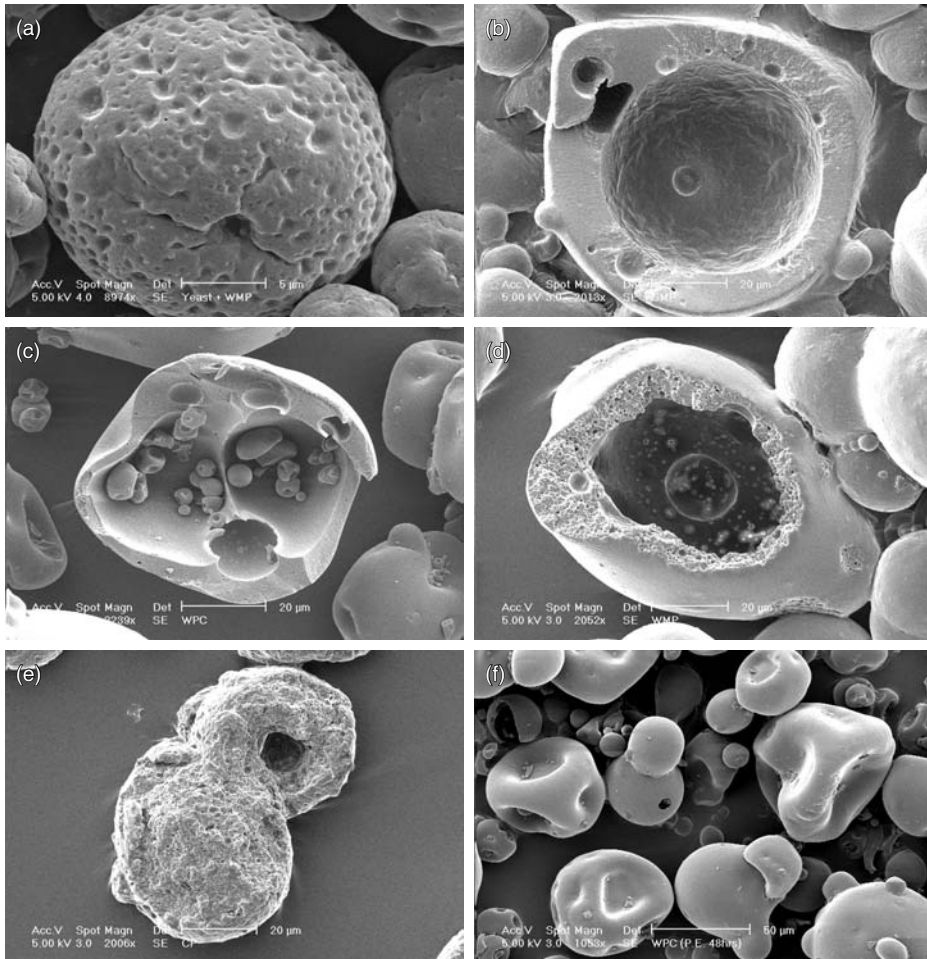


Fig. 4.10 Micro-structure and surface morphology of various spray dried powders. (a) Whole milk + yeast; (b) skim milk; (c) whey proteins concentrate; (d) whole milk; (e) cream powder; (f) whey proteins concentrate.

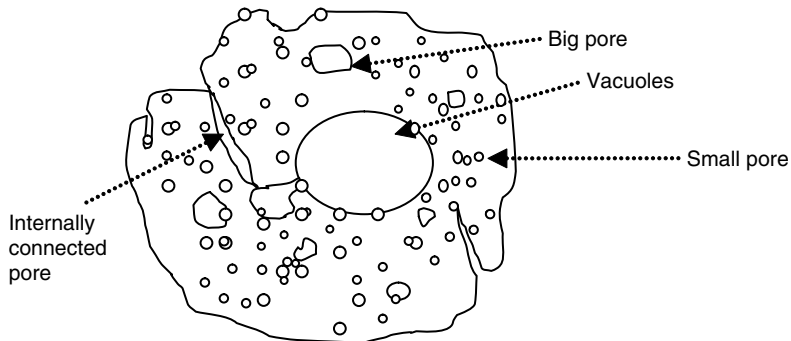


Fig. 4.11 Schematic diagram of a spray-dried particle depicting irregular surface, internal structure and pores.

somewhat blurry. The moisture movement within the particle during drying of food materials is known to influence the distortion, shrinkage and inflation behavior of the particle (King, 1995, Hecht and King, 2000). During drying of moist droplets, the diffusion of moisture molecules toward the surface is accompanied by an opposite diffusion of solute molecules toward the center. During migration of solute molecules, molecules with larger molecular weight (i.e. bigger molecules) would diffuse slowly compared to those with smaller molecular weight (i.e. smaller molecules). Understanding this molecular migration is very useful in determining the surface composition of the powder. The surface composition may severely affect the powder's functionality (wetting and dispersion) and stability as well as stickiness and cohesiveness. When studying the surface composition of a skim milk particle (SMP) and whole milk particle (WMP), a higher fat content was observed on the surface of the WMP (Kim *et al.*, 2002, 2003). With the SMP of 58% lactose, 41% protein and 1% fat, the surface of the particle was covered with 36% lactose, 46% protein and 18% fat. The surface fat content of the WMP was noted to be 98%. Migration of surface active proteins at the particle surface during drying has also been reported (Fäldt and Bergenståhl, 1994; Kim *et al.*, 2003; Shrestha *et al.*, 2007).

Characterizing the micro-structure and surface composition is relatively easier these days due to great advancements in various techniques such as SEM, ESEM, TEM, AFM, XPS, X-ray diffraction, FTIR, NMR, DSC, etc., but the difficulty is how to apply the outcomes to favor a higher quality product. Understanding how a typical micro-structure of the particle is formed during drying and how the specific micro-structure, particle morphology or surface properties affect the quality of the product may provide a valuable insight into the fundamentals of droplet drying, quality control, reconstitution of the powder, selection of process conditions and drier designing.

4.7.2 Particle morphology

Spray-dried particles can be categorized into three distinct particle morphologies: skin-forming, crystalline and agglomerate (Walton and Mumford, 1999). It is very complicated to assess the effect of individual process variables (feed, drying gas and atomization conditions and particle's residence time data) on the particle morphology due to the specific drying nature of the food materials. Most spray-dried food and dairy particles can be placed in the skin-forming group. The outermost layer of the particle, which is composed of a continuous solid phase, is generally referred as the 'skin' of the particle. Some common examples of skin-forming powders are skim milk, whole milk, yoghurt, protein powders, coffee, instant drink powder, custard, starch, gelatin, lactose, fructose, etc. The literature shows that skin-forming particles (see Figure 4.10) have most diverse morphological features, such as dents, wrinkles, blowholes, craters, cracks, vacuoles, etc. and micro-structural features such as hollow particles, shriveled particles, solid (yet porous) particles, collapsed particles, fractured particles, etc. compared to particles of crystalline and agglomerate morphology. Most industrial food particles have a regular shape, normally spherical.

A crystalline particle is composed of large crystal nuclei grouped together by a continuous micro-crystalline phase (Walton and Mumford, 1999). Inorganic materials are commonly known to have a crystalline morphology. Crystalline particles were noticed to have limited morphological features, mainly cracks and occasionally craters and blowholes. Dust or fractured shell formation is usually high with particles of crystalline morphology. Furthermore, crystalline particles may not be regular in shape, unlike skin-forming particles. Some

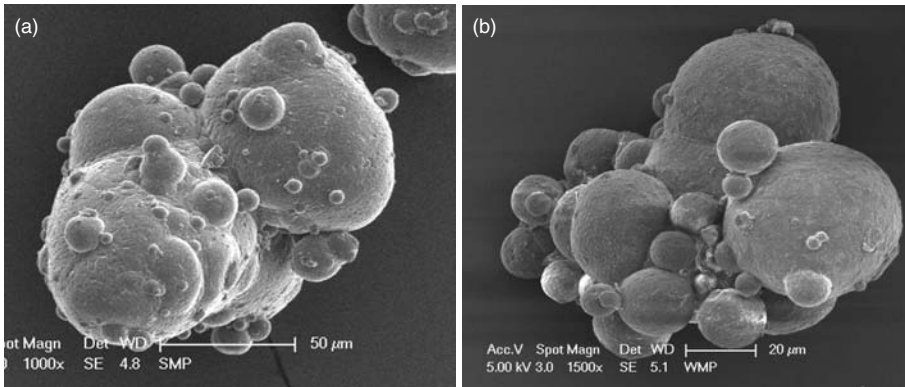


Fig. 4.12 Agglomerates from (a) skim milk and (b) whole milk powders.

carbohydrates, for instance glucose, may have a well-defined crystalline micro-structure, but still have a skin-forming morphology on the surface.

An agglomerate is composed of two or more individual particles (of crystalline or skin forming morphologies), which are bonded together by sub-micron particles or a binder (see Figure 4.12). Agglomerates tend to offer an ‘instant’ property to the powder. This means agglomerates disperse and dissolve quickly into solvents such as water, milk, tea, etc. during reconstitution. The reconstitution performance of the agglomerated powder is enhanced because the open porous structure of the agglomerate allows the solvent to penetrate and disperse throughout, forcing the agglomerate to sink faster compared to individual particles (Pietsch, 1999). In addition, agglomeration of the particles provides a dust-less, free-flowing powder that facilitates the handling of the powder to the benefit of manufacturers (Retsina, 1988).

Agglomerates can be produced in the drying chamber by encouraging coalescences between droplets of the same spray or two sprays in the case of multiple nozzle atomization. In modern spray drying plants, the dried fine powder of the same material being dried is mixed with fresh droplets near the atomization zone in order to produce larger particles or agglomerates. The secondary agglomeration is generally provided by incorporating internal and external fluidized-bed driers with the spray driers. The majority of agglomeration takes place during this secondary drying stage. Due to great advances in the fluidized-bed drying technique, the extent of agglomeration and thus bulk density of the powder can be well controlled during the secondary agglomeration process. A binder or a lubricant may be used during secondary agglomeration to increase the strength of agglomerates.

Agglomeration is widely used in food industries, for example in the production of skim milk, whole milk, whey proteins, instant coffee, instant soup, instant drink powder, etc (see Figure 4.12). The majority of food agglomerates are composed of spherical particles of a solid or hollow micro-structure. The size of primary particles present in the agglomerate can be uniform or vary widely, depending on the completeness of atomization, the droplet trajectory, the drier design and the number of drying stages (i.e. involvement of the fluidized-bed drying step). The surface composition of the droplets or the semi-dried particles plays a big role in manufacturing agglomerates in the drying chamber or fluidized-bed driers. Pores and wrinkles can be observed on the surface of primary particles of the agglomerate. Morphological features such as craters, fissures and blowholes are uncommon with agglomerated food particles.

Table 4.7 Key powder properties and their typical values.

1. Moisture (2–5%, w/w)
2. Particle density (1.0–1.5 g ml ⁻¹)
3. Particle size and distribution (10–200 μm)
4. Bulk density (loose and packed) (0.4–0.7 g ml ⁻¹)
5. Flowability (free flowing, angle of repose <35°)
6. Reconstitution property
Wettability (10–60 s for instant powder)
Dispersibility (fast dispersion)
Sinkability (rapid sinking)
Solubility (92–99%)

4.7.3 Physical and functional properties of powder

The surface morphology and internal micro-structure of the spray-dried particles highly influence the physical and functional characteristics of the powder. Powder characteristics have to consider the properties of both individual particles and the bulk powder. The fundamental (physical) properties of the powder include bulk density, particle density, particle size and distribution, particle shape and residual moisture content. These fundamental properties have a big influence on the market value, the storage conditions, the handling properties, the packaging requirements, the transport properties in a duct, and also the functional properties such as stability during storage, dispersibility, flowability, solubility and mixing with other dry ingredients. Some of these key powder properties (fundamental and functional) which are of main interest to the food industries and consumers are listed in Table 4.7.

4.7.3.1 Particle density and bulk density

Particle density is the mass of single particles per unit volume. Alternatively, particle density (g ml⁻¹) is defined as the mass of particles having a total volume of 1 ml. This property is significantly influenced by the density of individual components comprising the solid (proteins, carbohydrates, fat and minerals) and the presence of occluded air in the particles. The density of the mixture of various components can be calculated using mass fractions and true density of each component. True density (moisture free) for various food ingredients is listed in Table 4.8. A simple technique to measure particle density is to add a weighed amount of powder to petroleum ether in a measuring cylinder. Particle density would be the weight of powder divided by the volume increase of petroleum ether. Particle density is less frequently used compared to bulk density to characterize the final powder. A Pycnometer can also be used to calculate particle density. Particle density provides significant information to researchers when simulating a droplet drying process. If particle density is known, the porosity or the volume of occluded air of the particle can be estimated. Occluded air, usually expressed in ml per 100 g, is defined as the difference between the volume of a given mass of particles and the volume of the same mass of air-free solids.

The bulk density of a powder, normally expressed in g ml⁻¹, is the weight of the given amount of powder divided by the volume it occupies. Bulk density is greatly influenced by interstitial air along with particle density, particle size and its distribution, particle shape, electrostatic effect and moisture content. Interstitial air is defined as the difference between the volume of a given mass of particles and the volume of the same mass of the powder that is tapped 100 times. For common dairy and food powders, the interstitial air content

Table 4.8 True density of various dairy materials (moisture free).

Powder material (moisture free)	True density at 20°C (g ml⁻¹)
Milk fat in powder	0.940
Whole milk powder (28% fat)	1.280
Calcium-caseinate phosphate complex	1.390
Glutamine	1.460
Amorphous sucrose	1.507
Amorphous lactose	1.520
Non-fat milk solids	1.520
Demineralized whey powder	1.525
Glucose	1.540
α -Lactose monohydrate	1.545
Anhydrous α -lactose	1.545
Spray-dried whey powder	1.580
Sucrose crystal	1.586
β -Lactose	1.590
Residual whey components	1.800

is approximately 127 ml per 100 g of powder. Feed concentration, drying conditions and atomization pressure are also known to have a significant influence on the bulk density of the final product. Spherical particles have a higher bulk density because they have a low interstitial air content.

Bulk density in dairy industries is usually expressed as loose, 100 times tapped and 1250 times tapped. To measure the bulk density of the powder, a stainless-steel cylinder of a known volume is filled with the powder, and weighed before tapping. A Stampf volumeter (Engelsmann tapping machine) is generally used for regular tapping of the cylinder. The cylinder is weighed after 100 taps and 1250 taps.

The term 'bulk density' is frequently used by manufacturers and consumers to characterize bulk powder. A high bulk density is preferable for shipping the powder long distance because the transport and packaging costs would be smaller for a powder with a higher bulk density. In some instances, a low bulk density is preferred to illustrate optically a larger amount of the powder. Agglomerated particles or instant powders have a lower bulk density compared to individual particles of the same volume. For instance, the bulk density of instant coffee powder (agglomerated particles) is 0.147 g ml⁻¹, whilst it is 0.633 g ml⁻¹ for high-density skim milk powder.

4.7.3.2 Particle size and particle size distribution

The particle size and distribution of granular or food powders is very important from the processing, mixing and packaging point of views. The size of the particle is an essential reflection, especially for drying of heat-sensitive food materials. Small particles have the largest residence time as well as heat and mass transfer coefficients. They hold a small initial moisture content, drying times are usually smaller compared to bigger particles, and they are more prone to thermal degradation if exposed to high temperatures for an extended time. Particle size is most commonly expressed as a mean (or average) diameter of the particle. There could be a large variation of particle size in the powder sample from the same production run. Particle diameters, in general, range from sub-micron level up to 800 μm for various

spray-dried products. Optical microscopes and scanning electron microscopes (SEM) are generally used to measure the particle diameter. There are several ways to illustrate the mean diameter of the particles such as arithmetic mean, surface mean, volume–surface mean and geometric mean diameters.

The particle size distribution is particularly important to the value of the final product. A large particle size distribution is often referred to as poor quality, especially for high-value food powders. Recently, the trend in the market is to produce powders with stringent product quality. The narrow size distribution is therefore intended during production. The particle size and size distribution can be analyzed using a sieving technique (conventional method) or a laser diffraction particle size analyzing method (e.g. Malvern instrument). The latter technique is less time consuming, and provides a lot of information at a time, such as surface-averaged diameter, volume-averaged diameter, Sauter mean diameter, etc. Measurements are made difficult particularly if a large number of agglomerates are present in the powder sample. A log-normal graph (manual determination) can be plotted using a simple Microsoft Excel program or other software by collecting data from sieving analyses or a laser diffraction instrument.

4.7.3.3 Powder flowability

Particle flowability is an average rheological property of the heterogeneous particle population of a particular powder (Ilari, 2002). Flow of the powder starts with the initial movement of some individual particles in an unbalanced physical situation, and flow becomes continuous and regular (more like plastic deformation) under a continuous stress condition. The ability of powder to flow, or powder flowability, is an important property in storage and gravitational flow through pipes, for example, in coffee vending machines, unloading/loading from or to storage silos, filling bags, etc. Evaluation of the flowability of any powder is a very important issue for many industries. A good flow capacity is considered useful for all commercial or household practical applications. This rheological property of the powder is a complex phenomenon, and greatly influenced by particle size and size distribution, particle morphology/shape, interparticle forces (molecular forces, van der Waals forces, solid bridges, etc.), co-ordination number (packing density), residual moisture content, presence of fat (and free fat) on the particle surface, presence of lumps, the degree of caking, etc. (Peleg, 1983; Peleg and Hollenbach, 1984).

An inclinometer is a common tool for measurement of the flowability of the given powder. An angle of repose of less than 30° is considered a free-flowing powder, whilst more than 57° is considered a cohesive powder (Walton and Mumford, 1999). In between these average angle of repose values, the powder is considered a semi-free-flowing powder. Many other techniques are available these days to measure powder flowability. Ilari (2002) has comprehensively presented and compared commonly used flowability measurement techniques in context to industrial dairy powders. The same author found that the physical properties tester from Hosokawa is the most suitable tool to measure the flow capacity of the powder.

4.7.3.4 Insolubility index

The solubility index or insolubility index is usually considered a post-drying property of the food powder (Mistry and Hassan, 1991). In simple terms, the insolubility index is the ability of powder to dissolve in the solvent (water, milk, etc.). The insolubility index is also considered to be an indicator of the presence of insoluble materials in the particle/powder. This property

is often used by commercial milk powder manufacturers as a criterion to indicate the quality of milk powders. The insolubility index can be related to the feed composition (mainly the protein content), and it may affect the reconstitution property of powders in an aqueous medium. The insolubility index of a given powder is expressed as the volume of the insoluble material in milliliter. A simple method to determine the insolubility index of the powder is to dissolve it in water at a specific temperature. The solution is then placed in a centrifuge followed by the removal of supernatant. The residue or sediment is mixed with fresh water, and then centrifuged again. The volume of the sediment (ml) left in the tube after the second centrifugation indicates the insolubility index of the powder at a given temperature.

The rate of insoluble material formation during drying mainly depends on the protein content of the feed, drying conditions, and temperature and moisture content profiles of the droplet in the drying chamber. Kudo *et al.* (1990) carried out some experimental work by heating skim milk powders with moisture content in the range of 3–7 wt% to study the insolubility kinetics during storage. They evaluated the effect of various processes and feed parameters on the final solubility of the powder. Straatsma *et al.* (1999) proposed a zero-order kinetic model to determine the insolubility index for milk powders assuming that the insoluble material forms only when the particle moisture content is between 10 wt% and 30 wt%. The rate of insoluble material formation (r_{isi}) was then described by the following empirical equation:

$$r_{isi} = k_{isi} \exp\left(\frac{-E_{isi}}{R_g} \left(\frac{1}{T_{avg}} - \frac{1}{T_0}\right)\right) \quad (4.33)$$

where k_{isi} and E_{isi} are kinetic constants at a reference temperature T_0 , and T_{avg} is average product temperature. They evaluated constants $k_{isi} = 0.054 \text{ ml s}^{-1}$ and $E_{isi} = 2.7 \times 10^5 \text{ J mol}^{-1}$ at a $T_0 = 348 \text{ K}$ for skim milk powders. Since it is difficult to obtain a qualitative model to show the effect the moisture content on the rate of formation of insoluble material, this idealistic kinetic model may provide ‘first-guess’ information within the limited operating range. The drying kinetics model has to be incorporated with the above model if the solubility behavior of individual droplets during drying is of interest. Prediction of the insolubility index along the drying time may offer control on driers for minimizing the insolubility of the powder during a drying process. The insolubility index has to be established for a wider range of food products.

4.7.3.5 Glass-transition temperature

The glass-transition temperature (T_g) is a characteristic property of an amorphous component of the food material, and could be related to the stickiness behavior of the powder during storage or processing. The glass-transition is primarily a state transition of amorphous materials (lactose, fructose, glucose, maltose, galactose, maltodextrins, etc.) occurring between the solid, glassy and super-cooled liquid states (Roos, 1995; Slade and Levine, 1999). Many food powders contain amorphous sugars as a primary constituent. For instance, dairy powders contain lactose along with proteins, fat and minerals. Amorphous materials are considered as thermodynamically non-equilibrium systems (Roos and Karel, 1992), and they may undergo substantial changes when they are stored above the T_g due to the increment in the molecular mobility of those glassy materials. For food materials, the glassy state is reached in the viscosity range of 10^7 – 10^9 Pa s . Above T_g , the viscosity of the food matrix may decrease to a point where amorphous materials may deform and crystallize, leading to several problems

such as stickiness, caking, lump formation and diffusion-controlled deterioration reactions which can threaten the stability of individual particles or powders (Aguilera *et al.*, 1995). The higher the difference between the product temperature and the glass-transition temperature, the higher the threat to the stability of the product. Therefore, the food is considered to most stable below the T_g .

In the drying chamber, when the temperature of droplets or semi-dried particles rises above the corresponding T_g , the amorphous material transforms itself into a rubbery state. In that case, the surface of the droplets or particles remain plastic depending on the product characteristics, composition and the drying conditions, resulting in droplets sticking on the drier wall or among themselves. The sticky-point temperature, which is considered to be responsible for caking and wall deposition inside the drier, is generally 5–20°C higher than the glass-transition temperature (Bhandari and Howes, 1999). The drier wall temperatures, therefore, should be maintained well below the T_g during production in order to minimize the wall deposition and fouling problems. The glass-transition temperature of the material can be determined in the laboratory using a differential scanning calorimetry (DSC) that detects changes in the heat capacity of the amorphous component between glass and rubbery states. Other analytical methods for determining T_g are differential thermal analysis (DTA) and thermal mechanical analysis (TMA). The latter method detects changes in the elastic modulus of the amorphous material upon transition.

The glass-transition temperature of the food material is mostly estimated using a Gordon–Taylor equation or its modified expressions such as the Couchmann–Karasz equation, considering the T_g of individual components and average water and solid fractions in a single droplet. The Gordon–Taylor equation, which seems to be capturing the water content effect on the T_g , can be presented as:

$$T_g(\text{mixture}) = \frac{\sum w_i T_{g,i} + k_g w_{\text{water}} T_{g,\text{water}}}{\sum w_i + k w_{\text{water}}} \quad (4.34)$$

where w_i and w_{water} are mole fractions of individual solid components and water, respectively and $T_{g,i}$ and $T_{g,\text{water}}$ are glass-transition temperatures of individual solid components and water, respectively, and k_g is a solid–water constant that has to be determined using experiments. The glass-transition temperature of some common amorphous food compounds are listed in Table 4.9. The glass-transition temperature of water was reported to be –135°C. Since predicting the time-dependent glass-transition temperature during drying requires temperature–time and moisture content–time profiles of single droplets, an accurate drying kinetics model has to be combined with the glass-transition model, such as equation (4.34).

4.7.3.6 Powder solubility

Powder solubility or functionality is one of the most important functional properties of food powders that signify how the bulk powder behaves when reconstituted in water. Dissolution of food powders is of particular importance, both to the manufacturers and to the consumers, being one of the critical benchmarks of food powder quality for consumption. Food powders are normally added to water or other solvents such as milk at normal temperatures, or sometimes at higher temperatures, to form a reconstituted mix. Powders are expected to dissolve as quickly as possible and make a uniform solution when dissolved in the water to gain its original properties such as color, taste, nutrients, etc. An example is reconstituted milk powder, where it is important for the powder to dissolve instantly to form a stable colloidal

Table 4.9 Glass-transition temperatures of various amorphous food materials.

Material (moisture free)	Glass transition temperature (°C)	Constant (kg)
Fructose	5	3.18
Glucose	31	4.07
Galactose	32	
Skim milk with hydrolyzed lactose	49	8.00
Sucrose	62	
Maltose	87	
Low-fat milk (10.7% fat)	88	
Skim milk (0% fat)	92	
Whole milk (32.4% fat)	92	
Amorphous lactose	97	6.70
Medium-fat milk (18.6% fat)	98	
Maltodextrins (Dextrose Equivalent 36)	100	
Maltodextrins (Dextrose Equivalent 25)	121	
Maltodextrins (Dextrose Equivalent 20)	141	
Maltodextrins (Dextrose Equivalent 10)	160	
Maltodextrins (Dextrose Equivalent 5)	188	

Source: Roos and Karel (1991) and Roos (1995).

suspension of fat and protein, thus leaving little or no visible residue suspended in water or lumped on the container surface. Many factors can be influential in reconstitution of the powder such as particle size, shape, composition, surface properties, micro-structure, and the presence of additives and insoluble components.

Reconstitution of a given powder represents four process steps: wetting of particles, sinking of particles below the liquid surface, dispersion of particles in the liquid and complete dissolution of particles into the liquid. However, there is no sharp line between each of these processes. Each of these processing steps can be related to the properties of powders, which are wettability, sinkability, dispersibility and solubility, respectively. Wettability is the ability of the powder to absorb water on its surface and get wet completely. In generally, wettability is measured as the time taken for a prescribed amount of powder to sink below the liquid surface from the moment of being dropped on the liquid surface to the moment when all the powder is below. Powders with a particle size of less than 100 μm have very little inter-particulate space, and thus they are difficult to get wet. Agglomeration of small particles will improve the wettability, as discussed in Section 4.7.2.

Sinkability signifies the ability of powder to sink below the liquid surface once the particles are wet. Particle density, size and shape can have a big impact on the sinkability property of the powder. Dispersibility is defined as the ability to be evenly distributed throughout the water. This property also includes the behavior of the lumps or agglomerates falling apart into individual particles. Mechanically strong agglomerates tend to have good wettability, but poor dispersibility (Chen and Özkan, 2007).

Once the particles are dispersed in the liquid, the solubility property of the particle becomes an important parameter. In simple terms, solubility is a measure of the actual soluble or insoluble solids in the powder. Fat-containing particles do not dissolve easily in aqueous solution. Fat will rather be dispersed in the solution as small globules. Some powders such as ice-cream mix may require gentle stirring for quicker and better dissolution. The insolubility index is commonly used to evaluate the solubility of the powders after manufacturing

or during reconstitution. When producing protein-rich materials such as high milk protein powders, whey protein powders and casein-rich powders, the insolubility index is an important property that relates the functional behavior of proteins to the solubility property. The protein state is affected during spray drying because protein molecules may face emulsion, foaming and gelation during drying, leading to a denatured state. The solubility of proteins, which are trapped in the particle structure, depends on their native or denatured state and also on environmental factors such as temperature and pH of the liquid medium. Unfavorable changes in pH or temperature disrupt the normal folded structure into a random-shaped unfolded structure, which is a biologically inactive or a denatured state (Anandharamakrishnan *et al.* 2007). It is important to recognize that denaturation of proteins alone is not significant enough to cause a measurable loss of solubility, because proteins must also aggregate and/or coagulate and finally precipitate. High temperatures are known to favor protein aggregation, coagulation and precipitation. Therefore, increasing liquid temperatures do not necessarily help to improve the dissolution behavior of the powder.

4.7.4 Drying parameters

There are three main spray drying parameters, which can greatly influence the functional properties of the powder including protein functionality. These parameters are feed concentration, atomization parameters, and drying gas temperatures at inlet and outlet of the drier. Appropriate control and regulation of these parameters are very important to favor an easy operation, a predictable product quality and improved economy.

Concentration of the liquid feed can vary from 20 to 50 wt% depending on the properties of the feed (such as viscosity, heat-sensitivity), the type of the atomizer and the final product requirements. Higher feed concentrations improve the commercial viability of the process through thermal efficiency. Furthermore, feed with higher solids content minimizes the mean residence time of the particles leading to less thermal degradation for heat-sensitive materials. If the material is dried at low solid concentrations, the resulting powder will have relatively smaller particles (see Figure 4.13) which promote poor reconstitution. In addition, the recovery of the powder in cyclones and filters will be lower for smaller particles.

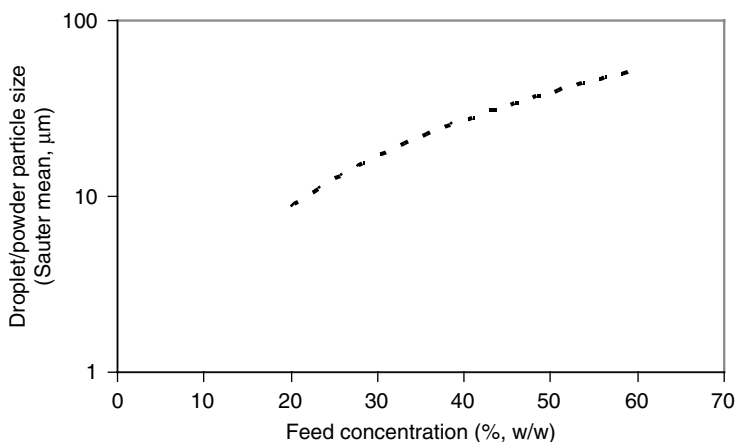


Fig. 4.13 Indicative diagram to show the effect of feed concentration on the droplet/particle size (ignoring the shrinkage of droplets during drying).

Table 4.10 Spray drying conditions used for drying various food liquids.

Product	Feed temperature (°C)	Feed solids (% w/w)	Inlet air temperature (°C)	Outlet air temperature (°C)
Skim milk	50–55	45–52	180–230	80–95
Whole milk	50–55	40–50	180–200	80–90
Whey, lactose	40–50	40–50	150–180	70–80
Coffee	20–30	30–50	180–220	80–95
Maltodextrin	50–80	50–60	150–300	80–100
Fruit juices, honey	40–50	50–60	150–160	65–80
Bacterial cultures	20–30	35–50	140–150	55–60
Cheese powder	40–50	30–40	150–180	60–75
Flavor powder	40–50	30–40	170–190	75–85

It was recognized that initial feed concentrations have a big impact on the particle microstructure that is a key characteristic for many functional and fundamental properties of the final powder.

Atomization is believed to be the first and most important step of the drying process. This processing step offers desirable sizes to the droplets. The initial droplet size greatly influences the final particle size and its size distribution, which affects almost all physical, transport, handling and functional properties of the food powder. Furthermore, occluded air in the particle, foaming ability of the functional proteins during drying and inactivation of bioactive components (enzymes, vitamins, etc.) are also influenced by the atomization step. Selection of atomizers is therefore considered an important criterion during the designing of spray driers. The mixing of spray with the hot drying medium is also very important for effective drying of dispersed droplets near the atomization zone, which is the hottest zone in the drying chamber.

High drying gas temperatures facilitate rapid drying inside the drying chamber leading to shorter residence times for particles being dried. In food applications, high inlet air temperatures (160–300°C) and low outlet air temperature (60–100°C) are used in order to achieve the higher thermal efficiency of the drier (Table 4.10). When the inlet temperature is increased during drying, the outlet air temperature is also increased. As a rule of thumb, increments of 1°C outlet air temperature can be achieved by elevating the inlet air temperature by 5°C. The upper limit of the inlet air temperature is usually limited by the heat-sensitivity of the food material to be dried. For instance, milk-based products are normally dried at the inlet air temperatures from 180°C to 200°C. When drying food materials, the nutrients (e.g. proteins, enzymes, vitamins, etc.) are intended to be preserved in the dried particles. The influence of outlet air temperature on the product quality is more prominent than any other drying parameters. The outlet air temperature can be regulated by controlling the feed rate and inlet air temperature. The low outlet air temperature is important to avoid protein denaturation because at the drier exit the product has both high reactant (proteins, carbohydrates and fat) concentrations and elevated temperatures to favor deterioration reactions. If all other feed and operating conditions are constant, elevated outlet air temperatures result in a product with small moisture content, whilst increase in inlet air temperatures cause higher residual moisture content in the powder (see Figure 4.14). A moderate temperature range is recommended to minimize thermal degradation of the product and other heat-related issues such as stickiness of the product in the drier. Also, it is advisable to facilitate the drying process

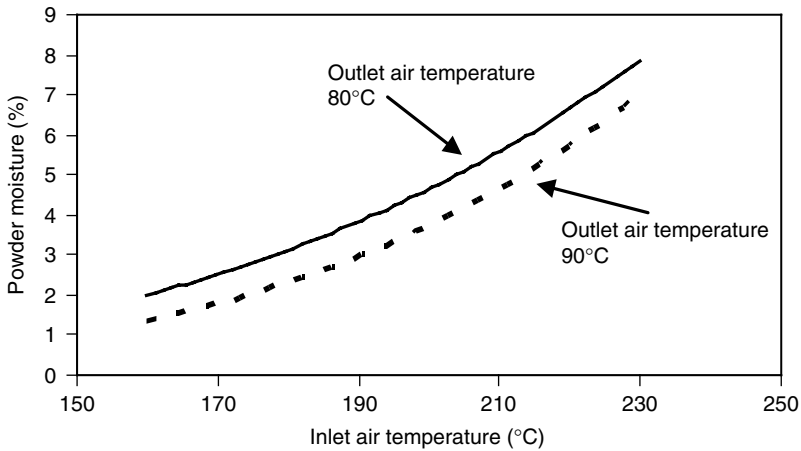


Fig. 4.14 A schematic diagram to show the effect of inlet and outlet air temperatures on the residual moisture content of powders.

in combination with fluidized-bed drying because particle agglomeration can be carried out with improved economy in the fluid-bed drier.

4.8 SPRAY DRYING OF VARIOUS FOOD PRODUCTS

4.8.1 Dairy powders

The dairy industry is the major food sector utilizing the spray drying technique in order to meet the ever-increasing demand of dried milk products. This unit operation has been employed for about 150 years to produce dairy powders at industrial scales. Skim milk, whole milk and whey are the most important milk-based liquid products, and are dried in large quantities. Other dairy materials such as butter milk, lactose, caseinates, cheese, ice-cream and yoghurt are also dried to meet consumer demand. Drying conditions and feed concentrations can vary from the product to product, depending on the feed properties and the expected product quality.

4.8.1.1 Skim milk powder

Skim milk powder is the most common dried dairy product, and is manufactured up to a production capacity of 25 ton powder per hour. Drying of skim milk involves evaporation of raw skim milk of 12–14 wt% solids content to around 50–55 wt% solids content. The inlet and outlet air temperatures are usually in the range of 180–230°C and 70–95°C, respectively. The final moisture content of the powder is 3–3.5 wt% (dry basis). Skim milk powders with different functional properties are manufactured with varying amount of whey proteins denatured during the preheating treatment. Different types of skim milk powders and their application are presented in Table 4.11. Denaturation of whey proteins and their mixtures with casein micelles provide desired functionalities to the powder, such as high water absorption capacity, high volume in bakery products and improvement of flavor in the confectionery products.

Table 4.11 Different types of skim milk powders with distinct whey protein nitrogen index (WPNI) values.

Type of SMP	WPNI	Pretreatment prior to spray drying	Applications
Low heat	>6	70–80°C/15–50 s	Reconstituted/recombined milk
Medium heat	1.5–5.9	90–100°C/30–50 s	Confectionery, ice-cream, sweetened condensed milk
High heat	<1.5	115–125°C/1–4 min	Bakery products

Lactose is the main ingredient of skim milk powder. The final skim milk powder may contain more than 50% lactose. During spray drying, lactose forms an amorphous structure in the solid matrix. The hygroscopicity of the skim milk powder containing high lactose content is greater, and therefore skim milk powders have to be handled, transported and stored under controlled-humidity conditions. To minimize the water absorption and subsequent caking, lactose in the milk is sometime crystallized prior to drying. Crystallization of lactose produces a relatively stable non-hygroscopic skim milk powder.

4.8.1.2 Whole milk powder

Whole milk is dried in similar drying conditions to those of skim milk. The residual moisture content in the final powder is generally 2.5–3 wt% (dry basis). Slightly lower air temperatures compared to skim milk drying are preferred due to the presence of high fat in the whole milk droplets which exhibit some stickiness due to a high free-fat content on the particle surface. To minimize the coalescence of the semi-dried particles and their deposition on the drier wall, moderate air temperature conditions are used. Application of an electric hammer to dislodge the particles from the chamber wall is also common practice. The rapid cooling of the powder (<30°C) is more critical during whole milk powder production. Removal of excess moisture can promote rapid oxidation of fat. Due to the presence of surface fat, whole milk powders are difficult to agglomerate and also to dissolve into water. Often, lecithin is sprayed on the powder during fluidized-bed drying in order to coat the free-fat on the surface. Sometimes extra heat treatments are given to the whole milk for initiating browning reaction products, which seem to contribute an antioxidant to fat. The whole milk powder is usually packaged in an inert environment.

4.8.1.3 Whey products

Whey is the by-product of cheese manufacturing plants. Whey can also be obtained during the acid coagulation of skim milk for casein manufacture. The cheese whey is termed as sweet whey, and can be dried without significant problems. In contrast, acid whey is difficult to dry due to high hygroscopicity of acids (such as lactic acid) and their contribution to lowering the overall glass-transition temperature of whey. Acid whey may be spray dried by neutralizing the acid first by mixing with other dairy materials with a low acid content. Whey solids contain mainly lactose with concentrations ranging from 65 to 88% of the total solids. The whey has to be concentrated prior to spray drying because the initial solid concentration of the whey solutions is about 6 wt% (dry basis). The final concentration of the whey solutions can go up to 45–50 wt% total solids.

Lactose and whey protein concentrate are commonly used whey products. Depending on their suitability, two types of whey products are manufactured using a spray drying method: ordinary whey powder and non-hygroscopic whey powder. Ordinary whey powders are extremely hygroscopic due to the high lactose content. They quickly absorb moisture from the environment, and can form lumps or cake during storage and handling. The non-hygroscopic whey powder is made by pre-crystallizing lactose in the whey solutions. Crystallization of lactose is facilitated by seeding with micron-size crystals of α -lactose. Lactose crystallizes in α -lactose monohydrate form which is relatively non-hygroscopic in nature compared to the amorphous lactose. Whey is dried to a slightly higher moisture content (12–14 wt% by dry basis) in the drying chamber, and further crystallization of supersaturated lactose continues in a fluidized-bed drier.

Whey proteins concentrate (WPC) is widely used in food applications due to its higher nutritional value and versatile functional properties compared to any other animal proteins. Industries manufacture WPC with a few different grades which differ in its protein content, mostly varying from 35% WPC to 80% WPC. The manufacturing process involves ultrafiltration of raw whey, obtained from the cheese production, followed by evaporation and spray drying. Lower inlet air temperatures (160–190°C) are used for manufacturing WPC in order to preserve as much protein as possible. High protein WPC requires additional water to be added to reduce the viscosity of the concentrated whey during ultrafiltration, now called diafiltration, which also removes the residual quantities of lactose and unwanted minerals. The trend today is to produce agglomerated instant whey protein powders. Fluidized-bed drying is necessary for producing agglomerates of high protein WPC as there is only a small amount of lactose present in the feed which acts as a binding agent.

Lactose powders are generally produced as food-grade, industrial-grade and pharmaceutical-grade products, which specifically differ in their purity considering their final applications. Variables controlling the performance of each grade must be understood to choose the right lactose product for a desired application. Food-grade lactose is generally manufactured from fresh sweet whey, a by-product during the manufacture of cheese, by crystallizing or permeating an oversaturated whey solution and drying it into a powder form. Industries offer several types of lactose that differ from each other regarding their physical form, purity, particle size and distribution. In solution form, lactose exists as equilibrium of 60% β -lactose and 40% α -lactose. The ratio of α - to β -lactose is usually unchanged during spray drying, especially at high temperatures. Spray-dried agglomerated lactose powder typically contains 9–12% of β -lactose that is present in an amorphous matrix, which is usually 15–20 wt% of the total product. Transformation of lactose from amorphous to crystalline form is likely to alter the performance and characteristics of the bulk powder, for instance, flowability, stability, drug dispersion, etc.

4.8.2 Micro-encapsulated powders

Spray drying is emerging as an important process to produce encapsulated powders. Various food flavor oils, essential oils, vitamins, useful bacteria, probiotics, butter oil, fish oil, vegetable oil and food colors can be encapsulated in a solid matrix during spray drying. A micro-encapsulation technique converts food ingredients (in solid or liquid form) into a more useable and shelf-stable solid form. The micro-encapsulation process also dilutes the core material, facilitating a uniform dispersion of these materials throughout the mixes. Encapsulated powders have found applications in cake mixes, biscuit mixes, ice-cream mixes,

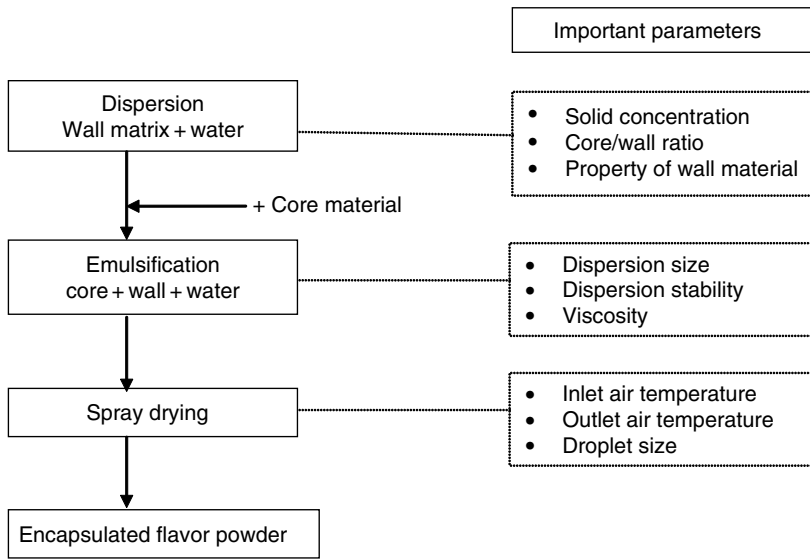


Fig. 4.15 A schematic process diagram for micro-encapsulation using a spray drying technique and some important parameters influencing the efficiency of encapsulation during drying.

oatmeal, instant beverages and a wide variety of snacks. Minimum loss of valuable volatile products during storage and controlled release properties are other benefits offered by micro-encapsulated powders.

The process of encapsulation by spray drying is described using a flowchart, shown in Figure 4.15. The solid matrix or shell materials used for these purposes are maltodextrins, acacia gum, lactose, sucrose, milk proteins (e.g. sodium caseinate, micellar casein, whey protein), soy protein isolates and modified starches. The core materials or active ingredients are dispersed in the aqueous solution of shell materials. If the core materials are not soluble in water (such as oils), they are emulsified by selecting appropriate shell materials with an emulsifying property or adding an emulsifier to the solution. The actual encapsulation of core material occurs during spray drying when the water evaporates rapidly and the matrix is fixed due to rapid solidification.

One of the important types of encapsulated powders produced by spray drying is flavor powders. The micro-encapsulated flavor powder produced by spray drying usually contains a relatively high flavor load. Stability of flavor is moderate in spray-dried micro-encapsules, mainly due to the presence of surface oil (non-encapsulated oil) on the particles.

The retention of volatile flavors when water evaporates during the course of spray drying is an interesting phenomenon. In fact, the volatility of these compounds is much higher than water itself. Nevertheless, flavor volatiles remain locked into the particle matrix. The retention of volatiles during the spray drying process is explained by a 'selective diffusion' theory, which was first described by Thijssen (Rulkens and Thijssen, 1972). This theory postulates that there is retention of flavors in the drying droplets for two reasons. Firstly, there is a semi-permeable film formation around the droplets that is permeable to water but impermeable to volatile compounds. Secondly, as water evaporates from the droplets, the diffusivity of the flavor compounds in the droplet system reduces drastically as compared to water. The difference between the diffusivity of volatiles and water becomes important when

the water activity of the droplet attains 0.9 or lower (King, 1995; Upadhyaya and Kilara, 1984). Flavor compounds are characterized by a larger molecular size and a lower diffusivity compared to those of water. Thus the controlling factor for the loss is molecular size, not the boiling point temperature. As a result, though some flavor compounds are relatively more volatile and have a lower boiling point than water, they are retained in the particles during the drying process. The retention of volatiles strongly increases with increasing molecular size of the volatiles, but is independent of the relative volatility.

4.8.3 Sugar-rich products

Fruit and vegetable products and honey are rich in sugars and organic acids. These products are normally dried by the addition of some carrier materials due to the difficulty in drying them in a pure form. The problem of stickiness during spray drying of sugar-rich food products such as fruit juices, honey and some starch derivatives (e.g. glucose syrups and maltodextrin at higher dextrose equivalent values) has been well recognized in the literature (Bhandari *et al.*, 1997; Vega *et al.*, 2005; Truong *et al.*, 2005). The physical state of the sugar-rich product changes as it passes through the drier from solution to syrup and finally to a solid form. During drying, these materials may remain as syrup or stick on the drier chamber wall. There is also a problem of unwanted agglomeration in the drier chamber, cyclones, conveying systems and packaging containers. This can lead to lower product yields and many other operating problems.

In recent years, the stickiness problem of sugar-rich products has been related to their low glass-transition temperatures. The dried particles which comprise the final powder may be called glass particles. The solutes in the liquid droplet will pass through a supersaturation state (rubbery) to an amorphous solid state (glass) by the virtue of a glass-transition. The time required for the nucleation or crystallization of solute(s) to occur during spray drying is not enough due to the fast removal of water and solidification of droplets. Many sugar- and acid-rich products have a glass-transition temperature lower than the outlet air temperature of the drier. This means that they remain in a liquid or sticky form in the drier, even though they are dried to a very low moisture content. In a practical sense, it has been shown that the temperature of the surface of the particle during spray drying should not reach 10–20°C above T_g . The glass-transition temperature of some sugar-rich products is so very low that spray drying of the pure product is generally not economically feasible. The most common approach to dry such products is to add high molecular weight additives. Additives have the effect of raising the glass-transition temperature (see Figure 4.16).

As an example, maltodextrin is generally added to honey during the production of dried honey powders. Honey is a mixture of different sugars with 90 wt% of glucose and fructose. The T_g of honey is around -45°C ($\approx 16\%$ moisture by w/w). Considering the T_g of principal components of honey (glucose and fructose), the glass-transition temperature of an anhydrous honey may lie between the T_g of fructose (5°C) and glucose (32°C). This means that spray drying of honey is not possible (Bhandari and Hartel, 2005). Addition of carrier materials such as maltodextrin at levels up to 50 wt% is necessary to dry products like honey (Sopade *et al.*, 2001). The indicative sticky curve with or without maltodextrin is schematically shown in Figure 4.16. The addition of a carrier material means dilution of the honey, but in terms of honey flavor it may not matter much if a strong flavored honey is selected for spray drying. Spray dried honey with maltodextrin is commercially available in the market, and used mainly for premixes and flavoring purposes.

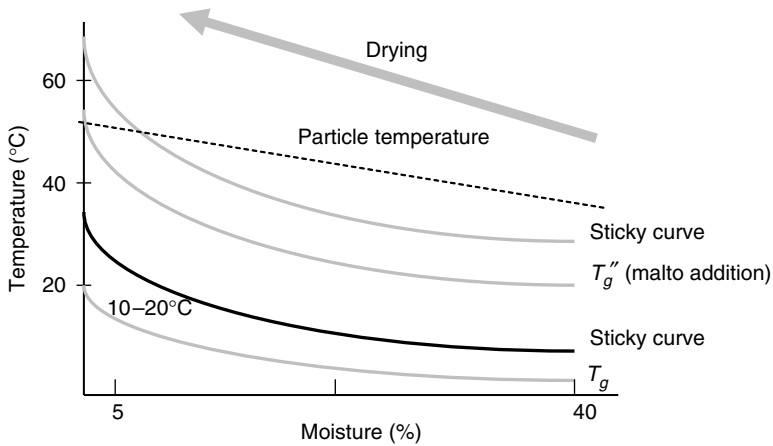


Fig. 4.16 Illustration of rising T_g of honey by adding maltodextrin. T_g of the feed increases as drying proceeds. The product will remain sticky if T_g is lower than the particle temperature.

4.8.4 Egg

Whole egg, egg yolk or egg white (egg albumin) can be spray dried by using the same spray drying system. The popularity of dried whole egg products for use in fine bakery goods is increasing because dried products have some advantages regarding their use, storage, handling and micro-biological safety. The whole egg and egg yolk can be dried at 25–45 wt% total solids. However, the egg white is normally dried at a lower solid content (around 10–12 wt%) due to the high viscosity and foaming ability of the egg white. The glucose in the egg albumin is normally removed by fermentation in order to avoid Maillard reactions and color deterioration during storage. Glucose removal is done mainly by adding bacteria, enzymes (glucose oxidase) or yeast. The glucose level is normally reduced to below 0.1 wt%. The egg white is pasteurized at 56–59°C for several minutes. Salt is normally added to the egg white to avoid heat damage to the protein during heating or spray drying. Prior to drying the raw feed is homogenized and then filtered to remove chalazae. The inlet and outlet air temperatures used in egg drying vary from 145 to 200°C and 80 to 90°C, respectively. The final moisture content of the powder is around 4–9 wt%.

4.8.5 Enzymes

Various types of spray-dried enzymes are used in the textile, paper, pharmaceutical, biological and food industries. The spray-dried enzymes include trypsin, amylase (starch hydrolysis and textile industries), protease (for detergents), glucose oxidase, pectinase (for fruit juice industries), glucose isomerase, lactase, pepsin, etc. In order to preserve the enzymatic activity, these bioactive compounds are dried in the presence of shell materials such as lactose, sucrose, mannitol, gums, maltodextrins and cyclodextrins (Daeman and van der Stege, 1982). Enzymes are encapsulated in the solid glassy matrix during spray drying. The activity of the enzyme is regained after reconstitution of micro-encapsules in water. Relatively low air temperatures are used for drying enzyme suspensions. Typically, inlet and outlet gas temperatures can be varied from 120 to 140°C and 50 to 65°C, respectively. Drying processes substantially affect the enzymatic activity. The overall activity loss depends on the severity of drying conditions and the extent of shear during atomization.

Recently it was found that the enzyme concentration on the surface of the particle is higher (40–50%) compared to the inner matrix due to the surface active property of enzymes (as they are proteins). Enzymes on the surface may experience most severe drying-induced stress during drying. Also, surface enzymes will degrade faster during storage primarily due to the loss of their secondary structure caused by unfavorable temperature, moisture and other environmental factors. It was recognized that the surface concentration of proteins in the spray-dried powders could be controlled by adding a surfactant to the initial feed before drying, since the surfactant is preferentially adsorbed at the air–liquid interface of the droplets, thus expelling proteins from the surface (Millqvist-Fureby, 1999). The loss of enzymatic activity can be estimated by incorporating the inactivation kinetics model with the drying kinetics model, since the inactivation rate is temperature–time and moisture content–time dependent. Chen and Patel (2007) have recently reviewed some existing inactivation kinetics models and relevant issues in the context of spray drying of food materials with bioactive compounds, and also proposed an appraisal to show the effect of surface and center water concentrations on the inactivation rate.

4.9 CONCLUDING REMARKS

A rise in world food powder production is forecast to continue since new markets have opened up for the consumption of food materials in a powder form. Spray drying is a proven economical and versatile technology to manufacture powders. Successful application of advanced process control to the spray drying operations has led to the emergence of a new generation of spray drier, which is capable of producing 25 tons of skim milk powder per hour. The advance in technology has permitted the production of powders with a strict food safety and quality control on this large scale. In this chapter, basic fundamentals of the spray drying operation and several important powder characteristics are presented which will be helpful to new graduates and also existing workers associated with spray drying-based food powder manufacture. The spray drying process is still the subject of extensive research in order to manufacture high-value innovative products with extraordinary health benefits. Innovation in spray drying technology is mainly facilitated by combining other existing novel technologies and the most recent knowledge of the processing and production sides. Several innovative designs and equipment modifications such as superheated steam drying, horizontal spray driers, spray-freeze drying, cyclone spray driers, spray driers with bag filters on the roof, etc. have been reported in the last few decades. Several challenges regarding the product development, product quality, health and safety matters, environmental issues and energy consumption are still ahead, and are encouraging researchers associated with food powder production to develop innovative research work.

4.10 NOTATION

A_d	surface area of single droplet or particle, m^2
Bi	<i>Biot</i> number
C	centrifugal force,
C_D	drag coefficient
C_p	specific heat, $J/kg\ K$
d	diameter, m

D_d	diffusion coefficient, $\text{m}^2 \text{s}^{-1}$
\dot{E}_c	evaporation capacity, kg water per s
E_{isi}	solubility kinetics constant, J mol^{-1}
ΔE_v	apparent activation energy, J mol^{-1}
F	feed rate, kg h^{-1}
g	gravitational constant
G	mass flow rate of the drying gas, kg s^{-1}
h	heat transfer coefficient, $\text{W m}^{-2} \text{K}$
h_m	external mass-transfer coefficient, m s^{-1}
h_v	volumetric heat transfer coefficient, $\text{kJ m}^{-3} \text{h}^\circ\text{C}$
k	thermal conductivity, $\text{W m}^{-1} \text{K}$
k_{isi}	solubility kinetics constant, ml s^{-1}
m	mass, kg
P	product rate, kg h^{-1}
Pr	Prandtl number ($=c_p\mu_b/k_b$)
r_{isi}	rate of insoluble material formation, ml s^{-1}
R	droplet radius, m
R_g	universal gas constant
Re	Reynolds number ($=d_d v_d \rho_b / \mu_b$)
T	temperature, K
T_g	glass-transition temperature, K
T_{wb}	wet-bulb temperature, K
ΔT_{AMTD}	arithmetic temperature difference
ΔT_{LMTD}	log mean temperature difference
t	time, s
v	velocity, m s^{-1}
V_{ch}	volume of the chamber, m^3
\dot{V}	volumetric flow rate, $\text{m}^3 \text{s}^{-1}$
w	mole fractions of solids
W	mass flow rate of water, kg h
X	droplet moisture content, kg water per kg dry-solids
X_e	equilibrium moisture content, kg water per kg dry-solids
Y	absolute humidity, kg water per kg dry-air

Greek symbols

λ	latent heat of vaporization, J kg^{-1}
θ	number of droplets
μ	viscosity, $\text{kg m}^{-1} \text{s}$
ε	volume fraction
ω	mass fraction of water
ρ	density, kg m^{-3}

Subscripts

0	initial conditions
a	ambient, atmospheric conditions

<i>av</i>	average
<i>b</i>	bulk drying gas phase
<i>d</i>	droplet or particle
<i>f</i>	liquid feed
<i>i</i>	inlet conditions
<i>o</i>	outlet conditions
<i>p</i>	product
<i>s</i>	solid
<i>v</i>	vapor
<i>sat</i>	saturated conditions

REFERENCES

- Alamilla-Beltrán, L., Chanona-Pérez, J.J., Jiménez-Aparicio, A.R. and Gutiérrez-López, G.F. (2005) Description of morphological changes of particles along spray drying. *Journal of Food Engineering*, **67**, 179–184.
- Anandharamkrishnan, C., Reilly, C.D. and Stapley, A.G.F. (2007) Effects of process variables on the denaturation of whey proteins during spray drying. *Drying Technology*, **25**(5), 799–807.
- Aguilera, J.M., de Valle, J.M. and Karel, M. (1995) Caking phenomenon in amorphous food powders. *Trends in Food Science and Technology*, **6**, 149–155.
- Avvaru, B., Patil, M.N., Gogate, P.R. and Pandit, A.B. (2006) Ultrasonic atomization: Effect of liquid phase properties. *Ultrasonics*, **44**, 146, 158.
- Bayvel, L.P. and Orzechowski, Z. (1993) *Liquid Atomization*. Taylor & Francis, Washington, DC.
- Bhandari, B.R., Datta, N. and Howes, T. (1997) Problems associated with spray drying of sugar-rich foods. *Drying Technology*, **15**(2), 671–684.
- Bhandari, B.R. and Hartel, R.W. (2005) Phase transitions during food powder production and powder stability. Chapter 11. In: *Encapsulated and Powdered Foods* (ed. C. Onwulata). Taylor & Francis, New York, pp. 261–291.
- Bhandari, B.R. and Howes, T. (1999) Implication of glass transition for the drying and stability of dried foods. *Journal of Food Engineering*, **40**, 71–79.
- Cakaloğlu, T., Akbaba, H., Yesugey, E.T. and Periz, A. (1997) Drying model for α -amylase in a horizontal spray dryer. *Journal of Food Engineering*, **31**(4), 499–510.
- Chen, X.D. (2004) Heat–mass transfer and structure formation during drying of single food droplets. *Drying Technology*, **22**(1–2), 179–190.
- Chen, X.D. and Lin, S.X.Q. (2005) Air drying of milk droplet under constant and time-dependent conditions. *AIChE Journal*, **51**(6), 1790–1799.
- Chen, X.D. and Özkan, N. (2007) Stickiness, functionality and microstructure of food powders. *Drying Technology*, **25**(6), 969–979.
- Chen, X.D. and Patel, K.C. (2007) Micro-organism inactivation during drying of small droplets or thin-layer slabs – A critical review of existing kinetics models and an appraisal of the drying rate dependent model. *Journal of Food Engineering*, **82**(1), 1–10.
- Chen, X.D. and Xie, G.Z. (1997) Fingerprints of the drying behavior of particulate or thin layer food materials established using a reaction engineering model, *Transactions of the IChemE (Part C): Food and Bioproducts Processing*, **75**(C4), 213–222.
- Daeman, A.L.H. and van der Stege, H.J. (1982) The destruction of enzymes and bacteria during the spray drying of milk and whey. 2. The effect of the drying conditions. *Netherlands Milk Dairy Journal*, **36**, 211–229.
- Fäldt, P. and Bergenståhl, B. (1994) The surface composition of spray-dried protein–lactose powders. *Colloids and Surfaces A: Physicochemical and Engineering Aspects*, **90**, 183–190.
- Ferrari, G., Meerdink, G. and Walstra, P. (1989) Drying kinetics for a single droplet of skim milk. *Journal of Food Engineering*, **10**, 213–222.

- Hecht, J.P. and King, J.C. (2000) Spray drying: Influence of developing drop morphology on drying rates and retention of volatile substances. 1. Single-drop experiments. *Industrial Engineering and Chemical Research*, **39**, 1756–1765.
- Huang, L., Kumar, K. and Mujumdar, A.S. (2003) Use of computational fluid dynamics to evaluate alternative spray chamber configurations. *Drying Technology*, **21**(3), 385–412.
- Huang, L. and Mujumdar, A.S. (2005) Development of a new innovative conceptual design for horizontal spray dryer via mathematical modeling. *Drying Technology*, **23**(6), 1169–1187.
- Ilari, J.L. (2002) Flow properties of industrial dairy powders. *Lait*, **82**, 383–399.
- Katta, S. and Gauvin, W. (1976) Basic concepts of spray dryer design. *AIChE Journal*, **22**(4), 713–724.
- Keey, R.B. (1991) *Drying of Loose and Particulate Materials*. Hemisphere Publishing Corporation: New York.
- Kentish, S., Davidson, M., Hassan, H. and Bloore, C. (2005) Milk skin formation during drying. *Chemical Engineering Science*, **60**, 635–646.
- Kim, E.H.-J., Chen, X.D. and Pearce, D. (2002) Surface characterization of four industrial spray-dried dairy powders in relation to chemical composition, structure and wetting property. *Colloids and Surfaces B: Biointerfaces*, **26**, 197–212.
- Kim, E.H.-J., Chen, X.D. and Pearce, D. (2003) On the mechanisms of surface formation and the surface compositions of industrial milk powders. *Drying Technology*, **21**(2), 265–278.
- King, C.J. (1995) Spray drying food liquids and the retention of volatiles revisited. *Drying Technology*, **13**, 1221–1240.
- Kudo, N., Hols, G. and van Mil, P.J.J.M. (1990) The insolubility index of moist skim milk powder: Influence of the temperature of the secondary drying air. *The Netherlands Milk and Dairy Journal*, **44**, 89–98.
- Kundu, K.M., Das, R., Datta, A.B. and Chatterjee, P.K. (2005) On the analysis of drying process. *Drying Technology*, **23**(5), 1093–1105.
- Langrish, T.A.G. and Fletcher, D.F. (2001) Spray drying of food ingredients and applications of CFD in spray drying. *Chemical Engineering and Processing*, **40**, 345–354.
- Langrish, T.A.G. and Kockel, T.K. (2001) The assessment of a characteristic drying curve for milk powder for use in computational fluid dynamics modelling. *Chemical Engineering Journal*, **84**, 69–74.
- Lin, S.X.Q. and Chen, X.D. (2006) A model for drying of an aqueous lactose droplet using the reaction engineering approach. *Drying Technology*, **24**(11), 1329–1334.
- Lin, S.X.Q. and Chen, X.D. (2007) The reaction engineering approach to modelling the cream and whey protein concentrate droplet drying. *Chemical Engineering and Processing*, **46**(5), 437–443.
- Masters, K. (1991) *Spray Drying Handbook*, 5th edn. Longman Scientific and Technical, Singapore.
- Masters, K. (1998) Developments in spray drying. *Drying '98. Proceedings of the 11th International Drying Symposium (IDS '98)*. Halkidiki, Greece. August 19–22. Volume A: 666–667.
- Masters, K. (2004) Current market-driven spray drying development activities. *Drying Technology*, **22**(6), 1351–1370.
- Mistry, V.V. and Hassan, H.N. (1991) Delactosed high milk protein powder. 2. Physical and functional properties. *Journal of Dairy Science*, **74**, 3716–3723.
- Millqvist-Fureby A., Malmsten, M. and Bergenstahl (1999) Spray-drying of trypsin-surface characterisation and activity preservation. *International Journal of Pharmaceutics*, **188**, 243–253.
- Mujumdar, A.S. (2004) Research and development in drying: Recent trends and future prospects. *Drying Technology*, **22**(1&2), 1–26.
- Nijdam, J.J. and Langrish, T.A.G. (2006) The effect of surface composition on the functional properties of milk powders. *Journal of Food Engineering*, **77**, 919–925.
- Oakley, D.E. (1997) Produce uniform particles by spray drying. *Chemical Engineering Progress*, **10**, 48–54.
- Patel, K.C. and Chen, X.D. (2007) Sensitivity analysis of the reaction engineering approach to modeling spray drying of whey proteins concentrate. In *Proceedings of the 5th Asia-Pacific Drying Conference*, pp. 276–281, August 13–15, 2007, Hong Kong.
- Patel, K.C. and Chen, X.D. (2008) Drying of aqueous lactose solutions in a single stream dryer. *Transactions of the IChemE (Part C): Food and Bioproduct Processing*, in press.
- Peleg, M. (1983) Physical characteristics of food powders. In: *Physical Properties of Foods* (eds M. Peleg and E.B. Bagley). AVI Publishing Company, Inc., Westport, CT, pp. 293–323.

- Peleg, M. and Hollenbach, A.M. (1984) Flow conditioners and anticaking agents. *Food Technology*, March, 93–99.
- Pietsch, W. (1999) Readily engineer agglomerates with special properties from micro- and nanosized particles. *Chemical Engineering Progress*, **95**(8), 67–81.
- Pisecky, J. (1997) *Handbook of Milk Powder Manufacture*. Niro A/S, Copenhagen, Denmark.
- Retsina, T. (1988) Agglomeration: A process to improve fine powder handling. *Food Technology International Europe*, 37–39.
- Roos, Y. and Karel, M. (1991) Water and molecular weight effects on glass transitions in amorphous carbohydrates and carbohydrates solutions. *Journal of Food Science*, **56**(1), 1676–1681.
- Roos, Y. and Karel, M. (1992) Crystallization of amorphous lactose. *Journal of Food Science*, **57**, 775–777.
- Roos, Y.H. (1995) *Phase Transitions in Foods*. Academic Press, Inc., San Diego, CA, USA.
- Rulkens, W.H. and Thijssen, H.A.C. (1972) The retention of organic volatiles in spray drying aqueous carbohydrate solutions. *Journal of Food Technology*, **7**, 95–105.
- Shi, M. and Wang, X. (2004) Investigation on moisture transfer mechanism in porous media during rapid drying process. *Drying Technology*, **22**(1–2), 111–122.
- Shrestha, A.K., Howes, T., Adhikari, B., Wood, B. and Bhandari, B.R. (2007) Effect of protein concentration on the surface composition, water sorption and glass transition temperature of spray-dried skim milk powders. *Food Chemistry*, **104**, 1436–1444.
- Slade, L. and Levine, H. (1999) A food polymer science approach to structure property relationships in aqueous food systems: Non-equilibrium behavior of carbohydrate–water systems. In: *Water Relationships in Food* (eds H. Levine and L. Slade). Plenum Press, New York.
- Sopade, P.A., Bhandari, B., Halley, P., D’Arcy, B. and Caffin, N. (2001) Glass transition in Australian honeys. *Food Australia*, **53**(9), 399–404.
- Straatsma, J. (1990) Reduction of energy consumption of the milk powder production by computer optimization. Innovation Energetique et Industrie Agro-alimentaire. Internationale Symposium AFME, Amiens, pp. 209–217.
- Straatsma, J., Van Houwelingen, G., Steenbergen, A.E. and De Jong, P. (1999) Spray drying of food products: 2. Prediction of insolubility index. *Journal of Food Engineering*, **42**(2), 73–77.
- Truong, V., Bhandari, B.R. and Howes, T. (2005) Optimization of co-current spray drying process of sugar-rich foods. Part I—Moisture and glass transition temperature profile during drying. *Journal of Food Engineering*, **71**(1), 55–65.
- Upadhyaya, R.L. and Kilara, A. (1984) Drying heat sensitive products. *Proceedings of 4th International Drying Symposium, 1*. Kyoto, Japan (July 9–12), pp. 316–321.
- Vega, C., Goff, H.D. and Roos, Y.H. (2005) Spray drying of high sucrose dairy emulsions: Feasibility and physicochemical properties. *Journal of Food Science*, **70**(3), 244–251.
- Walton, D.E. (2000) The morphology of spray-dried particles: A qualitative view. *Drying Technology*, **18**, 1943–1986.
- Walton, D.E. and Mumford, C.J. (1999) Spray dried products – Characterization of particle morphology. *Transactions of the IChemE: Chemical Engineering Research and Design (Part A)*, **77**, 21–38.
- Zbicinski, I., Strumillo, C. and Delag, A. (2002) Drying kinetics and particle residence time in spray drying technology. *Drying Technology*, **20**(9), 1751–1768.
- Zhang, J. and Datta, A.K. (2004) Some considerations in modeling of moisture transport in heating of hygroscopic materials. *Drying Technology*, **22**(8), 1983–2008.

5 Low-pressure superheated steam drying of food products

Sakamon Devahastin and Peamsuk Suvarnakuta

5.1 INTRODUCTION

Although the concept of superheated steam drying (SSD) was originally proposed over a century ago and the first industrial applications were reported some 60 years ago (Mujumdar, 2000, 2007), SSD has only recently re-emerged as an alternative drying technology for a wider array of products including woods (Pang, 1997; Pang and Dakin, 1999), paper (Douglas, 1994) as well as foods and biomaterials (Devahastin and Suvarnakuta, 2004). SSD involves the use of superheated steam in a direct (convective) drier in place of hot air, combustion, or flue gases as the drying medium to supply heat for drying and to carry away the evaporated moisture. Any direct or direct/indirect (e.g. combined convection/conduction) drier can be, in principle, operated as a superheated steam drier although, in practice, this conversion may not always be straightforward.

In addition to the energy-related advantages reported by many researchers (Mujumdar, 2000; Devahastin and Suvarnakuta, 2004), SSD also possesses many other advantages that are of special interest to processors of foods and biomaterials. Generally, no oxidative reactions, e.g. enzymatic browning (Nimmol *et al.*, 2007; Thomkapanish *et al.*, 2007), lipid oxidation or aerobic degradation of vitamins (Suvarnakuta *et al.*, 2005a), are possible in SSD due to lack of oxygen.

SSD can also help decontaminate micro-organisms, toxins and spores due to its normally high-temperature environment, even during an early stage of drying (Pronyk *et al.*, 2006; Cenkowski *et al.*, 2007). A combination of drying with other thermal treatments, for example, blanching (Iyota *et al.*, 2001; Prachayawarakorn *et al.*, 2002; Namsanguan *et al.*, 2004; Sotome *et al.*, 2006), deodorization (Furukawa and Akao, 1983), parboiling (Soponronnarit *et al.*, 2006), pasteurization and sterilization (Abe and Miyashita, 2006) as well as popping (Iyota *et al.*, 2005) is also possible.

Another advantage of SSD is that, for certain foods or vegetables, the porosity of the products dried in superheated steam is higher than that dried in hot air. This is due to the evolution of steam within the product, which decreases the bulk density of the product while enhancing its rehydration characteristics. This feature is especially attractive for the instant food as well as confectionary industries (Devahastin *et al.*, 2004).

Higher drying rates (comparing with hot air drying or in the case of the low-pressure superheated steam drying, vacuum drying) are possible in both constant and falling rate periods of SSD, depending on the steam temperature. The higher thermal conductivity and heat capacity of superheated steam leads to higher rates of surface moisture removal above the so-called inversion temperature (Schwartz and Brocker, 2002; Suvarnakuta *et al.*, 2005b). Below the inversion temperature drying in air is faster. In the falling rate period the higher

product temperature in SSD (over 100°C at 1 bar) and lack of diffusional resistance to water vapor lead to faster drying rates.

On the other hand, since most foods and biomaterials are damaged or degraded at the saturation temperature of superheated steam corresponding to atmospheric or higher pressures, these products cannot suitably be dried in SSD even if they contain only surface moisture. Lowering the drier operating pressure is clearly a feasible option that could lead to preservation of the quality of dried products and additionally, in some cases, to enhanced drying rates as well.

In the following section a short description of the basic principles of SSD and low-pressure superheated steam drying (LPSSD) is first illustrated. This is followed by a review of the recent advances in LPSSD of foods and biomaterials. For superheated steam drying of foods at near-atmospheric pressure the reader is referred to Devahastin and Suvarnakuta (2004).

5.2 BASIC PRINCIPLES OF SUPERHEATED STEAM DRYING

A simple schematic sketch of a superheated steam drying system is shown in Figure 5.1. Saturated steam from a boiler or a steam generator is heated up in a heater (steam superheater) and becomes superheated steam. Drying takes place through direct contact between superheated steam and the product to be dried. As mentioned earlier, the exhaust of the drier is also steam, albeit at lower specific enthalpy. Steam may be recirculated and reheated in a closed loop; only the amount of steam that corresponds to the amount of evaporated water is removed from the closed loop and used either directly or indirectly after its energy is recovered via a heat exchanger. The closed loop of SSD implies that emissions coming from the drying product are not emitted to the environment but are included in the condensate; toxic or expensive organic liquids can therefore be recovered more easily than in the case of hot air drying.

In the case of LPSSD the same basic concept applies except for the fact that an external steam superheater may not be required. As the saturated steam is introduced to

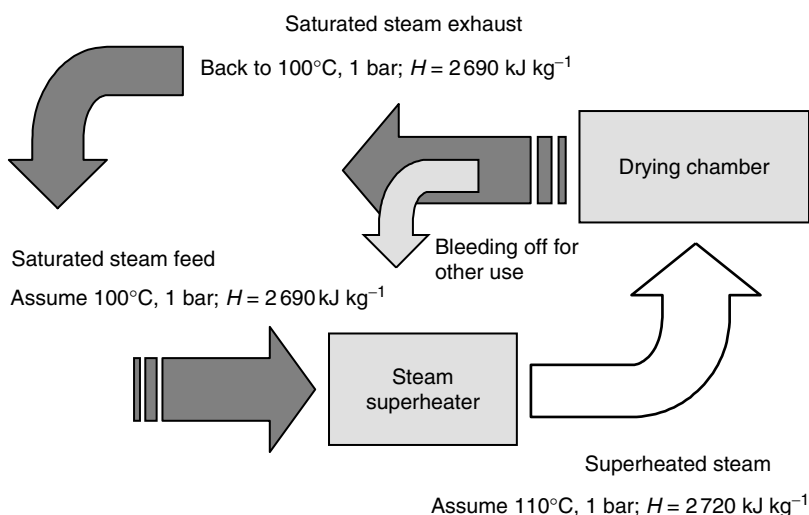


Fig. 5.1 A schematic sketch of a superheated steam drying system.

the low-pressure drying chamber, saturated steam becomes low-pressure superheated steam since its temperature is already well above the saturation temperature at the reduced pressure of the drying chamber. To minimize the effect of adiabatic expansion of steam that may occur in the low-pressure drying chamber, a heater is generally installed in the drying chamber to help control the low-pressure superheated steam temperature at a desired value (Devahastin *et al.*, 2004).

Since there is no resistance to diffusion of the evaporated water in its own vapor, the drying rate in the constant rate period is dependent only on the heat transfer rate q . If sensible heat effects, heat losses and other modes of heat transfer are neglected, the rate at which surface moisture evaporates in steam is given simply by:

$$N = \frac{q}{\lambda} = \frac{h(T_{steam} - T_s)}{\lambda} \quad (5.1)$$

where N is the evaporation rate, h is the convective heat transfer coefficient, T_s is the drying surface temperature which corresponds to the saturation temperature at the drier operating pressure, T_{steam} is the temperature of the superheated steam and λ is the latent heat of vaporization. In hot air drying, $T_s = T_{wet-bulb}$ and hence at lower drying temperatures, ΔT is higher in air drying but h is lower since air has heat transfer properties inferior to superheated steam at the same temperature. It turns out that these counter-acting effects lead to the phenomenon of inversion; a temperature beyond which the superheated steam drying rate is greater than hot air drying rate (see Figure 5.2). This is confirmed experimentally as well as numerically for water as well as several organic solvent systems (superheated vapor drying). It is observed that the inversion temperature is in the order of 160–200°C for evaporation of water in superheated steam for various flow configurations and flow regimes, for example, laminar/turbulent boundary layer flows, impinging jet flows, free convective flow over complex geometries (Chow and Chung, 1983; Wu *et al.*, 1987, 1989; Haji and Chow, 1988; Sheikholeslami and Watkinson, 1992; Bond *et al.*, 1994).

Strictly speaking, the inversion temperature is defined only for surface moisture evaporation and not for internal moisture removal, although some researchers do not make this distinction

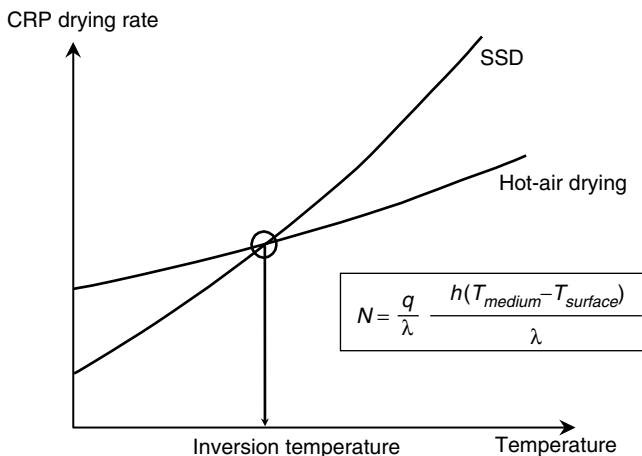


Fig. 5.2 An inversion phenomenon.

clear when reporting their results. However, the values of the inversion temperature calculated only from the surface moisture evaporation rates are obviously not the same as those calculated from the combined constant rate and falling rate drying rates (Suvarnakuta *et al.*, 2005b).

The convective heat transfer coefficient, h , between steam and the solid material surface can either be estimated using standard correlations for inter-phase heat transfer (Incropera and Dewitt, 2002) or from the experimental drying rates data. The following example illustrates how the values of the convective heat transfer coefficient are calculated from the experimental low-pressure superheated steam drying rates.

Example 1: Based on the data of Suvarnakuta *et al.* (2005b) who experimentally determined the drying rates of molecular sieve beads undergoing LPSSD at various operating pressures (see Figure 5.3), it is possible, through the use of equation (5.1), to determine the values of the convective heat transfer coefficient. First of all, it is recognized that equation (5.1) can be rewritten as:

$$h = \frac{N\lambda}{A(T_{\text{steam}} - T_{\text{surface}})} \quad (5.2)$$

As an illustrative case, consider the case at the drying temperature of 80°C and absolute pressure of 7 kPa (Figure 5.3a). Since the drying rates reported by Suvarnakuta *et al.* (2005b) are in kg kg^{-1} (d.b.) min^{-1} , it is necessary to multiply the reported drying rates by the bone-dry mass of the sample (approximately 24 g). Hence, $N = 1.4 \times 10^{-2} \text{ kg kg}^{-1}$ (d.b.) $\text{min}^{-1} \times 0.024 \text{ kg} = 3.36 \times 10^{-4} \text{ kg min}^{-1}$. In this case, A is the surface area of all molecular sieve particles used in each experiment and is equal to 0.044 m^2 .

At the pressure of 7 kPa the surface temperature is around 40°C, which corresponds to the saturation temperature at 7 kPa. Also at this pressure $\lambda = 2406.0 \text{ kJ kg}^{-1}$. Hence, $h = [3.36 \times 10^{-4} \text{ kg min}^{-1} \times 2406.0 \text{ kJ kg}^{-1}] / [0.044 \text{ m}^2 \times (80 - 40) \text{ K}] = 0.4593 \text{ kJ min}^{-1} \text{ m}^{-2} \text{ K}^{-1}$ or $7.66 \text{ W m}^{-2} \text{ K}^{-1}$.

The values of the heat transfer coefficient at other conditions are listed in Table 5.1. As expected, the values of the heat transfer coefficient increase with the operating pressure of the drier as there is more mass (steam) available for convection heat transfer in the drier.

5.3 LOW-PRESSURE SUPERHEATED STEAM DRYING OF FOODS AND BIOMATERIALS

Although there exist a number of publications on low-pressure superheated steam drying of other products, both from the fundamental (e.g. Shibata *et al.*, 1988, 1990; Sano *et al.*, 2005; Shibata, 2006; Tatemoto *et al.*, 2007) and application-oriented points of view (e.g. Chen *et al.*, 1992; Pang and Dakin, 1999; Defo *et al.*, 2004), this section is focused only on a more limited pool of information on LPSSD of foods and biomaterials. Near-atmospheric pressure superheated steam drying is not included either; the reader is referred to Devahastin and Suvarnakuta (2004) for a review on near-atmospheric pressure superheated steam drying and also to the literature for some recent advances of this drying technique applied to foods and biomaterials (e.g. Taechapairoj *et al.*, 2004; Rordprapat *et al.*, 2005; Prachayawarakorn *et al.*, 2006; Nathakaranakule *et al.*, 2007; Jamradloedluk *et al.*, 2007).

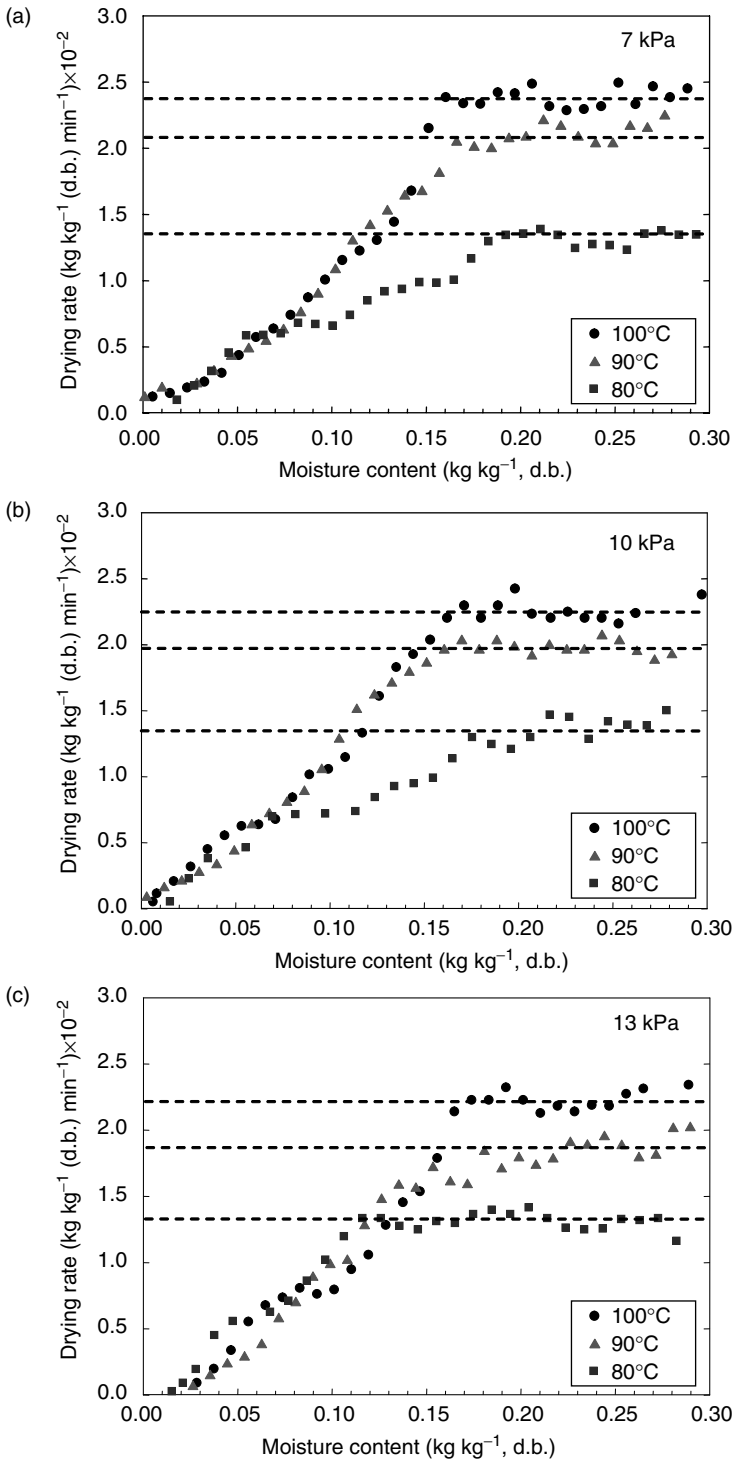
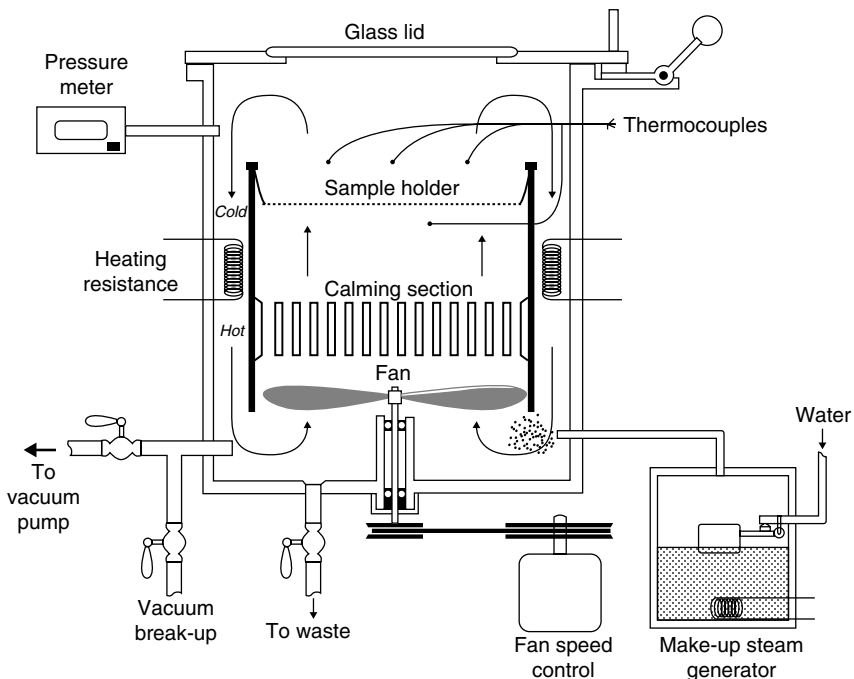


Fig. 5.3 Drying rate curves of molecular sieve beads undergoing LPSSD at various operating pressures. Reproduced with permission from Suvarnakuta *et al.* (2005b). Copyright 2005 American Chemical Society.

Table 5.1 Values of heat transfer coefficient ($\text{W m}^{-2} \text{K}^{-1}$) calculated from equation (5.2).

Absolute pressure					
7 kPa		10 kPa		13 kPa	
Mean	SD	Mean	SD	Mean	SD
7.661	0.61	8.353	0.44	9.168	0.33

**Fig. 5.4** Schematic of the experimental set up of Elustondo *et al.* (2001). Copyright 2001, reproduced with permission from Elsevier.

Among the first reported works on LPSSD of foods and biomaterials is the work of Elustondo *et al.* (2001) who studied LPSSD of foodstuffs both experimentally and theoretically. Wood slabs, shrimp, banana, apple, potato and cassava were dried using the steam pressures of 10 000–20 000 Pa, the steam temperatures of 60–90°C and the steam circulating velocities of 2–6 m s^{-1} in a set up shown schematically in Figure 5.4. A mathematical model was also developed based on a theoretical drying mechanism, which assumes that the water removal is carried out by evaporation in a moving boundary allowing the vapor to flow through the dry layer built as drying proceeds to predict the drying characteristics of foodstuffs undergoing this drying operation. A simplified expression, which has two experimentally determined parameters, was derived and used to predict the drying rate of test samples.

An example of the dimensionless drying rate curve is shown in Figure 5.5. The constant drying rate period cannot be observed in this figure (and all other experiments conducted).

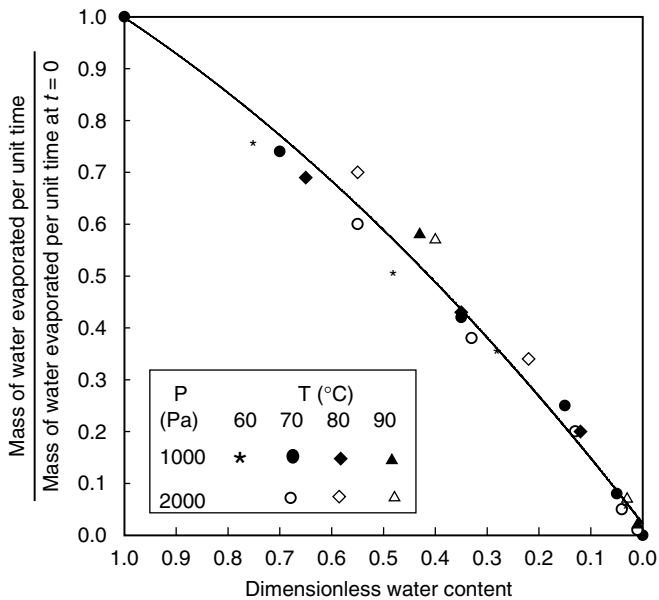


Fig. 5.5 Dimensionless drying rate of banana slices as a function of the instantaneous moisture content (Elustondo *et al.*, 2001). Copyright 2001, reproduced with permission from Elsevier.

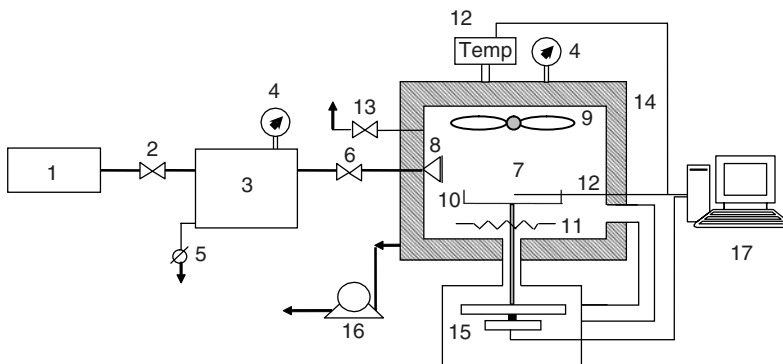


Fig. 5.6 A schematic diagram of the low-pressure superheated steam drier and associated units (Devahastin *et al.*, 2004). 1, boiler; 2, steam valve; 3, steam reservoir; 4, pressure gauge; 5, steam trap; 6, steam regulator; 7, drying chamber; 8, steam inlet and distributor; 9, electric fan; 10, sample holder; 11, electric heater; 12, on-line temperature sensor and logger; 13, vacuum break-up valve; 14, insulator; 15, on-line weight indicator and logger; 16, vacuum pump; 17, PC with installed data acquisition card.

An approximately linear relationship between the dimensionless drying rate and moisture content could be observed during an early stage of drying, whereas the slope of the curve increased toward the end of the drying process. A model proposed was found to predict the drying kinetics reasonably well. No mention about product quality was given, however.

Devahastin *et al.* (2004) developed another version of a low-pressure superheated steam drier, which can be operated by using steam supplied from a typical boiler available in a food plant. A schematic diagram of this drier is shown in Figure 5.6.

By using carrot as a model heat-sensitive material, experiments were conducted to examine the drying kinetics and various quality parameters of the product undergoing LPSSD. For comparison experiments were also performed under a vacuum condition (by using the same set-up but without the application of steam to the drier) at the same operating conditions, that is, absolute pressures of 7, 10 and 13 kPa and temperatures of 60, 70 and 80°C. Based on the experimental drying data it was observed that all samples undergoing LPSSD gained a small amount of moisture during the first few minutes of drying. Nevertheless, the condensation of steam was rather negligible if the operating pressure was low. It was also observed that the effect of temperature on the drying rates was greater than the effect of pressure in the case of LPSSD, especially at higher drying temperatures. The effect of operating pressure was less clear even at lower temperature (60°C) for the case of vacuum drying, however. This is probably due to the fact that the steam thermal properties were affected by temperature to a larger extent than those of air, especially at lower drying temperatures. No initial condensation was also observed, as expected, in the case of vacuum drying. It was also reported that the moisture content decreased faster, especially in the case of LPSSD at lower drying temperatures, at lower pressures since water boiled and evaporated at lower temperatures. It was found that the drying times of vacuum drying were shorter than those of LPSSD (at the same pressure) for all conditions tested. This is probably due to the fact that the electric heater was used more often during vacuum drying since it was the only source of energy for drying. This might increase the amount of radiation absorbed by the carrot surfaces, thus explaining the higher drying rate during vacuum drying. The initial steam condensation on the product surface might also contribute to the longer drying times for the case of LPSSD. The differences between the two sets of drying times, however, were smaller at higher drying temperatures. Raising the drying temperature further would eventually lead to equal rates of drying at an inversion temperature (due to increased temperature difference between the steam and the product as well as a reduction of the initial steam condensation).

Figure 5.7 illustrates changes of moisture content and temperature of carrot undergoing LPSSD at some selected conditions. It can be seen in this figure that the shapes of the drying and temperature curves were affected by both the drying temperature and pressure. At lower drying temperatures the temperature of carrot changed suddenly from its initial value and remained rather constant at the boiling temperature of water corresponding to the operating pressure until the first falling rate period drying ended (drying rate data are not shown here for the sake of brevity). Beyond this point, the carrot temperature rose again and finally approached the temperature of the drying medium. As the medium temperature increased (at the same operating pressure) it can be seen (for example, from Figure 5.7c) that the period of constant product temperature was shorter; the product temperature rose almost steadily from its initial value to the medium temperature. At the same drying temperature, however, increasing the operating pressure led to a lower rate of drying but a longer period of constant product temperature (as can be seen from Figures 5.7c and 5.7d). It may depend both on the characteristics of the drying product and on these effects to determine the optimum operating conditions of an LPSSD.

Figure 5.8 shows the evolutions of moisture content and temperature of carrot undergoing vacuum drying at the same operating as those used for LPSSD shown in Figure 5.7. It can be seen from this figure that the drying and heat transfer behavior of carrot undergoing vacuum drying was quite different from that of LPSSD; the product temperature, in this case, rose almost steadily from its initial value to the medium temperature. However, the rates of moisture reduction in the case of vacuum drying were higher than those belonged to LPSSD, especially at lower drying temperatures as mentioned earlier.

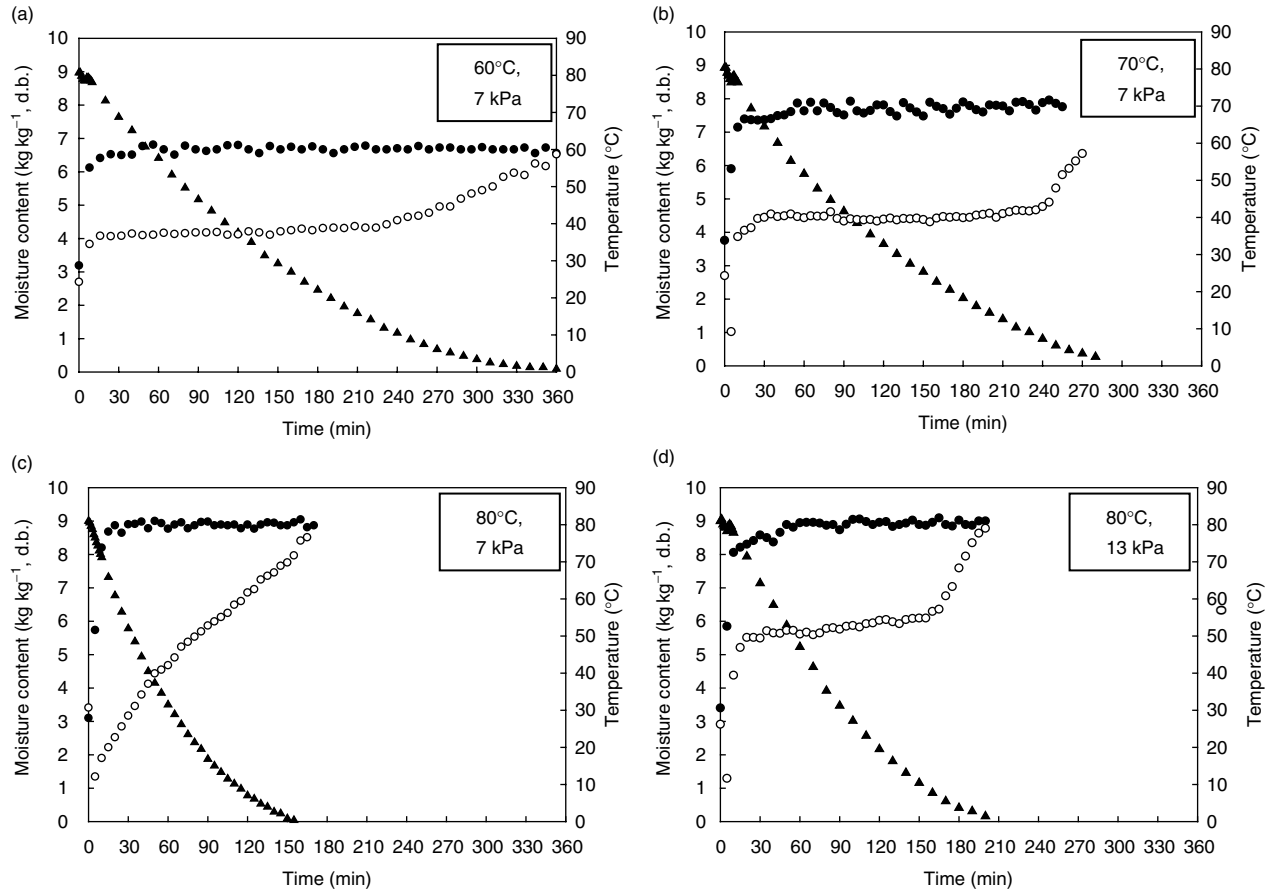


Fig. 5.7 Changes in moisture content and temperature of carrot undergoing LPSSD at different operating conditions. (▲), Moisture content; (●), steam temperature; (○), simple temperature.

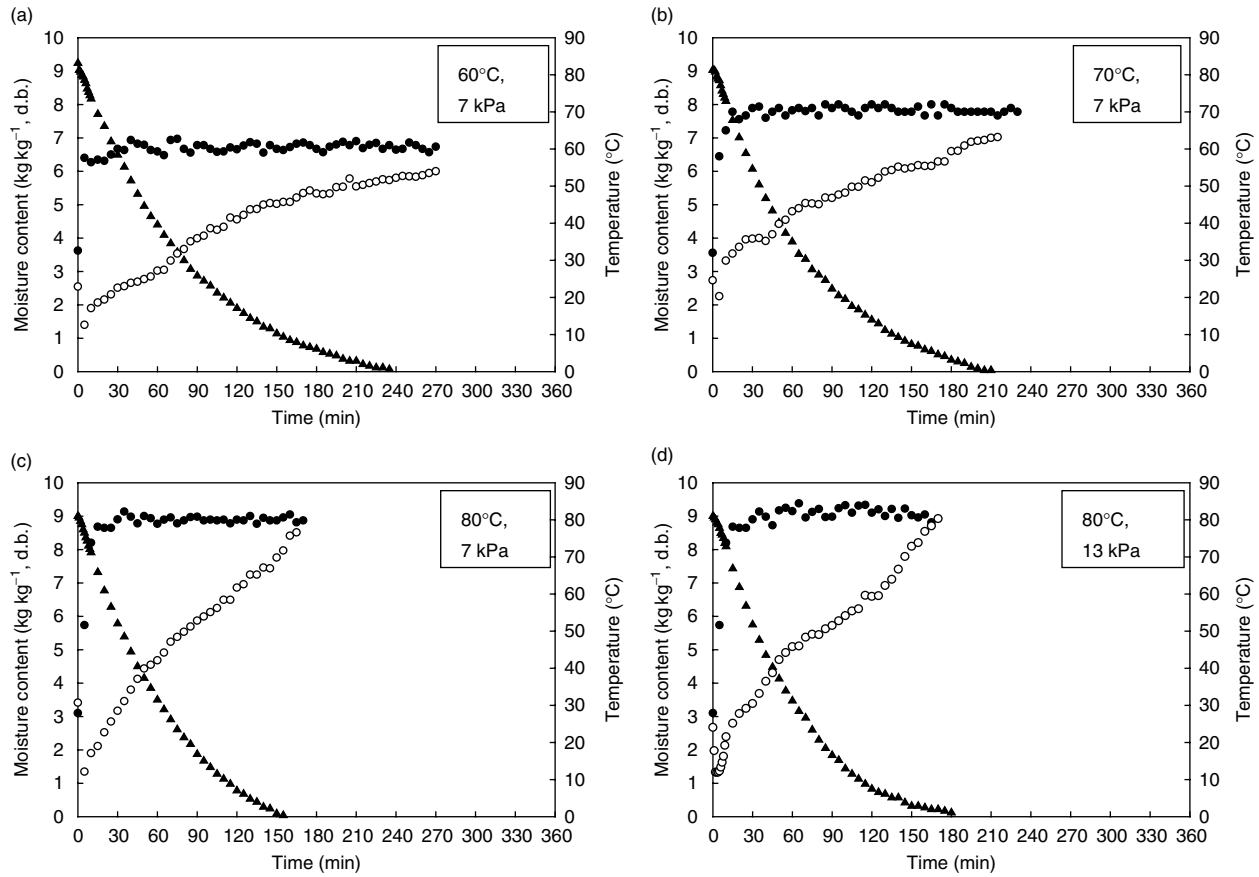


Fig. 5.8 Changes in moisture content and temperature of carrot undergoing vacuum drying at different operating conditions. (▲), moisture content; (●), steam temperature; (○), sample temperature.

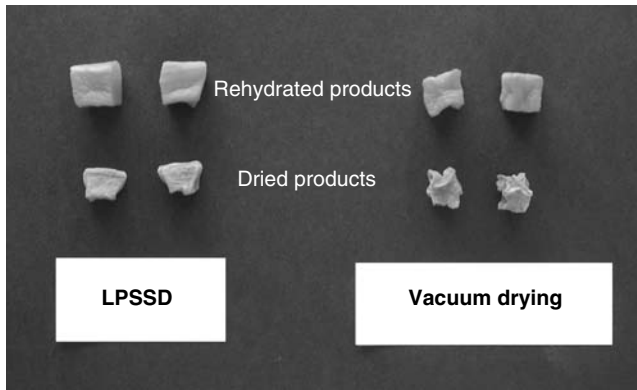


Fig. 5.9 Photographs of carrot cubes both after drying and after rehydration.

In terms of quality it was reported that the volume and apparent density of dried carrot undergoing both drying techniques slightly decreased and increased, respectively, as the operating pressure increased; both properties changed only slightly in this case, however, because of the narrow range of operating pressures tested. It was noted, however, that although the values of shrinkage of carrot that underwent LPSSD and vacuum drying were similar, the shrinkage patterns resulting from the two different drying processes were quite different. Carrot that underwent vacuum drying tended to shrink non-uniformly. In a more rapid drying (as in the case of vacuum drying when compared with LPSSD) the surface of the drying product became dry and rigid long before the center had dried out; the center dried and shrank much later than the outer surface did and hence pulled away from the rigid surface layers and caused a non-uniform shrinkage. Drying carrot in LPSSD, however, led to a more uniform shrinkage; in this case shrinkage seemed to occur because the carrot structure could not support its own weight and hence collapsed under gravitational force in the absence of moisture (Achanta and Okos, 2000). This is because LPSSD offered a milder drying condition (since the drying chamber was moister than in the case of vacuum drying). Dense or rigid large formations might not be formed as much in the case of LPSSD as in the case of vacuum drying. The photographs of carrot cubes both after drying and after rehydration are shown in Figure 5.9. These results are supported by the SEM photographs of Figures 5.10a and 5.10b, which show the micro-structure of LPSSD and vacuum dried carrot, respectively. It is seen from these figures that carrot that underwent vacuum drying developed a rather dense layer and its pore distribution was rather non-uniform compared to carrot that underwent LPSSD.

A simple technique has indeed been proposed to monitor deformation of a food product undergoing different drying techniques and conditions (Panyawong and Devahastin, 2007). The use of such a technique has confirmed the above-mentioned argument that the product undergoing LPSSD suffered less irregular deformation than the product undergoing vacuum drying although the percentage of the volumetric shrinkage of the two products was not significantly different.

Many studies were also performed to study the capability of LPSSD to retain some heat-sensitive chemical properties (e.g. various vitamins, flavors and aromas) of food products. Barbieri *et al.* (2004) compared the effects of hot air drying (40–60°C) and LPSSD (at a temperature of 50°C and pressure of around 5 kPa) on the retention of some volatile compounds in basil (*Ocimum basilicum*). It was found that the original aroma profiles were

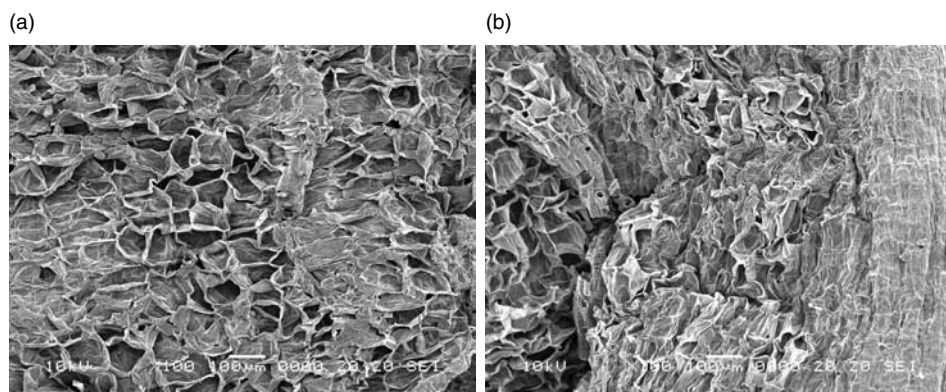


Fig. 5.10 SEM photographs of carrot undergoing (a) LPSSD and (b) vacuum drying.

kept almost constant in the case of basil dried by LPSSD. On the other hand, air-dried basil suffered significant variations in the relative proportions of aroma compounds.

Methakhup *et al.* (2005) dried Indian gooseberry (*Phyllanthus emblica* L.) flakes in both LPSSD and vacuum conditions using the same set-up as that used by Devahastin *et al.* (2004). Although vacuum drying took a shorter time to dry the product than did LPSSD at all drying conditions tested (temperatures in the range of 65–75°C and absolute pressures in the range of 7–13 kPa), it was found that LPSSD could retain ascorbic acid better than vacuum drying in almost all cases studied. In addition, LPSSD could preserve the colors of the sample better than vacuum drying at all drying conditions tested. In vacuum drying, temperature had a significant effect on ascorbic acid content and colors of the product while absolute pressure did not significantly affect the quality. In low-pressure superheated steam drying, on the other hand, the drying conditions did not affect the ascorbic acid and colors of the dried product. The quality results of their study are summarized in Tables 5.2 and 5.3.

From Table 5.2 it is seen that all dried Indian gooseberry flakes tended to lose some ascorbic acid as compared to fresh. The ascorbic acid retention was in the ranges of 64–94% for vacuum drying and 93–96% for LPSSD. For vacuum drying it was found that the ascorbic acid retention of the sample increased as the drying temperature increased. This may be due to the shorter drying time required to dry the samples to the desired moisture content. However, the pressure had only a little effect on the ascorbic acid retention. This may be explained by the fact that the drying time was not much affected by the operating pressure and that the level of oxygen content (which caused the aerobic degradation of vitamin C) was not much different at different pressures.

In LPSSD the ascorbic acid retention was not significantly different at different drying conditions even though the drying time was different. The results implied that no oxygen was available in the drying system and thus presented no effect on the ascorbic acid degradation during drying. The ability of the superheated steam drying system to maintain vitamin C has, in fact, been reported earlier by other investigators (e.g. Moreira, 2001)

From Table 5.3 it was found that LPSSD and vacuum drying at every condition resulted in a decrease of an *L* value and an increase of an *a* value of the dried sample compared with the fresh. However, *b* value of the dried sample was similar to that of the fresh sample. These results implied that the browning reaction and pigment destruction occurred in the dried sample. When considering the color retention of samples between two different drying

Table 5.2 Total ascorbic acid content of fresh and dried Indian gooseberry samples.

Drying method	Condition		Ascorbic acid (g per 100 g)		% Retention
	T (°C)	P _{ab} (kPa)	Fresh	Dried	
VD ¹	65	7	1.08 ± 0.07	3.67 ± 0.13	71.52 ^{ab} ± 1.97
		10	1.06 ± 0.09	3.50 ± 0.25	66.89 ^a ± 2.51
		13	0.94 ± 0.05	3.07 ± 0.30	64.84 ^a ± 6.01
	75	7	0.96 ± 0.02	3.84 ± 0.18	94.46 ^{cd} ± 2.57
		10	0.99 ± 0.02	3.72 ± 0.11	89.46 ^c ± 2.78
		13	0.98 ± 0.11	3.34 ± 0.03	78.13 ^b ± 2.83
LPSSD ²	65	7	1.05 ± 0.06	3.99 ± 0.22	93.46 ^{cd} ± 1.58
		10	—	—	—
		13	—	—	—
	75	7	1.06 ± 0.04	4.04 ± 0.08	95.35 ^d ± 3.49
		10	1.09 ± 0.08	4.03 ± 0.11	95.67 ^d ± 2.10
		13	1.04 ± 0.08	3.99 ± 0.11	94.96 ^{cd} ± 2.14

Means in the same column having the same letter are not significantly different ($\alpha < 0.05$).

¹ VD stands for vacuum drying.

² LPSSD stands for low-pressure superheated steam drying.

Table 5.3 Hunter parameters and total color difference (ΔE) of dried samples.

Drying method	Conditions		$\Delta L/L_0$	$\Delta a/a_0$	$\Delta b/b_0$	ΔE
	T (°C)	P _{ab} (kPa)				
VD ¹	65	7	0.06 ± 0.00	-0.91 ± 0.01	0.01 ± 0.01	3.83 ^b ± 0.09
		10	0.08 ± 0.00	-1.39 ± 0.07	0.02 ± 0.02	5.40 ^{cd} ± 0.10
		13	0.07 ± 0.01	-0.98 ± 0.22	0.00 ± 0.04	4.99 ^c ± 1.04
	75	7	0.08 ± 0.00	-0.71 ± 0.01	-0.02 ± 0.01	5.61 ^{cd} ± 0.28
		10	0.09 ± 0.00	-1.11 ± 0.01	-0.02 ± 0.00	6.42 ^d ± 0.26
		13	0.07 ± 0.01	-1.56 ± 0.58	0.03 ± 0.02	5.38 ^{cd} ± 0.66
LPSSD ²	65	7	0.04 ± 0.00	-0.88 ± 0.97	0.04 ± 0.01	3.09 ^{ab} ± 0.19
		10	—	—	—	—
		13	—	—	—	—
	75	7	0.03 ± 0.01	-0.64 ± 0.04	0.04 ± 0.02	2.48 ^a ± 0.44
		10	0.04 ± 0.00	-0.49 ± 0.18	0.04 ± 0.01	2.88 ^{ab} ± 0.18
		13	0.04 ± 0.04	-0.64 ± 0.23	0.02 ± 0.04	2.93 ^{ab} ± 0.39

Means in the same column having the same letter are not significantly different ($\alpha < 0.05$).

¹ VD stands for vacuum drying.

² LPSSD stands for low-pressure superheated steam drying.

methods it was found that LPSSD could retain the colors better than the vacuum drying system. This is because the degree of ascorbic acid and, probably, chlorophyll degradation of LPSSD was much lower than that of the vacuum drying system.

The drying methods were also found to affect the degradation and release of vitamin C (evaluated in terms of the total ascorbic acid, TAA) from Indian gooseberry flakes during preparation of Indian gooseberry tea (Kongsoontornkijkul *et al.*, 2006). LPSSD was indeed found to help retain TAA in dried gooseberry flakes better than hot air and vacuum drying.

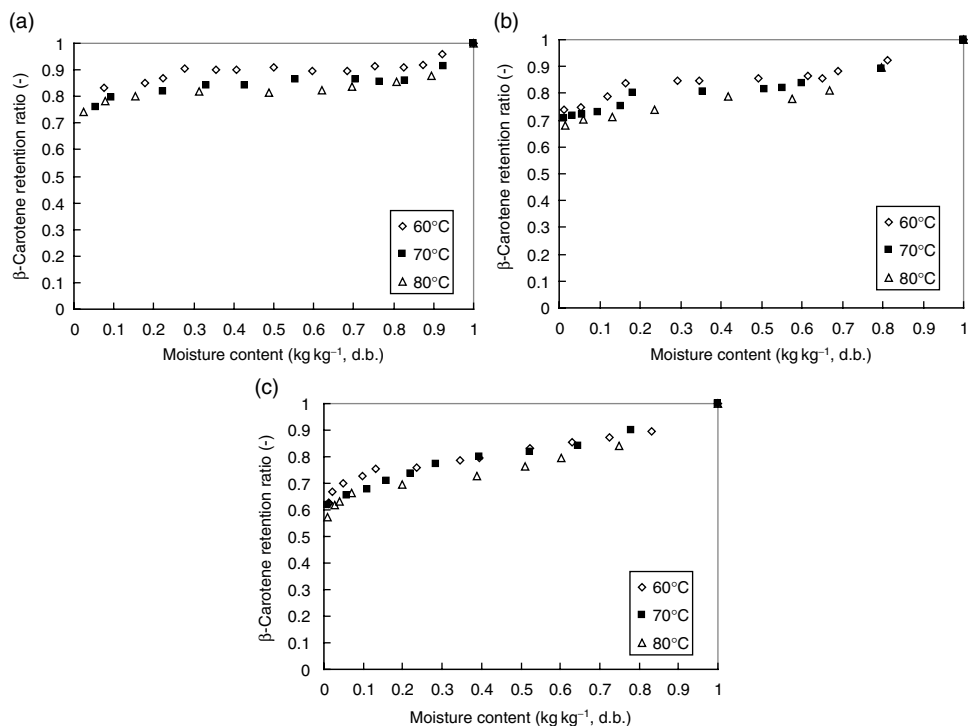


Fig. 5.11 Relationship between β -carotene content and moisture content of carrot undergoing different drying techniques: (a) LPSSD; (b) vacuum drying; (c) hot air drying.

Suvarnakuta *et al.* (2005a) experimentally studied the effects of LPSSD, vacuum and hot air drying on the drying and degradation kinetics of β -carotene in carrot. It was found that LPSSD and vacuum drying led to less degradation of β -carotene in carrot than in the case of hot air drying (see Figure 5.11 and Table 5.4). This is again due to the oxygen-free environment of LPSSD.

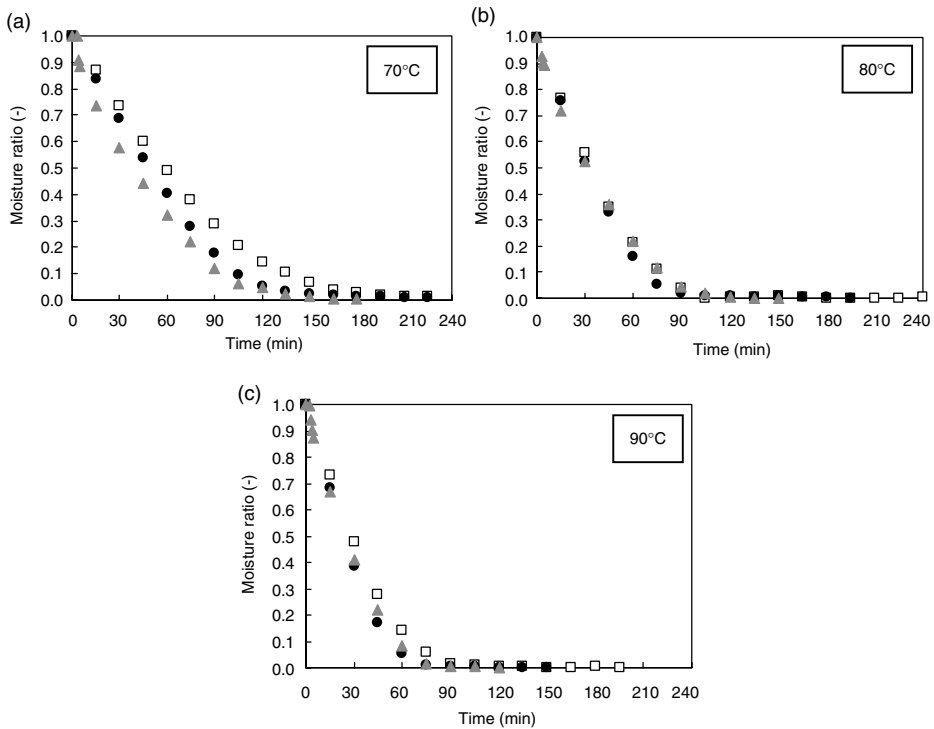
In terms of the texture of dried products (e.g. snacks) Leeratanarak *et al.* (2006) reported that the drying methods, in their case hot air drying (70–90°C) and LPSSD (at temperatures of 70–90°C and pressure of 7 kPa), had no significant effect on the texture (in terms of hardness) of dried potato chips. Hot-water blanching (95°C) of potato slices prior to drying, on the other hand, led to improved drying kinetics (due to structural softening leading to easier migration of moisture), colors (due to lower extents of browning reactions) and texture of the products. The degree of browning was also lowered. However, the use of different blanching periods (1–5 min) did not significantly affect the hardness of the chips.

Although blanching has been proved to enhance the quality of potato chips, the chips of Leeratanarak *et al.* (2006) were still observed to be of inferior quality to those available commercially. Pimpaporn *et al.* (2007) therefore investigated the use of different combined pretreatments prior to LPSSD (at temperatures of 70–90°C and pressure of 7 kPa) to improve the quality of potato chips, especially in terms of their texture. Both physical pre-treatments, such as blanching, combined blanching and freezing, as well as chemical pre-treatments, such as dipping raw potato slices in several chemicals including glycerol and monoglyceride, were evaluated. In terms of the drying kinetics it was noted (see Figure 5.12) that the combination

Table 5.4 Average drying times and losses of β -carotene of dried carrot (at moisture content of 0.1 kg kg^{-1} d.b.) undergoing different drying methods.

Sample	Average drying time (min)	β -Carotene content (mg per 100)		β -Carotene retention ratio (β_f/β_i)
		Wet basis	Dry basis	
Fresh carrot	—	4.86 ± 0.65	51.11 ± 6.89	—
LPSSD carrot				
$T = 60^\circ\text{C}$	420	54.92	43.94	0.83 ± 0.02^a
$T = 70^\circ\text{C}$	330	50.32	41.24	0.76 ± 0.04^b
$T = 80^\circ\text{C}$	210	38.81	31.55	0.74 ± 0.02^b
Vacuum-dried carrot				
$T = 60^\circ\text{C}$	300	26.95	24.28	0.74 ± 0.03^c
$T = 70^\circ\text{C}$	250	25.81	24.05	0.71 ± 0.03^{cd}
$T = 80^\circ\text{C}$	180	31.61	27.85	0.68 ± 0.03^d
Hot air-dried carrot				
$T = 60^\circ\text{C}$	420	22.56	21.46	0.62 ± 0.02^e
$T = 70^\circ\text{C}$	300	35.66	23.30	0.62 ± 0.03^e
$T = 80^\circ\text{C}$	240	36.26	22.05	0.58 ± 0.03^e

Means in the same column having the same letter are not significantly different ($\alpha < 0.05$).

**Fig. 5.12** Drying kinetics of unblanched (\square), blanched (\bullet) and blanched-frozen (\blacktriangle) potato slices.

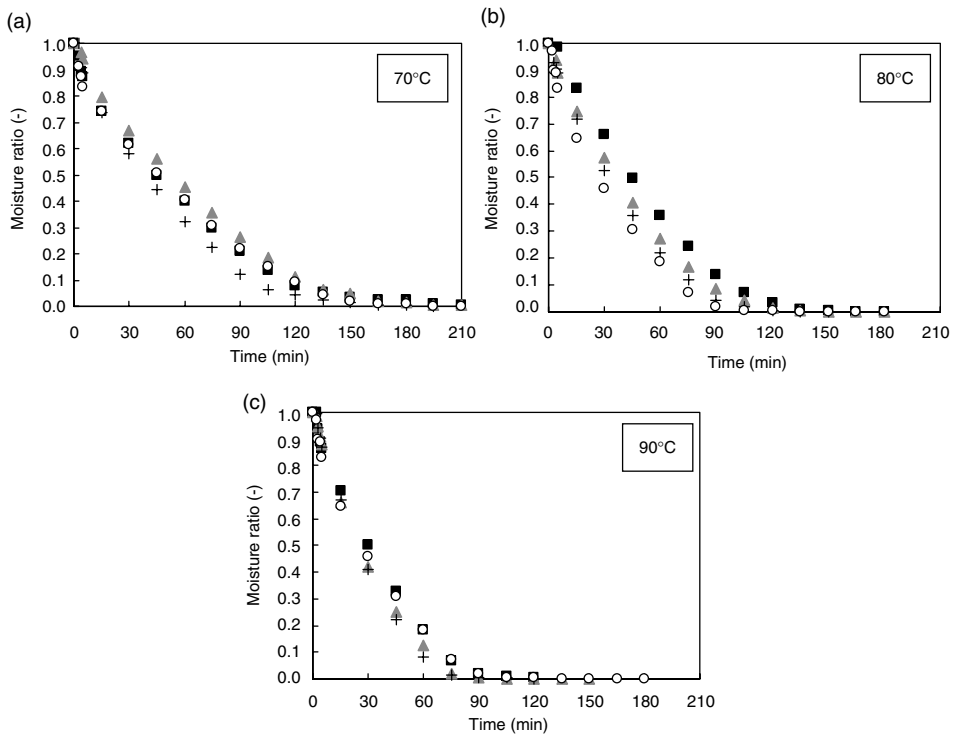


Fig. 5.13 Drying kinetics of blanched potato slices with glycerol immersion at concentrations of 0% (+), 1% (■), 3% (▲), and 5% (◊) followed by freezing at different drying temperatures.

of blanching and freezing led to a shorter drying time compared to that of unblanched samples at all drying temperatures. This is probably due to structure softening during blanching. In addition, freezing affects the physical tissue of potato due to the large size of ice crystals formed during slow freezing. The ice crystals might cause openings of the cell wall and semi-permeable membrane that could facilitate moisture transfer during drying. Chemically treated samples showed different drying behavior, however. As can be seen in Figure 5.13, which shows the drying curves of glycerol-treated samples, all glycerol-treated samples needed a longer time to reach their desired final moisture contents than those that underwent blanching and freezing pre-treatment. This is because glycerol has three hydroxyl groups that form hydrogen bonds with water in potato slices. Therefore, evaporation of free water on the surface of sliced potato becomes more difficult. However, the effect of glycerol was reduced at high drying temperatures, especially at 90°C. The drying time of each case was nearly the same as that of combined blanched-frozen samples. However, the results showed an unclear effect of monoglyceride on the drying kinetics of the samples.

In terms of quality it was found that the lightness of dried potato chips was improved by the use of freezing pre-treatment; nevertheless, the lightness values were not significantly different among all freezing pre-treated samples. Redness and yellowness of dried potato chips were not significantly affected by drying temperature but were significantly affected by the methods of pre-treatment.

The hardness of dried potato chips was not significantly influenced by the pre-treatment methods but was better at higher drying temperatures. However, in the cases of crispness

Table 5.5 Effects of pre-treatments and drying temperature on final thickness, hardness, crispness and toughness of LPSSD potato chips.

Pretreatment method	Drying temperature (°C)	Hardness (N)	Toughness (N mm ⁻¹)	Crispness (N mm ⁻¹)
Blanching	70	12.75 ± 2.38 ^{efg}	18.81 ± 4.46 ^f	3.43 ± 1.65 ^{ab}
	80	8.59 ± 2.30 ^{cdef}	17.59 ± 1.87 ^f	6.22 ± 0.94 ^{abcde}
	90	8.21 ± 0.64 ^{bcdef}	16.22 ± 0.21 ^{ef}	5.07 ± 0.43 ^{abcd}
Blanching + freezing	70	10.21 ± 0.58 ^{def}	9.13 ± 1.38 ^{bcde}	14.82 ± 2.86 ^{fghi}
	80	8.00 ± 2.60 ^{bcdef}	4.14 ± 1.97 ^{ab}	13.00 ± 0.67 ^{fghi}
	90	6.77 ± 0.25 ^{abcd}	3.35 ± 1.37 ^{ab}	15.98 ± 3.58 ^{fghi}
B + I (0.1% monoglyceride) + F	70	9.94 ± 1.30 ^{fg}	14.28 ± 1.38 ^{def}	11.37 ± 0.84 ^{defgh}
	80	9.60 ± 0.74 ^{cdef}	8.38 ± 0.92 ^{bcd}	12.54 ± 3.94 ^{efghi}
	90	7.03 ± 0.67 ^{abcd}	3.59 ± 2.08 ^{ab}	14.96 ± 3.02 ^{fghi}
B + I (0.3% monoglyceride) + F	70	10.34 ± 3.87 ^{def}	13.25 ± 1.02 ^{cdef}	9.26 ± 1.44 ^{bcdef}
	80	8.73 ± 0.13 ^{cdef}	7.88 ± 1.70 ^{abcd}	10.55 ± 1.47 ^{cdefgh}
	90	4.72 ± 0.48 ^{abc}	3.49 ± 2.05 ^{ab}	13.08 ± 2.68 ^{fghi}
B + I (0.5% monoglyceride) + F	70	10.33 ± 0.39 ^{def}	16.34 ± 0.72 ^{ef}	11.00 ± 1.19 ^{defgh}
	80	9.47 ± 1.70 ^{cdef}	5.75 ± 2.49 ^{abc}	13.09 ± 2.34 ^{fghi}
	90	7.54 ± 2.17 ^{abcde}	5.06 ± 2.41 ^{ab}	16.49 ± 1.15 ^{ghi}
B + I (1% glycerol) + F	70	11.30 ± 2.10 ^{def}	18.95 ± 4.59 ^f	2.25 ± 0.18 ^a
	80	9.40 ± 1.03 ^{cdef}	14.75 ± 1.68 ^{def}	13.10 ± 1.38 ^{fghi}
	90	7.48 ± 1.25 ^{abcde}	3.28 ± 1.44 ^{ab}	14.47 ± 2.57 ^{fghi}
B + I (3% glycerol) + F	70*	9.92 ± 0.51 ^h	18.63 ± 0.96 ^f	9.10 ± 2.97 ^{bcdef}
	80	8.13 ± 1.87 ^{bcdef}	14.08 ± 1.61 ^{def}	12.39 ± 1.50 ^{efghi}
	90	7.59 ± 0.76 ^{abcde}	3.07 ± 1.01 ^{ab}	18.34 ± 2.99 ⁱ
B + I (5% glycerol) + F	70*	17.52 ± 0.59 ^g	34.09 ± 6.92 ^g	4.29 ± 0.64 ^{abc}
	80	9.47 ± 2.06 ^{cdef}	13.35 ± 2.27 ^{cdef}	6.28 ± 2.42 ^{abcde}
	90	7.41 ± 2.06 ^{abcde}	6.30 ± 2.12 ^{abc}	14.96 ± 1.41 ^{hi}

B: blanching, I: immersion in solution and F: freezing

Different superscripts in the same column mean that the values are significantly different ($p \leq 0.05$).

*Denotes the cases where the final moisture content of 3.5% (d.b.) was not achievable.

and toughness, the drying temperature affected these parameters significantly, especially at 90°C. More importantly, freezing pre-treatment could improve the crispness and also toughness of dried chips. The crispness increased as the drying temperature increased but the toughness decreased with increased drying temperature. The textural results are summarized in Table 5.5.

A micro-structural evaluation of the potato chips was also performed. It was noted that the drying temperature significantly affected the micro-structure of dried potato chips. On the other hand, the effects of pre-treatments on the micro-structure were only that combined blanching and freezing pre-treatments led to the best integrity of micro-structure (in terms of pore size, pore distribution and also less formation of rigid dense layer). This superior integrity of the micro-structure might lead to the favorable texture of dried potato chips as summarized earlier.

Based on the aforementioned arguments, combined blanching and freezing without any chemical pre-treatments, followed by drying in LPSSD at a higher temperature (90°C in this

case) was recommended. It is important to note, however, that a sensory study is needed prior to being able to make a definitive conclusion on the validity of the results.

5.4 SOME ADVANCES IN LPSSD OF FOODS AND BIOMATERIALS

In addition to drying foods and biomaterials in LPSSD tray driers, some researchers have applied LPSSD to other types of driers. It should be noted that the concept of combining different modes of drying by itself is obviously not new.

Kozanoglu *et al.* (2006) dried coriander and pepper seeds in a low-pressure (in the range of 40–66 kPa) superheated steam fluidized-bed drier over the temperature range of 90–110°C. General trends of drying kinetics were observed. At a given temperature lowering the operating pressure led to a higher degree of steam superheat and higher fluidizing air velocity. The degree of steam superheat was found to have the most important effect on the drying behavior of both types of seeds.

Nimmol *et al.* (2007) combined LPSSD and far-infrared radiation (FIR) as an external heat source to enhance the rates of the drying process. The combined process (LPSSD-FIR) was also compared with combined vacuum drying and FIR (VACUUM-FIR) for banana slices, both in terms of the drying kinetics and quality of the dried chips (in terms of color, shrinkage, rehydration behavior, texture and micro-structure), over the temperature range of 70–90°C and pressures of 7 and 10 kPa. Moreover, the quality of dried banana chips was compared with that of banana slices undergoing LPSSD alone.

The changes in moisture ratio and temperature of banana slices undergoing LPSSD-FIR and VACUUM-FIR at some selected conditions are shown in Figures 5.14 and 5.15, respectively. After a slight drop of the sample temperature due to the rapid reduction of the chamber pressure, which led to some flash evaporation of surface moisture, the temperature of the sample (in the case of LPSSD-FIR) rose rapidly to a level close to the boiling point of water corresponding to the chamber pressure (not at the boiling point, as is seen in Figure 5.7, since far-infrared radiation was also present in this case) and then remained unchanged at this level until the surface of the sample started to dry. Another important aspect is that the temperature of the sample rose steadily to a level higher than the pre-determined medium temperature because heat transfer, in the case of LPSSD-FIR, simultaneously took place by radiation from the far-infrared radiator and by convection from superheated steam. After this period the temperature of the sample remained almost unchanged because during the later stage of the process moisture content within the sample was smaller leading to lower absorptivity of the sample.

Comparing the changes in the temperature of banana slices undergoing LPSSD-FIR and VACUUM-FIR reveals that, at the same pre-determined medium temperature, the sample temperature during the later stage of LPSSD-FIR was higher than that in the case of VACUUM-FIR. This is due to the fact that in the case of LPSSD-FIR, radiation intensity at the position of the thermocouple used for sending the signal to the temperature controller (30 mm above the sample surface) was less intense due to the higher absorptivity of superheated steam compared to that of air. The far-infrared radiator was thus used more often during LPSSD-FIR to maintain the desired level of drying medium temperature, leading to a higher surface temperature of the far-infrared radiator. Consequently, the radiation intensity, which depends on the surface temperature of the far-infrared radiator, experienced by LPSSD-FIR samples was greater, hence higher levels of the sample temperature.

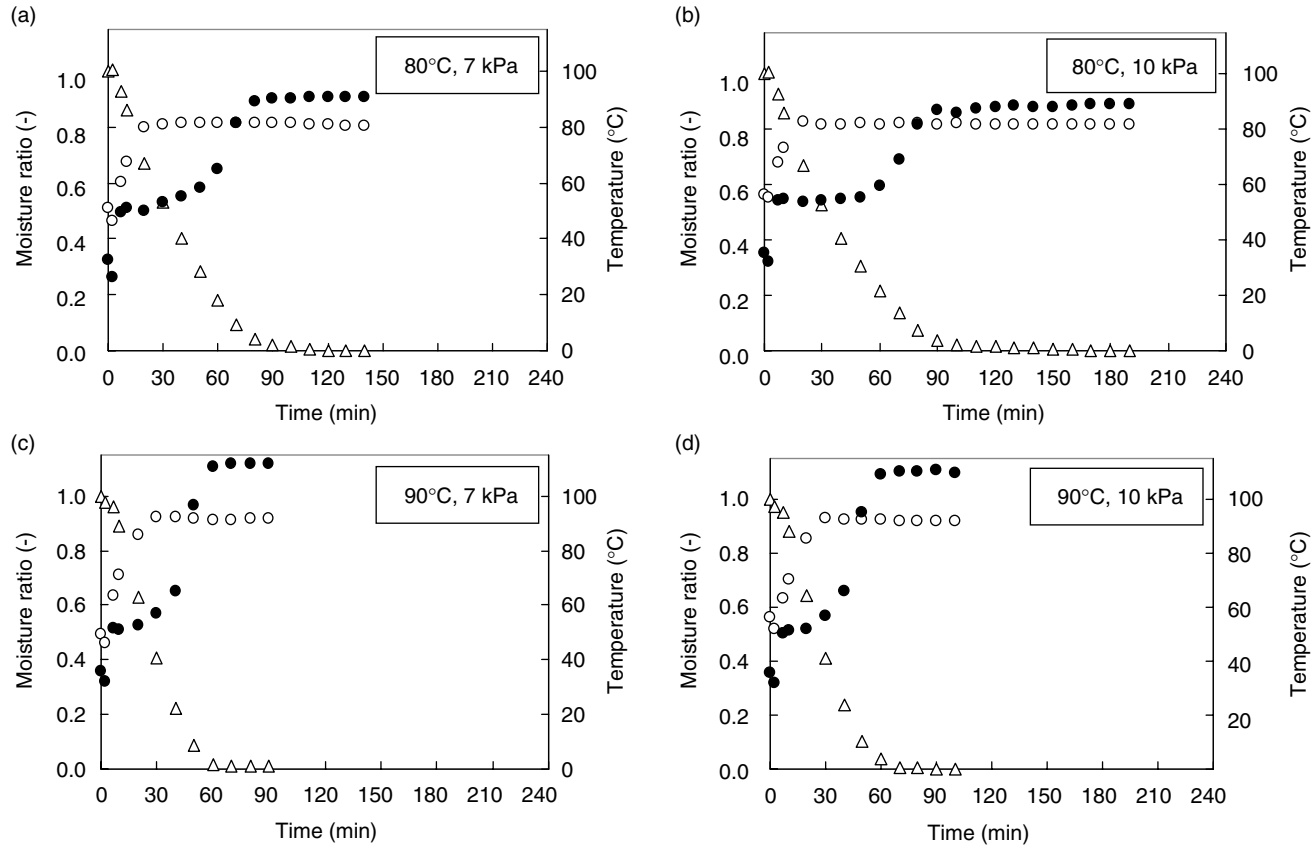


Fig. 5.14 Changes in moisture ratio and temperature of banana slices undergoing LPSSD-FIR. (○), Drying medium temperature; (●), sample temperature; (Δ), moisture ratio.

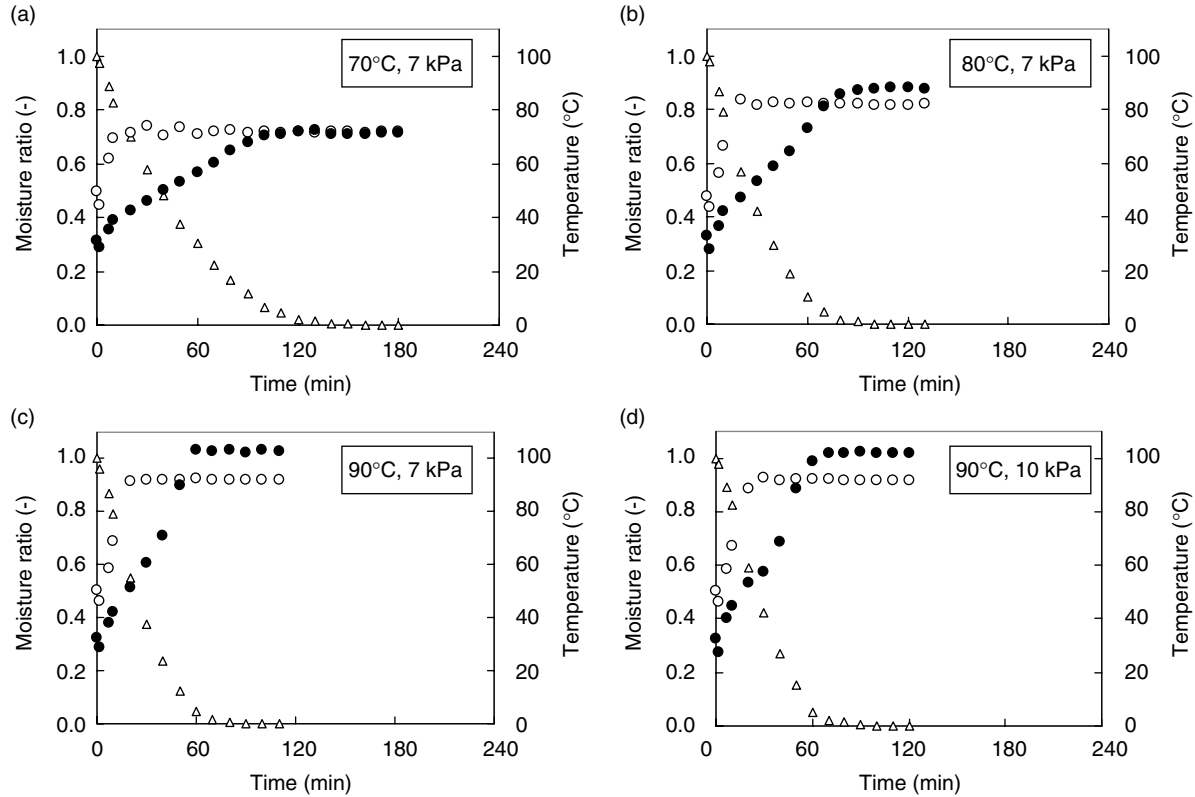


Fig. 5.15 Changes in moisture ratio and temperature of banana slices undergoing VACUUM-FIR. (○), drying medium temperature; (●), sample temperature; (△), moisture ratio.

In terms of quality it was observed that banana dried by LPSSD-FIR was significantly darker and redder than that dried by VACUUM-FIR at all drying conditions. This is because the temperature of banana slices undergoing LPSSD-FIR increased more rapidly and stayed at higher levels than that of samples dried by VACUUM-FIR as mentioned earlier.

When comparing the colors of banana chips dried either by LPSSD-FIR or VACUUM-FIR with those of banana chips dried only by LPSSD (Thomkapanish *et al.*, 2007) it is noted that bananas dried by FIR-assisted processes had higher values of color changes, especially in the case of lightness and redness. This is due to the fact that banana slices undergoing LPSSD-FIR and VACUUM-FIR were subjected to the higher temperature for a longer period than those dried by LPSSD, especially during the later stage of the process.

In terms of shrinkage it was noted that drying at lower temperatures (70° and 80°C in this case) yielded dried products with lower degrees of area shrinkage because case hardening (rigid layers) on the sample perimeter, which retarded shrinkage (surface area change) of the samples, occurred less at these conditions. Case hardening also developed faster during LPSSD-FIR and VACUUM-FIR compared with the case of LPSSD alone due to the higher sample temperatures mentioned earlier. Regarding the rehydration behavior, it was noted that banana slices dried at higher temperatures had higher rehydration ability than those dried at lower temperatures. This is because higher drying temperatures led to dried banana slices with a more porous structure, thus facilitating rehydration ability. It was also noted that banana slices dried by LPSSD-FIR generally had higher rehydration ability than those dried by VACUUM-FIR. This is due to the fact that the temperature of bananas dried by LPSSD-FIR suddenly rose to a level close to boiling temperature (as can be seen in Figure 5.14). Consequently, moisture in the banana rapidly boiled leading to rigorous evolution of steam within the samples. Larger and more pores were developed compared with the samples dried by VACUUM-FIR (see Figure 5.16, which clearly shows that when drying was performed at lower temperature banana slices dried by LPSSD-FIR had larger and more pores compared with those dried by VACUUM-FIR). However, the rehydration ability of banana slices dried by LPSSD-FIR and VACUUM-FIR was not significantly different in the case of drying at 90°C. This is probably due to the fact that moisture within the samples dried by VACUUM-FIR boiled as rigorously as in the case of LPSSD-FIR at this higher temperature. This hypothesis was confirmed by the fact that the micro-structure of banana slices dried by both methods was similar in the case of drying at 90°C (see Figures 5.16c and 5.16d).

Table 5.6 shows the results of the texture of banana chips in terms of the maximum force (hardness) and the number of peaks in the force-deformation curve (crispness). In the case of hardness it was found that banana slices dried by VACUUM-FIR were harder than those dried by LPSSD-FIR, as indicated by the higher value of the maximum force. This is probably due to the fact that VACUUM-FIR, especially at a lower drying temperature (80°C in this case), yielded dried banana slices with a more dense structure (smaller and less pores), as can be seen in Figures 5.16a and 5.16b. However, the statistical analysis showed that the effects of drying temperature and drying pressure as well as drying methods on the hardness were not significant. It should be noted that, at the same drying temperature, the hardness of banana chips was lower than that of samples dried by LPSSD alone.

In terms of crispness it can be seen again from Table 5.6 that LPSSD-FIR yielded banana chips with a larger number of peaks (hence indicating that the products were crispier) compared with VACUUM-FIR, especially at 80°C. This might be due to the larger and more numerous pores that occurred during LPSSD-FIR. Comparing these results with those obtained using LPSSD it was found that LPSSD-FIR and VACUUM-FIR provided banana

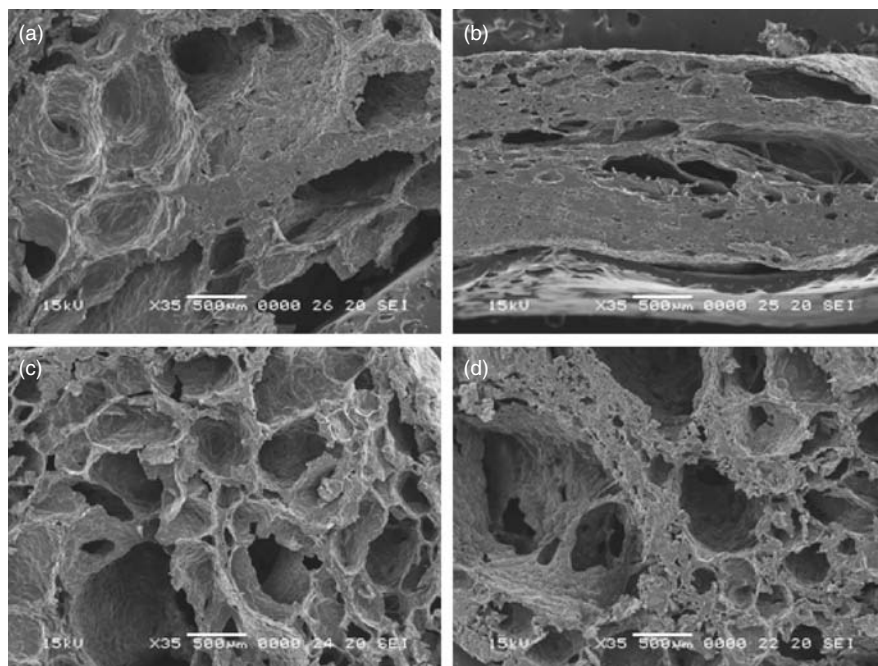


Fig. 5.16 SEM photographs showing cross section of banana slices dried by (a) LPSSD-FIR at 80°C–7 kPa, (b) VACUUM-FIR at 80°C–7 kPa, (c) LPSSD-FIR at 90°C–7 kPa, (d) VACUUM-FIR at 90°C–7 kPa.

Table 5.6 Effects of drying methods, drying temperature and pressure on maximum force and number of peaks of dried banana slices.

Drying method	Drying temperature (°C)	Drying pressure (kPa)	Maximum force (N)	Number of peaks
LPSSD-FIR	70	7	N/A	N/A
		10	N/A	N/A
	80	7	17.09 ± 3.15 ^a	37 ± 3 ^d
		10	17.30 ± 3.60 ^a	36 ± 4 ^d
		7	16.39 ± 3.57 ^a	38 ± 4 ^d
90	7	16.39 ± 3.57 ^a	38 ± 4 ^d	
	10	16.89 ± 4.58 ^a	38 ± 5 ^d	
VACUUM-FIR	70	7	18.44 ± 3.80 ^a	22 ± 4 ^{ab}
		10	19.12 ± 4.07 ^a	21 ± 5 ^a
	80	7	19.95 ± 3.55 ^a	25 ± 5 ^{bc}
		10	18.16 ± 4.51 ^a	26 ± 5 ^c
	90	7	16.72 ± 3.19 ^a	36 ± 3 ^d
		10	17.81 ± 3.63 ^a	36 ± 4 ^d
		7	17.81 ± 3.63 ^a	36 ± 4 ^d
LPSSD ^a	70	7	N/A	N/A
	80	7	21.52 ± 2.23	27 ± 3
	90	7	24.09 ± 1.26	28 ± 6

^a Data obtained from Thomkapanish *et al.* (2007).

N/A implies that the final moisture content of 0.035 kg kg⁻¹ (d.b.) was not obtainable at this condition.

Values in the same column with different superscripts mean that the values are significantly different ($p < 0.05$).

chips with a slightly larger number of peaks. This is again due to the larger and more numerous pores presented during LPSSD-FIR and VACUUM-FIR.

Instead of supplying thermal energy (via the application of low-pressure superheated steam or via the use of an electric heater) and vacuum condition continuously, Thomkapanish *et al.* (2007) implemented intermittent LPSSD of a food product (banana slices). Two intermittent modes, namely, intermittent temperature and intermittent pressure LPSSD, were tested. The effects of intermittent drying schemes, along with the other drying parameters viz. drying temperature (70–90°C) and pressure as well as the intermittency (on/off) period (10:5, 10:10 and 10:20 min in the case of intermittent supply of energy and 5:0, 5:5 and 5:10 min in the case of intermittent supply of vacuum) on the drying kinetics and various quality attributes (color, shrinkage, texture and ascorbic acid retention) of the dried banana chips were evaluated. The energy consumption values for intermittent LPSSD were also monitored through the effective (or net) drying time at various intermittent drying conditions and the results compared to those using continuous LPSSD.

In the case of intermittent temperature LPSSD the overall drying rates of intermittent and continuous LPSSD were not significantly different. However, the effective or net drying time of intermittent drying was significantly shorter than that of continuous drying, especially with a longer tempering period leading to high energy savings (up to 65%). It was also noted that the drying rates of intermittent pressure LPSSD were higher than those of continuous drying (in the range of 50–58%).

In terms of the quality of the dried chips it was found that the effect of intermittency in intermittent temperature drying in almost all cases, when compared with continuous drying, was not significant. However, intermittent temperature drying led to higher level of ascorbic acid retention, especially at longer tempering (off) periods.

On the other hand, it was noted that the colors of the products in the case of intermittent pressure drying were worse than those in the case of continuous drying. Shrinkage of the samples dried by intermittent pressure drying was also more obvious than in the case of continuous drying at all conditions. In addition, intermittent pressure drying led to greater degradation of ascorbic acid. This drying scheme is therefore not appropriate for heat- and, in particular, oxygen-sensitive products, as oxygen (air) is necessarily introduced to the drying chamber during the off period.

5.5 MATHEMATICAL MODELING OF LPSSD OF FOODS AND BIOMATERIALS

Several models with different degrees of complexity and predictability have been proposed for LPSSD. In this section only selected models applied to LPSSD of foods and biomaterials are reviewed, however. Mathematical models for LPSSD of other products are available in the literature (e.g. Shibata *et al.*, 1990; Pang, 1997; Elustondo *et al.*, 2002; Defo *et al.*, 2004; Suvarnakuta *et al.*, 2005b).

Elustondo *et al.* (2001) developed a mathematical model based on a theoretical drying mechanism, which assumes that the water removal is carried out by evaporation in a moving boundary allowing the vapor to flow through the dry layer built as drying proceeds to predict the drying characteristics of foodstuffs undergoing LPSSD. A simplified expression, which has two experimentally determined parameters, was derived and used to predict the drying rate of test samples. Despite its simplicity it was noted that the model could predict the drying kinetics of the tested materials adequately.

Suvarnakuta *et al.* (2007) proposed the use of a simple three-dimensional liquid diffusion based model to predict the evolutions of the moisture content and temperature of a biomaterial (carrot cube) undergoing LPSSD. The model consists of coupled heat conduction and mass diffusion equations along with an empirical equation, which describes shrinkage of the product during drying. An empirical equation that expresses the β -carotene degradation in carrot is also included in the model so as to predict the evolution of β -carotene content in carrot during drying.

The model assumes that the sample is isotropic and homogenous. Initial condensation of steam is also neglected in the model. In addition, mass transfer within the material is controlled only by liquid diffusion; it is thus assumed that no vaporization occurs within the drying material. Finally, it is assumed that shrinkage of the material is significant, and that it is accounted for in all three directions. The volumetric shrinkage depends on the operating temperature and moisture content and is described by an empirically determined correlation.

The conduction equation to describe energy transfer is written as follows:

$$\rho C_p \frac{\partial T}{\partial t} = \frac{\partial}{\partial x} \left(k_x \frac{\partial T}{\partial x} \right) + \frac{\partial}{\partial y} \left(k_y \frac{\partial T}{\partial y} \right) + \frac{\partial}{\partial z} \left(k_z \frac{\partial T}{\partial z} \right) \quad (5.3)$$

where $k_x = k_y = k_z = k$ due to the product isotropy.

The equation to describe the mass transfer during LPSSD is:

$$\frac{\partial X_f}{\partial t} = \frac{\partial}{\partial x} \left(D_{eff} \frac{\partial X_f}{\partial x} \right) + \frac{\partial}{\partial y} \left(D_{eff} \frac{\partial X_f}{\partial y} \right) + \frac{\partial}{\partial z} \left(D_{eff} \frac{\partial X_f}{\partial z} \right) \quad (5.4)$$

At the onset of the LPSSD process the temperature and moisture content of the material are uniform.

$$T = T_i \quad (5.5)$$

$$X = X_{f_i} \quad (5.6)$$

For the material subjected to convective drying the boundary condition (equation (5.7)) at the surface is used:

$$-k(\nabla T \cdot n) = h(T_{steam} - T_s) - \rho \lambda D_{eff} (\nabla X_f \cdot n) \quad (5.7)$$

where the term on the left-hand side refers to heat conducted from the outer surface to the inside of the cube, the first term on the right-hand side is heat penetrating from low-pressure superheated steam to the solid body by means of convection and the second term on the right-hand side denotes the latent heat of vaporization.

Mass transfer at the surface is modeled by assuming that there is no mass transfer resistance at the surface of the material since water possesses no self-resistance in its own body. This is certainly not a very realistic assumption and a model should be developed in future to better represent the phenomenon (by, for example, recognizing that the driving force for mass transfer from the surface is the difference between the vapor pressure of moisture at the surface temperature and the steam pressure in the bulk phase).

$$X_f = 0 \quad (5.8)$$

where X_f denotes free moisture content ($X_f = X - X_{eq}$). This condition simply implies that the moisture content at the surface was always at its equilibrium value at the corresponding operating condition.

The detailed estimation of the parameters required in the model is described in Suvarnakuta *et al.* (2007). It is only important to note here that the values of the effective diffusion coefficient (D_{eff}) obtained, assuming that the material suffers no shrinkage, are different from those obtained assuming that the material suffers uniform shrinkage.

The above-mentioned model was validated by the available experimental data. The estimated values of the heat transfer coefficient were set in the range of $\pm 20\%$ (see Table 5.1) to investigate the sensitivity of this parameter on the predictability of the product temperature and moisture content.

Figure 5.17 illustrates the sample evolutions of the moisture ratio and the center temperature of carrot cube undergoing LPSSD. It was found that the trends of moisture ratio prediction are in good agreement with the experimental data. However, at the highest operating pressure (13 kPa) the model was not able to predict the experimental data well (see Figures 5.18 and 5.19). This is due to the fact that a larger amount of steam condensation occurred during the start-up period at a higher operating pressure (since steam at a lower degree of superheat tended to condense more easily) and this led to under-prediction of the moisture ratio since the model, as mentioned earlier, did not take into account the effect of initial condensation. The same reason could also be used to explain a rather larger discrepancy between simulated and experimental results at lower drying steam temperatures as well.

Representative product center temperature profiles over time are also presented in Figures 5.17–5.19. The center temperature increased over time until it reached the boiling point of water at the corresponding operating pressure; after this point, the temperature slowly increased while latent heating prevented a temperature rise. It is seen from these figures that the simulated predictions did not quite agree with the experimental data. This is due to the fact that carrots undergoing LPSSD in fact shrank non-uniformly. Thus, the assumption of

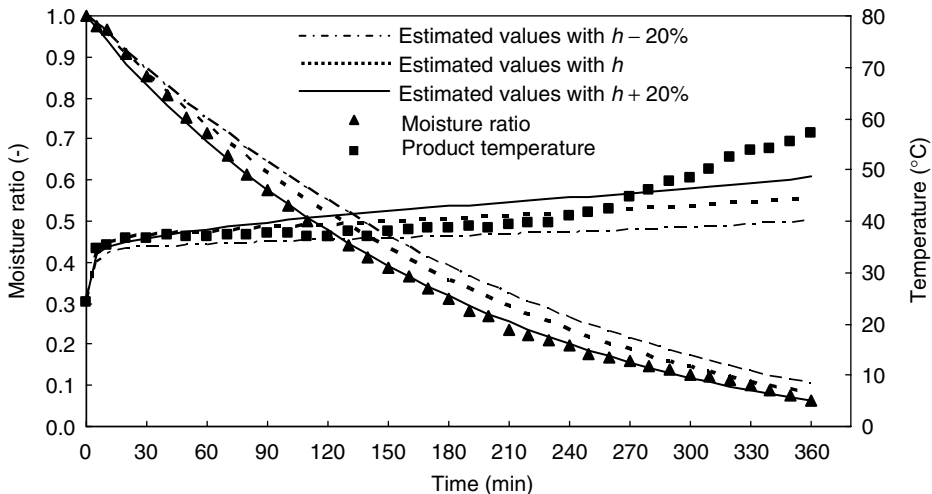


Fig. 5.17 Comparison between predicted (assuming shrinkage) and experimental moisture content and temperature variation with time of carrot cube at 60°C and 7 kPa ($X_{eq} = 0.10\text{ kg kg}^{-1}$ (d.b.)). Lines represent predicted data; symbols represent experimental data.

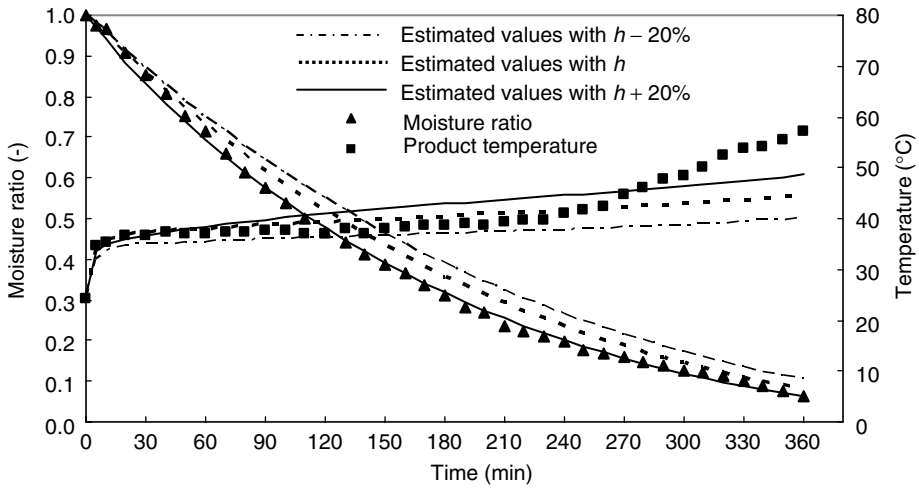


Fig. 5.18 Comparison between predicted (assuming shrinkage) and experimental moisture content and temperature of carrot cube at 70°C and 13 kPa ($X_{eq} = 0.10 \text{ kg kg}^{-1}$ (d.b.)).

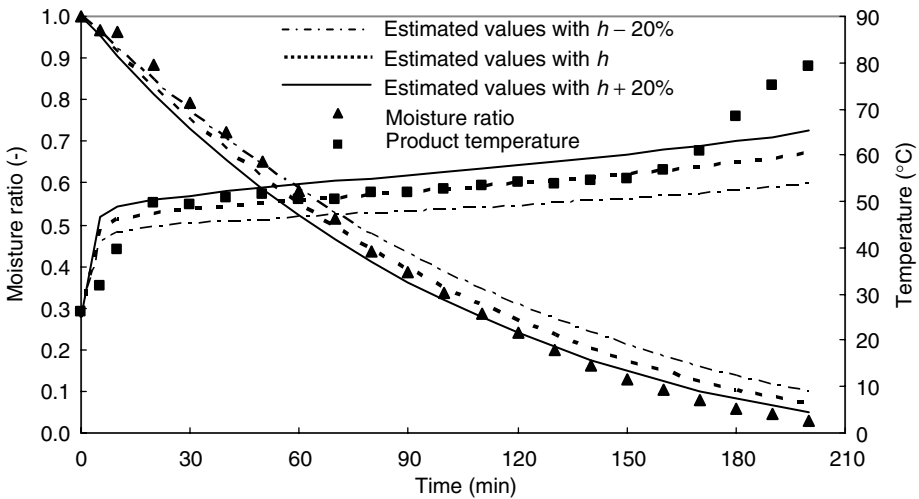


Fig. 5.19 Comparison between predicted (assuming shrinkage) and experimental moisture content and temperature of carrot cube at 80°C and 13 kPa ($X_{eq} = 0.10 \text{ kg kg}^{-1}$ (d.b.)).

uniform shrinkage used in this study was not quite correct. Another factor that contributed to the deviation of the simulated results from the experimental data is the fact that once the boiling point was reached there was vapor generation, which could give rise to an increase in the internal pressure in pores. Thus, it was possible that hydrostatic pressure gradients were generated within the product, which could in turn drive the liquid-form moisture out of the product faster than that permissible by liquid diffusion alone. Furthermore, the change in porosity and physical structure of carrot during drying could, in principle, change the diffusivity from what was predicted by the empirical correlations used.

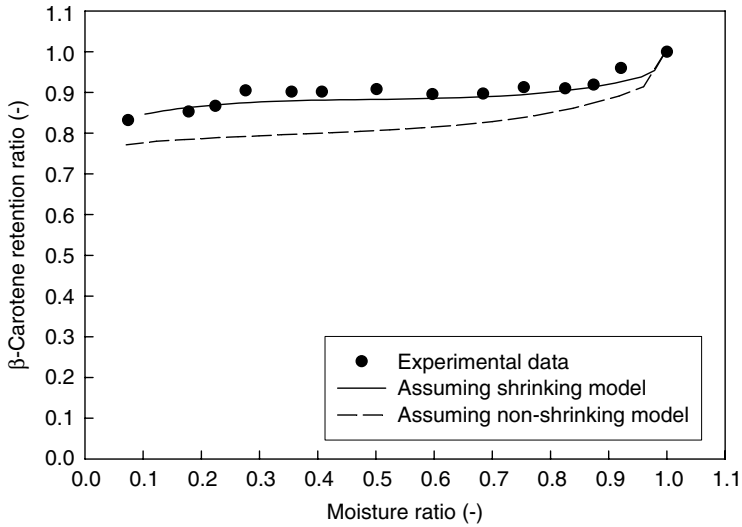


Fig. 5.20 Comparison between predicted and experimental β -carotene degradation of carrot at 60°C.

Figure 5.20 shows a sample predicted β -carotene degradation in carrot during LPSSD using the middle values of heat transfer coefficients. The β -carotene degradation predictions, which follow from the simulated moisture content and temperature based on the assuming shrinking model, show good agreement with the experimental data under all conditions.

The next step for model development should be directed towards the use of more realistic assumptions, boundary conditions and inclusion of phenomena that really occur during LPSSD, for example, vaporization of moisture within the drying material.

5.6 CONCLUDING REMARKS

Owing to several limitations of near-atmospheric pressure superheated steam drying, low-pressure superheated steam drying (LPSSD) has emerged as an alternative for drying heat- and/or oxygen-sensitive food products. Over the past several years, many attempts have been made to apply this technology to a wide array of foods and it has been shown that LPSSD could produce dried products with superior quality, either in terms of physical or chemical (nutritional) quality, compared with products dried by conventional hot air drying or vacuum drying. In addition to applying this technology to drying foods *per se*, LPSSD also has the potential to produce engineered biomaterials for different applications in food engineering, for example, production of antioxidant/antimicrobial edible films for active packaging applications. Preliminary results have indeed shown that LPSSD could yield edible films with higher strength, compared with films obtained from vacuum drying, due to its ability to enhance crystallinity of the film structure.

Future developments in this area should aim towards developing a more realistic mathematical model that enables predictions of moisture content and temperature evolutions within the drying material. Further use of the technology for the production of advanced materials should also be investigated.

5.7 NOTATION

C_p	heat capacity, $\text{J kg}^{-1} \text{K}^{-1}$
D_{eff}	effective diffusivity, $\text{m}^2 \text{s}^{-1}$
h	heat transfer coefficient, $\text{W m}^{-2} \text{K}^{-1}$
k	thermal conductivity, $\text{W m}^{-1} \text{K}^{-1}$
MR	moisture ratio, $\frac{X - X_{eq}}{X_i - X_{eq}}$
n	unit vector
N	evaporation rate, kg s^{-1}
q	heat transfer rate, W
t	time, s
T	temperature, $^{\circ}\text{C}$
T_i	initial temperature, $^{\circ}\text{C}$
X	total moisture content, $\text{kg water per kg dry solid (d.b.)}$
X_{eq}	equilibrium moisture content, $\text{kg water per kg dry solid (d.b.)}$
X_f	free moisture content, $\text{kg water per kg dry solid (d.b.)}$

Greek letters

λ	latent heat of vaporization, J kg^{-1}
ρ	density, kg m^{-3}

Subscripts

f	free
i	initial
s	surface of product
<i>steam</i>	superheated steam

REFERENCES

- Abe, T. and Miyashita, K. (2006) Surface sterilization of dried fishery products in superheated steam and hot air. *Nippon Shokuhin Kagaku Kogaku Kaishi*, **53**, 373–379.
- Achanta, S. and Okos, M.R. (2000) Quality changes during drying of food polymers. In: *Drying Technology in Agriculture and Food Science* (ed. A.S. Mujumdar). Science Publishers, Enfield, NH, pp. 133–147.
- Barbieri, S., Elustondo, M. and Urbicain, M. (2004) Retention of aroma compounds in basil dried with low pressure superheated steam. *Journal of Food Engineering*, **65**, 109–115.
- Bond, J.F., Mujumdar, A.S., van Heiningen, A.R.P. and Douglas, W.J.M. (1994) Drying paper by impinging jets of superheated steam. Part 2: Comparison of steam and air as drying fluids. *Canadian Journal of Chemical Engineering*, **72**, 452–456.
- Cenkowski, S., Pronyk, C., Zmidzinska, D. and Muir, W.E. (2007) Decontamination of food products with superheated steam. *Journal of Food Engineering*, **83**, 68–75.
- Chen, S.R., Chen, J.Y. and Mujumdar, A.S. (1992) Preliminary study of steam drying of silkworm cocoons. *Drying Technology*, **10**, 251–260.
- Chow, L.C. and Chung, J.N. (1983) Evaporation of water into a laminar stream of air and superheated steam. *International Journal of Heat and Mass Transfer*, **26**, 373–380.
- Defo, M., Fortin, Y. and Cloutier, A. (2004) Modeling superheated steam vacuum drying of wood. *Drying Technology*, **22**, 2231–2253.

- Devahastin, S. and Suvarnakuta, P. (2004) Superheated-steam-drying of food products. In: *Dehydration of Products of Biological Origin* (ed. A.S. Mujumdar). Science Publishers, Enfield, NH, pp. 493–512.
- Devahastin, S., Suvarnakuta, P., Soponronnarit, S. and Mujumdar, A.S. (2004) A comparative study of low-pressure superheated steam and vacuum drying of a heat-sensitive material. *Drying Technology*, **22**, 1845–1867.
- Douglas, W.J.M. (1994) Drying paper in superheated steam. *Drying Technology*, **12**, 1341–1355.
- Elustondo, D., Elustondo, M.P. and Urbicain, M.J. (2001) Mathematical modeling of moisture evaporation from foodstuffs exposed to subatmospheric pressure superheated steam. *Journal of Food Engineering*, **49**, 15–24.
- Elustondo, D.M., Mujumdar, A.S. and Urbicain, M.J. (2002) Optimum operating conditions in drying of foodstuffs with superheated steam. *Drying Technology*, **20**, 381–402.
- Furukawa, T. and Akao, T. (1983) Deodorization by superheated steam drying. *Drying Technology*, **2**, 407–418.
- Haji, M. and Chow, L.C. (1988) Experimental measurement of water evaporation rates into air and superheated steam. *Journal of Heat Transfer*, **110**, 237–242.
- Incropera, F.P. and DeWitt, D.P. (2002) *Fundamentals of Heat and Mass Transfer*, 5th edn. Wiley, New York.
- Iyota, H., Konishi, Y., Inoue, T., Yoshida, K., Nishimura, N. and Nomura, T. (2005) Popping of Amaranth seeds in hot air and superheated steam. *Drying Technology*, **23**, 1273–1287.
- Iyota, H., Nishimura, N., and Nomura, T. (2001) Drying of sliced raw potatoes in superheated steam and hot air. *Drying Technology*, **19**, 1411–1424.
- Jamradloedluk, J., Nathakaranakule, A., Soponronnarit, S. and Prachayawarakorn, S. (2007) Influences of drying medium and temperature on drying kinetics and quality attributes of durian chips. *Journal of Food Engineering*, **78**, 198–205.
- Kongsontornkijkul, P., Ekwongsupasarn, P., Chiewchan, N. and Devahastin, S. (2006) Effects of drying methods and tea preparation temperature on the amount of vitamin C in Indian gooseberry tea. *Drying Technology*, **24**, 1509–1513.
- Kozanoglu, B., Vazquez, A.C., Chanes, J.W. and Patino, J.L. (2006) Drying of seeds in a superheated steam vacuum fluidized bed. *Journal of Food Engineering*, **75**, 383–387.
- Leeratanarak, N., Devahastin, S. and Chiewchan, N. (2006) Drying kinetics and quality of potato chips undergoing different drying techniques. *Journal of Food Engineering*, **77**, 635–643.
- Methakhup, S., Chiewchan, N. Devahastin, S. (2005) Effects of drying methods and conditions on drying kinetics and quality of Indian gooseberry flake. *LWT – Food Science and Technology*, **38**, 579–587.
- Moreira, R.G. (2001) Impingement drying of foods using hot air and superheated steam. *Journal of Food Engineering*, **49**, 291–295.
- Mujumdar, A.S. (2000) Superheated steam drying – Technology of the future. In: *Mujumdar's Practical Guide to Industrial Drying* (ed. S. Devahastin). Exergex Corp., Brossard, Canada, pp. 115–138.
- Mujumdar, A.S. (2007) Superheated steam drying. In: *Handbook of Industrial Drying*, 3rd edn. (ed. A.S. Mujumdar). CRC Press, Boca Raton, FL, pp. 439–452.
- Namsanguan, Y., Tia, W., Devahastin, S. and Soponronnarit, S. (2004) Drying kinetics and quality of shrimp undergoing different two-stage drying processes. *Drying Technology*, **22**, 759–778.
- Nathakaranakule, A., Kraiwanchikul, W. and Soponronnarit, S. (2007) Comparative study of different combined superheated-steam drying techniques for chicken meat. *Journal of Food Engineering*, **80**, 1023–1030.
- Nimmol, C., Devahastin, S., Swasdisevi, T. and Soponronnarit, S. (2007) Drying of banana slices using combined low-pressure superheated steam and far-infrared radiation. *Journal of Food Engineering*, **81**, 624–633.
- Pang, S. (1997) Some considerations in simulation of superheated steam drying of softwood lumber. *Drying Technology*, **15**, 651–670.
- Pang, S. and Dakin, M. (1999) Drying rate and temperature profile for superheated steam vacuum drying and moist air drying of softwood lumber. *Drying Technology*, **17**, 1135–1147.
- Panyawong, S. and Devahastin, S. (2007) Determination of deformation of a food product undergoing different drying methods and conditions via evolution of a shape factor. *Journal of Food Engineering*, **78**, 151–161.

- Pimpaporn, P., Devahastin, S. and Chiewchan, N. (2007) Effects of combined pretreatments on drying kinetics and quality of potato chips undergoing low-pressure superheated steam drying. *Journal of Food Engineering*, **81**, 318–329.
- Prachayawarakorn, S., Soponronnarit, S., Wetchacama, S. and Jaisut, D. (2002) Desorption isotherms and drying characteristics of shrimp in superheated steam and hot air. *Drying Technology*, **20**, 669–684.
- Prachayawarakorn, S., Prachayawasin, P. and Soponronnarit, S. (2006) Heating process of soybean using hot-air and superheated-steam fluidized-bed dryers. *LWT – Food Science and Technology*, **39**, 770–778.
- Pronyk, C., Cenkowski, S. and Abramson, D. (2006) Superheated steam reduction of deoxynivalenol in naturally contaminated wheat kernels. *Food Control*, **17**, 789–796.
- Rordprapat, W., Nathakaranakule, A., Tia, W. and Soponronnarit, S. (2005) Comparative study of fluidized bed paddy drying using hot air and superheated steam. *Journal of Food Engineering*, **71**, 28–36.
- Sano, A., Senda, Y., Oyama, K., Tanigawara, R., Bando, Y., Nakamura, M., Sugimura, Y. and Shibata, M. (2005) Drying characteristics in superheated steam drying at reduced pressure. *Drying Technology*, **23**, 2437–2447.
- Schwartz, J.P. and Brocker, S. (2002) A theoretical explanation for the inversion temperature. *Chemical Engineering Journal*, **86**, 61–67.
- Sheikholeslami, R. and Watkinson, A.P. (1992) Rate of evaporation of water into superheated steam and humidified air. *International Journal of Heat and Mass Transfer*, **35**, 1743–1751.
- Shibata, H., Mada, J. and Shinohara, H. (1988) Steam drying of sintered glass bead spheres under vacuum. *Industrial & Engineering Chemistry Research*, **27**, 2385–2387.
- Shibata, H., Mada, J. and Funatsu, K. (1990) Prediction of drying rate curves on sintered spheres of glass beads in superheated steam under vacuum. *Industrial & Engineering Chemistry Research*, **29**, 614–617.
- Shibata, H. (2006) Drying rate curves of porous solids in steam and in air under low-pressure conditions. *Drying Technology*, **24**, 37–43.
- Soponronnarit, S., Nathakaranakule, A., Jirajindalert, A. and Taechapairoj, C. (2006) Parboiling brown rice using superheated steam fluidization technique. *Journal of Food Engineering*, **75**, 423–432.
- Sotome, I., Suzuki, K., Koseki, S., *et al.* (2006) Blanching of potato with superheated steam containing micro-droplets of hot water. *Nippon Shokuhin Kagaku Kogaku Kaishi*, **53**, 451–458.
- Suvarnakuta, S., Devahastin, S. and Mujumdar, A.S. (2005a) Drying kinetics and β -carotene degradation in carrot undergoing different drying processes. *Journal of Food Science*, **70**, S520–S526.
- Suvarnakuta, S., Devahastin, S. and Mujumdar, A.S. (2007) A mathematical model for low-pressure superheated steam drying of a biomaterial. *Chemical Engineering and Processing*, **46**, 675–683.
- Suvarnakuta, S., Devahastin, S., Soponronnarit, S. and Mujumdar, A.S. (2005b) Drying kinetics and inversion temperature in a low-pressure superheated steam-drying system. *Industrial & Engineering Chemistry Research*, **44**, 1934–1941.
- Taechapairoj, C., Prachayawarakorn, S. and Soponronnarit, S. (2004) Characteristics of rice dried in superheated-steam fluidized-bed. *Drying Technology*, **22**, 719–743.
- Tatemoto, Y., Yano, S., Mawatari, Y., Noda, K. and Komatsu, N. (2007) Drying characteristics of porous material immersed in a bed of glass beads fluidized by superheated steam under reduced pressure. *Chemical Engineering Science*, **62**, 471–480.
- Thomkapanish, O., Suvarnakuta, S. and Devahastin, S. (2007). Study of intermittent low-pressure superheated steam and vacuum drying of a heat-sensitive material. *Drying Technology*, **25**, 205–223.
- Wu, C.-H., Davis, D.C. and Chung, J.N. (1989) Simulated dehydration of wedge-shaped specimens in turbulent flow of superheated steam and air. *Drying Technology*, **7**, 761–782.
- Wu, C.-H., Davis, D.C., Chung, J.N. and Chow, L.C. (1987) Simulation of wedge-shaped product dehydration using mixture of superheated steam and air in laminar flow. *Numerical Heat Transfer*, **11**, 109–123.

6 Heat pump-assisted drying

Md Raisul Islam and Arun S. Mujumdar

6.1 INTRODUCTION

In the search for hygienic, energy efficient and well-controlled drying processes for high value heat-sensitive drying products, heat pump drying technologies have emerged as an attractive and viable option. Conventional driers dump the energy of evaporated moisture into the atmosphere. To reduce the energy consumption of drying processes, the energy of the evaporated moisture should be recovered and the temperature of the recovered energy raised high enough for reuse in the drying process. A heat pump-assisted drier (HPD) extracts the latent heat of vaporization from the exhaust's moist air by vapor condensation at the evaporator coil, and delivers the recovered energy as sensible heat to the drying air stream passing through the condenser coil. Excellent control over a wide range of operating conditions makes the HPD suitable for a number of high value products such as timber (Ceylan *et al.*, 2007), herbs (Fatouh *et al.*, 2006), fruits (Chua *et al.*, 2002), agricultural products (Chua *et al.*, 2001) etc. Moreover, a suitably designed heat pump can be conveniently fitted with driers such as superheated steam driers (Mujumdar *et al.*, 1992; Namsanguan *et al.*, 2004), fluidized bed driers (Strommen *et al.*, 1999), infrared driers (Tan *et al.*, 2001; Marshall and Metaxas, 1998), microwave driers (Jia *et al.*, 1993) etc.

Numerous experimental and numerical studies have been conducted by researchers on heat pump drying systems to achieve better product quality, increase energy efficiency and optimize components and system design. Soylemez (2006) presented thermal analyses of all system components together with a thermo-economic optimization to estimate the optimum operating conditions of heat pump driers with auxiliary heating. Chua and Chou (2005) experimentally studied the performance of a two-stage heat pump drying system and reported that up to 35% more heat could be recovered using a two-stage evaporator system in comparison to a single evaporator system. Saensabai and Prasertsan (2003) investigated the performance of five heat pump drier configurations which covered the fully open, the partially open and the fully closed systems with external condenser or external cooler. They reported that the best operating mode of the HPD depends on both the drying rate and the ambient conditions. Queiroz *et al.* (2004) studied the drying kinetics of tomato using HPD and electric resistance driers with parallel and crossed airflow arrangements and reported that the energy economy of HPD was about 40% when compared to the drying system with electric resistance. Chen *et al.* (2002) examined a dual-purpose heat pump dehumidifier drier to dry pine cones and pine pollen catkins. Their experimental results exhibit significant improvement in the product quality and seed germination rate.

Ogura *et al.* (2003) tested a novel chemical heat pump-assisted convective drier system and found it to be energy-efficient over a wide temperature range of industrial interest.

Commercial viability of chemical heat pumps for drying operations is still not established, however. Sarkar *et al.* (2006a, 2006b) studied the effect of key operating parameters such as the bypass air ratio, re-circulation air ratio, drier efficiency, ambient conditions (temperature and relative humidity), and air mass flow rate on the performance of a transcritical CO₂ HPD. They found that the effects of drier efficiency, recirculation air ratio, ambient temperature and air mass flow rate are very significant for the performance of the HP-drier. Teeboonma *et al.* (2003) identified recycled air ratio, evaporator bypass air ratio, airflow rates, and drying air temperature as the most important factors for optimization of a heat pump fruit drier. Namsanguan *et al.* (2004) experimentally investigated the drying kinetics and quality of shrimp using a superheated steam drier followed by a heat pump (SSD/HPD) and hot air drier (SSD/AD). They found that SSD/HPD dried shrimp had a much lower degree of shrinkage, higher degree of rehydration, better color, was less tough, softer and more porous than single-stage SSD dried shrimp. Klocker *et al.* (2002) provided the details for design and construction of a batch-type cabinet heat pump drier using carbon dioxide as the working fluid.

Hawladar *et al.* (2006) used nitrogen and carbon dioxide as the drying media and experimentally investigated the drying kinetics and quality of HP-dried products. They reported reduced browning, faster rehydration, and enhanced vitamin C retention in the final products and highlighted the great potential of the modified atmosphere heat pump drier in the food drying industry. Braun *et al.* (2002) investigated the feasibility of the air heat pump cycle for clothes tumble driers and found that an air cycle heat pump drier with practical components is capable of significant efficiency improvements as compared with conventional driers. Hawladar and Jahangeer (2006) investigated the performance of a solar-assisted heat pump drier and water heater. They reported a coefficient of performance value of 7.0 for a compressor speed of 1800 rpm and identified solar radiation, compressor speed and the total load placed in the drying chamber as the most important parameters that affect system performance. Alves-Filho (2002) presented combined HPD and cold extrusion technique for the production of instant foods and reported that besides being energetically efficient and environmentally friendly, heat pump drying technology provides a wide range of drying conditions that are required to produce dried products with improved characteristics.

6.2 CLASSIFICATION OF HEAT PUMP DRIERS

Properly designed heat pumps can be fitted to almost any conventional drier that uses convection as the primary mode of heat input. Moreover, the control strategy and design of the heat pump driers can be modified to obtain optimum drying conditions for a wide range of drying materials. A generalized classification scheme for heat pump driers is shown in Figure 6.1.

6.3 FUNDAMENTALS OF HEAT PUMP DRIERS

Transfer of heat from a lower temperature to a higher temperature region requires special devices called refrigerators. Heat pumps and refrigerators are essentially the same devices. The objective of a refrigerator is to remove heat from a refrigerated space or flow stream of low-temperature to the high-temperature medium. In this case, rejection of heat to the high-temperature medium is not the objective, but a necessary part of the process. The objective

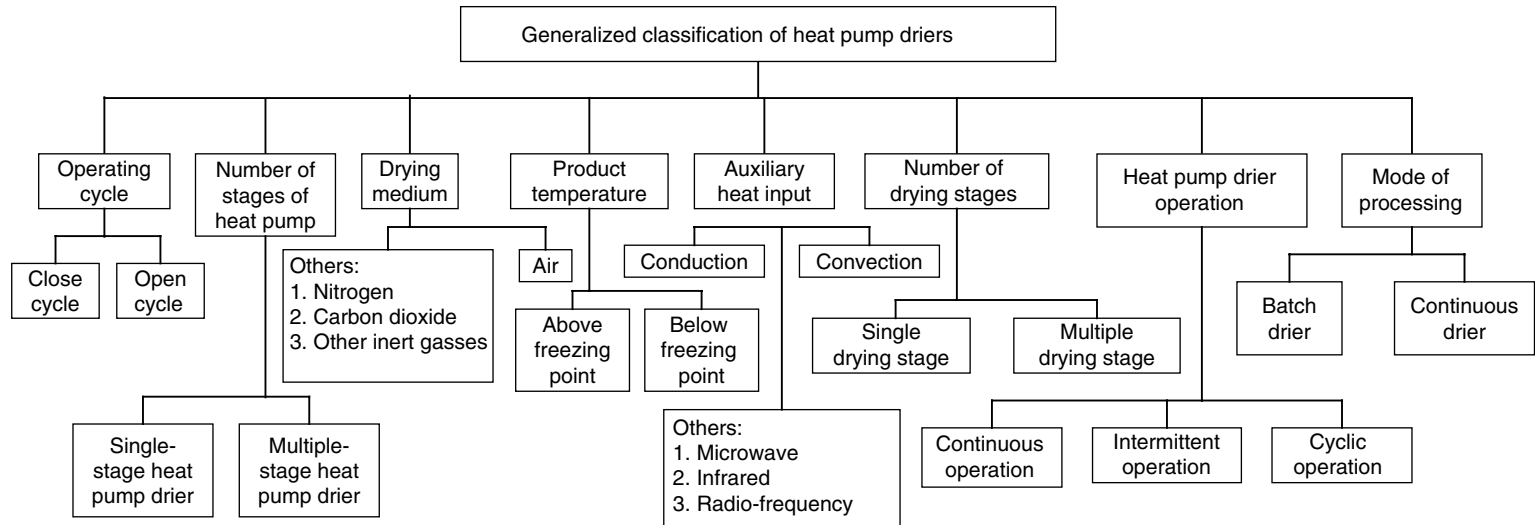


Fig. 6.1 Generalized classification scheme for heat pump drier.

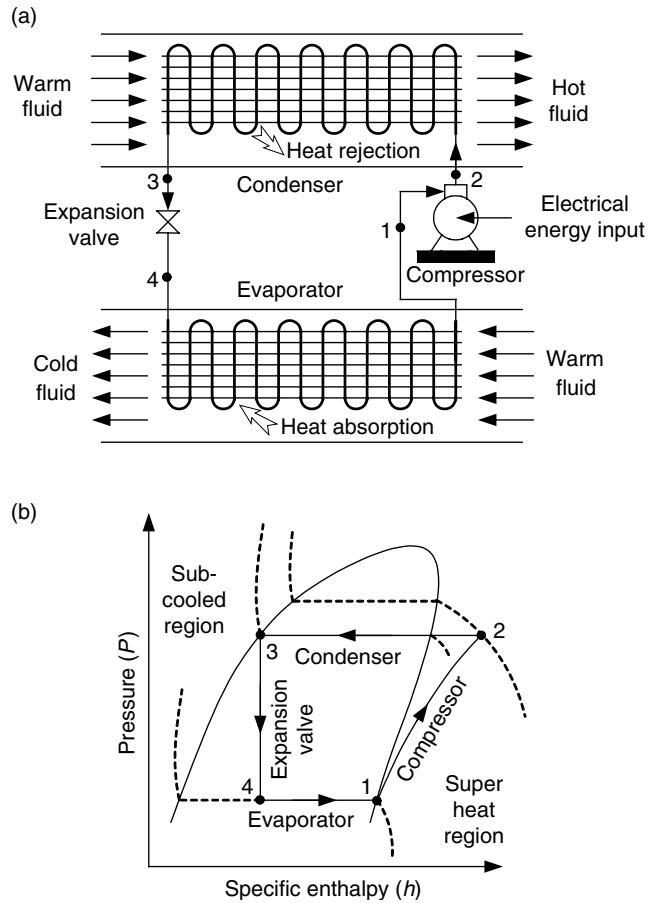


Fig. 6.2 (a) Schematic diagram of an ideal vapor compression refrigeration/heat pump cycle and (b) the P - h diagram of the cycle.

of a heat pump is to supply heat to a space or flow stream of high-temperature by absorbing heat from a low-temperature medium. A schematic diagram of a simple saturated vapor compression refrigeration/heat pump cycle and the variation of pressure and enthalpy at different stages of the process are shown in Figure 6.2. The working fluids used in the cycle are known as refrigerants. The main components of a vapor compression refrigeration/heat pump are: compressor, condenser, expansion valve and evaporator. The low-pressure liquid refrigerant evaporates in the evaporator by absorbing the latent heat of vaporization from the surrounding fluid and produces the cooling effect. The resulting refrigerant vapor is compressed to the condenser pressure by a compressor that usually consumes electrical energy. In the condenser, the high-pressure refrigerant is condensed and the resulting heat is released to the surrounding fluid. The condensed refrigerant is finally expanded to the evaporator pressure through the expansion valve and continues the cycle. Although the actual cycle usually deviates somewhat from the simple saturated cycle, it is worthwhile analyzing a simple saturated cycle for easily identifying and understanding the fundamental processes, which are the basis for every actual cycle.

The performance of refrigerators and heat pumps is expressed in terms of the coefficient of performance (COP), which is defined as

$$\text{COP}_{\text{Refrigerator}} = \frac{\text{Desired output}}{\text{Required input}} = \frac{\text{Cooling effect}}{\text{Work input}} = \frac{h_1 - h_4}{h_2 - h_1} \quad (6.1)$$

$$\text{COP}_{\text{Heat pump}} = \frac{\text{Desired output}}{\text{Required input}} = \frac{\text{Heating effect}}{\text{Work input}} = \frac{h_2 - h_3}{h_2 - h_1} \quad (6.2)$$

As the expansion of refrigerant in the expansion valve is a steady flow constant enthalpy process, the vertical line on the P - h diagram shows $h_3 = h_4$.

$$\text{Combining equations (6.1) and (6.2) gives : } \text{COP}_{\text{Heat pump}} = \text{COP}_{\text{Refrigerator}} + 1 \quad (6.3)$$

Figure 6.2(b) shows that the heating effect ($h_2 - h_3$) of a heat pump is equal to the summation of the input electrical energy ($h_2 - h_1$) to the compressor and the energy absorbed ($h_1 - h_4$) in the evaporator. The heat pumps used in the drying processes generally have COP in the range 4–7. This means it is possible to achieve heat energy about 4–7 times higher than the electrical energy input to the compressor. Of course higher grade energy (electricity) is converted to lower grade (thermal) energy in this process.

During drying, the temperature and relative humidity of the drying medium, which is usually air, needs to be maintained at the desired level to achieve optimum drying conditions. Figure 6.3 shows a conventional tunnel drier coupled with a heat pump. The main components of the drier are the drying chamber, air blower, heat pump and auxiliary air heater. The thermodynamic cycle for the air stream is shown on a psychrometric chart, Figure 6.4. Hot, moist air from the drying chamber flows through the evaporator section (A) and the by-pass duct (B). The flow rate of air in the evaporator section $\dot{m}_{\text{air},e}$ and the by-pass duct $\dot{m}_{\text{air},d}$ is adjusted based on the desired relative humidity at the entrance of the drying chamber.

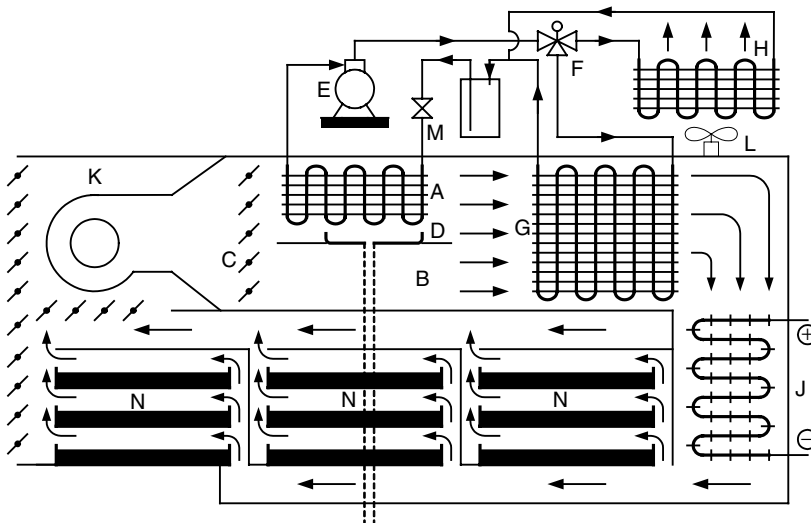


Fig. 6.3 Schematic diagram of a heat pump drier.

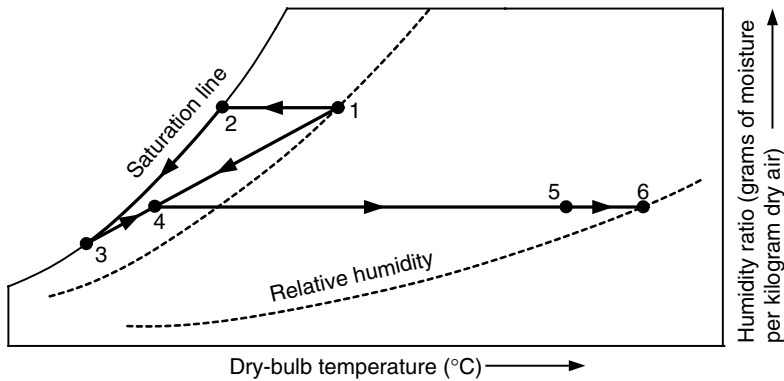


Fig. 6.4 Thermodynamic cycle of air stream in a heat pump drier.

The volumetric flow rate of the drying air through the evaporator coil and the by-pass duct is usually controlled using conventional butterfly dampers (C). As the air passes over the evaporator coils, its temperature falls and its relative humidity increases while the specific humidity is constant in the initial section of the evaporator coil (state 1 to 2 of Figure 6.4). Finally, the air stream reaches its dew-point. Further transfer of heat from the air stream in the remaining section of the evaporator coil results in condensation of part of the moisture in the air stream. The air stream remains saturated during the entire condensation process, which follows the 100% relative humidity line until the final state 3 is reached at the exit of the evaporator coil. The refrigerant that flows through the evaporator coil recovers the sensible and latent heat of condensation from the air stream and causes the refrigerant to evaporate. The condensed water is drained out from the evaporator section through a channel (D). Point-3 of the psychrometric chart (Figure 6.4) represents the temperature of the condensed water while leaving the evaporator. The quantity of energy recovered by the refrigerant under ideal conditions can be determined using a simple mass and energy conservation equation as:

$$\text{Mass of dry air: } \dot{m}_{air,e,1} = \dot{m}_{air,e,3} = \dot{m}_{air,e} \quad (6.4)$$

$$\text{Mass of water: } \dot{m}_{air,e}\omega_1 = \dot{m}_{air,e}\omega_3 + \dot{m}_{water} \quad (6.5)$$

Energy recovered by the refrigerant in evaporator:

$$\dot{Q}_{evaporator} = \dot{m}_{air,e}h_1 - \dot{m}_{air,e}h_3 - \dot{m}_{water}h_f \text{ at } T_3 \quad (6.6)$$

The sizes of the evaporator coil and the compressor of the heat pump are selected based on the design rate of energy recovered in the evaporator coils $\dot{Q}_{evaporator}$ and the $COP_{Refrigerator}$ of the machine. The refrigerant vapor is compressed to high pressure and temperature in the compressor (E) and then flows through a three-way control valve (F) to the main (G) and auxiliary condenser coils (H). The air stream of low temperature and moisture content that exits the evaporator coil mixes with the by-pass air at the exit of the by-pass duct (B) and then flows over the main condenser coil (G). Assuming adiabatic mixing and neglecting changes in the kinetic and potential energies, state 4 (before the main condenser coil) can be analyzed

with the conservation of mass and energy equations as:

$$\text{Mass of dry air: } \dot{m}_{air,e} + \dot{m}_{air,d} = \dot{m}_{air} \quad (6.7)$$

$$\text{Mass of water vapor: } \dot{m}_{air,e}\omega_3 + \dot{m}_{air,d}\omega_1 = \dot{m}_{air}\omega_4 \quad (6.8)$$

$$\text{Energy: } \dot{m}_{air,e}h_3 + \dot{m}_{air,d}h_1 = \dot{m}_{air}h_4 \quad (6.9)$$

As the air flows over the condenser coil, its temperature increases and relative humidity decreases at constant specific humidity (state 4 to 5 in Figure 6.4). Based on the set temperature of drying air, the flow rates of refrigerant in the main and auxiliary condenser coils are controlled by the three-way control valve. Finally, the air stream flows over the auxiliary air heater (J) to reach the set temperature (state 6) at the entrance of the drying chamber.

Conservation of mass and energy equations for state 4 and 5:

$$\text{Mass of dry air: } \dot{m}_{air,4} = \dot{m}_{air,5} = \dot{m}_{air} \quad (6.10)$$

$$\text{Mass of water vapor: } \dot{m}_{air}\omega_4 = \dot{m}_{air}\omega_5 \quad (6.11)$$

$$\text{Energy: } \dot{m}_{air}h_4 + \dot{Q}_{condenser} = \dot{m}_{air}h_5 \quad (6.12)$$

Conservation of mass and energy equations for state 5 and 6:

$$\text{Mass of dry air: } \dot{m}_{air,5} = \dot{m}_{air,6} = \dot{m}_{air} \quad (6.13)$$

$$\text{Mass of water vapor: } \dot{m}_{air}\omega_5 = \dot{m}_{air}\omega_6 \quad (6.14)$$

$$\text{Energy: } \dot{m}_{air}h_5 + \dot{Q}_{air\ heater} = \dot{m}_{air}h_6 \quad (6.15)$$

Flow uniformity of drying air inside the drying chamber is an important factor to ensure uniform drying of the products. Non-uniformity in velocity translates into different drying kinetics in different regions of the trays/drying chamber resulting in over- or under-drying of the products. Trays and air flow channels in the drying chamber of compact driers need to be designed more carefully since flow non-uniformities can be severe in these cases. Arrangement of the trays shown in Figure 6.3 is an example where the drying air will flow uniformly over the trays. Stainless-steel plates and nets are commonly used to fabricate the trays. Moisture can then evaporate from the top and bottom surfaces of the product placed in a netted tray. On the other hand, trays made of solid plate will be more rigid, but moisture evaporates only from the top exposed surface. Perforated plates and honeycombs are commonly installed at the entrance of the evaporator coil, condenser coil, air heater and drying chamber to make the flow of the drying air uniform. However, perforated plates and honeycomb increase resistance to the flow of air. Major sources of head loss for the heat pump driers are the trays, evaporator coil, condenser coil, auxiliary air heater, butterfly dampers, bends, turning vane and the converging and diverging sections of the air flow ducts. Readers are referred to any standard textbook or manual of duct design to calculate the pressure drops. The air blower is selected based on the head loss and the required flow rate of drying air. Thermocouples, relative humidity sensors, velocity probes, camera and automatic controllers are installed at different locations of the drier to monitor and accordingly control the temperature, relative humidity, velocity distribution of the drying air. With advanced PID controllers, it is possible to regulate the drying conditions at different stages of the drying process to follow the optimum operating conditions.

Heat pump driers can be operated both in the open and close cycles. In the initial stage of drying when the moisture content of the products is high, and the resulting higher moisture evaporation rate or the specific humidity of atmospheric air is low, the heat pump could be operated more efficiently in the open cycle. Heat sensitive products with relatively low moisture content can be dried more efficiently in the close cycle. The content of organic volatile matters, such as the aroma of the dried product, can be enhanced in close cycle drying. Color is another major quality parameter of dried food products. During drying the color of the drying products may change due to a number of chemical or biochemical reactions. Fruits and vegetables often contain different enzymes. Oxidation of the enzymes during drying leads to the formation of brown pigments. For effective control of the oxidative reactions, the level of oxygen in the drying medium should be held below 1% and the remainder can be an inert gas such as nitrogen. This condition also provides an effective control against insects. Inert gas (e.g. nitrogen) can be conveniently used as the drying medium in a closed cycle heat pump drier. Drying products also have a tendency to absorb odors from external sources, which is minimized in close cycle driers.

The performance of the driers is commonly expressed in terms of the specific moisture evaporation rate (SMER), which is defined as:

$$\text{SMER} = \frac{\text{Amount of water evaporated}}{\text{Energy used}}, \text{ kg kWh}^{-1}$$

The reciprocal of the SMER, which is the energy required to evaporate 1 kg of water, known as heat pump drier efficiency (HPDE), is also used as efficiency indicator of HPD. The SMER depends on temperature, relative humidity and velocity of the drying air as well as the moisture content, thermophysical and transport properties of the drying product. For HPD, the SMER also depends on the evaporation and condensation temperatures and the efficiency of the refrigeration system. The SMER of HPD decreases with the decrease of drying air temperature mainly because of the low COP of the refrigeration cycle at low evaporator temperature. Therefore, a higher drying air temperature should be used unless the quality of the dried product is degraded. The energy consumed by the fans or blowers to circulate the drying air is not considered in the classical definition of SMER. For low-temperature drying, the energy consumed by the fans or blowers can be a significant fraction of the total energy consumption and should be included in the calculation of SMER. The typical value of SMER of HPD is about 3 kg kWh⁻¹ which is only about 0.5–1 kg kWh⁻¹ for conventional convection driers. It is possible to achieve the SMER of HPD to about 10 kg kWh⁻¹ by using advanced heat pump and optimizing the drying conditions.

6.4 HEAT AND MASS TRANSFER MECHANISMS

In low-temperature drying of heat-sensitive products, liquid moisture migrates from the bulk of the product to the exposed drying surface by a process that can be modeled as a diffusion process. In convection drying processes, heat is transferred from the drying gas to the exposed surface of the product by convection. A major part of this heat is absorbed by the liquid moisture at the drying surface as latent heat of vaporization and evaporates. The remaining heat is conducted inside the product. Because of the difference of vapor pressure between the drying air and the surface of the drying product, evaporated moisture transfers to the drying medium.

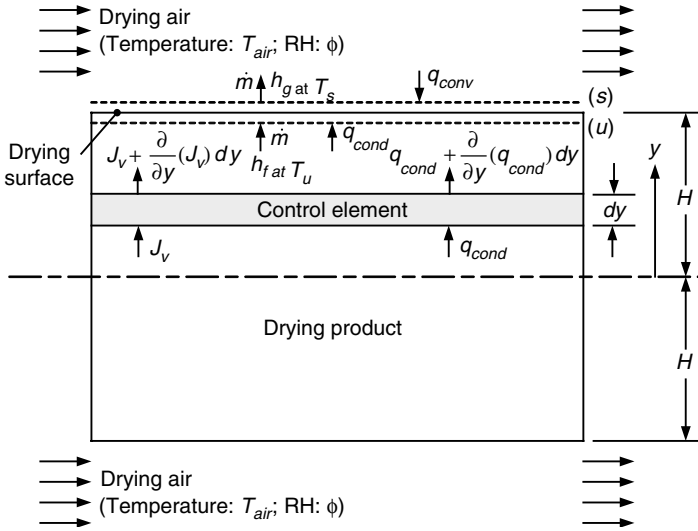


Fig. 6.5 Schematic diagram of the drying material.

To model the heat and mass transfer processes, a rectangular piece of the drying material of thickness $2H$ is considered as shown schematically in Figure 6.5. Unlike temperature, the distribution of moisture over the drying surface is discontinuous. In order to define moisture concentrations at the interface, two imaginary surfaces, denoted by u and s , are introduced on both sides of the real interface. u and s surfaces are infinitesimally close to the drying surface. Temperatures at u and s surfaces are the same; however, the concentrations of moisture are different.

Energy balance at the exposed drying surface gives:

$$\dot{m} h_{f \text{ at } T_u} + q_{cond} A + q_{conv} A = \dot{m} h_g \text{ at } T_s$$

or

$$\dot{m} (h_g \text{ at } T_s - h_f \text{ at } T_s) - A (q_{cond} + q_{conv}) = 0$$

or

$$\frac{\dot{m}}{A} (h_{fg} \text{ at } T_s + \Delta H_w) = q_{conv} + q_{cond}$$

or

$$J_v (h_{fg} \text{ at } T_s + \Delta H_w) = \bar{h}_c (T_{air} - T_s) - k_p \left. \frac{dT}{dy} \right|_u \tag{6.16}$$

where ΔH_w is the heat of wetting, which increases significantly at lower moisture contents (Kee, 1972). The average convective air-to-product heat transfer coefficient \bar{h}_c can be calculated using an appropriate correlation such as (Saravacos and Maroulis, 2001):

$$Nu = 0.664 Re^{1/2} Pr^{1/3} \quad Pr \geq 0.6, Re < 2300 \tag{6.17}$$

Where the heat transfer Nusselt number is $Nu = \bar{h}_c L / k_{air}$; Reynolds number is $Re = \rho_{air} U_{\alpha} L / \mu_{air} = U_{\alpha} L / \nu_{air}$ and the Prandtl number is $Pr = \nu_{air} / \alpha_{air} = c_p \mu_{air} / k_{air}$. Thermophysical properties of the air stream are evaluated at the average temperature $T = (T_s + T_{air}) / 2$.

The mass transfer rate of vapor from the drying surface to the drying air is:

$$\frac{\dot{m}}{A} = J_v = k_m (m_{v,s} - m_{v,air}) \quad (6.18)$$

The mass transfer coefficient k_m can be determined using a heat and mass transfer analogy. If a convective mass transfer problem has the same geometry, flow pattern and boundary conditions as a known heat transfer problem, then the heat transfer correlations may be converted to mass transfer correlations by replacing the Nusselt number for heat transfer Nu by the Nusselt number for mass transfer Nu_m and the Prandtl number Pr by the Schmidt number Sc . Therefore, the mass transfer equation analogous of the heat transfer equation (6.17) is:

$$Nu_m = 0.664 Re^{1/2} Sc^{1/3} \quad (6.19)$$

where $Nu_m = k_m L / \rho_{air} D_{v,air}$ and $Sc = \nu_{air} / D_{v,air}$.

Mass fraction of vapor at the s-surface is determined as:

$$m_{v,s} = \frac{\rho_{v,s}}{\rho_{total,s}} = \frac{\rho_{v,s}}{\rho_{v,s} + \rho_{air,s}} \quad (6.20)$$

Density of vapor at s-surface can be determined using ideal gas law as:

$$\rho_{v,s} = \frac{M_v P_{v,s}}{R_u T} \quad (6.21)$$

Similarly, density of dry air at s-surface:

$$\rho_{air,s} = \frac{M_{air} P_{air,s}}{R_u T} = \frac{M_{air} (P_{total} - P_{v,s})}{R_u T} \quad (6.22)$$

Combining equations (6.20), (6.21) and (6.22) gives

$$m_{v,s} = \frac{M_v P_{v,s}}{M_v P_{v,s} + M_{air} (P_{total} - P_{v,s})} \quad (6.23)$$

The ratio of partial vapor pressure at the drying surface (s-surface) to the saturation vapor pressure at drying surface temperature is defined as water activity that changes with moisture content and temperature of the drying surface. Equation (6.23) can be written in terms of the water activity and saturation vapor pressure as:

$$m_{v,s} = \frac{M_v a_w P_{v, sat} \text{ at } T_s}{M_v a_w P_{v, sat} \text{ at } T_s + M_{air} (P_{total} - a_w P_{v, sat} \text{ at } T_s)} \quad (6.24)$$

Similarly, mass fraction of vapor in the free stream is:

$$m_{v,air} = \frac{M_v P_{v,air}}{M_v P_{v,air} + M_{air} (P_{total} - P_{v,air})} \quad (6.25)$$

If the temperature T_{air} and relative humidity ϕ of the drying air is known, equation (6.25) can be expressed as:

$$m_{v,air} = \frac{M_v \phi P_{v \text{ sat at } T_{air}}}{M_v \phi P_{v \text{ sat at } T_{air}} + M_{air} (P_{total} - \phi P_{v \text{ sat at } T_{air}})} \quad (6.26)$$

If the thickness of the drying product is small relative to its width and length, it is reasonable to assume that heat and mass transfer occur exclusively in the y -direction (Figure 6.5). Considering the one-dimensional flow of liquid moisture inside the drying product, the distribution of liquid moisture inside the product can be determined using the conservation of moisture in the control element shown in Figure 6.5 as:

$$J_v A - \left[J_v + \frac{\partial}{\partial y} (J_v) dy \right] A = \frac{\partial}{\partial t} (\rho_v A dy)$$

or

$$\frac{\partial \rho_v}{\partial t} = - \frac{\partial}{\partial y} (J_v)$$

or

$$\frac{\partial \rho_v}{\partial t} = \frac{\partial}{\partial y} \left[\rho_p D_{m,p} \frac{\partial m_{v,p}}{\partial y} \right] \quad (6.27)$$

Similarly, the conservation of energy in the control element gives:

$$\rho_p c_p \frac{\partial T_p}{\partial t} = \frac{\partial}{\partial y} \left(k_p \frac{\partial T_p}{\partial y} \right) \quad (6.28)$$

The thermophysical and transport properties of the drying product, such as density, specific heat, thermal conductivity and moisture diffusivity, are functions of moisture content and temperature of the product which change along the depth of the drying product. Consequently, moisture and heat transport equations (6.27) and (6.28) become non-linear and must be solved numerically using appropriate boundary conditions. Effects of different modes of heat input such as conduction, radiation and microwave on the improvement of drying rate can be investigated by incorporating corresponding boundary conditions. Islam *et al.* (2003a) have solved the coupled energy and moisture transport equations simultaneously under different modes of heat input using the fourth-order Runge–Kutta scheme. Saravacos and Maroulis (2001), Sablani *et al.* (2000) and Rahman (1995) have presented empirical correlations for the variation thermophysical and transport properties with moisture content and temperature for a large number of drying products.

To obtain an analytical solution to the moisture and energy transport equations with reasonable accuracy, the thermophysical and transport properties of the drying product can be assumed to be a constant (since the temperature variation is small when drying heat-sensitive materials) that reduces equations (6.27) and (6.28) to:

$$\frac{\partial m_{v,p}}{\partial t} = D_{m,p} \frac{\partial^2 m_{v,p}}{\partial y^2} \quad (6.29)$$

$$\frac{\partial T_p}{\partial t} = \alpha_p \frac{\partial^2 T_p}{\partial y^2} \quad (6.30)$$

where $\alpha_p = k_p / \rho_p c_p$ thermal diffusivity.

The solutions of the moisture and energy transport equations (6.29) and (6.30) are similar. Schneider (1955) has provided an analytical solution to the energy transport equation of one-dimensional form for an infinite flat plate, long cylinder and sphere.

For the initial and boundary conditions of:

$$\text{At } t = 0, T_p = T_{p,i}$$

$$\text{At } y = 0, dT_p/dy = 0$$

$$\text{At } y = \pm H, -k_p(dT_p/dy)|_{y=\pm H} = \bar{h}_c(T_{p,y=\pm H} - T_{air})$$

The analytical solution of the energy equation for an infinite flat plate is:

$$\frac{T_p(y) - T_{air}}{T_{p,i} - T_{air}} = \sum_{n=1}^{\infty} \frac{4 \sin \zeta_n}{2\zeta_n + \sin(2\zeta_n)} \exp\left(-\frac{\alpha \zeta_n^2 t}{H^2}\right) \cos\left(\frac{\zeta_n y}{H}\right) \quad (6.31)$$

The discrete values of ζ_n are positive roots of the transcendental equation $\zeta_n \tan(\zeta_n) = Bi = \bar{h}_c H / k_p$

For a long cylinder of radius R :

$$\frac{T_p(r) - T_{air}}{T_{p,i} - T_{air}} = \sum_{n=1}^{\infty} \frac{2}{\zeta_n} \frac{J_1(\zeta_n)}{J_0^2(\zeta_n) + J_1^2(\zeta_n)} \exp\left(-\frac{\alpha \zeta_n^2 t}{R^2}\right) J_0\left(\frac{\zeta_n r}{R}\right) \quad (6.32)$$

The discrete values of ζ_n are positive roots of the transcendental equation:

$$\zeta_n \frac{J_1(\zeta_n)}{J_0(\zeta_n)} = Bi = \frac{\bar{h}_c R}{k_p}.$$

J_1 and J_0 are Bessel functions of the first kind.

Similarly, for sphere of radius R :

$$\frac{T_p(r) - T_{air}}{T_{p,i} - T_{air}} = \sum_{n=1}^{\infty} \frac{4[\sin(\zeta_n) - \zeta_n \cos(\zeta_n)]}{2\zeta_n + \sin(2\zeta_n)} \exp\left(-\frac{\alpha \zeta_n^2 t}{R^2}\right) \frac{R}{\zeta_n r} \sin\left(\frac{\zeta_n r}{R}\right) \quad (6.33)$$

The discrete values of ζ_n are positive roots of the transcendental equation $1 - \zeta_n \cot(\zeta_n) = Bi = \bar{h}_c R / k_p$.

The roots of the transcendental equations for a flat plate, cylinder and sphere have been tabulated by Schneider (1955) among many others. It is worth noting that the above solutions change with a change of initial and boundary conditions. The variation of average moisture content of the drying products with drying time is determined by integrating the solution of moisture transport equation across the thickness of the product. The final form of the solutions for some simple geometries are summarized in Table 6.1.

Here X^* is the equilibrium moisture content which corresponds to the drying conditions. For relatively large drying times, the average moisture content of the product can be determined with only small error by considering only the first term of the equations presented in Table 6.1.

Illustrative example: Consider a potato slice of length, width and thickness of 30 mm, 30 mm and 5 mm, respectively, which is being dried using a conventional convection drier. An electric heater is installed in the drier to heat up the ambient air temperature of 30°C and relative

Table 6.1 Solution of moisture transport equation for some simple geometries.

Geometry	Initial and boundary conditions	Dimensionless average free moisture content
Long flat plate of thickness $2H$	At $t = 0$; $-H < y < H$; $X = X_i$; At $t > 0$; $y = \pm H$; $X = X^*$	$\frac{X - X^*}{X_i - X^*} = \frac{8}{\pi^2} \sum_{n=1}^{\infty} \frac{1}{(2n-1)^2} \exp \left[-(2n-1)^2 \frac{\pi^2}{4H} \left(\frac{D_{m,p}t}{H} \right) \right]$
Long cylinder of radius R	At $t = 0$; $0 < r < R$; $X = X_i$; At $t > 0$; $r = R$; $X = X^*$	$\frac{X - X^*}{X_i - X^*} = 4 \sum_{n=1}^{\infty} \frac{1}{R^2 \alpha_n^2} \exp(-D_{m,p} \alpha_n^2 t)$ where α_n are positive roots of the equation $J_0(R\alpha_n) = 0$
Sphere of radius R	At $t = 0$; $0 < r < R$; $X = X_i$; At $t > 0$; $r = R$; $X = X^*$	$\frac{X - X^*}{X_i - X^*} = \frac{6}{\pi^2} \sum_{n=1}^{\infty} \frac{1}{n^2} \exp \left[-\frac{n^2 \pi^2}{R} \left(\frac{D_{m,p}t}{R} \right) \right]$

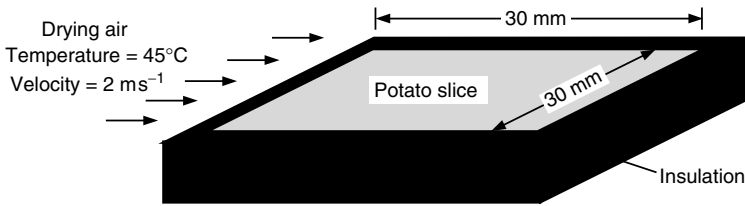


Fig. 6.6 Schematic sketch of a potato slice subjected to convective drying.

humidity 85% to 45°C before entering to the drying chamber. The air flows parallel to the drying surface of the slice at a velocity of 2.0 ms⁻¹. The sides and bottom of the slice are insulated as shown in Figure 6.6 and thus the heat and mass transfer processes can be considered as one-dimensional.

1. The exposed surface of the slice contains surface water during the initial period of drying. Determine the evaporation rate of surface water. Assume the average convective heat transfer coefficient can be calculated using the following correlation:

$$Nu = 0.664Re^{1/2}Pr^{1/3}$$

2. If the slice is placed in the drying chamber of a heat pump drier that supplies drying air at 45°C and a relative humidity of 10%, estimate the evaporation rate for surface water?
3. The water activity of potato is expressed using the following equation:

$$a_w = 1232.3X^4 - 646.14X^3 + 98.541X^2 - 0.3406X - 0.0008 \quad \text{for } X < 0.22$$

where X = moisture content, kg of moisture per kg db. Calculate the equilibrium moisture content of the potato slice for cases 1 and 2.

4. Calculate the time required to reduce the average moisture content of the potato slice from an initial moisture content of 4.5–2.5 kg water per kg db and from 2.5 to 0.5 kg water per kg db using a heat pump drier. Assume the diffusivity of liquid moisture in the potato slice is fixed and equal to $5.7 \times 10^{-10} \text{ m}^2 \text{ s}^{-1}$.
5. At a particular instant of drying, the moisture content of the bottom and exposed drying surfaces of the product are 3.5 and 0.2 kg water per kg db and the corresponding water activities are 0.97 and 0.42, respectively. The product is at a uniform temperature of 35°C. Calculate the moisture evaporation rate. Determine the rate of change of temperature of the product. If the product is suddenly flipped, calculate the new evaporation rate. What will the rate of change of temperature be after flipping? Assume:

$$\text{Density of potato slice} = 1100 \text{ kg m}^{-3}$$

$$\text{Specific heat of potato slice} = 3515 \text{ J kg}^{-1} \text{ K}$$

$$\text{Diffusivity of water vapor in air} = 2.6 \times 10^{-5} \text{ m}^2 \text{ s}^{-1}$$

$$\text{Molecular weight of water vapor} = 18 \text{ kg kmol}^{-1}$$

$$\text{Molecular weight of air} = 29 \text{ kg kmol}^{-1}$$

Solution:

Part 1:

$$\text{Length of potato slice along air flow } L = 30 \text{ mm} = 0.03 \text{ m}$$

$$\text{Velocity of drying air } U_\infty = 2.0 \text{ m s}^{-1}$$

$$\text{Temperature of ambient air } T_{amb} = 30^\circ\text{C} = 303.15 \text{ K}$$

$$\text{Relative humidity of ambient air } \phi_{amb} = 85\% = 0.85$$

$$\text{Temperature of drying air } T_{drying} = 45^\circ\text{C} = 318.15 \text{ K}$$

From the psychrometric chart:

$$\text{For } T_{amb} = 30^\circ\text{C} \text{ and } \phi_{amb} = 85\% \Rightarrow \text{Humidity ratio } \omega \approx 0.023 \text{ kg water per kg dry air}$$

During heating the drying air from 30°C to 45°C, humidity ratio in the air stream remains constant. Using the psychrometric chart: for $T_{drying} = 45^\circ\text{C}$ and humidity ratio $\omega = 0.023 \text{ kg water per kg dry air}$

$$\Rightarrow \text{wet-bulb temperature } T_{wb} \approx 31^\circ\text{C}, \text{ and relative humidity } \phi_{drying} \approx 37.5\%.$$

Surface water behaves like pure water and evaporates at a constant rate at the wet-bulb temperature.

Energy balance at the evaporating surface of the surface water (see Figure 6.7) gives:

$$\dot{m}h_f \text{ at } T_u + q_{cond}A + q_{conv}A = \dot{m}h_g \text{ at } T_s$$

Here, $T_s = T_u = T_{wb}$.

As entire surface water is at T_{wb} , temperature gradient and resulting q_{cond} at u-surface will be zero.

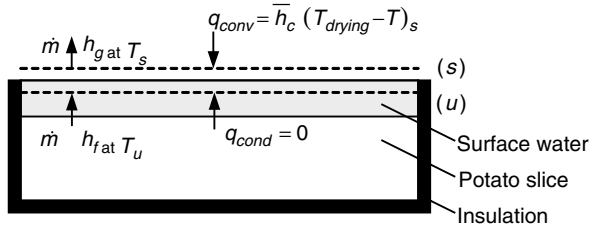


Fig. 6.7 Energy balance at the evaporating surface.

Therefore, $J_v(h_{fg} \text{ at } T_{wb}) = \bar{h}_c(T_{drying} - T_{wb})$ (Heat of wetting for surface water is zero.)

Physical properties of air at average temperature of air stream:

$$T = (T_{drying} + T_{wb})/2 = (45 + 31)/2 = 38^\circ\text{C are :}$$

$$\text{Density of air } \rho_{air} = 1.1358 \text{ kg m}^{-3}$$

$$\text{Viscosity of air } \mu_{air} = 1.898 \times 10^{-5} \text{ kg m}^{-1} \text{ s}$$

$$\text{Thermal conductivity of air } k_{air} = 0.0271 \text{ W m}^{-1} \text{ K}$$

$$\text{Prandtl number of air } Pr = 0.705$$

Therefore, the Reynolds number $Re = \rho_{air} U_\infty L / \mu_{air} = 3590.5$

$$Nu = 0.664 Re^{1/2} Pr^{1/3}$$

or

$$\frac{\bar{h}_c L}{k_{air}} = 0.664 (3590.5)^{1/2} (0.705)^{1/3}$$

Substituting the values of the variables gives $\bar{h}_c = 31.98 \text{ W m}^{-2} \text{ K}$

From the steam table, latent heat of vaporization at T_{wb} is $h_{fg} \text{ at } T_{wb} = 2428.12 \times 10^3 \text{ J kg}^{-1}$

Therefore, $J_v(h_{fg} \text{ at } T_{wb}) = \bar{h}_c(T_{drying} - T_{wb})$

or

$$J_v(2428.12 \times 10^3) = 31.98(45-31)$$

Therefore, evaporation rate of surface water $J_v = 0.000184 \text{ kg m}^{-2} \text{ s} = 0.66 \text{ kg m}^{-2} \text{ h}$.

Note: Relative humidity of drying air can also be determined from the known temperature and relative humidity of ambient air using the following empirical correlations:

Saturation vapor pressure at T_{amb} is:

$$P_{v, sat} \text{ at } T_{amb} = 100e^{[27.0214 - (6887/T_{amb})]} - 5.31 \ln\left(\frac{T_{amb}}{273.16}\right) = 4252.66 \text{ Pa}$$

$$\text{Humidity ratio } \omega = \frac{0.622 \phi_{amb} P_{v, sat} \text{ at } T_{amb}}{101000 - \phi_{amb} P_{v, sat} \text{ at } T_{amb}} = 0.02309 \text{ kg water per kg dry air}$$

Saturation vapor pressure at T_{drying} is:

$$P_{v, sat \text{ at } T_{drying}} = 100e^{[27.0214 - (6887/T_{drying})]} - 5.31 \ln \left(\frac{T_{drying}}{273.16} \right) = 9604.22 \text{ Pa}$$

$$\text{Relative humidity of drying air } \phi_{drying} = \frac{101\,000\omega}{(0.622 + \omega)P_{v, sat \text{ at } T_{drying}}} = 0.3764 = 37.64\%$$

which is close to the value (37.5%) obtained using the psychrometric chart. These empirical correlations are especially useful for numerical simulation.

Part 2:

From the psychrometric chart: for $T_{drying} = 45^\circ\text{C}$ and $\phi_{drying} = 10\%$

\Rightarrow Wet-bulb temperature $T_{wb} \approx 21.2^\circ\text{C}$ and

humidity ratio $\omega = 0.006$ kg water per kg dry air.

Physical properties of air at $T = (T_{drying} + T_{wb})/2 = (45 + 21.2)/2 = 33.1^\circ\text{C}$ are:

$$\text{Density of air } \rho_{air} = 1.1539 \text{ kg m}^{-3}$$

$$\text{Viscosity of air } \mu_{air} = 1.875 \times 10^{-5} \text{ kg m}^{-1} \text{ s}$$

$$\text{Thermal conductivity of air } k_{air} = 0.0267 \text{ W m}^{-1} \text{ K}$$

$$\text{Prandtl number } Pr = 0.706$$

Therefore, the Reynolds number $Re = \rho_{air}U_{\infty}L/\mu_{air} = 3692.5$

$$\text{Now, } Nu = 0.664Re^{1/2}Pr^{1/3}$$

or

$$\frac{\bar{h}_c L}{k_{air}} = 0.664(3692.5)^{1/2}(0.706)^{1/3}$$

Substituting the values of the variables gives $\bar{h}_c = 31.9756 \text{ W m}^{-2} \text{ K}$

From the steam table, latent heat of vaporization at T_{wb} is $h_{fg \text{ at } T_{wb}} = 2451.26 \times 10^3 \text{ J kg}^{-1}$

Therefore, $J_v(h_{fg \text{ at } T_{wb}}) = \bar{h}_c(T_{drying} - T_{wb})$

or

$$J_v(2451.26 \times 10^3) = 31.9756(45 - 21.2)$$

Therefore, evaporation rate of surface water $J_v = 0.00031 \text{ kg m}^{-2} \text{ s} = 1.1177 \text{ kg m}^{-2} \text{ h}$ which is $(1.1177/0.66) \approx 1.7$ times higher than that of convection drier.

Part 3:

Water activity is defined as the ratio of the partial vapor pressure at the drying surface (s-surface) to the saturation vapor pressure at the drying surface temperature.

Therefore, water activity $a_w = P_{v,s-surface}/P_{v, sat \text{ at } T_s}$

The drying product will reach equilibrium, when (i) the temperature of product is equal to the drying air temperature resulting in zero heat transfer and (ii) the partial vapor pressure at s-surface is equal to the vapor pressure of the drying air resulting in zero mass transfer of water vapor.

Therefore, at equilibrium:

$$a_w = \frac{P_{v,s-surface}}{P_{v,sat \text{ at } T_s}} = \frac{P_{v,drying \text{ air}}}{P_{v,sat \text{ at } T_{drying}}} = \frac{\phi_{drying} P_{v,sat \text{ at } T_{drying}}}{P_{v,sat \text{ at } T_{drying}}} = \phi_{drying}$$

For case 1: At equilibrium: $\phi_{drying} = 37.5\% = 0.375 = a_w$

A 'trial and error' method is needed to determine the equilibrium moisture content.

Putting $X = 0.0897$ kg water per kg db in the expression of water activity gives:

$$\begin{aligned} a_w &= 1232.3(0.0897)^4 - 646.14(0.0897)^3 + 98.541(0.0897)^2 - 0.3406(0.0897) - 0.0008 \\ &= 0.374955 \approx 0.375 \end{aligned}$$

Therefore, equilibrium moisture content for convection drying $X^* = 0.0897$ kg water per kg db.

For case 2: At equilibrium: $\phi_{drying} = 10\% = 0.1 = a_w$

Putting $X = 0.039$ kg water per kg db in the expression of water activity gives

$$\begin{aligned} a_w &= 1232.3(0.039)^4 - 646.14(0.039)^3 + 98.541(0.039)^2 - 0.3406(0.039) - 0.0008 \\ &= 0.10032 \approx 0.1 \end{aligned}$$

Therefore, equilibrium moisture content for heat pump drying $X^* = 0.039$ kg water per kg db.

Note: The final moisture content of the product is lower in heat pump drying.

Part 4:

Equilibrium moisture content for heat pump drying $X^* = 0.039$ kg water per kg db

Liquid moisture diffusivity in potato $D_{ab} = 5.7 \times 10^{-10} \text{ m}^2 \text{ s}^{-1}$.

Thickness of potato slice $H = 5 \text{ mm} = 0.005 \text{ m}$

Drying from initial moisture content of 4.5–2.5 kg water per kg db

Initial free moisture content $X_{initial} = 4.5 - 0.039 = 4.461$ kg water per kg db

Final free moisture content $X_{final} = 2.5 - 0.039 = 2.461$ kg water per kg db

Keeping only the first term of the infinite series of analytical solutions of the one-dimensional diffusion equation in Cartesian coordinates:

$$\frac{X_{final}}{X_{initial}} = \frac{8}{\pi^2} e^{-tD_{m,p}(\pi/2H)^2}$$

or

$$t = -\frac{4H^2}{D_{m,p}\pi^2} \ln \frac{\pi^2 X_{final}}{8X_{initial}} = 6839.8 \text{ s} = 1.89 \text{ h}$$

Again for drying from initial moisture content of 4.5–0.5 kg water per kg db
 Initial free moisture content $X_{initial} = 4.5 - 0.039 = 4.461$ kg water per kg db
 Final free moisture content $X_{final} = 0.5 - 0.039 = 0.461$ kg water per kg db

Therefore,

$$t = -\frac{4H^2}{D_{m,p}\pi^2} \ln \frac{\pi^2 X_{final}}{8X_{initial}} = 36612.8 \text{ s} = 10.17 \text{ h}$$

Therefore, the estimated time required to reduce the moisture content from 2.5 to 0.5 kg water kg^{-1} db

$$= 10.17 - 1.89 = 8.28 \text{ h.}$$

Note: To reduce the same quantity of moisture ($4.5 - 2.5 = 2.0$ kg water per kg db and $2.5 - 0.5 = 2.0$ kg water per kg db), the drying time is $8.28/1.89 = 4.38$ times longer for the final stage of drying. Liquid moisture diffusivity of the products decreases with the decrease of moisture content. Consequently, the drying rate slows down further in the final stage of drying.

Part 5:

Density of potato $\rho_p = 1100 \text{ kg m}^{-3}$

Specific heat of potato $c_p = 3515 \text{ J kg}^{-1} \text{ K}$

Diffusivity of water vapor in air $D_{v,air} = 2.6 \times 10^{-5} \text{ m}^2 \text{ s}^{-1}$

Molecular weight of water vapor $M_v = 18 \text{ kg kmol}^{-1}$

Molecular weight of air $M_{air} = 29 \text{ kg kmol}^{-1}$

Area of exposed drying $A = (30/1000)^2 = 0.0009 \text{ m}^2$

Evaporation rate of moisture from drying surface:

$$\dot{m} = Ak_m(m_{v,s} - m_{v,air})$$

Correlation for convective heat transfer coefficient:

$$Nu = 0.664Re^{1/2}Pr^{1/3}$$

From heat and mass transfer analogy:

$$Nu_m = 0.664Re^{1/2}Sc^{1/3}$$

Physical properties of air at the average temperature of air stream

$$T = (T_{\text{drying}} + T_{\text{product}})/2 = (45 + 35)/2 = 40^\circ\text{C are:}$$

$$\text{Density of air } \rho_{\text{air}} = 1.1284 \text{ kg m}^{-3}$$

$$\text{Viscosity of air } \mu_{\text{air}} = 1.907 \times 10^{-5} \text{ kg m}^{-1} \text{ s}$$

$$\text{Thermal conductivity of air } k_{\text{air}} = 0.0273 \text{ W m}^{-1} \text{ K}$$

$$\text{Prandtl number } Pr = 0.707$$

Therefore, the Reynolds number $Re = \rho_{\text{air}}U_{\infty}L/\mu_{\text{air}} = 3550.3$

$$Nu = 0.664Re^{1/2}Pr^{1/3}$$

or

$$\frac{\bar{h}_c L}{k_{\text{air}}} = 0.664(3550.3)^{1/2}(0.707)^{1/3}$$

Substituting values of the variables gives: $\bar{h}_c = 32.07 \text{ W m}^{-2} \text{ K}$

$$\text{And } Nu_m = 0.664Re^{1/2}Sc^{1/3}$$

$$\frac{k_m L}{\rho_{\text{air}}D_{v,\text{air}}} = 0.664Re^{1/2} \left(\frac{\mu}{\rho_{\text{air}}D_{v,\text{air}}} \right)^{1/3}$$

Substituting values of the variables gives: mass transfer coefficient $k_m = 0.0335 \text{ kg m}^{-2} \text{ s}$

Now water activity at the drying surface $a_w = 0.42$

Atmospheric pressure $P_{\text{total}} = 101330 \text{ Pa}$

From the steam table, saturation vapor pressure at surface temperature of 35°C is

$$P_{v \text{ sat at } T_s} = 5628 \text{ Pa}$$

Mass fraction of vapor at the drying surface:

$$m_{v,s} = \frac{M_v a_w P_{v \text{ sat at } T_s}}{M_v a_w P_{v \text{ sat at } T_s} + M_{\text{air}}(P_{\text{total}} - a_w P_{v \text{ sat at } T_s})}$$

Substituting values of the variables gives $m_{v,s} = 0.0146083$

Relative humidity of drying air $\phi = 10\% = 0.1$

From the steam table, saturation vapor pressure at drying air temperature of 45°C is:

$$P_{v \text{ sat at } T_{\text{air}}} = 9593 \text{ Pa}$$

Mass fraction of vapor in the free stream of drying air is:

$$m_{v,\text{air}} = \frac{M_v \phi P_{v \text{ sat at } T_{\text{air}}}}{M_v \phi P_{v \text{ sat at } T_{\text{air}}} + M_{\text{air}}(P_{\text{total}} - \phi P_{v \text{ sat at } T_{\text{air}}})}$$

Substituting values of the variables gives $m_{v,\text{air}} = 0.0058973$

Therefore, evaporation rate of moisture from drying surface:

$$\begin{aligned} \dot{m} &= Ak_m(m_{v,s} - m_{v,\text{air}}) = 0.0009 \times 0.0335(0.0146083 - 0.0058973) \\ &= 2.626 \times 10^{-7} \text{ kg s}^{-1} \end{aligned}$$

From the steam table, latent heat of vaporization at drying surface temperature of 35°C is:

$$h_{fg} = 2418600 \text{ J kg}^{-1}$$

Heat transfer rate from drying surface to the air due to evaporation:

$$Q_{eva} = \dot{m}h_{fg} = 2.626 \times 10^{-7} \times 2418600 = 0.635 \text{ W}$$

Convection heat transfer rate from drying air to drying surface:

$$Q_{conv} = A\bar{h}_c(T_{drying} - T_s) = 0.0009 \times 32.07(45 - 35) = 0.28863 \text{ W}$$

Energy conservation for the product gives:

$$\begin{aligned} V_p \rho_p c_p dT_p &= Q_{conv} dt - Q_{eva} dt \\ \frac{dT_p}{dt} &= \frac{Q_{conv} - Q_{eva}}{V_p \rho_p c_p} \\ &= \frac{0.28863 - 0.635}{(5 \times 30 \times 30 \times 10^{-9})1100 \times 3515} = -0.0199^\circ\text{C s}^{-1} = -1.19^\circ\text{C min}^{-1} \end{aligned}$$

where V_p = volume of the drying product.

Negative sign above indicates that the temperature of the product is decreasing.

If the product is flipped, water activity at the exposed surface becomes $a_w = 0.97$

Mass fraction of vapor at the drying surface:

$$m_{v,s} = \frac{M_v a_w P_{v \text{ sat at } T_s}}{M_v a_w P_{v \text{ sat at } T_s} + M_{air}(P_{total} - a_w P_{v \text{ sat at } T_s})}$$

Substituting values of the variables gives $m_{v,s} = 0.0341373$

Mass fraction of vapor in the drying air remains unchanged to $m_{v,air} = 0.0058973$

Therefore, evaporation rate of moisture will be:

$$\begin{aligned} \dot{m} &= Ak_m(m_{v,s} - m_{v,air}) = 0.0009 \times 0.0335(0.0341373 - 0.0058973) \\ &= 8.51436 \times 10^{-7} \text{ kg s}^{-1} \end{aligned}$$

Heat transfer rate from drying surface to air by evaporation:

$$Q_{eva} = \dot{m}h_{fg} = 8.51436 \times 10^{-7} \times 2418600 = 2.0593 \text{ W}$$

Convection heat transfer rate from air to drying surface remains unchanged to $Q_{conv} = 0.28863 \text{ W}$

Therefore, rate of change of product temperature:

$$\begin{aligned} \frac{dT_p}{dt} &= \frac{Q_{conv} - Q_{eva}}{V_p \rho_p c_p} = \frac{0.28863 - 2.0593}{(5 \times 30 \times 30 \times 10^{-9})1100 \times 3515} \\ &= -0.1018^\circ\text{C s}^{-1} = -6.1^\circ\text{C min}^{-1} \end{aligned}$$

Note:

- (i) As the bottom surface of the product contains higher moisture, the evaporation rate is increased $(8.51436 \times 10^{-7}) / (2.626 \times 10^{-7}) \approx 3.25$ times due to simple flipping of the product.
- (ii) Product temperature drops more rapidly after flipping due to the higher evaporation rate of moisture. To maintain the higher evaporation rate after flipping or during the initial period of drying when the products contain more moisture, other modes of heat input such as radiation or microwave could be included.

6.5 OPTIMUM USE OF HEAT PUMPS IN DRYING SYSTEMS

Numerous papers have been published on experimental studies and numerical simulation to optimize the use of heat pumps in drying systems. Mujumdar (1991) has identified and proposed for the first time the use of multiple modes of heat input, simultaneous and/or consecutive, as well as cyclical variations of drying conditions, as technologies of the future for batch as well as continuous heat pump drying processes. Islam *et al.* (2003a,b) among others solved simple liquid diffusion models under continuous and time varying conduction, convection, radiation and microwave modes of heat input, drying air velocity, temperature and relative humidity to match the drying conditions to the drying kinetics of the material and thereby optimize the heat pump drying processes. An on/off type temperature controller was simulated in the simulation program to predict control strategy for the power of the heaters and thereby maintain the product temperature always within the pre-specified range to avoid degradation of quality. Simulation results showed that heat pump driers can increase moisture evaporation rate of products significantly in comparison with the convection drier in the initial stage of drying when the moisture content of the products is high. In the initial stage of drying, moisture evaporation rate depends on the external driving potential of vapor transfer which is the difference of partial vapor pressure at the surface of the product and the drying air. Partial vapor pressure of the drying air decreases due to the dehumidification of drying air in heat pump driers. The vapor pressure at the drying surface is proportional to its moisture content and temperature. The higher initial moisture content of the products results in the higher vapor pressure at the drying surface and thus the higher moisture evaporation rate in the initial stage of drying. As the moisture content of the products decreases with drying time, the vapor pressure at the drying surface and resulting moisture evaporation rate also decreases.

At low moisture content of the product the internal moisture migration rate governed by local moisture diffusivity controls the drying process (internally controlled drying) and the effect of low relative humidity of the drying air becomes less significant. Therefore, the heat pump is not required to run for the entire period of drying. To reduce the initial as well as operating cost, the heat pump drier could be designed with multiple drying chambers. One heat pump will be used to supply dehumidified air sequentially for different predetermined times in different drying chambers. Based on the type of material to be dried in different chambers, the relative humidity and the duration of the supply of dehumidified air in different chambers could be adjusted. Hot air (without dehumidification) can be supplied to the drying chambers for the remaining period of drying. Figure 6.8 shows a possible arrangement using one heat pump in a drier with multiple drying chambers.

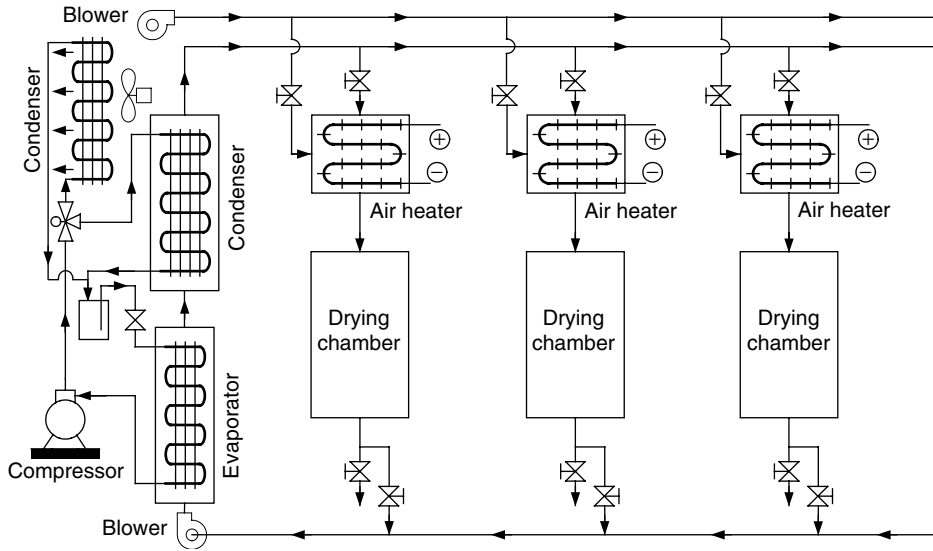


Fig. 6.8 Suggested arrangement for using only one heat pump to service a multiple chamber drier.

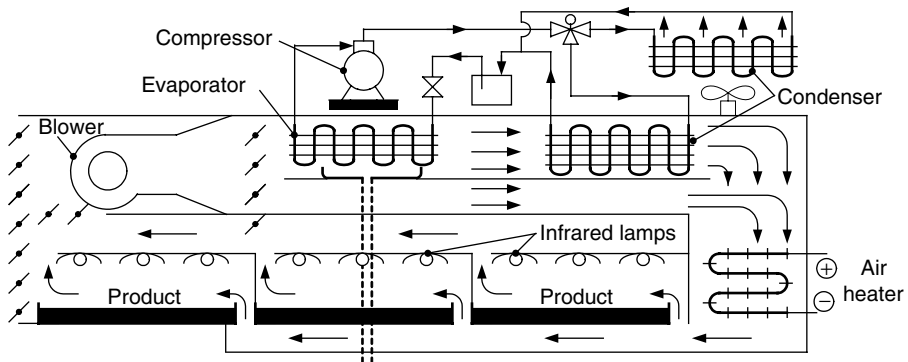


Fig. 6.9 Schematic diagram of infrared heat-assisted heat pump drier.

Simulation and experimental results show that radiation and microwave modes of heat input improve the evaporation rate of moisture remarkably in the initial stage of drying. Infrared heater and microwave magnetron can easily be installed in the heat pump drier as shown in Figures 6.9 and 6.10. Radiation heaters supply heat directly to the drying surface where heat is required for the evaporation of moisture. Microwave energy generates heat internally (volumetrically) in the products and maintains a high, as well as uniform, temperature throughout the product that increases the diffusivity of moisture inside the products. Generated internal heat develops increased vapor pressure within the product which can 'pump' the internal moisture to the surface of the product and prevent case hardening.

As the evaporation rate of moisture decreases with the decrease of product moisture content, input heat should also be decreased gradually to maintain the heat flux that matches the evaporation rate and prevents overheating of the products. A PID or on/off type controller

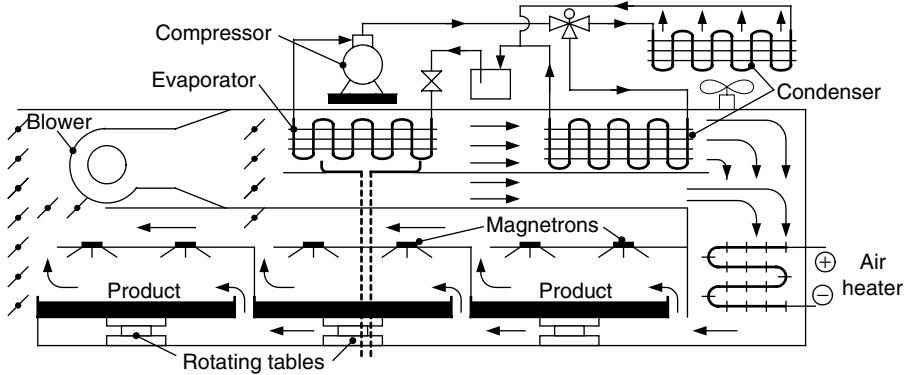


Fig. 6.10 Schematic of a microwave-assisted heat pump drier.

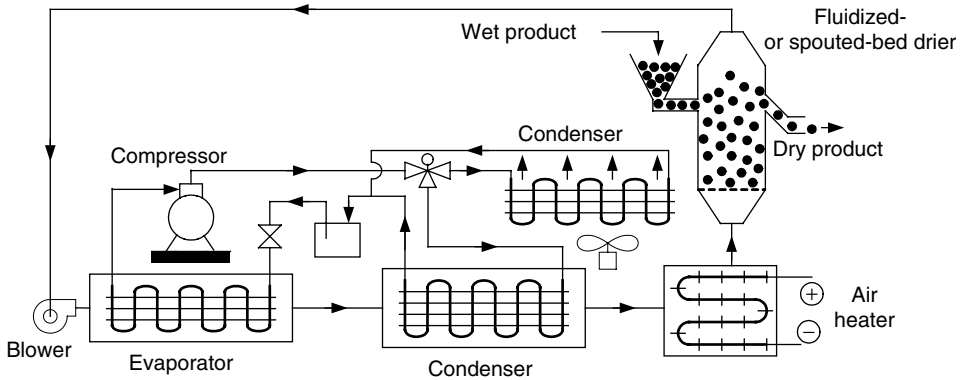


Fig. 6.11 Use of a heat pump in a fluidized- or spouted-bed drier system.

could be installed to measure product temperature and thereby control the input power of the heaters.

Any conventional drier (e.g. fluid bed, spouted bed, tunnel, rotary etc.) that uses convection as the primary mode of heat input can be fitted with a suitably designed heat pump. Figure 6.11 shows the use of a heat pump in the fluidized- or spouted-bed drier. The desired temperature of the drying air is obtained by adjusting the capacity of the condenser and auxiliary air heater. The power of the compressor is regulated using a frequency inverter to maintain the required humidity of the drying air. Due to the excellent gas-particle contact during fluidization of drying particles, fluidized-bed heat pump driers enable the drying rate to increase significantly.

6.6 INNOVATIVE HEAT PUMP DRYING SYSTEMS

The ordinary vapor-compression heat pump cycle operates in a two-pressure system and is adequate for most small-scale heat pump drying applications. The advantages of the ordinary heat pumps are that they are simple, inexpensive, reliable and almost maintenance-free.

However, the major concern for large drying industries is the efficiency, not simplicity. To optimize the drying process for different products, the simple vapor-compression heat pump cycle is often inadequate and needs to be modified.

Some drying applications require a moderately low temperature of evaporator coil to reduce the moisture content of drying air to the desired lower value. On the other hand, to achieve the desired temperature of the drying air at the inlet of the drying chamber, the temperature of condenser coil should be high enough for effective heat transfer from the condenser coil to the drying air. Consequently, the temperature and corresponding pressure differences involved between the evaporator and condenser become too large for a single stage vapor-compression cycle to be practical. As the slope of the isentropic lines on the $P-h$ diagram of refrigerants decreases away from the saturated vapor line, the power consumption of reciprocating compressors, that work closely to the isentropic process, increases remarkably with the increase of pressure difference between the evaporator and condenser. Moreover, the volumetric efficiency of the reciprocating compressor and hence the cooling and heating capacity of the heat pump decreases with the increasing of pressure difference between the evaporator and condenser.

Multi-stage or compound compression is an effective method of reducing the work of the compressor by working on isentropic lines closer to the saturation curve and thereby improving the overall performance of the heat pump. Multi-stage compression may also become essential due to the requirement of feeding of the refrigerant to multiple evaporators and condensers to optimize the drying processes at different stages of drying. One of the unique features of the heat pump drier is its ability to control the temperature and humidity of the drying air by controlling the flow of refrigerant at different components of the heat pump using advanced PID controllers and pneumatic valves. A few modifications and refinements of the heat pump used in the drying industries are illustrated in the following sections.

6.6.1 Multi-stage compression heat pump drying

Multi-stage compression of the refrigerant is an attractive solution to reduce the power consumption and increase COP for heat pump drying systems where low evaporator temperature and/or high condensing temperature are necessary. Schematic diagrams of a multi-stage compression heat pump drying system and $P-h$ diagram for the cycle are shown in Figures 6.12 and 6.13, respectively. The liquid refrigerant from the condenser first expands in a high pressure expansion valve (located between point-6 and 7 of Figure 6.12) to the flash chamber pressure, which is equal to the compressor interstate pressure. Part of the liquid refrigerant evaporates in the flash chamber. The remaining liquid refrigerant of relatively low temperature further expands in the low pressure expansion valve (located between point-8 and 9 of Figure 6.12) to the evaporator pressure and picks up heat by condensing moisture from the drying air at low temperature. Evaporated liquid from the evaporator is compressed by low-pressure compressor to the flash chamber pressure. Finally, high-pressure compressor compresses the refrigerant vapor from interstate to the condenser pressure where high pressure refrigerant vapor rejects heat to the drying air at high temperature and condenses. As the low and high pressure compressors work on isentropic lines (*state 1-2 and 4-5*) closer to the saturation line in comparison to the single stage compression (*state 1-2*) as shown in Figure 6.13, the work of the compressors decreases and thus COP of the cycle increases. The quantity of pick-up heat in the evaporator coils for multi-stage compression ($h_1 - h_9$) could be greater than that of single stage compression ($h_1 - h_7$). It is worth noting that because of the evaporation of refrigerant in the flash chamber, the refrigerant flow rate in the evaporator coils

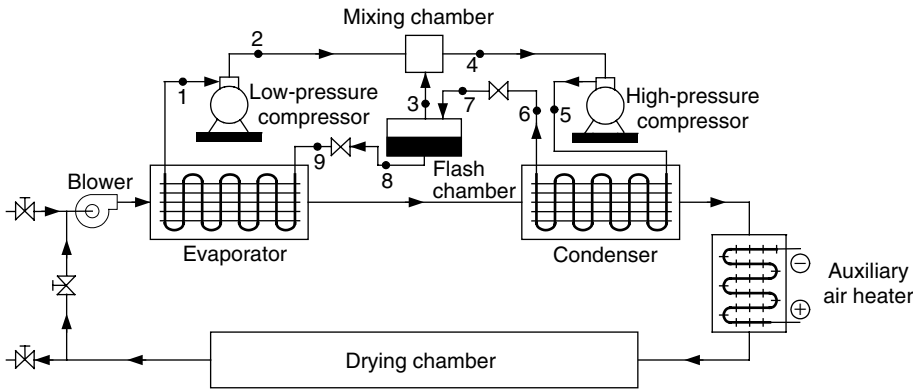


Fig. 6.12 Schematic diagram of a multi-stage compression heat pump drier.

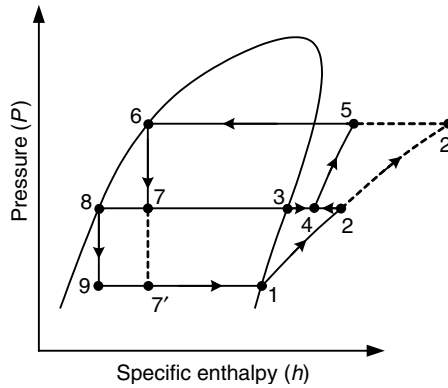


Fig. 6.13 P-h (pressure-specific enthalpy) diagram of the multi-stage compression heat pump cycle.

for multi-stage compression is less than single stage compression. To increase the quantity of pickup heat in the evaporator coils for multi-stage compression, the proper selection of refrigerant and designing of flash chamber pressure are crucial.

6.6.2 Cascade heat pump drying systems

In the multi-stage compression heat pump drying systems the same refrigerant is used in both high- and low-pressure cycles. Although better heat transfer characteristics can be achieved in the flash chamber by direct mixing of the refrigerant of high and low pressure cycles, the same refrigerant often cannot work efficiently over the wide pressure difference of the evaporator and condenser. In the cascade heat pump drying systems shown in Figure 6.14, different refrigerants can be used in the high- and low-pressure cycles. Therefore, refrigerants with more desirable characteristics can be used in each cycle. The saturation dome for each refrigerant would be different. The high and low pressure cycles are connected through a heat exchanger which serves as the evaporator for high-pressure cycle and the condenser for the low-pressure cycle. The temperature of the evaporator of high-pressure cycle should be somewhat lower than the condenser of low-pressure cycle for efficient transfer of heat. Mass

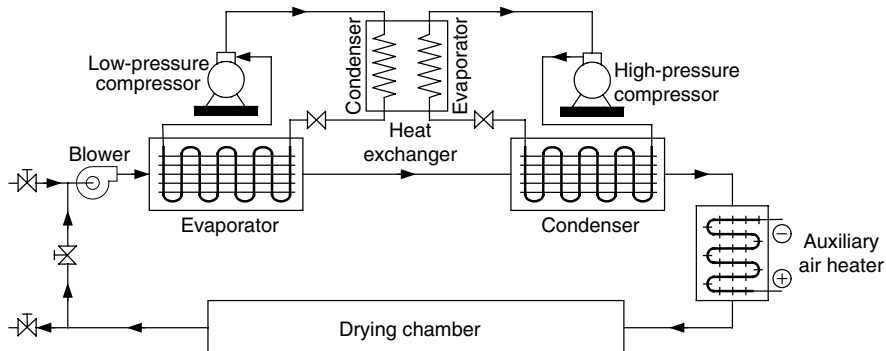


Fig. 6.14 Schematic diagram of a cascade heat pump drier.

flow rate of the refrigerants of the two cycles should be controlled to ensure the heat transfer from the refrigerant in the low-pressure cycle should be equal to the heat transfer to the refrigerant in the high-pressure cycle. Like multi-stage compression, the cascading improves COP for the heat pump drying systems and reduces compression work.

6.6.3 Heat pump drying systems with multiple evaporators in series and in parallel

During the falling rate period of drying, the evaporation rate depends on the internal potential for moisture migration from bulk to the exposed drying surface. The internal potential of moisture migration depends on the moisture diffusivity of the product, which usually decreases with the decrease of product moisture content. To optimize the drying processes, the external potential of mass transfer should be varied with the internal potential of moisture migration rate of the product. Therefore, the heat pump should be run in part load during the falling rate period and the percentage of the part load, that is, the refrigerant flow rate, should be decreased with the decrease of moisture content of the product. However, the COP of the heat pump decreases when operating in part load. Moreover, different temperatures of the evaporator and condenser coils could be required to maintain the desired relative humidity and temperature of the drying air at different stages of drying of different products. This can be accomplished by using different driers containing individual heat pumps of different capacities. Based on the moisture content of the product at different stages of drying, the product will be shifted to different driers that provide optimum conditions of drying air. However, using individual small compressors for different driers will probably be uneconomical and bulky. A small compressor may not be able to operate efficiently in the large pressure difference of the condenser and evaporator to achieve the required temperature of the condenser and evaporator coils. A more practical and economical approach is to route all the exit streams of refrigerant from different evaporators to a single large compressor. Compressed refrigerant at high pressure and temperature will flow in different sections of the entire drier based on the requirement. Flow rates of refrigerant in different condenser and evaporator coils are regulated using automatic control pneumatic valves. Separate expansion valves are installed in the flow circuits to maintain the required pressures of refrigerant in the evaporator coils. As a result, control of the optimum drying conditions for a wide range of products becomes possible and the driers become more versatile.

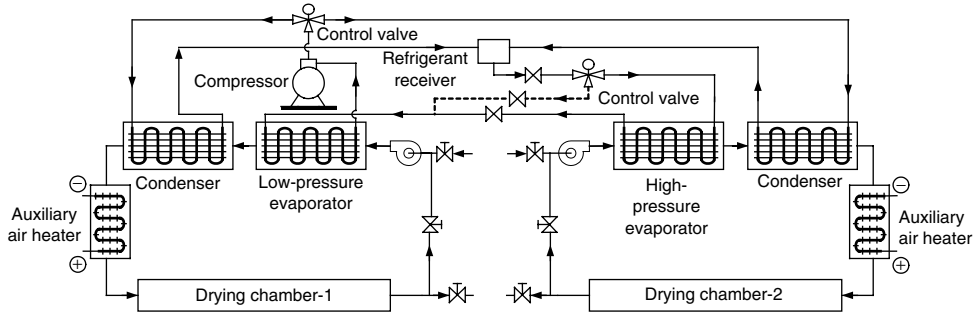


Fig. 6.15 Heat pump drying systems with multiple evaporators in series.

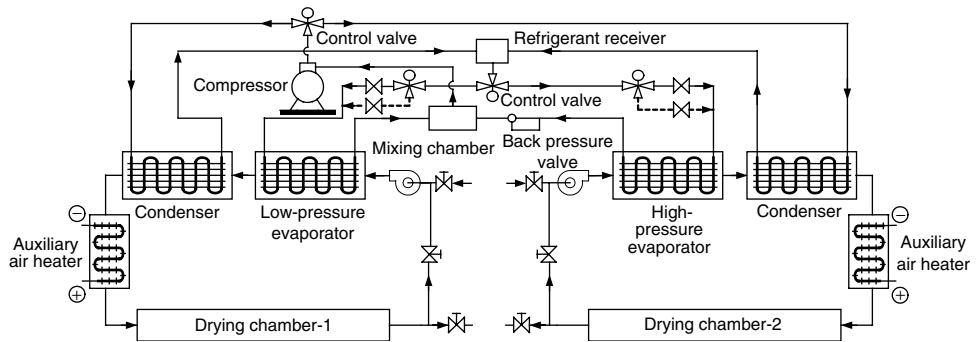


Fig. 6.16 Heat pump drying systems with multiple evaporators in parallel.

Figures 6.15 and 6.16 show two possible designs of heat pump driers where the evaporators are operated in series and parallel, respectively. When the evaporators are operated in series (Figure 6.15), the liquid refrigerant from refrigerant receiver is first expanded using high-pressure expansion valve to a relatively higher pressure for use in the high-pressure evaporator. The refrigerant is then further expanded using low-pressure expansion valve to use in the low-pressure evaporator. As the pressure and hence temperature of the evaporator coils are different, it is possible to maintain different relative humidities of the drying air at the entrance of the drying chambers 1 and 2. The products should be shifted to the appropriate drying chambers during the drying process to attain optimum drying conditions. Under normal operating conditions, the flow rate of refrigerant to the evaporators will be the same. However, the flow rates of refrigerant to the high- and low-pressure evaporators could be changed continuously using the control valve, and thereby changes the drying conditions of both the drying chambers, as the drying progresses. It is worth noting that as two different flow circuits of drying medium are used for drying chambers 1 and 2, two different drying media could conveniently be used for drying chambers 1 and 2. Moreover, each of the flow circuit could be operated as closed or open loop.

When the evaporators are operated in parallel as shown in Figure 6.16, the liquid refrigerant from the refrigerant receiver flows through the high- and low-pressure expansion valves and expands to the design preset pressures of high- and low-pressure evaporators. A back pressure valve is used at the exit of the high-pressure evaporator to equalize the vapor pressure to

the low-pressure evaporator before entering the compressor. Flow rate of refrigerant to the evaporators can be regulated using control valve to maintain optimum drying conditions of the drying chambers. The shifting cost of the drying product from one drying chamber to the other in order to attain optimum drying conditions can be avoided by changing refrigerant pressure of the evaporators. High- and low-pressure expansion valves could be installed in parallel with a control valve at the inlet of the evaporators as shown in Figure 6.16. Based on the desired drying conditions at different stages of the drying processes, the control valve will switch the flow of refrigerant through high- or low-pressure expansion valve and accordingly the evaporator will work as either high- or low-pressure evaporator. Such types of controlling can easily be done using commercially available PID controllers which are cheap as well as reliable.

6.6.4 Vapor absorption heat pump drier

In recent years, the refrigeration and air-conditioning industry has been experiencing major changes due to the decision by several countries to phase out chlorofluorocarbon (CFC) refrigerants that have been in use on a wide scale. CFC-refrigerants are known to cause 'global warming' and deplete the protective ozone layer of the atmosphere. Due to these detrimental effects of chlorofluorocarbon refrigerants, considerable efforts have been devoted to the development of alternative refrigerants that are considered less harmful to the environment. In this search for alternative refrigerants and refrigeration systems, vapor absorption refrigeration and heat pump systems have emerged as viable alternatives to vapor compression refrigeration machines. Vapor absorption systems use inexpensive thermal energy at a temperature of about 100°C as the main input energy form. This makes it possible to use energy forms such as natural gas, solar energy, geothermal energy, waste heat from cogeneration or process steam plants and others to operate vapor absorption systems.

Vapor compression and vapor absorption systems are shown schematically in Figure 6.17. Vapor absorption systems are very similar to vapor compression systems. A condenser, expansion valve and evaporator are common in both systems. The compressor of the vapor compression system, that uses electricity as the input energy, is replaced by absorber-generator unit consisting of an absorber, generator, solution pump and expansion valve. In order to accomplish the function of the compressor, the absorber-generator unit includes a secondary fluid called the absorbent. The ammonia-water, lithium bromide-water and lithium chloride-water solutions are widely used in the vapor absorption systems. For the ammonia-water system, water serves as the absorbent and ammonia as the refrigerant. However, water serves as refrigerant and lithium bromide and lithium chloride as absorbent for lithium bromide-water and lithium chloride-water systems respectively.

The refrigerant vapor from the evaporator is absorbed by the absorbent in the absorber unit, which operates at a low pressure close to that of the evaporator. As the absorption of refrigerant process evolves the heat of absorption, it is necessary to cool the absorber using an external cooling system. The solution, which is rich in refrigerant, is pumped using a solution pump from the absorber to the generator that operates at high pressure close to that of the condenser. In the vapor absorption system, liquid solution is pumped from a low-pressure absorber to a high-pressure generator instead of vapor for the vapor compression system. The steady-flow work is proportional to the specific volume, and thus the work input for the vapor absorption system is very small (on the order of about one percent of the heat supplied to the generator). The solution in the generator is heated with an external energy source to evolve the refrigerant out of the solution. The hot solution, which is weak in refrigerant,

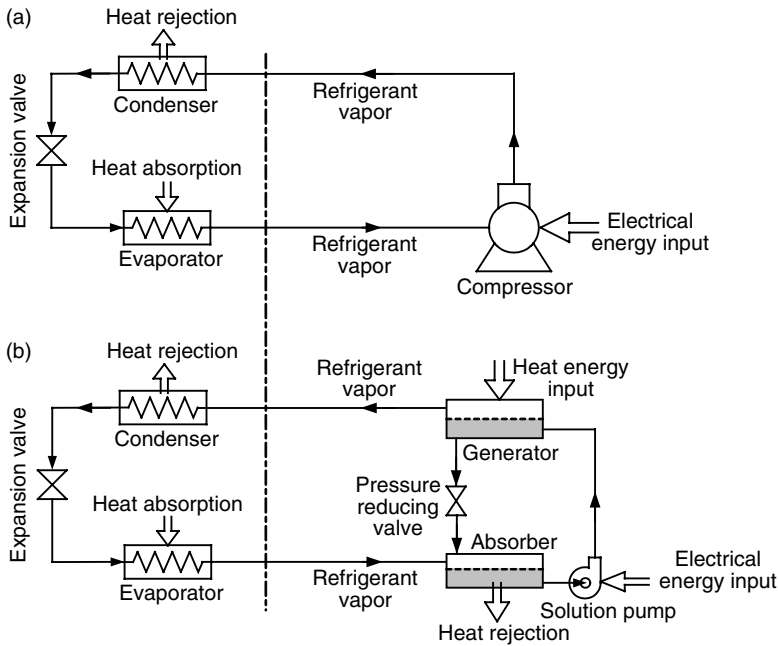


Fig. 6.17 Schematic diagrams of (a) vapor compression and (b) vapor absorption cycles.

then passes through a regenerator, where it transfers some heat to the rich solution leaving the solution pump, and is throttled to the absorber pressure. The refrigerant continues its passage through the rest of the cycle in a manner similar to that of a vapor compression system.

A schematic diagram of the vapor absorption heat pump drier is shown in Figure 6.18. It is possible to supply heat to the generator from multiple available sources. Absorption refrigeration and heat pump systems could be conveniently incorporated in total energy plants that produce both electricity and heat. For lithium bromide–water and lithium chloride–water systems, water serves as refrigerant and the minimum temperature of the refrigerant is above the freezing point of water, which is suitable for most heat pump drying applications. The minimum temperature of the refrigerant of ammonia–water system reaches below the freezing point of water. For effective heat transfer from the drying air to the evaporator coil, which is required for the condensation of moisture of the drying air, the temperature of the evaporator coil should be sufficiently lower than the dew-point temperature of the drying air. The refrigerant–absorbent pair should be selected based on the required conditions of the drying air.

The vapor-absorption heat pump systems are much more expensive than the vapor-compression heat pump systems. The vapor-absorption systems are more complex, occupy more space and the COP is low. However, vapor-absorption heat pump drying systems could be an attractive option for large-scale drying applications when the unit cost of thermal energy is low and is projected to remain low relative to electricity.

Illustrative example: A single-stage vapor-compression heat pump has been selected for a heat pump drier. The heat pump uses refrigerant-134a as the working fluid and operates between the evaporator and condenser pressures of 0.3 and 1.6 MPa, respectively. The mass

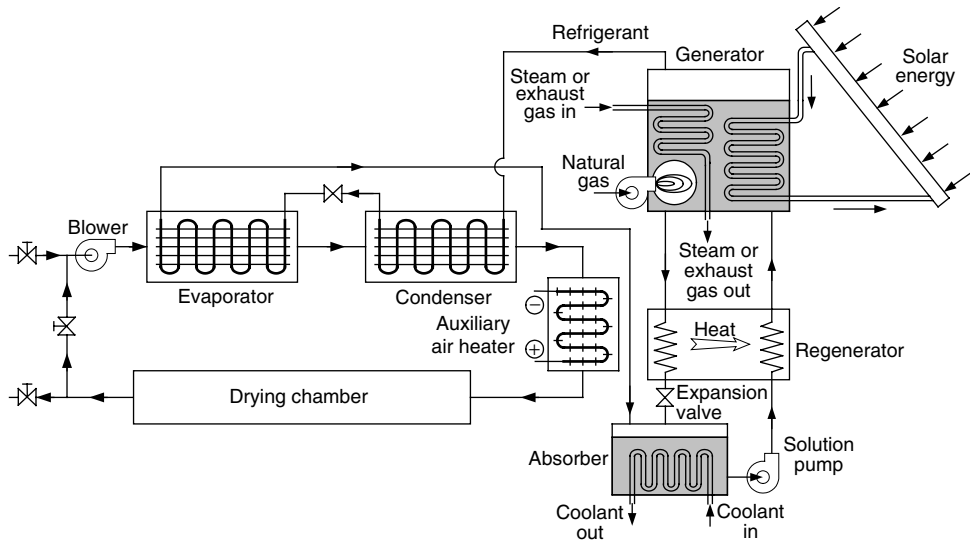


Fig. 6.18 Schematic diagram of a vapor absorption heat pump drier.

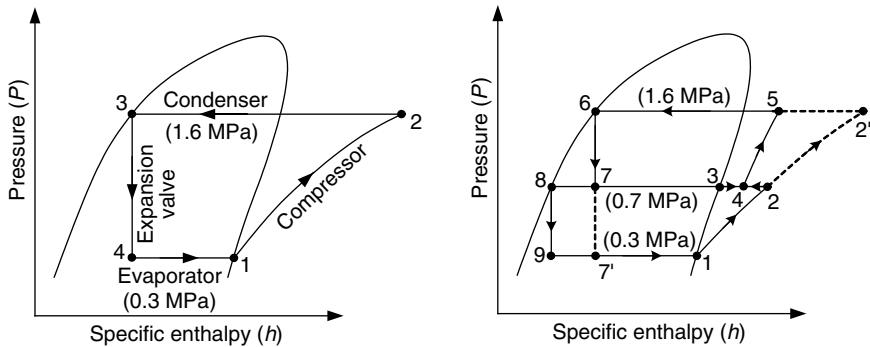


Fig. 6.19 The P - h diagrams of ideal (a) single and (b) two-stage vapor-compression heat pump cycles.

flow rate of the refrigerant is 0.1 kg s^{-1} . Calculate (a) the rate of heat absorption in the evaporator coil, (b) the rate of heat rejection from the condenser coil, and (c) the COP of the heat pump.

If the single-stage heat pump is replaced with a two-stage heat pump as shown in Figure 6.19 where the refrigerant leaves the condenser is throttled to the flush chamber operating at 0.7 MPa , calculate (a) the rate of heat absorption in the evaporator coil, (b) the rate of heat rejection from the condenser coil and (c) the COP of the two-stage heat pump. For both cases assume that the cycles can be treated as ideal and thus the compressors are isentropic; the refrigerant leaves the condensers as a saturated liquid and enters the compressors as a saturated vapor.

Solution:

Part 1: Single-stage vapor-compression heat pump cycle

From refrigerant-134a tables:

At pressure $P_1 = 0.3 \text{ MPa} \Rightarrow$ Enthalpy $h_1 = h_g \text{ at } 0.3 \text{ MPa} = 247.5984 \text{ kJ kg}^{-1}$

and entropy $s_1 = s_g \text{ at } 0.3 \text{ MPa} = 0.91866 \text{ kJ kg}^{-1} \text{ K}$

At pressure $P_2 = 1.6 \text{ MPa}$ and $s_1 = s_2$ (Isentropic) \Rightarrow Enthalpy $h_2 = 282.1808 \text{ kJ kg}^{-1}$

At pressure $P_2 = 1.6 \text{ MPa} \Rightarrow$ Enthalpy $h_3 = h_f \text{ at } 1.6 \text{ MPa} = 133.9826 \text{ kJ kg}^{-1}$

$h_3 = h_4$ (throttling) \Rightarrow Enthalpy $h_4 = 133.9826 \text{ kJ kg}^{-1}$

(a) Rate of heat absorption in the evaporator coil:

$$Q_{eva} = \dot{m}(h_1 - h_4) = 0.1(247.5984 - 133.9826) = 11.36 \text{ kW}$$

(b) Rate of heat rejection from the condenser coil:

$$Q_{con} = \dot{m}(h_2 - h_3) = 0.1(282.1808 - 133.9826) = 14.82 \text{ kW}$$

(c) Power input to the compressor:

$$W_{in} = \dot{m}(h_2 - h_1) = 0.1(282.1808 - 247.5984) = 3.458 \text{ kW}$$

Therefore, COP of the heat pump $\text{COP}_{hp} = Q_{con}/W_{in} = 14.82/3.458 = 4.28$.

Part 2: Two-stage vapor-compression heat pump cycle

At pressure $P_1 = 0.3 \text{ MPa} \Rightarrow$ Enthalpy $h_1 = h_g \text{ at } 0.3 \text{ MPa} = 247.5984 \text{ kJ kg}^{-1}$

and entropy $s_1 = s_g \text{ at } 0.3 \text{ MPa} = 0.91866 \text{ kJ kg}^{-1} \text{ K}$

At pressure $P_2 = 0.7 \text{ MPa}$ and $s_1 = s_2$ (Isentropic) \Rightarrow Enthalpy $h_2 = 265.0582 \text{ kJ kg}^{-1}$

At pressure $P_2 = 0.7 \text{ MPa} \Rightarrow$ Enthalpy $h_3 = h_g \text{ at } 0.7 \text{ MPa} = 261.8417 \text{ kJ kg}^{-1}$

and $h_8 = h_f \text{ at } 0.7 \text{ MPa} = 86.76428 \text{ kJ kg}^{-1}$

$h_8 = h_9$ (throttling) \Rightarrow Enthalpy $h_9 = 86.76428 \text{ kJ kg}^{-1}$

At pressure $P_3 = 1.6 \text{ MPa} \Rightarrow$ Enthalpy $h_6 = h_f \text{ at } 1.6 \text{ MPa} = 133.9826 \text{ kJ kg}^{-1}$

$h_6 = h_7$ (throttling) \Rightarrow Enthalpy $h_7 = 133.9826 \text{ kJ kg}^{-1}$

From steam table, latent heat of vaporization at $P_2 = 0.7 \text{ MPa} \Rightarrow$ Enthalpy $h_{fg} \text{ at } 0.7 \text{ MPa} = 175.08 \text{ kJ kg}^{-1}$.

The fraction of the refrigerant that evaporates as it is throttled to the pressure of flash chamber is:

$$x_7 = \frac{h_7 - h_8}{h_{fg} \text{ at } 0.7 \text{ MPa}} = \frac{133.9826 - 86.76428}{175.08} = 0.2697$$

Energy balance for the mixing chamber shown in Figure 6.12 gives:

$$\dot{m}_2 h_2 + \dot{m}_3 h_3 = \dot{m}_4 h_4$$

or

$$\dot{m}(1 - x_7)h_2 + \dot{m}x_7 h_3 = \dot{m}h_4$$

or

$$\begin{aligned} h_4 &= (1 - x_7)h_2 + x_7 h_3 = (1 - 0.2697)265.0582 + 0.2697 \times 261.8417 \\ &= 264.1907 \text{ kJ kg}^{-1} \end{aligned}$$

At pressure $P_2 = 0.7 \text{ MPa}$ and $h_4 = 264.1907 \text{ kJ kg}^{-1} \Rightarrow$ Entropy $s_4 = 0.91578 \text{ kJ kg}^{-1} \text{ K}$

At pressure $P_3 = 1.6 \text{ MPa}$ and $s_4 = s_5$ (isentropic) \Rightarrow Enthalpy $h_5 = 281.2051 \text{ kJ kg}^{-1}$

(a) Rate of heat absorption in the evaporator coil:

$$Q_{eva} = \dot{m}(1 - x_7)(h_1 - h_9) = 0.1(1 - 0.2697)(247.5984 - 86.76428) = 11.75 \text{ kW}$$

(b) Rate of heat rejection from the condenser coil:

$$Q_{con} = \dot{m}(h_5 - h_6) = 0.1(281.2051 - 133.9826) = 14.72 \text{ kW}$$

(c) Power input to the compressor

$$\begin{aligned} W_{in} &= \dot{m}(1 - x_7)(h_2 - h_1) + \dot{m}(h_5 - h_4) \\ &= 0.1(1 - 0.2697)(265.0582 - 247.5984) + 0.1(281.2051 - 264.1907) = 2.976 \text{ kW} \end{aligned}$$

Therefore, COP of the heat pump $\text{COP}_{hp} = Q_{con}/W_{in} = 14.72/2.976 = 4.95$.

Note:

- (i) The COP of the heat pump increases from 4.28 to 4.95 due to the use of two-stage vapor-compression heat pump cycle.
- (ii) It is possible to get 14.72 kW of heat energy in the condenser coil for an input of only 2.976 kW electrical energy in the compressor.

6.7 CLOSING REMARKS

The heat pump-assisted drier is an energy efficient option for the drying of heat-sensitive high-value products. The installation of a heat pump with different types of convection driers is discussed. A generalized classification of heat pump driers is presented. An introduction is given to the working principles of heat pump drying systems. Mechanisms of heat and moisture transfer processes involved in the drying operations are illustrated. For better understanding of different aspects of the drying processes and relative advantages of the heat

pump drying systems, two illustrative examples with detailed solutions are also presented. Some possible modifications and hybrid HPD technologies, such as use of one heat pump in multiple chambers drier, incorporation of radio frequency and infrared heaters in HPD are discussed. Possible integrations of advanced heat pump cycles in the driers are discussed in terms of their industrial potential. For further details the interested reader is referred to literature sources listed below.

6.8 NOTATION

Symbols

A	area, m^2
a_w	water activity
Bi	Biot number $\frac{\bar{h}_c H}{k_p}$
c_p	specific heat, $\text{J kg}^{-1} \text{K}$
$D_{m,p}$	diffusivity of moisture in product, $\text{m}^2 \text{s}^{-1}$
$D_{v,air}$	diffusivity of vapor in air, $\text{m}^2 \text{s}^{-1}$
H	half of product thickness, m
ΔH_w	heat of wetting, J kg^{-1}
h	enthalpy of refrigerant, J kg^{-1} ; enthalpy of moist air, J per kg dry air
\bar{h}_c	average convective heat transfer coefficient, $\text{W m}^{-2} \text{K}$
h_f	enthalpy of saturated water, J kg^{-1}
h_g	enthalpy of saturated vapor, J kg^{-1}
h_{fg}	latent heat of vaporization, J kg^{-1}
J_v	mass flux of water vapor, $\text{kg m}^{-2} \text{s}$
k	thermal conductivity, $\text{W m}^{-1} \text{K}$
k_m	mass transfer coefficient of vapor in air, $\text{kg m}^{-2} \text{s}$
L	length, m
M	molecular weight, kg kmol^{-1}
\dot{m}	moisture evaporation rate, kg s^{-1}
\dot{m}_{air}	total mass flow rate of dry air, $\text{kg of dry air s}^{-1}$
m_v	mass fraction of vapor, $\text{kg vapor per kg moist air}$; $\text{kg vapor per kg product}$
\dot{m}_{water}	water condensation rate, kg s^{-1}
Nu	heat transfer Nusselt number $\frac{\bar{h}_c L}{k}$
Nu_m	mass transfer Nusselt number $\frac{k_m L}{\rho_{air} D_{v,air}}$
P	pressure, Pa
Pr	Prandtl number, $\frac{\nu}{\alpha}$
\dot{Q}	heat flow rate, W
q_{cond}	conduction heat flux, W m^{-2}
q_{conv}	convection heat flux, W m^{-2}
R	radius, m
R_u	universal gas constant, $\text{J kmol}^{-1} \text{K}$
Re	Reynolds number $\frac{\rho U_{\infty} L}{\mu}$

Sc	Schmidt number $\frac{\nu_{air}}{D_{v,air}}$
T	temperature, °C
t	time, s
U_{∞}	velocity of drying air, $m\ s^{-1}$
X	moisture content, $kg\ kg^{-1}\ db$
y	axis along product thickness, m

Greek letters

α	thermal diffusivity, $m^2\ s^{-1}$
μ	dynamic viscosity, $kg\ m^{-1}\ s$
ν	kinematic viscosity, $m^2\ s^{-1}$
ρ	density, $kg\ m^{-3}$
ϕ	air relative humidity
ω	humidity ratio, kg moisture per kg dry air

Subscripts

air	drying air
d	through by-pass duct
e	through evaporator coil
i	initial
p	product
s	s-surface
sat	saturated
u	u-surface
v	vapor

REFERENCES

- Alves-Filho, O. (2002) Combined innovative heat pump drying technologies and new cold extrusion techniques for production of instant foods. *Drying Technology – An International Journal*, **20**(8), 1541–1557.
- Braun, J.E., Bansal, P.K. and Groll, E.A. (2002) Energy efficiency analysis of air cycle heat pump dryers. *International Journal of Refrigeration*, **25**, 954–965.
- Ceylan, I., Aktas, M. and Dogan, H. (2007) Energy and exergy analysis of timber dryer assisted heat pump. *Applied Thermal Engineering*, **27**, 216–222.
- Chen, G., Bannister, P., Carrington, C.G., Velde, P.T. and Burger, F.C. (2002) Design and application of a dehumidifier dryer for drying pine cones and pollen catkins. *Drying Technology – An International Journal, HPD special issue*, **20**(8), 1633–1643.
- Chua, K.J. and Chou, S.K. (2005) A modular approach to study the performance of a two-stage heat pump system for drying. *Applied Thermal Engineering*, **25**, 1363–1379.
- Chua, K.J., Mujumdar, A.S., Chou, S.K., Hawlader, M.N.A. and Ho, J.C. (2002) Heat pump drying of banana, guava and potato pieces: Effect of cyclic variations of air temperature on convective drying kinetics and color change. *Drying Technology – An International Journal*, **18**(5), 1583–1616.
- Chua, K.J., Mujumdar, A.S., Hawlader, M.N.A., Chou, S.K. and Ho, J.C. (2001) Study of stepwise change in drying air temperature during batch drying of agricultural products. *Food Research International*, **34**, 721–731.
- Fatouh, M., Metwally, M.N., Helali, A.B. and Shedid, M.H. (2006) Herbs drying using a heat pump dryer. *Energy Conversion and Management*, **47**, 2629–2643.

- Hawladar, M.N.A. and Jahangeer, K.A. (2006) Solar heat pump drying and aater heating in the tropics. *Solar Energy*, **80**, 492–499.
- Hawladar, M.N.A., Perera, C.O., Tian, M. and Yeo, K.L. (2006) Drying of guava and papaya: Impact of different drying methods. *Drying Technology – An International Journal*, **24**(1), 77–87.
- Islam, M.R., Ho, J.C. and Mujumdar, A.S. (2003a) Simulation of liquid diffusion-controlled drying of shrinking thin slabs subjected to multiple heat sources. *Drying Technology – An International Journal*, **21**(3), 413–438.
- Islam, M.R., Ho, J.C. and Mujumdar, A.S. (2003b) Convective drying with time-varying heat input: Simulation results. *Drying Technology – An International Journal*, **21**(7), 1359–1382.
- Jia, X., Clements, S. and Jolly, P. (1993) Study of heat pump assisted microwave drying. *Drying Technology – An International Journal*, **11**(7), 1583–1616.
- Keey, R.B. (1972) *Drying Principles and Practice*, 1st edn. Pergamon Press, Oxford, New York.
- Klöcker, K., Schmidt, E.L. and Steimle, F. (2002) A drying heat pump using carbon dioxide as working fluid. *Drying Technology – An International Journal, HPD special issue*, **20**(8), 1659–1671.
- Marshall, M.G. and Metaxas, A.C. (1998) Modeling the radio frequency electric field strength developed during the RF assisted heat pump drying of particulates. *International Microwave Power Institute*, **33**(3), 167–177.
- Mujumdar, A.S. (1991) Drying technologies of the future. *Drying Technology – An International Journal*, **9**(2), 325–347.
- Mujumdar, A.S., Nassikas, A.A. and Akritidis, C.B. (1992) Close-cycle heat pump dryer using superheated steam – an application to paper drying. *Drying '92, Part A*. Elsevier, Amsterdam, pp. 1085–1098.
- Namsanguan, Y., Tia, W., Devahastin, S. and Soponronnarit, S. (2004) Drying kinetics and quality of shrimp undergoing different two-stage drying processes. *Drying Technology – An International Journal*, **22**(4), 759–778.
- Ogura, H., Ishida, H., Hiroyuki Kage, H. and Mujumdar, A.S. (2003) Enhancement of energy efficiency of a chemical heat pump-assisted convective dryer. *Drying Technology – An International Journal*, **21**(2), 279–292.
- Queiroz, R., Gabas, A.L. and Telis, V.R.N. (2004) Drying kinetics of tomato by using electric resistance and heat pump dryers. *Drying Technology – An International Journal*, **22**(7), 1603–1620.
- Rahman, S. (1995) *Food Properties Handbook*. CRC Press, Inc., New York.
- Sablani, S., Rahman, S. and Al-Habsi, N. (2000) Moisture diffusivity in foods – an overview. In: *Drying Technology in Agriculture and Food Sciences* (ed. A.S. Mujumdar). Science Publishers, Inc., USA, pp. 35–59.
- Saensabai, P. and Prasertsan, S. (2003) Effects of component arrangement and ambient and drying conditions on the performance of heat pump dryers. *Drying Technology – An International Journal*, **21**(1), 103–127.
- Saravacos, G.D. and Maroulis, Z.B. (2001) *Transport Properties of Foods*. Marcel Dekker, Inc., New York.
- Sarkar, J., Bhattacharyya, S. and Gopal, M.R. (2006a). Transcritical CO₂ heat pump dryer: Part 1. Mathematical model and simulation. *Drying Technology – An International Journal*, **24**(12), 1583–1591.
- Sarkar, J., Bhattacharyya, S. and Gopal, M.R. (2006b) Transcritical CO₂ heat pump dryer: Part 2. Validation and simulation results. *Drying Technology – An International Journal*, **24**(12), 1593–1600.
- Schneider, P.J. (1955) *Conduction Heat Transfer*. Addison-Wesley, Reading, MA.
- Soylezmez, M.S. (2006) Optimum heat pump in drying systems with waste heat recovery. *Journal of Food Engineering*, **74**, 292–298
- Strommen, I., Eikevik, T.M. and Odilio A.-F. (1999) Optimum design and enhanced performance of heat pump dryers. In: *ADC'99, The First Asian-Australian Drying Conference* (eds K. Abdullah, A.H. Tamaunan and A.S. Mujumdar). Bali, Indonesia, pp. 68–80.
- Tan, M., Chua, K.J., Mujumdar A.S. and Chou S.K. (2001) Effect of osmotic pre-treatment and infrared radiation on drying rate and color changes during drying of potato and pineapple. *Drying Technology – An International Journal*, **19**(9), 2193–2207.
- Teeboonma, U., Tiansuwan, J. and Soponronnarit, S. (2003) Optimization of heat pump fruit dryers. *Journal of Food Engineering*, **59**, 369–377.

7 Freeze and vacuum drying of foods

Cristina Ratti

7.1 INTRODUCTION

Vacuum and freeze drying of biological materials are among the best methods of water removal to obtain final products of the highest quality. Both processes take place under different levels of vacuum and at lower temperatures than do other drying methods. The application of drying under vacuum to food products has been traditionally reduced to the production of heat- or oxygen-sensitive foodstuffs, or for those foods having a special end-use such as space shuttle goods, military or extreme-sport foodstuffs, and instant coffee. Recently, however, the market for 'natural' and 'organic' products has been increasingly strong along with the consumers' demand for foods with minimal processing and high quality. The market for higher quality food powders or ingredients is not only increasing in volume but also diversifying (Brown, 1999).

The high operating and maintenance costs are the main problem of drying processes under vacuum, particularly for freeze drying. The long drying times under continuous vacuum increase their energy consumption enormously and make the process considerably more expensive as compared to drying at atmospheric pressure. In addition, heat is not easily transferred under vacuum. These reasons have limited the industrial application of vacuum dehydration methods in the food industry.

In this chapter, the basis of vacuum and freeze drying will be analyzed, together with the heat and mass transfer phenomena occurring during these processes. Several transfer properties, which are fundamental in the design of the vacuum or freeze drying process, such as thermal conductivity, permeability and heat and mass transfer coefficients, as well as their functionality with water content, total pressure and temperature, will be described. The practical use of the glass-transition temperature concept to interpret food quality, particularly in relation to the freeze drying process, will be discussed. To conclude, the latest innovations in vacuum and freeze drying and their application to food materials will be analyzed in order to draw conclusions on the state-of-the-art and future of these processes.

7.2 STATES OF WATER

Water exists in three different states: solid, liquid or gas (vapor). Figure 7.1 presents the phase diagram of water (pressure versus temperature) where the curve lines show the passage from solid to vapor (sublimation), or from liquid to vapor (evaporation) or from solid to liquid (fusion). Point T in Figure 7.1 represents the triple point of water (at 0.01°C and 0.612 kPa) where the three phases (liquid, vapor, solid) coexist, and point C is the critical point of water (374°C and 22 060 kPa).

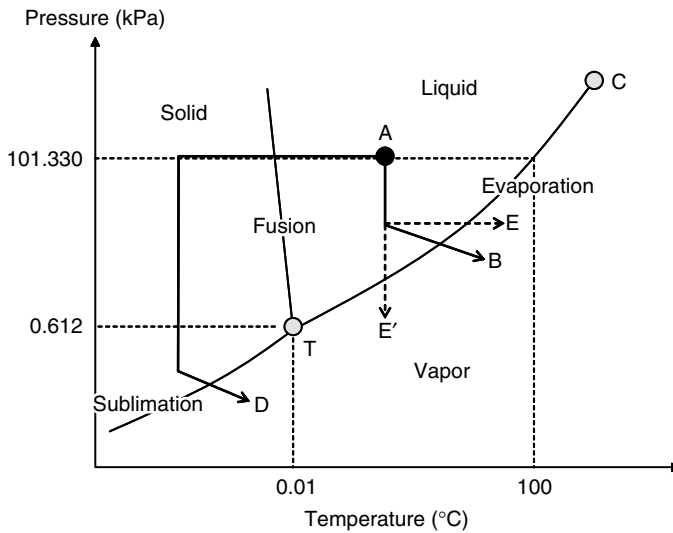


Fig. 7.1 Phase diagram of water (T: triple point of water, C: critical point of water).

Drying under vacuum lies below the atmospheric pressure line (101.330 kPa) in Figure 7.1. While freeze drying makes use of the *sublimation* phenomenon (at temperatures lower than 0.01°C, and vapor pressures below 0.612 kPa), ordinary vacuum drying involves *evaporation* (at temperatures above 0.01°C and pressures between 0.612 and 101.330 kPa). In Figure 7.1, if a product being at a pressure and temperature corresponding to ambient conditions (marked with the point A) is to be dried by vacuum drying, then it should follow the line from A to point B (i.e. it should be placed in equipment where pressure is reduced below the atmospheric pressure and then heat should be applied to favor the evaporation). However, if the same product is to be freeze dried, then it will follow the path from A to point D (i.e. the product should be first frozen by decreasing its temperature, then the water vapor pressure should be lowered below the pressure corresponding to the triple point, and finally some heat should be supplied to help the ice to convert into vapor by sublimation).

In order to understand better the underlying phenomena during vacuum drying, the difference between ordinary evaporation and boiling should be noted. During evaporation, the vapor pressure is less than the total pressure and bubbles cannot form inside the liquid, therefore evaporation is a *surface* phenomenon. At the boiling point, however, the saturated vapor pressure is equal to the total pressure, thus bubbles can form inside the liquid and rise, and the vaporization becomes a *volume* phenomenon. Certainly, drying under vacuum can be done at temperatures and pressures where water boiling is possible (i.e. in Figure 7.1, the path from point A to point E by increasing the temperature to the boiling point at the prevailing total pressure, or the path from point A to point E', by decreasing the total pressure sufficiently to reach the boiling pressure at the prevailing temperature). This can enormously enhance the water loss rate at low temperatures.

Table 7.1 shows the pressure–temperature data for water from -70 to 100°C . As Torr is a common unit for expressing vacuum, the conversion to this unit can be found in Table 7.1 together with the corresponding SI units.

The total pressure during vacuum drying is generally between 35 and 150 Torr (5–20 kPa). Thus, as can be seen from Table 7.1, water boils at approximately 32 and 60°C at 35 and

Table 7.1 Pressure–temperature data for pure water. ΔH_s and ΔH_v are the latent heat of sublimation or vaporization, respectively.

T (°C)	P_w^o (Pa)	P_w^o (Torr)	ΔH_s (kJ kg ⁻¹)	ΔH_v (kJ kg ⁻¹)	T (°C)	P_w^o (Pa)	P_w^o (Torr)	ΔH_v (kJ kg ⁻¹)
-70	0.261	0.00196	2834.2		25	3167.01	23.75	2442.5
-60	1.080	0.0081	2836.7		30	4242.23	31.82	2430.7
-50	3.936	0.0295	2837.9		35	5621.92	42.16	2418.8
-40	12.84	0.0963	2838.8		40	7374.88	55.31	2406.9
-35	22.35	0.1676	2838.9		45	9581.33	71.86	2395.0
-30	38.01	0.2851	2838.8		50	12333.96	92.50	2383.0
-25	63.29	0.4747	2838.5		55	15739.14	118.04	2370.8
-20	103.26	0.7745	2838.1		60	19917.85	149.38	2358.5
-15	165.30	1.2398	2837.5		65	25006.83	187.55	2346.0
-10	259.90	1.9493	2836.6		70	31159.57	233.70	2333.9
-5	401.76	3.0132	2835.0		75	38547.23	289.10	2321.0
0	614.91	4.6118	2834.4	2501.6	80	47359.47	355.20	2309.5
5	873.01	6.5476		2489.8	85	57805.41	433.54	2295.5
10	1228.23	9.2117		2477.9	90	70114.2	525.86	2283.2
15	1705.18	12.7889		2466.1	95	84535.81	634.02	2270.0
20	2337.74	17.5331		2454.4	100	101330.00	760	2257.5

150 Torr, respectively. This is the reason why vacuum drying is appropriate to dry heat-sensitive materials.

Freeze drying on the other hand, works at higher vacuum (adequate total pressure levels range from 0.01 to 1 Torr). It was historically believed that lowering the vacuum and the condenser temperature as much as possible would accelerate freeze drying. It is now well known that allowing the condenser temperature to rise and bleed air or inert gas into the freeze drying chamber can actually accelerate sublimation (Rowe, 1976).

7.3 FOOD AND AIR PROPERTIES IN RELATION TO VACUUM AND FREEZE-DRYING

Porosity (ε) of dried food materials has been investigated in the literature regarding the drying method (vacuum or freeze drying) or the effect of some variables such as drying process temperature (Tsami *et al.*, 1999; Krokida *et al.*, 1998; Rahman *et al.*, 2002). While some works do not report a difference in porosity for vacuum- or freeze-dried products (Tsami *et al.*, 1999), others showed a significant increase in porosity for foodstuffs that underwent freeze drying (Rahman *et al.*, 2002). Rahman *et al.* (2002) also found completely different pore size distribution curves for dried samples produced by different drying methods. Krokida *et al.* (1998) reported a decrease in porosity of freeze-dried apple, potato, carrot and banana as shelf temperature increased, which was related to the collapse phenomena and the glass-transition temperature of the product. These results were confirmed by shrinkage experiments during freeze drying of strawberry, apple and pear (Khalloufi and Ratti, 2003).

Thermal conductivity is an important material property when dealing with drying under vacuum, particularly for freeze drying. This food property is not only dependent on total pressure, nature of the surrounding gas and temperature, but also on porosity and total solid concentration. Information on average thermal conductivity of dried foodstuffs (i.e. beef,

whole milk, apple, peach, tomato juice, coffee, avocado) in the region of the very low pressures used in freeze drying can be found in Kessler (1975). However, scarce information on experimental values of thermal conductivity of freeze-dried foods as a function of total pressure or other variables, as well as models to represent this property, can be found in the literature (Harper, 1962; Qashou *et al.*, 1972; Fito *et al.*, 1984; Sagara and Ichiba, 1994; Lombraña and Izkara, 1996). Figure 7.2 shows typical curves for thermal conductivity as a function of total pressure (for freeze-dried milk based on data found in Fito *et al.*, 1984, and for turkey and beef based on data found in Qashou *et al.*, 1972). As shown in Figure 7.2, thermal conductivity curves present a distinct shape which is found for most materials: low constant thermal conductivity at low pressures, with a smooth increase at pressures between 0.1 and 10 Torr to a higher asymptotic value. It should be pointed out that the operating pressures normally encountered during freeze drying under vacuum (0.01–1 Torr, as mentioned earlier) are in the range of thermal conductivity transition.

A simple one-constant model representing thermal conductivity as a function of total pressure over the entire pressure range has been proposed by Harper (1962):

$$\frac{k_d}{k_{go}} = \frac{1}{1 + (C'/P)} \quad (7.1)$$

where k_{go} is the thermal conductivity of free gas and C' is the model constant. Constant C' has been found to be 1.5, 1.6 and 1.8 for beef, apple and peach, respectively (Harper, 1962). The applicability of this simple equation has been seriously questioned due to the use of k_{go} , which is the thermal conductivity of 'free' gas and not the gas trapped in the voids (Fito *et al.*, 1984).

Porosity is an important factor influencing thermal conductivity of freeze-dried foods (Fito *et al.*, 1984; Sagara and Ichiba, 1994). Figure 7.2(a) shows that for freeze-dried milk, distinct curves of thermal conductivity can be found even with slight changes in porosity (similar results were found for freeze-dried orange pulp by Fito *et al.*, 1984; and for coffee by Sagara and Ichiba, 1994). Logically, as porosity increases thermal conductivity decreases. This knowledge should be taken into account when working with freeze drying in order to optimize the preamable freezing process. Fito *et al.* (1984) proposed an equation to correlate the effect of porosity on thermal conductivity:

$$\frac{1}{k_d} = \frac{1 - a}{(1 - \varepsilon)K_s + \varepsilon K_G} + a \left(\frac{1 - \varepsilon}{K_s} + \frac{\varepsilon}{K_G} \right) \quad (7.2)$$

where a is a constant determined from experimental values, K_s and K_G are the thermal conductivities of the solid and the gas entrapped in the porous matrix, respectively.

Porosity, pressure and temperature also affect mass transport properties. Data for permeability or diffusion coefficients of freeze-dried beef, peach, apple, potato, coffee and for a model food can be found in the literature (Harper, 1962; Saravacos, 1967; Kessler, 1975; Sagara and Ichiba, 1994; Lombraña and Izkara, 1996). In spite of the behavior shown for thermal conductivity, a decrease in total pressure and an increase in porosity will enhance permeability and diffusion coefficients in the porous freeze-dried matrix (Lombraña and Izkara, 1996; Sagara and Ichiba, 1994). This change in mass transport parameters with the operating conditions is crucial for determination of the controlling transport process during freeze drying.

Moisture equilibrium of vacuum- and freeze-dried foods has been thoroughly studied at different pressures and/or temperatures (Saravacos and Stinchfield, 1965; Mazza, 1982; Kim

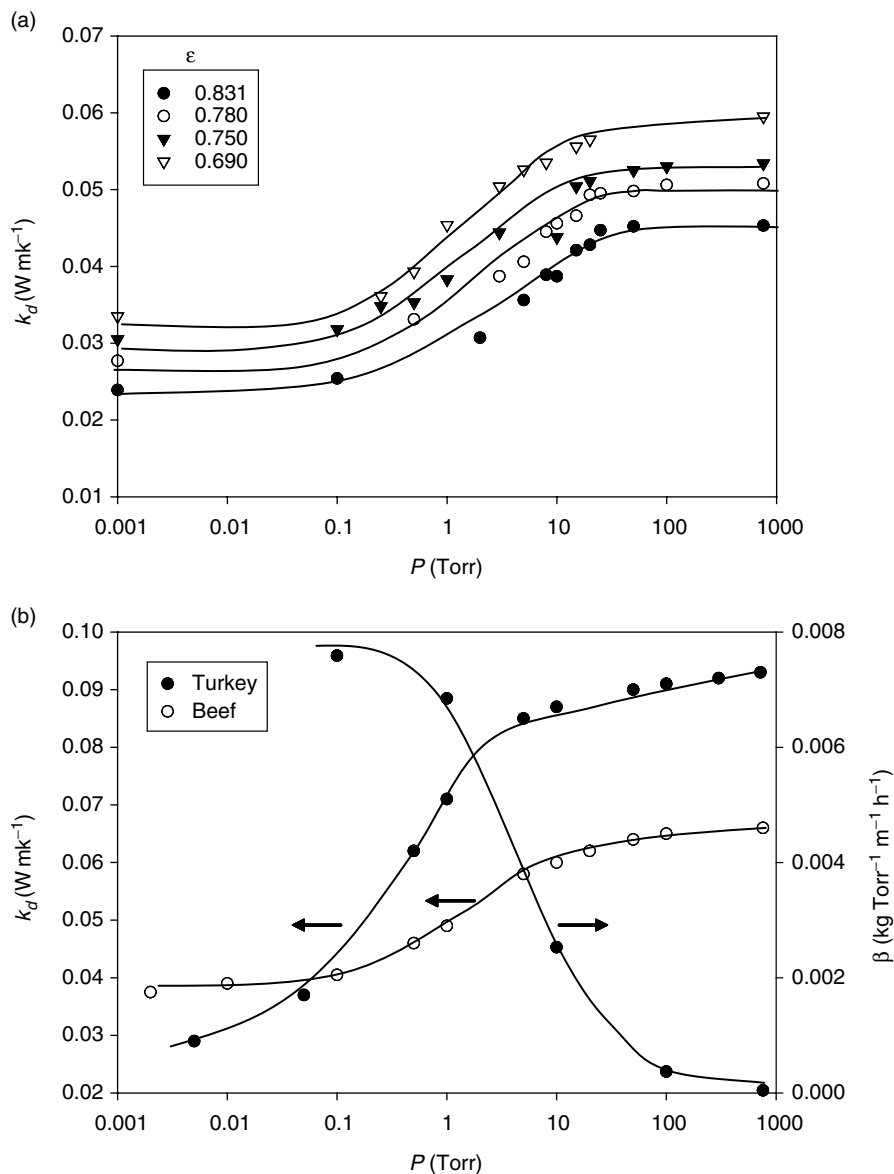


Fig. 7.2 Thermal conductivity of freeze-dried milk at different porosities (a) and meat (parallel to fiber) (b), as a function of total pressure (based on data from Fito *et al.*, 1984 and Qashou *et al.*, 1972). In (b), values of vapor permeability of turkey are included.

and Bhowmik, 1994; Tsami *et al.*, 1999; Khalloufi *et al.*, 2000a). Figure 7.3 shows a comparison of sorption equilibrium isotherms at 25°C for vacuum- or freeze-dried potato (a) and pectin (b). As can be seen, the drying method has an important influence on sorptional equilibrium, probably due to the difference in porosity produced by the different drying methods, as reported earlier. Total pressure was not found to have an impact on moisture equilibrium values of freeze-dried foodstuffs (Saravacos and Stinchfield, 1965). Above-zero temperatures

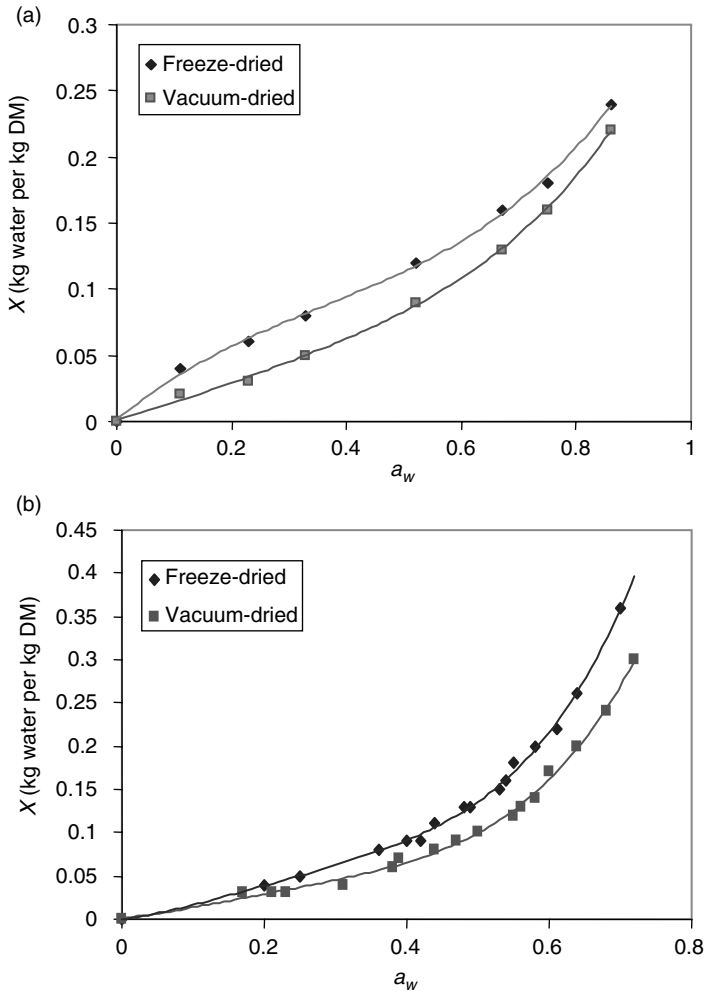


Fig. 7.3 Sorption isotherms for freeze-dried and vacuum-dried potato (a) and pectin (b) at 25°C, based on data from Mazza (1982) and Tsami *et al.* (1999).

affect the sorption isotherms in the expected Clapeyron–Clausius behavior (Khalloufi *et al.*, 2000a; Mazza, 1982). However, sub-zero temperatures may have the opposite effect, depending on the sugar content of the sample (Saravacos and Stinchfield, 1965). For vacuum- or freeze-dried foodstuffs, the Guggenheim–Anderson–deBoer (GAB) equation is one of the most frequently used (Ratti *et al.*, 1989):

$$\frac{X_e}{X_m} = \frac{X_m C k a_w}{(1 - k a_w)(1 - k a_w + C k a_w)} \quad (7.3)$$

where X_e is the equilibrium water content, a_w is the water activity, X_m , C and k are the GAB constants (C and k depend on temperature).

Among the main parameters affecting the quality of dried products are process temperatures. According to King *et al.* (1968), the appearance of freeze-dried turkey meat seemed to

depend upon freezing conditions. Quick-frozen meat samples maintained a whiter color than those frozen slowly. Similar results were found by Karel *et al.* (1975) and Flink (1975) for freeze-dried coffee. Freezing temperatures could therefore have an impact on final product quality. In addition, increasing the shelf temperature certainly reduces costs associated with energy consumption during freeze drying, but it could lead to product deterioration. Volume reduction due to freeze drying is minimal if operating pressures and temperatures are appropriate (Janković, 1993; Hammami and René, 1997; Krokida and Maroulis, 1997; and Shishegharha *et al.*, 2002). However, collapse may occur causing the sealing of capillaries, which in turn leads to reduced dehydration and puffiness. Thus, in the case of the freeze drying process, both freezing and drying temperatures appear to have an impact on final product quality. Therefore, the control and optimization of operating parameters during product manipulation and processing could prove essential to achieving a viable and efficient operation, and one might expect that the optimal operating conditions are influenced by the type of product being processed. Glass-transition temperature, T_g , is a product property linked to deterioration during thermal processing (Karel, 1993; Chuy and Labuza, 1994; Sapru and Labuza, 1993; Taoukis *et al.*, 1997). It can be defined as the temperature at which an amorphous system changes from a glassy state to a rubbery state (Karmas *et al.*, 1992; Roos and Karel, 1991a), which is mainly a function of water content, molecular weight (M_w) and nature of the dry matter compounds (e.g. nature of sugars) in a given substance (Genin and René, 1995; Roos, 1995; Slade and Levine, 1991). The effect of moisture on the T_g of foods has often been reported in the literature (Khalloufi *et al.*, 2000b; Liyod *et al.*, 1996; Pääkkönen and Roos, 1990; Roos, 1987). When prediction of this property is necessary, the Gordon–Taylor equation (Gordon and Taylor, 1952) is nowadays widely used to fit experimental data on glass-transition temperatures of food products as a function of water content and composition:

$$T_g = \frac{x_1 T_{g1} + k' x_2 T_{g2}}{x_1 + k' x_2} \quad (7.4)$$

where T_g and x are the glass transition temperature and mass fraction, k' is a parameter determined from experimental data, and subscripts 1 and 2 correspond to the dry solids and water, respectively. On this basis, two temperature limits were shown to be essential to avoid quality problems during freeze drying of a particular product (Karel, 1975; Hamanni et René, 1998; Roos, 1987; Khalloufi and Ratti, 2003): the frozen core has to be below the ice melting onset temperature, and the dry matrix temperature lower than the T_g of the dry solids. Unfortunately, the first thermal limit is difficult to corroborate in practice due the scarce data on the ice melting onset temperature for foods and, in addition, to the difficulty of measuring precisely the frozen core temperature during freeze drying of solid foods. It could be supposed that if the vacuum level in the freeze drier is low enough, then this first thermal limit is always achieved. The second thermal limit is accomplished when the final temperature of the product is lower than the maximum permissible surface temperature, which is usually dictated by quality considerations (Karel, 1975). This latter limit could be supposed as the glass-transition temperature of dry solids (Khalloufi and Ratti, 2003). Shrinkage and T_g are interrelated in that significant changes in volume and collapse can be noticed only if the temperature of the process is higher than the T_g of the material at that particular moisture content (Genin and René, 1995; Levi and Karel, 1995). Khalloufi and Ratti (2003) showed that equal freeze drying conditions had different impacts on the quality attributes of freeze-dried strawberry, apple and pear. In this publication, shrinkage and quality changes during

freeze drying were related to glass-transition temperature and micro-structure of the samples. The knowledge of the micro-structural arrangement of a heterogeneous food can also help to understand quality deterioration and collapse during processing. Pore formation during freeze drying of apples and dates was studied at different shelf temperatures (Sablani and Rahman, 2002). From these results, it was concluded that glass-transition theory alone could not explain pore formation during freeze drying. Further research on the relationship of freeze drying and glass-transition is required to fully develop this concept from a practical standpoint.

Psychrometric properties change when total pressure decreases. For medium vacuum levels (i.e. vacuum drying) this variation should be taken into account in order to calculate the driving force for mass transfer. Air relative humidity, dew-point and wet-bulb temperatures decrease as vacuum is applied in a chamber. On the other hand, the humid volume increases strongly as total pressure decreases, which reduces the relative space available for the load inside the vacuum chamber as compared to a conventional drier (Keey *et al.*, 2000).

7.4 HEAT TRANSFER MECHANISMS AT LOW PRESSURES

The rate of heat transfer by convection between a fluid and a solid, q_h , is expressed by:

$$q_h = h(T_s - T_f) \quad (7.5)$$

where T_s and T_f are the temperatures of the solid surface and the fluid, respectively, and h is the heat transfer coefficient ($\text{J m}^{-2} \text{s}^{-1} \text{ } ^\circ\text{C}^{-1}$), which has a strong direct functionality with total pressure. When total pressure decreases, h decreases as well. Under high vacuum, the heat transfer coefficient is negligible.

Conduction heat is transferred through a solid or fluid medium by contact. Thermal conductivity, k , is the property representing heat transfer by conduction, q_C (Fourier's law):

$$q_C = -k \frac{\partial T}{\partial x} \quad (7.6)$$

the thermal conductivity (k) of solids is, as shown previously, dependant of total pressure having its lowest value at high vacuum.

The only heat mechanism that does not need a medium to be transferred is radiation. It is usually predominant at high temperatures and under vacuum. Heat radiation between real bodies is a complicated process to describe mathematically, but fairly accurate results can be obtained using simplifying suppositions (Brülls and Rasmuson, 2002). The following expression for the radiation heat exchange, q_R , between non-black bodies can be found in the literature (Bird *et al.*, 1960):

$$q_R = \sigma \frac{(T_{s_1}^4 - T_{s_2}^4)}{(1/\varepsilon_1 + 1/\varepsilon_2 - 1)} \quad (7.7)$$

where A is the area of heat exchange; σ , the Boltzmann constant, T_s is the temperature of the surface, and ε the material emissivity. Subscripts 1 and 2 refer to each of the two non-black bodies. However, some models present for radiation heat transfer a simpler expression, which is similar to equation (7.5) for convection heat transfer, but with a radiation heat transfer

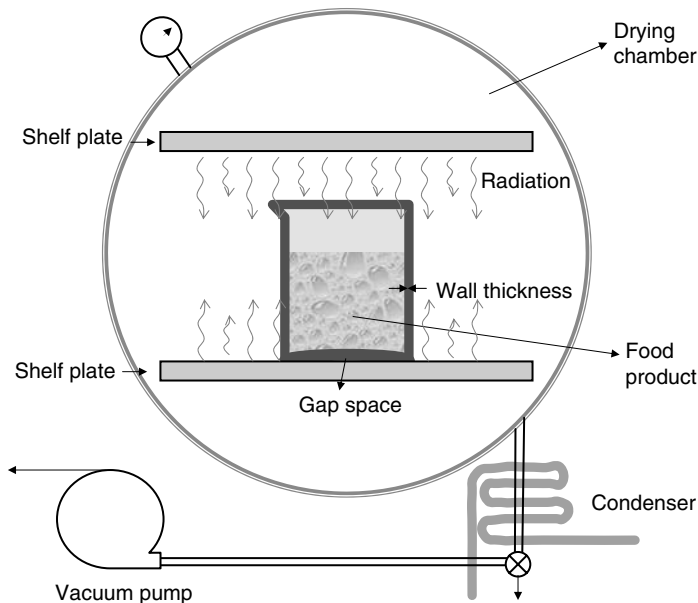


Fig. 7.4 Vacuum drying chamber with a food product.

coefficient determined experimentally. Usually this coefficient is a ‘combined’ radiation–convection parameter.

Heat transfer is poorly transferred under vacuum, which is a major drawback of vacuum drying. Under low pressures, heat is generally transferred to the product by conduction and sometimes by radiation. Convection is rare since very few fluid molecules are available under vacuum so, as mentioned previously, the heat transfer coefficient could be negligible in high vacuum situations (i.e. freeze drying). Figure 7.4 shows a schema of a food product that is being dried under vacuum or freeze drying. The food to be dehydrated is placed in a vacuum chamber on a shelf plate which can supply the necessary energy by conduction. Also, the product can receive heat from the top shelf by radiation. Thus, in the drying chamber heat is mainly transferred to the product by radiation and/or by conduction from the shelf plates. It should be taken into account, however, that conduction heat transfer from the bottom shelf plate to the product could be reduced significantly if there is not good contact between the beaker and the shelf (i.e. through the gap space shown in the picture), thus conduction will only take place through contact points. On the other hand, conduction heat transfer is predominant *within* the product. Nevertheless, vacuum reduces thermal conductivity and low moisture also, and thus heat transfer within the product is poor as dehydration proceeds leaving a dry layer of product.

Internal heat generation by application of microwaves has long been tested in drying in order to improve the poorly transmitted heat under vacuum (Karel, 1975; Steele, 1987; Saravacos and Kostaropoulos, 2002). Microwave heating provides an energy input that not only is essentially unaffected by the dry layers of the material undergoing vacuum or freeze drying, but is absorbed mainly in the humid region (Sunderland, 1982b). Since the humid region has a high thermal conductivity, microwave energy helps sublimation to decrease freeze drying times up to 60–75% (Rosenberg and Bögl, 1987; Peltre *et al.*, 1977). In addition, when compared to conventional freeze drying, microwave-assisted freeze drying leads to

products of similar or even higher quality (Barret *et al.*, 1997; Rosenberg and Bögl, 1987). Nevertheless, microwave freeze drying is still not widely used in the industry since many technical problems can be encountered, some related to the extreme low pressures used during freeze drying (i.e. corona discharges, melting and overheating of the frozen kernel, non-uniform heating, etc.) so it remains of academic interest only.

Heating with microwaves during ordinary vacuum drying of yogurt, model fruit gels, carrot, banana and other fruits, has been the subject of many recent publications (Cui *et al.*, 2004; Mousa and Farid, 2002; Drouzas *et al.*, 1999; Drouzas and Schubert, 1996; Kim and Bhowmik, 1995). Vacuum drying with microwave application certainly has potential because the process can be accelerated producing high-quality dried products, comparable to freeze drying. However, special care should be taken to maintain the temperature level below the maximum permissible values in order to avoid local product destruction due to overheating (Drouzas and Schubert, 1996). Finally, process costs are unfortunately not significantly lower than those for conventional vacuum or freeze drying. From the economic point of view, microwave vacuum drying ranks between spray drying and freeze drying (Mousa and Farid, 2002).

7.5 VACUUM DRYING: PRINCIPLES AND DEHYDRATION MODELS

Vacuum drying is the result of lowering the total pressure in the drying chamber. As shown earlier, water boils at lower temperatures under vacuum and thus drying times are shortened by enhanced drying rates. Also, water circulation through the product increases at lower pressures, resulting in a greater internal mass transfer under vacuum. Vacuum drying allows temperature-sensitive materials to dry under a reduced oxygen atmosphere, which is certainly favorable to the quality of final products.

If the temperature of the product during vacuum drying is lower than the water boiling point at the prevailing total pressure, then the drying mechanisms are similar to those encountered during atmospheric conventional drying. On the other hand, if during drying the material temperature is at the boiling point of water, then internal evaporation is produced with the consequent increase in drying rate. In this case, it is possible to suppose that a receding front moves inward as the product dries (Figure 7.5). Water in the product would evaporate at the interface and move out through the dry layer, leaving a humid core. Heat should be supplied sufficiently to keep the product temperature above the boiling point of water, which due to the heat transfer limitations under vacuum already described could be a difficult task. A good analysis of drying mechanisms with internal evaporation has been reported in the literature (Perré, 1995).

Heat could reach the product by radiation/convection from both sides (Figure 7.5a), therefore mass and heat transfer takes place in opposite directions through the dry layer. On the other hand, heat can be supplied by conduction through the shelf where the product is placed (Figure 7.5b). This latter type of heating is particularly efficient when drying products have good contact with the shelf. Table 7.2 shows simple mathematical equations that can represent both cases shown in Figures 7.5a and b (these equations have been adapted from the freeze drying equations introduced by Sandall *et al.* (1967), Karel (1975) and Geankoplis (1993), which could be applied to vacuum drying since both types of drying methods have internal vaporization or sublimation). In the case of radiation from both sides, equation (7.8) represents a single straight line between p_{wh} and T_h (p_{ws} , k_d , T_s , β , ΔH are constant). This

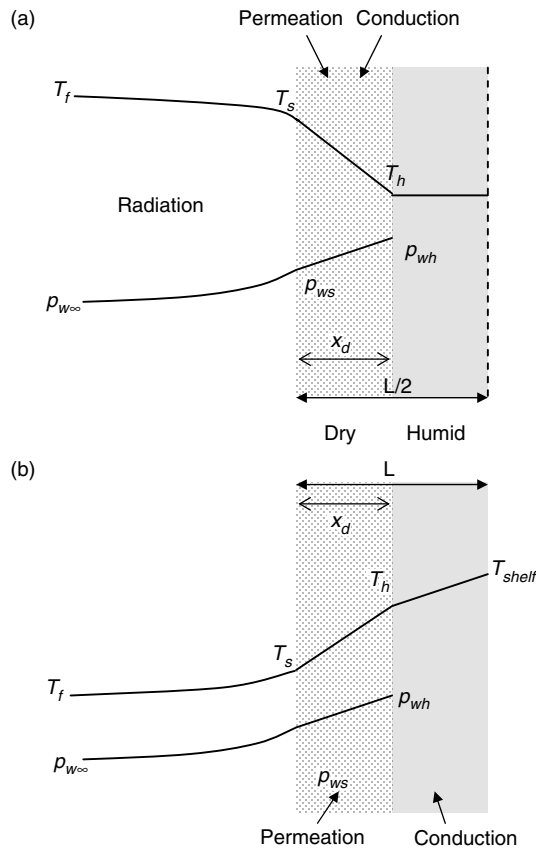


Fig. 7.5 Temperature and vapor pressure profiles during drying under vacuum. Heat and mass transfer in the dry layer (a), heat transfer in the humid layer and mass transfer in the dry layer (b).

single straight line should be combined with the vapor saturation curve in order to solve the temperature and vapor pressure in the interface (p_{wh} and T_h). Once these two parameters are solved, then equation (7.9) is applied when heat transfer is controlling and, (7.10) when mass transfer controls. In the case of conduction heat through the wet layer (equations (7.11) and (7.12), Figure 7.5b), equation (7.11) represents several straight lines as x_d is at different stages as time proceeds. Thus, the temperature and pressure of the vapor at the interface changes continuously with time in this case. The simple models presented in equations (7.8)–(7.12) are applicable only when internal evaporation is predominant. However, during the removal of bound water (the last part of the drying process), internal mass transfer becomes the controlling transfer. This last part of the drying process can take longer than the removal of the free water and it is not predicted by the internal evaporation model. Diffusion models are widely used in describing the mass transfer mechanisms; they are based on the resolution of Fick's law (equation (7.13)). The popularity of the diffusion models can be widely attributed to their ease of formulation. In many situations, diffusion models give satisfactory results by including all the complexity of the phenomena in an 'effective' diffusion coefficient which is determined from experimental data (Akpınar and Dincer, 2005). This approach was used for the calculation of diffusion coefficients during vacuum drying of coconut, carrot and

Table 7.2 Simple mathematical models representing drying kinetics under vacuum.

Type	Equations
Heat and mass transfer through the dry layer – Figure 7.5(a)	$p_{wh} = \left(p_{ws} + \frac{k_d}{\beta \Delta H} T_s \right) - \frac{k_d}{\beta \Delta H} T_h \quad (7.8)$
Equations based on previously reported models (Sandall <i>et al.</i> , 1967; Karel, 1975; Geankoplis, 1993)	$t = \frac{L^2}{8k_d} \frac{\Delta H \rho_s}{(T_f - T_h)} \left[\frac{4k_d(X_o - X)}{Lh} + \frac{(X_o - X)^2}{(X_o - X_e)} \right] \quad (7.9)$
	$t = \frac{L^2 \rho_s}{8\beta} \frac{1}{(p_{wh} - p_{ws})} \left[\frac{(X_o - X)^2}{(X_o - X_e)} \right] \quad (7.10)$
Heat transfer through the humid layer and mass transfer through the dry layer – Figure 7.5(b)	$p_{wh} = p_{ws} + \left(\frac{k_h}{\Delta H \beta} \right) \left(\frac{x_d}{L - x_d} \right) (T_{shelf} - T_h) \quad (7.11)$
Equations based on previously reported models (Karel, 1975)	$t = \frac{\rho_s(X_o - X_f)}{\beta} \int_0^L \frac{x_d}{(p_{wh} - p_{ws})} dx_d \quad (7.12)$
Fick's law	$\frac{\partial X}{\partial t} = D_{eff} (\nabla^2 X) \quad (7.13)$

pumpkin, mushroom, and yogurt (Jena and Das, 2007; Arévalo-Pinedo and Xiedieh Murr, 2007; Walde *et al.*, 2006; Kim and Bhowmilk, 1995).

Industrially, vacuum drying is only used when the product is heat-sensitive (i.e. maximum allowable temperature is lower than 40°C) or if it is easily oxidized. The vacuum tray drier is the simplest, although its loading capacity is low (Baker, 1997). The product must usually be sieved to break down any agglomerates (van't Land, 1991), thus mechanically agitated vacuum driers are widely used.

Superheated steam vacuum drying is a technique which has recently been getting increased attention (Defost *et al.*, 2004). This technique uses superheated steam as a heating medium for water evaporation from a solid which is at a temperature above its boiling point. The evaporated moisture becomes part of the drying medium and does not need to become exhaust (Cenkowski *et al.*, 2005) and, because the steam is superheated and not saturated, a drop in its temperature due to heat transfer to the solid will not cause condensation. In addition, no oxygen is present in the superheated steam medium, which can make it a choice heating method for oxygen-sensitive materials. Superheated steam vacuum drying has been successfully applied to foods (Methakhup *et al.*, 2005; Suvarnakuta *et al.*, 2005; Devahastin and Suvarnakuta, 2004; Martinello *et al.*, 2003; Elustondo *et al.*, 2001). However, although the final product quality is superior to other tested methods, the drying time is longer than that for vacuum drying at the same temperatures (Methakhup *et al.*, 2005; Suvarnakuta *et al.*, 2005). Semi-empirical drying kinetics models have been tested against actual food dehydrated with this method giving excellent results (Elustondo *et al.*, 2001).

7.6 FREEZE DRYING: PRINCIPLES AND DEHYDRATION MODELS

Freeze drying is based on dehydration by sublimation of the ice fraction of a frozen product. It has three distinct phases; freezing, primary drying stage (sublimation) and secondary drying

stage (desorption). Drying is faster during the primary drying stage due to the availability of large amount of unbound water in a frozen state. Ice sublimation leaves a porous dry layer that increases as drying proceeds (receding front). During the secondary drying stage, bound water has to be dried. A major portion of the bound water is in an unfrozen state and the drying rate will be very slow (Mellor, 1978; Vega-Mercado *et al.*, 2001).

Due to the absence of liquid water and the low temperatures required for the process, most of the deterioration reactions and micro-biological activities are stopped, which gives a final product of excellent quality. The solid state of water during freeze drying protects the primary structure and the shape of the products with minimal reduction of volume. Freeze-dried products have a long shelf life without refrigeration – two years for a 2% residual moisture content product being usual (Williams-Gardner, 1971). This technique has been applied with success to several biological materials, such as meats, coffee, juices, dairy products, cells, bacteria, and is now standard practice for penicillin, protein hydrolysates, hormones, blood plasma, vitamin preparations, etc. Despite many advantages, freeze drying has always been recognized as the most expensive process for manufacturing a dehydrated product.

Its cost varies depending on the type of raw material, the products, the packaging, the capacity of the plant, duration of cycle, etc. (Lorentzen, 1979; Sunderland, 1982a). As compared to air drying, freeze drying costs are 4–8 times higher (Flink, 1977a; Mafart, 1991). However, it is important to include all energy uses when evaluating or comparing different processes. For example, the comparison between freeze drying costs to other methods of food preservation such as freezing is quite advantageous if the energy spent at the home storage freezer is taken into account (calculations based on Flink, 1977b; Judge *et al.*, 1981). Also, the energy spent in the freeze drying process itself becomes insignificant when dealing with high-value raw materials. Freeze drying should therefore not be regarded as a prohibitively expensive preservation process if it gives a reasonable added value to the product, or if it keeps its high-value, as compared to other preservation methods (Lorentzen, 1979).

An important part of freeze drying investigations aimed to reduce operation times and consequently to lower the energy consumption, analyzing the possibilities of controlling the heat intensity and vacuum pressure, and therefore investigating possible ways of optimizing the freeze drying process. Several studies were carried out in laboratories and pilot scale plants (Liapis *et al.*, 1996; Kuu *et al.*, 1995; Sagara and Ichiba, 1994). Simulation was also used as a preliminary tool for evaluation of the freeze drying process. Several theoretical models concerning the heat and mass transfer phenomena during freeze drying can be found in the literature (Lombraña *et al.*, 1997; Lombraña and Izkara, 1996; Mellor, 1978; Karel, 1975; Liapis and Bruttini, 1995a).

One of the earliest and most simple models is one considering a receding front inside the product during freeze drying and energy used just for ice sublimation (Sandall *et al.*, 1967; Karel, 1975). If the heat and mass transfer takes place through the dry layer, then equation (7.9) is applied (Table 7.2) which, because of simultaneous heat and mass transfer process, is equivalent to equation (7.10). This model is usually applied in the case of heating by radiation to both faces of the solid undergoing freeze drying. If conduction through the frozen layer is the prevailing heating mechanism, then equation (7.12) is applicable. As in the case of vacuum drying, the temperature and vapor pressure at the interface should be evaluated in order to obtain the drying time (equations (7.8) or (7.11)) in combination with the saturated vapor pressure curve. Sandall *et al.* (1967) stated that the model satisfactorily predicted the drying time for removal of 65–90% of the total initial water content against experimental data (Geankoplis, 1993). Although easier to use than complex mathematical models, these

equations have several key assumptions not usually applicable: (a) the maximum allowable surface temperature T_s is reached instantaneously, (b) the heat output of the external supply is adjusted to maintain T_s constant throughout the drying cycle, (c) partial pressure in the drying chamber is constant, and (d) all the heat is used for sublimation of water vapor (Khalloufi *et al.*, 2005; Karel, 1975).

More recently, numerical models having highly detailed freeze drying equations have been developed (Nastaj and Ambrozek, 2005; Khalloufi *et al.*, 2005; Brülls and Rasmuson, 2002; George and Data, 2002; Lombraña *et al.*, 1997; Lombraña and Izkara, 1996; Liapis and Bruttini, 1995a). However, in most cases adjustable parameters are needed to match the model predictions to experimental data (Nastaj and Ambrozek, 2005; George and Datta, 2002; Sharma and Arora, 1993; Lipais and Marchello, 1984; Millman *et al.*, 1985; Sadikoglu and Liapis, 1997; Sheehan and Liapis, 1998). In other cases, no comparison with experimental data is presented (Liapis and Bruttini, 1995b; Nastaj, 1991). In addition, most of the models were developed for liquids and not for solid products such as foodstuffs (Sadikoglu and Liapis, 1997; Sheehan and Liapis, 1998; Brülls and Rasmuson, 2002). Khalloufi *et al.* (2005) built a freeze drying model for solid foods based on energy and mass microscopic balances in the dried and frozen regions of the product. All the parameters involved in the model (i.e. thermal conductivity, permeability, heat transfer coefficients, etc.) were obtained independently from actual experimental data. Simulation results closely agreed to apple and potato freeze drying data (Khalloufi *et al.*, 2005). The model presented recently by Nastaj and Ambrozek (2005) is interesting because it deals with multi-component freeze drying (simultaneous desorption of water and other organic compounds), which could be applied to simulate aroma retention during the process.

From the energy point of view, the freeze drying process has four main operations: freezing, vacuum, sublimation and condensing. Each of these operations shares the total energy consumption and, while sublimation takes almost half of the total energy of the process, the freezing step is not highly energy consuming. Vacuum and condensation shares are practically equal (Ratti, 2001). Any technological improvement to the classical vacuum freeze drying in order to reduce energy costs should be addressed to the following goals: (a) to improve heat transfer in order to help sublimation; (b) to cut drying times, in order to reduce the vacuum; (c) to avoid using condensers.

As explained previously, microwave heating has been tested thoroughly in order to reduce freeze drying times, but unfortunately the many technical problems encountered with this type of heating means its use is still restricted to laboratory tests.

Adsorption freeze drying uses a desiccant (e.g. silica gel) to create a high vapor drive at low temperatures (Bell and Mellor, 1990a). The adsorbent replaces the condenser, and gives a reduction of 50% in total costs as compared to traditional freeze drying. Despite the many advantages as compared to regular freeze drying (Bell and Mellor, 1990b), the quality of adsorption freeze-dried foods is slightly reduced, and sometimes poor, as compared to that obtained by traditional freeze drying.

Another method that has recently been developed, which is becoming popular, is the fluidized atmospheric freeze drier (Figure 7.6, Wolff and Gibert, 1990). This process can be defined by three words: adsorption, fluidization and atmospheric pressure (Wolff and Gilbert, 1987). It is a freeze drying operation at atmospheric pressure utilizing a fluidized bed of adsorbent particles (Di Matteo *et al.*, 2003). The adsorbent particles should be compatible with the material being dried, since it can be difficult to separate the adsorbent from the freeze-dried product (Kudra and Mujumdar, 2001). The cut off energy by using this method is approximately 34% as compared to vacuum freeze drying (Wolff and Gilbert, 1990).

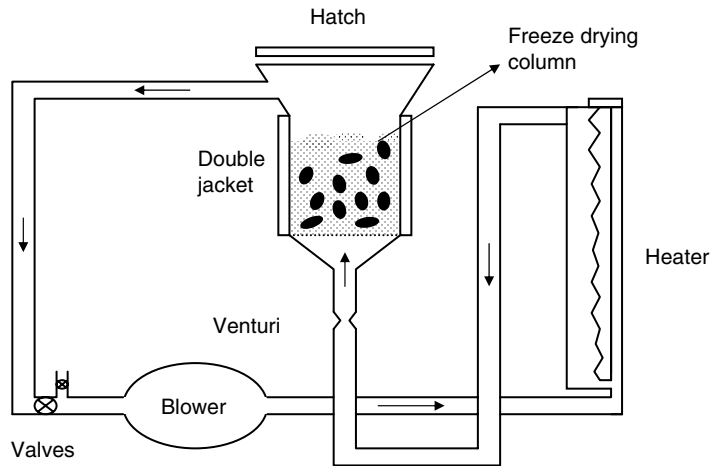


Fig. 7.6 Atmospheric fluidized freeze drier (adapted from Wolff and Gibert, 1990).

However, drying times are increased 1–3 times since the use of atmospheric pressure turns the control of the process from heat to mass transfer, which makes the kinetic extremely slow. Other studies showed that, in addition, the quality of products is not excellent when atmospheric pressure is used instead of vacuum, since the risk of product collapse is increased (Lombraña and Villarán, 1996, 1997). Di Matteo *et al.* (2003) concluded after a study of heat and mass transfer during atmospheric freeze drying in a fluidized-bed, that the choice of a proper set of variables (sample size, bed temperature and nature of the adsorbent being the main ones) are the key to success in the application of this technique to the food industry.

Recently, Mujumdar (2007) has reported ongoing work on the potential of a vibrated-bed atmospheric freeze drier for cost-competitive drying of heat-sensitive materials like fruits and vegetables. Using a vortex tube to provide the cooled air and combined conduction and radiation modes for supplying the heat of sublimation, their results on a laboratory scale unit show that a vibrated-bed drier can operate successfully without using the large volumes of air required for fluidization in the conventional manner. By ensuring that the product temperature is always above the triple point (considering the freezing point depression caused by soluble sugars or salts) they were able to obtain dried product quality (e.g. color, porosity and rehydration characteristics) which closely matched those obtained in vacuum freeze drying. By addition of suitable adsorbents to the bed of model materials they tested (carrot and potato cubes and slices) they showed that the drying time can also be reduced by up to 20%. This work may lead to cost-competitive atmospheric freeze drying processes that can compete with vacuum drying, which tends to be generally expensive in capital and operating costs.

7.7 ILLUSTRATIVE EXAMPLE

An instant soup is prepared by mixing dry pasta, dehydrated turkey pieces and spices. Because of quality concerns, the soup manufacturer decides to change the meat drying method from conventional hot-air drying to vacuum drying, expecting to improve the texture and nutritional content of rehydrated turkey pieces. The proposition is to test ordinary vacuum drying as well

as freeze drying of the turkey pieces. But, before performing laboratory tests, the manufacturer asks the food engineer in his company to present a preliminary study showing drying times and heat energy requirements associated with both possible drying methods.

The preliminary study will be done for a 10 g turkey piece having 0.8 cm thickness (L), which is vacuum or freeze dried in a chamber similar to the one shown in Figure 7.4. The chamber can operate at diverse vacuum levels, has only one shelf (the lower one), the temperature of which can be controlled from -40 to 80°C . The condenser can operate at different temperatures as well. The initial moisture content of turkey is about 74% (wet basis), and the final desired moisture content, 3% (wet basis).

Solution

Vacuum drying: A total pressure of 30 Torr is selected for vacuum drying. At this pressure water boils at approximately 30°C (Table 7.1), so in order to assure internal evaporation in the turkey during vacuum drying, the shelf temperature is set at 40°C (T_{shelf}). The heat will be transferred by conduction from the shelf to the turkey piece; thus, to obtain the drying time, equations (7.11) and (7.12) can be applied.

First, the expression for the vapor pressure at the interface between the dry and wet zones (p_{ws}) as a function of the temperature (T_h) should be obtained from equation (7.11):

$$p_{wh} = p_{ws} + \left(\frac{k_h}{\Delta H \beta} \right) \left(\frac{x_d}{L - x_d} \right) (T_{shelf} - T_h)$$

To solve the previous equation, some parameters should be estimated. The vapor pressure at the surface (between the dry layer and the environment, please refer to Figure 7.5b), p_{ws} , can be supposed as the vapor pressure in equilibrium at the condenser temperature, thus we can suppose the condenser operates with water at 5°C , therefore p_{ws} is estimated as 6.55 Torr. The thermal conductivity of the humid *fresh* turkey (k_h) is $0.5019 \text{ W m}^{-1} \text{ K}$ (Heldman, 1975). The latent heat of vaporization at 30°C (temperature at which water boils at 30 Torr), ΔH_v , is $2430.7 \text{ kJ kg}^{-1}$ (see Table 7.1). The value of permeability, β , in the dry layer at 30 Torr total pressure can be found from Figure 7.2b as $0.00175 \text{ kg Torr}^{-1} \text{ m h}$. Under these suppositions, equation (7.11) becomes:

$$p_{wh} = 6.55 \text{ Torr} + 0.425 \text{ Torr}^\circ\text{C}^{-1} \left(\frac{x_d}{0.8 \text{ cm} - x_d} \right) (40^\circ\text{C} - T_h)$$

The previous equation gives several straight lines between p_{wh} and T_h as x_d increases from 0 to 0.8 cm. At the interface, p_{wh} and T_h are in equilibrium, thus these straight lines should be combined with the water saturation curve in order to determine the pressure and temperature at the interface for each x_d . Figure 7.7 shows the combination of lines.

The following functionality between p_{wh} and x_d can be obtained from the intersection of each straight line (at different x_d) with the saturation vapor pressure curve (see the intersections marked with circles in Figure 7.7).

From Table 7.3, the following quadratic regression between p_{wh} and x_d can be obtained using Excel:

$$p_{wh} = 54.167x_d^2 - 3.155x_d + 8.286 \quad r^2 = 0.989$$

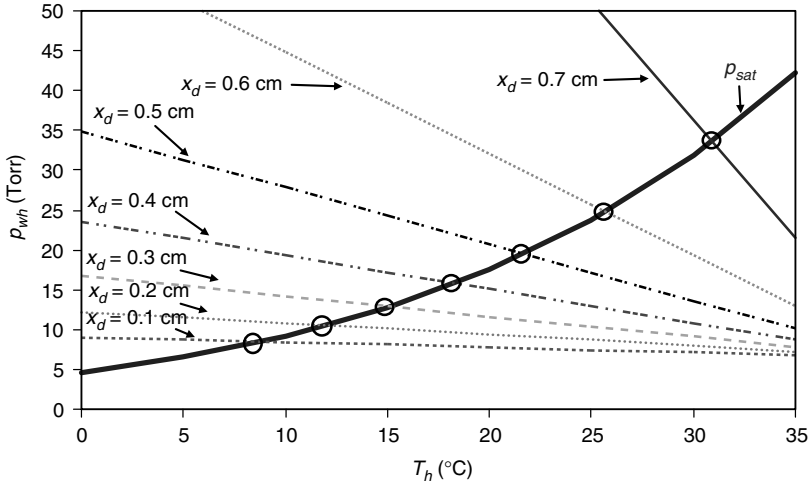


Fig. 7.7 Resolution diagram to obtain product temperature at the interface.

Table 7.3 Temperature and pressure at the interface as a function of dry layer thickness.

X_D (CM)	T_H ($^{\circ}$ C)	P_{WH} (Torr)
0.1	8.5	7.5
0.2	12.0	11.0
0.3	14.9	13.0
0.4	18.0	15.5
0.5	21.5	19.5
0.6	25.2	25.0
0.7	31.0	33.5

The previous expression can now be used in equation (7.12):

$$t = \frac{\rho_s(X_o - X_f)}{\beta} \int_0^{0.8 \text{ cm}} \frac{x_d}{(54.167x_d^2 - 3.155x_d + 8.286 - p_{ws})} dx_d$$

The integration required in the previous equation can be done numerically or graphically, its result value is $0.0337 \text{ cm}^2 \text{ Torr}^{-1}$.

The bulk density of the solids, ρ_s , can be estimated as $300 \text{ kg}_{ds} \text{ m}^{-3}$. The difference in moisture contents (initial and final) in dry basis is:

$$X_o - X_f = \left(\frac{0.74}{1 - 0.74} \right) - \left(\frac{0.03}{1 - 0.03} \right) = (2.84 - 0.03) \frac{\text{kg}_w}{\text{kg}_{ds}} = 2.81 \frac{\text{kg}_w}{\text{kg}_{ds}}$$

Including ρ_s , β and $(X_o - X_f)$ in the calculation, then the predicted time for vacuum drying a 0.8-cm thickness turkey piece is thus 1.63 h. It should be mentioned that this calculated drying time only includes water lost by internal evaporation, and not the water lost by desorption.

The heat energy requirements for vacuum drying (Earle, 1983) are calculated from the heat necessary to increase the turkey piece from the refrigerated storage temperature (i.e. 5°C) to the vacuum drying temperature (30°C at a total pressure of 30 Torr, from Table 7.1), and the heat required to evaporate the water contained in the turkey piece, which is:

Solids contained in 10 g of turkey having 74% (wb) moisture = 2.6 g

Initial water mass in 10 g turkey = 7.4 g

Final water mass at 3% (wb) moisture ($0.03 \text{ kg}_w/\text{kg}_{ds}$) = 0.08 g

Water mass to evaporate = $(7.4 - 0.08) \text{ g} = 7.32 \text{ g}$

$$Q = m_{turkey} C_{p_{turkey}} (30 - 5)^\circ\text{C} + m_{water} \Delta H_v$$

The specific heat for fresh turkey can be approximated as the value given in Heldman (1975) for fresh chicken, $3.31 \text{ J g}_{turkey}^{-1} \text{ K}$, and the evaporation heat is taken from Table 7.1 at 30°C, $2430.7 \text{ J g}_{water}^{-1}$. Thus:

$$Q = 10 \text{ g}_{turkey} * 3.31 \text{ J g}_{turkey}^{-1} \text{ K} * 25^\circ\text{C} + 7.32 \text{ g}_w 2430 \text{ J g}_w^{-1}$$

$$Q = 18620 \text{ J for 10 g of turkey} \rightarrow Q_m = 1862 \text{ kJ per kg turkey}$$

Freeze drying: For freeze drying, a condenser temperature of -50°C , a total pressure of 0.03 Torr and a shelf temperature of 0°C , are chosen. At this condenser temperature, p_{ws} is estimated as 0.0295 Torr (from Table 7.1). The thermal conductivity of the humid *frozen* turkey (k_h) is $1.416 \text{ W m}^{-1} \text{ K}$ (Heldman, 1975). The latent heat of sublimation does not change enormously with pressure and its value can be estimated as, ΔH_s , $2838.8 \text{ kJ kg}^{-1}$ (see Table 7.1). The value of permeability, β , in the dry layer at 0.03 Torr total pressure can be found from Figure 7.2b as $0.0077 \text{ kg Torr}^{-1} \text{ m h}$. Under these suppositions, equation (7.2) becomes:

$$p_{wh} = 0.0295 \text{ Torr} + 0.241 \text{ Torr } ^\circ\text{C}^{-1} \left(\frac{x_d}{0.8 \text{ cm} - x_d} \right) (0^\circ\text{C} - T_h)$$

Following the same steps shown for the case of vacuum drying:

$$p_{wh} = 1.607x_d^2 + 3.875x_d + 0.329 \quad r^2 = 0.998$$

Finally, the integration in equation (7.12) gives a value of $0.140 \text{ cm}^2 \text{ Torr}^{-1}$, and the freeze drying time calculated using this method is 1.52 h. As in the example for vacuum drying, it should be mentioned that this calculated drying time only includes water lost by sublimation, and does not include the removal of the last 10–35% of water. This last water removal constitutes the second freeze drying step, desorption, which can markedly increase total drying time (Geankoplis, 1993).

As can be seen, the drying times calculated for both drying methods, vacuum and freeze drying, are approximately the same. This is because although vacuum drying has a higher driving force due to increased product temperatures there is, on the other hand, an increase in permeability at lower total pressures which greatly favors freeze drying.

For freeze drying, the energy requirements include the refrigeration for freezing, Q_f , and the heat for sublimation, Q_s :

$$Q = Q_f + Q_s$$

The refrigeration energy for freezing 10 g of turkey from 25°C to -40°C can be calculated from:

$$Q_f = m_{turkey} C_{p_{turkey}} (25^\circ\text{C} - T_{if})^\circ\text{C} + m_{water} \Delta H_{freezing} \\ + m_{turkey} C_{p_{frozen\ turkey}} (T_{if} - (-40^\circ\text{C}))$$

The specific heat for fresh turkey can be approximated as the value given in Heldman (1975) for fresh chicken, $3.31 \text{ J g}_{turkey}^{-1} \text{ K}$, the value for specific heat for the *frozen* turkey can be estimated as 40% of the value for the fresh meat (Woolrich, 1966), thus $C_{p_{frozen\ turkey}} = 1.5 \text{ J g}_{turkey}^{-1} \text{ K}$, T_{if} is taken as -2°C , and the freezing enthalpy of water, $\Delta H_{freezing}$ as $335.5 \text{ J g}_{water}^{-1}$. Therefore,

$$Q_{fm} = 392 \text{ kJ per kg turkey}$$

Now, the necessary energy for sublimation is calculated:

$$Q_{sm} = (7.32 \text{ g}_w 2838 \text{ J g}_w^{-1}) / 10 \text{ g turkey} = 2077.4 \text{ kJ per kg turkey}$$

$$Q_m = (392 + 2077) \text{ kJ per kg turkey}$$

$$\rightarrow Q_m = 2469 \text{ kJ per kg turkey}$$

The previous calculation shows that freeze drying energy requirements are 32% higher than vacuum drying just by virtue of adding the freezing step and the sublimation (which consumes more energy per kilogram than evaporation). Energy requirements for vacuum have not been included in the previous estimation.

7.8 ADVANCES IN VACUUM AND FREEZE DRYING OF FOODS

The number of scientific articles on vacuum and freeze drying of foods (fruits, vegetables, meats, herbs) has been increasing over the last years. This is certainly due to a renewed interest in these processes for emerging applications such as 'natural' dehydrated fruits and vegetables, functional powders, value-added and nutraceutical products, etc. Foodstuffs have interesting bioactive compounds (i.e. isoflavones, carotenoids, anthocyanins, etc.) that nowadays are the center of consumer attention due to their action in preventing illnesses such as cancer, neurological and coronary diseases, etc. Some of these valuable compounds could be deteriorated by high temperatures, oxygen and light during processing, as well as other physical quality characteristics of the product. Therefore, many of the latest publications related to vacuum or freeze drying deal with:

- the effect of the process on the decrease of the activity or the content of a target *bioactive* compound (Ratti *et al.*, 2007; Santivarangkna *et al.*, 2006; Cui *et al.*, 2004; D'Andrea *et al.*, 1996; Lane *et al.*, 1995);

- the comparison of different *preservation* methods on the nutritional quality of the processed food (Vanamala *et al.*, 2005; Lester *et al.*, 2004; Asami *et al.*, 2003; Simone *et al.*, 2000);
- the comparison of different *dehydration* methods on the nutritional or physical quality of the dehydrated food (Walde *et al.*, 2006; Monsoor 2005; Beaudry *et al.*, 2004; Sunjka *et al.*, 2004; Nindo *et al.*, 2003; Hsu *et al.*, 2003; Abonyi *et al.*, 2001; Krokida *et al.*, 2001; King *et al.*, 2001; Kowsalya *et al.*, 2001; Martinez-Soto *et al.*, 2001; Yousif *et al.*, 2000);
- the quality deterioration during *storage* of dried products (Regier *et al.*, 2005; Çinar, 2004; Tang and Chen, 2000; Irzyniec *et al.*, 1993).

It is surprising to find that many of these articles indicate that freeze drying is not the best preservation method to preserve certain target bioactive compounds. Folic acid content was found to decrease in some vegetables after freeze drying (Lane *et al.*, 2005), although it increased in others. The activity of ascorbate oxydase purified from green zucchini squash slowed down on freeze drying, showing a potentially damaging effect of the process on enzyme activity (D'Andrea *et al.*, 1996). Vanamala *et al.* (2005) showed a decrease in vitamin C and volatile compounds after freeze drying of grapefruit. Garlic, however, could keep intact its capacity to form allicin after freeze drying at 20°C (Ratti *et al.*, 2007). The decrease in allicin retention with heating plate temperatures was marked only during freeze drying of whole garlic cloves (due to structural collapse), but it was not noticeable when freeze drying garlic slices.

Freezing did not cause a substantial loss in lutein and β -carotene in soybeans, but freeze drying did (Simone *et al.*, 2000). Freezing was also shown to be a better method than freeze drying to preserve ascorbic acid and total phenolics in marionberry, strawberry and corn (Asami *et al.*, 2003). Although freezing seems to be a better preservation method, freeze drying can be recommended to preserve bioactive compounds in powders when compared to other dehydration methods, such as air drying or drum drying (Hsu *et al.*, 2003; Asami *et al.*, 2003). In terms of final product quality, freeze drying is usually a winner over vacuum drying (Monsoor, 2005; Rahman *et al.*, 2002; Krokida *et al.*, 2001; Martinez-Soto *et al.*, 2001; Yousif *et al.*, 2000). This is particularly true when physical appearance, color, aroma, porous structure, and rehydration are evaluated. However, when retention of important bioactive compounds or functional properties are the quality targets, then both vacuum and freeze drying processes give similar results (Monsoor, 2005; Cui *et al.*, 2004). In the case of drying micro-organisms, vacuum drying seems to work fairly well and even better than freeze drying, especially for yeasts (Santivarangkna *et al.*, 2006; Cerrutti *et al.*, 2000). Walde *et al.* (2006) studied air drying, fluidized-bed drying, vacuum drying and microwave drying of mushrooms. They found that vacuum drying takes the longest drying time, and that fluidized-bed drying gave the best results in terms of drying rate and final quality. Sunjka *et al.* (2004) analyzed the application of microwaves during air and vacuum drying of cranberries. Microwave heating enhanced vacuum drying making this process the most energy efficient.

The porous structure created during freeze drying is interesting for manufacturing food powders, preparing instant foods or for adding freeze-dried fruits to cereal mixtures, etc. due to an improved and quick rehydration (Meda and Ratti, 2005). However, this feature could not be beneficial during long-term storage of freeze-dried products having bioactive compounds that could be affected by deterioration reactions depending on exposed area (i.e. oxidation). Chlorophyll in freeze-dried spinach was deteriorated during storage as compared to controlled low-temperature vacuum dehydrated samples (King *et al.*, 2001). The authors attributed the chlorophyll loss to the high porosity of freeze-dried products. On the other hand, low temperatures were pointed out as the key storage parameter for keeping the bioactive

quality in freeze-dried plant products (Çinar, 2004; Irzyniec *et al.*, 1993; Tang and Chen, 2000).

Chou and Chua (2001) presented a good revision on new hybrid drying technologies for heat-sensitive foodstuffs. Regarding freeze drying, some developments in this area have been made recently by a combination of hot-air drying followed by freeze drying of vegetables. Donsì *et al.* (1998) showed this combination to be a promising technique in the production of high-quality dehydrated fruits and vegetables. Kumar *et al.* (2001) also showed that this combination produces carrot and pumpkin dehydrated products that have a similar quality to freeze dried, and much superior quality to hot-air dried, products. The drying time and total energy consumption was 50 % lower than freeze drying alone. Yanyang *et al.* (2004) found that the combination of hot-air drying followed by microwave vacuum drying not only shortens drying time but also improves the retention of chlorophyll and ascorbic acid in wild cabbage.

7.9 CLOSURE

Vacuum and freeze drying are expensive processes used to manufacture functional food powders. Although some recent progress has been made in developing hybrid dehydration technologies in order to cut energy and costs associated with these processes, there is not yet a dehydration process that is superior to freeze drying in terms of final product nutritional and physical quality. By analyzing the world trends towards foods and eating habits, some predictions on the future of vacuum and freeze drying as methods for preserving foods can be made. Recently, the market for 'natural' and 'organic' products has been increasingly strong as well as the consumer's demand for foods with minimal processing and high quality. From this perspective, the demand for vacuum or freeze-dried foodstuffs or ingredients will certainly increase in the future years.

7.10 NOTATION

a	constant in Fito <i>et al.</i> (1984) model, equation (7.2)
a_w	water activity
C	constant in GAB model, equation (7.3)
C'	constant in Harper (1962) model, equation (7.1)
$C_{p_{turkey}}$	turkey specific heat, $\text{kJ kg}^{-1}\text{°C}$
$C_{p_{frozen\ turkey}}$	frozen turkey specific heat, $\text{kJ kg}^{-1}\text{°C}$
D_{eff}	effective diffusion coefficient, $\text{m}^2 \text{s}^{-1}$
h	heat transfer coefficient, $\text{W m}^{-2} \text{K}$
k	constant in GAB model, equation (7.3)
k'	constant in Gordon and Taylor (1952) model, equation (7.4)
k_d	thermal conductivity, W mK^{-1}
k_{go}	thermal conductivity of 'free gas', equation (7.1), W mK^{-1}
K_G	thermal conductivity of the gas entrapped in the porous matrix, equation (7.2), W mK^{-1}
K_s	thermal conductivity of the solid matter, equation (7.2), W mK^{-1}
L	total solid thickness, m
m_{turkey}	turkey mass, kg

m_{water}	water mass, kg
p_{wh}	water vapor pressure at the evaporation or sublimation front, Pa
p_{ws}	water vapor pressure at the solid surface, Pa
$p_{w\infty}$	water vapor pressure in bulk fluid, Pa
P	total pressure, Pa
P_w^o	saturated water vapor pressure, Pa
q_C	conduction heat flux, $W m^{-2}$
q_h	convection heat flux, $W m^{-2}$
q_R	radiation heat flux, $W m^{-2}$
Q	energy requirements for vacuum or freeze drying, kJ
Q_m	mass specific energy requirements for vacuum or freeze drying, $kJ kg^{-1}$
Q_f	freezing energy requirement, kJ
Q_{fm}	specific freezing energy requirement, $kJ kg^{-1}$
Q_s	sublimation energy requirement, kJ
Q_{sm}	specific sublimation energy requirement, $kJ kg^{-1}$
t	time, s
T	temperature, $^{\circ}C$
T_f	fluid temperature, $^{\circ}C$
T_g	glass-transition temperature, $^{\circ}C$
T_h	temperature at the evaporation or sublimation front, $^{\circ}C$
T_{if}	initial freezing temperature, $^{\circ}C$
T_s	solid surface temperature, $^{\circ}C$
T_{shelf}	shelf temperature, $^{\circ}C$
x	coordinate axis, m
x_d	dried layer thickness, m
x_1	dry solids mass fraction, equation (7.4)
x_2	water mass fraction, equation (7.4)
X	water content (dry basis), kg water per kg dry matter
X_e	equilibrium water content (dry basis), kg water per kg dry matter
X_f	final water content (dry basis), kg water per kg dry matter
X_m	constant in GAB model, equation (7.3), kg water per kg dry matter
X_o	initial water content (dry basis), kg water per kg dry matter
β	vapor permeability in dried product, $kg\ water\ Torr^{-1}\ m\ h$
ΔH	enthalpy of evaporation or sublimation, equation (7.8), (7.9) and (7.11), $kJ\ kg^{-1}$
ΔH_f	enthalpy of freezing, $kJ\ kg^{-1}$
ΔH_s	enthalpy of sublimation, $kJ\ kg^{-1}$
ΔH_v	enthalpy of evaporation, $kJ\ kg^{-1}$
ε	porosity
$\varepsilon_1\varepsilon_2$	emissivity for surfaces 1 or 2, respectively, equation (7.7)
ρ_s	density of dry solids, $kg\ m^{-3}$
σ	Boltzmann constant, equation (7.7)

REFERENCES

- Abonyi, B.I., Feng, H., Tang, J. *et al.* (2001) Quality retention in strawberry and carrot purees dried with Refractance Window™ system. *Journal of Food Science*, **67**(2), 1051–1056.

- Akpınar, E.K. and Dincer, I. (2005) Moisture transfer models for slabs drying. *International Communications in Heat and Mass Transfer*, **32**(1–2), 80–93.
- Arévalo-Pinedo, A. and Xiedieh Murr, F.E. (2007) *Journal of Food Engineering*, **80**, 152–156.
- Asami, D.K., Hong, Y.-J., Barret, D. and Mitchell, A.E. (2003) Comparison of the total phenolic and ascorbic acid content of freeze-dried and air-dried marionberry, strawberry and corn growth using conventional, organic, and sustainable agricultural practices. *Journal of Agricultural and Food Chemistry*, **51**, 1237–1241.
- Baker, C.G.H. (1997) *Industrial Drying of Foods*. Blackie Academic and Professional, Chapman & Hall, London.
- Beaudry, C., Raghavan, G.S.V., Ratti, C. and Rennie, T.J. (2004) Effect of four drying methods on the quality of osmotically dehydrated cranberries. *Drying Technology*, **22**(3), 521–539.
- Bell, G.A. and Mellor, J.D. (1990a) Adsorption freeze-drying. *Food Australia*, **42**(5), 226–227.
- Bell, G.A. and Mellor, J.D. (1990b) Further developments in adsorption freeze-drying. *Food Research Quarterly*, **50**(2), 48–53.
- Bird, R.B., Stewart, E.N. and Lightfoot, E.N. (1960) *Transport Phenomena*. John Wiley & Sons, Inc., New York.
- Brown, M. (1999) Focusing on freeze-drying. *Food Manufacture*, September, **74**(9), 34–36.
- Brülls, M. and Rasmuson, A. (2002) Heat transfer in vial lyophilization. *International Journal of Pharmaceutics*, **246**, 1–16.
- Cenkowski, S., Pronyk, C. and Muir, W.E. (2005) Current advances in superheated-steam drying and processing. *Stewart Postharvest Review*, **4**, 4.
- Cerrutti, P., Segovia de Huergo, M., Galvagno, M., Schebor, C. and Buera, M.P. (2000) Commercial baker's yeast stability as affected by intracellular content of trehalose, dehydration procedure and the physical properties of external matrices. *Applied Microbiology Biotechnology*, **54**, 575–580.
- Çınar, I. (2004) Carotenoid pigment loss of freeze-dried plant samples under different storage conditions. *Lebensmittel-Wissenschaft & Technologie*, **37**, 363–367.
- Chou, S.K. and Chua, K.J. (2001) New hybrid drying technologies for heat sensitive foodstuffs. *Trends in Food Science and Technology*, **12**, 359–369.
- Chuy, L.E. and Labuza, T.P. (1994) Caking and stickiness of dairy-based food powders as related to glass transition. *Journal of Food Science*, **59**(1), 43–46.
- Cui, Z.-W., Xu, S.-Y. and Sun, D.-W. (2004) Microwave-vacuum drying kinetics of carrots slices. *Journal of Food Engineering*, **65**, 157–164.
- D'Andrea, G., Salucci, M.L. and Avigliano, L. (1996) Effect of lyoprotectants on ascorate oxidase activity alter freeze-drying and storage. *Process Biochemistry*, **2**, 173–178.
- Defost, M., Fortin, Y. and Cloutier, A. (2004) Modeling superheated steam vacuum drying of wood. *Drying Technology*, **22**(10), 2231–2253.
- Devahastin, S. and Suvanakuta, P. (2004) Superheated steam drying of food products. In: *Dehydration of Products of Biological Origin* (ed. A.S. Mujumdar). Science Publishers Enfield, NH, USA.
- Di Matteo, P., Donsì, G. and Ferrari, G. (2003) The role of heat and mass transfer phenomena in atmospheric freeze-drying of foods in a fluidised bed. *Journal of Food Engineering*, **59**, 267–275.
- Donsì, G., Ferrari, G., Nigro, R. and Di Matteo, P. (1998) Combination of mild dehydration and freeze-drying processes to obtain high quality dried vegetables and fruits. *Transactions of the IChemE*, **76**, 181–187.
- Drouzas, E., Tsami, E. and Saravacos, G.D. (1999) Microwave/vacuum drying of model fruit gels. *Journal of Food Engineering*, **39**, 117–122.
- Drouzas, A.E. and Schubert, H. (1996) Microwave application in vacuum drying of fruits. *Journal of Food Engineering*, **28**, 203–209.
- Elustondo, D., Elustondo, M.P. and Urbicain, M.J. (2001) Mathematical modeling of moisture evaporation from foodstuffs exposed to subatmospheric pressure superheated steam. *Journal of Food Engineering*, **49**, 15–24.
- Fito, P.J., Piñaga, F. and Aranda, V. (1984) Thermal conductivity of porous bodies at low pressure: Part I. *Journal of Food Engineering*, **3**, 75–88.
- Flink, J.M. (1977a) Energy analysis in dehydration processes. *Food Technology*, **31**(3), 77–79.
- Flink, J.M. (1977b) A simplified cost comparison of freeze-dried food with its canned and frozen counterparts. *Food Technology*, **31**(4), 50.

- Flink, J.M. (1975) The influence of freezing conditions on the properties of freeze-dried coffee. Chapter 2. In: *Freeze-drying and Advanced Food Technology* (eds S.A. Goldblith, L. Rey and W.W. Rothmayr) Academic Press, London.
- Geankoplis, C.J. (1993) *Transport Processes and Unit Operations*. 3rd edn. Prentice-Hall, NJ, USA.
- George, J.P. and Datta, A.K. (2002) Development and validation of heat and mass transfer models for freeze-drying of vegetable slices. *Journal of Food Engineering*, **52**, 89–93.
- Genin, N. and René, F. (1995) Analyse du rôle de la transition vitreuse dans les procédés de conservation agroalimentaires. *Journal of Food Engineering*, **26**, 391–408.
- Gordon, M. and Taylor, J.S. (1952) Ideal co-polymers and the second order transitions of synthetic rubbers. *Journal of Applied Chemistry*, **2**, 493–500.
- Hammami, C. and René, F. (1997) Determination of freeze-drying process variables for strawberries. *Journal of Food Engineering*, **32**, 133–154.
- Harper, J.C. (1962) Transport properties of gases in porous media at reduced pressures with reference to freeze-drying. *AIChE Journal*, **8**(3), 298–302.
- Heldman, D. (1975) *Food Process Engineering*. Avi Publishing Company, USA.
- Hsu, Ch-L., Chen, W., Weng, Y.-M. and Tseng, Ch-Y. (2003) Chemical composition, physical properties, and antioxidant activities of yam flours as affected by different drying methods. *Food Chemistry*, **83**, 85–92.
- Irzywiec, Z., Klimczak, J. and Michalowski, S. (1993) Effect of storage temperature on vitamin C and total anthocyanins of freeze-dried strawberry juices. *Proceedings of Bioavailability'93 – Nutritional, Chemical and Food Processing Implications of Nutrient Availability*, pp. 398–403, Ettingen, Germany.
- Janković, M. (1993) Physical properties of convectively dried and freeze-dried berrylike fruits. *Faculty of Agriculture, Belgrade*, **38**(2), 129–135.
- Jena, S. and Das, H. (2007) Modelling for vacuum drying characteristics of coconut presscake. *Journal of Food Engineering*, **79**, 92–99.
- Judge, M.D., Okos, M.R., Baker, T.G., Potthast, K. and Hamm, R. (1981) Energy requirements and processing costs for freeze-dehydration of Prerigor meat. *Food Technology*, **35**(4), 61–62, 64–67.
- Karel, M. (1975) Heat and mass transfer in freeze drying. In: *Freeze Drying and Advanced Food Technology* (eds S.A. Goldblith, I. Rey and W.W. Rothmayr). Academic Press, London.
- Karel, M. (1993) Temperature-dependence of food deterioration processes. *Journal of Food Science*, **58**(6), ii.
- Karel, M., Fennema, O.R. and Lund, D.B. (1975) *Principles of Food Science – Part II, Physical Principles of Food Preservation*. Marcel Dekker, Inc., New York.
- Karmas, R., Buera, M.P. and Karel, M. (1992) Effect of glass transition on rates of nonenzymatic browning in food systems. *Journal of Agriculture Food Chemistry*, **40**, 873–879.
- Key, R.B., Langrish, T.A.G. and Walker, J.C.F. (2000) *Kiln-Drying of Lumber*. Springer, Berlin.
- Kessler, H.G. (1975) Heat and mass transfer in freeze drying of mixed granular particles. In: *Freeze Drying and Advanced Food Technology* (eds S.A. Goldblith, I. Rey and W.W. Rothmayr). Academic Press, London.
- Khalloufi, S., Robert, J.-L. and Ratti, C. (2005) A mathematical model for freeze-drying simulation of biological materials. *Journal of Food Process Engineering*, **28**, 107–132.
- Khalloufi, S. and Ratti, C. (2003) Quality deterioration of freeze-dried foods as explained by their glass transition temperature and internal structure. *Journal of Food Science*, **68**(3), 892–903.
- Khalloufi, S., Giasson, J. and Ratti, C. (2000a) Water activity of freeze-dried berries and mushrooms. *Canadian Agricultural Engineering*, **42**(1), 51–56.
- Khalloufi, S., El Masloui, Y. and Ratti, C. (2000b) Mathematical model for prediction of glass transition temperature of fruit powders. *Journal of Food Science*, **65**(5), 842–848.
- Kim, S.S. and Bhowmik, S.R. (1994) Moisture sorption isotherms of concentrated yogurt and microwave vacuum dried yogurt powder. *Journal of Food Engineering*, **21**, 157–175.
- Kim, S.S. and Bhowmik, S.R. (1995) Effective moisture diffusivity of plain yogurt undergoing microwave vacuum drying. *Journal of Food Engineering*, **24**, 137–148.
- King, C.J., Lam, W.K. and Sandal, O.C. (1968) Physical properties important for freeze-drying poultry meat. *Food Technology*, **22**, 1302.
- King, V.A.-E., Liu, Ch-F. and Liu, Y.-J. (2001) Chlorophyll stability in spinach dehydrated by freeze-drying and controlled low-temperature vacuum dehydration. *Food Research International*, **34**, 167–175.
- Kowsalya, S., Chandrasekhar, U., Balasasirekha, R. (2001) Beta carotene retention in selected green leafy vegetables subjected to dehydration. *The Indian Journal of Nutrition and Dietetics*, **38**, 374–383.

- Krokida, M.K. and Maroulis, Z.B. (1997) Effect of drying method on shrinkage and porosity. *Drying Technology*, **15**(10), 2441–2458.
- Krokida, M.K., Maroulis, Z.B. and Saravacos, G.D. (2001) The effect of the method of drying on the colour of dehydrated products. *International Journal of Food Science and Technology*, **36**, 53–59.
- Krokida, M.K., Karathanos, V.T. and Maroulis, Z.B. (1998) Effect of freeze-drying conditions on shrinkage of dehydrated agricultural products. *Journal of Food Engineering*, **35**, 369–380.
- Kudra, T. and Mujumdar, A.S. (2001) Atmospheric freeze-drying. In: *Advanced Drying Technologies*. Marcel Dekker, New York. Also, CRC Press, Boca Raton, FL.
- Kumar, H.S.P., Radhakrishna, K., Nagaraju, P.K. and Rao, D.V. (2001) Effect of combination drying on the physico-chemical characteristics of carrot and pumpkin. *Journal of Food Processing Preservation*, **25**, 447–460.
- Kuu, W.Y., McShane, J. and Wong, J. (1995) Determination of mass transfer coefficient during freeze drying using modeling and parameter estimation techniques. *International Journal of Pharmaceutics*, **124**, 241–252.
- Lane, H.W., Nillen, J.L. and Kloeris, V.L. (1995) Folic acid content in thermostabilized and freeze-dried space shuttle foods. *Journal of Food Science*, **60**(3), 538–540.
- Lester, G.E., Hodges, D.M., Meyer, R.D. and Munro, K. (2004) Pre-extraction preparation (fresh, frozen, freeze-dried, or acetone powdered) and long-term storage of fruit and vegetable tissues: Effects on antioxidant enzyme activity. *Journal of Agricultural and Food Chemistry*, **52**, 2167–2173.
- Levi, G. and Karel, M. (1995) Volumetric shrinkage (collapse) in freeze-dried carbohydrates above their glass transition temperature. *Food Research International*, **28**, 145–151.
- Liapis, A.I., Pikal, M.J. and Bruttini, R. (1996) Research and development needs and opportunities in freeze-drying. *Drying Technology*, **14**(6), 1265–1300.
- Liapis, A.I. and Bruttini, R. (1995a) Freeze drying. In: *Handbook of Industrial Drying* (ed. A.S. Mujumdar), 2nd edn. Marcel Dekker, New York.
- Liapis, A.I. and Bruttini, R. (1995b) Freeze-drying of pharmaceutical crystalline and amorphous solutes in vials: Dynamic multi-dimensional models of the primary and secondary drying stages and qualitative features of the moving interface. *Drying Technology*, **13**(1&2), 43–72.
- Lombraña, J.I., De Elvira, C. and Villarán, M. (1997) Analysis of operating strategies in the production special foods in vials by freeze drying. *International Journal of Food Science and Technology*, **32**, 107–115.
- Lombraña, J.I. and Izkara, J. (1996) Experimental estimation of effective transport coefficients in freeze drying for simulation and optimization purposes. *Drying Technology*, **14**(3&4), 743–763.
- Lombraña, J.I. and Villarán, M. (1996) Interaction of kinetic and quality aspects during freeze drying in an adsorbent medium. *Industrial and Engineering Chemical Research*, **35**, 1967–1975.
- Lombraña, J.I. and Villarán, M. (1997) The influence of pressure and temperature on freeze-drying in an adsorbent medium and establishment of drying strategies. *Food Research International*, **30**(3/4), 213–222.
- Lorentzen, J. (1979) Freeze-drying of foodstuffs. Quality and economics in freeze-drying. *Chemistry and Industry*, **14**, 465–468.
- Mafart, P. (1991) Génie Industriel Alimentaire. *Les procédés physiques de conservation*. Vol. I. Lavoisier, Paris.
- Martinello, M.A., Mattea, M.A. and Crapiste, G.H. (2003) Superheated steam drying of parsley: A fixed bed model for predicting drying performance. *Latin American Applied Research*, **33**(3), 333–337.
- Martinez-Soto, G., Ocaña-Camacho, R. and Paredes-López, O. (2001) Effect of pretreatment and drying on the quality of oyster mushrooms (*Pleurotus ostreatus*). *Drying Technology*, **19**(3&4), 661–672.
- Mazza, G. (1982) Moisture sorption isotherms of potato slices. *Journal of Food Technology*, **17**, 47–54.
- Meda, L. and Ratti, C. (2005) Rehydration of freeze-dried strawberries at varying temperatures. *Journal of Food Process Engineering*, **28**, 233–246.
- Mellor, J.D. (1978) *Fundamentals of Freeze Drying*. Academic Press Inc., London.
- Methakup, S., Chiewchan, N. and Devahastin, S. (2005) Effects of drying methods and conditions on drying kinetics and quality of Indian gooseberry flake. *Lebensmittel-Wissenschaft & Technologie*, **38**, 579–587.
- Millman, M.J., Liapis, I.A. and Marchello, J.M. (1985) An analysis of lyophilization process using a sorption–sublimation model and various operational policies. *AIChE Journal*, **31**(10), 1594–1604.
- Mousa, N., and Farid, M. (2002) Microwave vacuum drying of banana slices. *Drying Technology*, **20**(10), 2055–2066.

- Monsoor, M.A. (2005) Effect of drying methods on the functional properties of soy hull pectin. *Carbohydrates Polymers*, **61**, 362–367.
- Mujumdar, A.S. (2007) Personal communication. National University of Singapore, April, 2007.
- Nastaj, J. (1991) A mathematical modeling of heat transfer in freeze drying. In: *Drying 91* (eds A.S. Mujumdar and I. Filkova), Elsevier Science Ltd., Amsterdam, pp. 405–413.
- Nastaj, J.F. and Ambrozek, B. (2005) Modeling of vacuum desorption in freeze-drying process. *Drying Technology*, **23**, 1693–1709.
- Nindo, C.I., Sun, T., Wang, S.W., Tang, J. and Powers, J.R. (2003) Evaluation of drying technologies for retention of physical quality and antioxidants in asparagus (*Asparagus officinalis* L.). *Lebensmittel-Wissenschaft & Technologie*, **36**, 507–516.
- Pääkkönen, K. and Roos, Y.H. (1990) Effects of drying conditions on water sorption and phase transitions of freeze-dried horseradish roots. *Journal of Food Science*, **55**(1), 206–209.
- Peltre, R.P., Arsen, H.B. and Ma, Y.H. (1977) Applications of microwave heating to freeze-drying: Perspective. *AIChE Symposium Series*, **73**(163), 131–133.
- Perré, P. (1995) Drying with internal vaporization: Introducing the concept of identity drying card (IDC). *Drying Technology*, **13**(5–7), 1077–1097.
- Qashou, M.S., Vachon, R.I. and Touloukian, Y.S. (1972) Thermal conductivity of foods. ASHRAE Semi-Annual Meeting, 23–27.
- Rahman, M.S., Al-Amri, O.S. and Al-Bulushi, I.M. (2002) Pores and physico-chemical characteristics of dried tuna produced by different methods of drying. *Journal of Food Engineering*, **53**, 301–313.
- Ratti, C. (2001) Hot air and freeze-drying of high-value foods: A review. *Journal of Food Engineering*, **49**(4), 311–319.
- Ratti, C., Araya, M., Mendez, L. and Makhlof, J. (2007) Drying of garlic (*Allium sativum*) and its effect on allicin retention. *Drying Technology*, **25**(2), 349–356.
- Ratti, C., Crapiste, G.H. and Rotstein, E. (1989) A new water sorption equilibrium expression for solid foods based on thermodynamic considerations. *Journal of Food Science*, **54**(3), 738–742.
- Regier, M., Mayer-Miebach, E., Behsnilian, D., Neff, E. and Schuchmann, H.P. (2005) Influences of drying and storage of lycopene-rich carrots on the carotenoid content. *Drying Technology*, **23**, 989–998.
- Roos, Y.H. (1987) Effect of moisture on the thermal behavior of strawberries studied using differential scanning calorimetry. *Journal of Food Science*, **52**(1), 146–149.
- Roos, Y.H. (1995) *Phase Transitions in Foods*. Academic Press Inc., London.
- Roos, Y.H. and Karel, M. (1991) Applying state diagrams to food processing and development. *Food Technology*, **45**, 66–70, 107.
- Rosenberg, U. and Bögl, W. (1987) Microwave thawing, drying, and baking in the food industry. *Food Technology*, **41**(6), 85–91.
- Rowe, T.W.G. (1976) Optimization in freeze-drying. *Developments in Biological Standards*, **36**, 79–97.
- Sablani, S.S. and Rahman, M.S. (2002) Pore formation in selected foods as a function of shelf temperature during freeze-drying. *Drying Technology*, **20**(7), 1379–1391.
- Sadikoglu, H. and Liapis, A.I. (1997) Mathematical modeling of the primary and secondary drying stages of bulk-solution freeze-drying in trays: Parameter estimation and model discrimination by comparison theoretical results with experimental data. *Drying Technology*, **15**(3/4), 791–810.
- Sagara, Y. and Ichiba, J.-I. (1994) Measurement of transport properties for the dried layer of coffee solution undergoing freeze drying. *Drying Technology*, **12**(5), 1081–1103.
- Sandall, O.C., King, J. and Wilke, C.R. (1967) The relationship between transport properties and rates of freeze-drying of poultry meat. *AIChE Journal*, **13**(3), 428–438.
- Santivarangkna, C., Kulozik, U. and Foerst, P. (2006) Effect of carbohydrates on the survival of *Lactobacillus helveticus* during vacuum drying. *Letters in Applied Microbiology*, **42**, 271–276.
- Sapru, V. and Labuza, T.P. (1993) Glassy state in bacterial spores predicted by polymer glass-transition theory. *Journal of Food Science*, **58**(2), 445–448.
- Saravacos, G.D. (1967) Effect of the drying method on the water sorption of dehydrated apple and potato. *Journal of Food Science*, **32**, 81–84.
- Saravacos, G.D. and Kostaropoulos, A.E. (2002) *Handbook of Food Processing Equipment*. Kluwer Academic/Plenum Publishers, New York.

- Saravacos, G.D. and Stinchfield, R.M. (1965) Effect of temperature and pressure on the sorption of water vapor by freeze-dried food materials. *Journal of Food Science*, **30**, 779–786.
- Sharma, N.K. and Arora, C.P. (1993) Prediction transient temperature distribution during freeze drying of yoghurt. *Drying Technology*, **11**(7), 1863–1883.
- Sheehan, P. and Liapis, A.I. (1998) Modeling of primary and secondary drying stages of freeze-drying of pharmaceutical products in vials: Numerical results obtained from solution of dynamic and spatially multi-dimensional lyophilization model for different operational policies. *Biotechnology and Bioengineering*, **60**(6), 712–728.
- Shishegarha, F., Makhlof, J. and Ratti, C. (2002) Freeze-drying characteristics of strawberries. *Drying Technology*, **20**(1), 131–145.
- Simone, A.H., Smith, M., Weaver, D.B. *et al.* (2000) Retention and changes of soy isoflavones and carotenoids in immature soybean seeds (Edamame) during processing. *Journal of Agricultural and Food Chemistry*, **48**, 6061–6069.
- Slade, L. and Levine, H. (1991) Beyond water activity: Recent advances based on an alternative approach to the assessment of food quality and safety. *Critical Reviews in Food Science and Nutrition*, **30**, 115–360.
- Steele, R.J. (1987) Microwaves in the food industry. *CSIRO Food Research*, **47**, 73–78.
- Sunderland, J.E. (1982a) An economic study of microwave freeze-drying. *Food Technology*, **36**(2), 50–52, 54–56.
- Sunderland, J.E. (1982b) Microwave freeze-drying. *Journal of Food Process Engineering*, **4**(4), 195–212.
- Sunjka, P.S., Rennie, T.J., Beaudry, C. and Raghavan, G.S.V. (2004) Microwave-convective and microwave-vacuum drying of cranberries: A comparative study. *Drying Technology*, **22**(5), 1217–1231.
- Suvarnakuta, P., Devahastin, S. and Mujumdar, A.S. (2005) Drying kinetics and β -carotene degradation in carrot undergoing different drying processes. *Journal of Food Science*, **70**(8), S520–S526.
- Tang, Y.C. and Chen, B.H. (2000) Pigment change of freeze-dried carotenoid powder during storage. *Food Chemistry*, **69**, 11–17.
- Taoukis, P.S., Labuza, T.P. and Saguy, I.S. (1997) Kinetics of food deterioration and shelf-life prediction. Chapter 9. In: *Handbook of Food Engineering Practice* (eds K.J. Valentas, E. Rotstein and R.P. Singh) CRP Press LLC, Boca Raton, FL, USA.
- Tsami, E., Krokrida, M.K. and Drouzas, A.E. (1999) Effect of drying method on the sorption characteristics of model fruit powders. *Journal of Food Engineering*, **38**, 381–392.
- Vanamala, J., Cobb, G., Turner, N.D. *et al.* (2005) Bioactive compounds of grapefruit (*Citrus paradise* Cv. Rio Red) respond differently to postharvest irradiation, storage, and freeze-drying. *Journal of Agricultural and Food Chemistry*, **53**, 3980–3985.
- van't Land, C.M. (1991) *Industrial Drying Equipment. Selection and Application*. Marcel Dekker, Inc., New York, USA, pp. 21–25.
- Vega-Mercado, H., Gongora-Nieto, M. and Barbosa-Canovas, G.V. (2001) Advances in dehydration of foods. *Journal of Food Engineering*, **49**(4), 271–289.
- Walde, S.G., Velu, V., Jyothirmayi, T. and Math, R.G. (2006) Effects of pretreatments and drying methods on dehydration of mushroom. *Journal of Food Engineering*, **74**, 108–115.
- Williams-Gardner A. (1971) *Industrial Drying*. Gulf Publishing Company, Houston, TX, USA.
- Wolff, E. and Gibert, H. (1987) Lyophilisation sous Pression Atmosphérique. In: *Collection Récents progrès en Génie des procédés*. Lavoisier, Paris.
- Wolff, E. and Gibert, H. (1990) Atmospheric freeze-drying. Part 2: Modelling drying kinetics using adsorption isotherms. *Drying Technology*, **8**(2), 405–428.
- Woolrich, W.R. (1966) Specific heat and latent heat of foods in the freezing zone. *ASHRAE Journal*, **4**, 43–47.
- Yanyang, X., Min, Z., Mujumdar, A., Le-qun, Z. and Jin-cai, S. (2004) Studies on hot air and microwave vacuum drying of wild cabbage. *Drying Technology*, **22**(9), 2201–2209.
- Yousif, A.N., Durance, T.D., Scaman, C.H. and Girard, B. (2000) Headspace volatiles and physical characteristics of vacuum-microwave, air, and freeze-dried oregano (*Lipia berlandieri* Schauer). *Journal of Food Science*, **65** (6), 926–930.

8 Post-drying aspects for meat and horticultural products

Mohammad Shafiur Rahman

8.1 INTRODUCTION

Foods can be divided into three broad groups based on the value added through drying. In the case of cereals, legumes and root crops, very little value is added per kilogram processed. More value per unit mass is added to foods such as vegetables, fruits and fish; and considerably more to high value crops such as spices, herbs, medicinal plants, nuts, bioactive materials, and enzymes (Rahman and Perera, 2007). Drying reduces the water activity, thus preserving foods by avoiding microbial growth and deteriorative chemical reactions. The heating effects on micro-organisms and enzyme activity are also important in the drying of foods. In the case of foods to be preserved by drying, it is important to maximize micro-organism and/or enzyme inactivation for preventing spoilage and enhancing safety, and to reduce the components causing the deterioration of dried foods. On the other hand, in the case of drying bacterial cultures, enzymes, functional compounds or vitamins, minimum inactivation of micro-organisms and/or enzyme is required. Thus, detrimental effects of drying may be desirable or undesirable depending on the purpose of drying process.

8.2 STATE DIAGRAM AND STABILITY CONCEPTS OF DRIED PRODUCTS

A state diagram is a map of the different states of a food as a function of water or solid content and temperature. The main advantage of drawing a map is in identifying different states of a food, such as freezing point and glass transition, which help in understanding the complex changes that occur when a food's water content and temperature are changed. It also assists in identifying a food's stability during storage as well as selecting suitable conditions of temperature and moisture content for processing (Rahman, 2006). Figure 8.1 shows a state diagram indicating different states as a function of temperature and solid mass fraction. The components of a state diagram are discussed as follows.

Earlier state diagrams were constructed with only a freezing curve and glass-transition line. Recently, attempts have been made to add other structural changes with the glass line, freezing curve, and solubility line in the state diagram. Numbers of micro-regions and new terminologies are being included in construction. The state diagram shown in Figure 8.1 is updated from Rahman (2004). In Figure 8.1 the freezing line (ABC) and solubility line (BD) are shown in relation to the glass-transition line (EFS). The point F (X'_s and T'_g) lower than T'_m (point C) is a characteristic transition (maximal-freeze-concentration condition) in the state diagram defined as the intersection of the vertical line from T'_m to the glass line

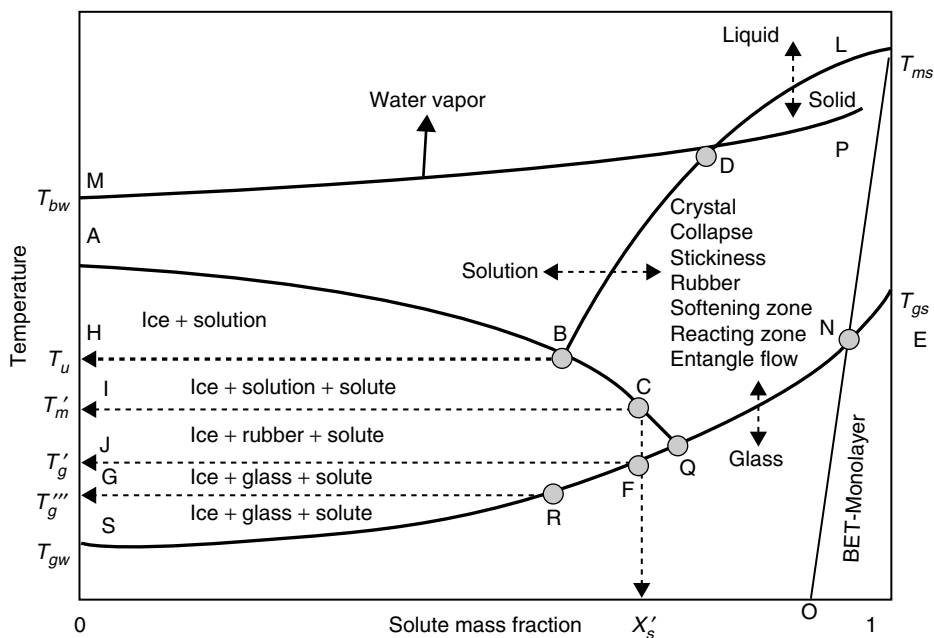


Fig. 8.1 State diagram showing different regions and state of foods (T_{bw} : boiling point, T_u : eutectic point, T'_m : end point of freezing, T'_g : glass transition at end point of freezing, T''_g : glass transition of water, T_{ms} : melting point of dry solids, T_{gs} : glass transition of dry solids (Rahman, 2006).

EFS. The water content at point F or C is considered as the un-freezeable water ($1 - X'_s$). Un-freezeable water mass fraction is the amount of water remaining unfrozen even at a very low temperature. It includes both un-crystallized free water and bound water attached to the solids matrix. The point Q is defined as T''_g and X'_s as the intersection of the freezing curve to the glass line by maintaining the similar curvature. Point R is defined as T'''_g as the glass transition of the solids matrix in the frozen sample, which is determined by DSC. This is due to the formation of same solid matrix associated with un-freezeable water and transformation of all free water into ice, although the sample contains a different level of total water before the start of DSC scanning (Rahman *et al.*, 2005a).

Different zones or regions are marked in the state diagram showing different characteristics. The line BDL is the melting line which is important when products experience high temperatures during processing, such as frying, baking, roasting and extrusion cooking. In the case of a multi-component mixture such as food, a clear melting point is difficult to observe at high temperature due to the reactions between components. In this case Rahman (2004) defined it as the decomposition temperature. Line MDP is the boiling line for water evaporation from the liquid (line MD) and evaporation from solid-liquid matrix (line DP). This line does not intersect the y-axis at the right. The line LNO is drawn from the BET-monolayer stability as a function of temperature, which is discussed later. The region of the drying and freezing process can be easily visualized in the diagram, and product stability could be assessed based on moisture content and temperature.

In the middle of the 20th century scientists discovered the existence of a relationship between the water contained in a food and its relative tendency to spoil (Scott, 1953). They began to realize that active water could be much more important to the stability of a food than

total amount of water present. Thus it was possible to develop generalized rules or limits for the stability of foods using water activity. For example, there is a critical water activity below which no micro-organisms can grow, at about 0.6 value of water activity. A food product is most stable at its monolayer moisture content, which varies with the chemical composition and structure.

Recently the limitations of water activity have been pointed out and alternatives have been proposed (Rahman, 2006). These limitations are: (i) water activity is defined at equilibrium, whereas foods may not be in a state of equilibrium, (ii) the critical limits of water activity may also be shifted to higher or lower levels by other factors, such as pH, salt, anti-microbial agents, heat treatment and temperature, (iii) the nature of the solute used also plays an important role, (iv) it does not indicate the state of the water present and how it is bound to the substrate (Rahman and Labuza, 1999; Chirife, 1994; Scott, 1953; Hardman, 1986). The glass-transition concept was put forward considering the limitations of water activity.

Glass-transition is by nature of a second-order time-temperature dependent transition, which is characterized by a discontinuity in the physical, mechanical, electrical, thermal, and other properties of a material (Rahman, 1995). The process is considered to be a second-order thermodynamic transition in which the material undergoes a change in state but not in phase. It is more meaningful to define as the nature second-order change in the properties since each measurement technique is based on monitoring change in a specific property, and since a change or break in properties are achieved within a certain temperature range rather than a specific temperature. A perfect second-order transition occurs at a specific temperature (Allen, 1993; Kasapis, 2005).

The rules of the glass-transition concept are: (i) the food is most stable at and below its glass transition, and (ii) the higher the $T-T_g$ (i.e. above glass-transition), the higher the deterioration or reaction rates. Similarly mechanical and transport properties could also be related to glass transition. It is very interesting to see that this concept has been so widely tested in foods. In many instances the glass-transition concept does not work alone, thus it is now recommended to use both the water activity and glass-transition concepts in assessing process-ability, deterioration, food stability and shelf-life predictions (Roos, 1995). Recently the concept of a state diagram based on glass transition and freezing curve has been proposed. The food industry is currently using the water activity concept in determining food stability. The scientific evidence shows that the glass-transition concept could be added to their existing criterion on water activity and that this should give better confidence to the food industry in determining the food stability. The food industry could locate their products in the state diagram as a function of solid content and temperature. Based on the location they could determine the stability of their product (Rahman, 2006).

Recently many papers have presented data on water activity as well as the glass transition as a function of water content. However the link between them has not been identified in order to determine stability. Karel *et al.* (1994) attempted to relate water activity and glass-transition by plotting equilibrium water content and glass transition as a function of water activity. By drawing a vertical line on the graph, stability criterion could be determined from isotherm curve and glass-transition line. At any temperature (say 25°C) stability moisture content from the glass-transition line was much higher than the stability moisture from the isotherm. The question is how to use both? At present it is a real challenge to link them. As a first attempt Rahman (2006) plotted a BET-monolayer value as LO line in the state diagram shown in Figure 8.1. It intersects at point N with the glass line ES, which shows that at least in one location (point N) glass and water activity concepts provide the same stability criterion. This approach forms more micro-regions, which could give different stability in the state

Table 8.1 Quality characteristics of dried foods.

Microbial	Chemical	Physical	Nutritional
Pathogens	Browning	Rehydration	Vitamin loss
Spoiling	Oxidation	Solubility	Protein loss
Toxin	Color loss	Texture	Functionality loss
	Aroma development	Aroma loss	Fatty acid loss
	Removal of undesired components	Porosity	
		Shrinkage	
		Pores' characteristics	
		Crust formation	
		Structure	

diagram. More studies regarding stability need to be done on the left (above and below glass) and right sides (above and below) of the line LO. A successful combination of water activity and glass transition could open up more in depth knowledge on stability criteria. In addition it is important to know how other factors, such as pH and preservatives could be linked with these concepts.

8.3 CONTROLLING QUALITY ATTRIBUTES

The quality characteristics of dried foods can be grouped as: microbial, chemical, physical and nutritional or medical (Table 8.1). Initial or optimum freshness plays an important role in determining the quality of dried foods, the fresher or more optimum the raw material, the more stability and quality of the product. Suitable varieties of produce with desired maturity should be used to achieve a desired product with best quality (Su and Chang, 1995).

8.3.1 Microbial quality

Multiplication of micro-organisms should not occur in properly processed dehydrated foods, but they are not immune to other types of food spoilage. If dried foods are safe in terms of pathogenic microbial count and toxic or chemical compounds, then acceptance depends on the flavor or aroma, color, appetizing appearance, texture, taste and nutritional value of the product. Microbial standards are usually based on the total number of indicator organisms or number of pathogens (Rillo *et al.*, 1988). The microbial load and its changes during drying and storage are important information for establishing a standard that will ensure food safety. Poor processing, handling and storage practices often result in a limited storage life of dried fish, for example (Wheeler *et al.*, 1986).

Perishable foods, such as meat and fish are prone to rapid microbial spoilage, thus adequate care must be taken in drying. The microbial load for dried mackerel ranged from 3×10^3 colonies per gram sample to too numerous to count. No evidence of spoilage was detected in the samples with water activity from 0.72 to 0.74. The isolates found were *Alcaligenes*, *Bacillus*, *Leuconostoc*, *Micrococcus*, *Halobacterium*, *Flavobacterium*, *Halococcus*, *Aspergillus*, and *Penicillium*. All the samples were positive for coliform, Streptococcus, and Staphylococcus. *Vibrio* and *Clostridium* were not detected while Salmonella was detected only in some samples (Rillo *et al.*, 1988). Brining and drying decreased the microbial load but did not eliminate

the pathogens. Wheeler *et al.* (1986) studied the common fungi involved in spoiling of dried salted fish. They studied the micro-organisms of dried salted fish with an emphasis on visible spoiled fish and spoilage fungi. A total of 364 isolates from 74 fish were cultured and identified. Wheeler and Hocking (1993) studied the effect of water activity and storage temperature on the growth of fungi associated with dried salted fish. Micro-organisms did grow during drying of highly perishable products such as fish (Trevally) in a heat pump dehumidifier drying at low temperatures of 20–40°C. Lower temperatures gave a lower count regardless of the relative humidity of drying. Sulfur-producing organisms were a significant portion of the total flora in dried fish. Rahman *et al.* (2000) studied the endogenic micro-organism changes in tuna mince during convection air-drying between 40 and 100°C. A drying temperature of 50°C or below showed no lethal effect on the micro-organisms and showed a significant growth. The drying temperature of fish must be above 60°C to avoid microbial risk in the product. The actual optimum temperature above 60°C should be determined based on other quality characteristics of the dried fish (Rahman *et al.*, 2000).

Reducing the water activity of a product inhibits growth, but does not result in a sterile product. The highest possible drying temperatures should be used to maximize thermal death even though low drying temperatures are best for maintaining organoleptic characteristics (Okos *et al.*, 1989). Another alternative is to use a high drying temperature initially at high moisture content and then dry at a low temperature. The microbial deactivation kinetics depends on several factors: variety, water content (i.e. water activity), temperature and compositions of the medium (acidity, types of solids, pH, etc.) as well as heating method (Lopez *et al.*, 1998; Schaffner and Labuza, 1997; Juneja and Marmer, 1998). Models to predict the *D*-values were also developed as a function of temperature, pH, and water activity for isothermal conditions (Gaillard *et al.*, 1998; Cerf *et al.*, 1996). These models could not be used in the case of drying conditions since the level of water content does not remain same for each temperature studied. Bayrock and Ingledew (1997b) measured the *D*-values for the changing moisture content (i.e. drying) and for moist conditions (i.e. no change of moisture during heating). The heat resistance of micro-organisms increased significantly during drying compared to the moist heat conditions. During drying of tuna, Rahman *et al.* (2000) found that decimal reduction time (*D*-value) for endogenous micro-organisms varied from 12.66 to 2.64 h when drying temperature varied from 60 to 100°C, respectively. As expected the values were decreased with the increase of temperature, which indicates that an increase in drying temperature increased the lethal effect also. The *D*-value at 100°C was much lower than the drying temperature at 90°C or below. This may be due to the high drying rate at 100°C (Rahman *et al.*, 2000; Bayrock and Ingledew, 1997a). Rahman *et al.* (2004) investigated the changes in endogenous bacterial counts in minced tuna during dry heating (convection air-drying) and moist heating (heating in a closed chamber) as a function of temperature. The *D*-values for total viable counts decreased from 2.52 to 0.26 h for moist heating and 2.57 to 0.34 h for dry heating, respectively, when temperature was maintained constant within 60–140°C. In both cases, increasing temperature caused significant decrease in *D*-values, whereas the effect of heating methods was not significant. The *Z*-values were found to be 144°C and 46°C for temperatures within 60–100°C and 100–140°C, respectively. Rahman *et al.* (2004) also identified the types and characteristics of endogenous microbes present in fresh and dried tuna. Initially tuna contained a mixture of different microbes, of which some are more heat and/or osmo-tolerant than others. In dried tuna, the predominant microbes were the moderate-osmo-tolerant, and the dominant microbes were heat sensitive.

Rahman *et al.* (2005b) studied the microbial (aerobic plate count, *Pseudomonas*, *Staphylococcus*, molds) and physico-chemical (pH, expressed juice, fatty acid profile, rehydration

ratio, color) characteristics of sun, air, vacuum, freeze, and modified atmosphere (nitrogen gas) -dried goat meat. The modified atmosphere drying showed significant improvement in selected quality attributes, such as shrinkage, color, types of molds and PV values.

8.3.2 Chemical changes and quality

8.3.2.1 Color and Browning reactions

Browning reactions change color, decrease nutritional value and solubility, create off-flavors, and induce textural changes. Browning reactions can be classified as enzymatic or non-enzymatic with the latter being more serious as far as the drying process is concerned. Two major types of non-enzymatic browning are caramelization and Maillard browning. In addition to the moisture level, temperature, pH and the composition are all parameters which affect the rate of non-enzymatic browning. The rate of browning is the most rapid in the intermediate moisture range and decreases at very low and very high moistures. Browning tends to occur primarily at the center of drying period. This may be due to migration of soluble constituents toward the center region. Browning is also more severe near the end of the drying period when the moisture level of a sample is low and less evaporative cooling is taking place which results in the product temperature rises. Several suggestions have been found to reduce browning during drying. In each case, it was emphasized that the product should not experience unnecessary heat when it is in its critical moisture content range (Okos *et al.*, 1989).

Maillard-type non-enzymatic browning reactions in processed meat products also contribute to their external surface color. The main browning reaction involves the reaction of carbonyl compounds with amino groups, although lesser amounts of carbonyl browning also occur. Muscle usually contains small amounts of carbohydrate in the form of glycogen, reducing sugars and nucleotides, while the amino groups are readily available from the muscle proteins. Browning occurs at temperatures of 80–90°C and increases with time and temperature (Chang *et al.*, 1996). A loss of both amino acids and sugars from the tissue occurs as a result of the browning reaction. Lysine, histidine, threonine, methionine and cysteine are some of the amino acids that may become involved in browning (Hsieh *et al.*, 1980a). Potter (1986) identified that Maillard browning proceeds most rapidly during drying if moisture content is decreased to a range of 15–20%. As the moisture content drops further, the reaction rate slows, so that in products dried below 2% moisture further color change is not perceptible even during subsequent storage. Drying systems or heating schedules generally are designed to dehydrate rapidly through the 15–20% moisture range so as to minimize the time for Maillard browning. In carbohydrate foods browning can be controlled by removing or avoiding amines and conversely in protein foods by eliminating the reducing sugars.

Development of a brown center sometimes occurs in macadamia nuts if high-moisture nuts are dried at elevated temperatures (Prichavudhi and Yamamoto, 1965). Heat pump drying of macadamia nuts did not result in the above defects, even when they were dried at 50°C (Van Blarcom and Mason, 1988). Mason (1989) studied the heat pump drying of macadamia kernels and herbs with temperature and relative humidity ranges of 30–50°C and 0.10–0.50, respectively. Freshly harvested macadamia nuts can be dried rapidly up to a moisture content of 0.015 with no loss in quality, and there was no significant difference of quality when dried under the conditions mentioned above. This may be due to the faster drying rates associated with the heat pump drying process (Perera and Rahman, 1997). The losses in color, flavor and nutritive value associated with dried products are attributed to non-enzymatic browning.

It is recognized that the rate of reaction for non-enzymatic browning in dried products is highest at moisture levels that are commonly attained toward the end of the drying cycle, when the drying rate is low and the product temperature approaches that of the drying medium. However, the lower drying temperatures used throughout the drying cycle in heat pump driers reduce the extent of non-enzymatic browning reactions. The sensory color and aroma of herbs (e.g. parsley, rosemary, and sweet fennel) were nearly doubled in case of heat pump dried compared to commercially dried products. In the case of drying in a modified atmosphere, O'Neill *et al.* (1998) showed that browning of apple cubes during drying could be arrested when the oxygen level in the atmosphere is less than 0.5%.

Smoking, mainly used for meat and fish, imparts desirable flavors and colors to the foods and provides preservative effects (bactericidal and antioxidant) (Cohen and Yang, 1995). The odor, composition of flavor compounds, and antimicrobial activity of the smoked product are recognized to be highly dependent on the nature of the wood. Some studies have recognized beech and oak woods as those which produce wood smoke with the best sensory properties (Guillen and Ibargoitia, 1996). Smoking is a slow process and it is not easy to control. Smoke contains phenolic compounds, acids, and carbonyls and smoke flavor is primarily due to the volatile phenolic compound (Deng *et al.*, 1974; Jarvis, 1987). Wood smoke is extremely complex and more than 400 volatiles have been identified (McIlveen and Valley, 1996; Guillen and Manzanos, 1999). Polycyclic aromatic hydrocarbons are ubiquitous in the environment as pyrolysis products of organic matter. Its concentrations in smoked food can reach levels hazardous for human health, especially when the smoking procedure is carried out under uncontrolled conditions (Moret *et al.*, 1999). Wood smoke contains nitrogen oxides, polycyclic aromatic hydrocarbons, phenolic compounds, furans, carbonylic compounds, aliphatic carboxylic acids, tar compounds, carbohydrates, pyrocatechol, pyrogallols, organic acids, bases and also carcinogenic compounds like 3:4 benzpyrene. Nitrogen oxides are responsible for the characteristic color of smoked food whereas polycyclic aromatic hydrocarbon components and phenolic compounds contribute to its unique taste. These three chemicals are also the most controversial from a health perspective (McIlveen and Valley, 1996). The level of fats in fish affects texture, oiliness, and color of smoked salmon during storage (Sheehan *et al.*, 1996; Deng *et al.*, 1974). Color development in smoked fish is a complex process. Maillard type browning with glycolic aldehyde, and methyglyoxal in the dispense phase of smoke is the dominant role. Several types of synthetic colors, paprika, caramel and seasoning can also be used (Abu-Bakar *et al.*, 1994).

8.3.2.2 Lipid oxidation

Dehydrated foods containing fats are prone to develop rancidity after a period, particularly if the water content is reduced too much. Fish oils or fats are more unsaturated than beef or butter, and they are usually classified as drying oils because they contain considerable proportions of highly unsaturated acids. The high degree of un-saturation of omega-3 fatty acids in fish and their close proximity to strong pro-oxidative systems predispose them to oxidation, which converts them to compounds that negatively affect the quality attributes of fish and have a hazardous effect on health. The best known quality attribute degradation is the development of rancid flavor. In addition, other quality attributes such as color and texture deteriorate as a consequence of lipid oxidation. The behavior of drying oils toward atmospheric oxygen is well known, and oxidation is a serious problem for commercial drying of fatty fish and seafood. The flesh of some fatty fish, such as herrings, contains a fat pro-oxidant that is not wholly inactivated by heat (Banks, 1950).

Lipid oxidation is responsible for rancidity, development of off-flavors, and the loss of fat-soluble vitamins and pigments in many foods, especially in dehydrated foods. Factors which affect oxidation rate include: moisture content, type of substrate (fatty acid), extent of reaction, oxygen content, temperature, presence of metals, presence of natural antioxidants, enzyme activity, UV light, protein content, free amino acid content and other chemical reactions. Moisture content plays a big part in the rate of oxidation. At water activities around the monolayer ($a_w \approx 0.3$), resistance to oxidation is greatest. Several hypotheses have been reported to explain the protective effect of water in retarding lipid oxidation. The most important ones are (Maloney *et al.*, 1966): (i) water has a protective effect due to retardation of oxygen diffusion, (ii) water decreases the effect of metal catalysts such as copper and iron, (iii) water is attached to sites on the surface, thereby preventing oxygen uptake by these sites, (iv) water promotes non-enzymatic browning, which may result in formation of antioxidant compounds, and (v) water forms hydrogen bonds with hydro-peroxides and retards hydro-peroxide decomposition.

The elimination of oxygen from foods can reduce oxidation, but the oxygen concentration must be very low to have an effect. The effect of oxygen on lipid oxidation is also closely related to the product porosity. Freeze-dried foods are more susceptible to oxygen because of their high porosity. Air-dried foods tend to have less surface area for pores due to shrinkage, and are thus not affected by oxygen. Minimizing the oxygen level during processing and storage, and adding antioxidants as well as sequesterants is recommended in the literature to prevent lipid oxidation (Okos *et al.*, 1989). Fish oils or fats are drying oils, which rapidly absorb oxygen from the air and harden, just as paints harden on exposure to air. Fatty fish must be dehydrated quickly in a vacuum, and must be stored in vacuum or in an atmosphere of an inert gas (Jarvis, 1987).

Antioxidants added to the herrings before drying are ineffective, but the addition to the air during drying of wood smoke, which contains some of the simple antioxygenic phenols, stabilizes the fat of the dehydrated products very considerably (Banks, 1950). Oxidation of the fat normally occurs during dehydration. Herrings and haddock dried at 80–90°C, compared to lower temperatures, were found more stable during storage (Banks, 1950). One factor that may be important is that the production of browning products from proteins or non-fatty parts give antioxidant activity. The effectiveness of non-enzymatic browning products in preventing lipid oxidation is demonstrated and is one of the mechanisms hypothesized by Karel (1986) to prevent lipid oxidation.

The effects of water on the destruction of the protective food structure in some specific dehydrated foods is probably involved in the prevention of lipid oxidation in heated meat systems (Karel, 1986). In systems in which there are both surface lipids and lipids encapsulated within a carbohydrate, polysaccharide or protein matrix, the surface lipids oxidize readily when exposed to air. The encapsulated lipids, however, do not oxidize until the structure of the encapsulated matrix is modified and/or destroyed by adsorption of water. Another reason is the increase of oxygen diffusion by increasing molecular mobility above the glass–rubber transition (Roos and Karel, 1992).

The peroxide values (PV) and thiobarbituric values (TBA) are the major chemical indices of oxidative rancidity. The primary product of lipid oxidation is the fatty acid hydro-peroxide, measured as PV. Peroxides are not stable compounds and they break down to aldehydes, ketones and alcohols which are the volatile products causing off-flavor in products. The TBA value measures secondary products of lipid oxidation. TBA consists mainly of malondialdehydes as a representative of aldehydes. Oxidized unsaturated fatty acids bind to protein and form insoluble lipid–protein complexes.

The peroxide values of different dried meat samples were studied by Rahman *et al.* (2005b). The values were significantly different according to the methods of drying. Freeze drying gave the highest value, while air drying gave the lowest. Similar results were also observed in case of air-dried, vacuum-dried and freeze-dried tuna meat (Rahman *et al.*, 2002). Rahman *et al.* (2002) indicated that this was due to the fact of increased oxygen diffusion and exposed surface area with the increase of porosity in the case of freeze-dried samples.

8.3.2.3 Changes in proteins

The protein matrix in muscle has a marked effect upon its functionality and properties (Schmidt *et al.*, 1981). The non-fatty part of fish is very susceptible to changes caused by the high temperature of initial cooking, drying and storage. Every process involved in the conversion of muscle to meat alters the characteristics of the structural elements (Stanley, 1983). Heating is believed to cause the denaturation of the muscle proteins, even below 60°C, but not enough to greatly shear resistance (Sebranek, 1988). The decrease in shear observed at 60°C was attributed to collagen shrinkage. Hardening at 70–75°C was believed to be due to increased cross-linking and water loss by the myofibrillar proteins, while decreasing shear at higher temperatures may indicate solubilization of collagen (Chang *et al.*, 1996). After 1 h at 50°C, the collagen fibrils of the endomysium appear beaded, which is brought about by their close association with the heat-denatured non-collagenous proteins in the extracellular spaces. Heat denaturation of the lipoprotein plasmalemma results at a temperature of 60°C for 1 h. The breakdown products of the plasmalemma are large granules and are often associated with the basement lamina, which appears to survive intact even after heating at 100°C for 1 h (Rowe, 1989a,b).

8.3.3 Physical changes and quality

8.3.3.1 Structural changes

Structural changes in food during drying are usually studied by microscopy. It provides a good tool to study this type of phenomena as well as other types of physical and chemical changes during the drying of food materials. Shrinkage occurs first at the surface and then gradually moves to the bottom with an increase in drying time (Wang and Brennan, 1995). The cell walls became elongated. As drying proceeds at higher temperatures, cracks are formed in the inner structure. From microscopy it was found that shrinkage of apple samples dried by convection is significantly an-isotropic, while less damage to the cell structure during freeze drying leads to a more isotropic deformation (Moreira *et al.*, 1998). The cellular structure of microwave-vacuum dried apple with and without osmotic treatment indicated collapse of the cellular structure in the untreated apple (Erle and Schubert, 2001). Osmotic treatment prior to vacuum drying preserved the cellular structure by keeping its three-dimensional nature. Electron microscopic investigations of the cell structure in dried carrots and green bean showed that drying leads to shrinkage and twisting of the cells and clumping of the cytoplasm (Grote and Fromme, 1984). Histological changes in air-dried, freeze-dried and osmotically treated freeze-dried samples showed that air-dried samples displayed the elongated and thinned cell wall and enlarged inter-cellular air spaces (Lee *et al.*, 1967).

Heating produces major changes in muscle structure. Voyle (1981) reviewed modifications in cooked tissue observable with the scanning electron microscope. Alteration in muscle structure due to heating includes coagulation of the perimysial and endomysial connective

tissue, sarcomere shortening, myofibrillar fragmentation and coagulation of sarcoplasmic proteins (Hsieh *et al.*, 1980b; Voyle, 1981). Heating and/or drying intensifies the detachment of the myofibrils from the muscle fiber bundles, which is caused mainly by electrical stunning or stimulation and improper conditioning following slaughter (Chang and Pearson, 1992).

Rehydration is maximized when cellular and structural disruption, such as shrinkage, is minimized (Okos *et al.*, 1989). Chang *et al.* (1991) illustrate the morphological changes that occur in the appearance of the muscle fiber bundles during cooking and drying in convection heated rotary drier. They found that after cooking the fibers are bound together in a compact bundle. The bundle size is gradually reduced due to the effects of heating and tumbling during the early stage of pre-drying in the modified clothes drier. Apparent bundle size is expanded with the endomysial capillary moisture being removed during drying.

8.3.3.2 Case hardening or crust formation

During drying, the concentration of moisture in the outer layers is less than in the interior, since outer layers necessarily lose moisture before interior. This surface shrinkage causes checking, cracking and warping. This type of shrinkage causes moisture gradient and resistance near the surface. In extreme cases, the shrinkage and drop in diffusivity may combine to give a skin practically impervious to moisture, which encloses the volume of the material so that interior moisture cannot be removed. This is called case hardening. In food processing, case hardening is also commonly known as crust formation. The extent of crust formation can be reduced by maintaining flattening moisture gradients in the solid, which is a function of drying rate. The faster the drying rate, the thinner the crust formation (Achanta and Okos, 1996). Crust (or shell) formation may be either desirable or undesirable in dried food products. In micro-encapsulation of flavors, rapid crust formation is required to prevent flavor losses. Achanta and Okos (1996) pointed out that crust formation may be inhibited by allowing the drying rate to be slow enough that moisture loss from the product surface is replenished by moisture from inside. Crust formation is also important in explosion puffing. In this case the high-moisture product is exposed to rapid drying conditions, such as high temperature and vacuum, which create crust. The impermeable crust coupled with the extreme drying conditions results in rapid moisture vaporization and causes large internal pressures to build up, resulting in product expansion/puffing. During the expansion stage, stress build up in the glassy surface may cause the surface to crack, allowing vapor to escape.

8.3.3.3 Shrinkage or collapse and pore formation

Two types of shrinkage are usually observed in the case of food materials: isotropic and an-isotropic shrinkage. Isotropic shrinkage can be described as the uniform shrinkage in all geometric dimensions of the materials. An-isotropic shrinkage is described as the non-uniform shrinkage in the different geometric dimensions. In many cases, it is important to estimate the changes in all characteristic geometric dimensions to characterize a material. In the case of muscle, such as fish and seafood, shrinkage in the direction parallel to muscle fibers was significantly different from that perpendicular to the fibers during air drying. This is different from the very isotropic shrinkage of most fruits and vegetables (Balaban and Pigott, 1986; Rahman and Potluri, 1990).

Shrinkage is an important phenomenon impacting on dried food product quality by reducing product wettability, changing product texture and decreasing product absorbency. Depending on the end use, crust and pore formation may be desirable or undesirable. If a long

bowl life is required for a cereal product, a crust product that prevents moisture re-absorption may be preferred. If a product (such as dried vegetables in instant noodles) with good rehydration capacity is required, a highly porous product with no crust is required. Rahman (2001) provides the present knowledge on the mechanism of pore formation in foods during drying and related processes. The glass-transition theory is one of the proposed concepts to explain the process of shrinkage and collapse during drying and other related process. According to this concept, there is negligible collapse (more pores) in a material if it is processed below glass transition, and the higher the difference between the process temperature and the glass-transition temperature, the higher the collapse. The methods of freeze drying and hot air drying can be compared based on this theory. In freeze drying, since the temperature of drying is below T'_g (maximally freeze concentrated glass-transition temperature), the material is in the glassy state. Hence shrinkage is negligible. As a result the final product is very porous. In hot air drying, on the other hand, since the temperature of drying is above T'_g or T_g , the material is in the rubbery state and substantial shrinkage occurs. Hence the food produced from hot air drying is dense and shrivelled (Achanta and Okos, 1996). However, the glass-transition theory does not hold true for all products. Other concepts such as surface tension, structure, environmental pressure and mechanisms of moisture transport also play important roles in explaining the formation of pores. Rahman (2001) hypothesized that as capillary force is the main force responsible for collapse, so counterbalancing of this force causes formation of pores and lower shrinkage. The counterbalancing forces are due to generation of internal pressure, variation in moisture transport mechanisms and environmental pressure. Another factor could be the strength of the solid matrix (i.e. ice formation, case hardening and matrix reinforcement).

Cooking as a pre-treatment may cause excessive shrinkage or toughening (Potter, 1986) as well as a decrease in the water-holding capacity of meat (Stanley, 1983). Apple cubes dried in a nitrogen atmosphere had more open pores and uniform shrinkage than those air dried in air and vacuum (O'Neill *et al.*, 1998). Hawlader *et al.* (2006a) observed that apple tissues dried in a modified atmosphere showed lighter color, lower density values, porous (non-collapsed) structure and better rehydration properties, compared to those dried by most other commonly used drying methods.

8.3.3.4 Stress development and cracking or breakage

During air-drying, stresses are formed due to non-uniform shrinkage resulting from non-uniform moisture and/or temperature distributions. This may lead to stress crack formation, when stresses exceed a critical level. Crack formation is a complex process influenced interactively by heat and moisture transfer, physical properties and operational conditions (Liu *et al.*, 1997). Air relative humidity and temperature are the most influential parameters that need to be controlled to eliminate formation of cracks.

Breaking and breakage of dried foods has two undesirable consequences: loss of valuable product and loss of consumer satisfaction (Achanta and Okos, 1996). Cracking is detrimental to grain quality since affected kernels are more susceptible to mold attack during storage and pathogenic invasion after seeding. Cracked grains are also of lower organoleptic quality, which limits their use in direct food preparation. Internal cracking in the starchy endosperm of a grain is induced by mechanical stress due to the high humidity gradient inside the kernel and/or to thermal stress. The fissure is a large internal fracture usually found to be perpendicular to the long axis of grain (Sharma and Kunze, 1982). The drying rate, which is a function of drying temperature and humidity, is the main cause of fissures (Du-Peuty *et al.*, 1996;

Bonazzi *et al.*, 1994; Sarker *et al.*, 1996). The process of fissures also continues after drying. Most fissuring occurs within 48 h after drying, but additional fissures develop at a low rate for another 72 h thereafter (Kunze, 1979). In microwave drying, stress cracking can be even more pronounced due to superposition of the pressure gradient that may build up within the material under certain drying conditions (Turner and Jolly, 1991). In the case of wheat it is also depends on the variety (Kudra *et al.*, 1994). The higher humidity air damages grains to a lesser extent than low-humidity air. Grains are severely damaged by high drying temperatures (Sokhansanj, 1982).

In the case of plant materials, cracks are also formed. At higher drying rates the outer layers of the material become rigid and their final volume is fixed early in the drying. As drying proceeds, the tissues split and rupture internally, forming an open structure, and cracks are formed in the inner structure. When the interior finally dries and shrinks, the internal stresses pull the tissue apart (Wang and Brennan, 1995). Initial structure before drying can also create a different extent of cracks inside as well as on the surface.

8.3.3.5 Rehydration

Rehydration is the process of moistening dry material. Mostly it is done by abundant amounts of water. In most cases dried food is soaked in water before cooking or consumption, thus rehydration is one of the important quality criteria. In practice, most of the changes during drying are irreversible and rehydration cannot be considered simply as a reverse process to dehydration (Lewicki, 1998). In general, absorption of water is fast at the beginning and thereafter slows down. A rapid moisture uptake is due to surface and capillary suction. Rahman and Perera (1999), and Lewicki (1998) reviewed the factors affecting the rehydration process. These factors are porosity, capillaries and cavities near surface, temperature, trapped air bubbles, amorphous–crystalline state, soluble solids, dryness, anions and pH of soaking water. Porosity, capillaries and cavities near the surface enhance the rehydration process, whereas the presence of trapped air bubbles gives a major obstacle to the invasion of fluid. Until the cavities are filled with air, water penetrates to the material through its solid phase. In general, temperature strongly increases the early stages of water rehydration. There is a resistance of crystalline structures to solvation that causes development of swelling stresses in the material, whereas amorphous regions hydrate fast. The presence of anions in water affects the volume increase during water absorption.

8.3.3.6 Volatile development or retention

In addition to physical changes, drying generates flavor or releases flavor from foods. Drying changes the composition of volatiles by evaporating most and by forming new volatile odor compounds by chemical reactions (Luning *et al.*, 1995; Van-Ruth and Roozen, 1994). Such changes in volatiles may cause off-flavor when peanuts were dried above 35°C. In the case of the peanut, they observed that the amount of off-flavor detected appeared to be a function of drying air temperature and moisture content and that the off-flavor was more likely to occur in immature peanuts than in mature peanuts (Osborn *et al.* 1996). Off-flavors resulting from high-temperature drying can be passed on to peanut butter and roasted peanuts. Acetaldehyde and ethyl acetate may be better indicators of off-flavor. Higher temperature drying of pasta also related to off-color and off-flavor (Resmini *et al.*, 1996). The loss of a volatile varies with its concentration, with the greatest loss occurring during the early stages

of drying. Blanching time correlated with flavor and sensory attributes of dried fruits and vegetables (Shamaila *et al.*, 1996).

A substantial volatile loss occurs during the first three stages of spray drying, and there should be zero or very little loss of volatiles during the fourth stage due to selective diffusion (King, 1994). Losses can occur during atomization, from undisturbed drops and as a result of morphological development. Several factors affect volatile retention, including control of atomizer pressure or rotation speed, choice of spray angle, configuration of air input, alteration of air temperature profile, feed concentration, presence of an oil phase and/or suspended solids, foaming of the feed, feed composition, surfactant and steam blanketing of atomizer (King, 1984, 1994; Kieckbusch and King, 1980). The retention increased with increasing initial concentration of solids, increasing air temperature and velocity and decreasing humidity. This is due to the selective diffusion mechanism, when surface water content is reduced sufficiently so that the diffusion coefficients of volatile substances become substantially lower than that of water (Kieckbusch and King, 1980; King, 1984).

Ginger dried in a heat pump drier was found to retain over 26% of gingerol, the principal volatile flavor component responsible for its pungency, compared to only about 20% in rotary dried commercial samples (Mason *et al.*, 1994). The higher retention in heat pump dried samples may be due to the reduced degradation of gingerol at the lower drying temperature used compared with the commercial drier temperatures. Since heat pump drying is conducted in a sealed chamber, any compound that volatilizes will remain within it, and the partial pressure for that compound will gradually build up within the chamber, retarding further volatilization from the product (Perera and Rahman, 1997).

8.3.3.7 Caking and stickiness

Caking and stickiness of powders, desirable or undesirable, occurs in dried products. Caking is desirable for tablet formation and is undesirable when a dry free-flowing material is required. To reduce caking during drying, a logical option is to dry rapidly so that the moisture content drops to a level where caking is inhibited. The rapid drying will form a crust, which may be undesirable, thus product optimization or solutes in product formulation may be considered. Tendencies to form surface folds on particles during spray drying are governed by the viscosity of the concentrated solution. Stickiness and agglomeration tendencies also depend upon the viscosity of the concentrated solution, surface tension, particle size and exposure time (King, 1984). For viscosities below the critical value, stickiness usually occurs. The predicted critical viscosity was within the range of 10^8 – 10^{10} Pa s. The mechanism of sticking and agglomeration was postulated through viscous flow driven by surface tension and forming bridges between particles (Downton *et al.*, 1982). Adhikari *et al.* (2001) presented a complete review on stickiness in foods including mechanisms and factors controlling the process. The main factors affecting stickiness are temperature, viscosity and water followed by low molecular sugars, organic acids and compaction or pressure. The use of the glass-transition temperature-based model provides a rational basis for understanding and characterizing the stickiness of many foods.

8.3.3.8 Texture

Factors that affect texture include moisture content, composition, variety or species, pH, product history (maturation or age) and sample dimensions. Texture is also dependent on the method of dehydration and pre-treatments. Purslow (1987) stated that meat texture is

affected by the structure of the solid matrix. He concluded that it is important to have a fundamental understanding of the fracture behavior of meat and how it relates to the structure of the material. Stanley (1983) stated that many researchers now believe the major structural factors affecting meat texture are associated with connective tissues and myofibrillar proteins. Moreover, two other components, muscle membranes and water, also deserve consideration – not because of their inherent physical properties, but rather as a result of the indirect influence they have on the physical properties. It should be noted that sarcoplasmic proteins could be important for the same reason, although little information on their role is available.

Kuprianoff (1958) referred to the possible adverse effects of removing bound water from foods as: (i) denaturation of protein by concentration of the solutes, (ii) irreversible structural changes leading to textural modification upon rehydration, (iii) storage stability problems. Stanley (1983) stated that the water holding capacity of muscle is related to its sorption properties. The bound water in the muscle is primarily a result of its association with the myofibrillar proteins as indicated by Wismer-Pedersen (1971). Protein–water interactions significantly affect the physical properties of meat (Hamm, 1960). Changes in water holding capacity are closely related to pH and to the nature of muscle proteins.

8.3.4 Vitamins retention

In general, losses of B vitamins are usually less than 10% in dried foods. Dried foods do not greatly contribute to dietary requirements for thiamin, folic acid and vitamin B-6. Vitamin C is largely destroyed during drying due to heating (Chang *et al.*, 1996). Fruits dried in a modified atmosphere retained the highest level of nutrients, such as vitamin C and flavor compounds (Hawladar *et al.*, 2006b). From non-fatty vegetables, such as cabbage, as much water as possible should be removed, because this helps to conserve ascorbic acid. The loss of vitamin A and ascorbic acid in dried products could be avoided in the absence of oxygen. Even though most amino acids are fairly resistant to heating-drying, lysine is quite heat labile and likely to be borderline or low in the diet of humans and especially so in developing countries where high quality animal proteins are scarce and expensive (Erbersdobler, 1986).

8.4 CONCLUSION

Drying in earlier times was done in the sun, now many types of sophisticated equipment and methods are used to dehydrate foods. The quality aspect of dried foods during drying and after drying is a very complex phenomenon. Recently, considerable efforts have been made to understand the chemical and biochemical changes that occur during dehydration and to develop methods for preventing undesirable quality losses. Generic concepts of determining the stability of foods during drying and storage are far from reality. In this chapter, the concepts of glass transition and water activity are discussed in the state diagram. In addition, factors affecting the microbial, chemical, physical and nutritional quality of foods are discussed for dried foods.

REFERENCES

- Abu-Bakar, A., Abdullah, M.Y. and Azam, K. (1994) The effects of caramel on the quality of smoked fish. *ASEAN Food Journal*, 9(3), 116–119.

- Achanta, S. and Okos, M.R. (1996). Predicting the quality of dehydrated foods and biopolymers – research needs and opportunities. *Drying Technology*, **14**(6), 1329–1368.
- Adhikari, B., Howes, T., Bhandari, B.R. and Truong, V. (2001) Stickiness in foods: A review of mechanisms and test methods. *International Journal of Food Properties*, **4**(1), 1–33.
- Allen, G. (1993) A history of the glassy state. In: *The Glassy State in Foods* (eds J.M.V. Blanshard and P.J. Lillford). Nottingham University Press, Nottingham, pp. 1–12.
- Balaban, M. and Pigott, G.M. (1986) Shrinkage in fish muscle during drying. *Journal of Food Science*, **51**(2), 510–511.
- Banks, A. (1950) *Journal of the Science of Food and Agriculture*, **1**, 28–34.
- Bayrock, D. and Ingledew, W.M. (1997a) Fluidized bed drying of baker's yeast: Moisture levels, drying rates, and viability changes during drying. *Food Research International*, **30**(6), 407–415.
- Bayrock, D. and Ingledew, W.M. (1997b) Mechanism of viability loss during fluidized bed drying of baker's yeast. *Food Research International*, **30**(6), 417–425.
- Bonazzi, C., Courtois, F., Geneste, C., Pons, B., Lahon, M.C. and Bimbenet, J.J. (1994) Experimental study on the quality of rough rice related to drying conditions. In: *Drying '94* (eds V. Rudolph, R.B. Key and A.S. Mujumdar), *Drying Symposium*. Gold Coast, Australia, pp. 1031–1036.
- Cerf, O., Davey, K.R. and Sadoudi, A.K. (1996) Thermal inactivation of bacteria – a new predictive model for the combined effect of three environmental factors: Temperature, pH and water activity. *Food Research International*, **29**(3–4), 219–226.
- Chang, S.F., Huang, T.C. and Pearson, A.M. (1991) Some parameters involved in production of Zousoon – a semi-dry, long fibered pork product. *Meat Science*, **30**, 303–325.
- Chang, S.F. Huang, T.C. and Pearson, A.M. (1996) Control of the dehydration process in production of intermediate-moisture meat products: A review. *Advances in Food and Nutrition Research*, **39**, 71–161.
- Chang, S.F. and Pearson, A.M. (1992) Effect of electrical stunning or sticking without stunning a microstructure of Zousoon, a Chinese semi dry pork product. *Meat Science*, **31**, 309.
- Chirife, J. (1994) Specific solute effects with special reference to *Staphylococcus aureus*. *Journal of Food Engineering*, **22**, 409–419.
- Cohen, J.S. and Yang, T.C.S. (1995) Progress in food dehydration. *Trends in Food Science and Technology*, **6**, 20–25.
- Deng, J., Toledo, R. T. and Lillard, A. (1974) Effect of smoking temperatures on acceptability and storage stability of smoked Spanish mackerel. *Journal of Food Science*, **39**, 596–601.
- Downton, G.E., Flores-Luna, J.L. and King, C.J. (1982) Mechanism of stickiness in hygroscopic, amorphous powders. *Industrial and Engineering Chemistry Fundamentals*, **21**, 447.
- Du-Peuty, M.A., Themelin, A., Cruz, J.F., Arnaud, G. and Fohr, J.P. (1996) Improvement of paddy quality by optimizing of drying conditions. *Drying '94 Proceedings of the 9th International Drying Symposium*. Gold Coast, Australia, p. 929.
- Erbersdobler, H.F. (1986) In: *Concentration and Drying of Foods* (ed. D. MacCarthy). Elsevier, London, pp. 69–87.
- Erle, U. and Schubert, H. (2001) Combined osmotic and microwave-vacuum dehydration of apples and strawberries. *Journal of Food Engineering*, **49**, 193–199.
- Gaillard, S., Leguerinel, I. and Mafart, P. (1998) Modelling combined effects of temperature and pH on the heat resistance of spores of *Bacillus cereus*. *Food Microbiology*, **15**, 625–630.
- Grote, M. and Fromme, H.G. (1984) Electron microscopic investigations of the cell structure in fresh and processed vegetables (carrots and green bean pods). *Food Microstructure*, **3**, 55–64.
- Guillen, M.D. and Ibargoitia, M.L. (1996) Volatile components of aqueous liquid smokes from *Vitis vinifera* L. shoots and *Fagus sylvatica* L. wood. *Journal of the Science of Food and Agriculture*, **72**(1), 104–110.
- Guillen, M.D. and Manzano, M.J. (1999) *Journal of the Science of Food and Agriculture*, **79**, 1267–1274.
- Hamm, R. (1960) Biochemistry of meat hydration. *Advances in Food Research*, **10**, 355–463.
- Hardman, T.M. (1986) Interaction of water with food component. In: *Interaction of Food Components* (eds G.G. Birch and M.G. Lindley). Elsevier Applied Science Publishers, London and New York, pp. 19–30.
- Hawladar, M.N.A., Perera, C.O. and Tian Min (2006a) Properties of modified atmosphere heat pump dried foods. *Journal of Food Engineering*, **74**(3), 392–401.

- Hawladar, M.N.A., Perera, C.O. and Tian Min (2006b) Comparison of the retention of 6-gingerol in drying of ginger under modified atmosphere heat pump drying and other drying methods. *Drying Technology*, **24**(1), 51–56.
- Hsieh, Y.C., Pearson, A.M., Morton, I.D. and Magee, W.T. (1980a) Some changes in the constituents upon heating a model meat flavour system. *Journal of the Science of Food and Agriculture*, **31**, 943–949.
- Hsieh, Y.P.C., Cornforth, D.P. and Pearson, A.M. (1980b) Ultrastructural changes in pre- and post-rigor beef muscle caused by conventional and microwave cookers. *Meat Science*, **4**, 299.
- Jarvis, D. (1987) In: *Curing of Fishery Products*. Teaparty Books, Kingston, MA, USA.
- Juneja, V. K. and Marmer, B. S. (1998) Thermal inactivation of *Clostridium perfringens* vegetative cells in ground beef and turkey as affected by sodium pyrophosphate. *Food Microbiology*, **15**, 281–287.
- Karel, M. (1986). In: *Concentration and Drying of Foods* (ed. D. MacCarthy). Elsevier, London, pp. 37–68.
- Karel, M., Anglea, S., Buera, P., Karmas, R., Levi, G. and Roos, Y. (1994) Stability-related transitions of amorphous foods. *Thermochimica Acta*, **246**, 249–269.
- Kasapis, S. (2005) Glass transition phenomena in dehydrated model systems and foods: A review. *Drying Technology*, **23**(4), 731–758.
- Kieckbusch, T.G. and King, C.J. (1980) Volatiles loss during atomization in spray drying. *AIChE Journal*, **26**, 718.
- King, C.J. (1984) Transport processes affecting food quality in spray drying. In: *Engineering and Food. Volume 2: Processing and Applications* (ed. B.M. McKenna). Elsevier Applied Science Publishers Ltd., Essex, pp. 559–574.
- King, C. J. (1994) Spray drying: Retention of volatile compounds revisited. In: *Drying '94. Proceedings of the 9th International Drying Symposium (IDS '94)*. Gold Coast, Australia, August 1–4, 1994, pp. 15–26.
- Kudra, T., Niewczas, J., Szot, B. and Raghavan, G.S.V. (1994) Stress cracking in high-intensity drying: Identification and quantification. In: *Drying '94* (eds V. Rudolph, R.B. Keey and A.S. Mujumdar), *Proceedings of the 9th International Drying Symposium*. Gold Coast, Australia, p. 809.
- Kunze, O.R. (1979) Fissuring of the rice grain after heated air drying. *Transactions of the ASAE*, **22**, 1197.
- Kuprianoff, J. (1958) *Fundamental Aspects of Dehydration of Foodstuffs*. Society of Chemical Industry, London.
- Lee, C.Y., Salunkhe, D.K. and Nury, F.S. (1967) Some chemical and histological changes in dehydrated apple. *Journal of the Science of Food and Agriculture*, **18**, 89–93.
- Lewicki, P.P. (1998) Effect of pre-drying treatment, drying and rehydration on plant tissue properties: A review. *International Journal of Food Properties*, **1**(1), 1–22.
- Liu, H., Zhou, L. and Hayakawa, K. (1997) Sensitivity analysis for hygrostress crack formation in cylindrical food during drying. *Journal of Food Science*, **62**(3), 447–450.
- Lopez, M., Martinez, S., Gonzalez, J., Martin, R. and Bernado, A. (1998) Sensitization of thermally injured spores of *Bacillus stearothermophilus* to sodium benzoate and potassium sorbate. *Letters in Applied Microbiology*, **27**, 331–335.
- Luning, P.A., Yuksel, D., De Vries, R.V.D.V. and Roozen, J.P. (1995) Aroma changes in fresh bell peppers (*Capsicum annuum*) after hot-air drying. *Journal of Food Science*, **60**, 1269–1276.
- Maloney, J., Labuza, T.P., Wallace, D.H. and Karel, M. (1966) Autooxidation of methyl linoleate in freeze-dried model systems. I. Effect of water on the autocatalyzed oxidation. *Journal of Food Science*, **31**, 878–884.
- Mason, R.L. (1989) Application of heat pumps to drying food products. *Food Australia*, **41**(12), 1070–1071.
- Mason, R.L., Britnell, P.M., Young, G.S., Birchall, S., Fitz-Payne, S. and Hesse, B.J. (1994) Development and application of heat pump dryers to Australian food industry. *Food Australia*, **46**(7), 319–322.
- McIlveen, H. and Valley, C. (1996) Something's smoking in the development kitchen. *Nutrition Food Science*, **6**, 34–38.
- Moreira, R., Villate, J.E., Figueiredo, A. and Sereno, A. (1998) Shrinkage of apple slices during drying by warm air convection and freeze drying. In: *Drying '98. Proceedings of the 11th International Drying Symposium (IDS '98)*, Vol. B. Halkidiki, Greece, August 19–22, pp. 1108–1114.
- Moret, S., Contre, L. and Dean, D. (1999) Assessment of polycyclic aromatic hydrocarbon content of smoked fish by means of a fast HPL/HPLC method. *Journal of Agriculture Food Chemistry*, **47**, 1367–1371.
- O'Neill, M.B., Rahman, M.S., Perera, C.O., Smith, B. and Melton, L.D. (1998) Color and density of apple cubes in air and modified atmosphere. *International Journal of Food Properties*, **1**(3), 197–205.

- Okos, M.R., Bell, L., Castaldi, A. *et al.* (1989) *Design and Control of Energy Efficient Food Drying Processes with Specific Reference to Quality*. Report Purdue University, IN, USA.
- Osborn, G.S., Young, J.H. and Singleton, J.A. (1996) Measuring the kinetics of acetaldehyde, ethanol, and ethyl acetate within peanut kernels during high temperature drying. *Transactions of the ASAE*, **39**(3), 1039–1045.
- Perera, C.O. and Rahman, M.S. (1997) Heat pump drying. *Trends in Food Science and Technology*, **8**(3), 75.
- Potter, N.N. (1986). *Food Science*. AVI Publication, CT, USA.
- Prichavudhi, K. and Yamamoto, H.Y. (1965) Effect of drying temperature on chemical composition and quality of macadamia nuts. *Food Technology*, **19**, 1153.
- Purslow, P.P. (1987) The fracture behaviour of meat – a case study. In: *Food Structure and Behaviour* (eds J.M.V. Blanshard and P. Lillford). Academic Press Ltd., London, pp. 177–197.
- Rahman, M.S. (1995) *Food Properties Handbook*. CRC Press, Boca Raton, FL, USA.
- Rahman, M.S. (2001) Towards prediction of porosity in foods during drying: A brief review. *Drying Technology*, **19**(1), 3–15.
- Rahman, M.S. (2004) State diagram of date flesh using differential scanning calorimetry (DSC). *International Journal of Food Properties*, **7**(3), 407–428.
- Rahman, M.S. (2006) State diagram of foods: Its potential use in food processing and product stability. *Trends in Food Science and Technology*, **17**, 129–141.
- Rahman, M.S., Al-Amri, O.S. and Al-Bulushi, I. (2002) Pores and physico-chemical characteristics of dried tuna produced by different methods of drying. *Journal of Food Engineering*, **53**, 301–313.
- Rahman, M.S., Guizani, N. and Al-Ruzeiki, M.H. (2004) D- and Z-values of microflora in tuna mince during moist- and dry-heating. *Food Science and Technology*, **37**, 93–98.
- Rahman, M.S., Guizani, N., Al-Ruzeiki, M.H. and Al-Khalasi, S. (2000). Microflora changes in tunas during convection air drying. *Drying Technology*, **18**(10), 2369–2379.
- Rahman, M.S. and Labuza, T.P. (1999) Water activity and food preservation. In: *Handbook of Food Preservation* (ed. M.S. Rahman). Marcel Dekker, Inc., New York, pp. 339–382.
- Rahman, M.S. and Perera, C.O. (1999) Drying and food preservation. In: *Handbook of Food Preservation*, 1st edn. (ed. M.S. Rahman). Marcel Dekker, New York, pp. 173–216.
- Rahman, M.S. and Perera, C.O. (2007) Drying and food preservation. In: *Handbook of Food Preservation*, 2nd edn. (ed. M.S. Rahman). CRC Press, Boca Raton, FL, pp. 403–432.
- Rahman, M.S. and Potluri, P.L. (1990) Shrinkage and density of squid flesh during air drying. *Journal of Food Engineering*, **12**(2), 133–143.
- Rahman, M.S., Sablani, S.S., Al-Habsi, N., Al-Maskri, S. and Al-Belushi, R. (2005a) State diagram of freeze-dried garlic powder by differential Scanning Calorimetry and cooling curve methods. *Journal of Food Science*, **70**(2), E135–E141.
- Rahman, M.S., Salman, Z., Kadim, I.T., *et al.* (2005b) Microbial and physico-chemical characteristics of dried meat processed by different methods. *International Journal of Food Engineering*, **1**(2), 1–13.
- Resmini, P., Pagani, M. A. and Pellegrino, L. (1996) Effect of semolina quality and processing conditions on nonenzymatic browning in dried pasta. *Food Australia*, **48**(8), 362–367.
- Rillo, B.O., Magat, R.P., Miguel, M.M.S. and Diloy, M.L. (1988) Microbiological quality of dried salted mackerel (*Rastrelliger brachosomus*). In: *Food Science and Technology in Industrial Development* (eds S. Maneepun, P. Varangoon and B. Phithakpol). Institute of Food Research and Product Development, Bangkok, pp. 690–694.
- Roos, Y. (1995) Characterization of food polymers using state diagrams. *Journal of Food Engineering*, **24**, 339–360.
- Roos, Y. and Karel, M. (1992) Crystallization of amorphous lactose. *Journal of Food Science*, **57**, 775–777.
- Rowe, R.W.D. (1989a) Electron microscopy of bovine muscle. I – The native state of post rigor sarcolemma and endomysium. *Meat Science*, **26**, 271–279.
- Rowe, R.W.D. (1989b) Electron microscopy of bovine muscle. II – The effect of heat denaturation on post rigor sarcolemma and endomysium. *Meat Science*, **26**, 281.
- Sarker, N.N., Kunze, O.R. and Strouboulis, T. (1996) Transient moisture gradients in rough rice mapped with finite element model and related to fissures after heated air drying. *Transactions of the ASAE*, **39**(2), 625–631.

- Schaffner, D. W. and Labuza, T. P. (1997) Predictive microbiology: Where are we, and where are we going. *Food Technology*, **51**(4), 95–99.
- Schmidt, G.R., Mawson, R.F. and Siegel, D.G. (1981) *Food Technology*, **35**(5), 235.
- Scott, W.J. (1953) Water relations of *Staphylococcus aureus* at 30°C. *Australian Journal of Biological Science*, **6**, 549.
- Sebranek, J.G. (1988). *Meat Science and Processing*. Paladin House, WI, USA.
- Shamaila, M., Durance, T. and Girard, B. (1996) Water blanching effects on headspace volatiles and sensory attributes of carrots. *Journal of Food Science*, **61**(6), 1191–1195.
- Sharma, A.D. and Kunze, O.R. (1982) Post-drying fissure developments in rough rice. *Transactions of the ASAE*, **25**, 465.
- Sheehan, E.M., Connor, T.P.O., Sheehy, P.J.A., Buckley, D. J. and FitzGerld, R. (1996) Effect of dietary fat intake on the quality of raw and smoked salmon. *Irish Journal of Agriculture and Food Research*, **35**, 37–42.
- Sokhansanj, S. (1982) Quality of food grains in recirculating hot-air dryers. *Proceedings of the 3rd International Drying Symposium*, Vol. 2 (ed. J.C. Ashworth). Drying Research Ltd., Wolverhampton, p. 253.
- Stanley, D.W. (1983) Relation of structure to physical properties of animal material. In: *Physical Properties of Foods* (eds M. Peleg and E.B. Bagley). AVI Publishing Co. Inc., CT, USA, p. 157.
- Su, H.L. and Chang, K.C. (1995) Dehydrated precooked pinto bean quality as affected by cultivar and coating biopolymers. *Journal of Food Science*, **60**(6), 1330–1332.
- Turner, I.W. and Jolly, P.G. (1991) Combined microwave and convective drying of a porous material. *Drying Technology*, **9**, 1209.
- Van Blarcom, A. and Mason, R.L. (1988) Low humidity drying of macademia nuts. *Proceedings of the Fourth Australian Conference on Tree and Nut Crops*. Lismore, NSW, p. 239.
- Van-Ruth, S.M. and Roozen, J.P. (1994) Gas chromatography/sniffing port analysis and sensory evaluation of commercially dried peppers (*Capsicum annum*) after rehydration. *Food Chemistry*, **51**, 165.
- Voyle, C.A. (1981) *Scanning Electron Microscope*, **3**, 405.
- Wang, N. and Brennan, J.G. (1995) A mathematical model of simultaneous heat and moisture transfer during drying of potato. *Journal of Food Engineering*, **24**(1), 47–60.
- Wheeler, K.A. and Hocking, A.D. (1993) Interactions among xerophilic fungi associated with dried salted fish. *Journal of Applied Bacteriology*, **74**, 164–169.
- Wheeler, K.A., Hocking, A.D., Pitt, J.I. and Anggawati, A.M. (1986) Fungi association with Indonesian dried fish. *Food Microbiology*, **3**, 351–357.
- Wismer-Pedersen, J. (1971) In: *The Science of Meat and Meat Products* (eds J.F. Price and B.S. Schweigert). Freeman, San Francisco, pp. 177–191.

9 Food drier process control

Brent R. Young

9.1 INTRODUCTION – WHY PROCESS CONTROL?

The drying process is a major industrial unit operation and energy user that reportedly consumes up to 15% of all industrial energy use (e.g. Jumah *et al.*, 1995). The food industry is a significant user of process drying because food has such a direct impact on daily life. As a result there are many food drying applications and variations too numerous to exhaustively list here. A recent survey of drying process control research (Dufour, 2006) indicated that there are at least eight times more applications in food than in any other domain. From a product-engineering point of view, the drier is a very important unit operation in food processing as it typically controls the quality of end product. From a food engineering unit operations point of view, process drying is also well established – in fact it is perhaps the oldest unit operation (e.g. Keey, 1992). So why is food drier process control such a challenge?

From a transport phenomena point of view, food process drying is also a complex process that poses technical challenges for modelling and therefore in many cases is not well understood. The food drying process is typically multi-variable and highly non-linear. This modelling complexity further poses challenges for the development of adequate models for the subsequent development of food drier process control systems.

There are also sensor challenges that present further difficulties for food drier process control. In general there is a lack of direct, inexpensive and/or reliable methods for on-line sensing of the food product quality and the food product moisture content. Thus the major desired outputs or controlled variables typically are not measured and are instead inferred by indirect measurements of other variables.

Drying is theoretically an inherently self regulating process, which means that if the drier is not subject to changes from the environment (or *disturbance variables*) then the process will maintain its steady state. This seems to indicate that automatic control may not be necessary, but such a conclusion would be premature and false as disturbances do occur in real processes and therefore automatic control is necessary. Recent advances and applications (e.g. McFarlane, 1995) in statistical quality control (sometimes called statistical process control) have further emphasized the importance of process control for the maintenance of product quality.

9.1.1 Disturbance variables

Disturbances typically come in three types: input disturbances, load disturbances and set point disturbances. An *input disturbance or manipulated variable (mv) disturbance* is a change in the mass or energy of the supply, or input, to the process that may cause the condition of the process variable to drift from its set point value, *SP*. These may be adjusted either manually

or automatically. A *load disturbance* is any other upset, except for an input mass or energy change, which may alter the quality of the process variable from the desired set point value. A *set point disturbance* occurs when the desired state of the process variable (*PV*) changes and the process must adjust to a new state. The biggest difference between input disturbances and load disturbances – and the reason we distinguish between them – is that load disturbances cannot typically be anticipated, and they are often not measured directly. The only way we find out about them is by observing the effect they have on the product conditions or quality. While input disturbances may also be difficult to anticipate, they are often measured, and corrective action can more readily be taken.

Input disturbances or *manipulated variables*, *mv* (potential/actual) that are common for drying processes include:

1. Airflow rate – in the case of direct driers
2. Feed solids flow rate
3. Heating rate – for the case of direct driers e.g. via air inlet temperature
4. Rotational speed – for the case of rotary driers

Load disturbances that are common for drying processes include:

1. Air humidity
2. Air temperature
3. Feed composition
4. Feed moisture content

9.1.2 Control benefits

The challenge for any drier process control system is to perform in the face of these input and load disturbances. The potential benefits and indeed the objectives of a food drier process control system are:

1. Safety – reduced fire or explosion hazards and particulate emissions
2. Product quality assurance and desired properties – maintenance of desired product quality set point and properties such as colour or flavour
3. Throughput or desired yield – maximization of throughput
4. Energy savings – minimum cost and optimal eco-efficiency
5. Attenuation of load disturbances – minimal influence upon product quality and quantity
6. Stability of the drying process – no large, sustained oscillations in the process or product
7. Robustness – successful operation over a sufficiently large range of operating points and disturbances

9.1.3 Examples

For the reasons cited above regarding the challenge of food drier process control, the literature is sparse with only 47 papers published on drying process control between 1983 (the date of publication of the first paper) and 2006 (Dufour, 2006). Nevertheless, there are some good documented studies in a few good reviews and texts as listed in the bibliography (Jumah, 1995; McFarlane, 1995; Mittal, 1996; Dufour, 2006). With respect to controls benefit analysis,

manufacturers can also be understandably reluctant to release process economic data to the public. However, there are a few indicative examples:

1. Two studies on grain drier optimization and optimal control that quote operating cost savings of 33.6% (Rynieki and Nellist, 1991) and total cost savings of 1.3% (McFarlane and Bruce, 1996), respectively.
2. Model predictive control of beet sugar drying (CADDET, 2000) that produced energy savings of 1.2% in addition to increased downstream energy savings and product yield.
3. Model predictive control of milk powder driers (Pavilion, 2004) that achieved typical benefits of a 17% average throughput increase and a 49% product moisture decrease.

9.1.4 Chapter organization

Having now dealt with why drying process control is important and worthy of study, we will now consider ‘what, where, when and how’, that is, what to control, where to control it, when to control it and how to control it. More specifically the next sections will cover in detail the following topics: (1) manipulated and controlled variables, (2) control strategy, (3) control philosophy, (4) fundamental control methods and (5) advanced control methods.

9.2 WHAT TO CONTROL (MANIPULATED AND CONTROLLED VARIABLES)

9.2.1 Controlled variables

The *output variables* or *process variables* or *controlled variables (CV)* are the outputs of the drying process and represent the response of the process to the input disturbance variables (or manipulated variables, *mv*) and load disturbance variables, as well as the impact of the drying process on the surroundings.

Potential/actual *controlled variables (CV)* for food drying control include:

1. Product quality e.g. colour, flavour, etc.
2. Product moisture content
3. Exit air temperature
4. Exit air humidity

As mentioned previously, it is difficult to measure product quality on-line and/or it is expensive and/or unreliable. Therefore, product quality is often inferred based on the experience of the operator.

Product moisture content can theoretically be measured on-line in some cases, but as was also pointed out above, it is more typically not measured because of the expense and/or unreliability of the sensors. Therefore, the product moisture content is also often inferred from the exit air temperature and humidity. However, there is actually a low correlation between the exit air temperature and the real product moisture content. Therefore, indirect control can often result in poor control of the drier, especially if humidity is not included in the control scheme. If possible, direct control via on-line measurement of product moisture content is therefore preferred for attaining good control.

9.2.2 Manipulated variables

As mentioned above, we can also have a choice for manipulated variables depending on the drier type. The manipulated variables, mv , represent the variables in the process to which the PV are sensitive, and to which the final control elements (FCE) are attached.

Manipulated variables that are common for drying processes include:

1. Airflow rate (for direct driers)
2. Feed solids flow rate
3. Heating rate (for direct driers)
4. Rotational speed (for rotary driers)

Choice of mv and CV of course depends on the drier type. It may also depend on how the drier is integrated into the whole food process plant. Plant-wide control considerations and specific control schemes for various drier types will be dealt with in the next section.

9.3 WHERE TO CONTROL (CONTROL STRATEGY)

The drier is one unit operation of many in an entire food processing plant. Therefore it is important to consider the plant-wide control strategy configuration as a whole, before focusing on the drier alone.

9.3.1 Plant-wide control strategy configuration

The fundamental questions in plant-wide control are whether the feed rates can simply be set for a process and left unattended and whether the process is meeting the desired purity and quality specifications (e.g. Vogel, 1992). What happens when common disturbances occur, such as feed composition changes, production rate changes, product mix or purity specification changes, ambient temperature changes or measurement sensors either fail or are in error?

When applying a plant-wide control scheme, it is important to be aware of the propagation of variation and the transformation that each control system performs. Management of that variation is the key to good plant-wide operation and control. A healthy variation management strategy should have both a short-term and a long-term focus. The short-term focus is to use control strategies to transform the variation to less harmful locations in the plant. The long-term focus should concentrate on improvements that reduce or eliminate either the variations or the problems caused by variations.

The dynamics and control of continuous process units that operate as a cascade of units, either in parallel or in series, have been studied extensively for many years (e.g. Buckley, 1964). A wealth of knowledge is available to help design effective control systems for a large number of unit operations when these units are run independently (e.g. Considine, 1993). This knowledge can be directly applied to the plant-wide control problem if a number of process units are linked together as a sequence of units. Each downstream unit simply sees the disturbances coming from its upstream neighbour.

The design procedure was proposed over four decades ago (Buckley, 1964) and has since been widely used in industry. The first step of the procedure is to set out a logical and consistent 'material balance' control structure that handles the inventory controls, that is, the levels and

pressures. This hydraulic structure provides gradual and smooth flow rate changes from unit to unit. Thus, flow rate disturbances are filtered so that they are attenuated and not amplified as they work their way down through the cascade of units. Slow acting, proportional only level controllers provide the simplest and most effective way to achieve this flow smoothing.

Then, product quality control loops are closed on each of the individual units. These loops typically use fast proportional integral controllers to hold product streams as close as possible to specification values. Since these loops are considerably faster than the slow inventory loops, interaction between the two is generally not a problem. Also, since the manipulated variables used to hold product qualities are often streams that are internal to each individual unit, changes in these manipulated variables have little effect on the downstream process. The manipulated variables frequently are utility streams that are provided by the plant utility system, the cooling water, steam, refrigerant, etc. Thus, the boiler house will be disturbed, but the other process units in the plant will not see disturbances coming from upstream process units. Of course, this is only true when the plant utilities systems have effective control systems that can respond quickly to the many disturbances that they see coming in from units all over the plant.

If recycle streams exist in the plant, the procedure for designing an effective plant-wide control scheme becomes more complicated. Processes with recycle streams are quite common, but their dynamics are poorly understood at present.

The typical approach in the past for plants with recycle streams has been to install large surge tanks. This isolates the sequences of units and permits the use of conventional cascade process design procedures. However, this practice can be very expensive in terms of capital costs and working capital investment. In addition, and increasingly more importantly, the large inventories of chemicals can greatly increase safety and environmental hazards if dangerous or environmentally unfriendly chemicals are involved.

While there are a number of different ways to control a plant, it is helpful to keep in mind two fundamental rules of plant-wide control (Luyben *et al.*, 1998):

1. Only flow control a feed if it is sure to be fully consumed in the reaction.
2. Always put one stream in the recycle path on flow control.

9.3.2 Common loops and examples

In this section we examine the set up of two common food drier process control loops and applications – rotary driers and spray driers.

9.3.2.1 Rotary drier control

Rotary driers are commonly used for the drying of grains (e.g. Rynieki and Nellist, 1991; McFarlane and Bruce, 1996), but also other food materials such as granulated sugar (e.g. Douglas *et al.*, 1992). Rotary driers are commonly controlled via the measurement of the exit air temperature, which is used to control the air temperature. Note, however, that the direction of the flow is a very important parameter when considering these systems (Edgar *et al.*, 1997).

For co-current driers, for example, grain driers, the control of the exit air temperature is directly related to the moisture content control as long as the feed solids flow rate, airflow rate, feed moisture content and inlet air moisture content are reasonably constant. Control of

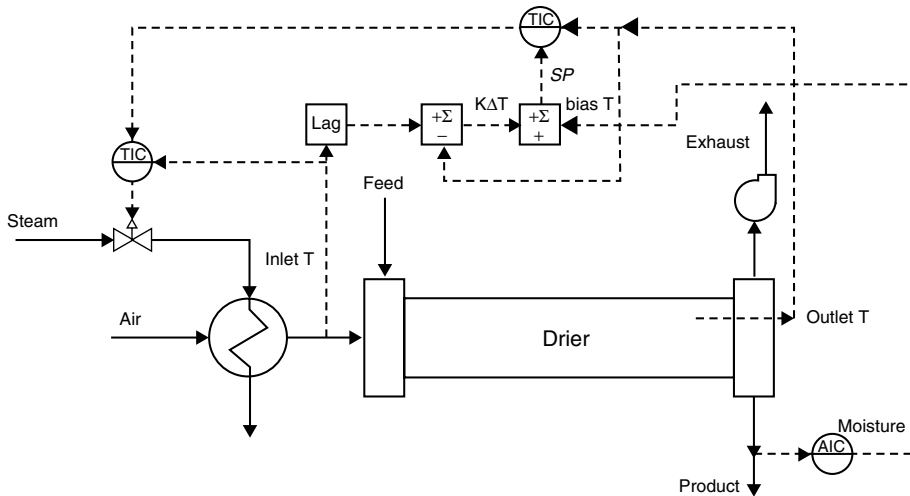


Fig. 9.1 Co-current rotary drier control scheme.

the product quality can be improved further by controlling the exit temperature in proportion to the evaporative load as shown in Figure 9.1.

For the counter-current flow case, for example, granulated sugar driers, exit temperature is not so correlated with product moisture. The control of product moisture can be better achieved by controlling product discharge temperature (Edgar, 1997). Control schemes for counter-current flow mentioned in the literature include the control of the rate of evaporation as indicated by the difference of the wet- and dry-bulb exit air temperatures (Jumah *et al.*, 1995) and control of moisture content and temperature by manipulating the air flow rate and the rotational speed (Douglas *et al.*, 1992).

9.3.2.2 Spray drier control

Spray drying process control can be considered to be similar in many respects to co-current rotary drier control discussed above, and the control strategy is similar (Edgar, 1997). However, the process dynamics are quite different (Jumah *et al.*, 1995). Spray driers have a much shorter residence time and the drying is much more rapid. Therefore, there is little process dead time and, all other things being equal, this theoretically allows good process control.

Four common control schemes are used:

1. Exit air temperature control via the air heater with manual feed rate control. This scheme is commonly used for nozzle atomizers and when wide variations in the feed rate cannot be accommodated.
2. Exit air temperature control via the feed rate and inlet air temperature control via the heater. This scheme is commonly used for rotary atomizers.
3. A cascade of moisture content to exit air temperature control via the feed rate. This control system is commonly used for rotary atomizers.
4. A cascade of moisture content to exit air temperature control via the feed rate with feed-forward from atmospheric humidity, feed density and inlet air temperature.

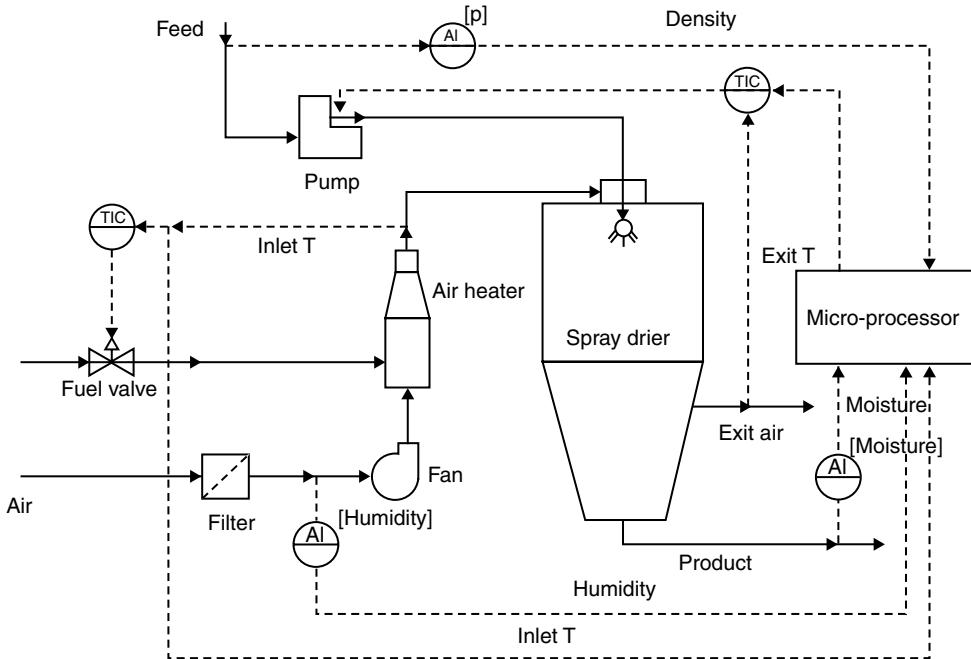


Fig. 9.2 Spray drier control scheme.

The latter control system is commonly used for rotary atomizers and is shown in Figure 9.2.

9.4 WHEN TO CONTROL (CONTROL PHILOSOPHY)

9.4.1 After something happens – feedback control

9.4.1.1 Automatic single input/single output feedback control

Manual or open loop control suffices when no disturbances are present to threaten the desired state of the product. However, this is almost never the case and ‘real’ processes must operate in the presence of disturbances, and, therefore, require some sort of closed loop control. Single input, single output automatic feedback control is the most common form.

The basic elements of a feedback controller (e.g. Svrcek *et al.*, 2006) are:

1. A single output or process variable, *PV*, which represents the variable that is important to maintain under control.
2. The set point, *SP*, which represents the desired value of the *PV*.
3. The error, *e*, which represents the magnitude of the difference between the *PV* and the *SP*.
4. The controller, whose ‘control law’ and tuning drive the corrective action and influence the response of the system.
5. A single input or final control element, FCE (typically a control valve) to which the controller output is attached and through which the controller exercises its influence on the *PV*.

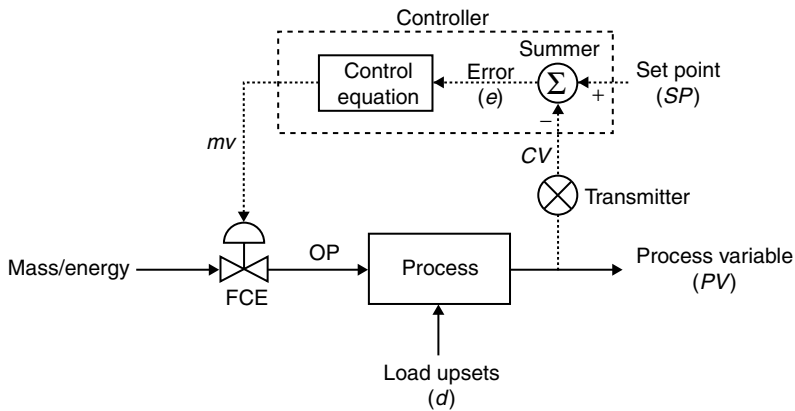


Fig. 9.3 Single input/single output feedback control loop schematic.

6. The manipulated variable, mv , which represents the variable in the process to which the PV is sensitive, and to which the FCE is attached.

A feedback controller works by measuring the PV and comparing it to the SP to generate an error. The error, conditioned by the controller type and tuning, drives appropriate changes in the FCE (and thus the mv) such that the PV is driven back in the direction of the SP . Figure 9.3 is a schematic of an automatic feedback control loop.

If an automatic feedback controller succeeds in keeping the PV at the desired SP in the presence of load disturbances then, by necessity, there will be changes in the mv dictated by the controller. So in effect, *process control takes variability from one place, and moves it to another* (Downs and Doss, 1991). Therefore, good process control involves knowing where variability can be tolerated and where it cannot, and designing schemes that manage variability to acceptable levels.

The advantages of the single input, single output automatic feedback controller are that it is easy to implement, robust (i.e. insensitive to modelling errors), regulates both known and unknown loads and operators have generally been taught to use and understand them. Disadvantages of the feedback controller include that the process must first be upset before the controller reacts, the PV must be measurable and not noisy, interaction with other control loops must be minimal, there should be no significant dead time, the mv must be adjustable over a large range and the dynamic process characteristics must not vary significantly with operating conditions or time (i.e. the process dynamics should be essentially linear and time invariant).

9.4.1.2 Cascade control

Cascade control is a common variation of feedback control that uses two controllers with one feedback loop nested inside the other (e.g. Svrcek *et al.*, 2006). The output of the primary controller acts as the set point for the secondary controller. The secondary controller controls the final control element (FCE). One of the most common forms of cascade is the output of a primary controller acting as a set point to a valve positioner. And we have already seen another example of cascade control in spray drying. Figure 9.4 is a schematic of a cascade control system.

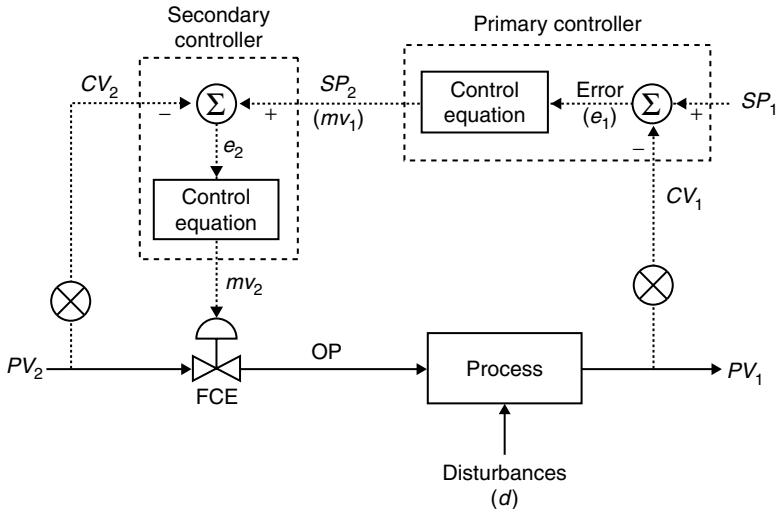


Fig. 9.4 Cascade control system schematic.

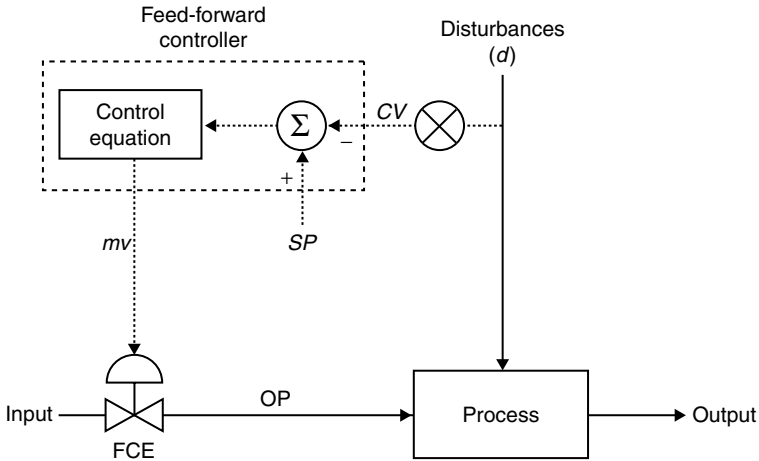


Fig. 9.5 Feed-forward control system schematic.

9.4.2 As something happens – feed-forward/predictive control

One of the disadvantages to using feedback control is that a disturbance must pass through the process before it is recognized and action is taken to correct it. This type of control is sufficient for processes in which some deviation from the set point is acceptable. However, there are certain processes where this set point deviation must be minimized. Feed-forward control can accomplish this because it corrects and/or minimizes disturbances before they enter the process (e.g. Svrcek *et al.*, 2006). A schematic of a feed-forward control system is shown in Figure 9.5.

In its simplest form, feed-forward control proportions the corrective action to the size of the disturbance. In other words, the control equation is a gain based on steady state, that is,

mass or energy balance at steady state. This does not take into account any of the process dynamics of the system. If there is a difference, or lag, in the speed of the process response to the control action when compared to that of the disturbance, it may be necessary to introduce some dynamic compensation into the control equation. The dynamic compensation correctly times the control action and response thus giving increased accuracy in the feed-forward control.

In general, the feed-forward dynamic elements will not be physically realizable. In other words, they cannot be implemented exactly. For instance, if the process disturbance measurement contains dead time, or lag, the feed-forward dynamic compensation would have to be a predictor, which of course is impossible unless an exact and very fast dynamic model of the process is available. In practice, the feed-forward dynamic elements are often approximated by a lead lag network (e.g. Svrcek *et al.*, 2006) that is adjusted to yield as much disturbance rejection as possible over as wide a range as possible.

When feed-forward control is used, equations are needed to calculate the amount of the manipulated variable needed in order to compensate for the disturbance. This sounds simple enough; however, the equations must incorporate an understanding of the exact effect of the disturbances on the process variable. Therefore, one disadvantage of feed-forward control is that the controllers often require sophisticated calculations as even steady models can be non-linear and thus need more technical and engineering expertise in their implementation.

Another disadvantage of feed-forward control is that all of the possible disturbances and their effects on the process must be precisely known. If unexpected disturbances enter the process when only feed-forward control is used, no corrective action is taken and the errors will build up in the system. If all the disturbances were measurable and their effects on the process precisely known, a feedback control system for regulatory purposes would not be needed. However, such complete and error free knowledge is never available, so feed-forward is generally combined with feedback, as illustrated in Figure 9.6. The intent of this union is that the feed-forward mitigates most of the effects of the principal disturbances and the feedback loops provide residual control and set point tracking.

Another, alternative form of predictive control to feed-forward is model predictive control or MPC. MPC is more complex than classical feed-forward control and is the form of advanced control that is most widely used in industry (e.g. Seborg, 1984). Therefore, we will deal with MPC in the final section of this chapter.

9.5 HOW TO CONTROL (FUNDAMENTAL CONTROL METHODS)

9.5.1 PID feedback control and tuning

9.5.1.1 PID controller modes

Proportional (P-only) control

Proportional control is the simplest continuous control mode that can damp out oscillations in the feedback control loop. This control mode normally stops the process variable, *PV*, from cycling but does not necessarily return it to the set point.

In equation form, the output of a proportional controller is proportional to the error, equation (9.1).

$$mv = K_c e + b \quad (9.1)$$

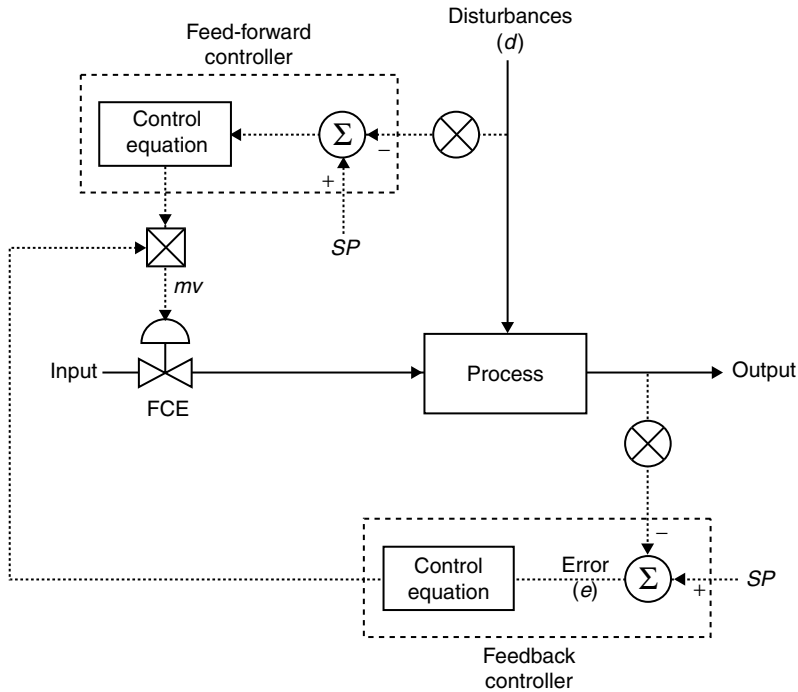


Fig. 9.6 Feed-forward/feedback control system schematic.

In equation (9.1), K_c is the controller gain, e is the error or deviation of the measurement CV from the set point SP , mv is the manipulated variable and b , is the bias or the output of the controller when the error is zero.

Note:

$$e = SP - CV \quad (\text{for reverse acting})$$

$$e = CV - SP \quad (\text{for direct acting})$$

Increasing K_c can decrease the error, but remember not to increase K_c such that it makes the loop unstable. There is a limit for each feedback control loop. If K_c has a value such that the loop gain, K_L , is equal to one, the loop will oscillate with a period that is a function of the natural characteristics of the process. This is called the natural period, τ_n . If K_c is adjusted such that the loop gain is equal to 0.5 and a change is made in F_o , the response shown in Figure 9.7 could be expected.

CV damps out with a quarter decay ratio and a period approximately equal to the natural period. It then stabilizes with an offset that is a function of both the controller gain and the bias. The offset is the sustained error, e , where CV does not return to the set point even when steady state is reached. This is a typical response for a loop under proportional only control.

Virtually all modern controllers use a gain adjustment, however a few older controllers exist that still use a proportional band, PB adjustment, where $K_c = 100\%/PB\%$, or as the PB gets larger, the gain gets smaller and vice versa. The equation for a proportional controller in

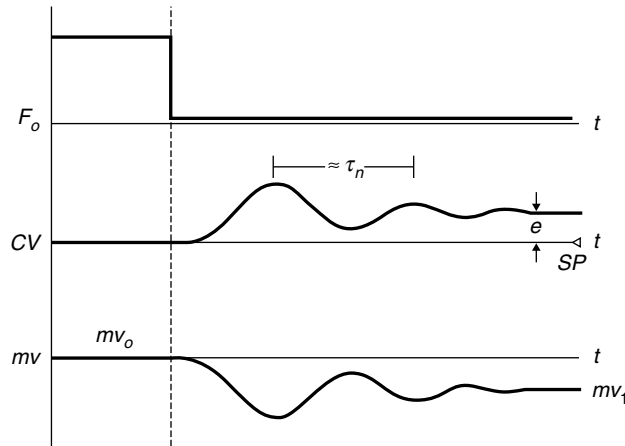


Fig. 9.7 Typical proportional only controller response.

terms of PB can be written as follows:

$$mv = \frac{100}{PB}e + b \quad (9.2)$$

Some controllers also have an adjustable bias to make the error zero, as in equation (9.3).

$$e = \frac{1}{K_c}(mv - b) \quad (9.3)$$

However, this approach is only an option for processes that experience few load upsets, since a manual readjustment of the bias is required each time there is a load upset. There would be no error as long as the bias was equal to the load. Hence, if the process had infrequent load upsets, the operators could readjust the bias to give zero error, and it would be possible to use a P-only controller.

In general, a proportional controller provides a fast response when compared to other controllers but a sustained error occurs where the PV does not return to the set point even when steady state is reached. This sustained error is called offset and is undesirable in most cases. Therefore, it is necessary to eliminate offset by combining proportional control with one of the other basic control modes.

Integral (I-only) action

The action of *integral control* is to remove any error that may exist. As long as there is an error present, the output of this control mode continues to move the FCE in a direction to eliminate the error. The equation for integral control is given in equation (9.4):

$$mv = \frac{1}{T_i} \int e dt + mv_o \quad (9.4)$$

mv_o is defined as either the controller output before integration, the initial condition at time zero, or the condition when the controller is switched into automatic.

The integral time, T_i , is defined as the amount of time it takes the controller output to change by an amount equal to the error. In other words, it is the amount of time required to duplicate the error. Thus T_i is measured in minutes per repeat.

Because of the form of equation (9.4) some manufacturers measure the reciprocal of T_i or repeats per minute in a controller. As a result of this reciprocal relationship, if the controller is adjustable in min/rep, then increasing the adjustment gives less integral action, whereas in rep/min, increasing the number produces greater integral action. Therefore, it is important to be aware of how an individual controller adjusts T_i . The rate of change of mv also depends on the magnitude of e .

Although an integral only controller provides the advantage of eliminating offset, there is a significant difference in its response time when compared to proportional only controller. As mentioned earlier, the output of the proportional only controller changes as quickly as the measurement changes; in other words, the controller tracks the error. So, if the measurement changes as a step, the controller output also changes as a step by an amount depending on the controller gain. For a step input to an integral controller, the output does not change instantaneously but rather by a rate that is affected by T_i and e .

Hence, integral only control, due to the additional lag introduced by this mode, has an overall response that is much slower than that for proportional only control. The period of response for the PV under integral only control can be up to ten times that for proportional only; so a trade off is made when using an I-only controller. If no offset is required then a slower period of response must be tolerated. If the requirement is a return to the set point with no offset, and a faster response time is necessary, then the controller must be composed of both proportional and integral action.

As a result of the above, controllers with both proportional and integral action are more common. However, a few examples of integral only controllers do occur.

Proportional plus integral (PI) control

A *proportional plus integral controller* will give a response period that is longer than a P-only controller but much shorter than an I-only controller. Typically, the response period of the process variable, PV , under PI control is approximately 50% longer than for the P-only ($1.5\tau_n$). Since this response is much faster than I-only ($\gg \tau_n$), and only somewhat longer than P-only control (τ_n), the majority (>90%) of controllers found in plants are PI controllers. Figure 9.8 illustrates the responses of P-only, I-only and PI controllers to a step input.

The equation for a PI controller is given in equation (9.5):

$$mv = K_c \left(e + \frac{1}{T_i} \int e dt \right) = K_c e + K_c \cdot \frac{1}{T_i} \int e dt \quad (9.5)$$

The PI controller gain has an effect not only on the error, but also on the integral action. When we compare the equation for a PI controller (equation (9.5)) to that for a P-only controller (equation (9.1)) we see that the bias term in the P-only controller has been replaced by the integral term in the PI controller. Thus, the bias term for PI control is given by equation (9.6):

$$b = K_c \cdot \frac{1}{T_i} \int e dt \quad (9.6)$$

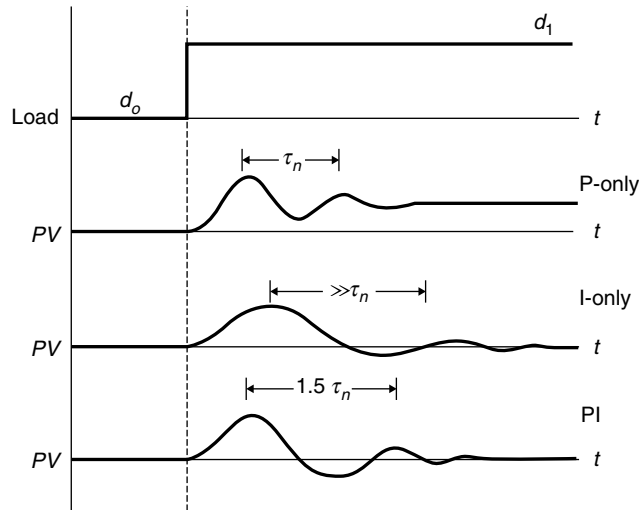


Fig. 9.8 Response of P-only, I-only and PI controllers.

Therefore, the integral action provides a bias that is automatically adjusted to eliminate any error. The PI controller is faster in response than the I-only controller because of the addition of the proportional action, as illustrated in Figure 9.8.

Although the response period of a loop under PI control is only 50% longer than that for a loop under P-only control, this may in fact be far too long if τ_n is as large as three or four hours. In order to increase the speed of the response it may be necessary to add an additional control mode.

Derivative action

The purpose of *derivative action* is to provide lead to overcome lags in the loop. In other words, it anticipates where the process is going by looking at the rate of change of error, de/dt . For derivative action, the output equals the derivative time, T_d , multiplied by the derivative of the input, which is the rate of change of error (equation (9.7)):

$$\text{output} = T_d \frac{de}{dt} \quad (9.7)$$

As the rate of change of the error gets larger, the output gets larger. Since the slope of each of these error signals is constant, the output for each of these rate inputs will also be constant. However, what happens as the slope approaches infinity as in the case of a step change? Theoretically, the output should be a pulse that is of infinite amplitude and zero time long. This output is not realizable since a perfect step with zero rise time is physically impossible, but signals that have short rise and fall times do occur. These types of signals are referred to as noise. Thus, the output from the derivative block would be a series of positive and negative pulses, which would try to drive the FCE either full open or full close. This would result in accelerated wear on the FCE and no useful control.

Consider a temperature measurement with a small amplitude and high-frequency noise. One might assume that since the noise is of such small amplitude in comparison to the average temperature signal that a controller would not even notice it. This is only the case

if the controller does not have derivative action. If the controller contains derivative action, the temperature signal would be completely masked by the noise into the derivative mode of the controller, and the controller output would be a series of large amplitude pulses, entirely masking any output contributed by the other control modes. Fortunately, in a case such as this the noise is either easily filtered out or is eliminated by modifying the installation of the primary sensor.

However, there are cases where noise is inherent in the measurement of *PV* and the rise and fall time of the noise is of the same magnitude as that of the measurement itself. In such a case, noise filtering would only serve to degrade the accuracy of the measurement of *PV*. A good example of a situation like this is a flow control loop. Flow measurement by its very nature is noisy; and, therefore, derivative action cannot be successfully applied.

It is important to note that derivative control would never be the sole control mode used in a controller. The derivative action does not know what the set point actually is and hence cannot control to a desired set point. Derivative action only knows that the error is changing.

Returning to equation (9.7) and a set point change, the derivative action acts on the error. Since $e = SP - CV$ for reverse action, de/dt is a function of both the derivative of the set point, dSP/dt , and the derivative of the controlled variable, dCV/dt .

If there is a load upset to the process, the process variable, *PV*, will change at some rate, dCV/dt which will result in the error also changing at the same rate ($de/dt = -dCV/dt$), assuming there is no set point change. Now, if a set point change of even a few percent is made and if the set point is changed quickly, then dSP/dt can become very large. This would cause a large pulse to be generated at the output of the controller. To overcome this potential problem, the controller can be made so that the derivative mode simply ignores set point changes as shown in equations (9.8) and (9.9):

$$\frac{de}{dt} = \frac{dSP}{dt} - \frac{dCV}{dt} \quad (9.8)$$

Ignoring set point changes gives:

$$\frac{de}{dt} = \frac{-dCV}{dt} \quad (9.9)$$

In a controller with derivative action, even by setting T_d to a very small value, there is still the possibility of a sizeable derivative contribution if there is a noisy input, that is, if dCV/dt is large. In electronic controllers and distributed control systems (DCS) the derivative action can be eliminated by setting T_d to zero. In a pneumatic controller the derivative action cannot be eliminated but can be reduced to a minimum value of approximately 0.01 min. If a PD controller is installed on a flow loop there will still be considerable derivative action due to the noisy flow measurement. It is therefore important, when applying a pneumatic controller to a noisy loop such as a flow loop, to make certain the controller does not contain a derivative block.

The main reason for interest in derivative action is to combine it with proportional and integral action to produce a three-mode controller, PID.

Proportional integral derivative (PID) control

The primary purpose of a *proportional integral derivative controller* (equation (9.10)) is to provide a response period, τ_n , that is much the same as with proportional control but which

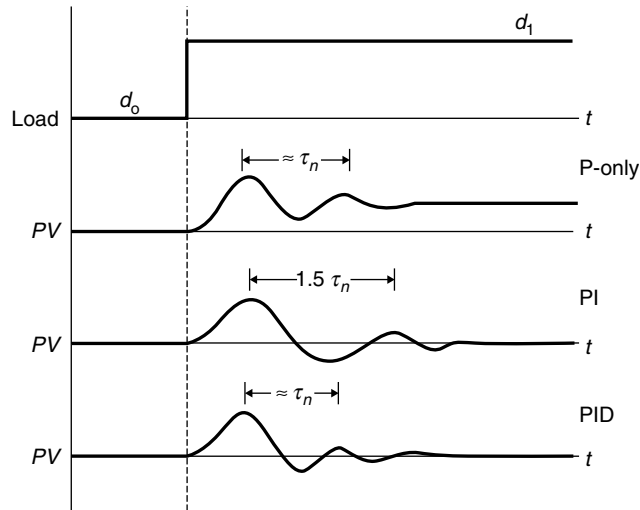


Fig. 9.9 P-only, PI and PID controller response to a load disturbance.

has no offset. The derivative action adds the additional response speed required to overcome the lag in the response from the integral action.

$$mv = K_c \left(e + \frac{1}{T_i} \int e dt - T_D \frac{CV}{dt} \right) \quad (9.10)$$

Figure 9.9 presents a comparison of the responses for a P-only, PI, and PID controller to a step change in load.

The addition of the derivative mode in the PID controller provides a response similar to that of a P-only controller but without the offset because of the integral action. Therefore, a PID controller provides a tight dynamic response, but since it contains a derivative block it cannot be used in any processes in which noise is anticipated.

Choosing the correct controller

Now that the various basic control modes have been described, it is desirable to be able to choose a particular control mode for a specific process. Figure 9.10 graphically outlines a procedure for control mode selection.

Starting at the top of the flow diagram, the first decision block asks the question: ‘Can offset be tolerated?’ If the answer is yes, a proportional only controller can be used. If the answer is no, proceed to the next block which asks: ‘Is there noise present?’ If there is noise, then use a PI controller. If there is no noise, proceed to the next block, which asks: ‘Is dead time excessive?’ If the ratio of the dead time to the process time constant is greater than 0.5, the process can be assumed to be dead time dominant and requires a PI controller. If the process has no excessive dead time, then the next block asks: ‘Is the capacitance extremely small?’ If the answer is yes, then a PI controller can be used. A process with a short dead time and small capacitance does not require derivative action to speed up the response since it is already fast enough, as is the case for a flow loop. In this instance we might even consider an I-only controller since the loop is so fast that slowing down the response through the use of integral only action will still provide a fast enough response for the majority of applications

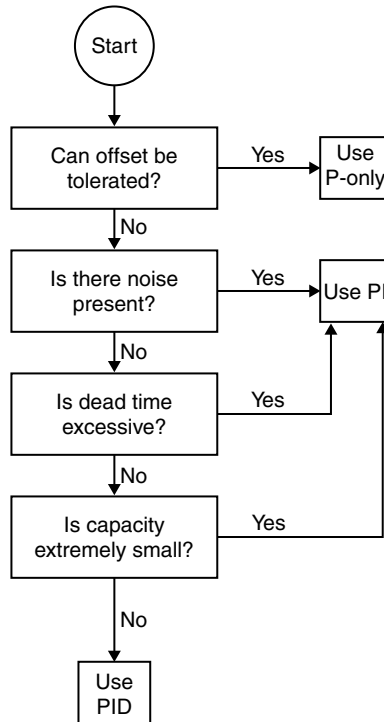


Fig. 9.10 Flow chart for controller selection.

in the fluid processing industries. Finally, if the process capacitance is large, a PID controller can be effectively used.

It was mentioned earlier that the PI controller is the most common controller found in the plant. Looking at this flow chart one can see why. There are three possible paths to the PI controller, while there are four decision blocks that must be passed through to reach a PID controller.

9.5.1.2 How to tune PID feedback controllers

The following presents a very brief description of some of the various accepted methods used for controller tuning. In each case the suggested controller settings are optimized for a particular error performance criterion, often quarter decay ratio. The first method described is based entirely on trial and error, while the rest are based upon some understanding of the physical nature of the process to be controlled. This understanding is generated from either open or closed loop process testing.

'Trial and error tuning method'

As the name suggests, tuning by trial and error is simply a guess and check type method. The following is a list of practical suggestions for tuning a controller by trial and error. These suggestions are also useful for fine tuning controllers tuned by other methods.

1. Proportional action is the main control. Integral and derivative actions are used to trim the proportional response.

2. The starting point for trial and error tuning is always with the controller gain, integral action and derivative action all at a minimum.
3. Make adjustments in the controller gain by using a factor of two, i.e. 0.25, 0.5, 1.0, 2.0, 4.0, etc.
4. The optimal response is the quarter decay ratio (QDR).
5. When in trouble, decrease the integral and derivative actions to a minimum and adjust the controller gain for stability.

Rules of thumb

The following rules of thumb should not be taken as gospel or as a methodology but rather are intended to indicate typical values encountered. As such, these rules can be useful when tuning a controller using the trial and error method. However, it is important to remember that controller parameters are strongly dependent upon the individual process and may not always abide by the rules outlined below.

Flow: When dealing with a flow loop, P-only control can be used with a low controller gain. For accuracy, PI control is used with a low controller gain and high integral action. Derivative action is not used because flow loops typically have very fast dynamics and flow measurement is inherently noisy.

Level: Levels represent material inventory that can be used as surge capacity to dampen disturbances. Hence, loosely tuned P-only control is sometimes used. However, most operators do not like offset, so PI level controllers are typically used.

Pressure: Pressure control loops show large variation in tuning depending on the dynamics of the pressure response.

Temperature: Temperature dynamic responses are usually fairly slow, so PID control is used.

Typical parameter values are given in Table 9.1.

Table 9.1 Typical controller parameter values (Svrcek *et al.*, 2006).

Process variable	Controller mode	Controller parameters
Flow (approximate)	P-only	Low gain
Flow (accurate control)	PI	$K_C = 0.4\text{--}0.65$, $T_i = 0.1$ min (or 6 s)
Level (averaging)	P-only	$K_C = 2$, Bias term (b) = 50%, Set point (SP) = 50%
Level (no offset)	PI	$K_C = 2\text{--}20$, $T_i = 1\text{--}5$ min
Vapour pressure	PI	$K_C = 2\text{--}10$, $T_i = 2\text{--}10$ min
Liquid pressure	PI	$K_C = 0.5\text{--}2$, $T_i = 0.1\text{--}0.25$ min
Temperature	PID	$K_C = 2\text{--}10$, $T_i = 2\text{--}10$ min, $T_d = 0\text{--}5$ min

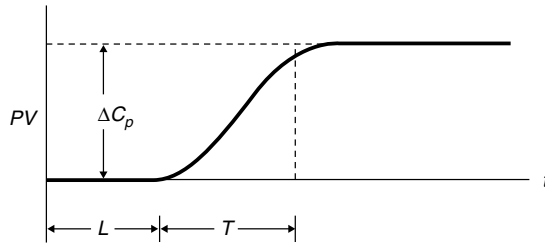


Fig. 9.11 Process reaction curve.

Process reaction curve methods

In process reaction curve methods a process reaction curve is generated in response to (typically) a step disturbance. This process curve is then used to calculate the controller gain, integral time and derivative time. These methods are performed in open loop so no control action occurs and the process response can be isolated.

To generate a process reaction curve, the process is allowed to reach steady state or as close to steady state as possible. Then, in open loop so there is no control action, a small step disturbance is introduced and the reaction of the process variable is recorded. Figure 9.11 shows a typical process reaction curve generated using the above method for a generic self-regulating process. The term self-regulating refers to a process where the controlled variable eventually returns to a stable value or levels out without external intervention.

The process parameters that may be obtained from this process reaction curve are as follows:

L = lag time (min)

T = time constant estimate (min)

P = initial step disturbance (%)

ΔC_p = change in PV in response to a step, (change in PV)/(PV span) \times 100 (%)

$N = \Delta C_p/T$ = reaction rate (%/min)

$R = L/T = NL/\Delta C_p$ = lag ratio (dimensionless)

Methods of process analysis with forcing functions other than a step input are possible and include pulses, ramps and sinusoids. However, step function analysis is the most common as it is the easiest to implement.

Ziegler–Nichols open-loop rules. In 1942, Ziegler and Nichols changed controller tuning from an art to a science by developing their open-loop step function analysis technique. They also developed a closed-loop technique, which is described in the next section on constant cycling methods.

The Ziegler–Nichols open-loop recommended controller settings for quarter decay ratio, QDR are as follows:

$$\text{P-only: } K_c = \frac{P}{NL}$$

$$\text{PI: } K_c = 0.9 \left(\frac{P}{NL} \right)$$

$$T_i = 3.33 (L)$$

$$\text{PID: } K_c = 1.2 \left(\frac{P}{NL} \right)$$

$$T_i = 2.0(L)$$

$$T_d = 0.5(L)$$

These settings should be taken as recommendations only and tested thoroughly in closed loop, fine-tuning the parameters to obtain QDR.

Internal model control tuning rules. Many practitioners have found that the Ziegler–Nichols open loop and other similar rules such as Cohen–Coon (1953) are too aggressive for most chemical industry applications since they give a large controller gain and short integral time. Rivera *et al.* (1986) developed the internal model control (IMC) tuning rules with robustness in mind. The tuning parameter from the IMC method (the closed-loop speed of response) relates directly to the closed-loop time constant and the robustness of the control loop. As a consequence, the closed-loop step load response exhibits no oscillation or overshoot. Lambda tuning (e.g. McMillan, 1999) is also a term that is also used to refer to controller tuning methods that are based on a specified closed-loop time constant.

Since the general IMC method is unnecessarily complicated for processes that are well approximated by first-order dead time or integrator dead time models, simplified IMC rules were developed by Fruehauf *et al.* (1993) for PID controller tuning (Table 9.2).

Of course, these recommendations need to be tested in the closed-loop situation and the final settings arrived at through the use of fine-tuning.

Constant cycling methods

Ziegler–Nichols closed-loop method. The closed-loop technique of Ziegler and Nichols (1942) is a technique that is commonly used to determine the two important system constants, ultimate period and ultimate gain. It was one of the first tuning techniques to be widely adopted.

When tuning using Ziegler–Nichols closed-loop method, values for proportional, integral and derivative controller parameters may be determined from the ultimate period and ultimate gain. These are determined by disturbing the closed-loop system and using the disturbance response to extract the values of these constants.

The following is a step-by-step approach to using the Ziegler–Nichols closed-loop method for controller tuning:

1. Attach a proportional only controller with a low gain (no integral or derivative action).
2. Place the controller in automatic.
3. Increase the controller gain until a constant amplitude limit cycle occurs.

Table 9.2 Simplified IMC rules (Fruehauf *et al.*, 1993).

	$(\tau/L) > 3$	$(\tau/L) < 3$	$L < 0.5$
K_c	$P/2(NL)$	$P/2(NL)$	P/N
T_i	$5L$	τ	4
T_d	$\leq 0.5L$	$\leq 0.5L$	$\leq 0.5L$

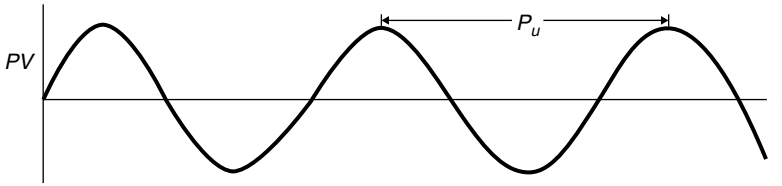


Fig. 9.12 Constant amplitude limit cycle.

4. Determine the following parameters from the constant amplitude limit cycle (Figure 9.12):

$P_u \equiv$ ultimate period = period taken from limit cycle

$K_u \equiv$ ultimate gain = controller gain that produces the limit cycle

5. Calculate the tuning parameters using the following equations:

$$\text{P-only: } K_c = \frac{K_u}{2}$$

$$\text{PI: } K_c = \frac{K_u}{2.2}$$

$$T_i = \frac{P_u}{1.2}$$

$$\text{PID: } K_c = \frac{K_u}{1.7}$$

$$T_i = \frac{P_u}{2}$$

$$T_d = \frac{P_u}{8}$$

6. Fine tune by adjusting K_c , T_i , and T_d as required to find the QDR.

Note that Ziegler–Nichols tuning is often considered aggressive with a large controller gain and a short integral time. This technique was originally developed for electromechanical systems control and is based on the aggressive QDR criterion.

Auto tune variation technique. The auto tune variation (ATV) technique of Åström and Hagglund (1984) is another closed-loop technique used to determine the two important system constants, the ultimate period and the ultimate gain. However, the ATV technique determines these system constants without unduly upsetting the process. Tuning values for proportional, integral and derivative controller parameters can be determined from these two constants. ATV tuning was developed for fluid and thermal processes and emphasizes minimizing overshoot. ATV is, therefore, often the preferred technique for process control. We recommend the use of Tyreus–Luyben (1992) settings for tuning that is suitable for chemical process unit operations.

All methods for determining the ultimate period and ultimate gain involve disturbing the system and using the disturbance response to extract the values of these constants. In the case of the ATV technique, a small limit cycle disturbance is set up between the manipulated variable (controller output) and the controlled variable (process variable). Figure 9.13 shows the instrument setup, and Figure 9.14 shows the typical ATV response plot with critical

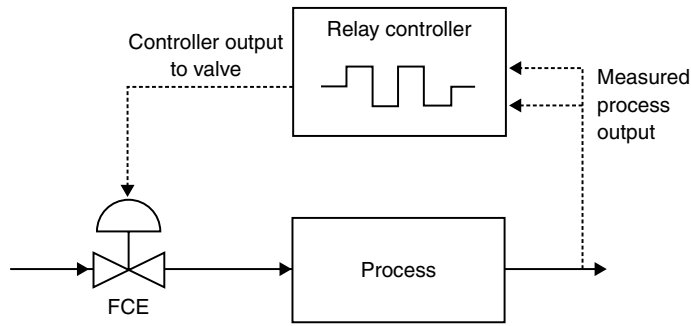


Fig. 9.13 ATV tuning instrument setup.

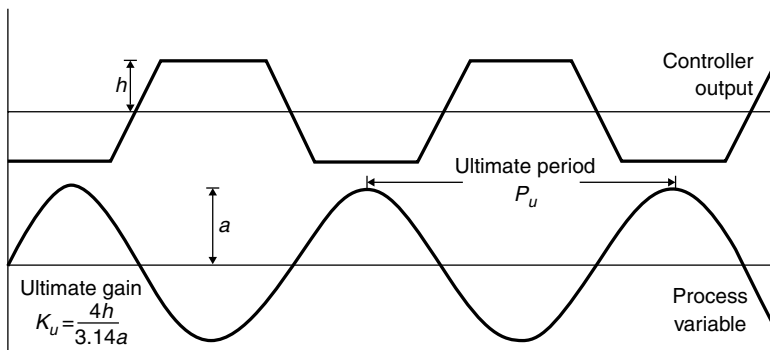


Fig. 9.14 ATV critical parameters.

parameters defined. It is important to note that the ATV technique is applicable only to processes with significant dead time. The ultimate period will just equal the sampling period if the dead time is not significant.

The general ATV Tuning Method for a PI Controller is as follows:

1. Determine a *reasonable* value for valve change, h (typically 0.05, i.e. 5%). The value for h should be small enough that the process is not unnecessarily upset but large enough that the amplitude, a , can be measured.
2. Move the valve $+h$ units.
3. Wait until the process variable starts to move, then move the valve $-2h$ units.
4. When the process variable (PV) crosses the set point, move the valve $+2h$ units.
5. Repeat until a limit cycle is established, as illustrated in Figure 9.14.
6. Record the value of a by picking it off the response graph.
7. Perform the following calculations to determine the ultimate period, ultimate gain, and the controller gain and integral time.

$P_u \equiv$ ultimate period = period taken from limit cycle

$K_u \equiv$ ultimate gain = $4h/3.14a$

$$K_c = \frac{K_u}{3.2}$$

$$T_i = 2.2(P_u)$$

Single and multiple loops

Since a manipulated variable generally affects more than one controlled variable in a multi-loop system, it may be challenging to properly tune the system. The easiest way to work with a multi-loop system is to treat it as a group of individual control loops. First tune each loop with all the other control loops in manual. Then, close all the control loops and retune the control loops until the system can ‘handle’ a known disturbance without losing its stability. It is often necessary to loosen the original tuning parameters to minimize interactions between control loops. This entails decreasing the controller gains and increasing the integral times (e.g. Svrcek *et al.*, 2006). Dynamic simulation can then be used to drastically reduce the time required and to simplify the above controller tuning procedure.

Cascade control. Tuning cascade control loops is a particular example of multiple loop tuning. Both the primary and secondary loops have their own response time, independent of whether they are in a cascade configuration or not. The response time of the primary loop is τ_1 and that of the secondary loop is τ_2 . The heuristic $\tau_1 \geq 4 \times \tau_2$ must be adhered to in order ensure that cascade control works effectively. What this rule of thumb means is that the primary loop should never know that there is a secondary loop and the secondary loop should be able to respond as quickly as the FCE. If this rule is followed then there will be little interaction between the two loops and the control scheme will function effectively.

When tuning the primary controller there should be no interaction between the primary and secondary loops. If there is, it means that the primary loop is not slow enough in comparison to the secondary. The procedure to put a cascade system into operation is as follows:

1. Place the primary controller in manual or the secondary controller to local set point. This will break the cascade and allow the secondary controller to be tuned.
2. Tune the secondary controller as if it were the only control loop present.
3. Return the secondary controller to remote set point and/or place the primary controller in auto.
4. Now tune the primary loop normally. If the system begins to oscillate when the primary controller is placed in auto, reduce the primary controller gain.

9.6 HOW TO DO ADVANCED CONTROL (ADVANCED CONTROL METHODS)

In this final section of the chapter we will consider how to control driers with advanced control methods.

First we need to define just what ‘advanced’ process control is. Advanced Process Control is typically abbreviated APC. APC is relative to process and technology, typically involves computer models, typically involves more complex mathematics than simple PID control, is implemented above the regulatory (PID) layer (APC sends set-points to regulatory layer) and may even involve dynamically manipulating either the PID tuning constants or the model parameters (in the case of Self Tuning and Adaptive Control).

Why would one want to use APC? APC is used when there are variations in process dynamics and variations in process disturbances that PID is insufficient to handle.

APC can allow a wider range of control and achieve the same or better efficiency of operation for wider operating range. Note however that this extra operational efficiency

comes at an increased but not necessarily exorbitant cost of commissioning and maintaining control loops.

Process control strategies including APC have been classified by a number of workers (e.g. Seborg, 1994) according to the following general classes:

1. Conventional control – manual and PID
2. Advanced control: classical techniques – e.g. ratio, cascade and feed-forward
3. Advanced control: widely used in industry – e.g. MPC, IMC and adaptive control
4. Advanced control: with some industrial application – e.g. expert systems, neuro-controllers and fuzzy control
5. Advanced control: proposed, with few applications – e.g. optimal control, robust control and most academic's papers!

We have dealt with the first two classes of process control in the previous sections of this chapter, that is, conventional control and advanced classical techniques. We have also touched on IMC as applied to controller tuning, which is where it is most commonly used in industry as well as the ATV method of self-tuning, which can be considered a form of adaptive control. In this section we will cover the next two classes of APC – APC widely used in industry and APC with some industrial application – by focusing on MPC, self-tuning and adaptive control, and computational intelligence in control.

9.6.1 Model predictive control (MPC)

Model predictive control or MPC is the most widely industrially used of all advanced control methods (Qin and Badgwell, 2003). MPC is a class of computer control scheme that uses a process model for explicit prediction of future plant behaviour and computation of appropriate control action required to drive the predicted output as close as possible to the desired target value.

Industrial control challenges include dealing with multiple variables, some variables not being measurable, difficult dynamics such as time delays, inverse-responses, instabilities and nonlinearities, equality and inequality, hard and soft constraints on absolute values and rates of change. The drying process exhibits all of these challenges.

MPC is capable of handling many of these challenges. MPC is easy for multi-variable and interacting processes, handles difficult dynamics with ease, uses a process model that can be simple, and controls both measured and unmeasured variables. MPC is posed as an optimization problem that optimizes control effort to meet objectives and is therefore capable of handling all constraints.

MPC works by employing a moving horizon algorithm that considers first how process output will behave in future if no further action taken. Control action is then targeted to rectify what is left to be corrected after the full effects of the previously implemented control action.

The basic elements of MPC include the specification of a reference trajectory, $y^*(k)$; the prediction of the process outputs over some horizon, $\hat{y}(k+i)$, based on a model, \mathbf{M} relating the process outputs to the process inputs, $u(k+j)$; computation, based on \mathbf{M} , of a control action sequence to satisfy an optimization objective, subject to pre-specified constraints (this is akin to using the model inverse, \mathbf{M}^{-1}); and an error prediction update, $e(k) = y_m(k) - \hat{y}(k)$.

'Standard' MPC uses linear models. MPC schemes are implemented on digital computers so discrete models are used. Three linear, discrete models are mostly used: finite convolution, discrete state space and discrete transfer function models.

Finite convolution models are presented either as impulse or step response forms. The finite impulse response (FIR) model form is:

$$y(k) = \sum g(i)u(k - i), \quad \text{for } i = 0 - k$$

where the parameters $g(i)$ constitute the impulse response function.

The step response model form is as follows:

$$y(k) = \sum \beta(i)\Delta u(k - i), \quad \text{for } i = 0 - k$$

where the parameters $\beta(i)$ constitute the step response function and $\Delta u(k) = u(k) - u(k - 1)$.

The step and impulse response functions are related as:

$$\begin{aligned} g(i) &= \beta(i) - \beta(i - 1) \\ \beta(i) &= \sum g(j), \quad \text{for } j = 1 - i \end{aligned}$$

where $g(0) = \beta(0) = 0$ for real, causal systems – that is, there is a mandatory one-step delay.

Discrete state space models are also known as Auto Regressive Moving Average with External input or ARMAX (e.g. Ljung, 1999) models:

$$y(k) = \sum a(i)y(k - i) + \sum b(i)u(k - i - m), \quad i = 0 - k$$

where $m =$ time delay and $a(0) = b(0) = 0$ for real, causal systems.

The discrete transfer function model form is:

$$y(z) = z^{-m}[B(z^{-1})/A(z^{-1})] u(z)$$

where $B(z^{-1}), A(z^{-1})$ are polynomials in the z -transform variable.

The parameters for these models are obtained from fitting noise-free plant data/other models. This system identification is the most critical part of developing an MPC controller and therefore is the biggest cost in terms of time and money (e.g. Qin and Badgwell, 2003).

Obtaining the model inverse is mostly carried out numerically as the solution of an optimization problem. For example, constrained least-squares minimization requires numerical solution with techniques such as quadratic programming, QP.

Many factors contribute to discrepancy between actual data and model predictions, including un-modelled, unmeasured disturbances, fundamental errors in model structure and errors in model parameter estimates. The MPC strategy is typically pragmatic. The simplest approach used assumes error caused by unmeasured disturbances and constant, so the current discrepancy is added to all predictions. This can be refined by estimating the discrepancy recursively on-line, for example, with Kalman filters.

Since the development of MPC in the early 1970s there have been many commercial versions and literally thousands of applications. Common commercial instantiations include Dynamic Matrix Control (DMC) originally from Shell, Quadratic DMC (QDMC) now an Aspen Technology product, Pavilion from Pavilion Technologies, Robust MPC Technology (RMPCT) from Honeywell and Shell Multivariable Optimizing Control (SMOC) from Shell Global Solutions. Food drying control has imitated chemical process control with MPC being the most common APC scheme used (Dufour, 2006).

9.6.2 Adaptive control

Adaptive control is an APC method that automatically adjusts controller parameters to take account of significant process dynamics changes with operating point change (i.e. non-linearity) and time (e.g. due to processes such as deactivation and fouling). There are three major classes or types of adaptive control. The types of adaptive control are, in order of complexity: gain scheduling, self-tuning and model reference adaptive control.

Gain scheduling is also referred to as scheduled adaptive control. Gain scheduling uses known process response information to pre-programme a schedule of controller parameters that are downloaded to the controller as the process moves from one operating regime to another. This form of adaptive control is easily implemented as a look-up table in the distributed control system.

Self-tuning control is a form of adaptive control where the parameters of a process model are identified repeated on-line. The newly re-identified process model parameters are then used to specify new values of the controller parameters. The controller can be a PID or MPC controller. The key aspect of self-tuning control is the identification of the process model parameters. This must be reliable and robust for industrial use. Methods such as ATV (Åström and Hagglund, 1984) are typically employed.

Model reference adaptive control uses a reference model whose output is compared to the process output and the resulting reference model error, $e_{rm} = PV_m - PV_{actual}$, is used to update the controller so that the error value becomes zero. Often the controller parameter adjustment reduces an integral error criterion such as integral time absolute error, ITAE.

Despite the simplicity of gain scheduled adaptive control it is interesting to note that adaptive control has not yet found great application in food process drying, at least in the public domain. Less than 5% of the reported drier control applications in literature have involved adaptive control (Dufour, 2006). This could be an area of opportunity.

9.6.3 Artificial intelligence in control

The application of artificial intelligence (AI) or computational intelligence is generally the next most common form of APC that has some industrial application.

The classical view of AI is that of the brain as a computer, for example, HAL in '2001: A Space Odyssey'. This is the computer science view of machine intelligence and this approach is based on the processing of symbols.

The dynamic systems view of AI is that of the brain as a dynamic system. This is machine intelligence engineering or cybernetics. It often involves large systems of differential or difference equations modelling natural phenomena.

In general we cannot articulate the mathematical rules that describe our behaviour, but instead we recognize patterns. Symbolic processing fits naturally into the brain-as-computer framework and allows us to present structured knowledge as rules, but prevents us from applying the tools of numerical mathematics – we cannot take the derivative of a symbol.

These considerations led to a framework of 'model free' estimators. Such estimators contain no explicit statement on how outputs depend on inputs. There are three basic classes: expert systems, artificial neural networks (ANN) and fuzzy systems. Expert systems exploit structured knowledge but store/process it symbolically. ANN exploit numerical frameworks with theorems, numeric algorithms and analogue and digital implementations. Fuzzy systems directly encode structured knowledge but in a numerical framework.

Expert systems

Expert systems (e.g. Liao, 2005) are AI systems that store and process rules, for example:

$$\text{IF A THEN B} \quad \text{or} \quad \text{A} \rightarrow \text{B}$$

Collections of rules are known as knowledge bases or trees, for example:

$$\text{A} \rightarrow \text{B} \rightarrow \text{C} \rightarrow \text{D} \rightarrow \dots$$

Knowledge engineers search the knowledge tree to enumerate logical paths – the inference process. Forward chaining inference answers the ‘what-if’ questions. Backward chaining inference answers the ‘why/how-come’ questions. Knowledge engineers acquire, store and process data rules as symbols from real experts. The difficulty is for the experts to articulate the propositional rules that approximate their expert behaviour.

Expert systems were a popular APC method in the late 1980s and early 1990s but there are few recently published food drying applications (Dufour, 2006).

Artificial neural networks (ANN)

ANN (e.g. Kosko, 1992) are a form of non-linear black box modelling via interconnected processing elements (neurons), which are specialized cells for transmission of information. An individual neuron acts as a summing device, adding weighted inputs and passing the sum through a non-linearity. ANN are taught to identify relationships between input and output data sets. ANN are in essence a regression technique, but they automatically produce the fitting form as well as simultaneously fitting this form to data.

ANN have found specific application in process control as soft sensors where other process variables that are easy to measure are used to produce an artificial measurement of quality that can be used for on-line control which is updated periodically by off line or at line quality analyses. Pavilion Technology employs ANN in just this way to produce effectively a non-linear MPC (Sayyar-Rodsari *et al.*, 2004) which has been employed widely for milk product spray drying control for Fonterra in New Zealand (Pavilion, 2004).

Fuzzy systems

Fuzzy systems (e.g. Davidson, 1996; Ross, 2004) make use of fuzzy logic as opposed to crisp logic. For example, instead of describing a temperature as 25.0°C according to crisp logic, we might say that the temperature is warm in fuzzy logic. To make use of fuzzy logic for control one needs to encode the fuzzy information numerically. There are three primary elements of fuzzy logic that must be defined – the fuzzy sets, for example, warm, cold etc.; the membership functions, for example, the percentage certainty that the system is warm; and the production rules for calculation of the controller output. A fuzzy logic controller therefore operates by performing two functions – fuzzy inference and de-fuzzification.

Fuzzy logic control is useful when intuition/judgement is required and the system is considered difficult to automate, for example, where there are tracking, tuning and interpolation problems. As a result, fuzzy logic control has found favour in food drying systems (e.g. Davidson, 1996) and represents approximately 10% of the published APC applications (Dufour, 2006).

REFERENCES

- Åström, K.J. and Hagglund, T. (1984) Automatic tuning of simple regulators with specifications on phase and amplified margins. *Automatica*, **20**, 645.
- Buckley, P.S. (1964) *Techniques of Process Control*. John Wiley & Sons, New York.
- CADDET (2000) Model predictive control system saves energy. *CADDET Technical Brochures*, **R371**.
- Cohen, G.H. and Coon, G.A. (1953) Theoretical consideration of retarded control. *Transactions of the ASME*, **75**, 827.
- Considine, D.M. (ed.) (1993) *Process Industrial Instrument and Controls Handbook*, 4th edn. McGraw-Hill, New York.
- Douglas, P.L., Kwade, A., Lee, P.L., Mallick, S.K. and Whaley, M.G. (1992) Modelling, simulation and control of rotary sugar dryers. *Drying '92, Part B*, 1928–1939.
- Davidson, V.J. (1996) Fuzzy control for food processes. Chapter 6. In: *Computerized Control Systems in the Food Industry* (ed. G.S. Mittal). Marcel Dekker, New York, pp. 179–205.
- Downs, J.J. and Doss, J.E. (1991) Present status and future needs – A view from North American industry. *Proceedings of 4th International Conference on Chemical Process Control*, Feb. 17–22, Padre Island, TX, USA, pp. 53–77.
- Dufour, P. (2006) Control engineering in drying technology: Review and trends. *Drying Technology*, **24**, 889–904.
- Edgar, T.F., Smith, C.L., Shinsky, R.G. *et al.* (1997) Process control. Chapter 8. In: *Perry's Chemical Engineering Handbook*, 7th edn. (eds R.H. Perry and D.W. Green). McGraw-Hill, New York, pp. 36–37.
- Fruehauf, P.S., Chien, I.-L. and Lauritsen, M.D. (1993) Simplified IMC-PID tuning rules. *ISA*, Paper# 93-414, p. 1745.
- Jumah, R., Mujumdar, A.S. and Raghavan, V.G.S. (1995) Control of industrial dryers. Chapter 43. In: *Handbook of Industrial Drying*, 2nd edn. (ed. A.S. Mujumdar). Marcel Dekker, New York.
- Keey, R.B. (1992) *Drying of Loose and Particulate Materials*. Hemisphere, New York.
- Kosko, B. (1992) *Neural Networks and Fuzzy Systems*. Prentice-Hall, Englewood Cliffs, NJ.
- Ljung, L. (1999) *System Identification – Theory for the User*, 2nd edn. PTR Prentice Hall, Upper Saddle River, NJ.
- Liao, S.-H. (2005) Expert system methodologies and applications – A decade review from 1995–2004. *Expert Systems with Applications*, **28**, 93–103.
- Luyben, W.L., Tyreus, B.D. and Luyben, M.L. (1998) *Plant Wide Process Control*. McGraw-Hill, New York.
- McFarlane, I. (1995) *Automatic Control of Food Manufacturing Processes*, 2nd edn. Blackie, London.
- McFarlane, N.J.B. and Bruce, D.M. (1996) A cost function for continuous-flow grain drying and its use in control. *Journal of Agricultural Engineering Research*, **65**, 63–75.
- McMillan, G.K. (ed.) (1999) *Process/Industrial Instruments and Controls Handbook*, 5th edn. McGraw-Hill, New York, NY.
- Pavilion (2004) Fonterra Co-operative Group Case Study. *Pavilion Technologies Technical Brochures*.
- Qin, S.J. and Badgwell, T.A. (2003) A survey of industrial model predictive control technology. *Control Engineering Practice*, **28**(8), 1169–1192.
- Rivera, D.E., Morari, M. and Skogestad, S. (1986) Internal model control, 4. PID Controller Design. *Industrial and Engineering Chemical Process Design and Development*, **25**, 252.
- Ross, T.J. (2004) *Fuzzy Logic with Engineering Applications*, 2nd edn. John Wiley and Sons, New York.
- Ryniaki, A. and Nellist, M.E. (1991) Optimization of control systems for near-ambient grain drying: Pt. 2. The optimizing simulations. *Journal of Agricultural Engineering Research*, **48**, 19–35.
- Sayyar-Rodsari, B., Hartman, E., Plumer, E., Liano, K. and Schweiger, C. (2004) Extrapolating gain-constrained neural networks – Effective modeling for nonlinear control. *Proceedings of the 43rd IEEE Conference on Decision and Control*. 14–17 December 2004, **5**, 4964–4971.
- Seborg, D.E. (1984) A perspective on advanced strategies for process control. *Modelling, Identification and Control*, **15**(3), 179–189.
- Svrcek, W.Y., Mahoney, D.P. and Young, B.R. (2006) *A Real-time Approach to Process Control*, 2nd edn. John Wiley and Sons, Ltd., Chichester, UK.

- Tyreus, B.D. and Luyben, W.L. (1992) Tuning of PI controllers for integrator/deadtime processes. *Industrial and Engineering Chemical Research*, **31**, 2625.
- Vogel, E.F. (1992) Plant wide process control. In: *Practical Distillation Control* (ed. W.L. Luyben). Van Nostrand Reinhold, New York, p. 86.
- Ziegler, J.G. and Nichols, N.B. (1942) Optimum settings for automatic controllers. *Transactions of the ASME*, **64**, 759.

10 Fire and explosion protection in food driers

Xiao Dong Chen

10.1 INTRODUCTION – THERMAL HAZARDS IN DRIERS

It is uncommon for a drying facility to process highly flammable materials, though most solid food products are combustible due to their chemical composition of elements such as proteins, carbohydrate and fatty acids. As such, elevated temperatures are highly undesirable, not just from the quality point of view. The single greatest ‘fear’ for a drying operation, or indeed any industrial operation, is a widespread fire and/or followed by a massive explosion due to the exothermic nature of the products involved. Explosion involves combustible gases (flammable vapour) or dusts. The consequences can be devastating. Some sort of fire may be initiated in the first place and propagated, triggering a greater hazard such as an explosion. Explosion, both the initiation and propagation of it, is the focus of this chapter.

Food processing normally does not use flammable solvent except when an extraction stage is needed, for example, to remove cholesterol from fatty foods, and the solvent would have to be removed as a ‘drying’ operation. In this chapter, the cases where flammable solvents are not used are focused upon. In many food-drying operations, combustible materials including combustible dusts do exist which can be potentially ignited and exploded.

10.1.1 Conditions for an explosion to occur

An explosion is an exothermic chemical process (a process that releases a large amount of heat in a short time) that, when occurring at constant volume, gives rise to a sudden and significant pressure rise (Eckhoff, 1991). A dust explosion occurs when a finely divided combustible solid is dispersed in air (oxygen is available) and subjected to an ignition source (a fire or an electrical spark, for instance). An illustration of the necessary combination of the conditions for a fire/explosion to start is shown in Plate 10.1. An analogy of the logical sequence is such an incident represented by the development of the combustion of wood blocks, to that of wood chips (smaller sizes), and then to the explosion of suspended wood sawdust (even smaller sizes) (Eckhoff, 1991).

Furthermore, several conditions also have to be satisfied before an explosion occurs: the dust must be airborne in sufficient concentration to fall within the explosion range (an explosion will not occur at either too low or too high concentrations); the ignition source must be powerful enough to initiate combustion emitting a greater amount of heat than that of the minimum ignition energy (MIE) required to trigger an explosion; and there must be sufficient oxygen in the atmosphere to support combustion. In addition, finer particles and higher ambient temperatures are more likely to lead to explosions. Once ignition has occurred, the propagation of the flame front through the dust suspension causes very rapid temperature and pressure rises (Beever, 1984, 1985).

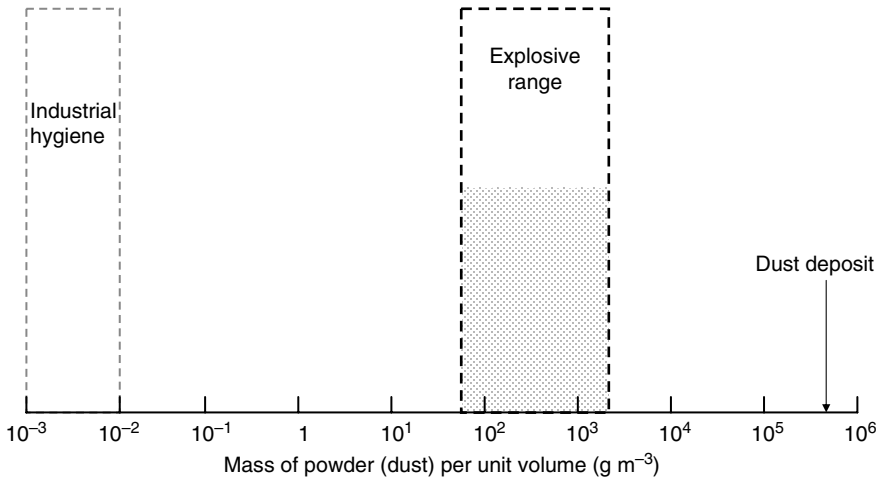


Fig. 10.1 Range of explosive concentrations in air at normal temperature and atmospheric pressure for a typical natural dust (maize starch) compared with a typical range of maximum permissible dust concentration for industrial hygiene, and typical density of dust deposits of natural organic dusts (modified from Eckhoff, 1991).

The key points are that the dust must (Eckhoff, 1991; Lunn, 1992):

1. be combustible
2. be airborne
3. have a particle size distribution capable of propagating flame
4. have concentrations that are within the explosive range (see Figure 10.1 for instance; too high (rich) or too low (lean) are not favourable for an explosion to occur)
5. have the cloud(s) in contact with an ignition source of sufficient energy to cause an ignition
6. be present in an atmosphere capable of supporting combustion

10.1.2 How serious is the problem?

Milling, grinding, filters and driers used in the food industry are the main process items which can be affected by fire and explosion. From statistics, about 50% of the known sources for dust explosions are in the following three categories (Lunn, 1992):

- Frictional/mechanical (bearings, rotating discs (in a spray drier) etc.)
- Self-heating/over-heating
- Open flames/burning materials

10.1.3 What affects the degree of violence of a dust explosion?

The particle size/specific surface area (i.e. the ratio between surface area and volume of a particle) is a central factor. The major factors are summarized in Table 10.1 (after Eckhoff, 1991).

Table 10.1 The major factors that influence the degree of violence in explosions.

Particle size	Finer dusts tend to make severe explosions. This is because the rate of the chemical reaction is a function of surface area.
Moisture	The lower the moisture content of the material the greater the explosive violence. It takes a significant part of the chemical energy to vapourize the water if significant amounts are present, before preceding the material's temperature to greater than 100°C.
Turbulence	Heat and mass transfer are enhanced by turbulence. The explosion can propagate through the dust cloud more rapidly if it is turbulent.
Temperature	If the rate of the reaction is controlled by the rate at which air can get to the powder, temperature has little effect. However, in a turbulent gas where the rate of the chemical reaction is a function of temperature, increasing temperature increases explosion violence. This is also true if there is an oxidant present in the dust itself.
Dust concentration	The explosiveness of a dust cloud increases with an increase in dust concentration until a maximum is reached. In higher dust concentrations, explosivity decreases or remains roughly the same.

There are two categories of dust explosions: *primary and secondary explosions*.

Primary explosion: Dust explosions which are primarily initiated are normally found inside process equipment, such as mills, mixers, spray driers, fluidized-bed driers, screens, cyclones, filters, bucket elevators, hoppers, silos, pipes for pneumatic transport of powders – by certain ignition sources. An important objective of dust explosion control is therefore to limit primary explosion in the process equipment in which they are initiated.

Secondary explosion: After a primary explosion occurs, the central concern is then to avoid secondary explosions due to the entrainment of dust layers by the blast wave from the primary explosion. Such an entrainment can be demonstrated in Plate 10.2 which shows how a resting deposit layer becomes hazardous.

In general, dispersible and combustible dust layers (can be airborne) anywhere in a process plant present a potential hazard for extensive secondary dust explosions.

10.1.4 How to reduce the risk of dust explosion

One can reduce the risk if one eliminates the explosive dust cloud, eliminates oxygen from gas or eliminates sources of ignition. These solutions are inferred in the *fire/explosion triangle* (Plate 10.1). Realistically, it is known that one can only minimize the risk or damage; one can never eliminate it 100%.

10.2 A PRACTICAL EXAMPLE: MILK POWDER PLANT SAFETY

Milk powders are explosive when they are suspended in an air flow in a concentration which is within the explosive range, and when there is an ignition source which emits energy that is greater than the minimum ignition energy of the dust cloud; sufficient oxygen is also necessary. The extent of explosion-induced damage depends on whether the device within which the explosion happens is properly vented and whether there are secondary explosions.

A number of incidents of fires and explosions in spray drying plants in New Zealand have been reported in milk powder manufacture (X.D. Chen, personal communication).

Because of the current drying operations in the milk powder manufacturing process, there is a very large demand for dry gas usage, it is not economic to use inert gas totally, for example, N₂. The technology to produce N₂ using membrane air separation is not yet cost effective. Oxygen is therefore always available for a fire or an explosion. There are a number of possible ways to achieve ignition of a fire, for example, self-ignition, electrostatic discharge, open fires – including welding operations in a dusty environment, cigarette smoking, over-heating by light bulb etc.

Human error can lead to disasters, and we are sometimes the main trouble makers. However, the 24-h operation itself presents a management problem that is related to human weakness, both of the managers and the operators (this will be discussed further in Section 10.4).

Milk powder production involves pre-concentration of milk by evaporation to about 45–50% total solids, followed by spray drying of the concentrate in hot air. Modern drier capacities are typically 4–12 tonnes of milk powder per hour. In milk drying plants there are certain regions (especially at the dry side of the operation) where all the conditions for an explosion, apart from the existence of an ignition source, are always present during normal operations. It is essential to understand the various possible mechanisms for a heating-to-ignition process to become reality, and the regions of concern, in order to decide on suitable prevention and protection measures.

10.2.1 Fires

The most well known (unintentional) causes for an explosion in a spray drying plant are the self-heating of milk powders in seemingly non-hazardous environments, or over-heating due to the high drying air temperature, or by other means, for example, over-shot of temperature control, mechanical friction or a series of electrostatic discharges. Generally, an ignition of a solid would occur when the rate of heat generation from the exothermic reactions of the particle (usually the oxidation in air) becomes greater than that of the heat dissipation (water evaporation, convective/radiative heat transfer to ambient from the particle).

10.2.1.1 Self-ignition

A review of explosion accidents in spray driers show that the by far most common cause of explosions in spray driers is self-ignition. This self-ignition (self-heating to ignition temperatures) process causes smouldering material to fall down into the conical part of the drier, directly igniting a flammable dust cloud there, or whirling up dust and igniting this (Alfert *et al.*, 1988). As the mass of the solid gets larger, the heat generated inside the solid domain (packed particles for instance) can only be partially retained due to the low thermal conductivity of the packed milk powders or the milk powder deposit layer (typically of 0.1–0.2 W m⁻¹ K when water content of the powders is of a few per cent). This accumulation of heat raises the temperature at the central part of the solid, which can lead to an ignition when the heat generated by oxidation overcomes the heat loss to ambient (Duane and Synnott, 1992).

Self-ignition of milk powder can occur in the deposit layers on drier walls, or on other pneumatic conveying devices, or bag houses or storage silos (although the oxygen content may be low here, the potential hazard of smouldering bulk solids does exist), or on rotating machinery. Cyclone blockage with milk powder may also induce a fire. Amongst the equipment used in a drying plant, the spray drier is perhaps the most expensive, and discussions

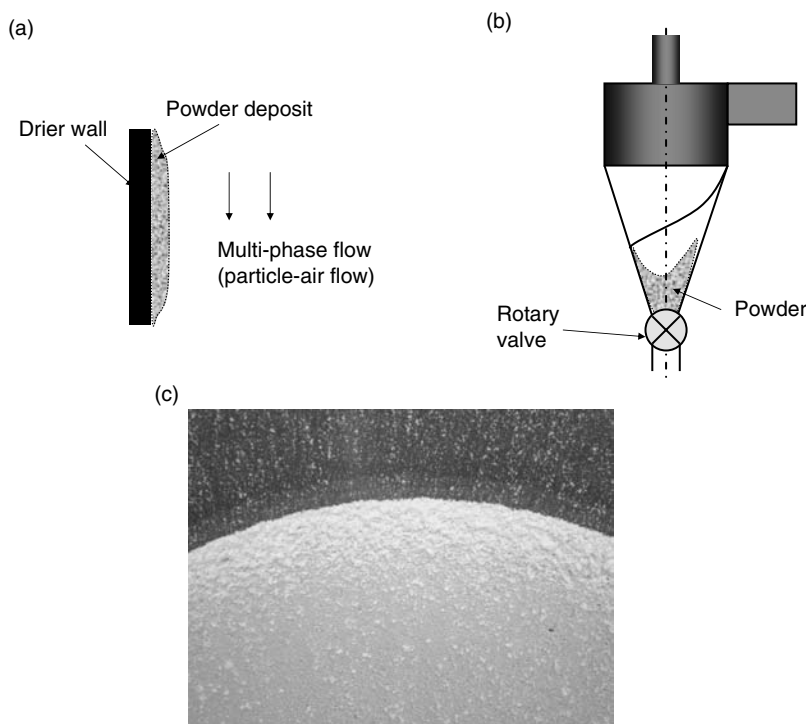


Fig. 10.2 Powder deposition on drier wall and blockage in cyclone. (a) Wall deposit; (b) cyclone blockage; (c) milk powder deposit at the region joining the straight (vertical) section and the cone (bottom) section of a lab scale spray drier.

around spray drier safety are often the major subject of explosion protection. The issues related to the spray drier are thus most thoroughly discussed in the following sections.

As the spray drying chamber itself is the major capital item, the powder deposition on the chamber walls should be of primary importance (see Figure 10.2).

The formation of milk powder deposit layer on drier wall

Milk powder deposits on the internal walls of spray driers are not desirable because of fire safety and hygiene requirements. These deposits have to be washed away after a few production runs. Frequent washing of the drier results in a high cleaning cost (labour, chemicals, effluent disposal) as well as increased down time. The regions in which deposits are likely to occur in the compact driers with rotating disc atomizers were first described by Masters (1991) and were then studied in more detail by Chen *et al.* (1993) and can be summarized below:

1. Deposits on the side wall due to direct impact of large wet concentrate particles with high velocities; this deposit may be minimized by deflecting the concentrate spray downwards by a suitable air flow. The production of large concentrate particles can be reduced by reducing the viscosity of the concentrate being dried, thus aiding atomization.
2. Deposits on the lower cone, which is caused either by the direct impact of the concentrate spray or by the dry particles swirling down with the air movement and striking and sticking

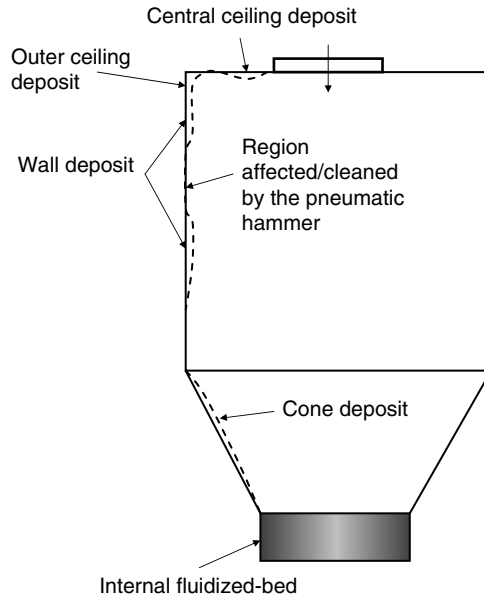


Fig. 10.3 The regions of milk powder deposition (modified after Chen *et al.*, 1993).

to the slope of the cone; this deposit may be removed during operation of the drier using 'air sweeps' consisting of jets of air (or by adjusting disc diameter and speed).

3. Deposits on the ceiling, which may be caused both by dispersion of the mist of the atomized concentrate and by entrainment of particles in the turbulent mixing zone caused by the sudden expansion imposed on the air stream entering the drying chamber (see Figure 10.3).

The mechanisms involving the direct impact of wet particles on drier walls have largely been confirmed for milk powder driers and occur in all commercial drying plants to a greater or lesser extent. Ceiling deposit is a major concern as it can catch fire spontaneously. In a high-temperature environment (the inlet air temperature is usually higher than 180°C so inside the drier it is very hot) if the deposit layer becomes very thick it can catch fire (Beever, 1984, 1985; Beever and Crowhurst, 1989; Duane and Synnott, 1992). Deposits undergo oxidation (particularly for whole milk powder) and browning or scorching (Raemy *et al.*, 1983), and will degrade the final product if they fall off and mix with it, giving rise to conspicuous 'scorched particles'. This appearance of scorched particles (dark brown or black) in the powder samples collected routinely for functional testing (from the sifter every half an hour during production) is often used as a means of fire alarm. Most milk powder specifications include a strict limitation on the permitted proportion of scorched particles, which is expected to be routinely tested in dairy factories. Humid conditions within deposited layers of milk powder in cooler parts of the drier may also encourage bacterial growth. The effects of the drier wall temperature on the physical characteristics of food powder deposits have not yet been well described; the deposits may exhibit different physical properties under different heating conditions. One good example along those lines is the study reported by Brennan *et al.* (1971), who investigated the deposition of fruit juice powder on spray drier walls, which were found to be largely dependent on the wall temperatures. More recent works on powder deposition on driers are those by Chen *et al.* (1993) and Chen *et al.* (1994) who carried out

work in a large industrial drier. The glass-transition phenomena of the lactose content in milk powder should also be recognized as responsible for the temperature effect on powder deposition in driers (Lloyd *et al.*, 1996).

For milk powders, the physical properties of the fat (typically 27% of whole milk powder) and the lactose (typically 50% of skin milk powder) in relation to temperature changes are believed to dominate the probability of a permanent powder deposition once the powders make contact with the steel walls at different temperatures. The melting points of milk fats of varying compositions (soft and hard fractions), at which the fats become liquid, range from -20°C to about 40°C (Mulder and Walstra, 1974). The 'sticking' temperatures, as defined by Wallack and King (1988) for amorphous carbohydrates range from room temperature to the melting temperature of their crystalline states (about 200°C) depending on the moisture content (Roos and Karel, 1990, 1991, 1992; Lloyd *et al.*, 1996). The amorphous lactose is formed during rapid drying where the time scale for full crystallization is much longer than the drying and solidification of a lactose-containing concentrated liquid droplet. The sticking phenomena has been postulated as being caused by the glass transition of the amorphous lactose as beyond the glass-transition point, which is affected greatly by the temperature of the powder and the relative humidity of its surrounding gas, the amorphous lactose begins to crystallize (Lloyd *et al.*, 1996). The higher the relative humidity, the lower is this sticking temperature. This aspect has also been discussed in Chapter 2.

As studied recently (Chen *et al.*, 1993), deposits from both a skim and a whole milk powder were found in similar positions in the drier (particle size dominating phenomenon), but the wall deposits of the whole milk powder were of larger, and ceiling deposits of smaller, mean particle size than those for skim milk powder (stickiness dominating phenomenon). There were more powder deposits on the walls and less on the ceiling for whole milk powder than for skim milk powder. However the deposits of whole milk powder were generally easier to remove. The non-uniformity of the deposit patterns was evident, which indicated the non-symmetrical temperature and air velocity distributions inside the drying chamber. It is expected that the ceiling deposits can be reduced by manipulating the internal surface temperatures, air flow patterns and by improving the vibration effect of the pneumatic hammers on the walls. The major conclusions of the work by Chen *et al.* (1993) were:

1. The Saunter mean particle diameter (d_{32}) of the deposits on the ceiling was significantly smaller than that of the deposits on the side walls of the upper region. The deposits in all these upper regions had much smaller particles than the bulk products. This supports the theory of air entrainment of fine particles and higher temperature promoting deposition in the upper region. Skim milk powder production produced more small particles than whole milk powder production, and this may have resulted in a heavier deposit on the outer region of the drier ceiling. The whole milk powder deposit was heavier than the skim milk powder deposit on the side walls and near the centre of the ceiling.
2. The temperature distribution either on the walls or on the airflow near the walls and the inlet was very important in determining the deposit distribution and type.

Modification of the temperature distribution of the air inlet and the explosion doors should change the deposition intensity in these particular regions. It appears that both too high and too low temperatures would promote deposition.

It should be noted that the powder concentration in the air, particle size, air velocity and turbulent mixing near the walls all play very important but complicated roles in increasing the probability of deposition.

In the lab work by Chen *et al.* (1994), it was interesting to note that although overall the particles deposited on the drier ceiling were finer than those on the side walls, the powder that went up to the ceiling had more medium size fraction particles compared with the bulk product. This was the first of the reported experiments to confirm the numerically simulated result at Harwell Laboratories, Oxford (Reay, 1989). There was also a strong relationship between the stickiness of a powder with its rate of deposition (Chen *et al.*, 1994). The higher the stickiness, the higher the rate of deposition would be.

The hazard potential of milk powder deposit on drier walls

All oxidative reactions are exothermic and the rates of such reactions depend on temperature, moisture content and availability of oxygen (Labuza *et al.*, 1971; Duane and Synnott, 1981). When conditions favouring oxidation are present (for example, elevated temperature and oxygen-rich environment) the reaction would proceed rapidly accompanied by an increase in the rate of heat evolution. If the rate of heat evolution exceeds the rate of heat loss, the temperature of the reacting material will increase. Consequently, the rate of oxidation increases, and the reaction will rapidly proceed to glowing heat.

High-temperature oxidation of milk powders may start a fire or an explosion in spray driers, which can also lead to dangerous situations for factory operators and may cause serious damage to plants and buildings (International Dairy Federation (IDF), 1987). Fire prevention in this area is promoted through efforts to avoid situations involving a fire hazard (Gibson and Schofield, 1977; Beever, 1984; Beever and Crowhurst, 1989). Any situation that signals a fire hazard must be quickly detected, either through a system of recording and automatic alarm, or through visual inspection.

Self-ignition of milk powder in a spray drier arises as a result of the oxidation of powder deposits exposed to elevated temperatures (Beever and Crowhurst, 1989). Beever (1984) determined the cause of a series of fires in a milk powder plant. It was discovered that many of the fires occurred soon after start-up. Wet patches which encourage deposition may be present on the wall of the drier following washing or incorrect start-up procedures. Chen *et al.* (1993) found sharp rises in temperature everywhere in an industrial spray drier during start-up and shut-down (at least 10°C higher than the steady-state operations). The layer of powder may build up to the thickness necessary for self-ignition and hence is regarded as a hazard.

Raemy *et al.* (1983) used the technique of differential thermal analysis (DTA) for studying spontaneous ignition of milk powder and various milk constituents. Their aim was to detect early exothermic phenomena; such reactions are often related to the deterioration or decomposition of the product. They found that if materials were heated under a large excess of oxygen, fat oxidation, carbohydrate and protein decomposition become so fast that they could bring milk powders to ignition, even at relatively low temperatures. The calorimetric curves of whole milk powders are shown in Figure 10.4.

The three peaks shown in Figure 10.4 correspond to (in order of increasing temperature) α -lactose crystallization, Mallard browning and oxidation, and carbohydrate decomposition. The result in Figure 10.4 was compared to the result of a test carried out under argon atmosphere. It was found that the second peak was not produced in the argon test, thus indicating that at least part of the second peak (between about 120°C and 170°C) could be attributed to fat oxidation.

Raemy *et al.* (1983) pointed out that the thermal release from the reaction was low and was difficult to detect. Several ideas for the type of reactor that could be used were found in research papers. One possibility is an isothermal calorimeter, similar to the one used by

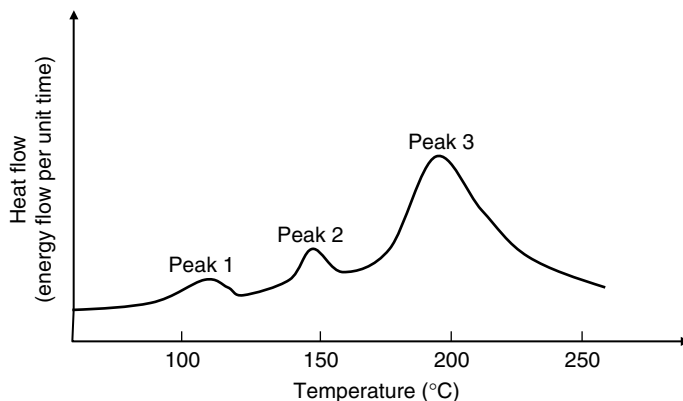


Fig. 10.4 Qualitative calorimetric curve of whole milk powder (modified after Raemy *et al.*, 1983).

Chen and Stott (1993) in their study of the effect of moisture content on coal oxidation. A similar calorimeter was used by Cheng *et al.* (1993) in their research on the validity of the steady-state calorimeter for measuring the total hemispherical emissivity of solids. Pham *et al.* (1994) used a smaller sized adiabatic calorimeter to determine the enthalpy of foods. In any case, this type of study helps identify the key chemical reactions that contribute to the ignition.

Minimum ignition temperature and critical deposit layer thickness

Much work has been carried out on the minimum ignition temperature of milk powder layer. Duane and Synnott (1981) defined *minimum ignition temperature (MIT)* as the average of the lowest ambient temperature that results in ignition and highest ambient temperature that results in non-ignition. The method by which MIT can be measured is based on a mathematical model derived for the one-dimensional case of self heating in a plane slab of reacting materials with a finite, and constant, thermal conductivity, as considered by Frank–Kamenetskii (Bowes, 1984).

The combined effect of percentage of fat and percentage of protein on MIT (°C) was investigated using multiple linear regressions. The following equation (for the 25 mm cube sample size) was found to describe the effect:

$$\text{MIT} = 282.6 + 1.35644(\% \text{protein}) - 2.3133(\% \text{fat}) \quad (10.1)$$

It can be seen that increasing protein content and reducing fat content give rise to the MIT for the milk powder layer and therefore reduces the hazard potential. Equation (10.1) cannot be literally applied in practice, as it is for specific size and shape (cube) of milk powders. It does, however, demonstrate the relative importance of each component in the self-ignition process.

It can be seen that the effects of protein and fat contents are of a similar order of magnitude, which leads to the conclusion that skim milk powder and whole milk powder would have similar ignition characteristics.

The times to ignition are likely to be of the order of an hour or less at 200°C and a few hours at 100°C (Beever, 1985).

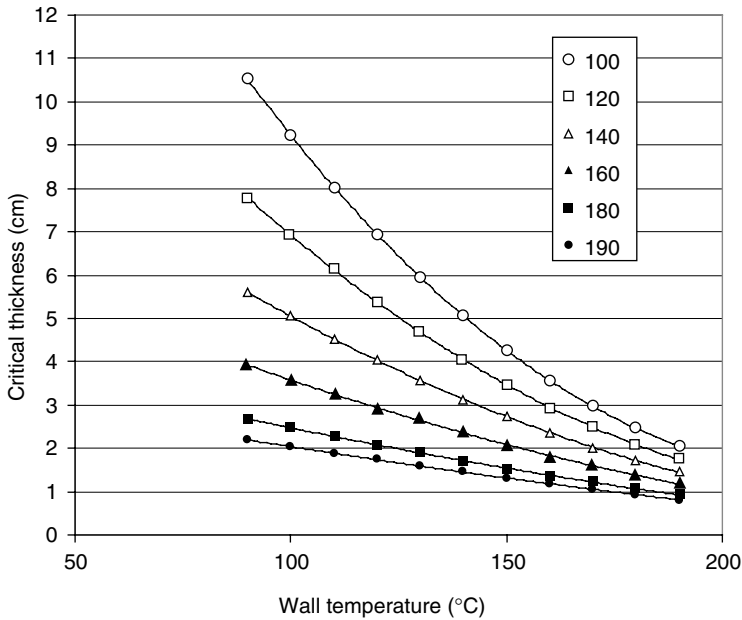


Fig. 10.5 Critical thickness as influenced by drying chamber air temperature (legend) predicted using the thermal ignition kinetics measured in the basket heating method (whole milk powder).

The wall temperature and the temperature at the solid–air interface of the milk powder deposit layer are assumed to be constants. The solid–air temperature is further assumed to be the same as that of the chamber hot air temperature (infinitely large heat transfer coefficient for convection). One can use a modified Frank–Kamnetskii solution catering for the two different temperatures (Wake *et al.*, 1992) and the measured ignition kinetics (reaction heat, rate constant and activation energy) such as those measured by Chong *et al.* (1996), the critical thicknesses of the milk powder deposits beyond which self-ignition is possible, under various combinations of the wall temperature and chamber air temperature, can be calculated. The typical results for whole milk powder and skim milk powder are shown respectively in Figures 10.5 and 10.6. At elevated temperature such as 180°C and above, the critical thickness is down to only a few millimetres. The composition of the food particles of concern plays a key role, so laboratory tests are useful in getting the precise data on the kinetics and the heat transfer properties which can then be used to estimate the critical thicknesses.

In practice, however, deposits may not be formed instantaneously. They may gradually accumulate on the walls to form layers which will tend to oxidize as they are formed and present less of a hazard. The aging effect tends to lead the process to a safer side. It is worth noting that low-temperature self-ignition of larger quantities of milk products is relevant to the processing and storage of the powders after leaving the drier. If stored or packed warm from one drying process, a large pile may, instead of cooling to room temperature, self-heat to ignition (Beever, 1985). Sometimes, the fine powder collected in the bag house can also be fairly hazardous, not only because of the self-heating tendency but also because of the potential of an electrostatic discharge due to the low-humidity environment as well as the very dryness of the fine powders (X.D. Chen, personal industrial experience, 1994).

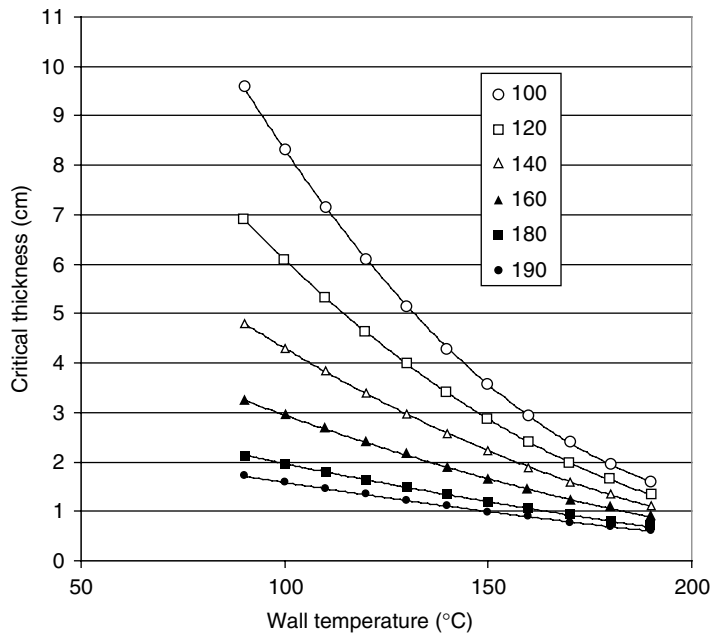


Fig. 10.6 Critical thickness as influenced by drying chamber air temperature (legend) predicted using the thermal ignition kinetics measured in the basket heating method (skim milk powder).

It is further noted that not only the deposit layer presents a self-ignition hazard, a large lump of powder, as is occasionally observed in the fluidized-beds, may also be hazardous. The larger the lump formed the higher the possibility of self-ignition.

Ignition of large stationary powder mass due to over-heating

Although the drier wall temperatures vary from one run to another, they are often greater than 50°C. The temperature is higher near the ceiling than lower down. The wall temperatures were raised transiently to above 100°C during both start-up and shut-down of the drier, and corresponded to changes in the drier feed, for example, starting water spray and switching from water to milk concentrate, or the other way around, and is reflected by the drier exhaust temperature. There are localized cold and hot-spots on the walls of a spray drier (Chen *et al.*, 1993). Over-heating can occur due to several reasons: mechanical friction, crushing of fell off metals, radiative heat from light bulbs, short circuits etc. A few incidents are described below:

1. In dairy plant A, a previous production run produced a blockage in a cyclone that was not found and cleaned out, the start-up of a new run introduced a high-temperature wave and then triggered an ignition in a fashion similar to that of the self-ignition described earlier. This ignition caused a small-scale explosion (Industrial communication, 1992).
2. In dairy plant B, a workman's light bulb was tied onto the handles of a viewing port when certain equipment in that area was checked, and was left on after the production run started. A fire was triggered by the over-heating induced by the radiative heat flux (about 300 W through a viewing port with a diameter of 10 cm going into a layer of milk

powder deposited on the port inside the chamber. A small-scale explosion also occurred (Industrial communication, 1994).

Routinely checking the parts of certain equipments, like rotary valves, bucket elevators and sifters, in terms of finding powder blockages (by knocking using a rubber hammer) or hot spots (by temperature probes), should be carried out wherever possible.

10.2.1.2 Fire protection

Once a fire has been detected by smell, by the appearance of scorched or charred particles at the outlet or by operation of some form of gas detector (sensing CO emission for instance), temperature sensors located at key positions or hot spot sensors (by an infrared sensor for example), action must be taken at once to avoid the risk of explosion.

A practical system for early fire detection in a spray drier has been developed by researchers in the Netherlands Institute for Dairy Research (NIZO) (Steenbergen *et al.*, 1991). Smouldering milk powder (an incomplete combustion state) was found to produce carbon monoxide at a rate of 30 mg s^{-1} per kilogram of smouldering skim milk powder and 20 mg s^{-1} per kilogram of smouldering whole milk powder (Steenbergen *et al.*, 1989). However, with the large quantity of air flow in the drier exhaust, this amount is dispersed to an almost undetectable limit of 1–2 ppm.

The fire detection system developed by NIZO consists of an air sampling and air sample preparation unit, and a sensitive CO analyser. The CO concentration in the spray-drier's inlet air is compared to that of the exhaust air. The CO detection system is currently priced at approximately US\$50k. Due to the small amounts of CO generated (compared with the large volume of air flow), the demand on such a system is great. In addition to detecting the rise in CO content, it is possible to increase the reliability of the system by including smoke point detection (Chong *et al.*, 2006).

Fire fighting within a drier may be extremely difficult unless some extinguishing system has been incorporated into the drier chamber itself. Once a fire has been detected the air flow (out from a drier during drying operation) should be switched off at once, the product feed switched off or switched to water and the extinguishing system (if available) activated. The same principles should be applied to ancillary equipment into which burning materials may have passed (Beever, 1985).

Water is the commonest extinguishing agent, though carbon dioxide is sometimes used. For driers greater than 8.4 m in diameter, a water flow rate of 10 L s^{-1} has been suggested by Pineau (1984). Even if this does not extinguish the fire, the flow over the drier walls will minimize heat damage to the structure (thermal shock). The extinguishing nozzles should be designed and maintained so that they do not become blocked with powder. Fire fighters opening the drier for access with a hose should be prepared for falling burning debris and should be aware of the danger of dust explosion. Smouldering fires are very difficult to put off and it may take many hours before the fire is entirely out (Beever, 1985).

10.2.2 Explosion protection

The biggest risk, in the event of a fire occurring in the plant, is that of a dust explosion. Beever and Crowhurst (1989) stated that in certain regions in a milk spray drying system all the conditions for an explosion, apart from the existence of an ignition source, are always present during normal operation. The possibility of a dust explosion occurring increases when

Table 10.2 Explosive characteristics of milk powder.

Dust	Minimum ignition temperature (°C)	Minimum explosive concentration (g m ⁻³)	Minimum ignition energy (J)	Maximum explosion pressure (MPa)	Maximum rate of pressure rise (MPa s ⁻¹)
Milk powder	440	60	—	0.58	2.8
Skim milk powder†	490	50	0.05	0.66–0.68	11.0–15.9
Skim milk powder‡	500	60	—	0.90	9.9

Code of Practice for the Prevention, Detection and Control of Fire and Explosion in New Zealand Dairy Industry Spray Drying Plant (1990).

† Data obtained from small-scale tests.

‡ Data obtained from large-scale tests.

there is an ignition source in the drier. In the right conditions, the milk powder can self-heat or heat by other mechanisms (e.g. over-heating etc.) and may reach temperatures well in excess of 700°C (X.D. Chen and L.V. Chong, 1994; unpublished data), presenting a serious ignition source for the dust cloud. The minimum ignition temperature for a milk powder cloud of the correct concentration is given in Table 10.2. It should be noted that this minimum ignition temperature should not be confused with the minimum ignition temperature of a layer of milk powder deposit mentioned in previous section on self-ignition.

Since it is not possible to entirely remove the risk of self-ignition, over-heating or other sources of ignition in milk drying plants, then it must be assumed that there is always a risk of explosion. Once an explosion has been initiated, in order to minimize damage to a plant and risk to operators, it must be contained, isolated, vented or suppressed (Gardner, 1994).

1. *Containment*: this is to make the drier and ancillary equipment so strong that an explosion can be sustained without damage. This is obviously not suitable for large spray driers because of the enormous strength required.
2. *Isolation*: explosions are isolated from other parts of the dust handling plant, limiting the destructive effects. Rotary valves, extinguishing barriers and explosion diverters are some of the methods for doing this.
3. *Venting*: weak panels open in the walls of the plant early in the development of the explosion, dissipating its main force to the atmosphere.

Although vents are in widespread use, the technology is not fully developed and there are different methods for calculating the area of a vent for a given dust in a known volume. Detailed accounts of explosion venting have recently been given by Schofield (1984) and Lunn (1992).

The system which has been used in the UK and USA for many years is the so-called vent ratio method. The vent ratio is defined as:

$$\text{Vent ratio} = \text{Area of vent/Volume of the vessel} \quad (10.2)$$

The appropriate vent ratios, based on the explosivity of milk powders, are given in Table 10.3 (Code of Practice, OSH, Wellington, NZ, 1990). It is assumed in Table 10.3 that the plant can withstand an overpressure of 0.14 bar. The disadvantage of this method is

Table 10.3 Vent ratios as a function of volume of equipment for milk powder.

Volume range (m ³)	Vent ratio (m ⁻¹)
<30	1/6.1
30–300	Linearly reduced from 1/6 to 1/25
300–600	Half-area of top
>700	Full-area of top

that it demands very large vent areas in the larger driers which may be difficult and costly to accommodate.

In summary, the parameters for explosion relief design are:

- Equipment/vessel volume (V)
- Force of the explosion K_{st}
- Equipment/vessel pressure strength
- Equipment/vessel interconnections
- Opening pressure of explosion panel or door

4. *Suppression*: An inert material is injected into the explosion as soon as possible after ignition. Explosion pressure is therefore kept low (refer to Figure 10.7).

Explosion suppression involves the early detection of an explosion (pressure transducer) and the injection of inert or inhibiting materials into the chamber to quench flame spread and consequent pressure rise. A large number of injection points are needed to protect the whole plant. At the present time, volumes up to 150 m³ can be protected by suppression methods, or larger if the cone region only is suppressed.

Typically, there is a time delay of 30–100 ms before destructive pressures are generated. This window of opportunity is too short for suppressive techniques to be feasible against top class (the most dangerous) dusts which have K_{st} values greater than 30 MPa m s⁻¹. Milk powders have values lower than this and it is possible to adopt the suppression technology. The K_{st} value is a characteristic value for explosion valence and is defined as follows:

$$(dP/dt)_{max} V^{1/3} = K_{st} \quad (10.3)$$

where $(dP/dt)_{max}$ is the maximum rate of pressure rise in a constant volume, MPa s⁻¹; V is the volume of the vessel, m³. The classification of dust explosions is given by Bartknecht (1981) (see Table 10.4).

The characteristics of venting of some typical equipment in dairy powder industry are summarized below:

Cyclones: Cyclones are usually of weak construction. The best place to vent is on the top surface of the cyclone body because it is relatively easy to access and maintain. Sometimes they are positioned on the top of the vortex tube.

Dust filter separator: Venting should always be placed on the dirty side and as close to a likely ignition source as can be arranged. It is essential that filter bags and internal baffles should not mask the vent area in any way. Most filters can withstand a pressure of 1.7 bar absolute, but is recommended that vent sizing should be based on a value of 1.035 bar absolute.

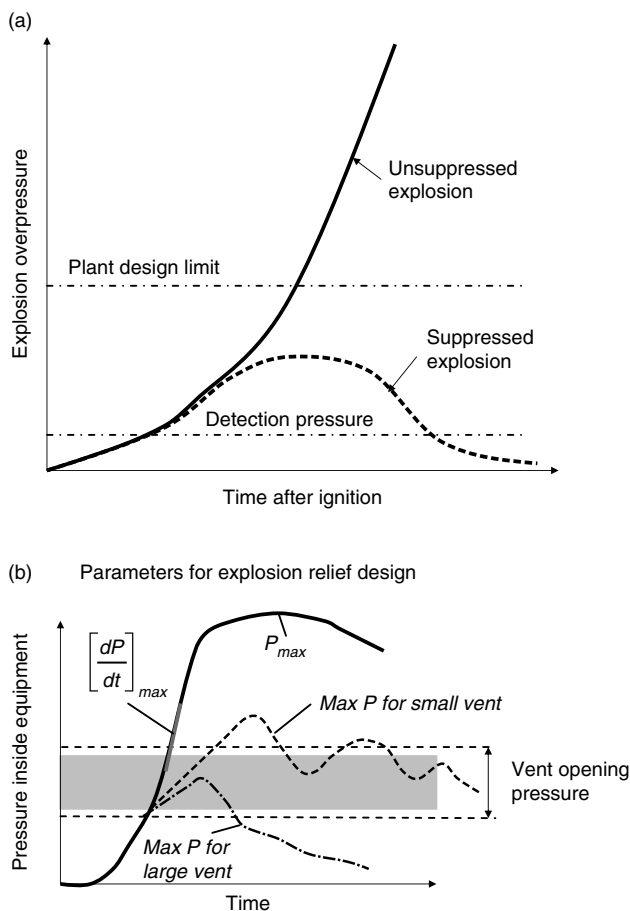


Fig. 10.7 (a) Pressure–time history for suppressed explosion (modified from Kee, 1992); (b) The effect of vent opening pressure and vent size.

Table 10.4 Classification of dust explosions.

Dust explosion class	K_{St} (MPa m s ⁻¹)
St0	0
St1	0–20
St2	20–30
St3	>30

Spray driers: Although the explosive dust rarely fills the whole spray drier, it is recommended that safe design should be based on the total vessel volume. Most of the spray driers have a design pressure of 1.2 bar. The vents are usually located at the upper part of the drier.

Mills: Usually mills are strong enough to contain a dust explosion, but they present a source of ignition to attached hoppers. Isolation techniques should be used to stop the spread of explosion with the basic equipment attached to a mill being fitted with venting.

Elevators: Bucket elevators are essentially vertical ducts partially blocked by buckets. Isolation valves should be fitted to stop the spread of explosions, and the unit itself should be vented at the top and bottom and along its length as if it were a duct.

Storage bins and silos: Isolation between adjacent units should be a feature. Explosion panels in the top of the unit are most favoured. This is also a feature of silo design where it suggests that the entire top area of the silo should be kept clear for venting.

Powder blenders: Venting should be provided. Isolation and speedy arrest of the operation are strongly advised. Special care should be taken with all blending operations to exclude all ignition sources during operation and loading.

The installation of a suppression system is, however, very expensive. In fact, it becomes a nightmare for such a system to be properly maintained in terms of skilled personal requirements and suppressant reloading after a fire etc.

10.3 TESTING FOR VARIOUS EXPLOSION PARAMETERS

It is generally accepted that the following parameters are the key factors in determining the explosion hazard potential for each type of powder:

MIT – Minimum ignition temperature.

MIE – Minimum ignition energy.

MIC – Minimum ignition concentration of dust suspension.

All these factors may be assessed by the following organizations:

Building Research Establishment	Imperial Chemical Industries PO Box 42	Chilworth Technology Ltd Beta House
Fire Research Station Borehamwood Hertfordshire WD6 3BL, UK	Hexagon House Blackley Manchester M9 3DA, UK	Chilworth Research Centre Southampton SO1 7NS, UK

Tests for the explosion parameters have often been carried out in the Hartmann tube apparatus (see Plate 10.3), which is a vertical cylinder of 1.3 L capacity (Bartknecht, 1981). However, there are a number of drawbacks associated with the Hartmann tube device. The alternative device is the 20 L capacity spherical apparatus shown in Plate 10.4 introduced by Bartknecht (1981), where the dust can be more evenly distributed throughout the explosion chamber. In these apparatus, dust, oxygen concentration and the powerfulness of the ignition source can be varied to yield threshold values.

10.4 THE HUMAN FACTORS

Proper build-up and maintenance of an integrated system, such as a milk drying plant, has been mentioned earlier, as preventing and mitigating dust explosions depends very much on

human relations and human behaviour. A number of different personnel categories may be involved, including:

- Workers in the plant
- Foreman in the plant
- Workers from the maintenance department
- Plant engineers
- Safety engineers
- Purchasing department officers
- Safety manager
- Middle management
- Top management
- Suppliers of equipment
- Dust explosion experts/consultants

Adequate prevention and mitigation of dust explosion cannot be realized unless there is meaningful communication between the various categories of personnel involved. If such communication is lacking, the result can easily become both unsatisfactory and confusing (Eckhoff, 1991).

In general terms meaningful communication may be defined as conveyance and proper receipt and appreciation of adequate information whenever required. However, in order to receive, appreciate and use the information in a proper way, one must have:

- Adequate knowledge
- Adequate motivation
- Adequate resources and deciding power

Knowledge about dust explosion can be acquired by reading, listening to lectures, talking to experts etc., although experience of actual explosion prevention and mitigation works is perhaps the best form of knowledge. Genuine motivation is more difficult to achieve. It seems to be a fact of life that it is people who have themselves experienced serious explosion accidents that possess the highest level of motivation. In particular if the accident caused injuries and perhaps even loss of life, the people in similar areas are much more alert to the facts and are very keen to address the safety issues around them. This applies the top management as well. High-level motivation can also result from good demonstrations of real explosions, including their initiation by various ignition sources, as well as their propagation and damaging effects. Video and film can be used as powerful tools for demonstration if used properly.

The final element, adequate resources and the authority to put the good plans into practice, is in reality controlled by the top management. The real responsibility for establishing and running a proper safety assurance system must always lie with the top management. Summarizing the experience of a large, multi-national chemical company, Verhaegen (1989) suggested that the following 10 essential elements be involved to ensure proper safety management.

- Top management responsibility
- Safety statement (explicit commitment from top management)
- Objectives and goals (specification of long- and short-term expectations)
- Stated standards (written guidelines and rules)

- Safety committees (a dedicated organization for handling safety issues at all levels)
- Accident recorders (written analyses of accidents. Why did they happen? How can similar future accidents be prevented?)
- Safety personnel (qualified specialists essential as advisers, but responsibility remains with top management)
- Motivation (by information and involvement etc.)
- Training (a continual process; courses essential; the message must get through)

10.5 CONCLUDING REMARKS

Foods in general are combustible, and can be ignited causing a fire. Rapid drying sometimes employs hot air as the drying medium. The worst scenario is perhaps a dust explosion when food powders are involved. Both fire and dust explosion can cause injuries or even death to humans and are highly undesirable. They can also cause tremendous production loss and lengthy down times. Awareness, adequate knowledge, appropriate actions taken – including laboratory testing, explosion vent design/implementation, careful management (and minimization) of the factors that can lead to a hazard, rapid warning system etc. – all contribute to a safer practice in the food drying industry. This chapter only covers some key aspects. In order to achieve a high standard in fire and explosion protection in food drying practice, one has to go through a more rigorous approach to address the matters of concern.

REFERENCES

- Alfert, F., Eckhoff, R.K. and Fuhre, K. (1988) Zündwirksamkeit von Glimmnestern und heißen Gegenständen in industriellen Anlagen. *VDI-Berichte*, **701**, 303–319.
- Bartknecht, W. (1981) *Explosions-Course Prevention Protection*. Springer-Verlag, New York.
- Beever, P.F. (1984) Spontaneous ignition of milk powders in a spray-drying plant. *Journal of the Society of Dairy Technology*, **37**, 68–71.
- Beever, P.F. (1985) Fire and explosion hazards in the spray drying of milk. *Journal of Food Technology*, **20**, 637–645.
- Beever, P. and Crowhurst, D. (1989) Fire and explosion hazards associated with milk spray drying operations. *Journal of the Society of Dairy Technology*, **37**, 68–71.
- Bowes, P.C. (1984) *Self-heating: Evaluation and Controlling the Hazards*. Elsevier, Amsterdam.
- Brennan, J.G., Herrera, J. and Jowitt, R. (1971) Spray drying of orange juice. *Journal of Food Technology*, **6**, 295–307.
- Chen, X.D. and Stott, J.B. (1993) The effect of moisture content on the oxidation rate of coal during near-equilibrium drying and wetting at 50°C. *Fuel*, **72**, 787–792.
- Chen, X.D., Lake, R. and Jebson, S. (1993) Study of milk powder deposition on a large industrial drier. *Transactions of IChemE Part C: Food and Bioproducts Processing*, **71**, 180–186.
- Chen, X.D., Rutherford, L. and Lloyd, R.J. (1994) A laboratory study of milk powder deposition at room temperature on the stainless steel surface mimicking the ceiling of a spray drier. *Transactions of IChemE Part C: Food and Bioproducts Processing*, **72(C)**, 170–175.
- Cheng, S.X., Ge, X.S., Yao, C.C., Gao, J.W. and Zhang, Y.Z. (1993) Research on the validity of the steady-state calorimeter for measuring the total hemispherical emissivity of solids. *Measurement Science and Technology*, **4**, 721–725.
- Chong, L.V., Shaw, I.F. and Chen, X.D. (1996) The exothermic reactivity of milk powders as measured using a novel procedure. *Journal of Food Engineering*, **30(1–2)**, 185–196.

- Chong, L.V., Chen, X.D. and Mackereth, A.R. (2006) Experimental results contributed to early detection of smouldering milk powder as an integrated part of maintaining spray drying plant safety. *Drying Technology*, **24**, 783–789.
- Code of Practice for the Prevention, Detection and Control of Fire and Explosion in New Zealand Dairy Industry Spray Drying Plant (1990) Occupational Safety and Health, Wellington, New Zealand.
- Duane, T.C. and Synnott, E.C. (1981) Effect of some physical properties of milk powders on minimum ignition temperature. *ICHEME Symposium Series* No. 68.
- Duane, T.C. and Synnott, E.C. (1992) Ignition characteristics of spray-dried milk product powders in oven tests. *Journal of Food Engineering*, **17**, 163–176.
- Eckhoff, R.K. (1991) *Dust Explosions in the Process Industries*. Butterworth–Heinemann, Oxford.
- Gardner, G. (1994) Explosion suppressions gain favour. *The Chemical Engineer*, **April issue**, 21–23.
- Gibson, N. and Schofield, F. (1977) Fire and explosion hazards in spray driers. *ICHEME Symposium Series* No. 49, 53–62.
- International Dairy Federation (1987) Recommendations for fire prevention in spray drying of milk powder. *Bulletin of the International Dairy Federation* No. 219.
- Labuza, T.P., Heidebaugh, N.D., Silver, M. and Karel, M. (1971) Oxidation at intermediate moisture contents. *Journal of the American Oil Chemist's Society*, **48**, 86–90.
- Lloyd, R.J., Chen, X.D. and Hargreaves, J. (1996) A study of the relationship between lactose caking and the glass-transition of spray-dried lactose. *International Journal of Food Science and Technology*, **31**, 305–311.
- Lunn, G. (1992) *Dust Explosion Prevention and Protection Part 1: Venting*. IChemE, London.
- Masters, K. (1991) *Spray Drying Handbook*, 5th edn. Landman, NJ.
- Mulder, H. and Walstra, P. (1974) The milk fat globule – emulsion science as applied to milk products and comparable foods. Centre for Agricultural Publishing and Documentation, Wageningen, The Netherlands, pp. 33–35.
- Pham, Q.T., Wee, H.K., Kemp, R.M. and Lindsay, D.T. (1994) Determination of the enthalpy of foods by an adiabatic calorimeter. *Journal of Food Engineering*, **21**, 137–156.
- Pineau, J.P. (1984) Protection against fire and explosion in milk powder plants. *EuropeX. Explosion Research in Practice: 1st International Symposium*, Antwerp, April, Part 2.
- Raemy, A., Hurrell, R.F. and Loliger, J. (1983) Thermal behaviour of milk powders studies by Differential Thermal Analysis and heat flow calorimetry. *Thermochemica Acta*, **65**, 81–92.
- Reay, D. (1989) Fluid flow, residence time simulation and energy efficiency in industrial driers. In: *Drying '89* (eds A.S. Mujumdar and M. Roques). Hemisphere Publishing Corporation, New York, pp. 1–8.
- Roos, Y. and Karel, M. (1990) Differential scanning calorimetry study of phase transitions affecting the quality of dehydrated materials. *Biotechnology Progress*, **6**, 159–163.
- Roos, Y. and Karel, M. (1991) Plasticizing effect of water on thermal behaviour and crystallization of amorphous food models. *Journal of Food Science*, **56**, 38–43.
- Roos, Y. and Karel, M. (1992) Crystallization of amorphous lactose. *Journal of Food Science*, **57**, 775–777.
- Schofield, C. (1984) *Guide to Explosion Prevention and Protection. Part 1 – Venting*. Rugby, IChemE, London.
- Steenbergen, A.E., van Houwelingen, G. and Straatsma, J. (1991) System for early detection of fire in a spray drier. *Journal of the Society for Dairy Technology*, **44**, 76–79.
- Verhaegen, H. (1989) Safety, a management task. *Proceedings of 6th International Symposium of Loss Prevention and Safety Promotion in the Process Industries (June)*. Norwegian Society of Chartered Engineers, Oslo, Norway.
- Wake, G.C., Sleeman, M., Chen, X.D. and Jones, J.C. (1992) Theory and application of ignition with sequential reactions. *Journal of Thermal Science*, **1**, 208–212.
- Wallack, D.A. and King, C.J. (1988) Sticking and agglomeration of hydroscopic, amorphous carbohydrate and food powders. *Biotechnology Progress*, **4**, 31–35.

Index

- activation energy for microbial and enzyme deactivation, 104
- activation energy level for deactivation of micro-organisms and enzymes, 104
- adaptive control, 295
- additive cell deactivation model, 107
- additive type of deactivation kinetics, 107
- advanced control methods, 292–3
- apple tissue, 14–16
- artificial intelligence in control, 295–6
- atomization, 118–21

- banana slices, 178, 181
- β -carotene retention, 185–6
- bio-deterioration in drying – sub-cell level approach, 106–8
- Biot* number, 24
- browning reactions, 257

- caking and stickiness, 264
- carrot tissue, 170–71
- case hardening/crust formation, 261
- Choi and Okos model of heat capacities of pure food substances, 26
- Choi and Okos model of pure densities, 20
- Choi and Okos model of thermal conductivities of pure food substances, 22
- CIELAB colour expression system, 27
- colour, 26–9, 257–8
- colour change kinetics, 29
- colour perception and like/dislike pattern, 27
- composition based water activity model, 59–65
- concept of synergistic drying, 43
- control philosophy, 276–8
- control strategies, 273–4
- control variables, 272
- cracking/breakage, 262

- dairy powders, 149–51
- deactivation kinetics for bacteria/cells, 100–106
- deactivation rate constant, 100, 102
- death rate constant k_d , 100

- degree of violence in explosions, 301
- desiccation (sorption isotherm determination), 80
- diffusion along pore wall surfaces (schematic), 34
- diffusion theories, 32–42
- drier control, 270–71
- driers, 42–3
- droplet drying kinetics, 126–9
- drying characteristic curve, 3, 7–8, 164
- drying flux, 7, 30
- dust concentration effect on explosion, 301
- dynamics of deactivation process, 106

- effective diffusivity, 32–4
- effect of temperature on water activity, 73–4
- egg products, 154
- energy balances for spray drying, 114
- enzymes, 154
- enzyme stability, 95
- equilibration time, 85
- equilibrium isotherms, 6, 29–30, 230
- examples
 - calculation of heat transfer coefficient in superheated steam drying, 163, 165
 - drier control, 271–2
 - drying of potato slices, 202–10
 - GAB model parameter determination, 71
 - heat and mass balance of a spray drier, 135
 - single stage vapor-compression heat pump drying operation, 218–21
 - sorption heat determination, 74–5
 - time to reach equilibrium, 86
 - vacuum drying of soup, 239–43
- explosion protection, 310
- explosive characteristics of milk powder, 311
- explosive concentration, 300

- feed-forward/predictive control, 278–9
- Fickian type diffusion, 36–7
- film parameters, 46
- fire and explosion, 299
- fires, 302

- freeze and vacuum drying, 225–7, 234–6, 236–9
 atmospheric fluidized bed freeze dryer, 239
 drying kinetics under vacuum, 236
 food and air properties, 227–32
 heat transfer mechanisms at low pressures, 232
 new advances, 243
 phase diagram of water and its critical point, 226
 pressure–temperature data for pure water, 227
 schematic diagram of food in a vacuum drying chamber, 233
- GAB model of equilibrium isotherm, 30
 Gibbs free energy, 56–7
 glass-transition, 144–5
 glass-transition temperature
 (Couchmann–Karasz equation), 145
 glass-transition temperatures (Gordon and Taylor equation), 231
 glass-transition temperatures of various amorphous food materials, 146
 gravimetric method (sorption isotherm determination), 78
- hazard potential of milk powder deposit on dryer walls, 306
 heat and mass balance for heat pump drying, 197–201
 heat and mass balances, 39–41
 heat flux, 20–22
 heating and cooling function, 25
 heat pump assisted drying, 190–91
 cascade heat pump drying systems, 214–15
 classification, 191–2
 coefficient of performance (COP), 194
 compression refrigeration/heat pump cycle (schematics), 193
 differential equations of heat and mass balances, 199–202
 drying systems with multiple evaporators, 215–17
 heat pump dryer (schematics), 194
 innovative systems, 213
 mass and energy balances, 195–6
 multi-stage compression heat pump drying, 213–14
 optimal use of heat pump in drying system, 210–212
 specific moisture evaporation rate (SMER), 197
 thermodynamics of air stream, 195
 vapor absorption heat pump dryer, 217–19
 heat pump classification, 192
 heat transfer coefficient, 26, 163
 heat transfer general, 20–26
- human factors in fire/explosion protection, 314–15
 hygroscopic methods (sorption isotherm determination), 84
 hysteresis of sorption isotherms, 58–9
- indicative energy consumption of various dehydration processes, 114
 in-drying problems, 95–6
 interactive cell deactivation kinetics, 107
 interactive type of deactivation kinetics, 108
 isotherm models, composition based
 Grover model (sorption isotherm), 63
 Money–Born model (sorption isotherm), 62
 Norrish model (sorption isotherm), 60
 Ross model (sorption isotherm), 61
 Salwin model (sorption isotherm), 64
 isotherm models, three-parameter models
 Ferro Fontan *et al.* equation, 68
 Guggenheim–Anderson–de Boer (GAB) model, 69, 230
 Schuchmann–Ray–Peleg equation, 69
 isotherm models, two-parameter models
 BET equation, 67–8
 Chung and Pfost equations, 67
 Halsey equation, 66–7
 Henderson equation, 66
 Langmuir equation, 65
 Oswin equation, 65–6
 Smith equation, 65
 isotherm measurement, 78–86
 isotherms (sorption) models, 65–78
- K_{st} values, 313
- $L^*-a^*-b^*$ system, 26–8
 lipid oxidation, 258
 local evaporation term, 42
 local temperatures in moist material being dried, 97
 local water content in moisture material being dried, 98
 Luikov theory of drying processes, 49–51
- manometric method (sorption isotherm determination), 83–4
 mass and heat balances for spray drying, 131–4
 mass transfer correlations, 46–8
 Meerdink and Van't Riet model of deactivation kinetics, 102
 micro-encapsulated products, 151
 microscopic images
 agglomerated milk powders, 140
 apple cells, xx

- avocado flesh, xviii
- banana cross-section, xxii
- banana skin cross-section, xxiii
- celery cross-section, xviii
- cooked apple tissue in environmental SEM, 15
- cooked potato cells, xx–xxi
- cream particle, xvi, 138
- fresh cut apple tissue in environmental SEM, 15
- gel bead particle with imbedded bacteria, xvii
- raw potato cells, xix
- shell-fish (Pipi) tissue, xxiv
- skim milk powder, xvi, 138
- whey protein concentrate powder, 138
- whole milk powder, xv, 138
- microstructural change during drying of potato issue (local shrinkage effect), 19
- microstructure (schematic) of a spray dried particle, 138
- microstructure schematics of a typical spore cross-section, 107
- minimum ignition temperature MIT, 307
- moisture effect on explosion, 301
- monolayer moisture contents, 70
- mixture densities, 23
- mixture glass-transition temperature, 145, 231
- mixture heat capacity model, 26
- model predictive control, 293–4
- multi-stage heat pump driers, 213–19

- natural pH values of foods, 99

- optimum pH for micro-organisms, 99
- optimal pH values of foods, 99
- overall heat transfer coefficient, 26

- page model, 8
- parallel and series model of thermal conductivity, 23–4
- particle density and bulk density, 141–2
- particle insolubility index, 144
- particle properties (typical), 141
- particle size and size distribution, 142–3
- particle size effect on explosion, 301
- PID control, 279–86
- pore channel length reduction, 36
- pore formation, 261
- pore narrowing, 35
- porosity effect on diffusivity, 38
- post-drying, 252–3
- potato tissue, 174–6, 202
- powder deposition, 303–4
- powder flowability, 143
- powder microstructure, 137–41
- powder separator, 122–4
- powder solubility, 145–7
- pre-drying, in-drying and post-drying concepts, 90
- pressure–time history for suppressed explosion, 313
- process reaction curve, 288
- proteins, 260
- psychrometric chart, 116
- pure densities, 20

- quality attributes for dried foods
 - caking/stickiness, 264
 - case hardening, 261
 - color and browning reactions, 257
 - crust formation, 261
 - D*-value, 256
 - lipid oxidation, 258–9
 - microbial, 255–7
 - protein structural change, 260–61
 - rehydration, 263
 - shrinkage, collapse and pore formation, 261–2
 - stress, cracking and breaking, 262
 - texture, 264
 - vitamins retention, 265
 - volatile retention, 263
- quality characteristics of dried foods, 255

- Raoult's law, 59
- rate of explosion pressure build-up, 312
- reducing risk of explosion, 301
- rehydration, 263
- relative humidity, 6
- residence time in spray drier, 129–30
- rheological fluid types, 13
- rheological properties of food liquids, 13
- rotary drier control, 274

- scale of food materials, 9
- self-ignition, 302
- shear-deformation behaviour of raw and cooked apple tissue, 16
- shear rate, 10–14
- shear stress, 10–14
- shrinkage and density, 16–20, 261
- shrinkage modelling, 17–18
- specific heat capacity, 26
- spore, 107
- spray dried products
 - egg products, 154
 - enzyme products, 154–5
 - microencapsulated products, 151–2
 - skim milk powder, 149
 - sugar-rich products, 153
 - whey products, 150–51

- whole milk powder, 150
- spray drier control, 275
- spray drier efficiencies, 134–7
- spray drying, 113–14, 117
- spray drying chamber, 121–2
- spray drying systems
 - advantages, 114
 - atomization systems, 118–20
 - chamber, 121–2
 - components of a spray drying system, 117
 - control, 275
 - droplet drying, 125–9
 - drying efficiencies, 134–7
 - drying gas supply, 117
 - drying parameters (feed conditions, feed solids, inlet/outlet air conditions), 147–9
 - heat and mass balances, 130–35
 - heating system, 117
 - mean droplet size correlations, 121
 - powder separators, 122–4
 - reaction engineering approach to droplet drying, 128–9
 - residence time, 129–30
 - single stage process, 115
- state diagram of food materials, 253
- stress–strain relationships for different foods, 14
- sub-cell level deactivation kinetics, 107
- sugar-rich products, 153
- superheated steam drying system
 - advances in drying of biological materials, 177–82
 - drying times, 174
 - flowchart, 161
 - inversion phenomena, 162
 - lab device schematics, 165–6
 - mathematical modeling, 182–6
 - pretreatment effects on final product properties, 176
 - sample products, 170–71
- super-heated steam drying (low pressure), 160–161
- suppression and K_{ST} value, 312–13
- surface-centre temperature and moisture content profiles, 97–8
- synergistic drying concept, 43
- temperature effect on explosion, 301
- thermal conductivity, 22, 228–9
- thermal-resistant *B. stearothermophilus* spores, 95
- tortuosity effect on diffusivity, 38
- turbulence effect on explosion, 301
- typical values of heat capacities of foods, 25
- Van der Waals molar volumes and molecular weights of sugars, 12
- Van Meel model of drying kinetics, 30–32, 51–2
- vent ratio, 311
- viscosity, 10–13
- viscosity models
 - Einstein model, 11
 - Krieger–Dougherty model, 11
 - maximum packing fraction, 11
 - order of magnitudes of viscosities, 11
 - Rao model on the effect of concentration, 11
 - Telis *et al.* model, 11–12
 - yield stress, 13
- viscosity-temperature function, 10
- vitamin retention, 265
- volatile development or retention, 263
- water activities of saturated salt solutions
 - as a function of temperature, 80
- water activity, 5–6, 56–8
- water activity above boiling point, 75
- water activity of sulphuric acid solutions at different concentrations and temperatures, 81
- water activity range that suits the growth of micro-organisms, 93
- water content dependent deactivation kinetics, 102–3
- whey protein nitrogen index (WPNI) values of skim milk powders, 150
- Young's modulus, 14

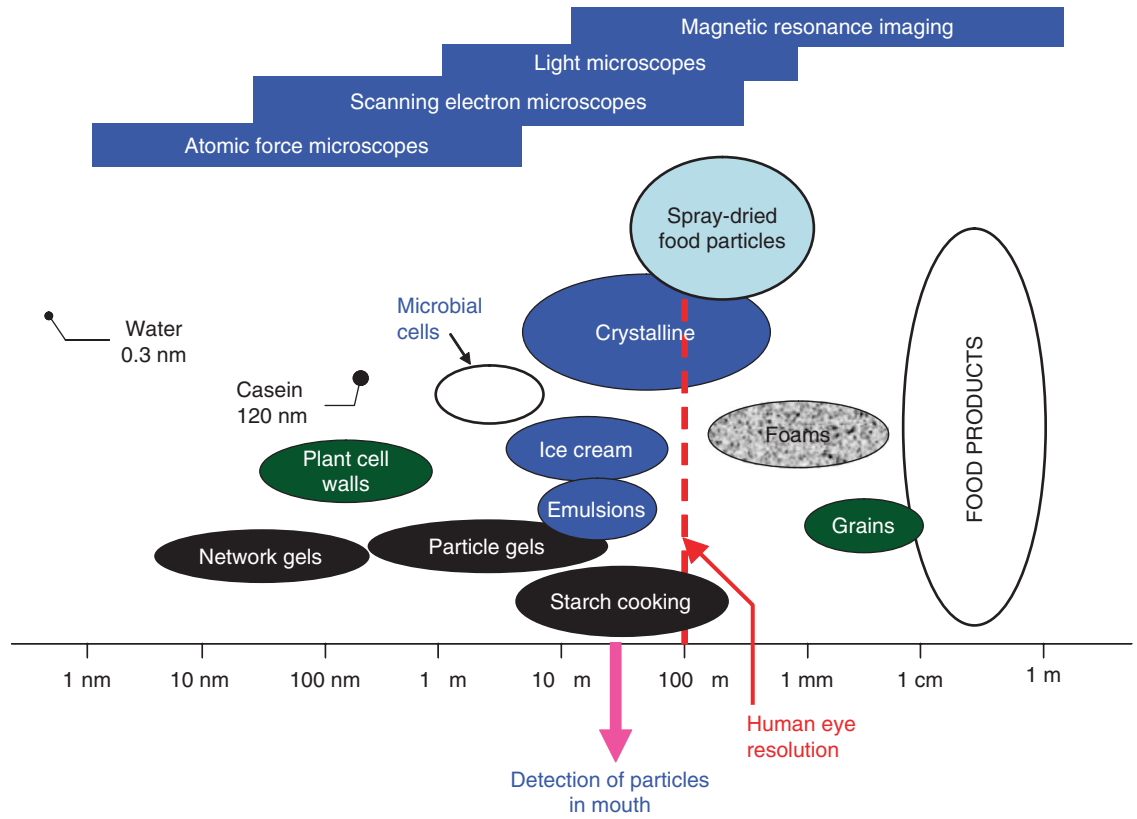


Plate 1.1 Scales of food components and products, and the visualisation tools for characterisation (modified from a diagram provided by Jose Aguilera (2004) by X.D. Chen).

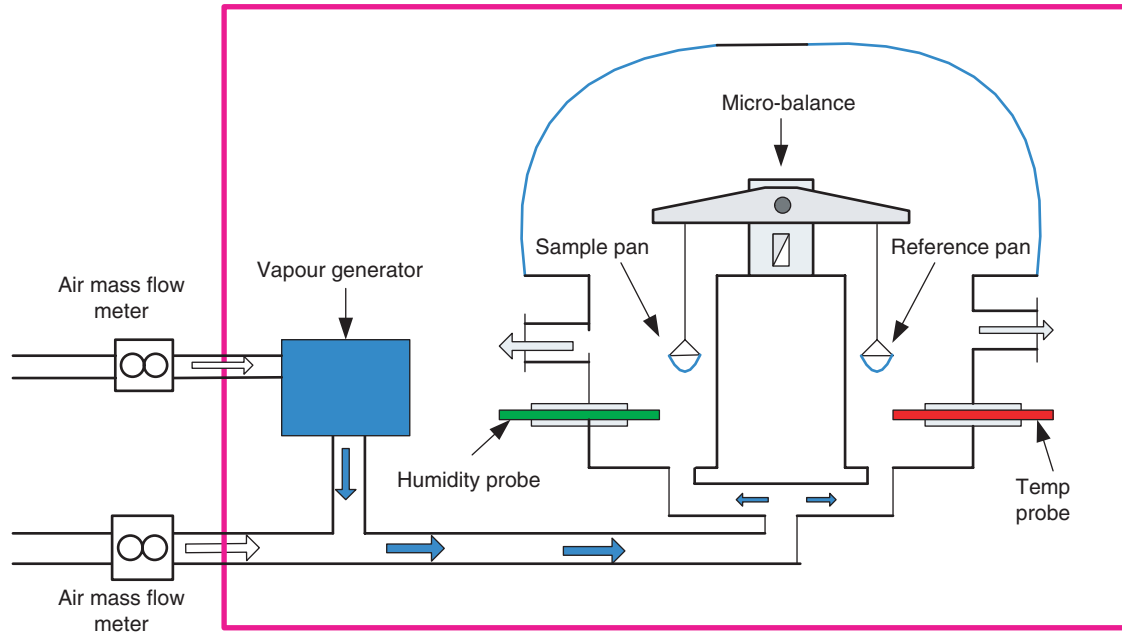


Plate 2.1 Schematic diagram of dynamic vapour sorption instrument.

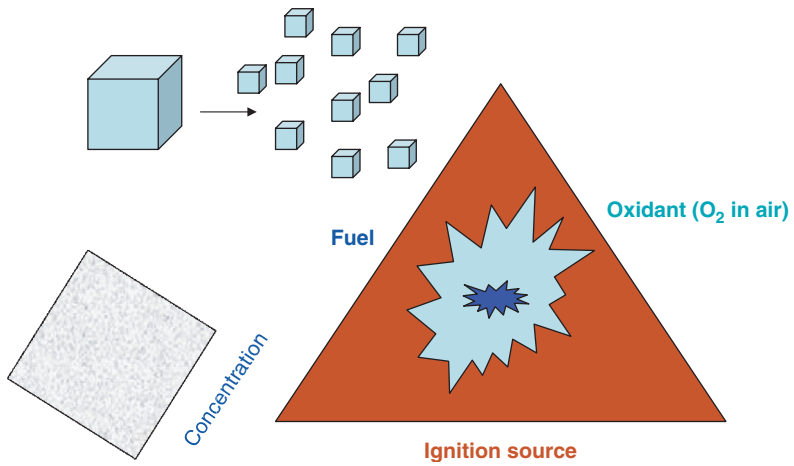


Plate 10.1 Fire triangle for a flammable dust cloud (drawn by X.D. Chen).

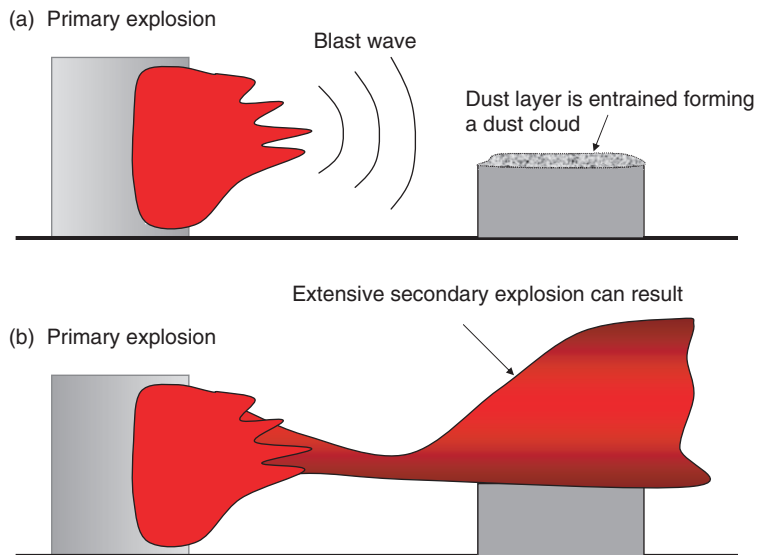


Plate 10.2 An illustration of the primary explosion and secondary explosion (modified from Eckhoff, 1991).

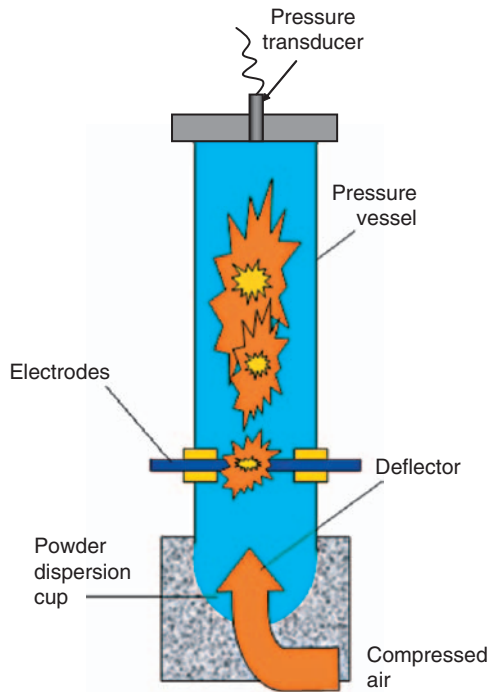


Plate 10.3 The Hartmann tube apparatus for testing the explosiveness of dust samples (drawn by X.D. Chen; after Bartknecht, 1981).

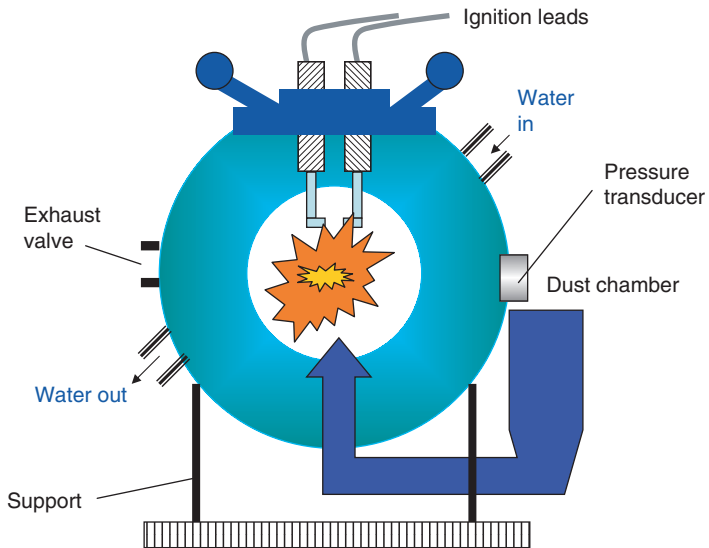


Plate 10.4 The spherical bomb apparatus for testing the explosiveness of dust samples (drawn by X.D. Chen; after Schofield, 1984).